AD-A107 662 PENNSYLVANIA STATE UNIV UNIVERSITY PARK APPLIED RESE--ETC F/G 20/4
INVERSE AXISYMMETRIC BODY STUDY.(U)
AUG 81 J J EISENHUTH, G H HOFFMAN N00024-79-C-6043
UNCLASSIFIED ARL/PSU/TM-81-177 NL

1 OF 3
ADA
107682

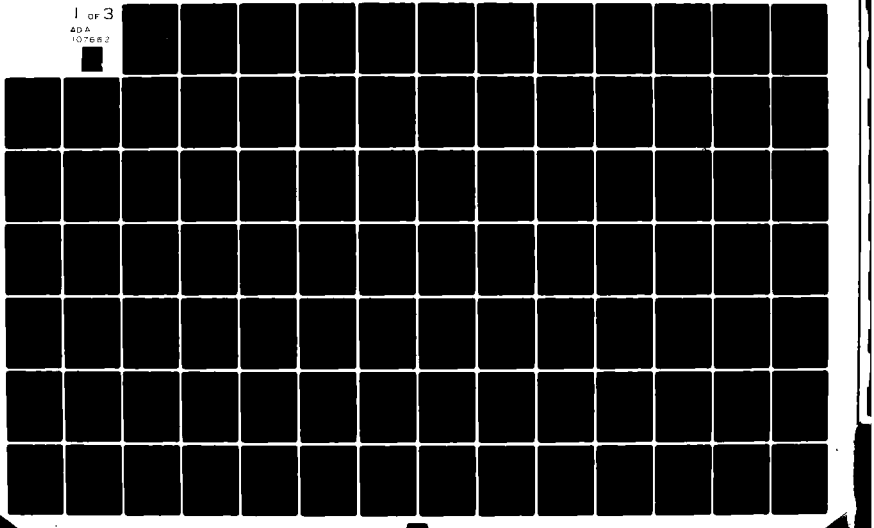

LEVEL II

(6)

AD A107662

INVERSE AXISYMMETRIC BODY STUDY

J. J. Eisenhuth, G. H. Hoffman

Technical Memorandum
File No. TM 81-177
19 August 1981
Contract No. N00024-79-C-6043

Copy No. 39

The Pennsylvania State University
APPLIED RESEARCH LABORATORY
Post Office Box 30
State College, PA 16801

NAVY DEPARTMENT

NAVAL SEA SYSTEMS COMMAND

UNCLASSIFIED

SECURITY CLASSIFICATION OF THIS PAGE (When Data Entered)

REPORT DOCUMENTATION PAGE		READ INSTRUCTIONS BEFORE COMPLETING FORM
1. REPORT NUMBER TM 81-177	2. GOVT ACCESSION NO. AD-A107662	3. RECIPIENT'S CATALOG NUMBER
4. TITLE (and Subtitle) INVERSE AXISYMMETRIC BODY STUDY		5. TYPE OF REPORT & PERIOD COVERED Technical Memorandum 6. PERFORMING ORG. REPORT NUMBER
7. AUTHOR(s) J. J. Eisenhuth, G. H. Hoffman		8. CONTRACT OR GRANT NUMBER(s) N00024-79-C-6043
9. PERFORMING ORGANIZATION NAME AND ADDRESS Applied Research Laboratory P. O. Box 30 State College, PA 16801		10. PROGRAM ELEMENT, PROJECT, TASK AREA & WORK UNIT NUMBERS
11. CONTROLLING OFFICE NAME AND ADDRESS Naval Sea Systems Command - Codes NSEA-63R3 and Department of the Navy NSEA-63R2 Washington, DC 20362		12. REPORT DATE 19 August 1981 13. NUMBER OF PAGES 278
14. MONITORING AGENCY NAME & ADDRESS(if different from Controlling Office)		15. SECURITY CLASS. (of this report) 15a. DECLASSIFICATION DOWNGRADING SCHEDULE

16. DISTRIBUTION STATEMENT (of this Report)

Approved for Public Release. Distribution Unlimited.
Per NAVSEA - November 3, 1981.

17. DISTRIBUTION STATEMENT (of the abstract entered in Block 20, if different from Report)

18. SUPPLEMENTARY NOTES

19. KEY WORDS (Continue on reverse side if necessary and identify by block number)

inverse, axisymmetric, body, potential, flow, laminar flow

20. ABSTRACT (Continue on reverse side if necessary and identify by block number)

A potential flow inverse body method was used to generate a family of underwater bodies that would generally possess extensive laminar flow by the use of surface heat addition. Parameters specifying the pressure coefficient distribution were varied in order to find the limits of these parameters beyond which a body could not physically be generated. Length-to-diameter ratios and prismatic coefficients were computed as a function of the parameters. Specific cases representing the limits of parameters are used

DD FORM 1 JAN 73 1473 EDITION OF 1 NOV 65 IS OBSOLETE

UNCLASSIFIED

SECURITY CLASSIFICATION OF THIS PAGE (When Data Entered)

20. (Continuing)

as examples in the graphical presentation of body contours and pressure coefficient distributions. Curves of temperature and heat flux distributions showing limits for the effective use of heat in suppressing boundary layer transition are also presented for these cases.

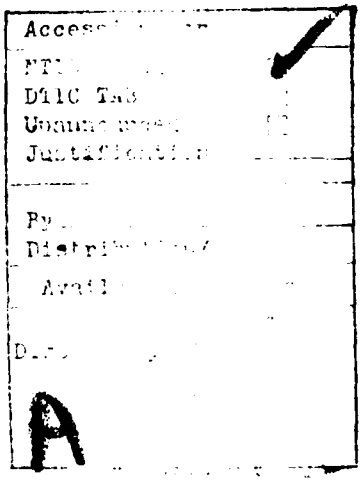

Subject: Inverse Axisymmetric Body Study

References: See Page 25

Abstract: A potential flow inverse body method was used to generate a family of underwater bodies that would generally possess extensive laminar flow by the use of surface heat addition. Parameters specifying the pressure coefficient distribution were varied in order to find the limits of these parameters beyond which a body could not physically be generated. Length-to-diameter ratios and prismatic coefficients were computed as a function of the parameters. Specific cases representing the limits of parameters are used as examples in the graphical presentation of body contours and pressure coefficient distributions. Curves of temperature and heat flux distributions showing limits for the effective use of heat in suppressing boundary layer transition are also presented for these cases.

Acknowledgment: This study was sponsored by the U. S. Naval Sea Systems Command, Codes NSEA-63R3 and NSEA-63R2. Acknowledgment is also given to D. W. Prather, L. Lantz, and K. C. Kaufman for their contributions in the numerical and computational aspects of this study.

Table of Contents

List of Figures

List of Symbols

C_p pressure coefficient = $\dfrac{p^* - p_\infty^*}{\frac{1}{2}\rho_\infty^* V_\infty^{*2}}$

C_Ψ prismatic coefficient = $\dfrac{\text{volume of body}}{\text{volume of cylinder}}$

L^* axial length of body

M pressure gradient parameter = $\dfrac{x}{u_e}\dfrac{du_e}{dx}$

n exponent in conical flow formulation

p^* local pressure

p_∞^* pressure in the free stream

r_o^* local body radius

r_o nondimensional local body radius = $\dfrac{r_o^*}{L^*}$

R_{δ^*} Reynolds number = $\dfrac{u_e^* \delta^*}{\nu_\infty^*}$

S slope of C_p curve in mid-body region = $\dfrac{C_{p_2} - C_{p_1}}{x_2 - x_1}$

u_e^* velocity at the edge of boundary layer

u_e nondimensional velocity at the edge of boundary layer = $\dfrac{u_e^*}{U_\infty^*}$

U_∞^*, V_∞ free-stream velocity

x^* length along body axis—also, arc length distance along body surface

x nondimensional distance = $\dfrac{x^*}{L^*}$

α constant = $\left[(n+1)(1 - C_{p_2}) - \dfrac{\eta_2}{2} S\right]$ [See Eq. (8)]

β pressure gradient parameter = $\dfrac{2M}{M + \lambda + 1}$, also

constant = $\left[n(1 - C_{p_2}) - \dfrac{\eta_2}{2} S\right]$ [See Eq. (8)]

δ^* boundary layer displacement thickness

η relative axial distance = $1 - x$

λ radius gradient parameter = $\frac{2x}{r_o} \frac{dr_o}{dx}$

ν_∞* kinematic viscosity in free stream

ξ normalized axial distance = $\frac{x}{x_1}$

ξ_m value of ξ where Segments I and II of C_p curve meet

Subscripts

1 end location of the C_p distribution's Segment I

2 beginning location of the C_p distribution's Segment III

I refers to Segment I of C_p distribution

II refers to Segment II of C_p distribution

III refers to Segment III of C_p distribution

c cone

crit critical value

Introduction

Inverse methods permit the specification of certain performance properties of a body and from this specification the generation of a compatible body profile. A potential flow inverse method, in which the pressure distribution of an axisymmetric body operating in water is specified, was developed at the Applied Research Laboratory, The Pennsylvania State University (ARL/PSU) and was reported in Reference 1. This method employs a higher order surface singularity technique using parabolic surface elements with linearly varying sources. The body shape is obtained through an iterative scheme which is rapidly convergent.

There is at present a strong need to exercise such a method in establishing some bounds on a class of bodies that lend themselves to extensive laminar flow in the forebody region, either by the shape alone or by a combination of shape and surface heat. This class of bodies requires that the pressure distribution change gradually over a major portion of the body extent and be free of abrupt peaks in the nose region. This insures the best possible environment for laminar flow.

In answer to this need, a study was undertaken in which the pressure distribution was specified in parametric form. Bodies were generated for a range of parameters and then analyzed with respect to surface heat requirements for a specific body diameter and a specific speed of operation. In the interest of presenting the data generated to date, no analysis of the turbulent boundary layer flow portion of the body nor the estimation of the overall drag is included in this report. This will be reported in a subsequent memorandum.

Pressure Distribution Specification

The approach that was used was to divide the pressure coefficient distribution into three segments as shown in Figure 1. Segment II, the largest of the three, has a constant pressure gradient and its limits are indicated by points (1) and (2). Segments I and III provide a transition from the C_p values at (1) and (2) to a value of $C_p = 1.0$ at the nose and tail, respectively. Four parameters that can, therefore, be specified are x_1, C_{p_1}, x_2, and C_{p_2}. If these are specified, so is the slope of Segment II,

$$S = \frac{C_{p_2} - C_{p_1}}{x_2 - x_1} \quad . \tag{1}$$

If S is chosen, only three of the original four parameters need be specified.

Other parameters that might enter the picture would be those associated with the type of curve that is used in either Segment I or Segment III. In this study, only one type of curve definition was used in each of these two segments. Therefore, as far as this study is concerned, only four parameters were used.

Segment I: After trying a number of defining curves, the one one that was used in this study was a portion of an ellipse. The semiminor axis is the value, x_1 , and the semimajor axis is approximately C_{p_1}. The semimajor axis is exactly equal to C_{p_1} when $S = 0$, but is slightly different for other S values because of a built-in requirement that curve Segments I and II meet with the same slope.

The defining equation for the C_p distribution curve in Segment I is given by:

$$C_{p_I} = 1 - \left\{ \left[1 - C_{p_1}' \right]^2 \left[1 - (1 - \xi)^2 \right] \right\}^{\frac{1}{2}} \qquad (2)$$

where

$$\xi = \frac{x}{x_1}$$

and

$$(1 - C_{p_1}')^2 = \frac{\left[(1 - C_{p_1}) - \dfrac{x_1^2 S^2}{(1 - C_{p_1})} \right]}{\left[1 - \left(\dfrac{S x_1}{1 - C_{p_1}} \right)^2 \right]} \quad .$$

The C_p calculations for Segment I should be made only to the point:

$$\xi = \xi_m = 1 + \frac{S x_1}{(1 - C_{p_1})} \quad . \qquad (3)$$

This type of defining curve produces rather blunt noses when the x_1 choices are relatively small. These noses do not have flat faces, but in some cases come fairly close to that type of shape.

Another type of defining curve that was tried, but not used in this study, was a parabolic one. The defining equation for this type can be written as:

$$C_{p_I} = C_{p_1}' + (1 - C_{p_1}')\ (1 - \xi)^2 \tag{4}$$

where

$$\xi = \frac{x}{x_1}$$

and

$$C_{p_1}' = -\frac{(1 + C_{p_1})}{2} - \left[\frac{(1 + C_{p_1})^2}{4} - \left(\frac{x_1^2\ S}{4} - C_{p_1}\right)\right]^{\frac{1}{2}} .$$

Again the C_p calculations for Segment I should be made only to a point ξ_m. In this case, ξ_m is given by:

$$\xi_m = 1 + \frac{x_1\ S}{2\ (1 - C_{p_1}')} . \tag{5}$$

The noses that result from this description are more pointed, even when the chosen x_1 value is relatively small.

Segment II: A great deal more need not be said about this segment. The slope of the C_p curve is constant and is given by Equation (1). The equation for C_p in Segment II then becomes

$$C_{p_{II}} = C_{p_1} + x_1(1 - \xi)\ S \tag{6}$$

with the calculations beginning at $\xi = \xi_m$. ξ is defined the same as it has been previously.

Segment III: The third segment was formulated by attempting to fair into the local potential flow of a cone. The local conical solution, originally derived by Mangler (see Reference 2), shows that:

$$u_c \sim \eta^n$$

from which

$$C_{p_c} = 1 - a\,\eta^{2n}$$

where

$$0 \leq 2n \leq 1$$

and

$$\eta = 1 - x \quad .$$

So that there will be continuity of C_p and (dC_p/dx) at point (2), the pressure coefficient can be written as:

$$C_p = 1 - a\,\eta^{2n} + b\,\eta^{(2n+2)} \quad . \tag{7}$$

Imposing these continuity conditions, the final equation that results is:

$$C_{p_{III}} = 1 - \alpha\,\bar{\eta}^{2n} + \beta\,\bar{\eta}^{(2n+2)} \tag{8}$$

where

$$\alpha = \left[(n+1)\,(1 - C_{p_2}) - \frac{\eta_2}{2}\,S\right] \quad , \tag{9}$$

$$\beta = + \left[n(1 - C_{p_2}) - \frac{\eta_2}{2}\,S\right] \quad , \tag{10}$$

and

$$\bar{\eta} = \frac{\eta}{\eta_2} = \frac{1 - x}{1 - x_2} \quad . \tag{11}$$

The choice of n = 0.1 was made in this study. This was somewhat arbitrary, but it was felt that what happens from a potential flow point of view in the tail region is not as important as it is in the nose portion. On reflection, it would probably have been just as good or better to use a different value of n or to formulate the distribution by use of a parabola as discussed in the Segment I description. In an extension of this work, when we pay more attention to the shaping of the aft part of the body, more care will be taken with this aspect.

Body Generation Procedure and Results

Bodies were generated by choosing combinations of x_2 and S as fixed parameters and then systematically varying x_1 and C_{p_1} to see what ranges of values of these latter parameters would permit the generation of possible bodies. When these ranges are exceeded, a body consistent with the prescribed pressure distribution is not possible.

In order to show graphically the ranges in question, contours enclosing the x_1 - C_{p_1} combinations for possible body shapes are shown in Figures 2-10. x_2 values of 0.7, 0.8, and 0.9 were chosen for each S value. The S values were chosen to be -0.075, 0.0, and +0.075. The n value in all cases was 0.1. Superimposed on the contour curves are lines of constant length-to-diameter ratio, L/D, and lines of constant prismatic coefficient, $C_\forall$ (volume of body/ volume of cylinder of same L/D).

The numbered points, shown in Figures 2-10, represent the calculations used to determine the contours. As can be seen, these points do not lie exactly on the faired contours.

In determining the right-hand portion of a contour, successive runs were made for increments of $\Delta x_1 = 0.01$ and a faired curve drawn through the results. Thus, the possible error in the location of the right-hand part of the contour is ±0.01.

Points on the left portion of the contour were restricted to $x_1 \geq 0.01$. The value $x_1 = 0.01$ represents a practical lower limit for possible body shapes which conform acceptably to the present C_p parameterization. For $x_1 < 0.01$ the direct program predicts an unacceptable overshoot in C_p in the vicinity of x_1.

This brings us then to the display of the specified C_p curves and the corresponding generated bodies for the cases shown with the contour curves. These cases will represent the extremes in body shape that can be generated within the range of fixed parameters that were chosen and are shown in Figures 11-87. In addition to the specified C_p curves and the body shapes, C_p values generated by a direct program are also shown. One can see that the direct program points match the specified distributions very well with the possible exception of the slight overshoot in the $x_1 = 0.01$ cases.

Temperature Distribution Calculations and Results

The type of body generated in this study is amenable to the use of wall heating as a means of extending the length of its stable boundary layer region. A procedure for estimating the distribution of wall temperature and heat flux necessary to attain this objective was developed at ARL/PSU and is reported in Reference 3. The procedure makes use of two criteria, the "minimum heat" and the "maximum heat" conditions. The minimum heat criterion implies that, for a particular free-stream velocity, enough heat is added to make the local operating Reynolds number $R_{\delta}*$, equal to the critical value of that Reynolds number. This should insure that there will never be any amplification of waves in the laminar boundary layer. The maximum heat criterion fixes the $R_{\delta*_{crit}}$ at its maximum value. Whether there is amplification depends upon the free-stream velocity and the local thickness $\delta*$ being high enough to have the local operating $R_{\delta}*$ exceed the maximum $R_{\delta*_{crit}}$.

A code embodying these criteria was used in this study to provide the temperature and heat flux information for the chosen body cases. The procedure is based on the laminar characteristics resulting from similar solution of the axisymmetric boundary layer equations for water with wall heat addition. The major parameters in this procedure are the pressure gradient parameter β and the differential temperature between the wall and the ambient temperature. It was shown in Reference 3 that the parameter β can be related to two other parameters, the pressure gradient parameter M and the radius gradient parameter λ through the equation:

$$\beta = \frac{2M}{M + \lambda + 1} \tag{12}$$

where

$$M = \frac{x}{u_e} \frac{du_e}{dx} \tag{13}$$

and

$$\lambda = \frac{2x}{r_o} \frac{dr_o}{dx} \quad . \tag{14}$$

x here is the arc length distance along the body surface, u_e is the velocity at the edge of the boundary layer (equivalent to the tangential velocity at the body surface via potential flow theory), and r_o is the local body radius. Therefore, from the C_p distributions and corresponding body shapes of this study, the local values of β can be calculated directly from the local values of M and λ.

Although not used in the calculations of this study, a recently developed reformulation permits β to be calculated somewhat more simply by:

$$\beta = 2 \times r_o^2 \frac{du_e}{d\zeta} \tag{15}$$

where

$$\zeta = x \, r_o^2 \, u_e \quad . \tag{16}$$

The development of this alternative formulation appears in the Appendix.

The specified C_p distributions and the derived body shapes were used as inputs to the temperature and heat flux estimating procedure. The results are shown in Figures 88-241 for a vehicle velocity, U_∞ = 50 fps and a maximum body diameter of 21 inches.

One of the first observations is that the temperature and heat flux distributions in the forward nose regions (Segment I) are never smooth. This is the result of the nature of the C_p and radius distributions at the nose. Although the curves of C_p (therefore u_e) and radius versus axial distance are both smoothly varying, u_e versus arc length curves have localized changes in slope that ultimately cause irregularities in the temperature and heat flux curves. The cause of these irregularities was studied in great detail to make sure they were not a function of numerical noise by way of the spline routines used in curve fitting or the number of points that were used. The conclusion was reached that the irregularities were the result of the combination of velocity and body radius distributions and is, therefore, a phenomenon that exists for this family of bodies. The temperature and heat flux curves were drawn by using straight line segments between points. Attempts to draw these as curves with continuous slopes were not at all successful.

Given along with the graphs are values of total heating power for the extent of arc length distance along which heat is added. As can be seen, the temperature and heat flux curves stop at distances less than the full length of the body. For the minimum heat, this is an indication that the operating displacement thickness Reynolds number has exceeded the peak critical Reynolds number beyond the point where the curves end.

This further indicates that the boundary layer is unstable beyond this point and that transition is imminent. The ends of these minimum heat curves can thus be used as a conservative estimate of the transition location on each body.

One other part of the temperature heat flux study is shown in Figures 242-251. In order to show the effects of free-stream velocity on the heating requirements, values of V_∞ of 30, 40, and 60 fps were used and are shown in Figures 242-247. Along with the computations at 50 fps already shown, these give the reader some idea of the effects of forward speed. The effects of body diameter (and therefore body length) are shown in the results displayed in Figures 248-251 along with the original results of Case 22 with a body diameter of 21 inches.

Discussion of Results

This study provides a basis for determining the range of body shapes that are possible for one type of parameterized pressure distribution. This type of distribution permits the maintenance of laminar flow over a major portion of the body by the addition of heat to the body wall. The results that are presented are intended to be used as a catalog for quickly making a preliminary choice of a body to fit some specific requirement.

To carry the range of parameters beyond those chosen is also possible, but time and the overwhelming bulk of data did not permit this. For instance, other values of the slope S could certainly have been used. A more negative value of S would provide a greater hedge against transition. The positive S value was used primarily to show that a small adverse pressure gradient could be used without disastrous results. The value of x_2 could also have been made larger, thus pushing aft the location of the body maximum diameter and again improving the chances of moving the transition location farther back on the body.

With regard to the temperature and heat flux distributions, one would certainly not provide heat in the irregular manner displayed near the nose for most of the cases. These curves could be smoothed making sure that the resulting distributions lie somewhere between the original maximum and minimum curves.

It is hoped that the presentation of these results will provide the designer with a practical means for making preliminary choices of body shapes. It should not be viewed as a final tool for the complete hydrodynamic design of an underwater body. Overall drag estimation,

including the contribution of the aft portion of the body with its own difficult computational problems must still enter the picture and eventually be included in a completely inverse design approach. Then too, the approximate similarity considerations used in the heating calculations should be checked by the use of more sophisticated nonsimilar procedures.

References

1. Fernandez, J., "A Higher Order Surface Singularity Method for the Axisymmetric Inverse Problem," ARL/PSU Technical Memorandum, File No. 79-125, June 25, 1979.

2. Rosenhead, L., Laminar Boundary Layers, Oxford at the Clarendon Press, 1963, pp. 428-430.

3. Eisenhuth, J. J. and Hoffman, G. H., "A Simplified Method for Predicting Body Temperature Distribution in the Preliminary Design of Heated Underwater Vehicles," ARL/PSU Technical Memorandum, File No. 79-02, January 4, 1979.

19 August 1981
JJE:GHH:mmj

Appendix

Calculation of β

By definition

$$\beta = \frac{2M}{M + \lambda + 1} \tag{A-1}$$

where

$$M = \frac{x}{u_e} \frac{du_e}{dx} \quad , \tag{A-2}$$

$$\lambda = \frac{2x}{r_o} \frac{dr_o}{dx} \quad . \tag{A-3}$$

A single expression for β can be found in which it is not necessary to perform the intermediate steps of calculating M and λ. This expression can be derived as follows:

$$\frac{M + \lambda}{x} = \frac{1}{u_e} \frac{du_e}{dx} + \frac{2}{r_o} \frac{dr_o}{dx} = \frac{1}{u_e r_o^2} \frac{d}{dx} (u_e r_o^2) \quad . \tag{A-4}$$

Therefore, the denominator of Equation (A-1) becomes:

$$M + \lambda + 1 = \frac{x}{u_e r_o^2} \frac{d}{dx} (u_e r_o^2) + 1 \quad ,$$

$$M + \lambda + 1 = \frac{1}{u_e r_o^2} \left[x \frac{d}{dx} (u_e r_o^2) + u_e r_o^2 \right] \quad ,$$

$$M + \lambda + 1 = \frac{1}{u_e r_o^2} \frac{d}{dx} (x r_o^2 u_e) \quad . \tag{A-5}$$

Substituting Equation (A-2) and Equation (A-5) in Equation (A-1):

$$\beta = \frac{\frac{2x}{u_e}\frac{du_e}{dx}}{\frac{1}{u_e r_o^2}\frac{d}{dx}(x r_o^2 u_e)} = \frac{2x r_o^2 \frac{du_e}{dx}}{\frac{d}{dx}(x r_o^2 u_e)}$$

or finally,

$$\beta = 2x r_o^2 \frac{du_e}{d\zeta} \qquad \text{(A-6)}$$

where

$$\zeta = x r_o^2 u_e \quad . \qquad \text{(A-7)}$$

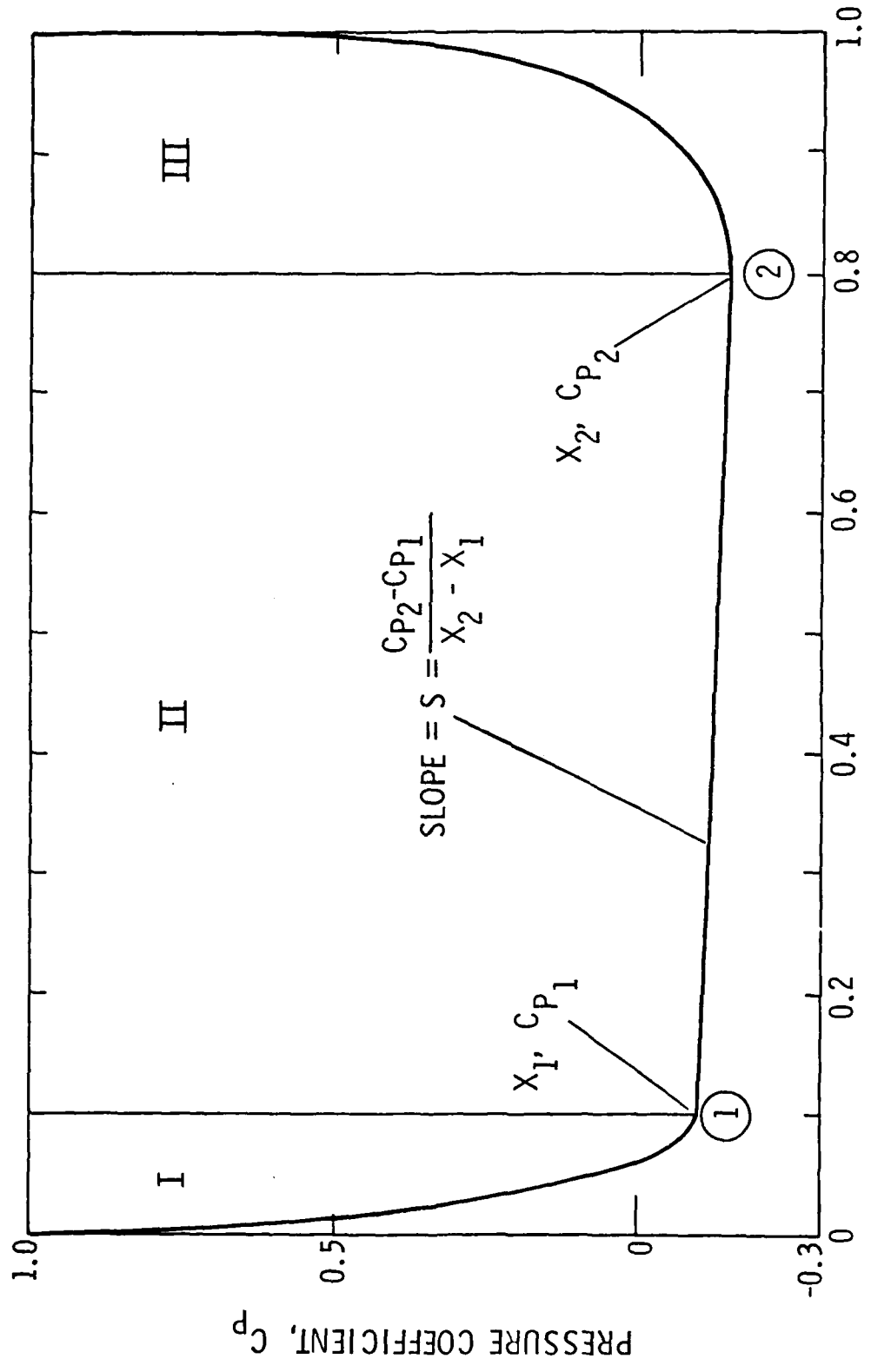

Figure 1. Parameterized Pressure Distribution.

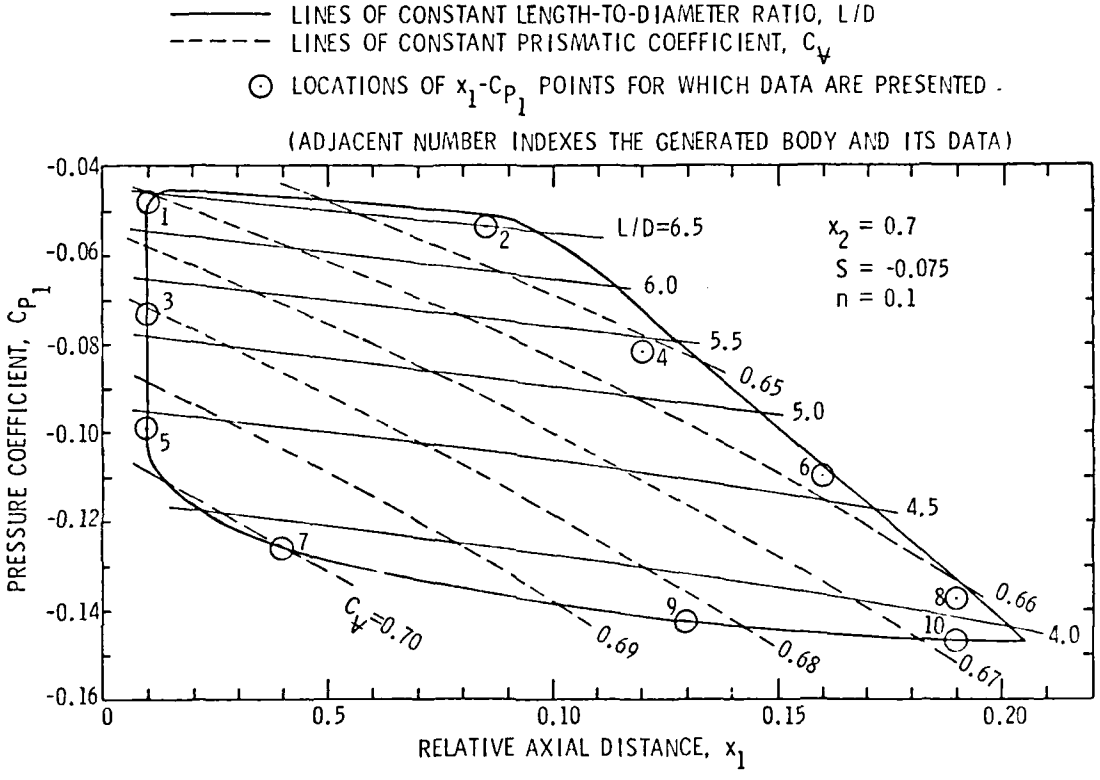

Figure 2. Parameter Contour for Possible Body Shapes (x_2 = 0.7, S = -0.075).

19 August 1981
JJE:GHH:mmj

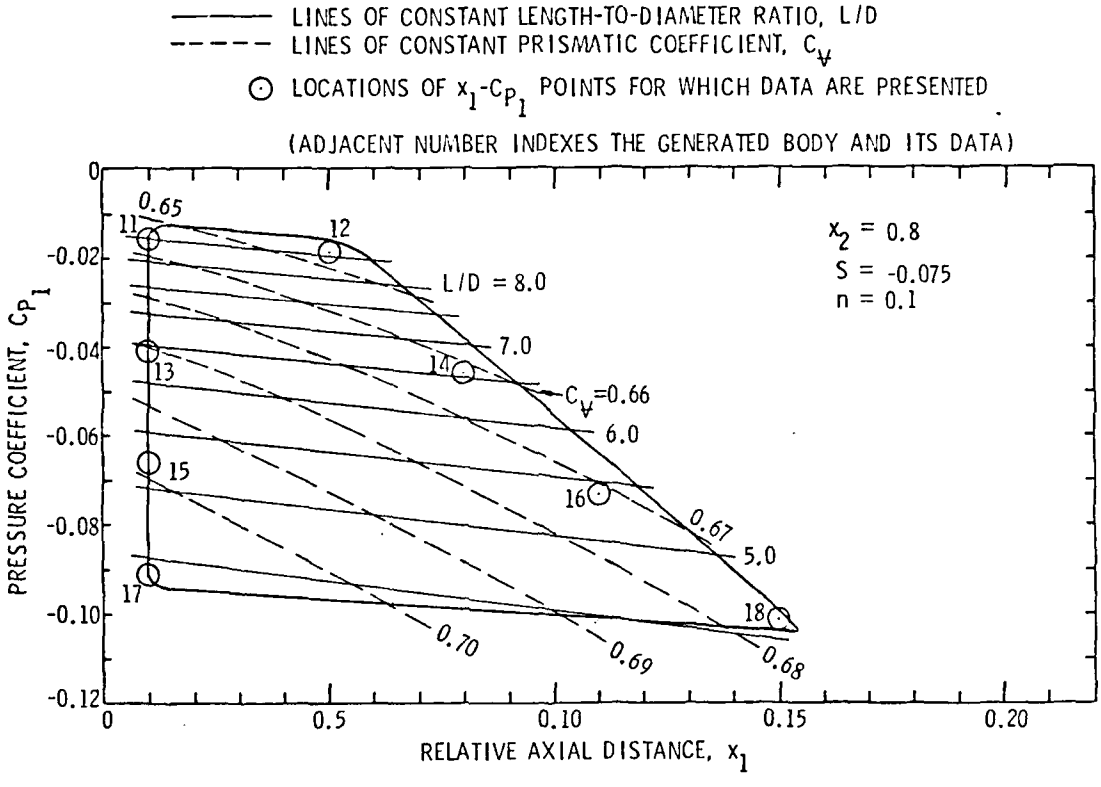

Figure 3. Parameter Contour for Possible Body Shapes (x_2 = 0.8, S = -0.075).

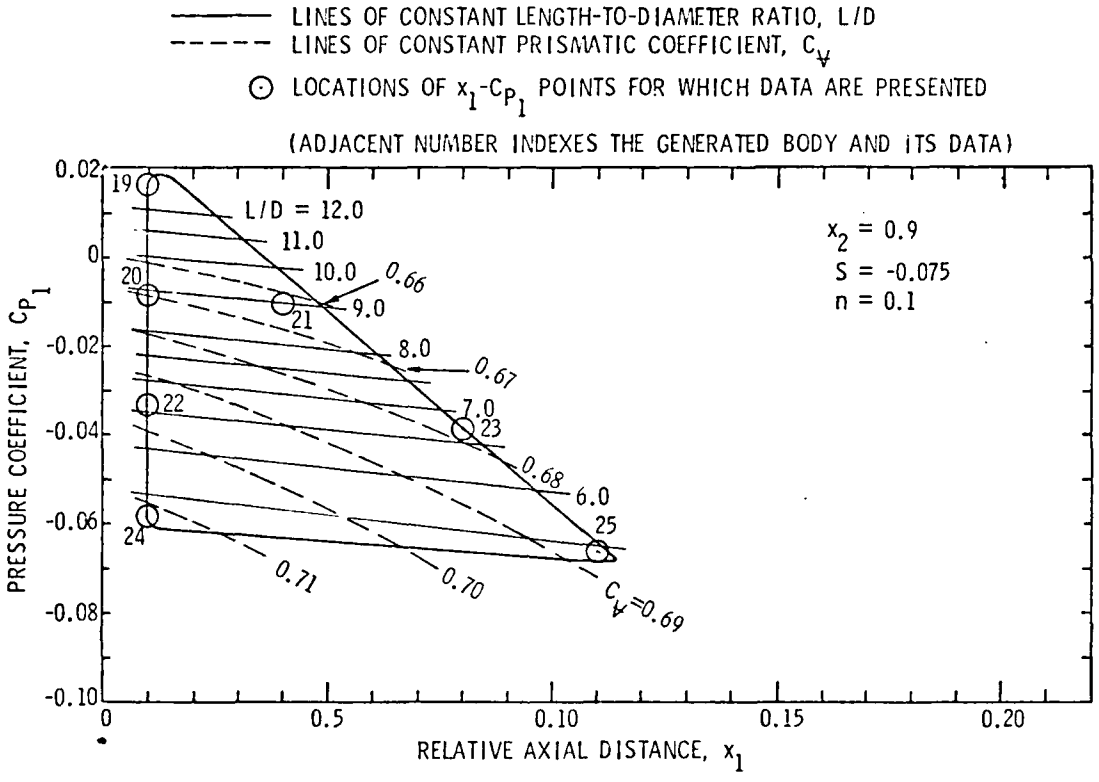

Figure 4. Parameter Contour for Possible Body Shapes (x_2 = 0.9, S = -0.075).

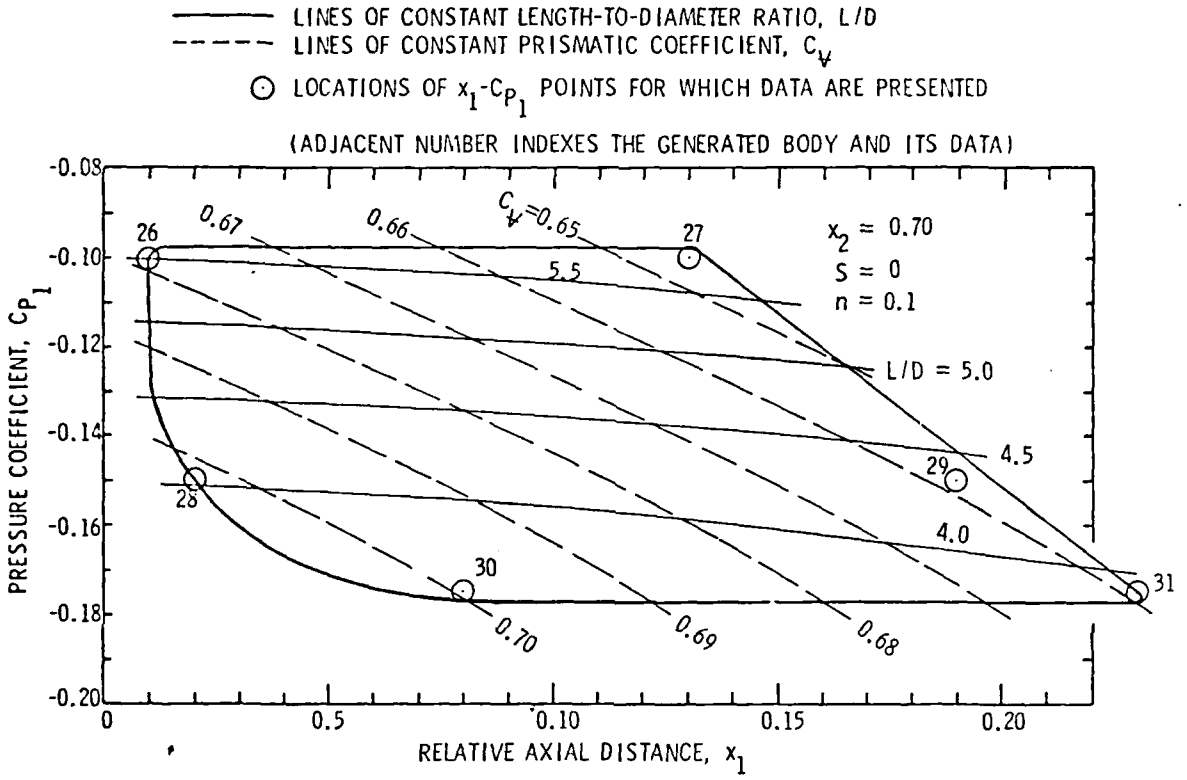

Figure 5. Parameter Contour for Possible Body Shapes (x_2 = 0.7, S = 0.0).

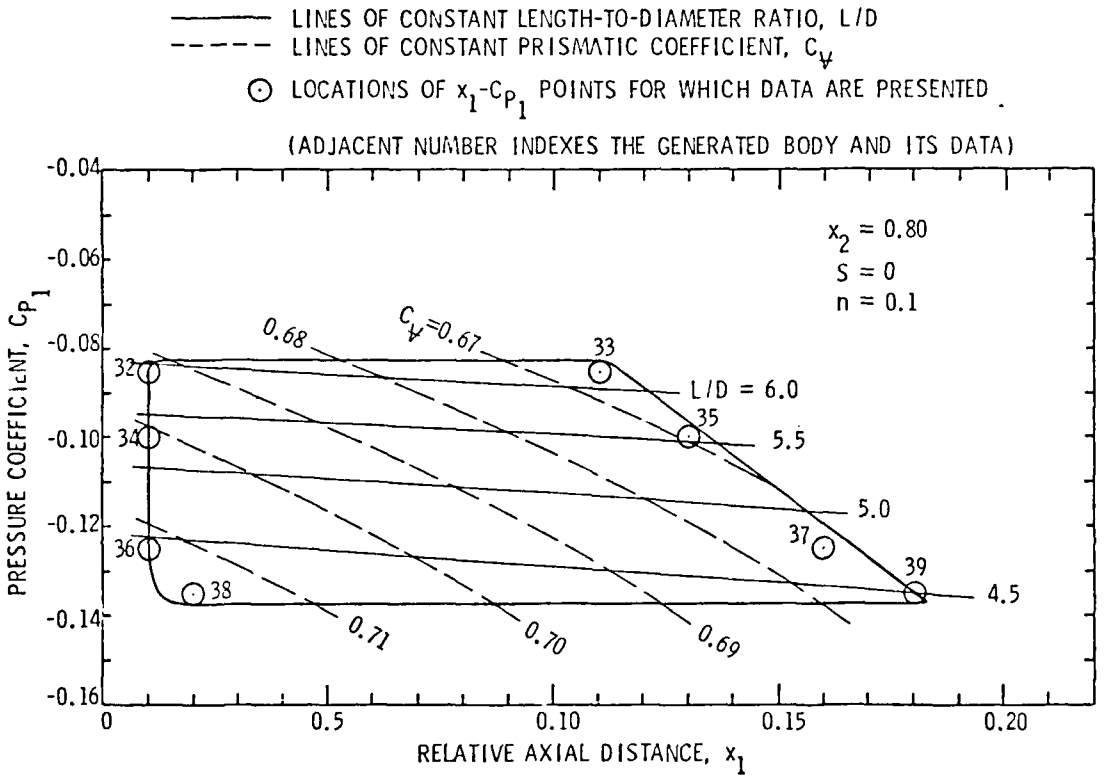

Figure 6. Parameter Contour for Possible Body Shapes (x_2 = 0.8, S = 0.0).

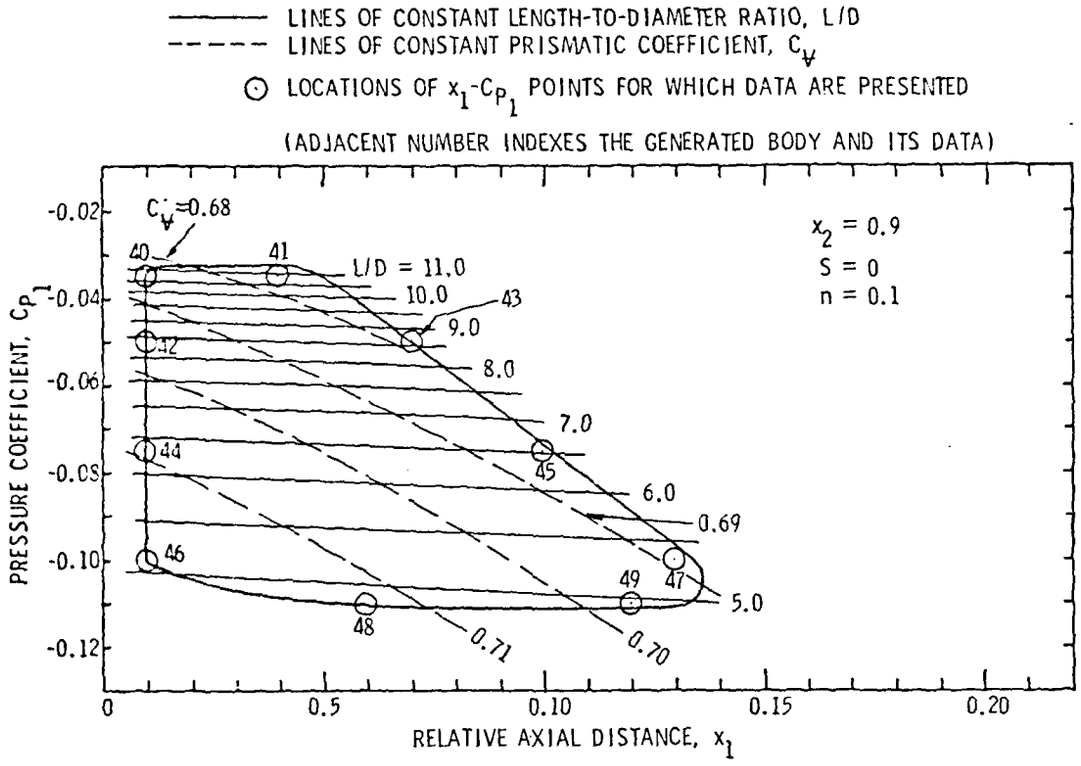

Figure 7. Parameter Contour for Possible Body Shapes (x_2 = 0.9, S = 0.0).

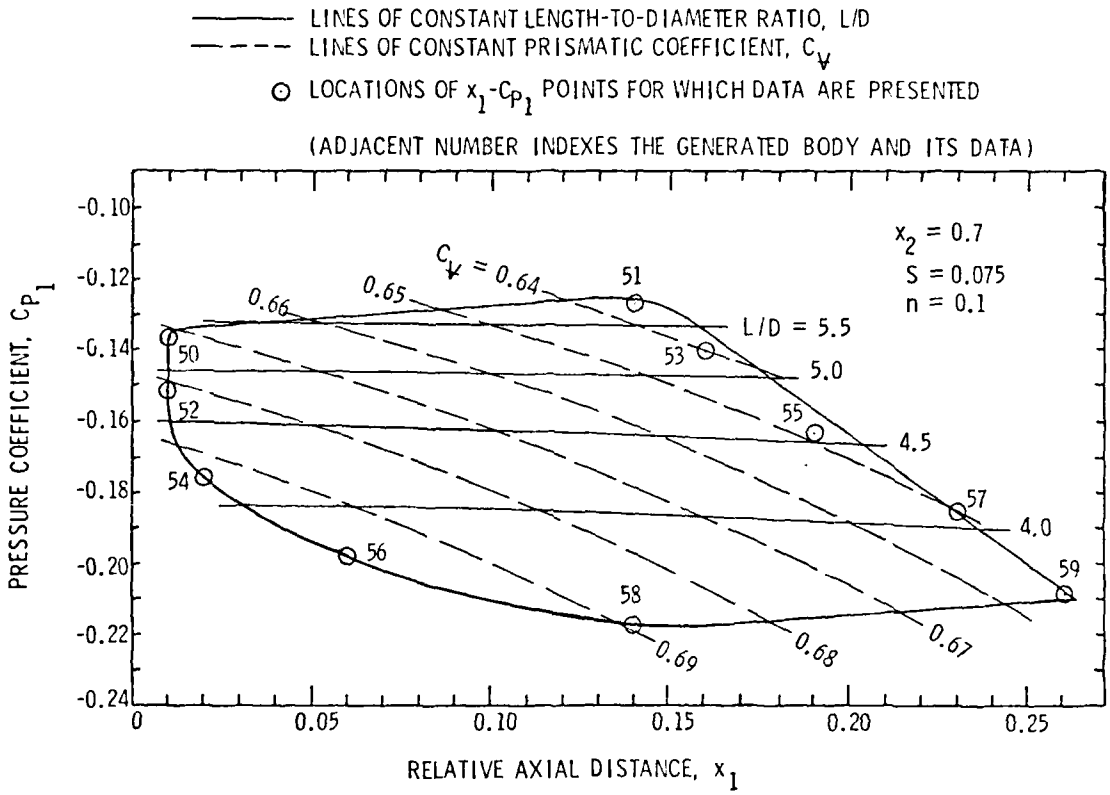

Figure 8. Parameter Contour for Possible Body Shapes (x_2 = 0.7, S = 0.075).

19 August 1981
JJE:GHH:mmj

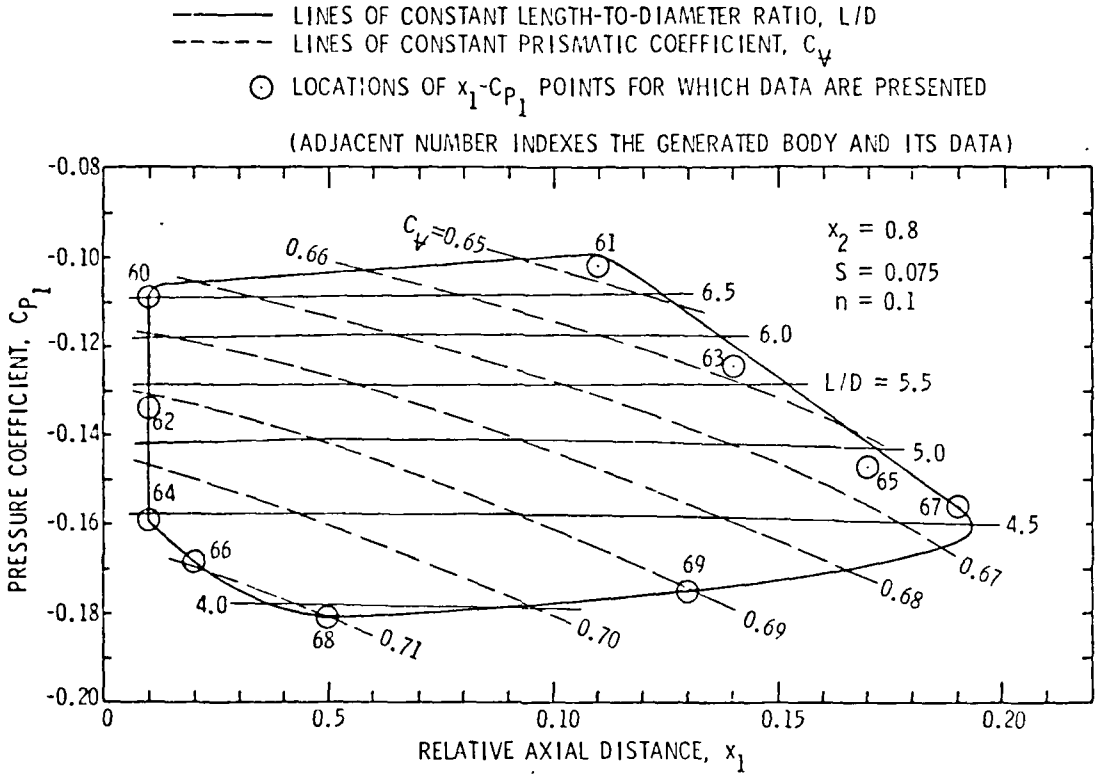

Figure 9. Parameter Contour for Possible Body Shapes (x_2 = 0.8, S = 0.075).

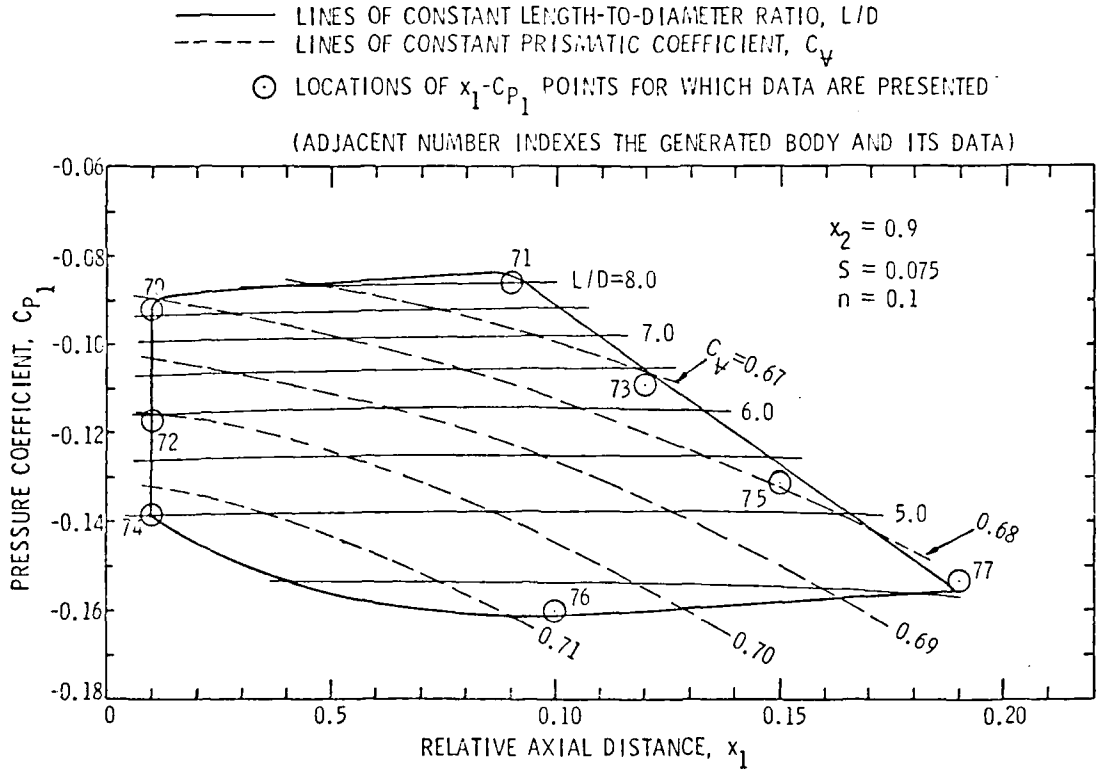

Figure 10. Parameter Contour for Possible Body Shapes (x_2 = 0.9, S = 0.075).

19 August 1981
JJE:GHH:mmj

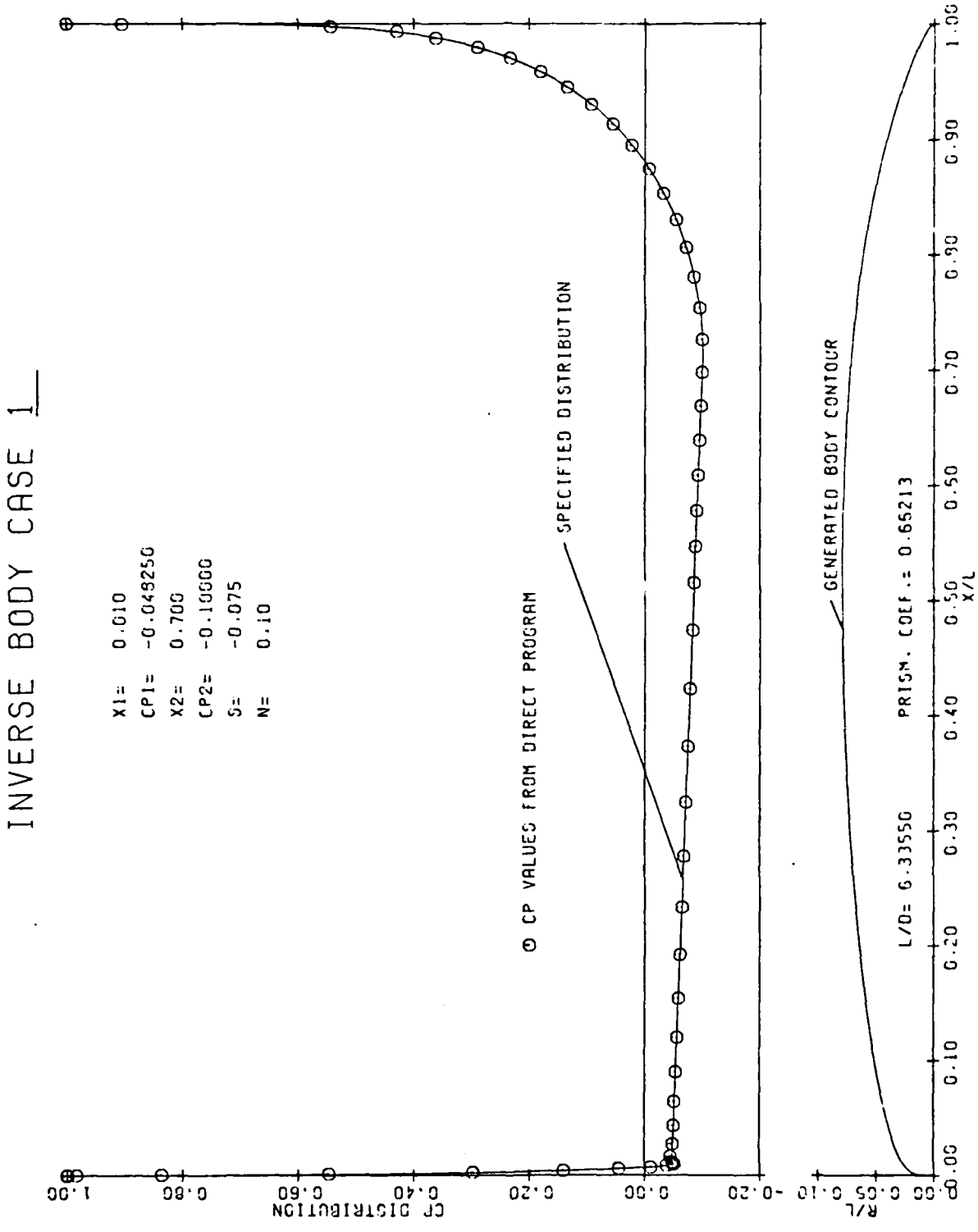

Figure 11. Pressure Distribution and Body Contour, Case No. 1.

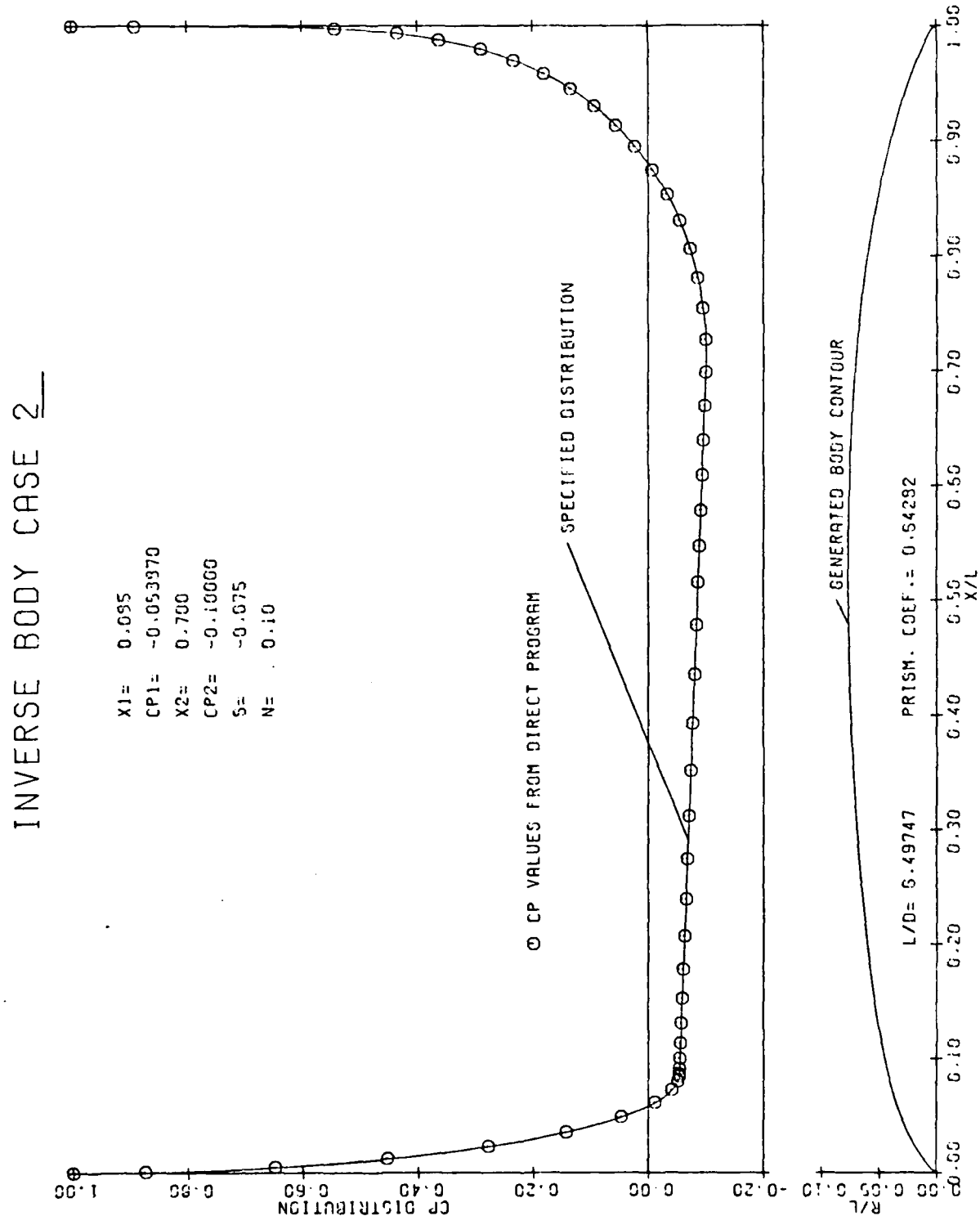

Figure 12. Pressure Distribution and Body Contour, Case No. 2.

19 August 1981
JJE:GHH:mmj

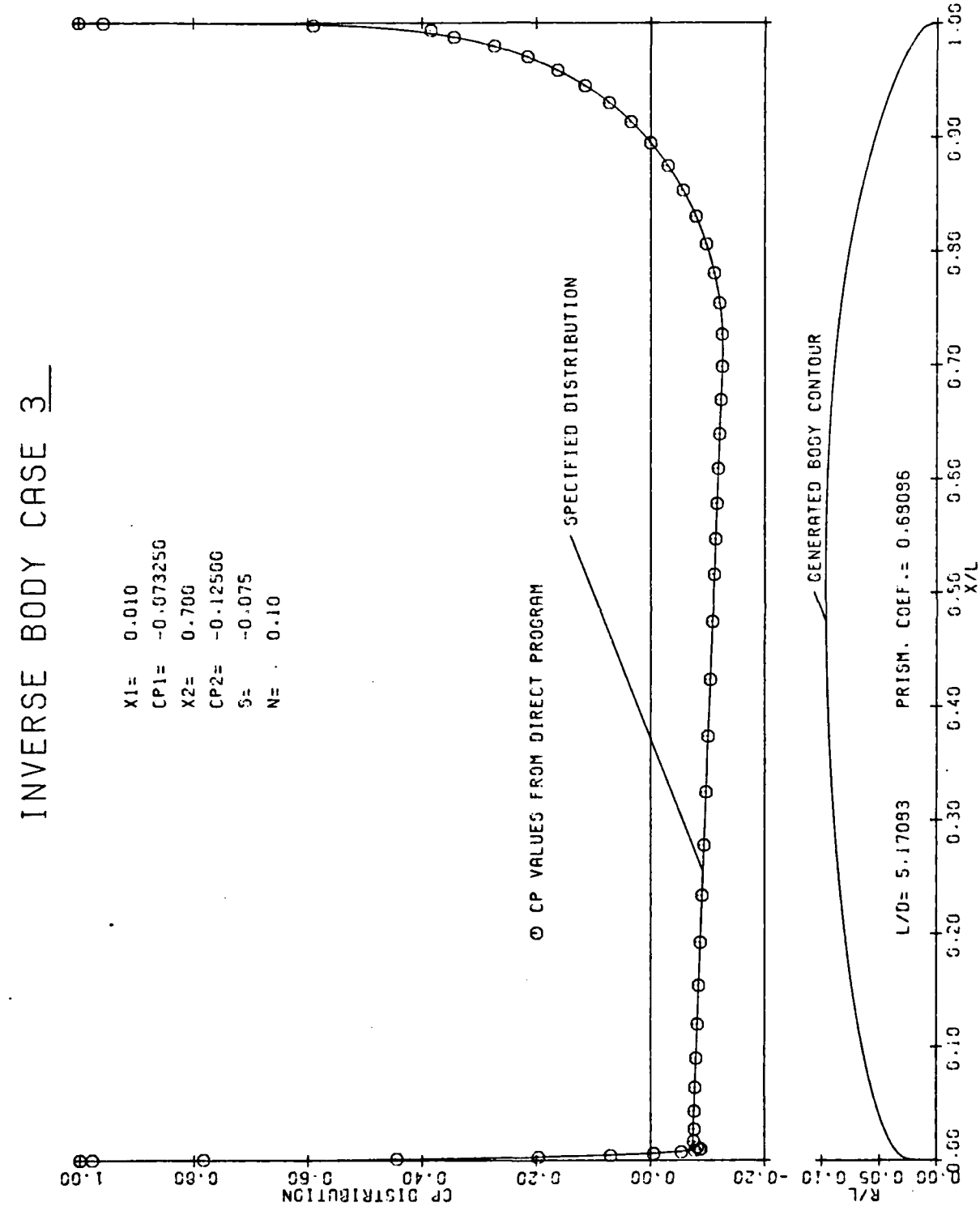

Figure 13. Pressure Distribution and Body Contour, Case No. 3.

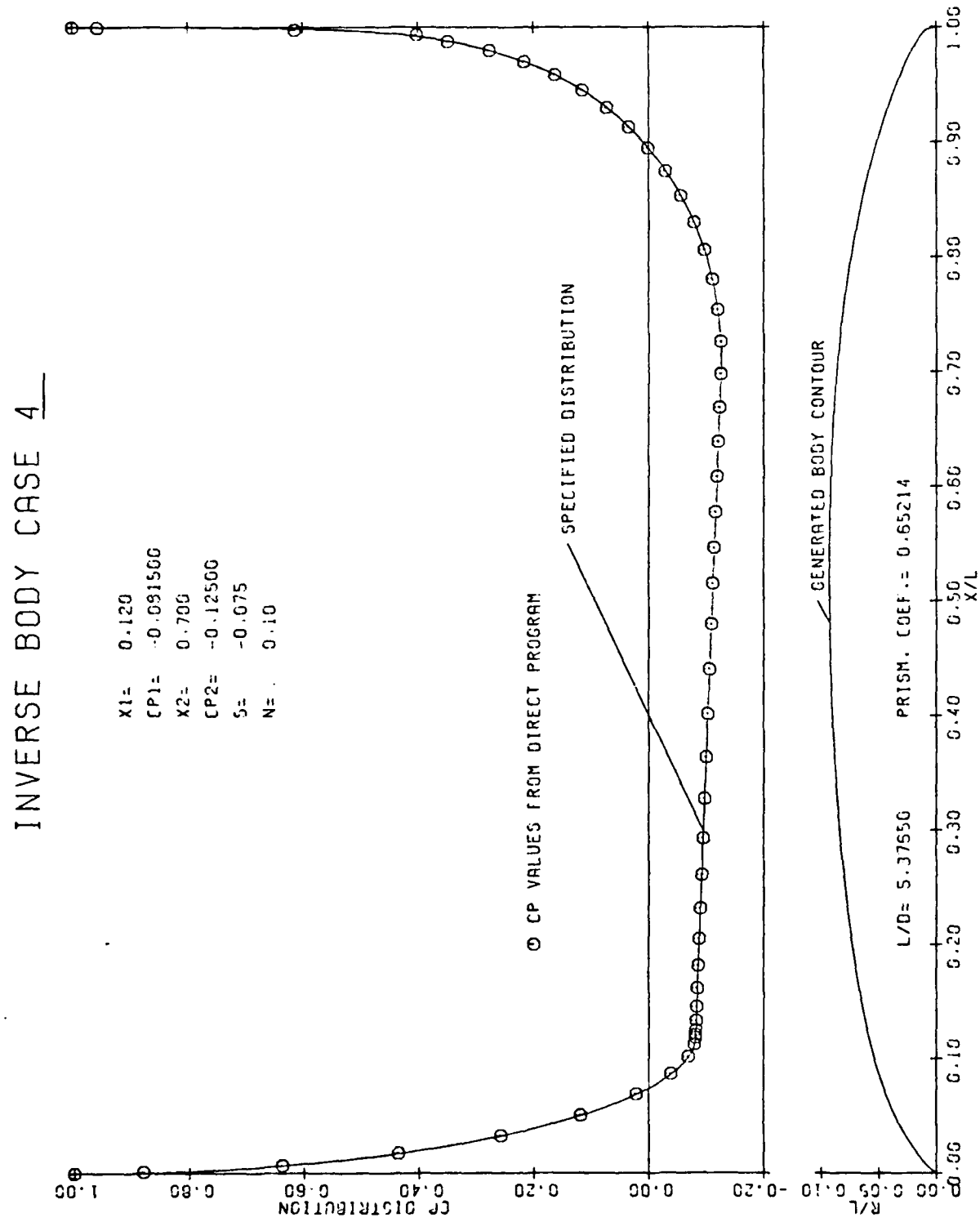

Figure 14. Pressure Distribution and Body Contour, Case No. 4.

19 August 1981
JJE:GHH:mmj

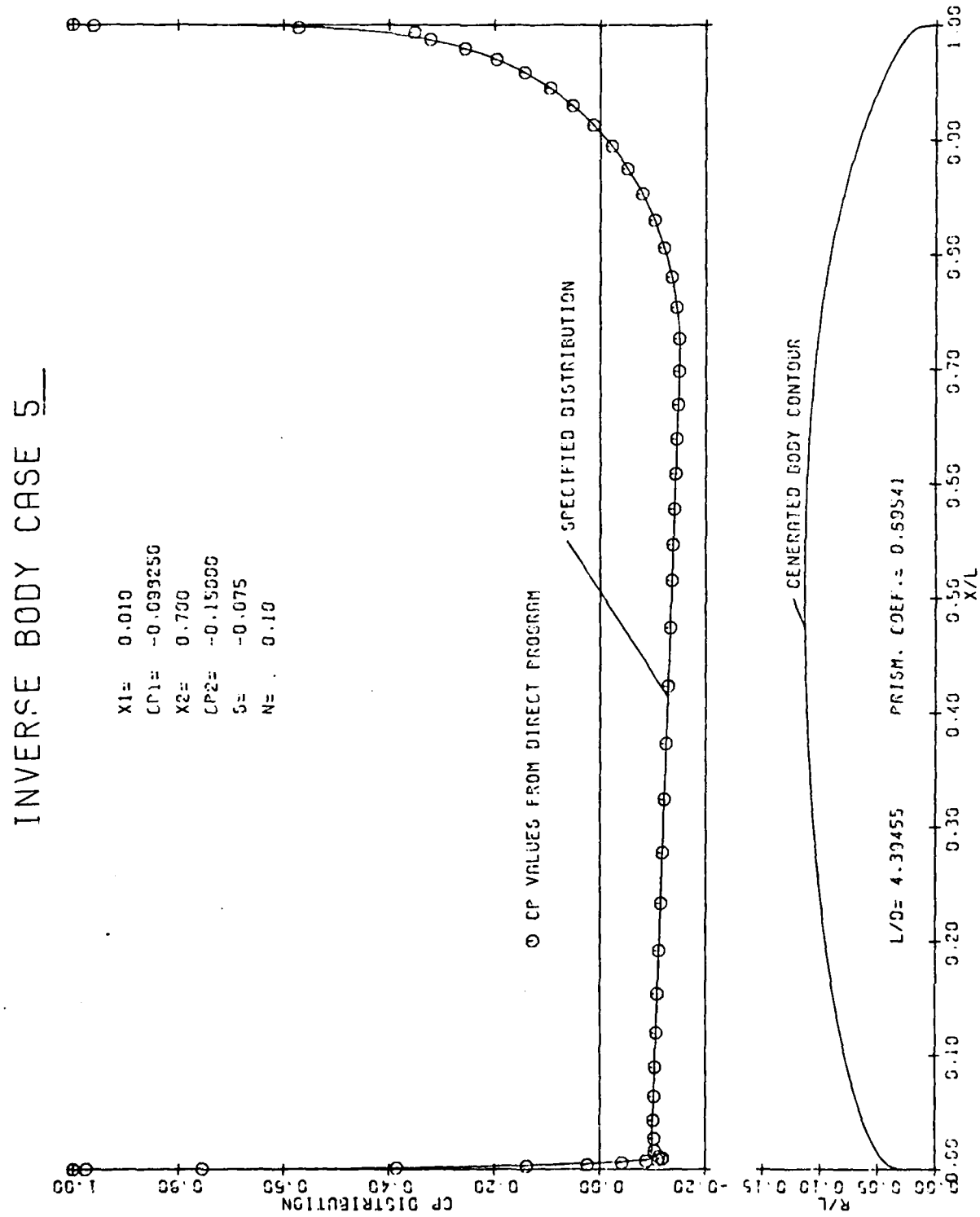

Figure 15. Pressure Distribution and Body Contour, Case No. 5.

19 August 1981
JJE:GHH:mmj

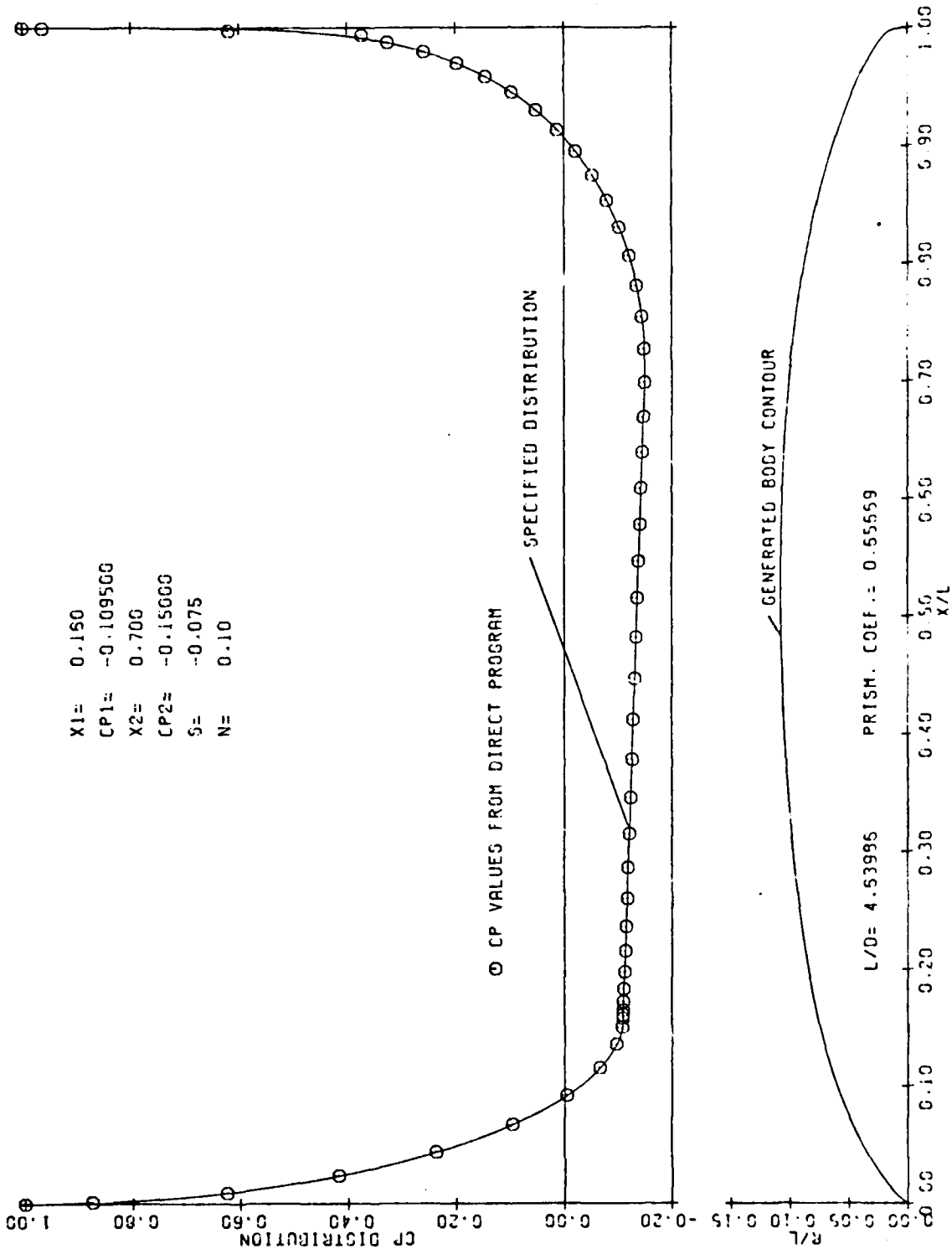

Figure 16. Pressure Distribution and Body Contour, Case No. 6.

19 August 1981
JJE:GHH:mmj

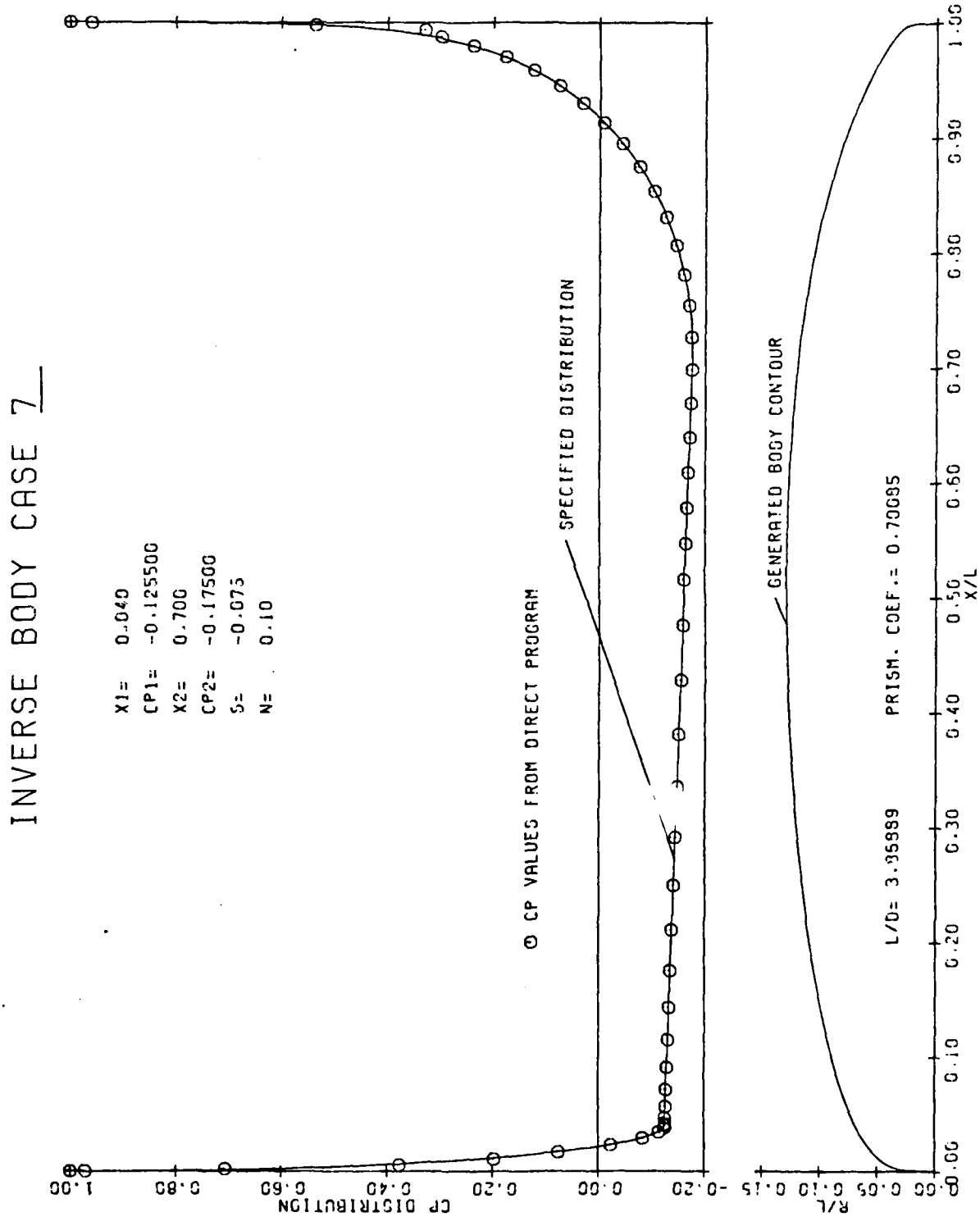

Figure 17. Pressure Distribution and Body Contour, Case No. 7.

19 August 1981
JJE:GHH:mmj

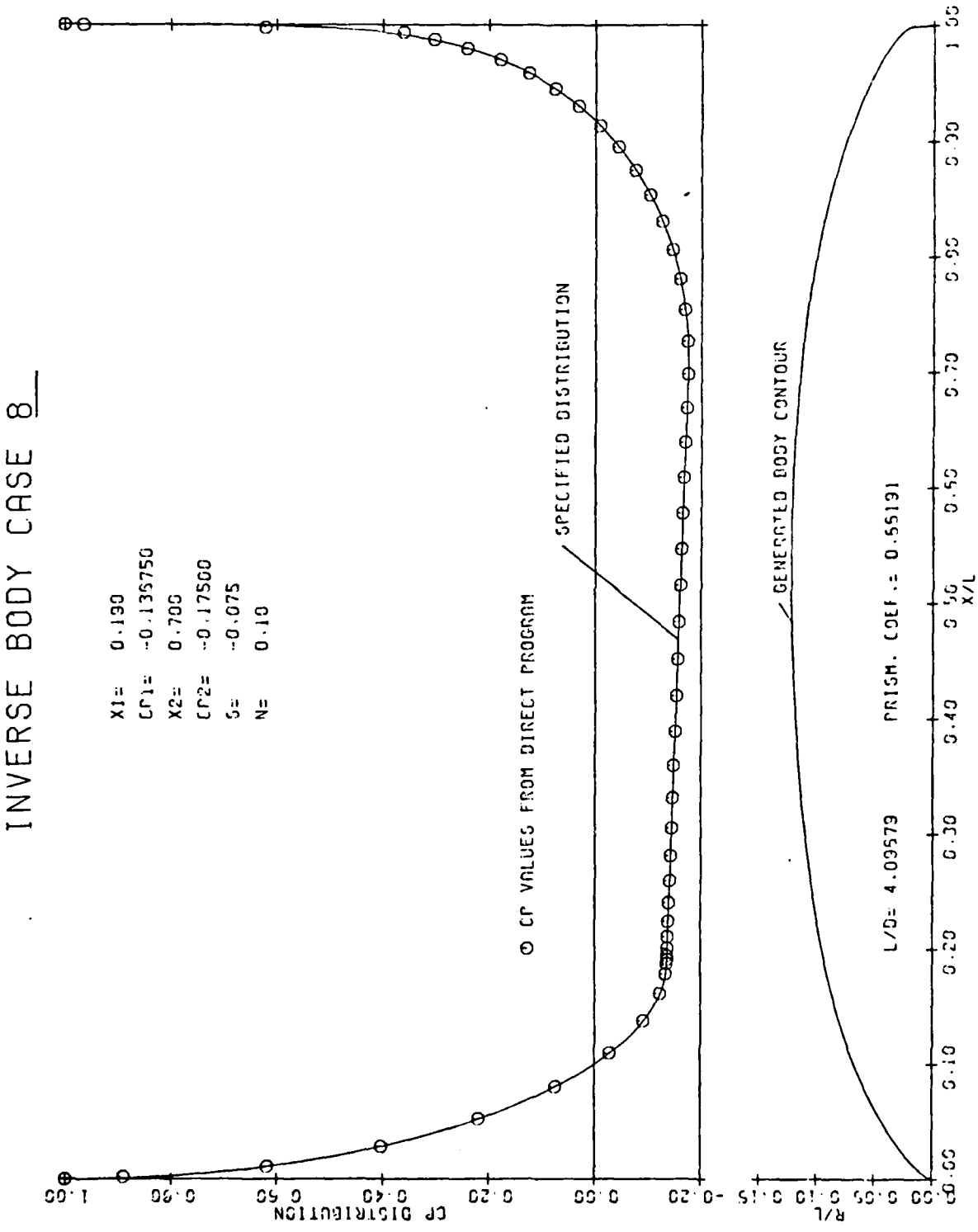

Figure 18. Pressure Distribution and Body Contour, Case No. 8.

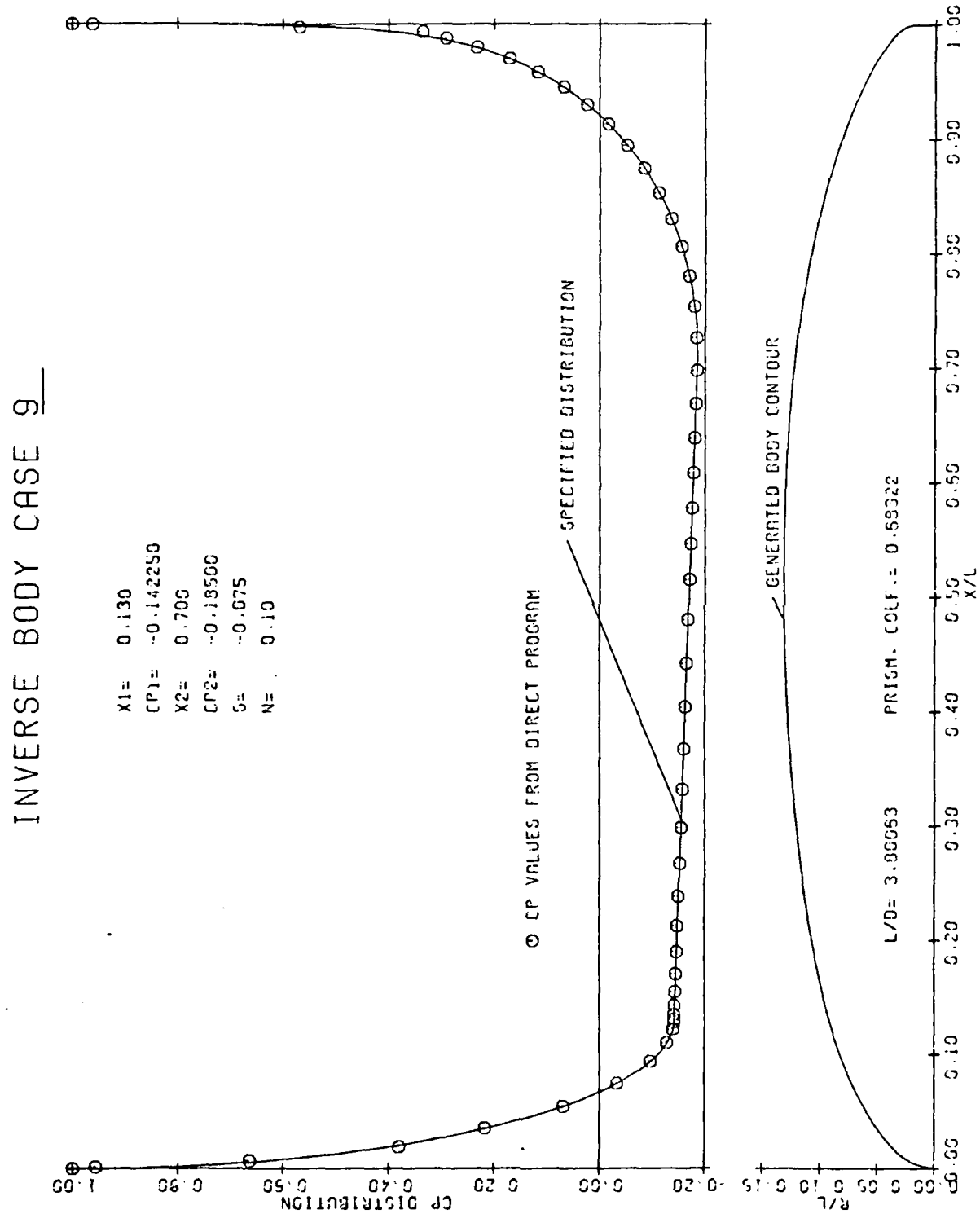

Figure 19. Pressure Distribution and Body Contour, Case No. 9.

19 August 1981
JJE:GHH:mmj

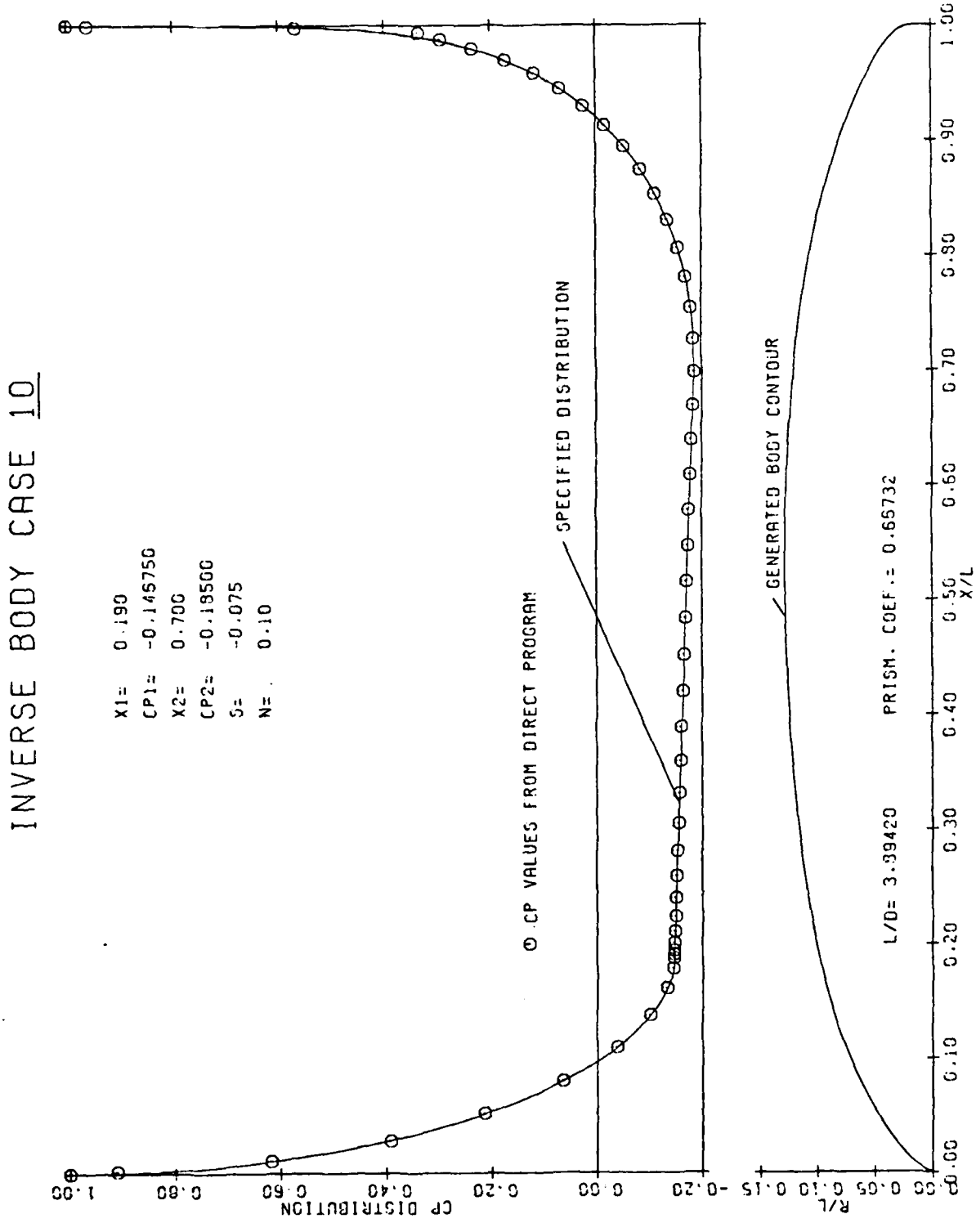

Figure 20. Pressure Distribution and Body Contour, Case No. 10.

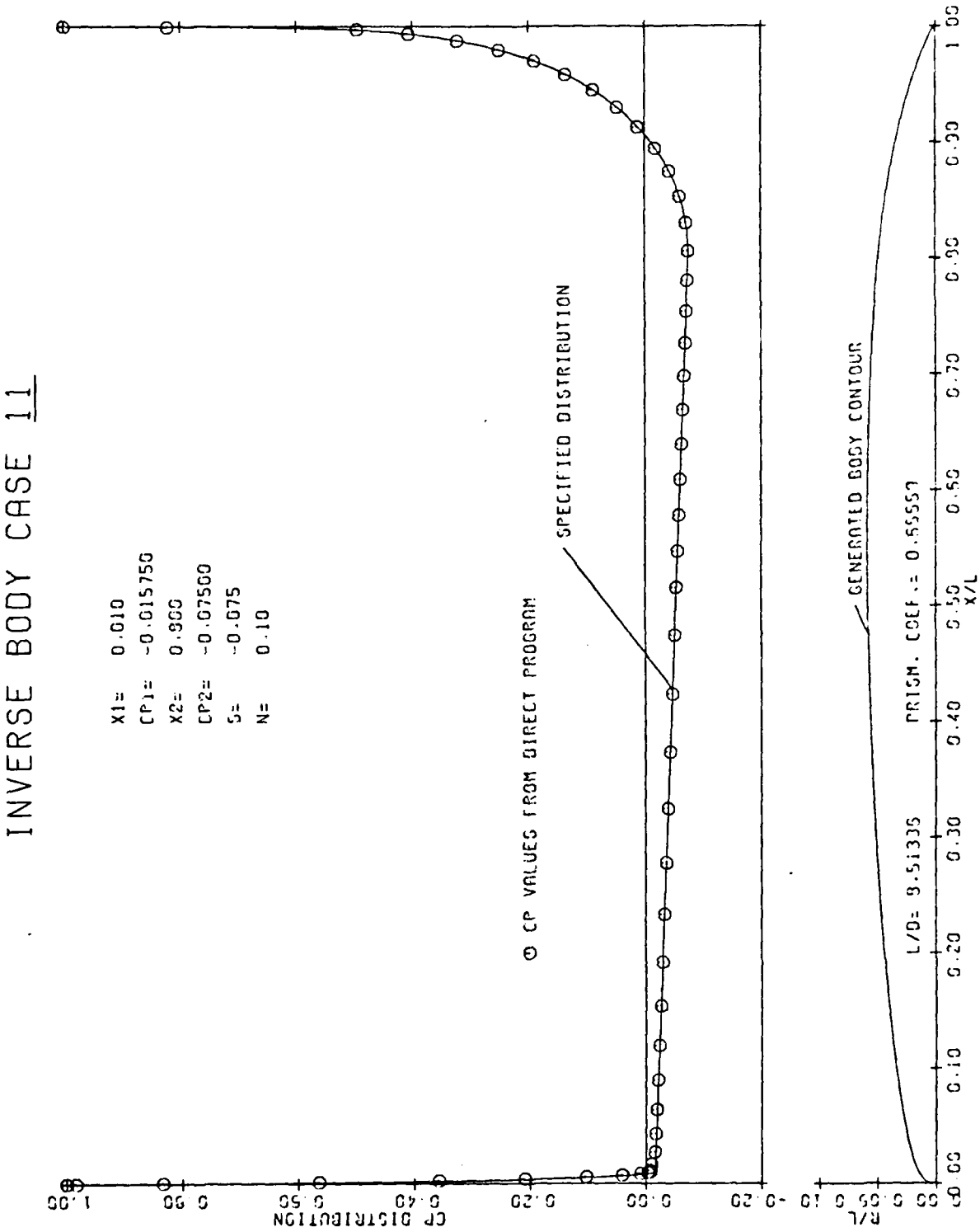

Figure 21. Pressure Distribution and Body Contour, Case No. 11.

19 August 1981
JJE:GHH:mmj

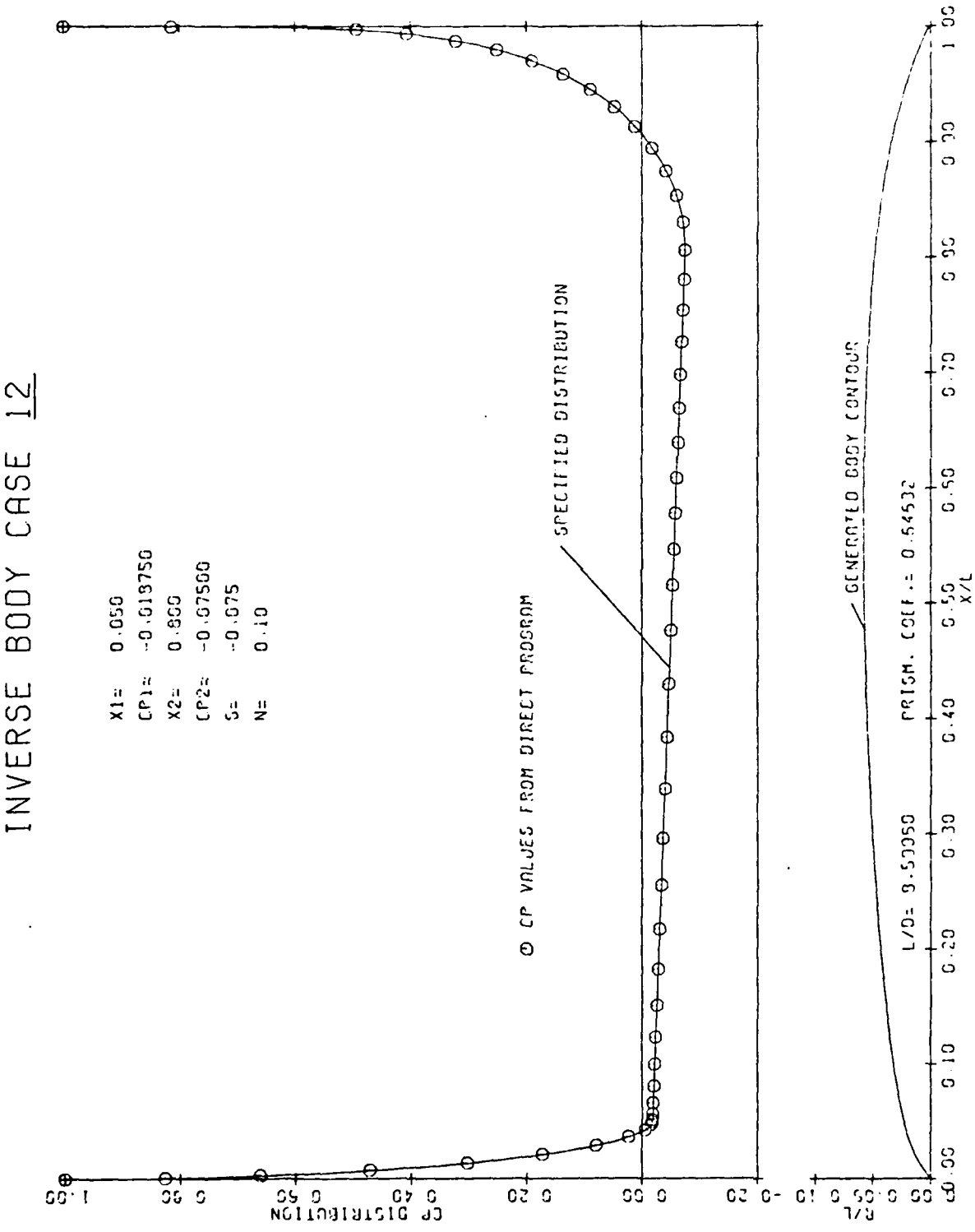

Figure 22. Pressure Distribution and Body Contour, Case No. 12.

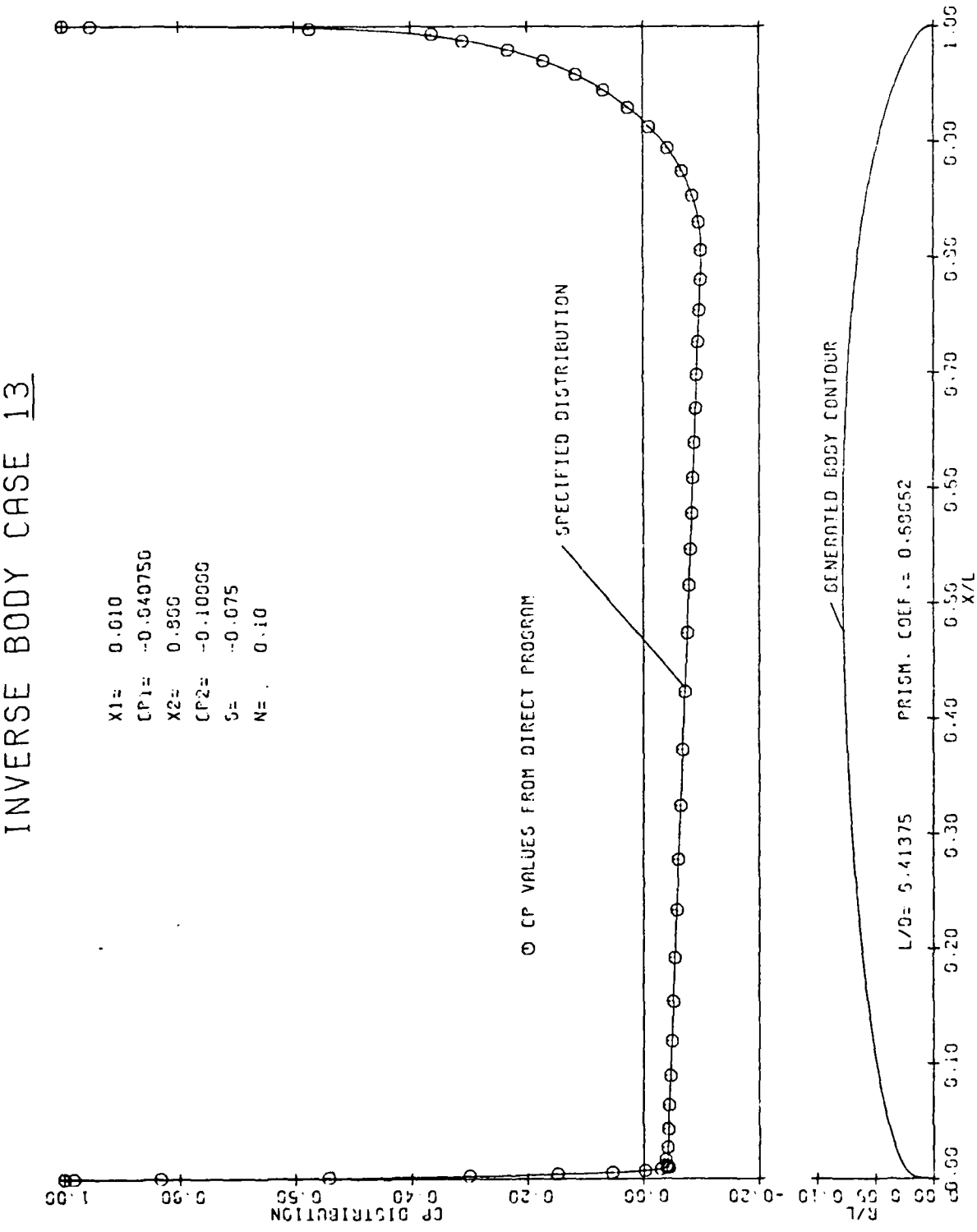

Figure 23. Pressure Distribution and Body Contour, Case No. 13.

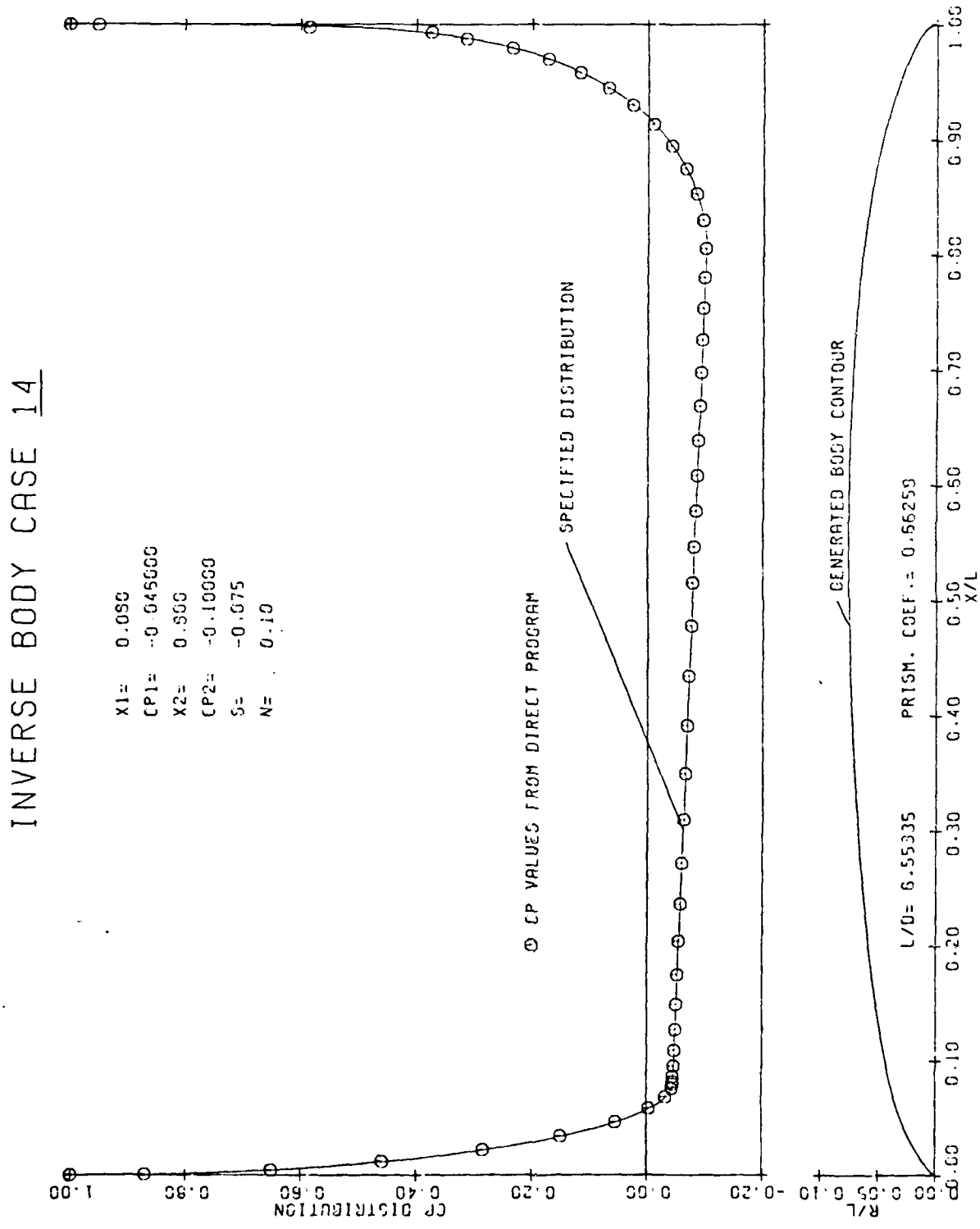

Figure 24. Pressure Distribution and Body Contour, Case No. 14.

19 August 1981
JJE:GHH:mmj

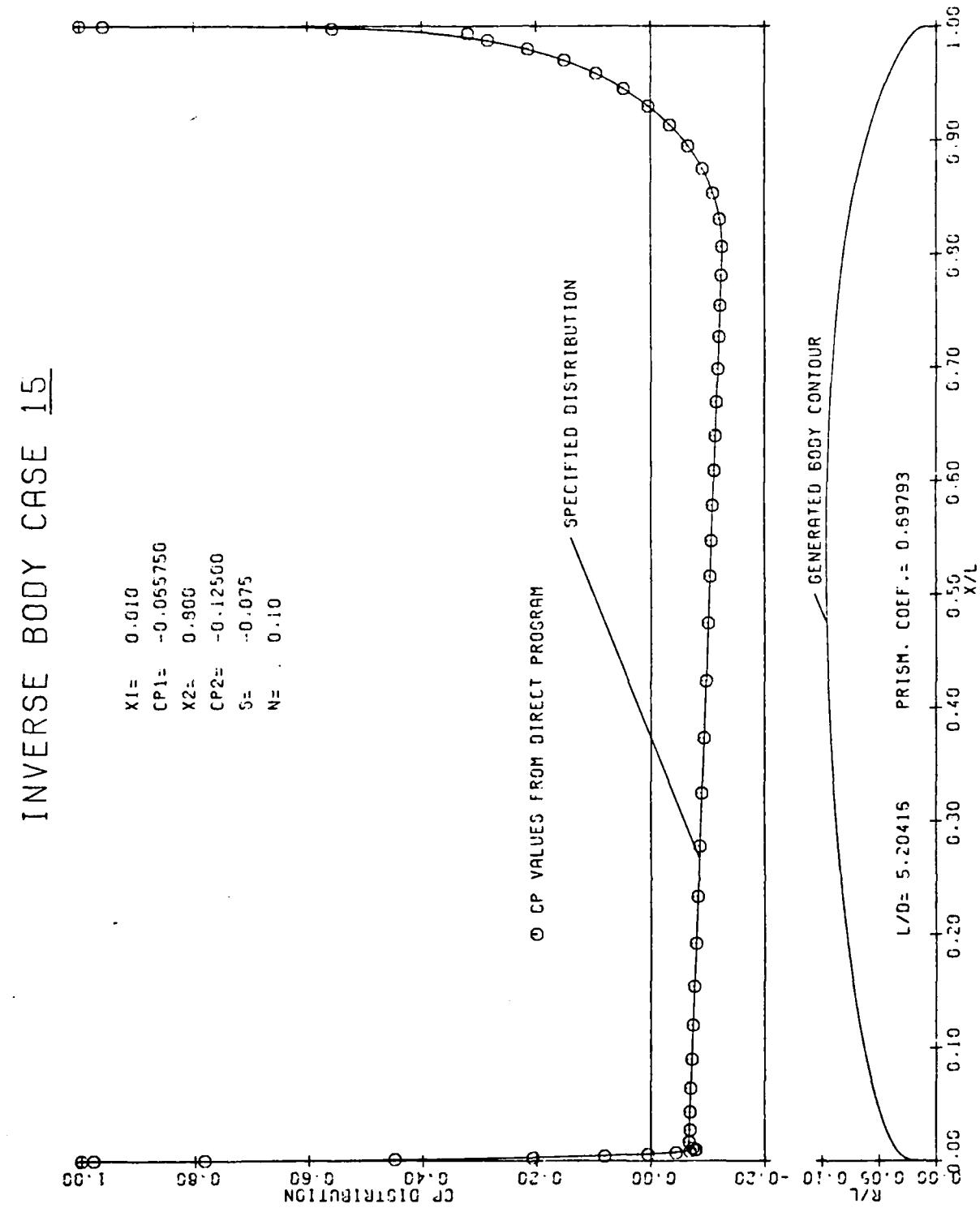

Figure 25. Pressure Distribution and Body Contour, Case No. 15.

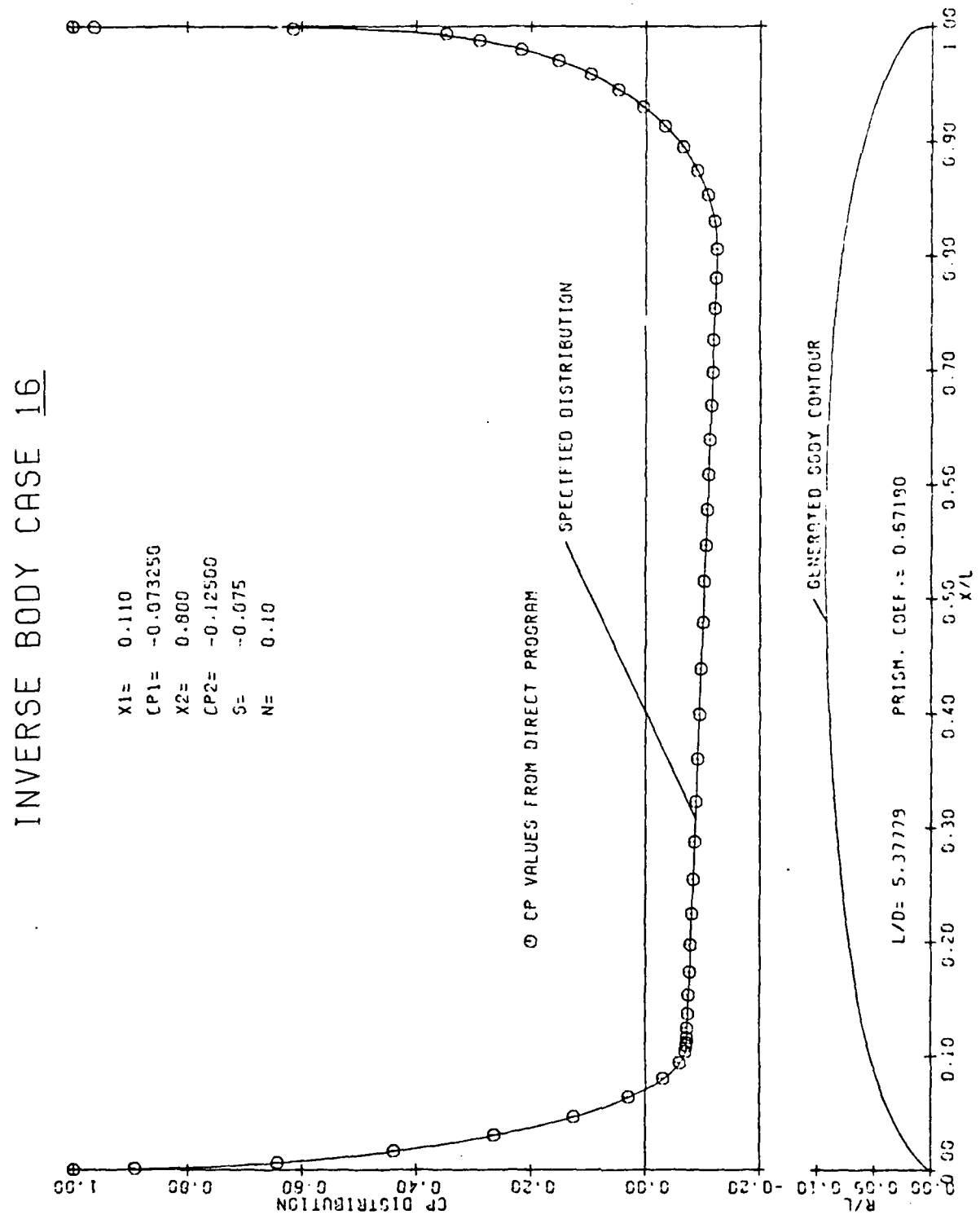

Figure 26. Pressure Distribution and Body Contour, Case No. 16.

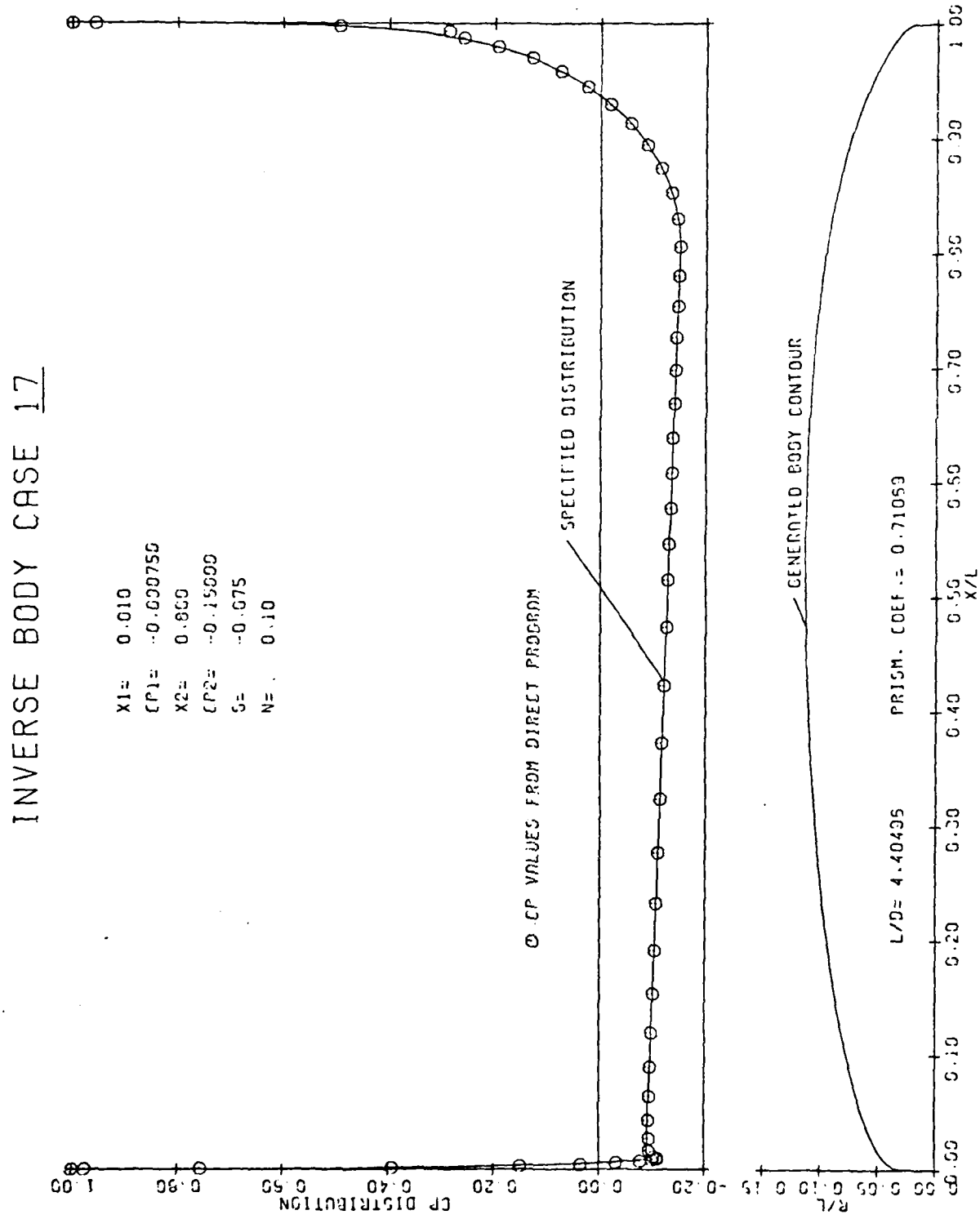

Figure 27. Pressure Distribution and Body Contour, Case No. 17.

19 August 1981
JJE:GHH:mmj

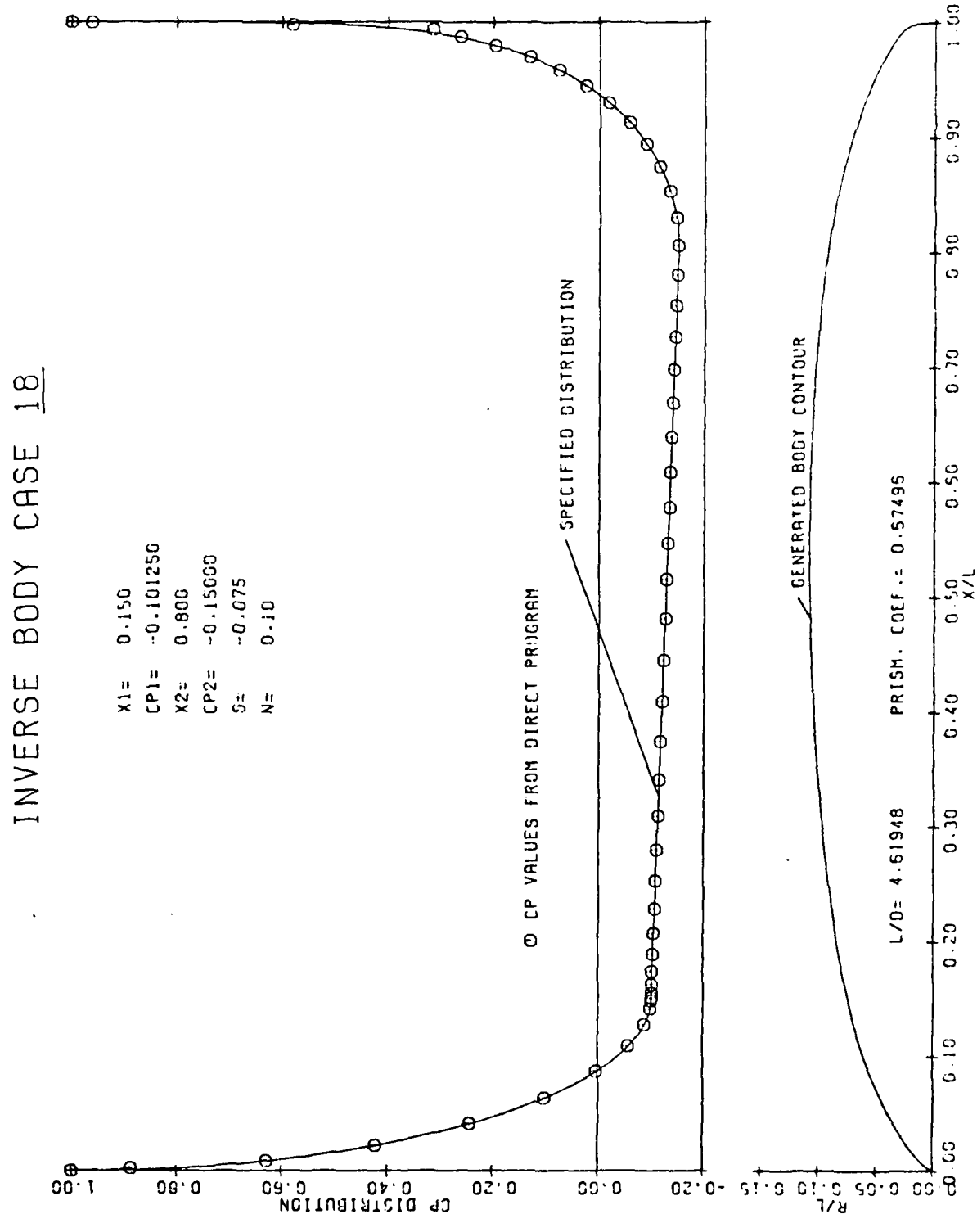

Figure 28. Pressure Distribution and Body Contour, Case No. 18.

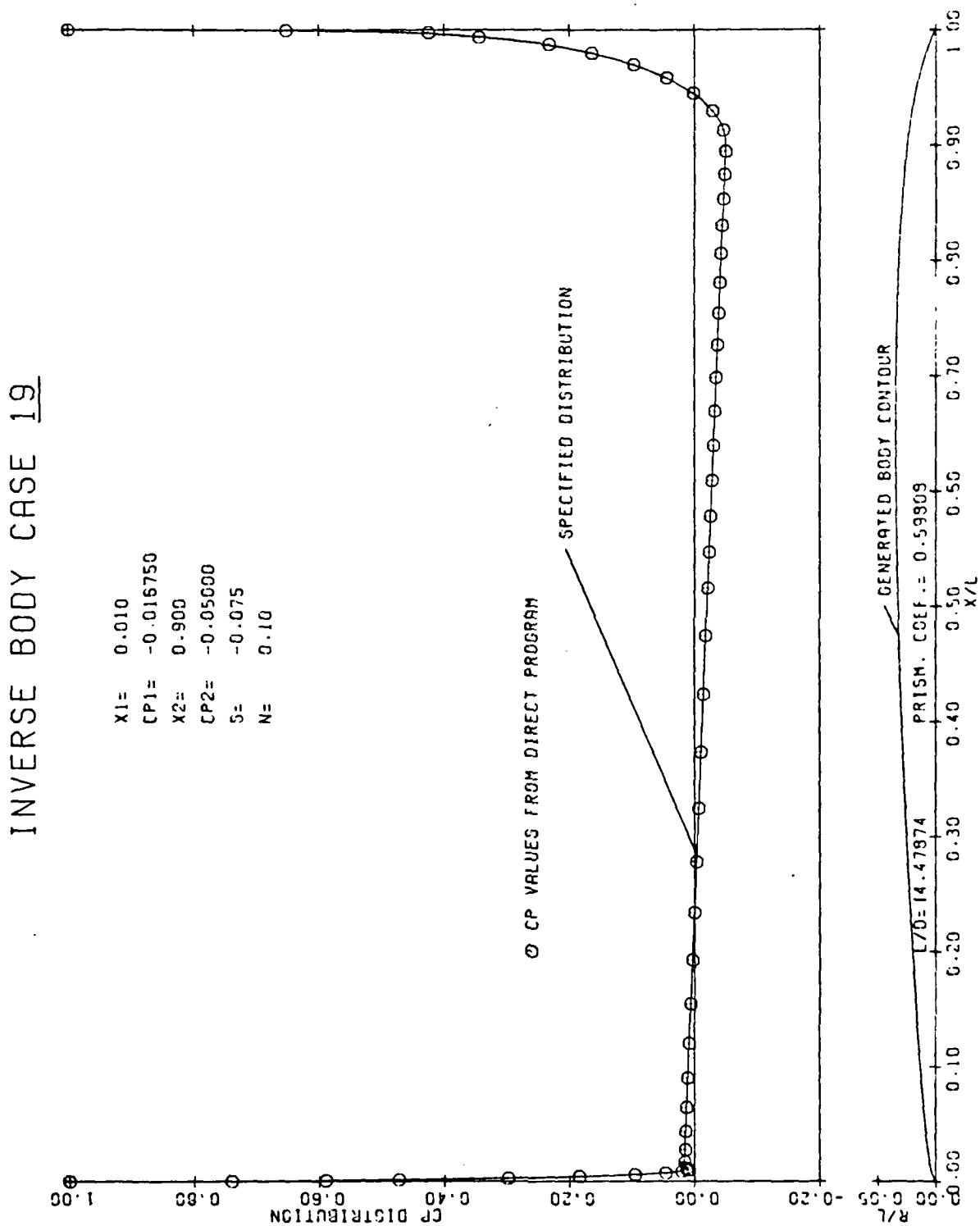

Figure 29. Pressure Distribution and Body Contour, Case No. 19.

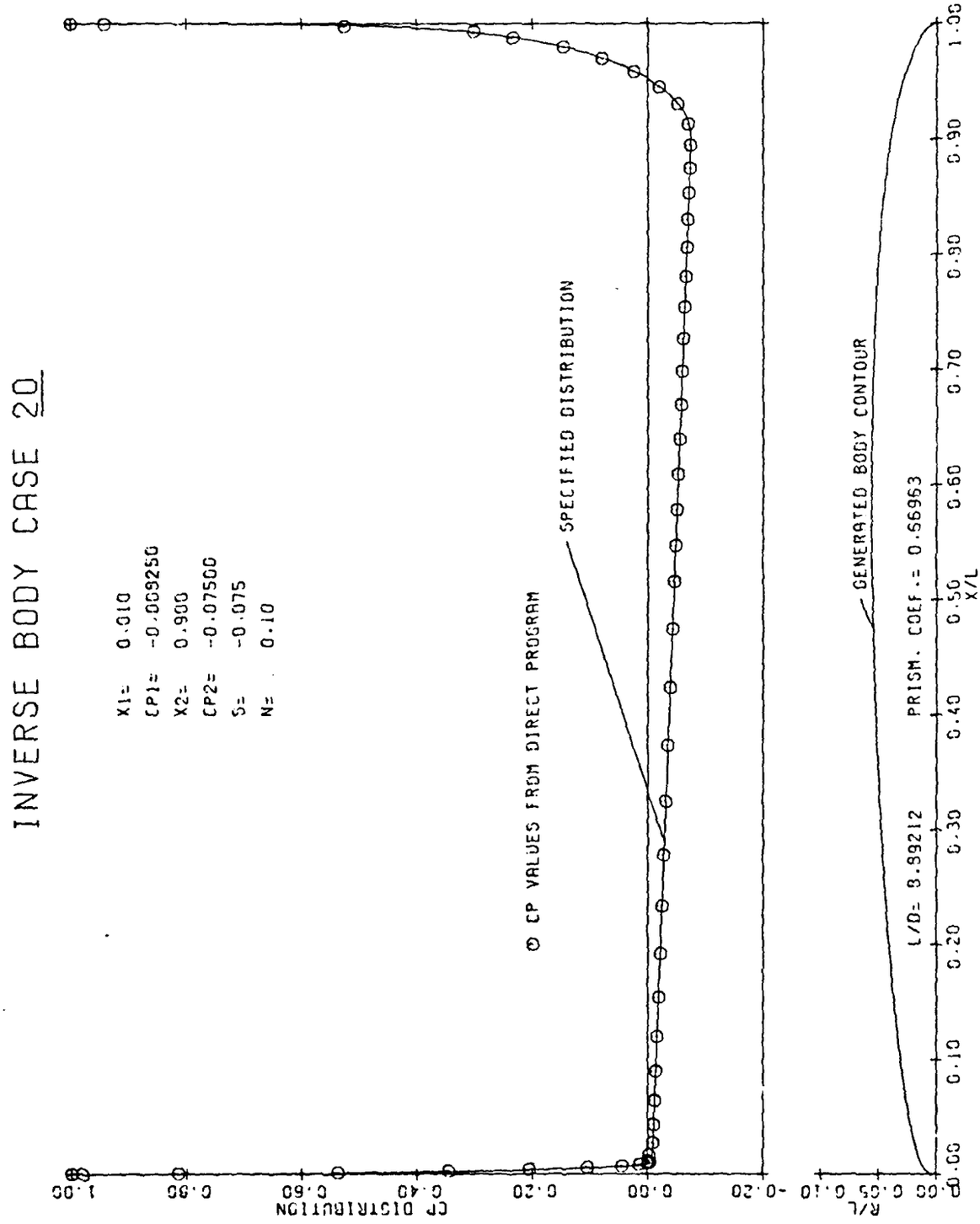

Figure 30. Pressure Distribution and Body Contour, Case No. 20.

19 August 1981
JJE:GHH:mmj

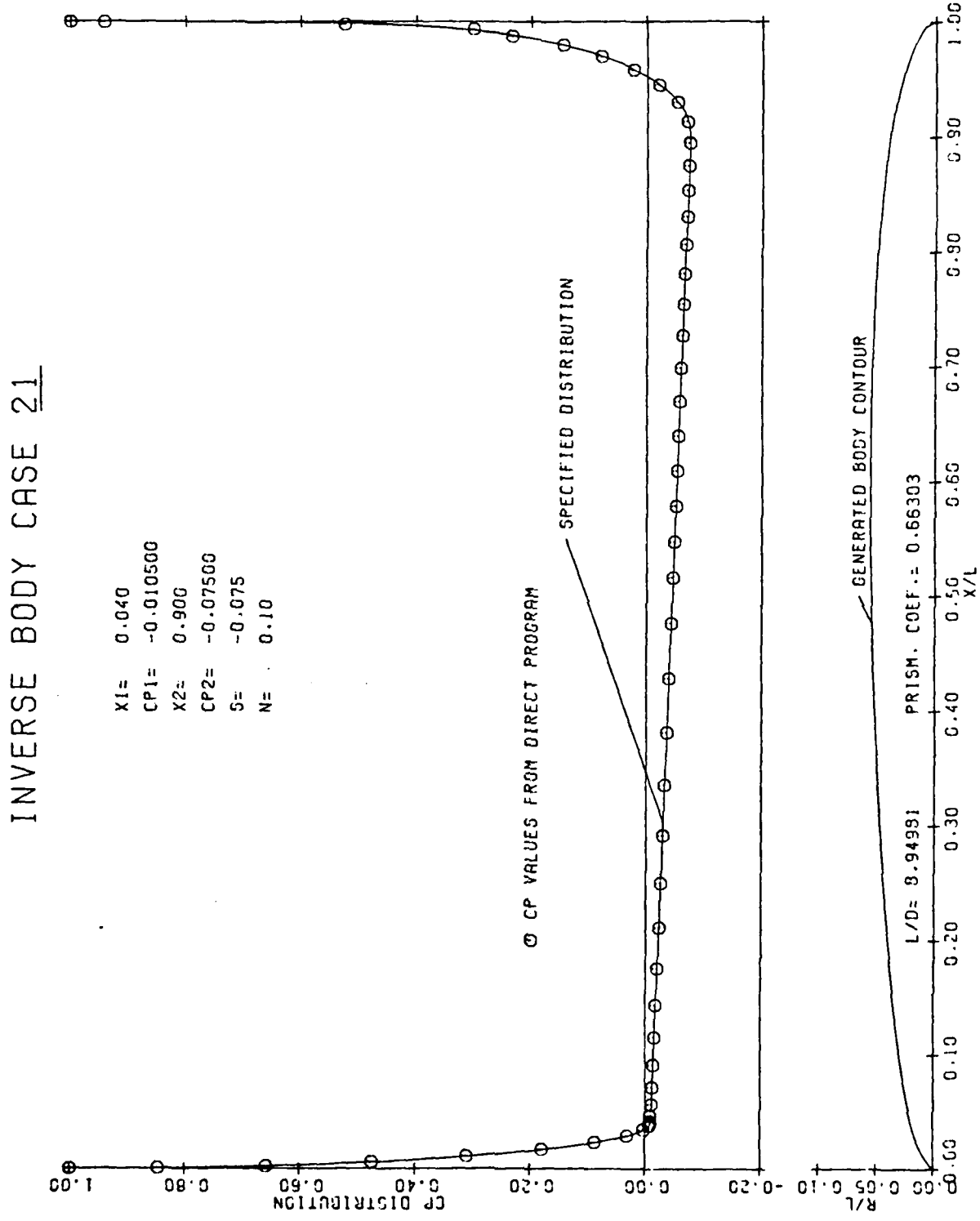

Figure 31. Pressure Distribution and Body Contour, Case No. 21.

19 August 1981
JJE:GHH:mmj

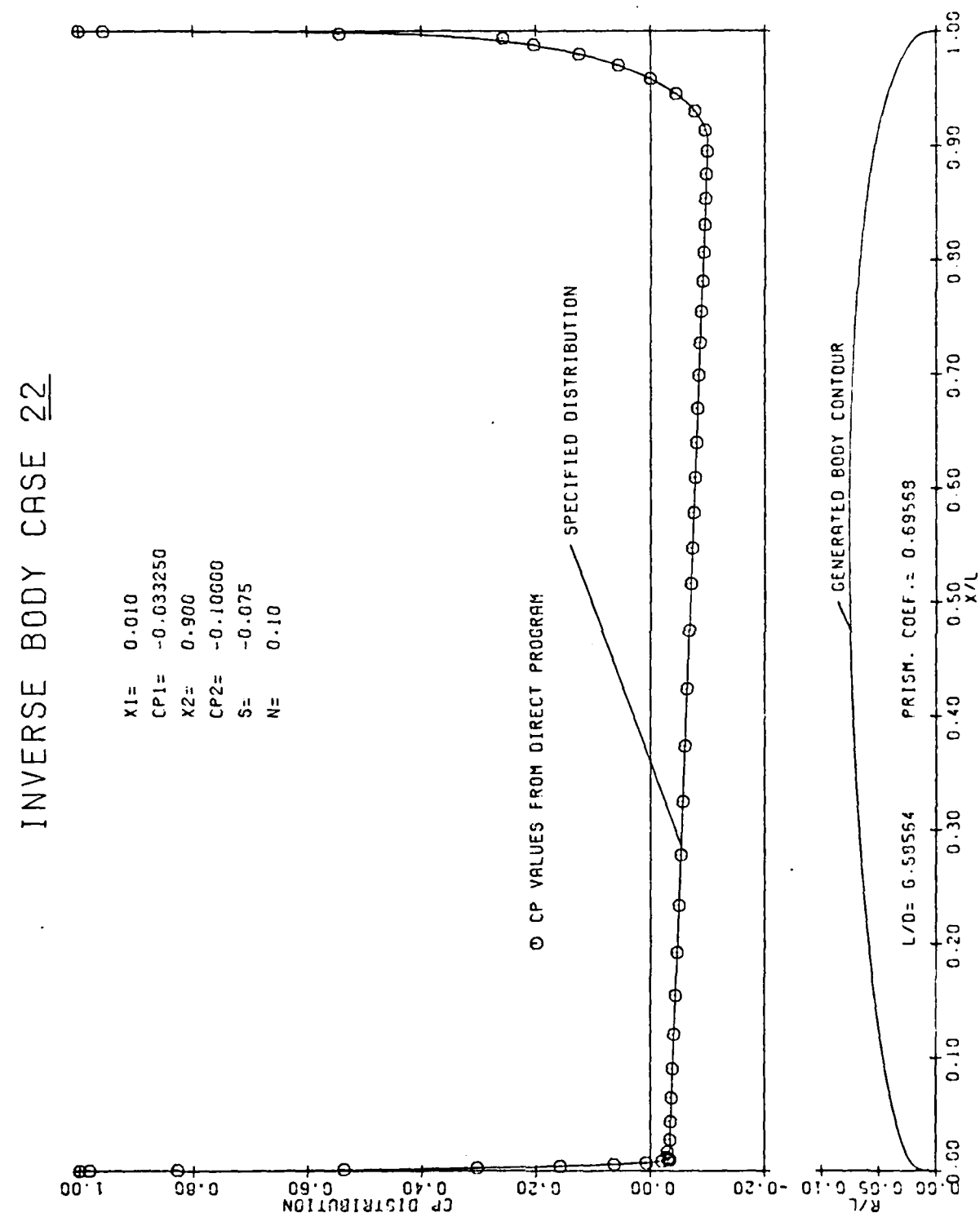

Figure 32. Pressure Distribution and Body Contour, Case No. 22.

19 August 1981
JJE:GHH:mmj

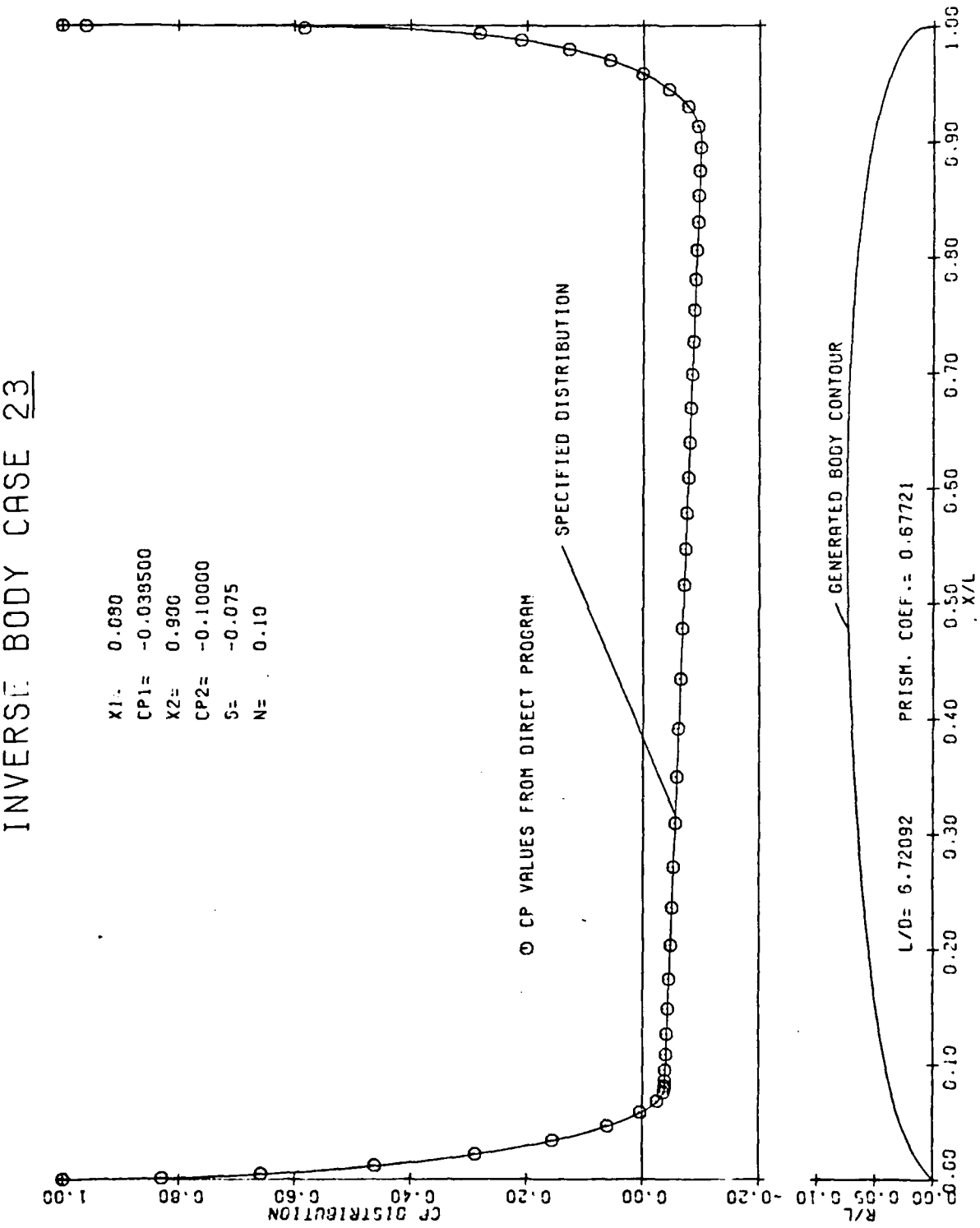

Figure 33. Pressure Distribution and Body Contour, Case No. 23.

19 August 1981
JJE:GHH:mmj

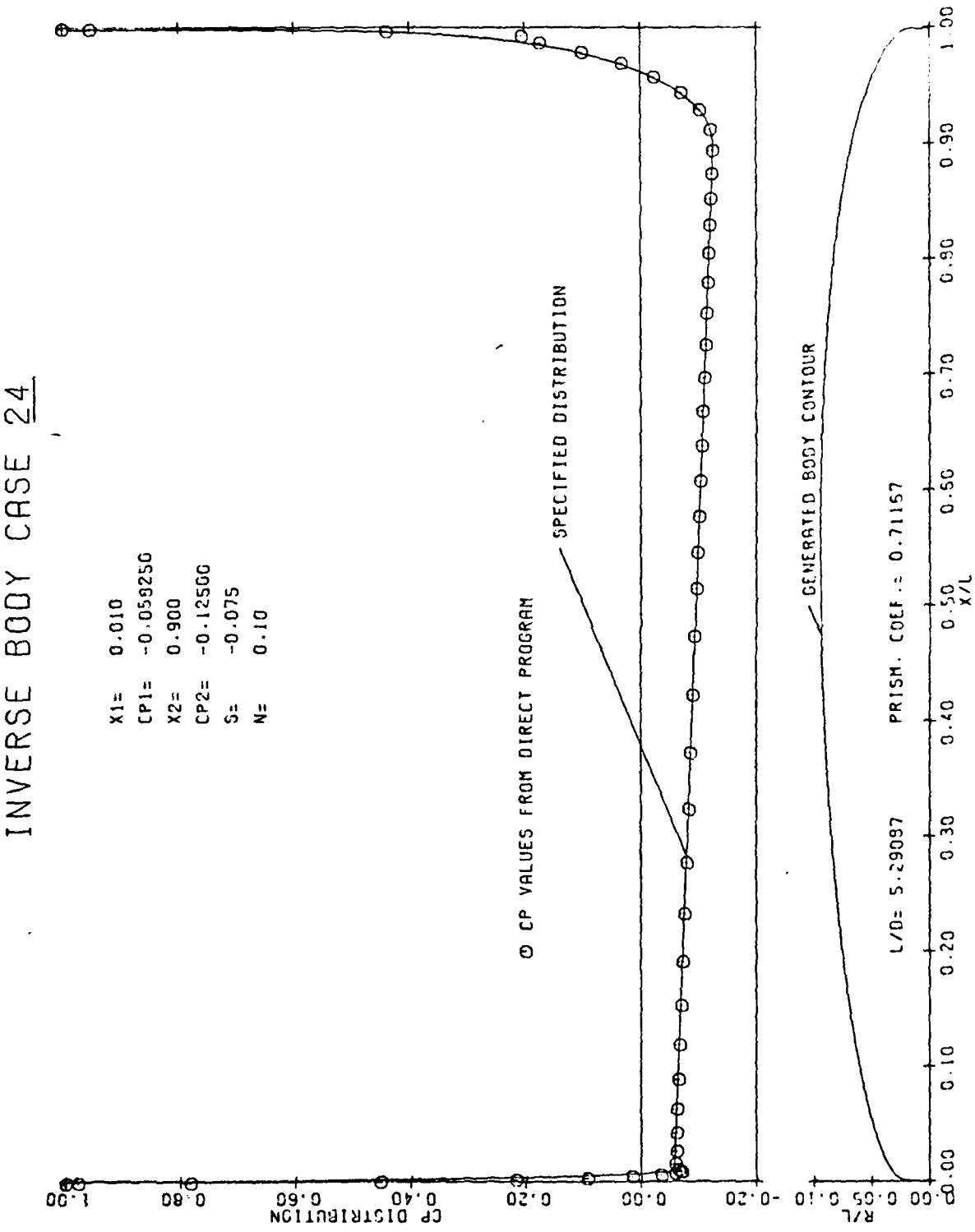

Figure 34. Pressure Distribution and Body Contour, Case No. 24.

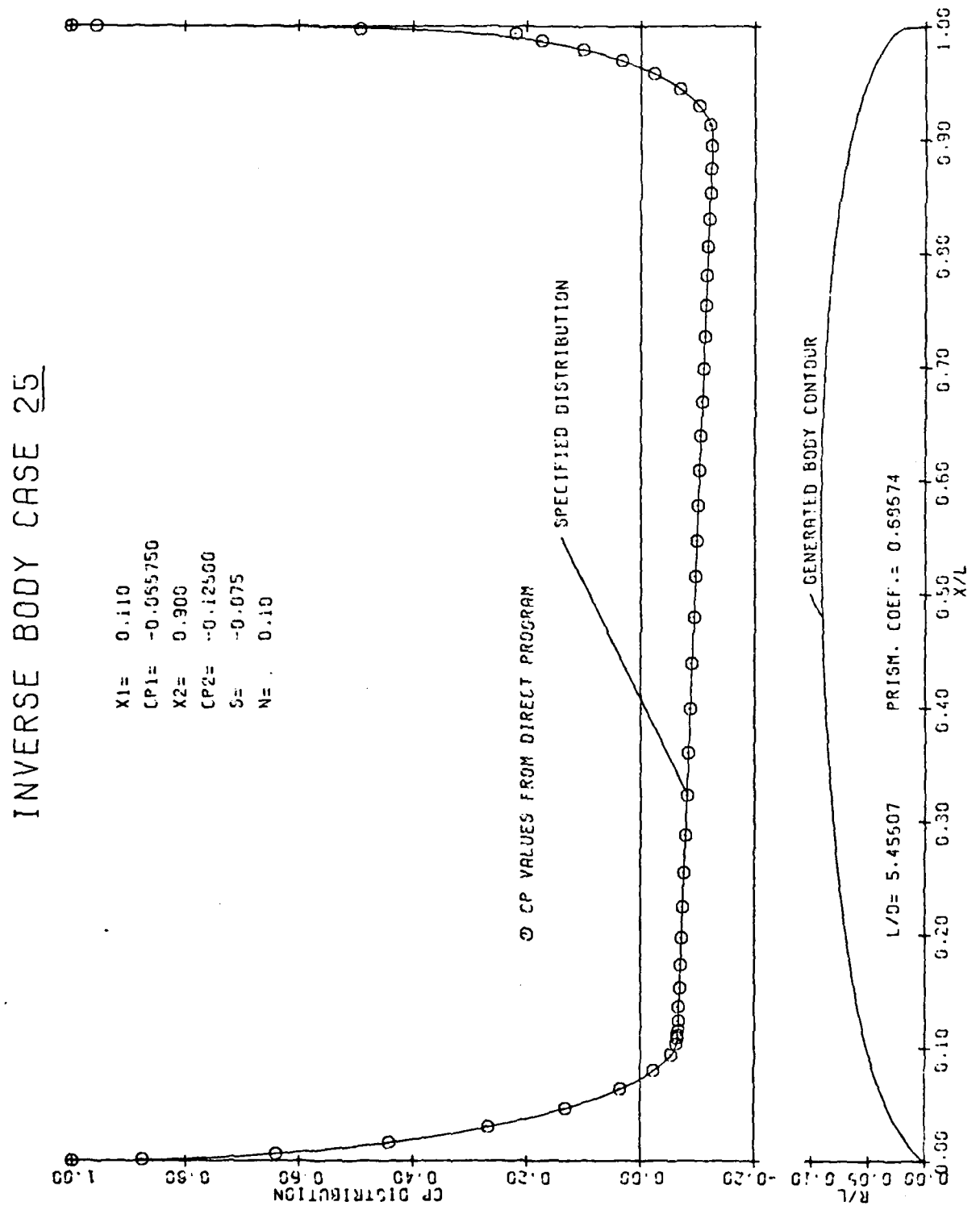

Figure 35. Pressure Distribution and Body Contour, Case No. 25.

19 August 1981
JJE:GHH:mmj

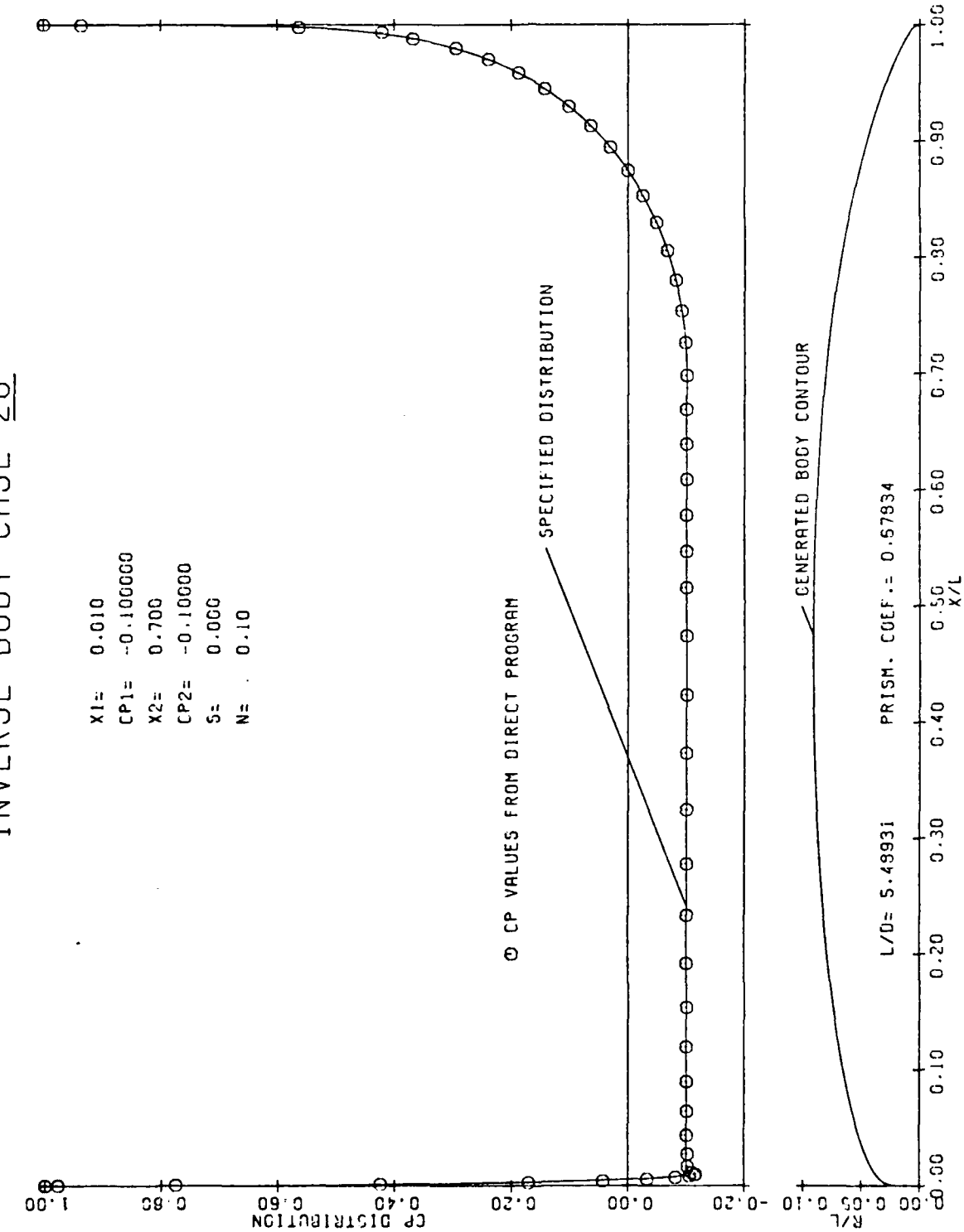

Figure 36. Pressure Distribution and Body Contour, Case No. 26.

19 August 1981
JJE:GHH:mmj

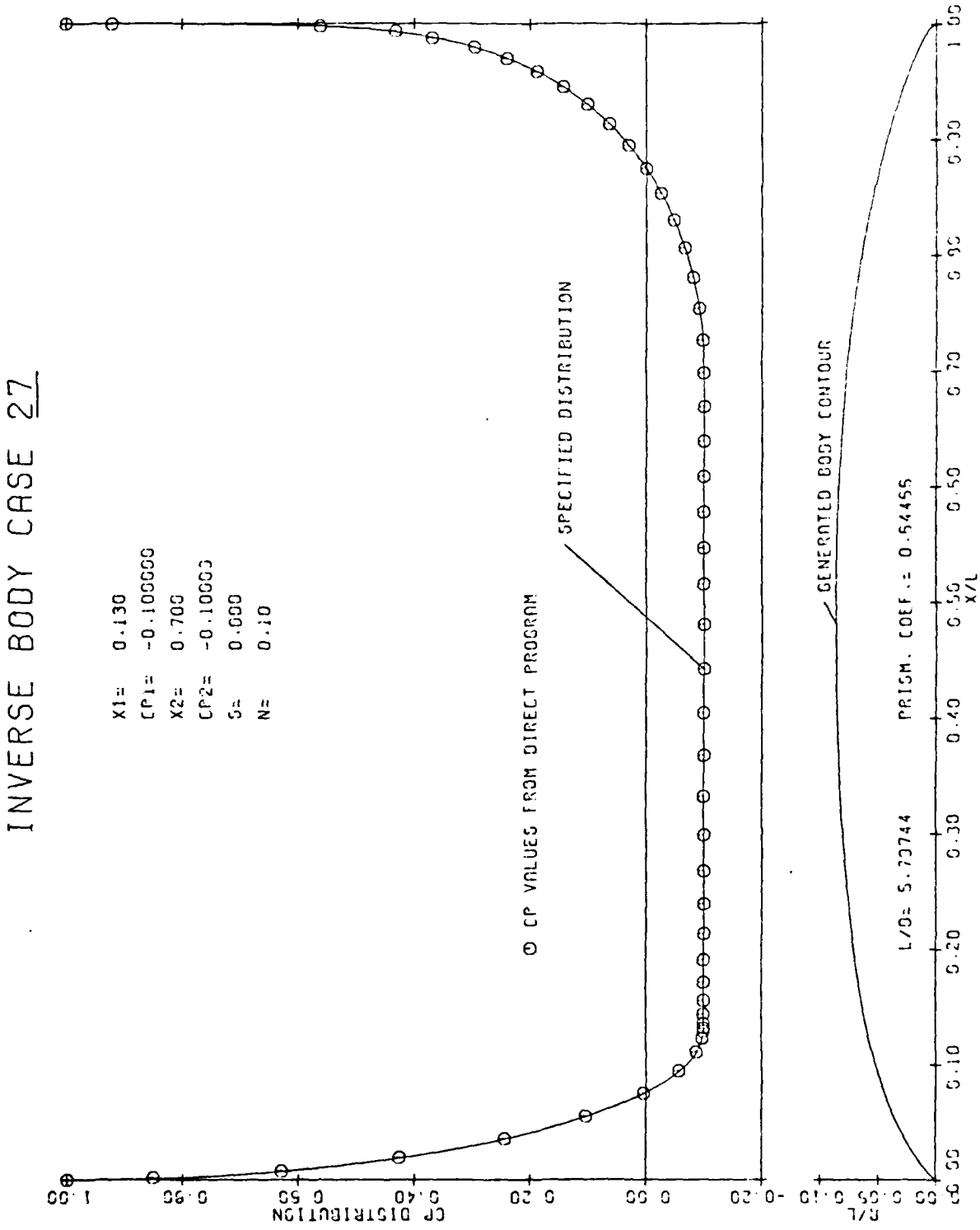

Figure 37. Pressure Distribution and Body Contour, Case No. 27.

19 August 1981
JJE:GHH:mmj

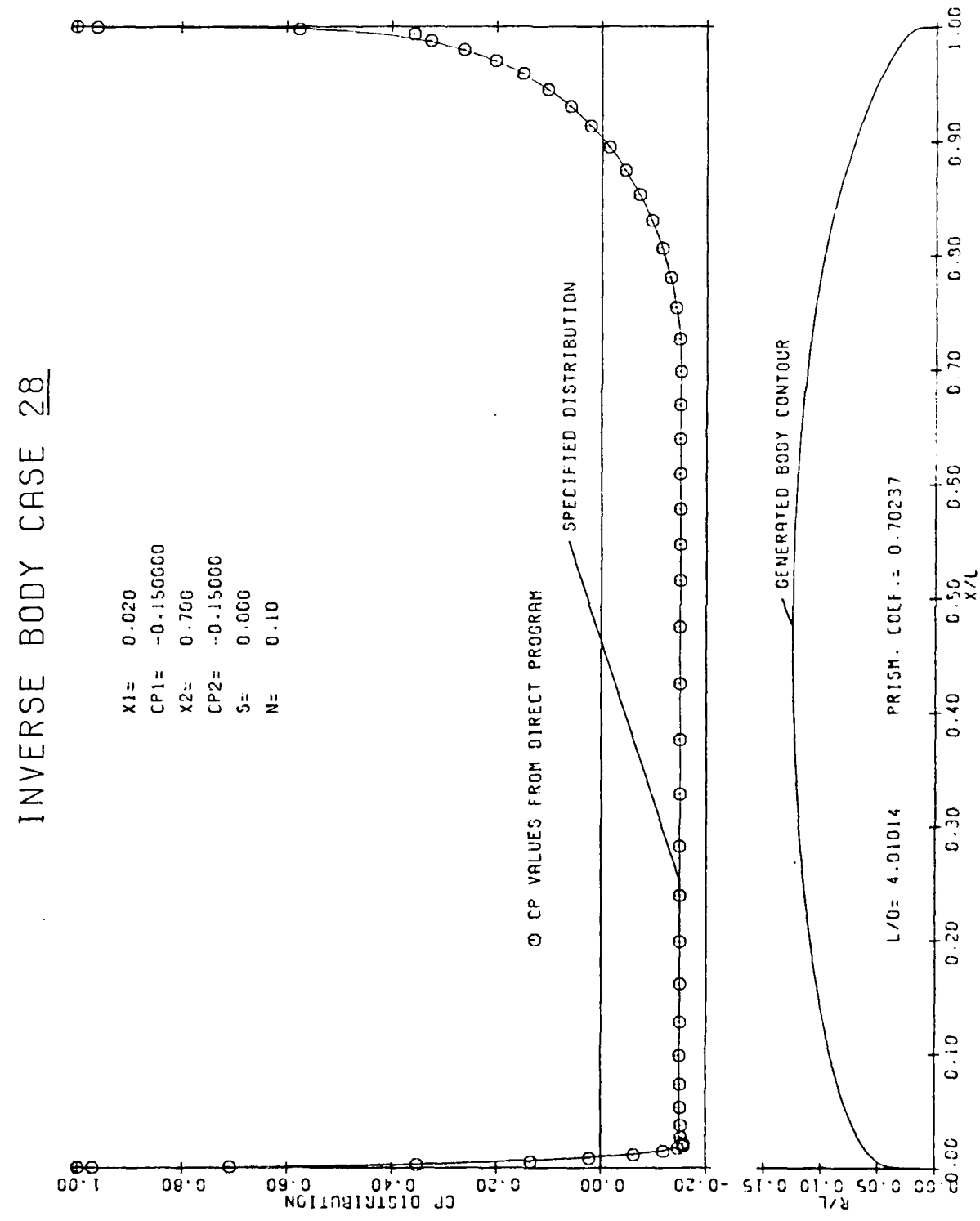

Figure 38. Pressure Distribution and Body Contour, Case No. 28.

19 August 1981
JJE:GHH:mmj

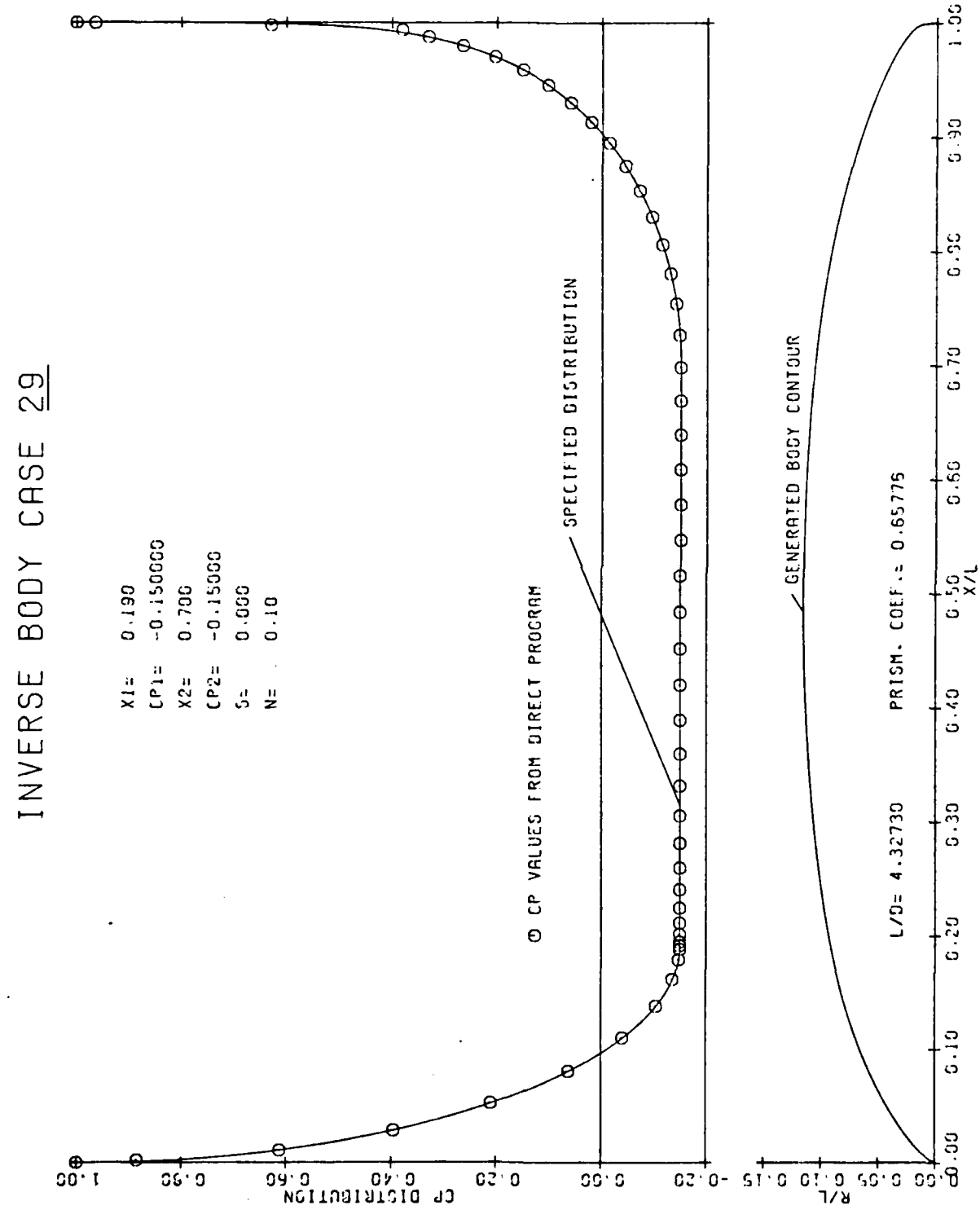

Figure 39. Pressure Distribution and Body Contour, Case No. 29.

19 August 1981
JJE:GHH:mmj

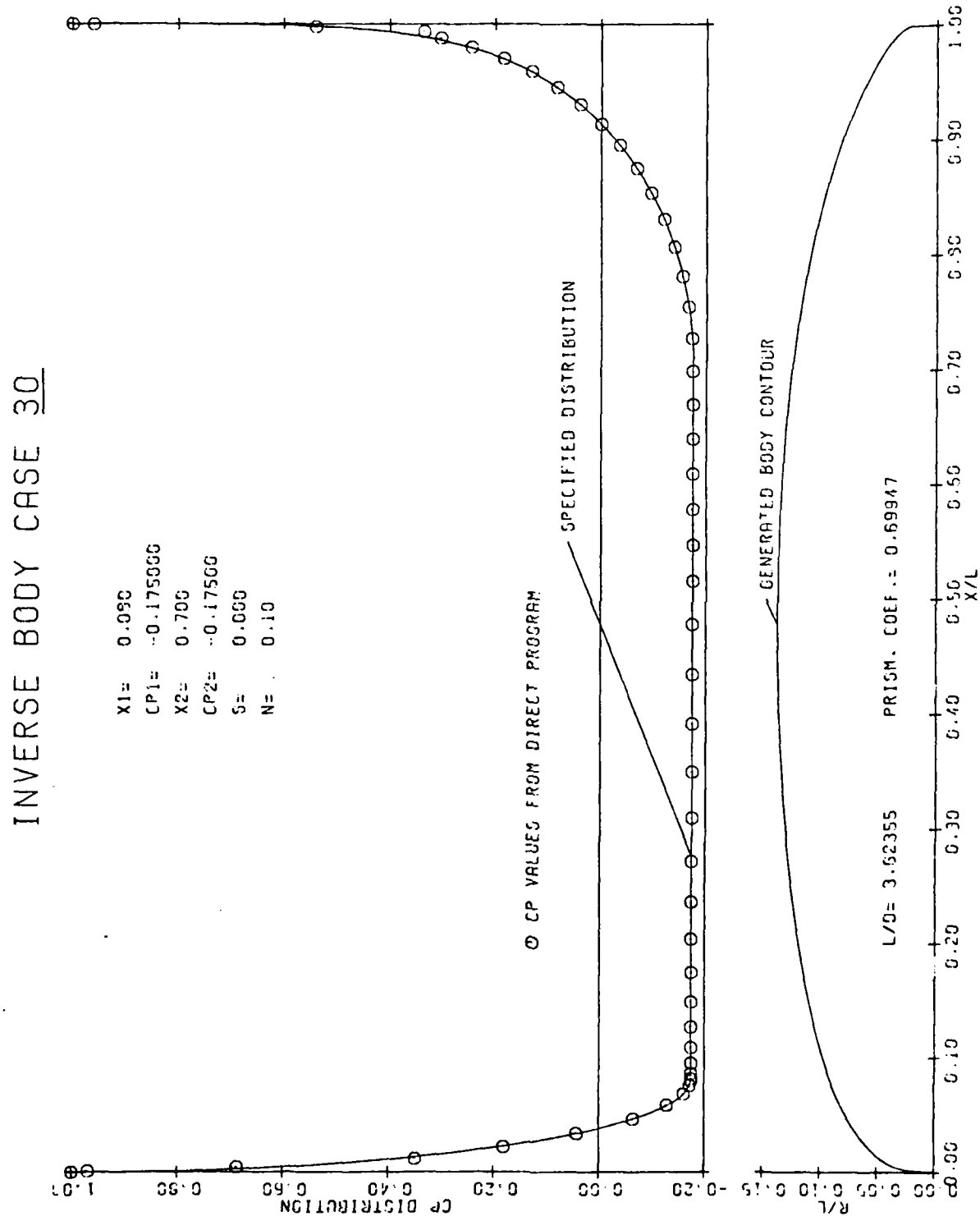

Figure 40. Pressure Distribution and Body Contour, Case No. 30.

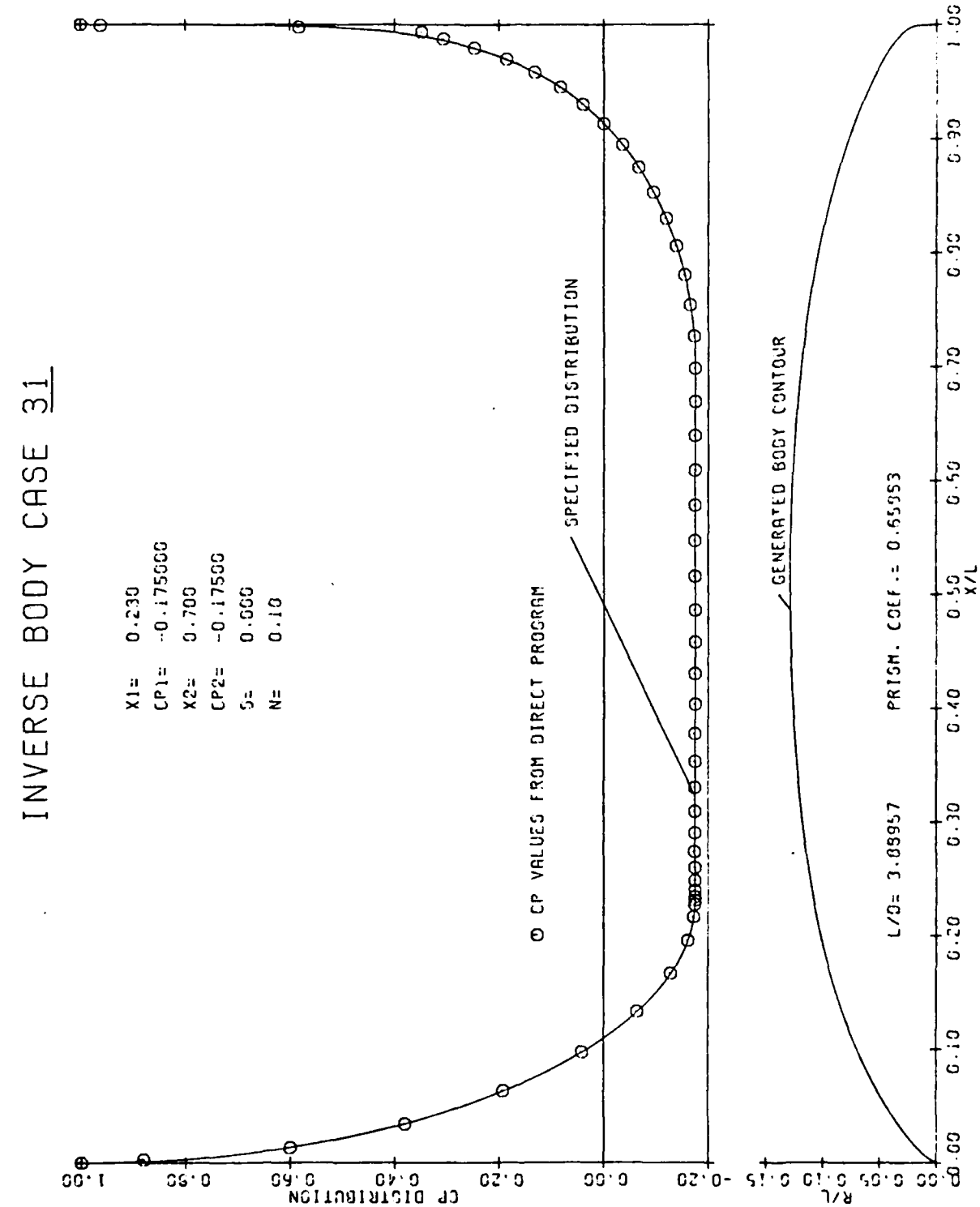

Figure 41. Pressure Distribution and Body Contour, Case No. 31.

19 August 1981
JJE:GHH:mmj

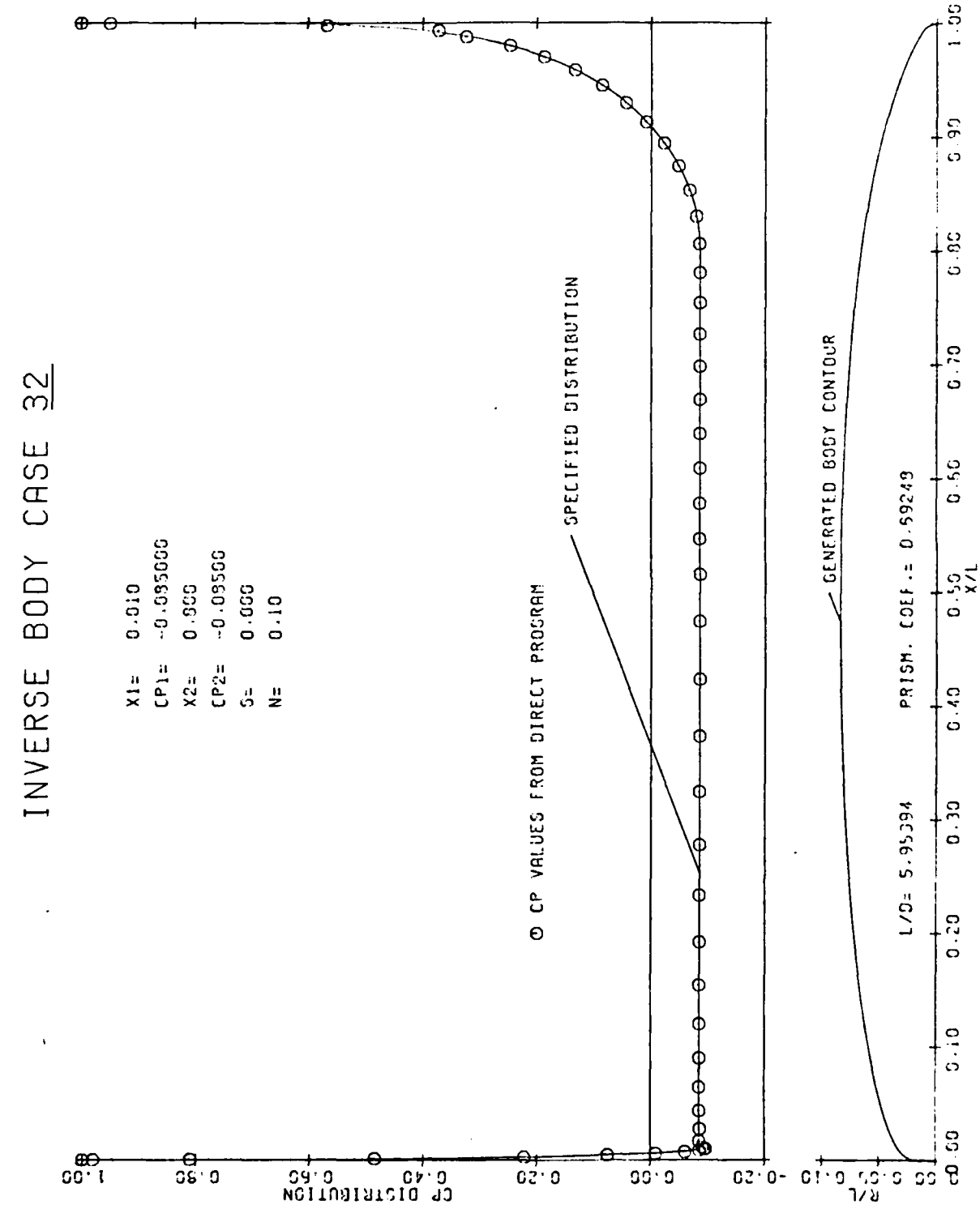

Figure 42. Pressure Distribution and Body Contour, Case No. 32.

19 August 1981
JJE:GHH:mmj

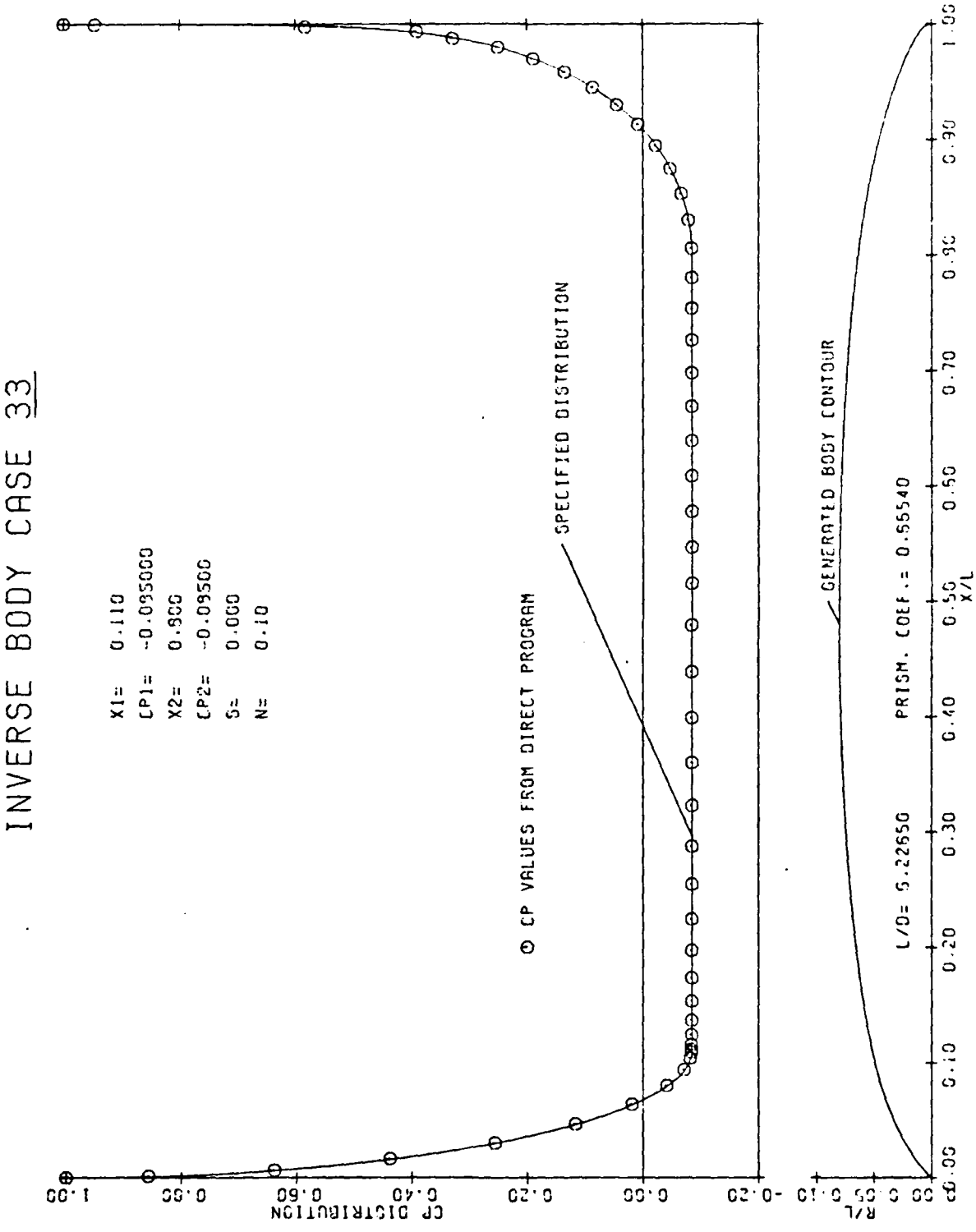

Figure 43. Pressure Distribution and Body Contour, Case No. 33.

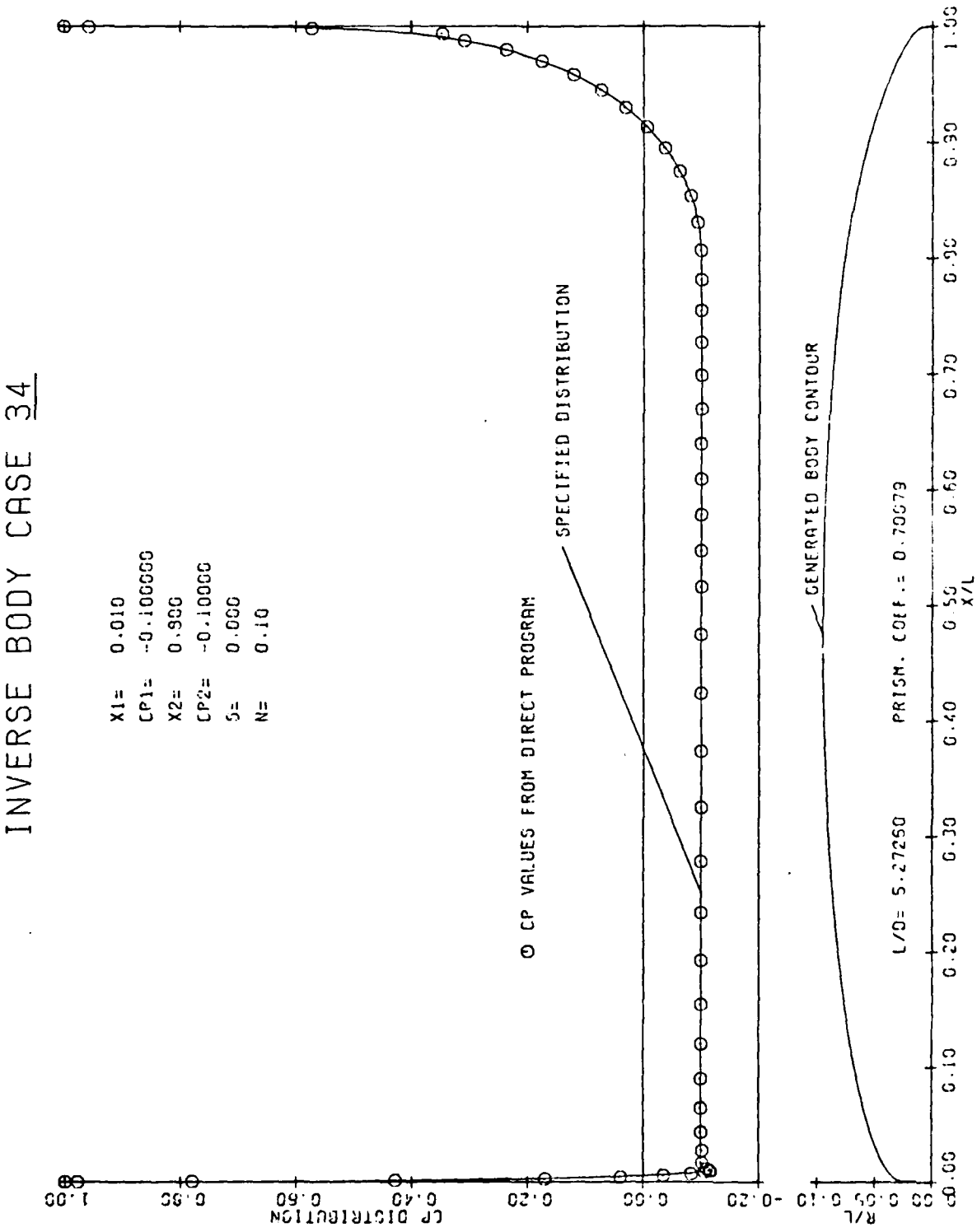

Figure 44. Pressure Distribution and Body Contour, Case No. 34.

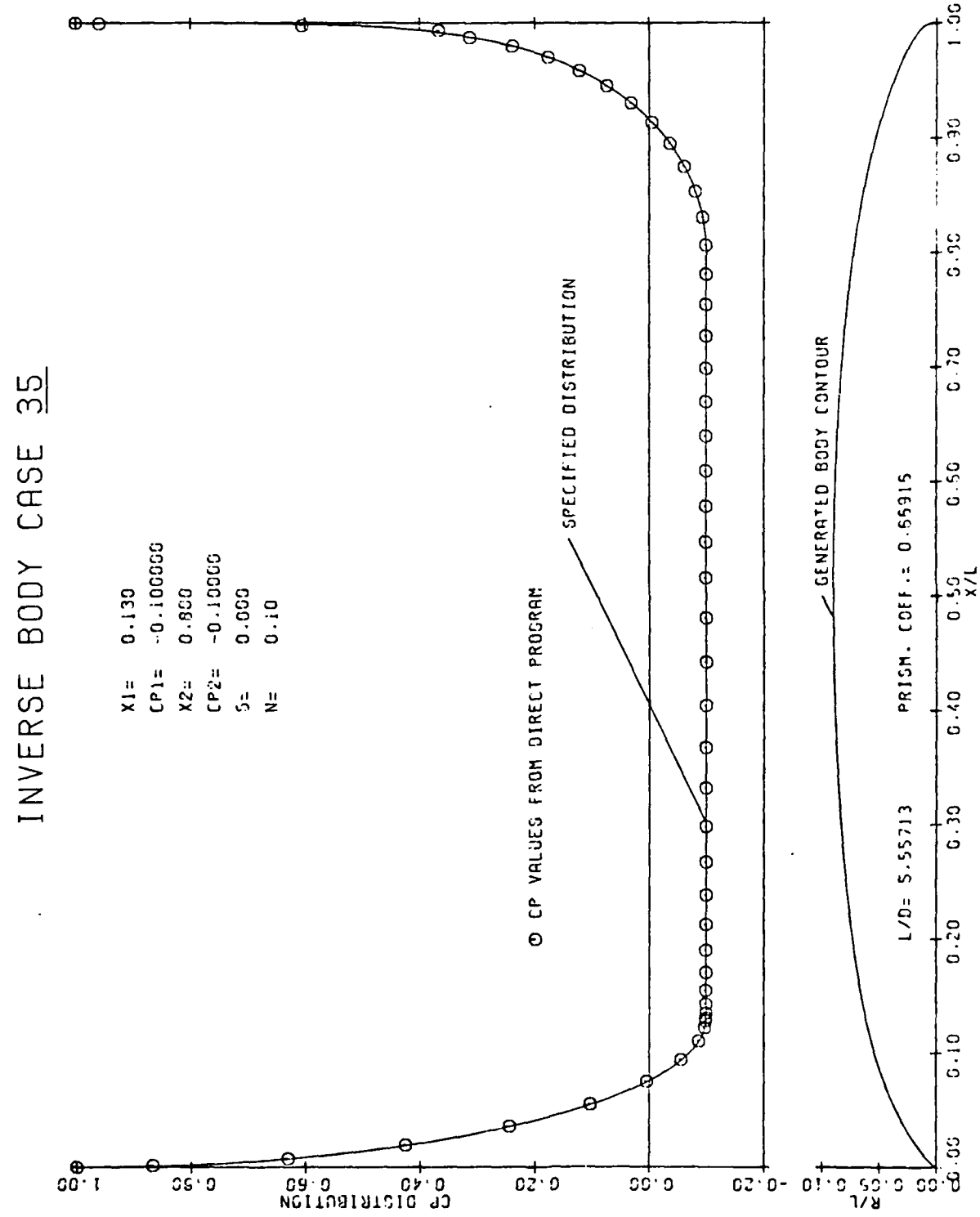

Figure 45. Pressure Distribution and Body Contour, Case No. 35.

19 August 1981
JJE:GHH:mmj

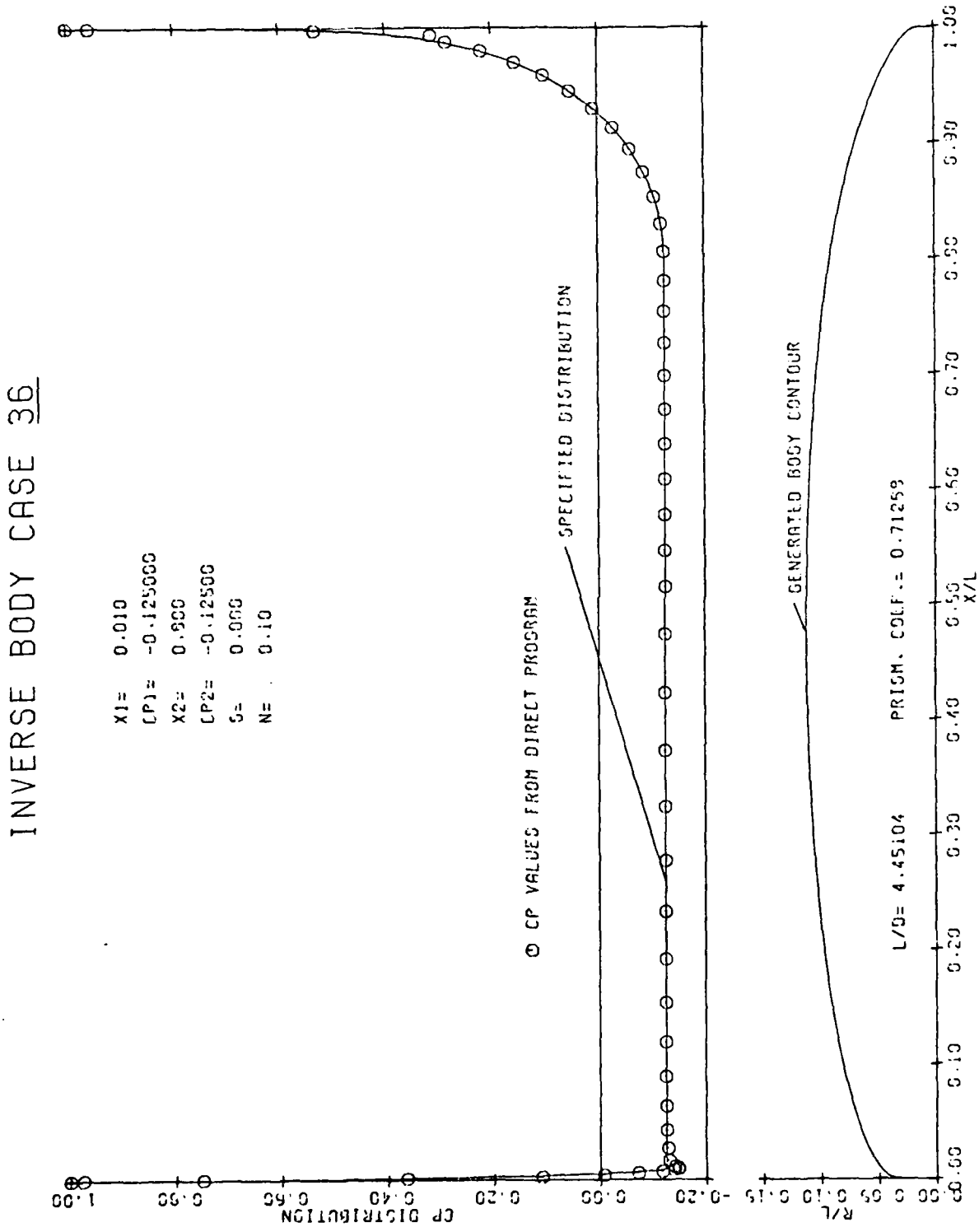

Figure 46. Pressure Distribution and Body Contour, Case No. 36.

19 August 1981
JJE:GHH:mmj

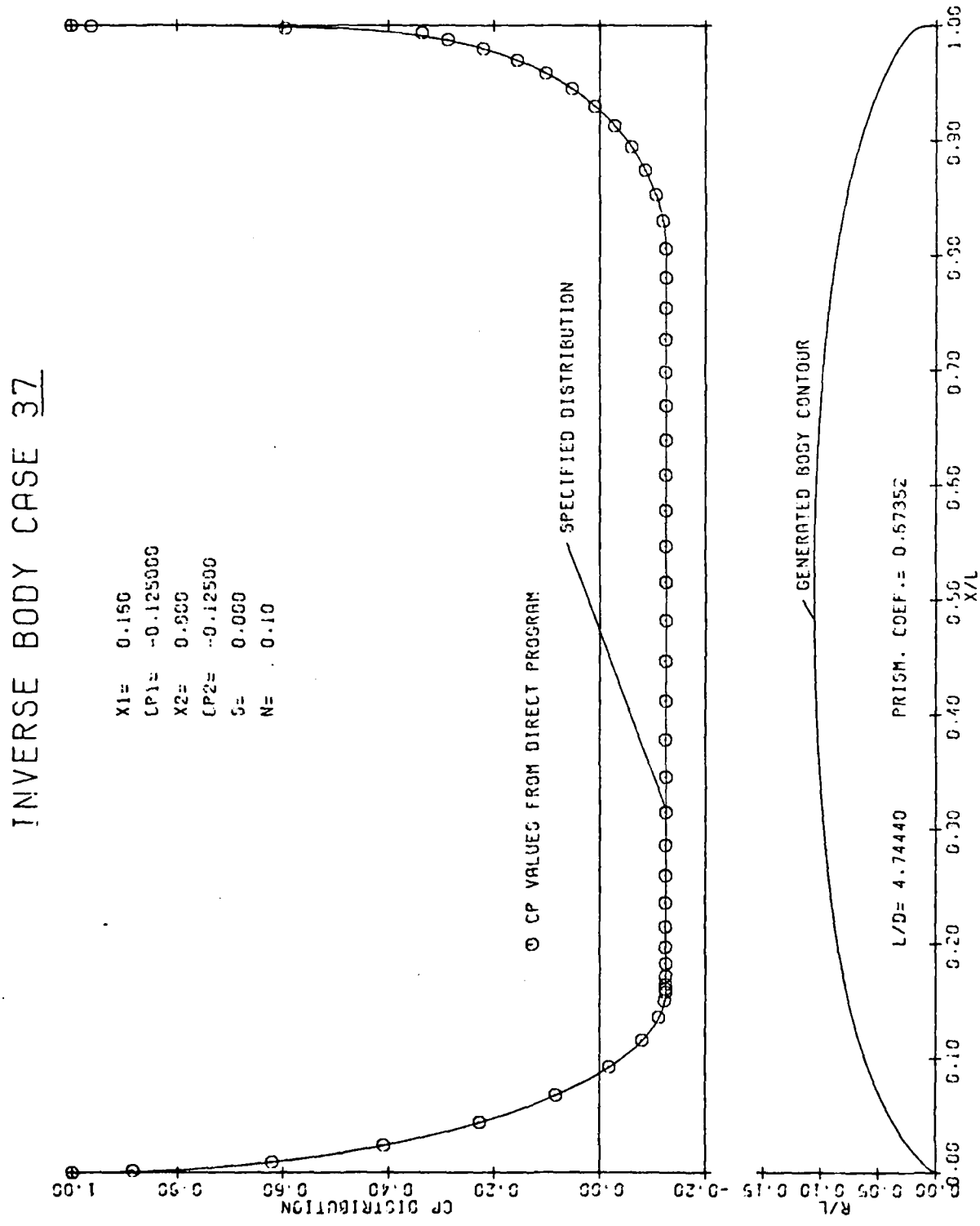

Figure 47. Pressure Distribution and Body Contour, Case No. 37.

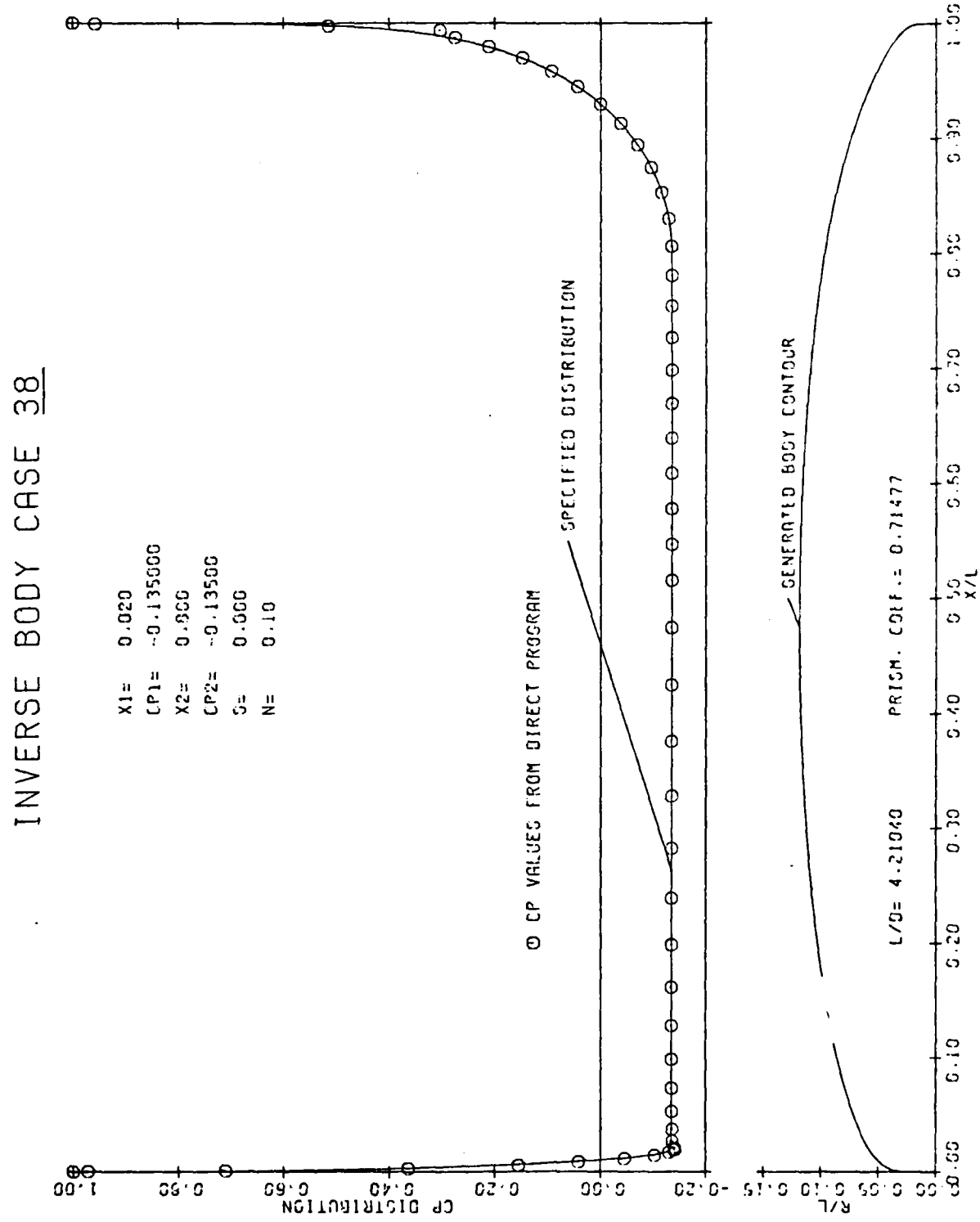

Figure 48. Pressure Distribution and Body Contour, Case No. 38.

19 August 1981
JJE:GHH:mmj

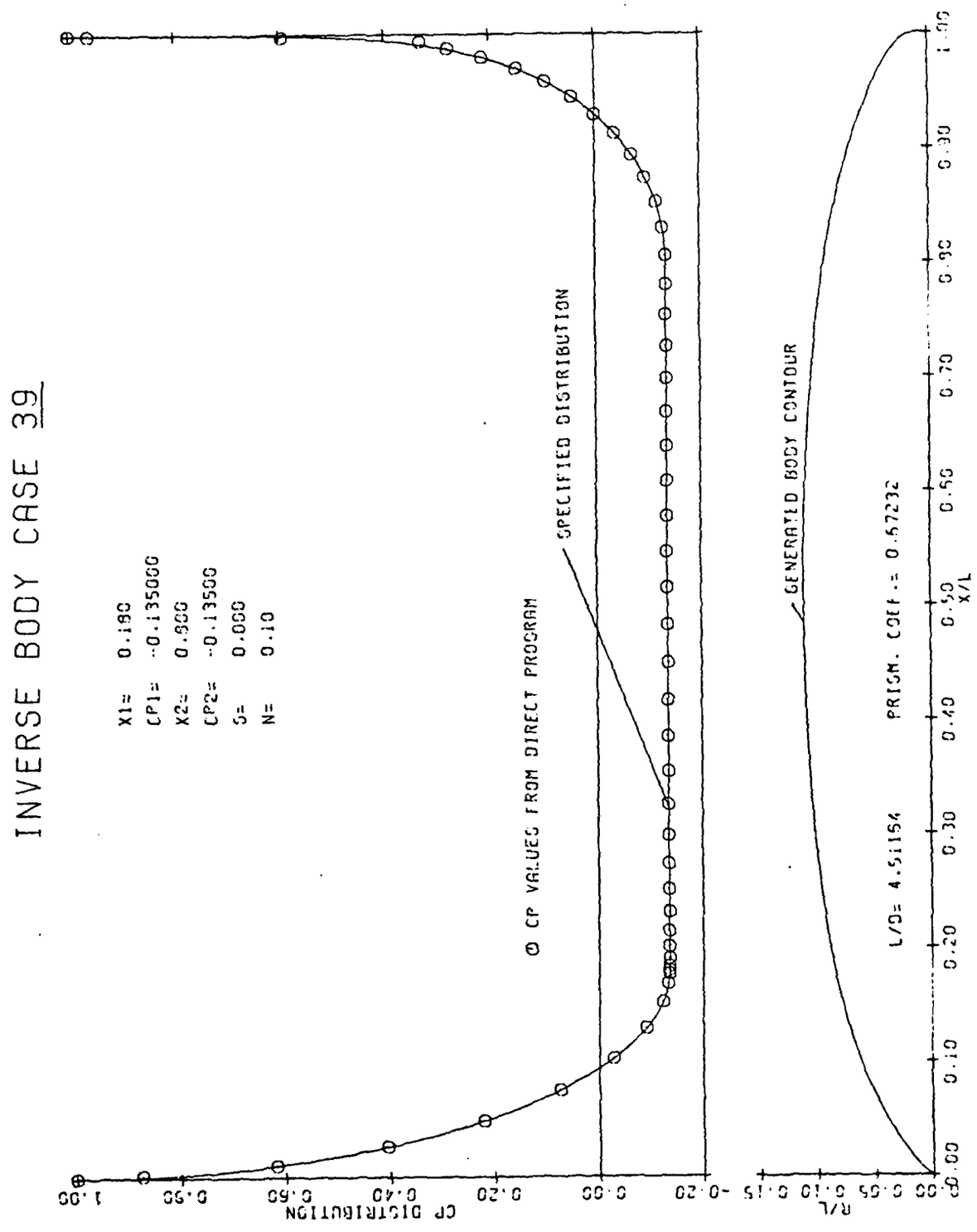

Figure 49. Pressure Distribution and Body Contour, Case No. 39.

19 August 1981
JJE:GHH:mmj

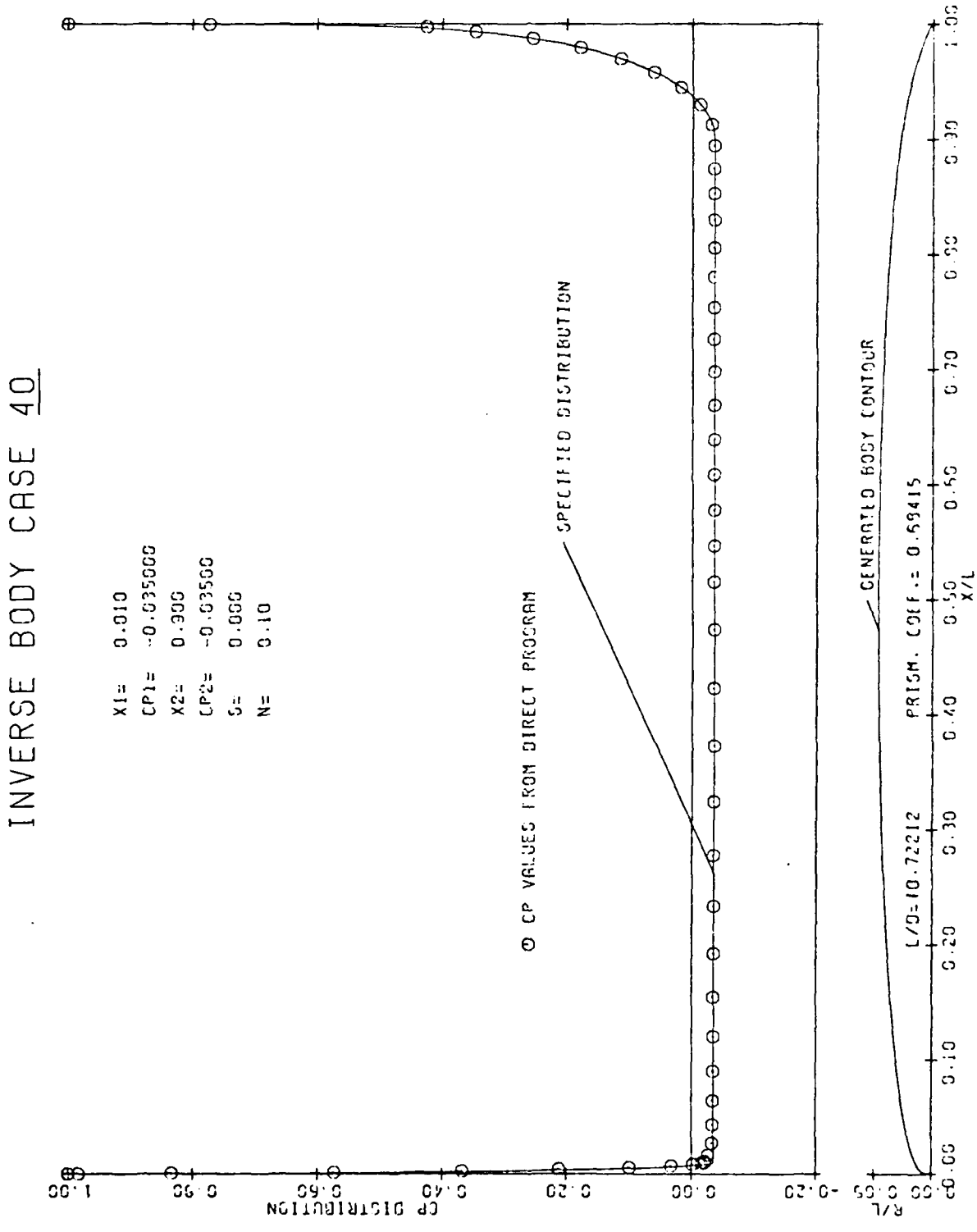

Figure 50. Pressure Distribution and Body Contour, Case No. 40.

19 August 1981
JJE:CHH:mmj

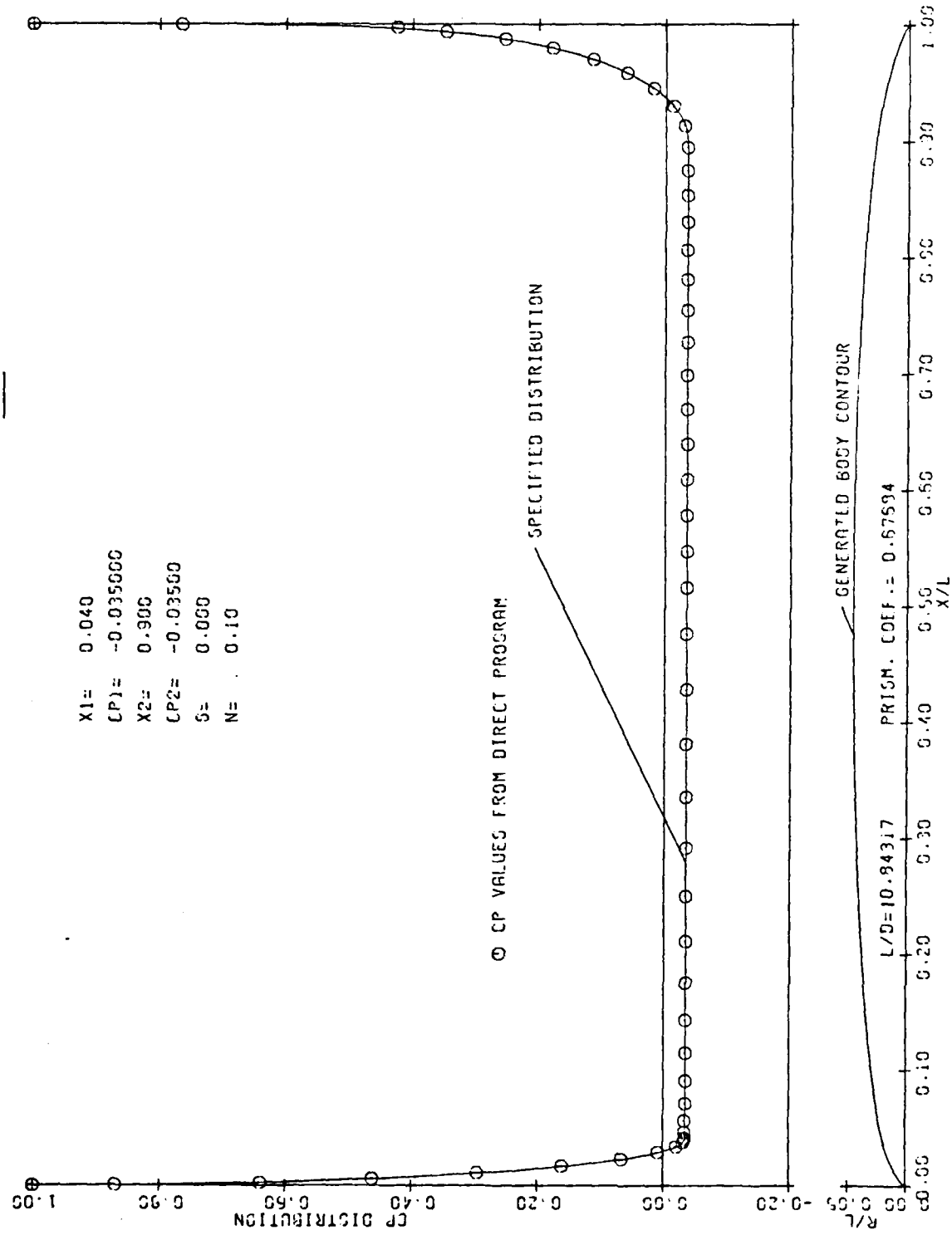

Figure 51. Pressure Distribution and Body Contour, Case No. 41.

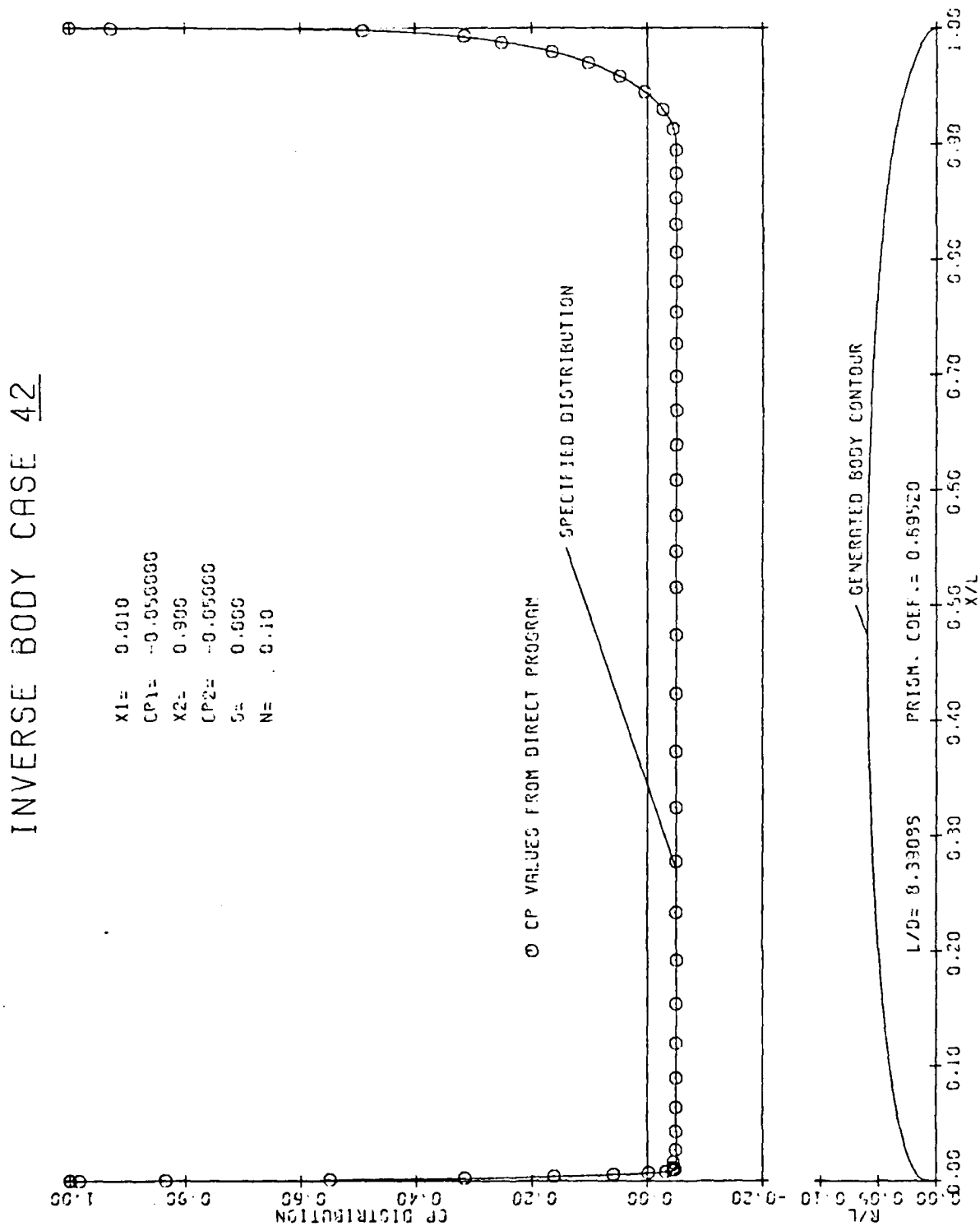

Figure 52. Pressure Distribution and Body Contour, Case No. 42.

19 August 1981
JJE:GHH:mmj

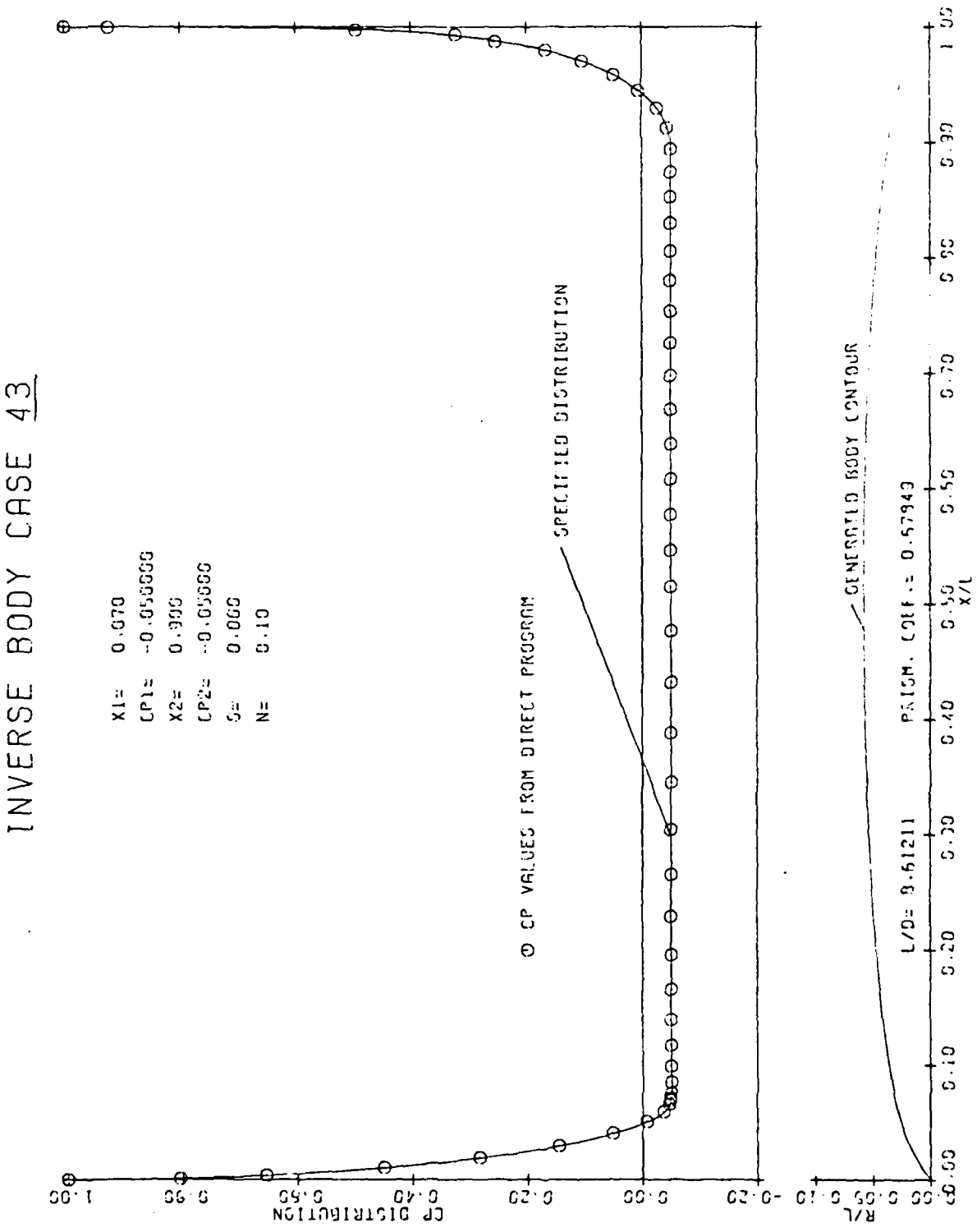

Figure 53. Pressure Distribution and Body Contour, Case No. 43.

19 August 1981
JJE:GHH:mmj

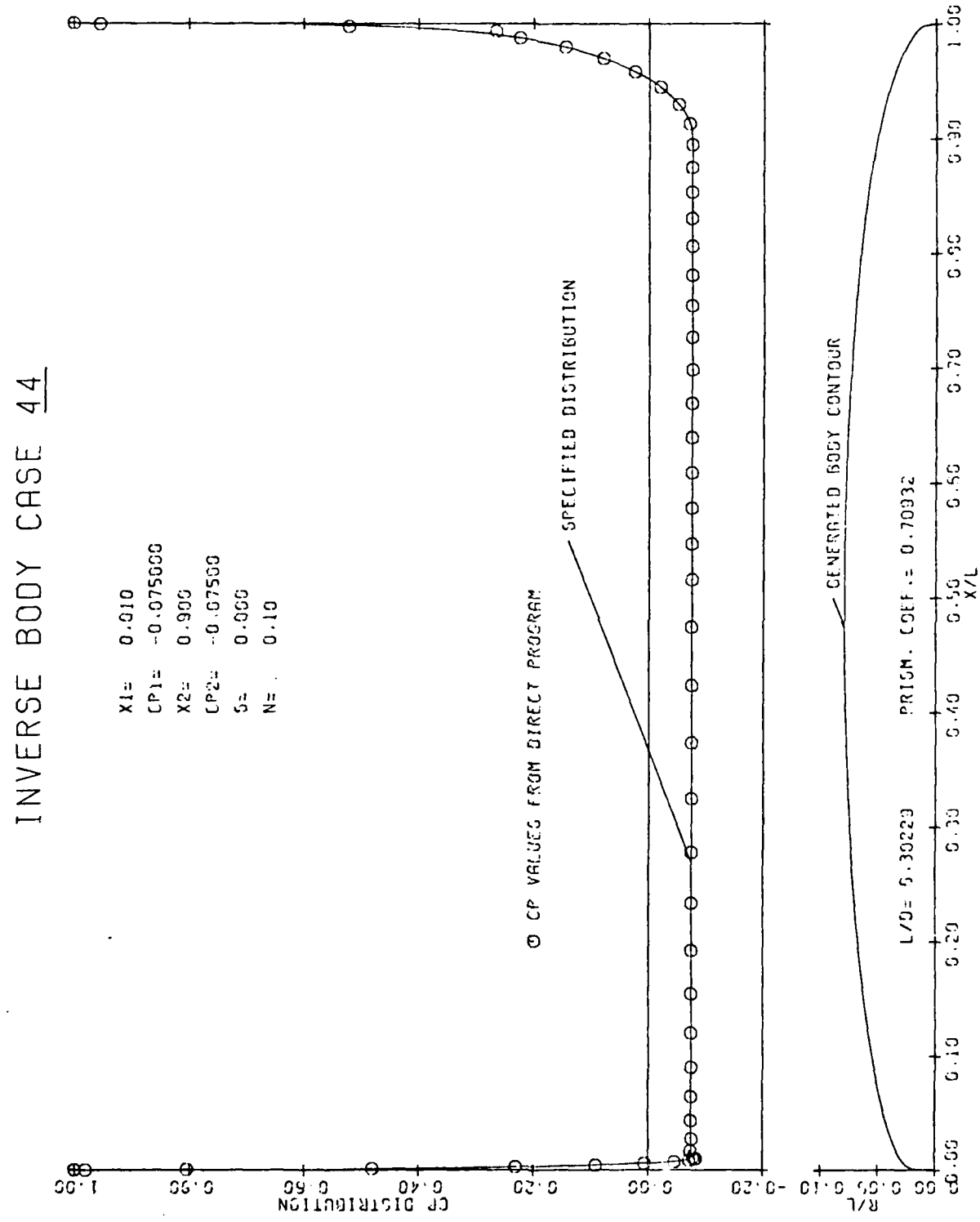

Figure 54. Pressure Distribution and Body Contour, Case No. 44.

19 August 1981
JJF:GHH:mmj

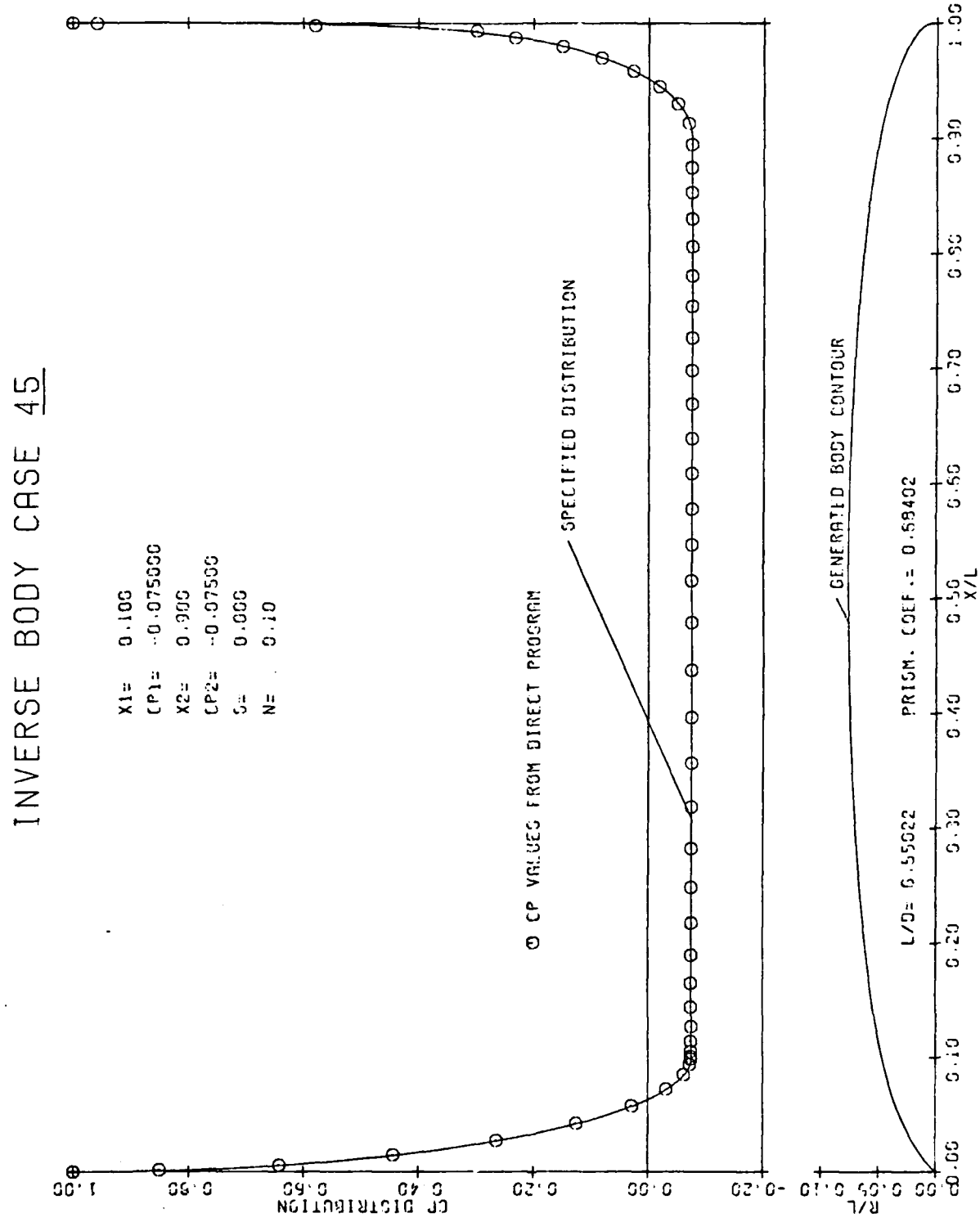

Figure 55. Pressure Distribution and Body Contour, Case No. 45.

19 August 1981
JJE:GHH:mmj

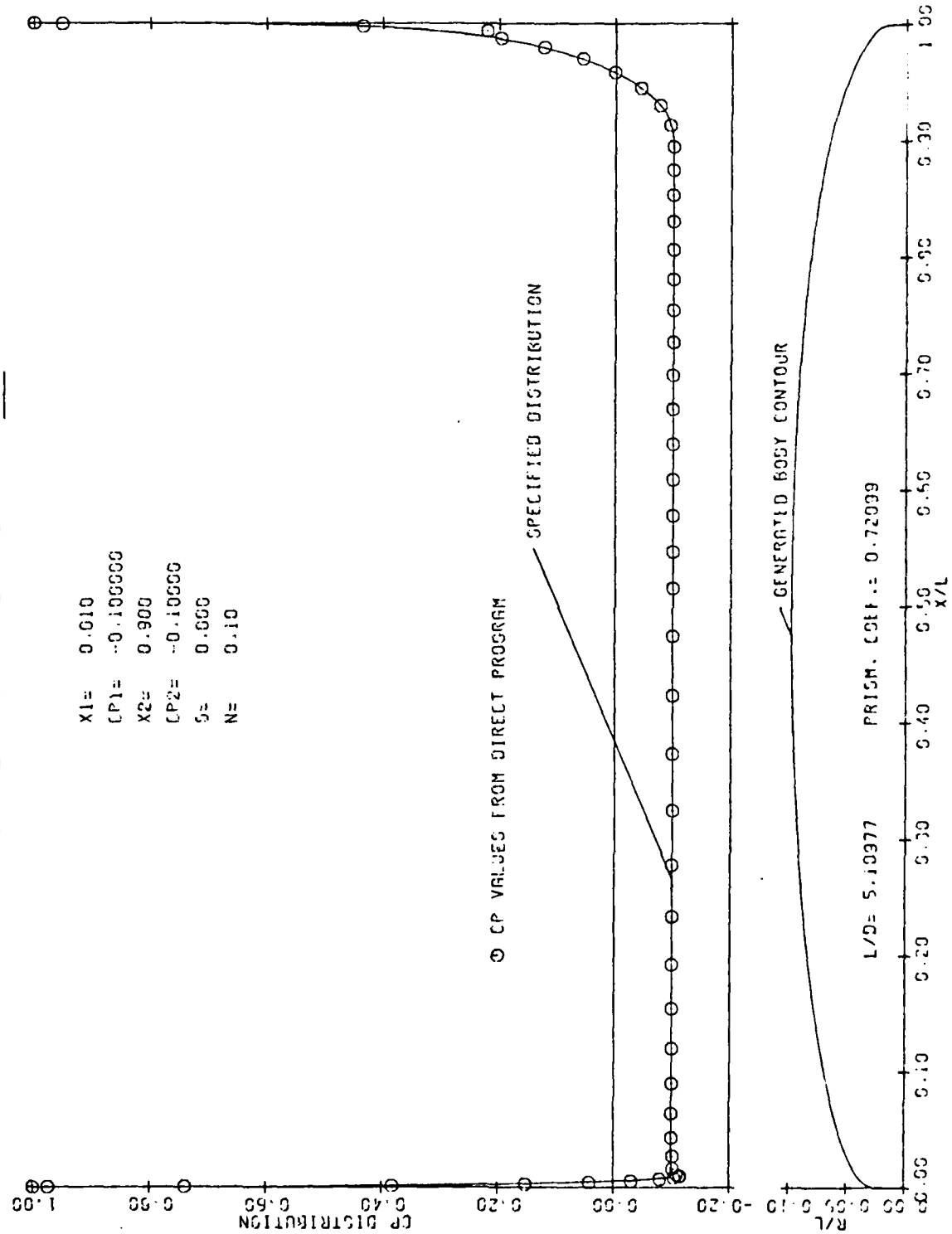

Figure 56. Pressure Distribution and Body Contour, Case No. 46.

19 August 1981
JJE:GHH:mmj

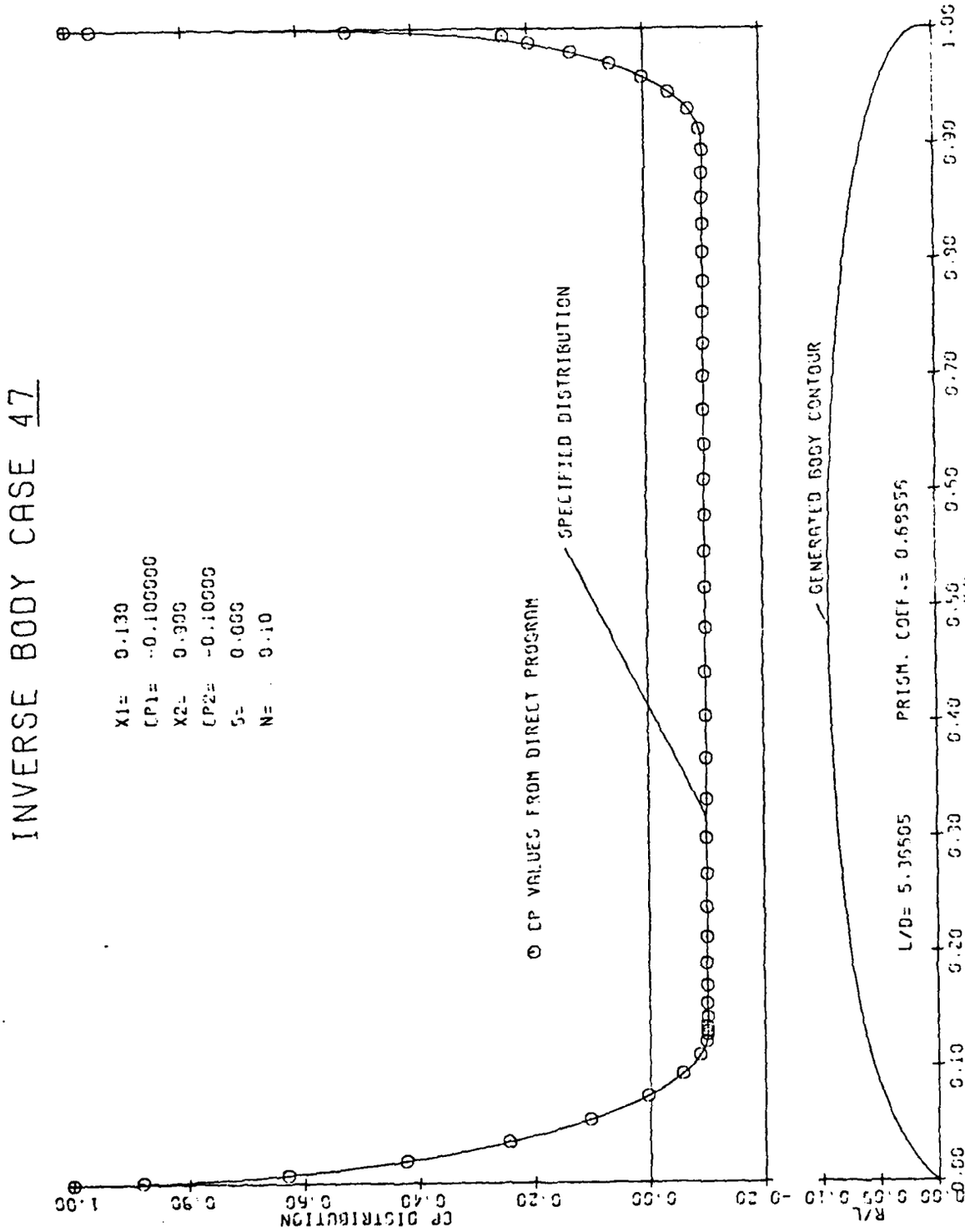

Figure 57. Pressure Distribution and Body Contour, Case No. 47.

19 August 1981
JJE:GHH:mmj

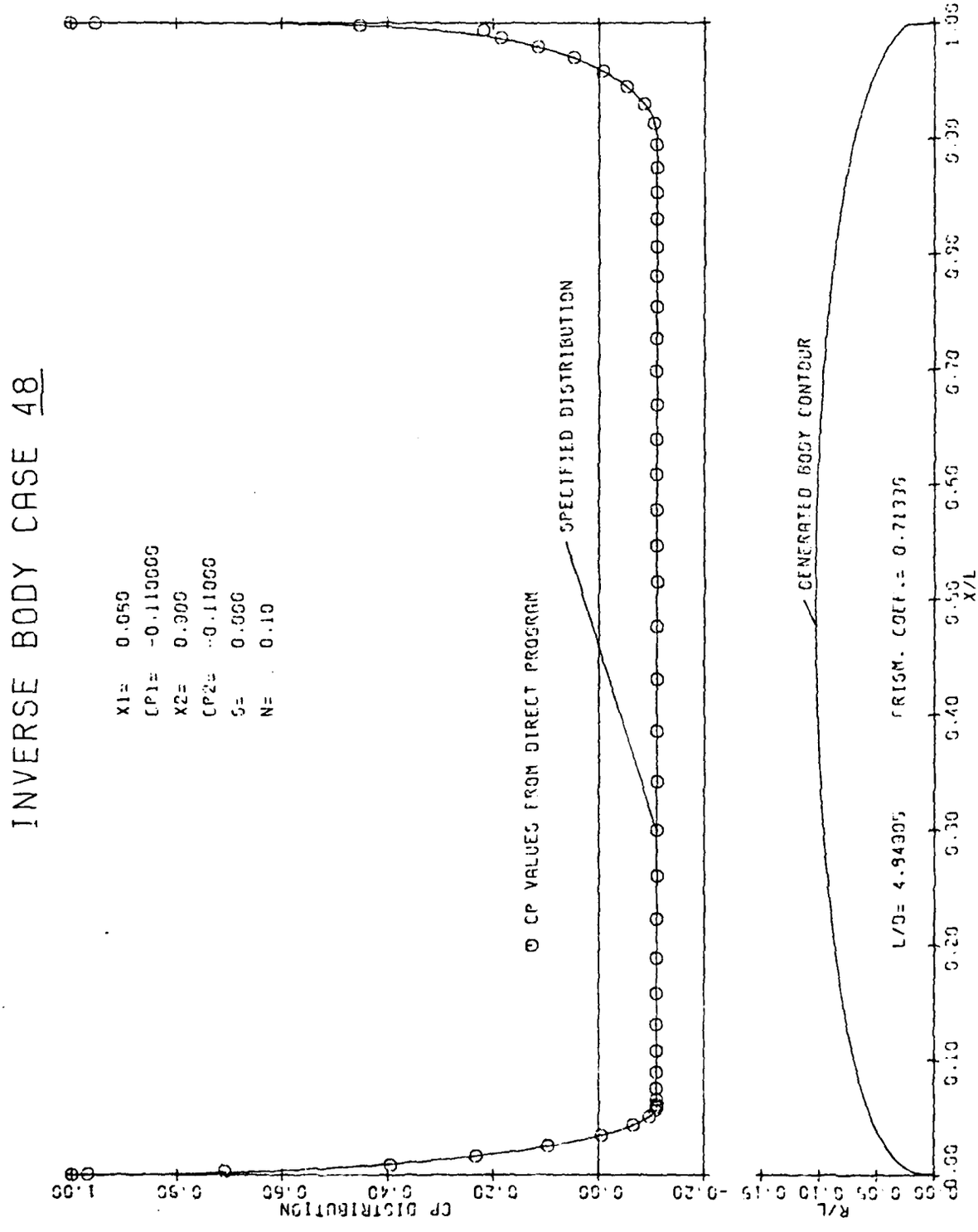

Figure 58. Pressure Distribution and Body Contour, Case No. 48.

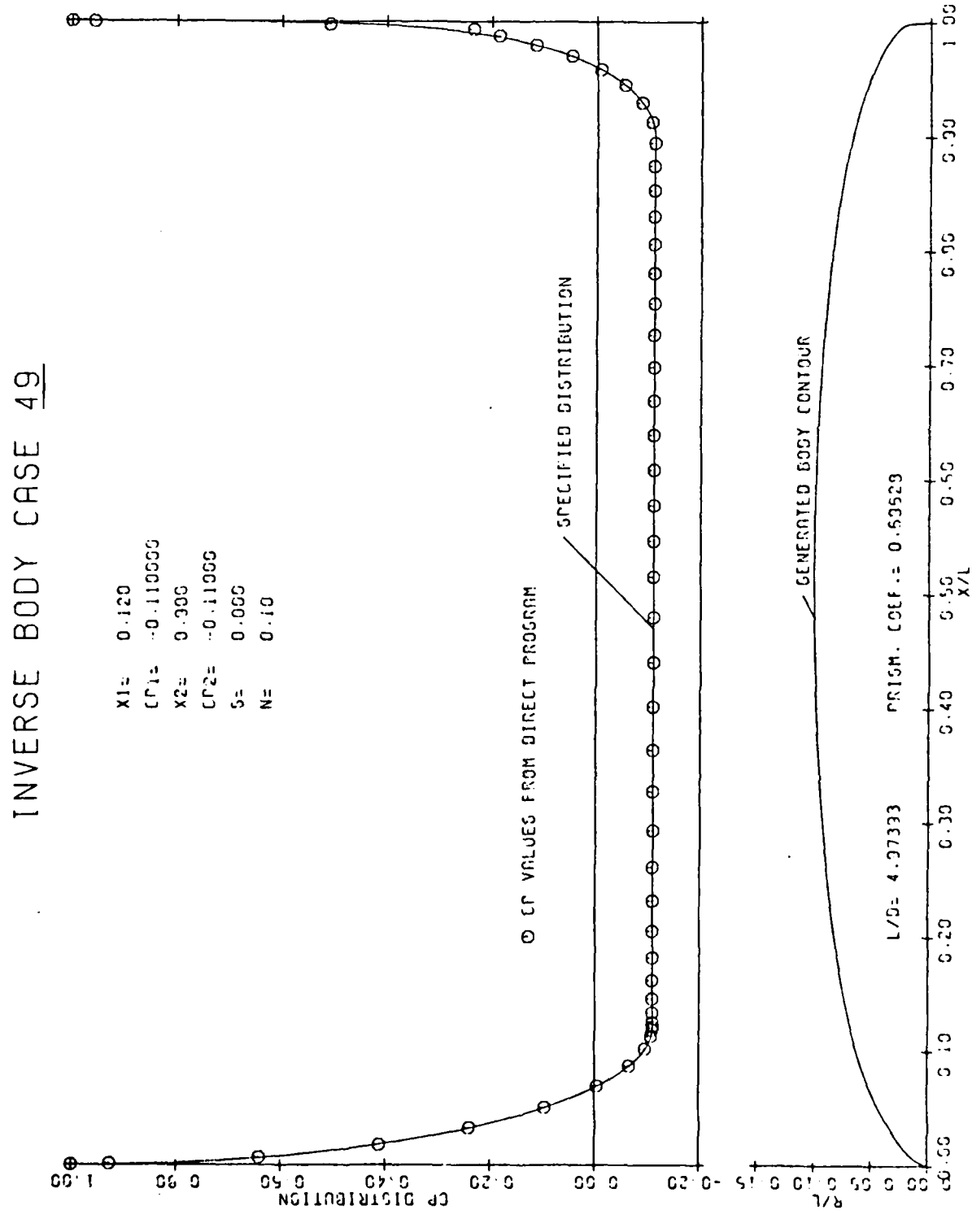

Figure 59. Pressure Distribution and Body Contour, Case No. 49.

19 August 1981
JJE:GHH:mmj

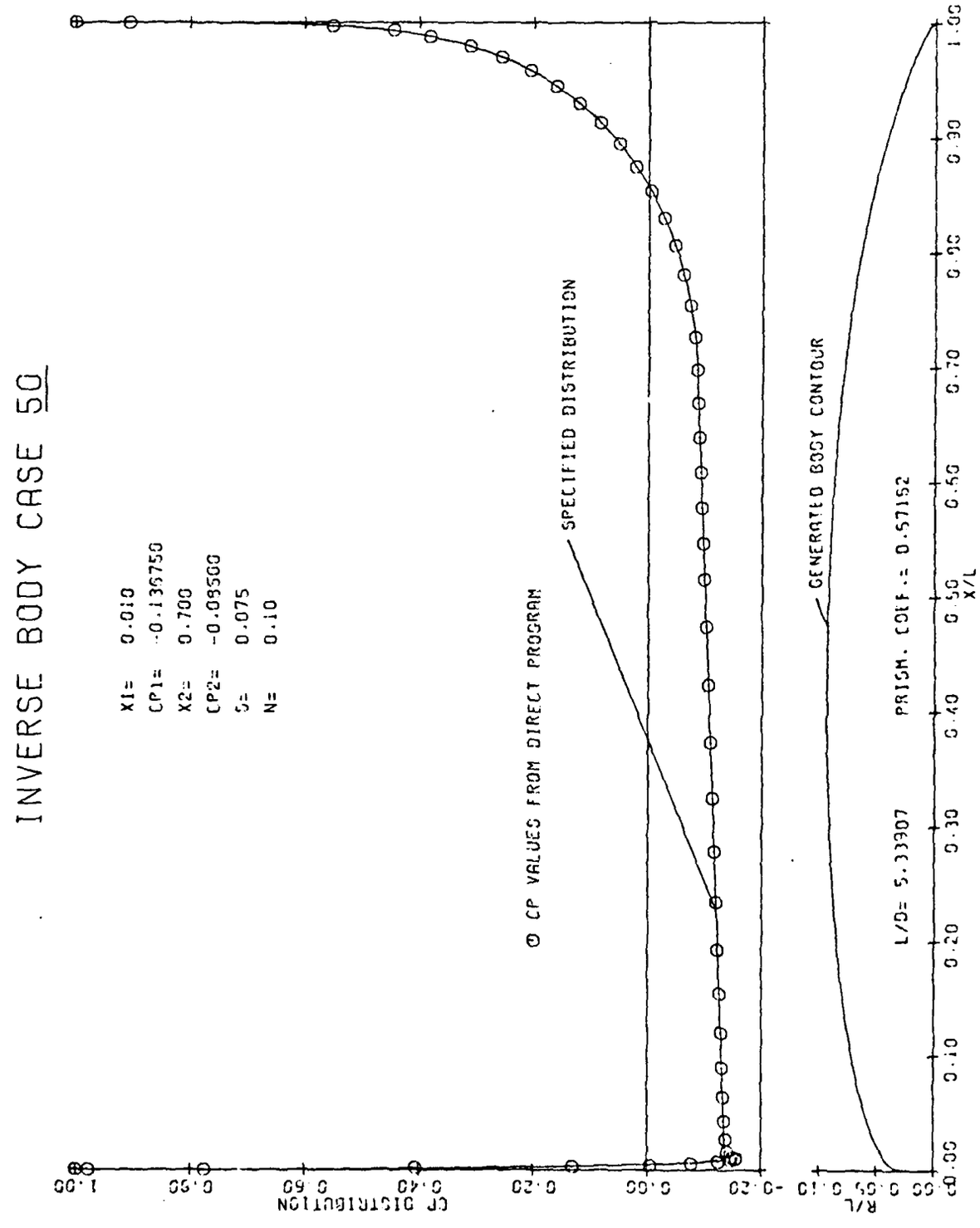

Figure 60. Pressure Distribution and Body Contour, Case No. 50.

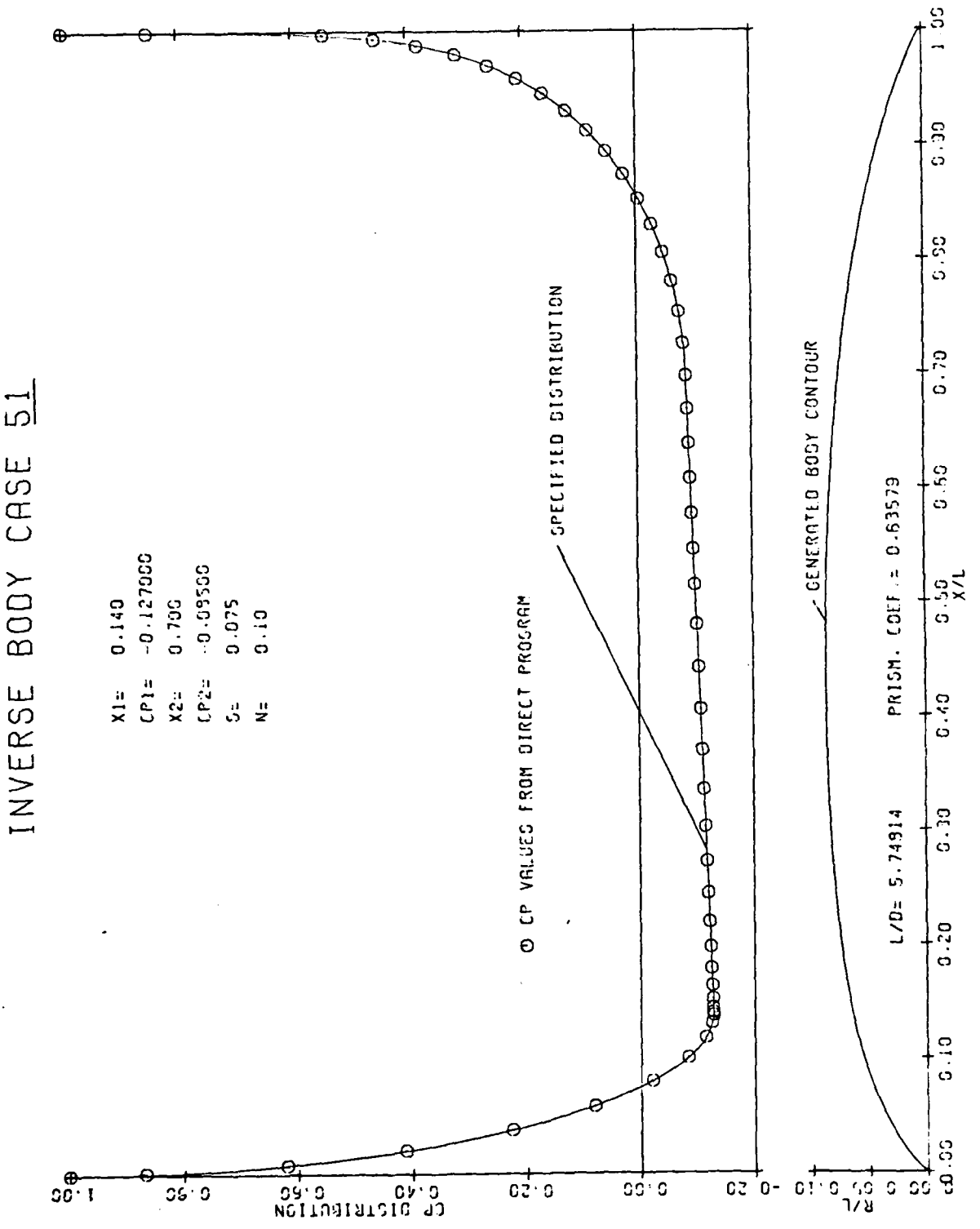

Figure 61. Pressure Distribution and Body Contour, Case No. 51.

19 August 1981
JJE;GHH:mmj

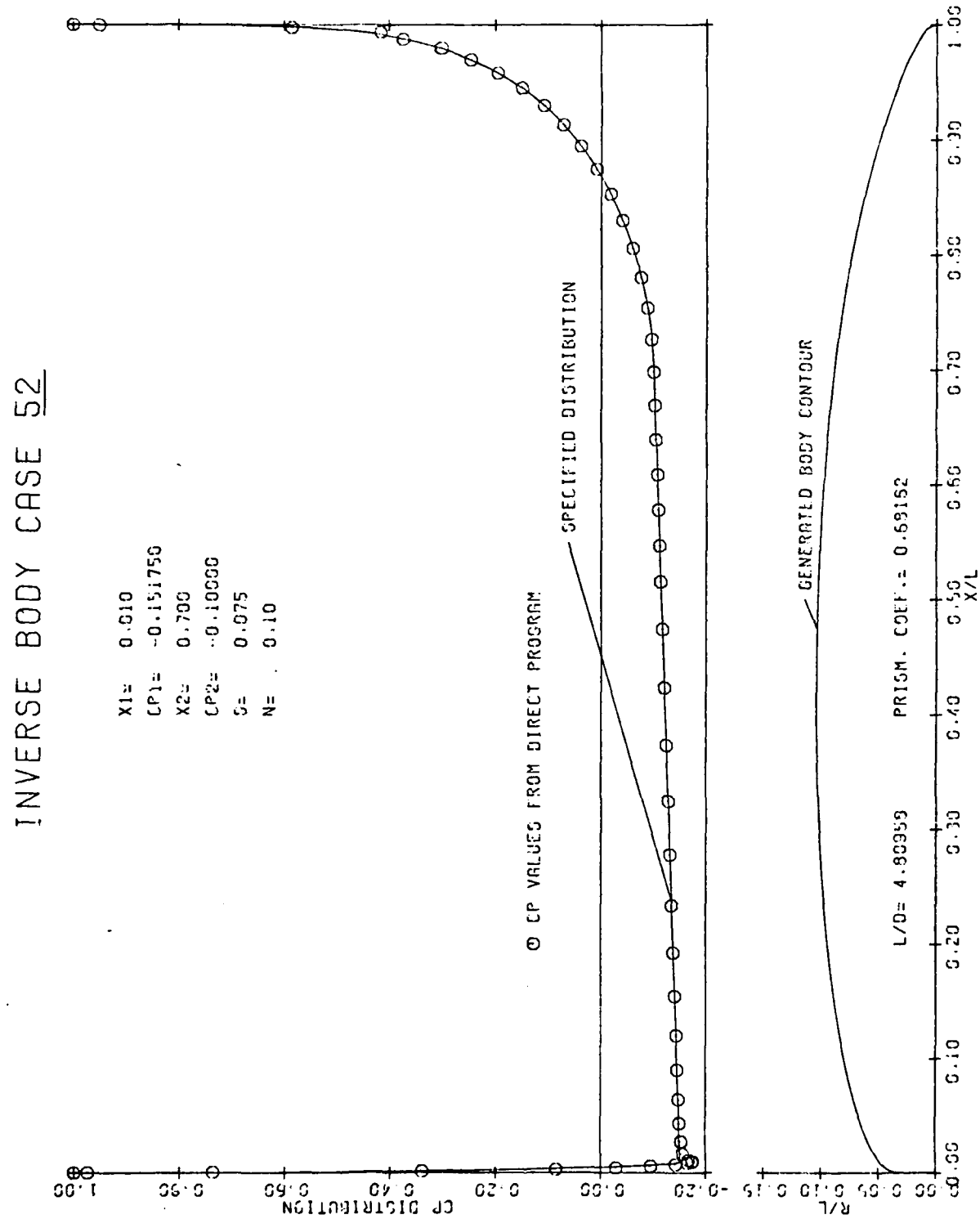

Figure 62. Pressure Distribution and Body Contour, Case No. 52.

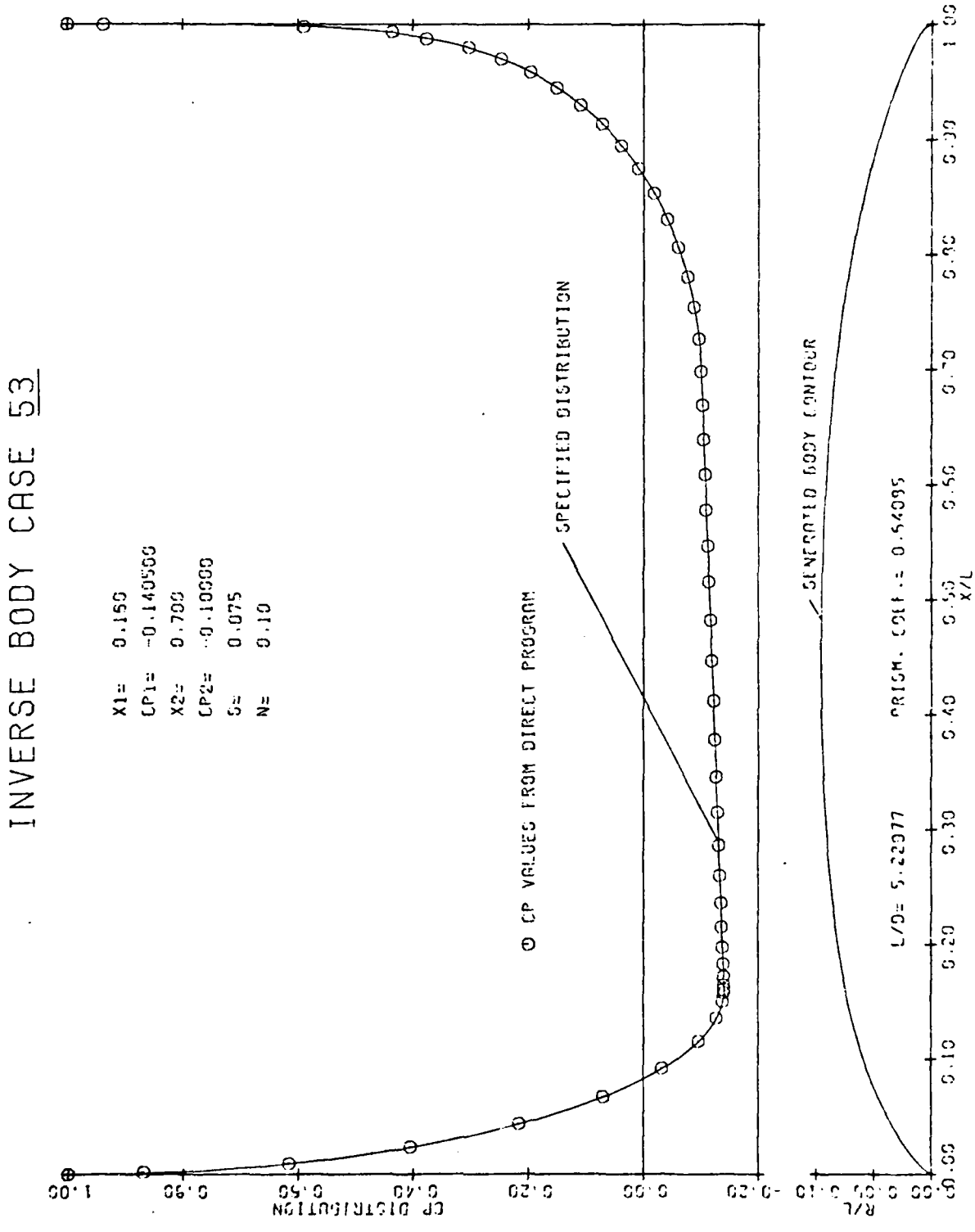

Figure 63. Pressure Distribution and Body Contour, Case No. 53.

19 August 1981
JJE:GHH:mmj

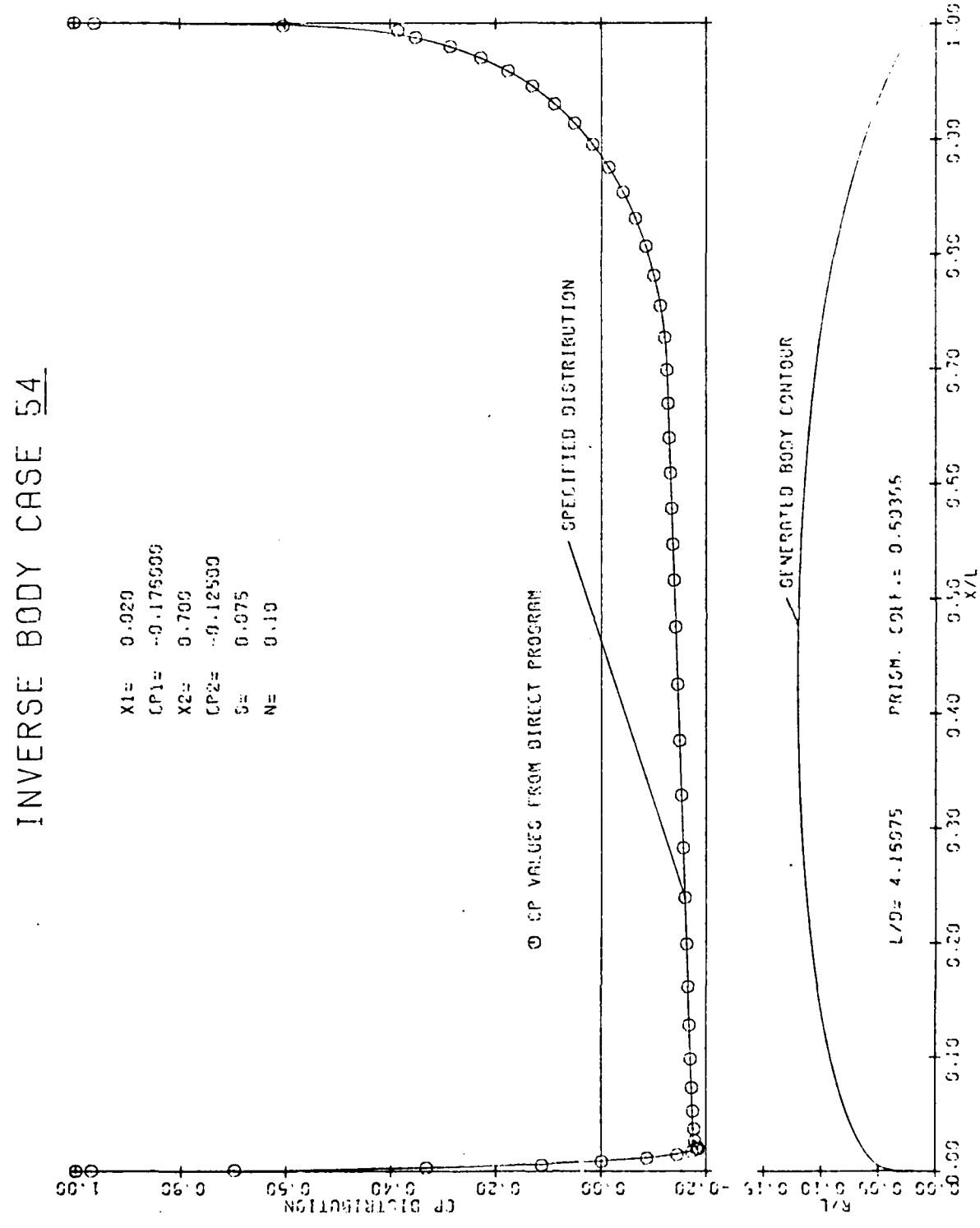

Figure 64. Pressure Distribution and Body Contour, Case No. 54.

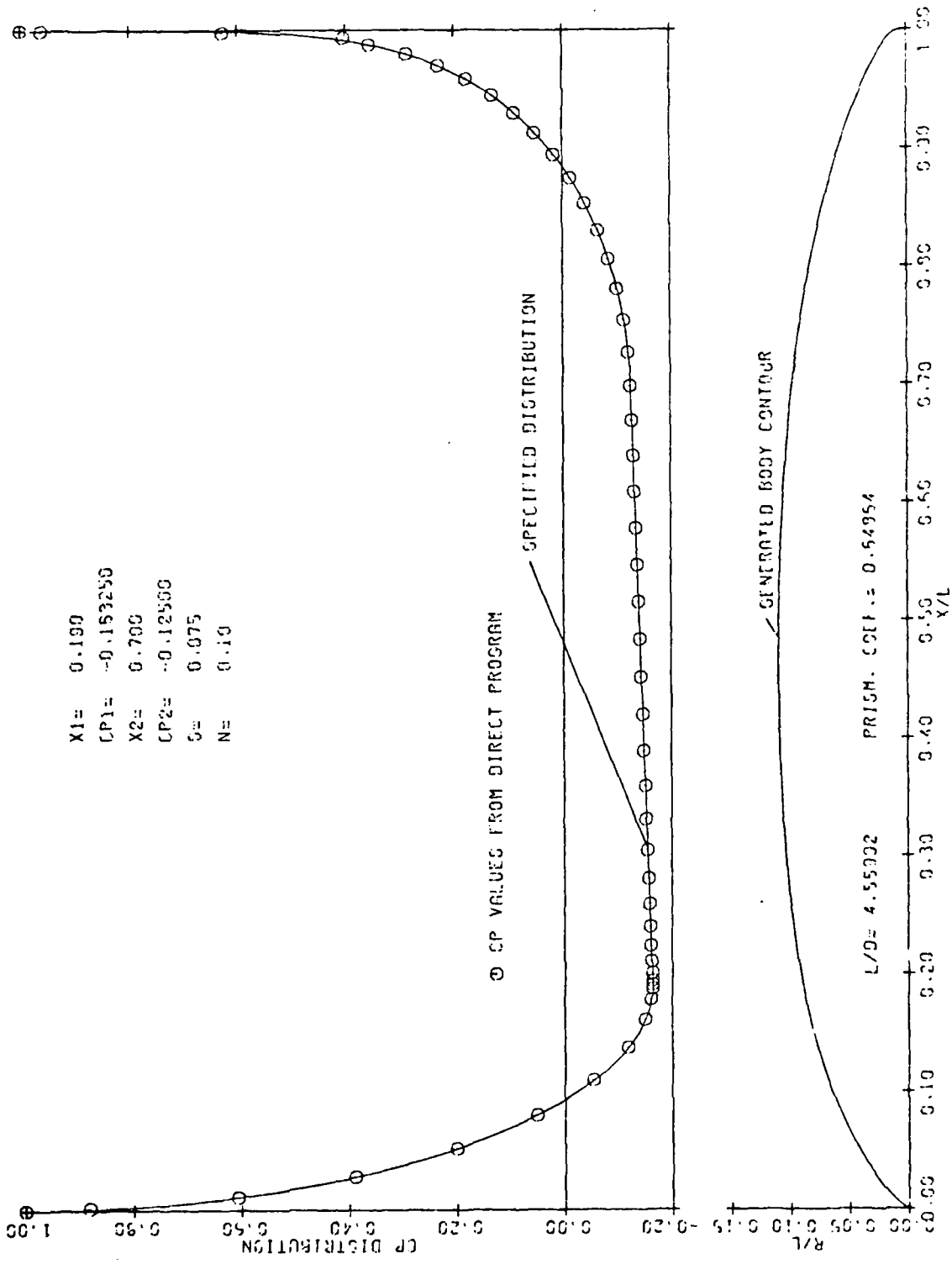

Figure 65. Pressure Distribution and Body Contour, Case No. 55.

19 August 1981
JJE:GHH:mmj

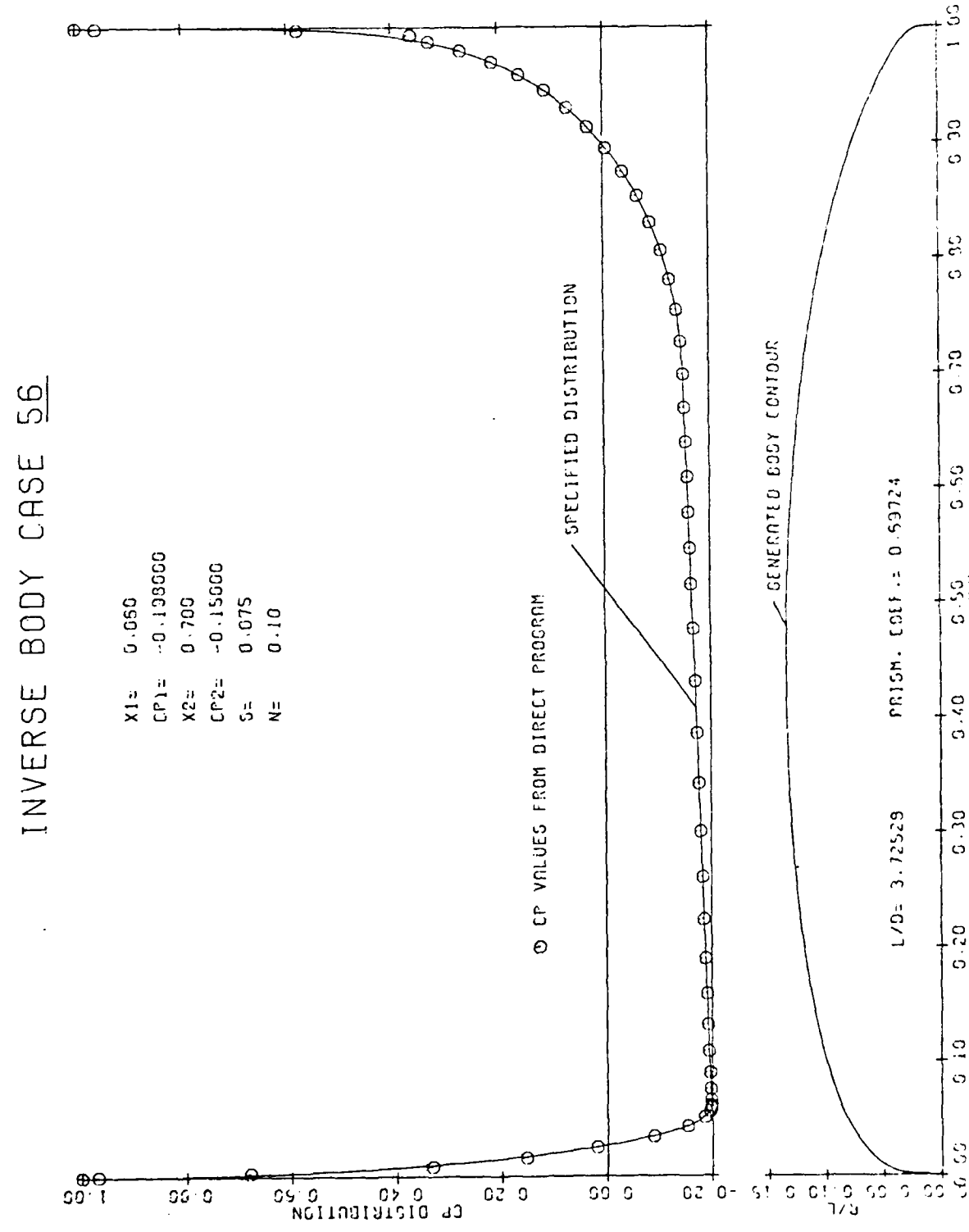

Figure 66. Pressure Distribution and Body Contour, Case No. 56.

AD-A107 662 PENNSYLVANIA STATE UNIV UNIVERSITY PARK APPLIED RESE--ETC F/G 20/4
INVERSE AXISYMMETRIC BODY STUDY.(U)
AUG 81 J J EISENHUTH, G H HOFFMAN N00024-79-C-6043
UNCLASSIFIED ARL/PSU/TM-81-177 NL

2 OF 3
AD A
107662

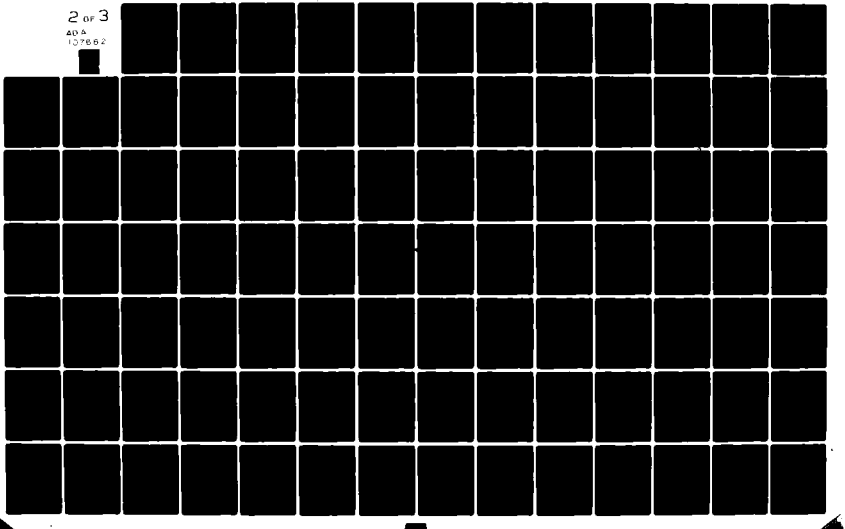

19 August 1981
JJE:GHH:mmj

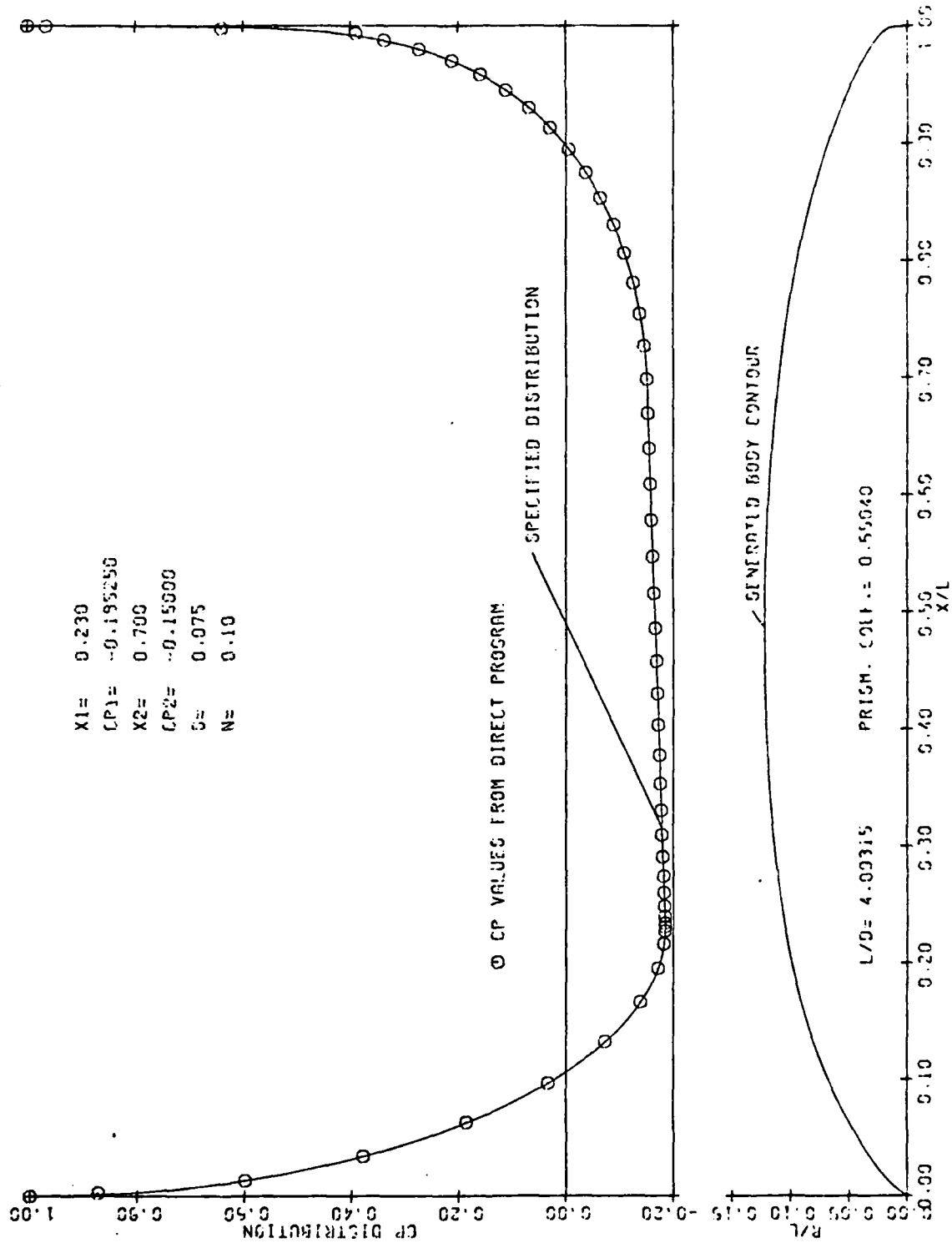

Figure 67. Pressure Distribution and Body Contour, Case No. 57.

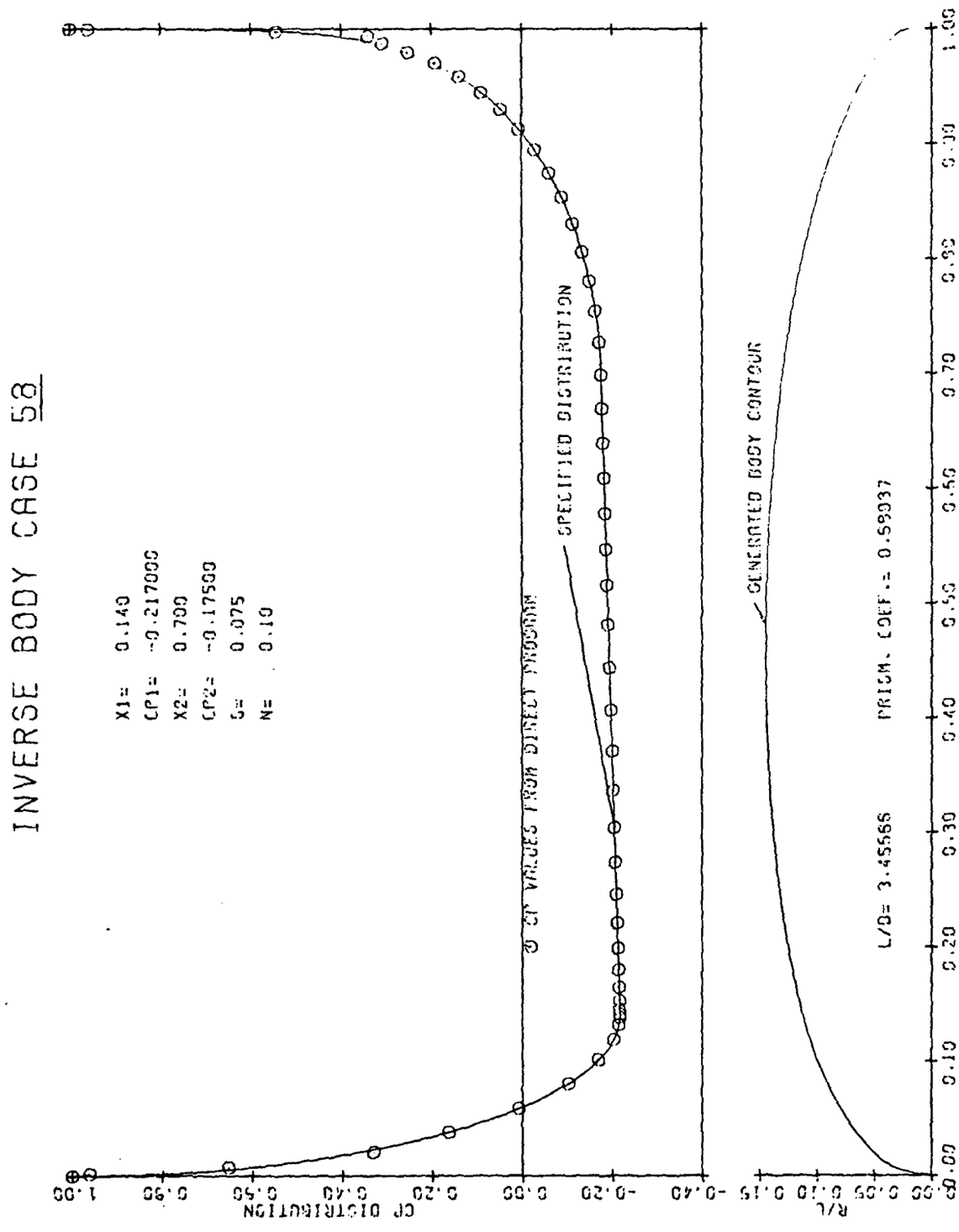

Figure 68. Pressure Distribution and Body Contour, Case No. 58.

19 August 1981
JJE:GHH:mmj

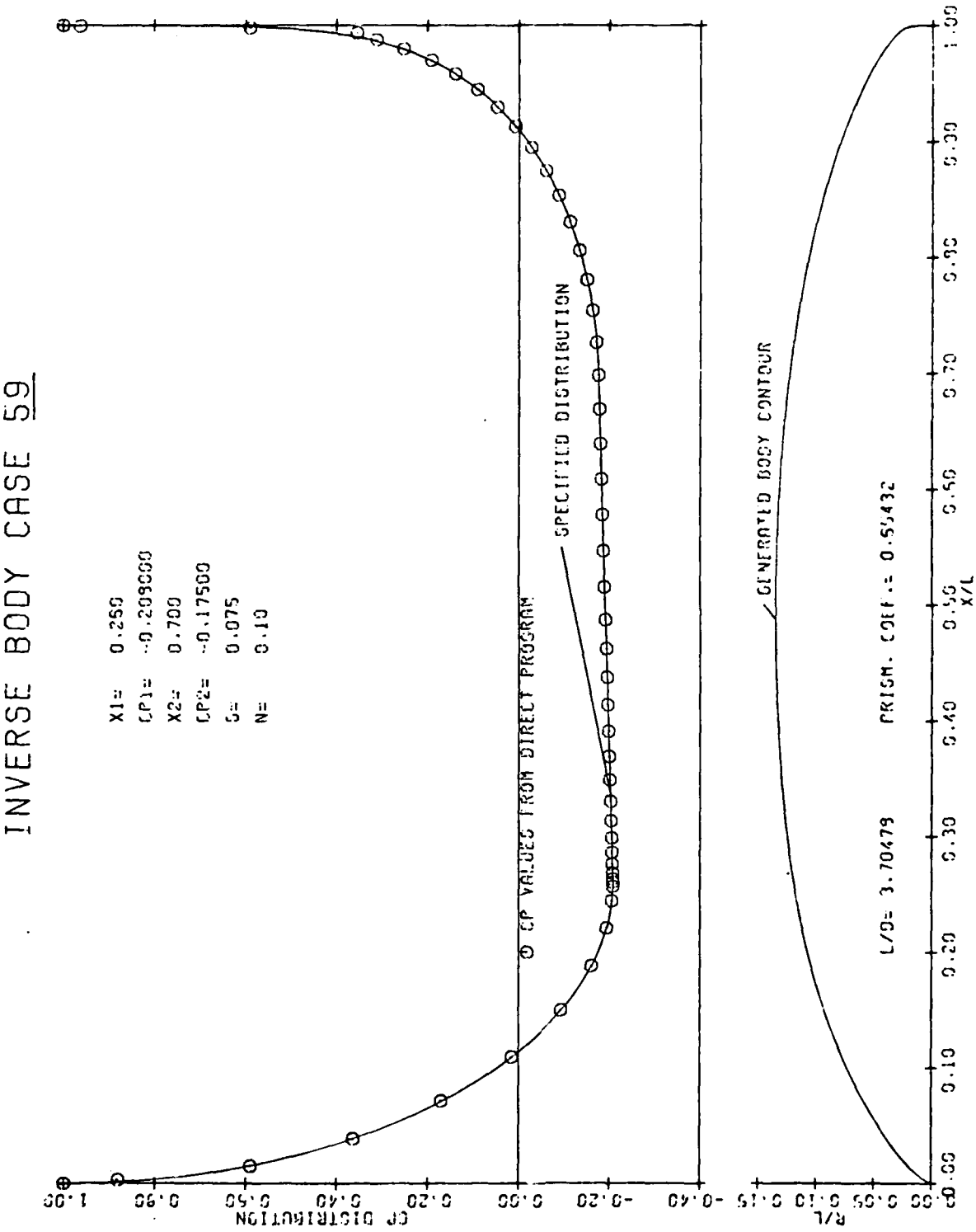

Figure 69. Pressure Distribution and Body Contour, Case No. 59.

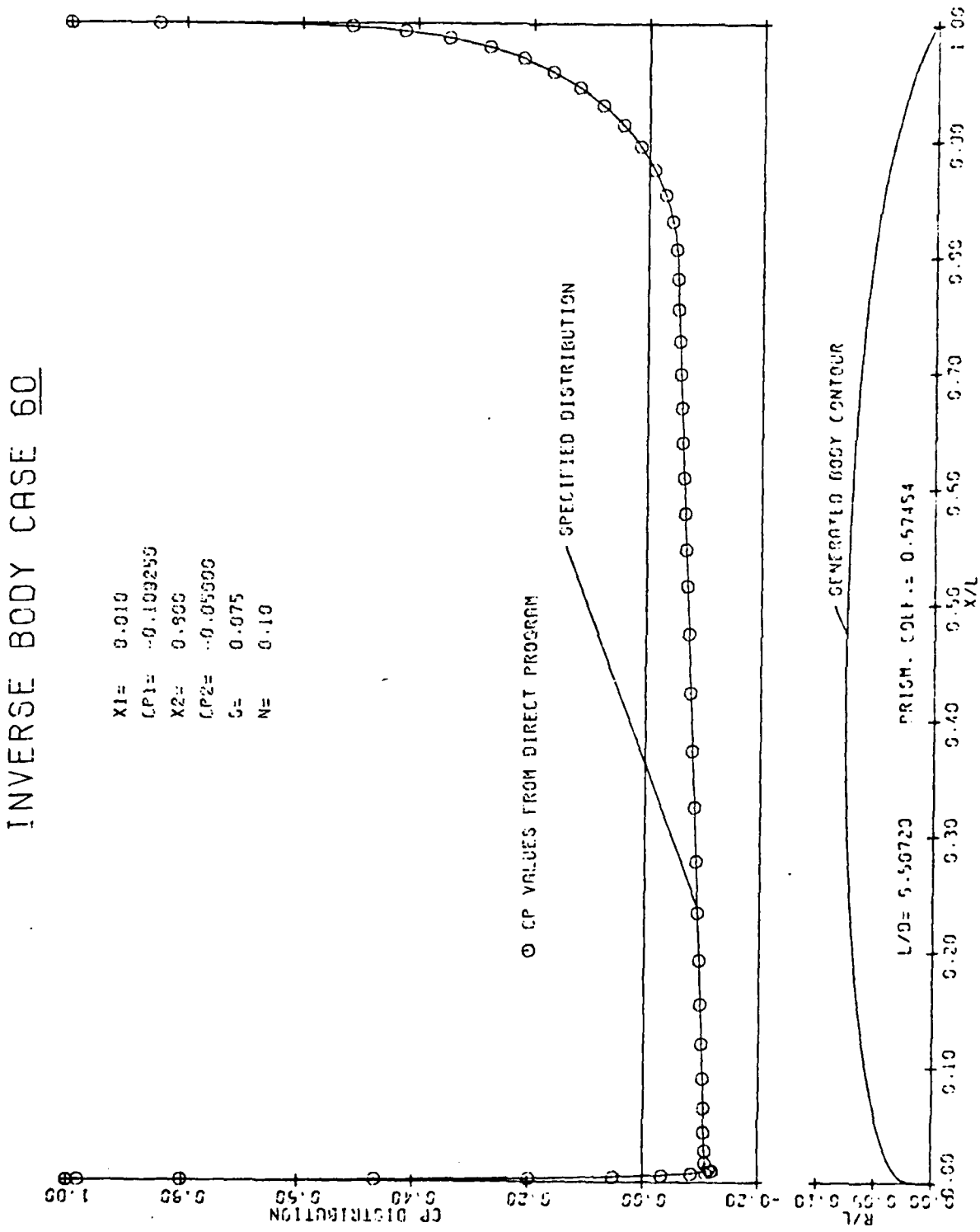

Figure 70. Pressure Distribution and Body Contour, Case No. 60.

19 August 1981
JJE:GHH:mmj

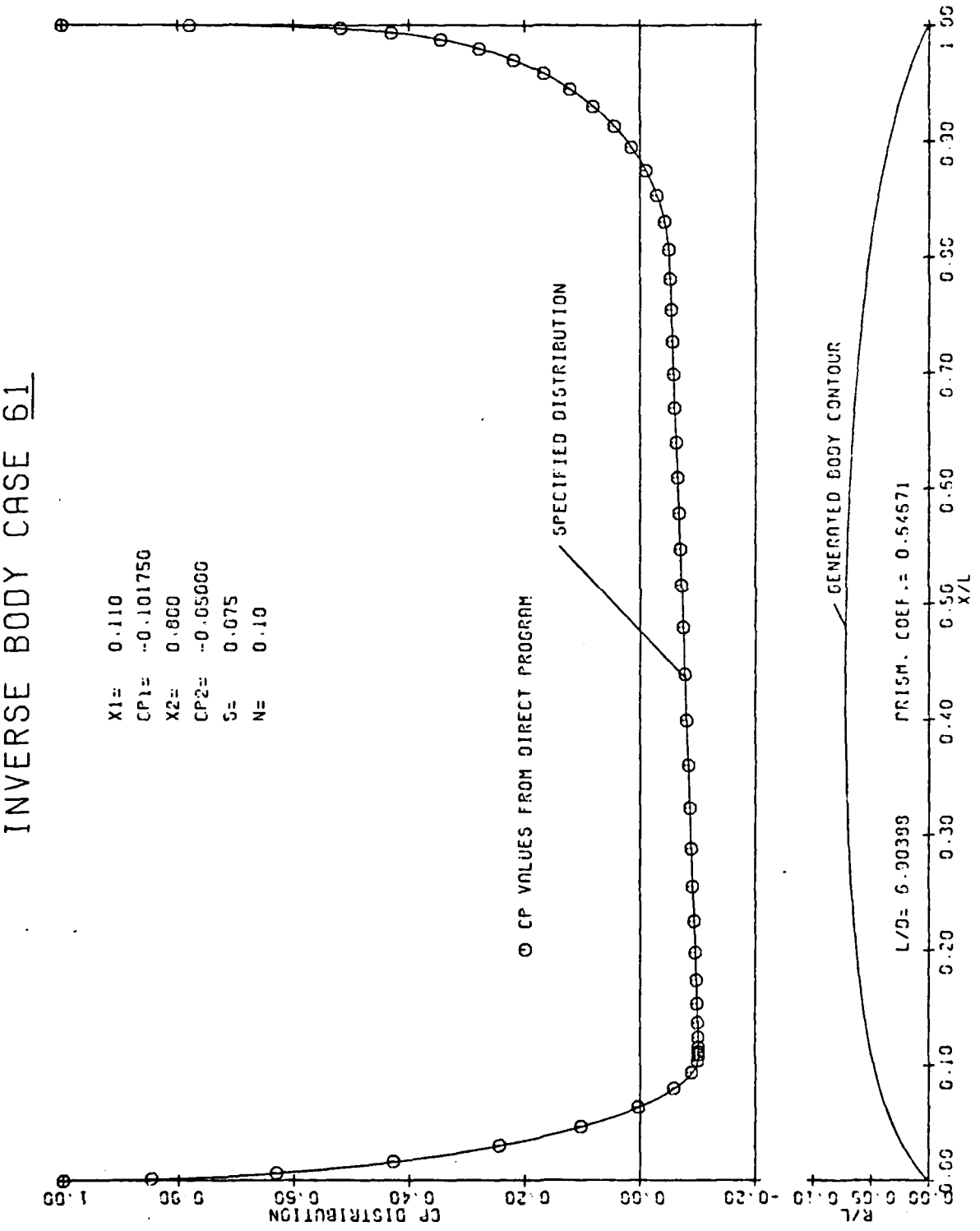

Figure 71. Pressure Distribution and Body Contour, Case No. 61.

19 August 1981
JJE:GHH:mmj

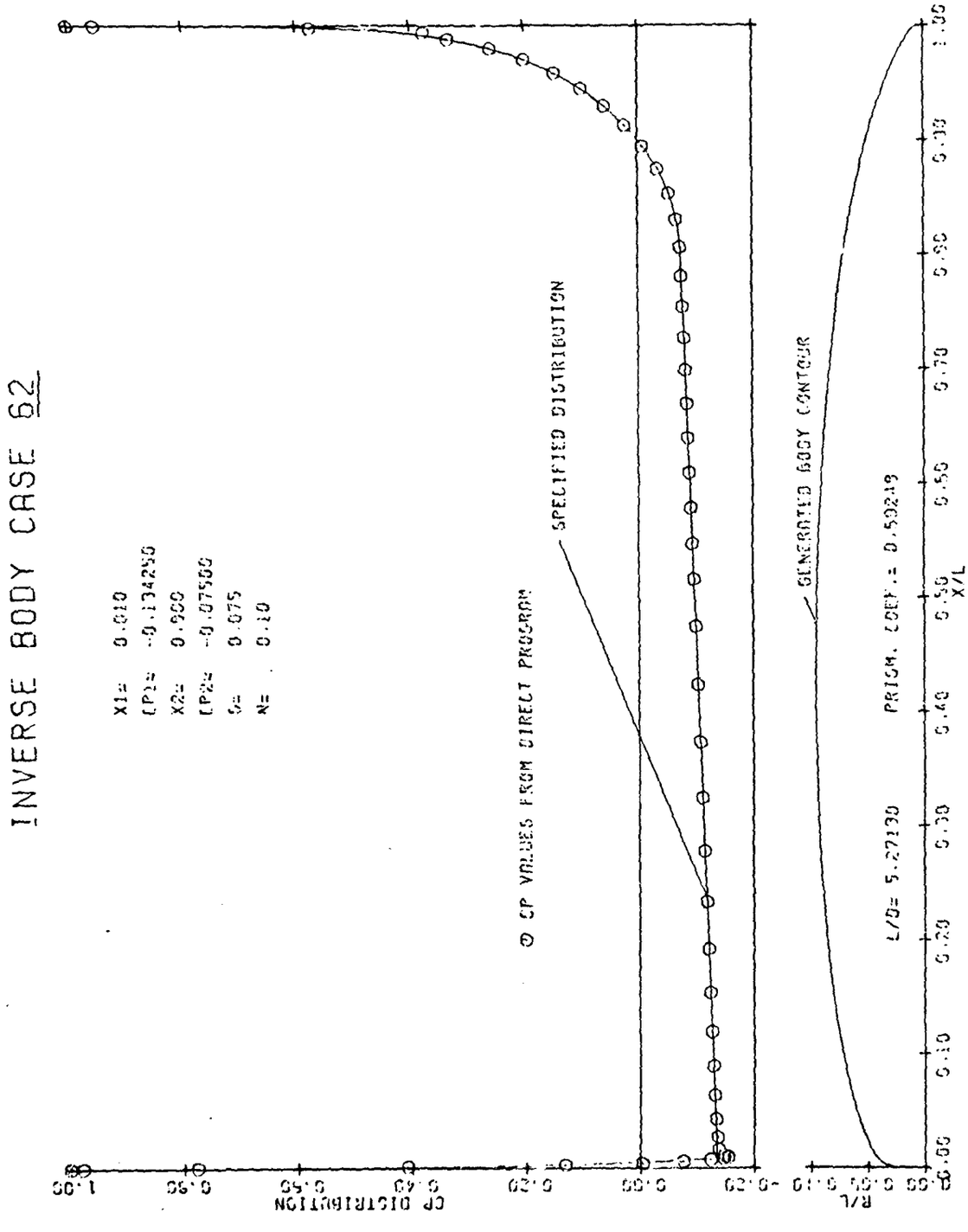

Figure 72. Pressure Distribution and Body Contour, Case No. 62.

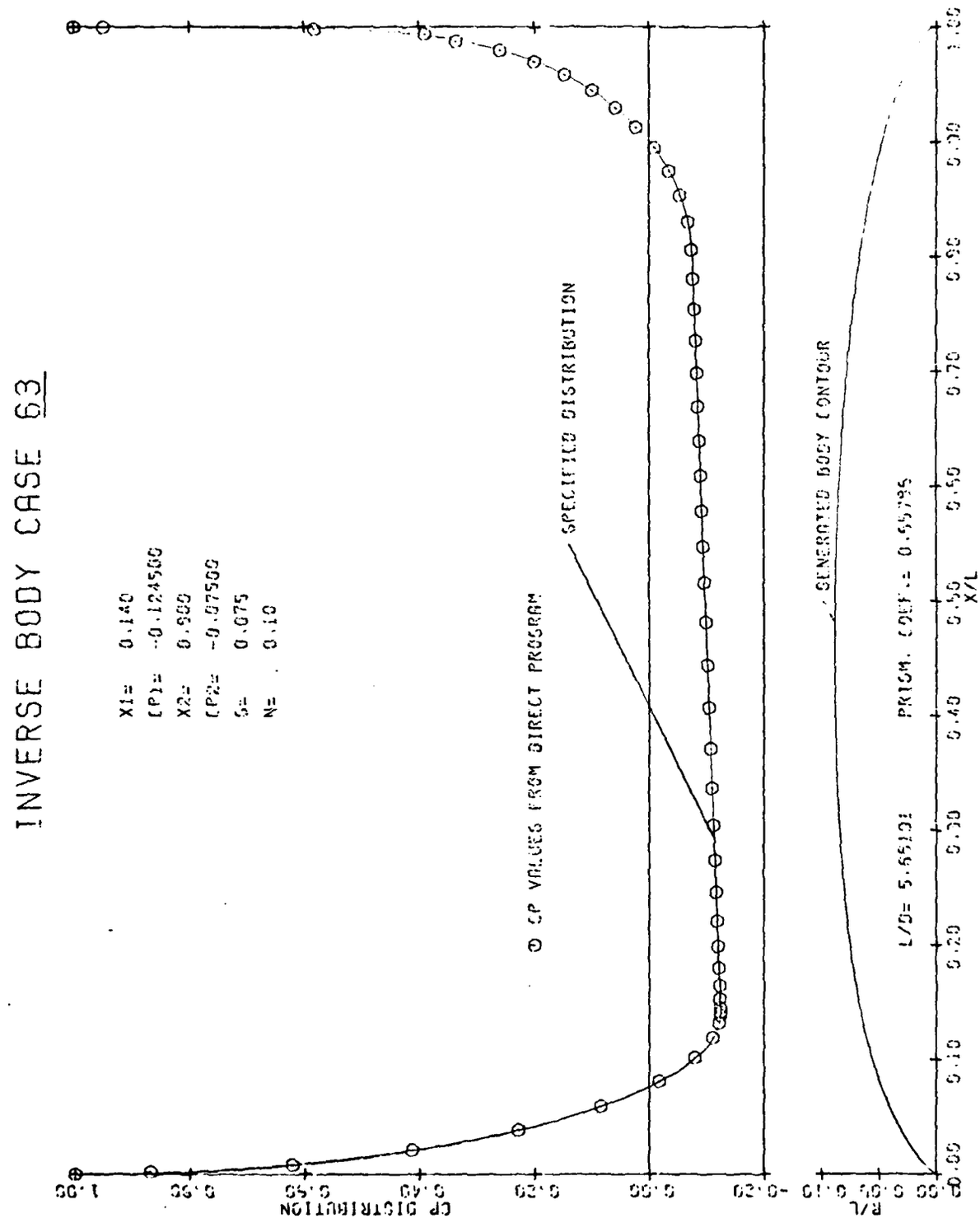

Figure 73. Pressure Distribution and Body Contour, Case No. 63.

19 August 1981
JJE:GHH:mmj

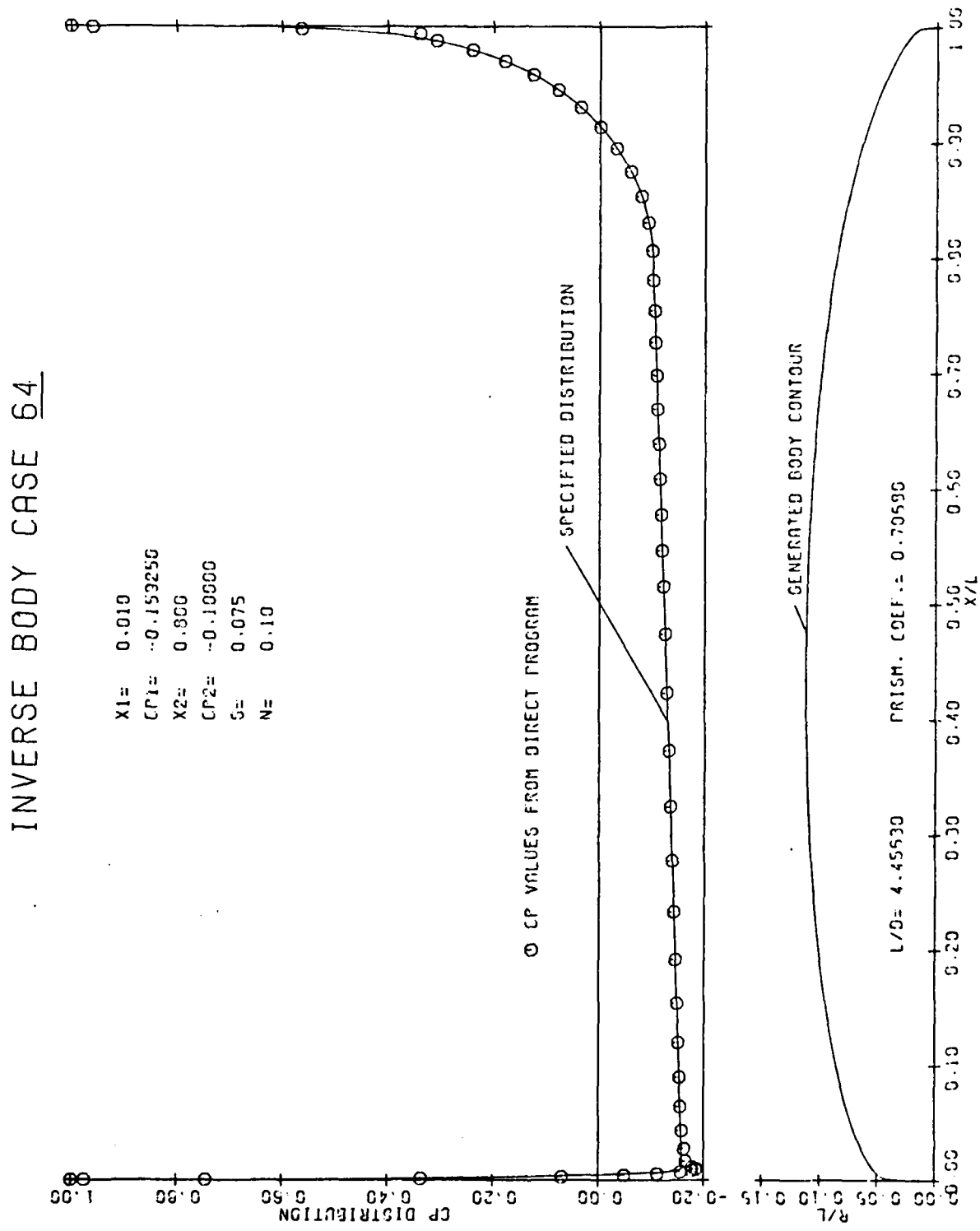

Figure 74. Pressure Distribution and Body Contour, Case No. 64.

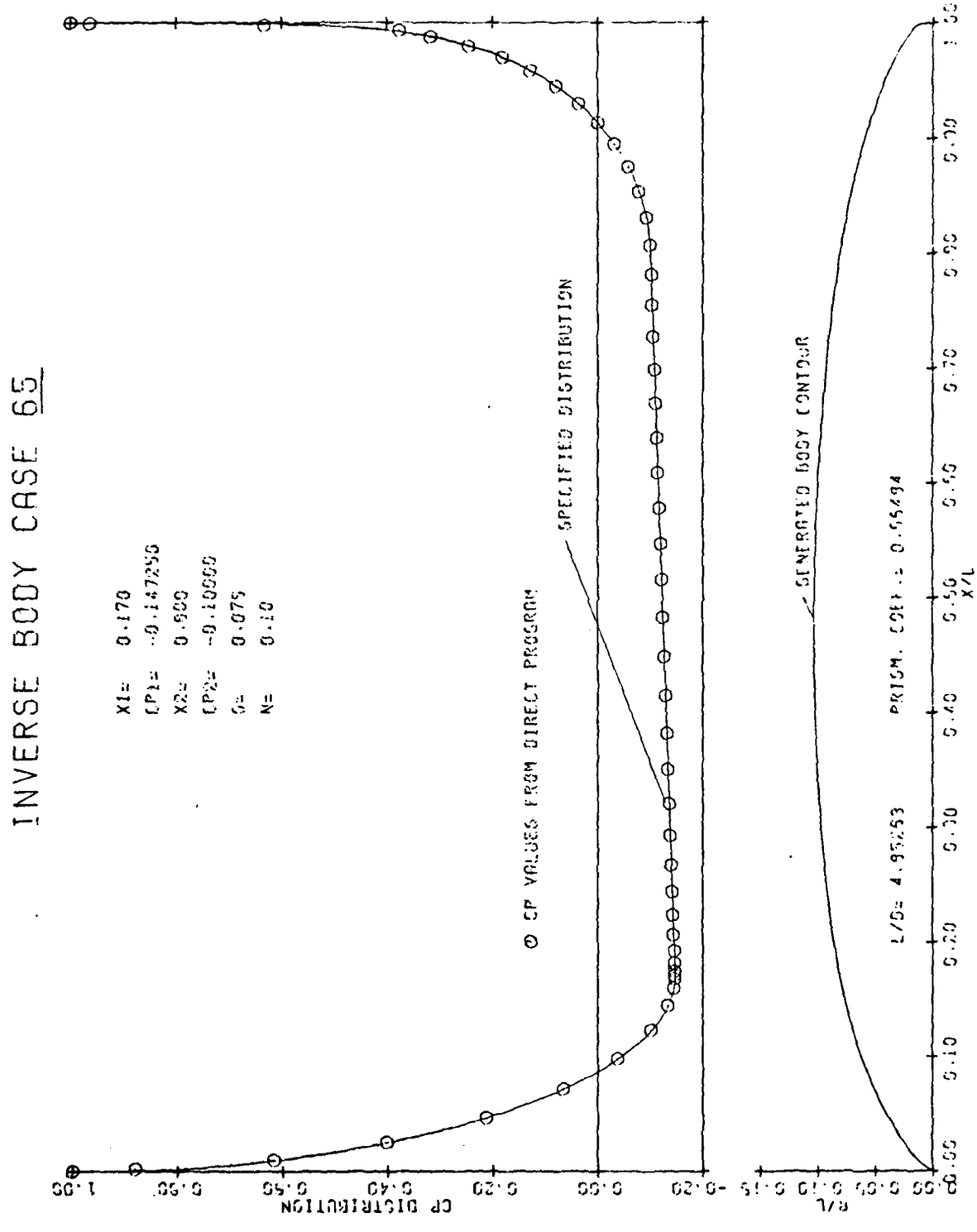

Figure 75. Pressure Distribution and Body Contour, Case No. 65.

19 August 1981
JJE:GHH:mmj

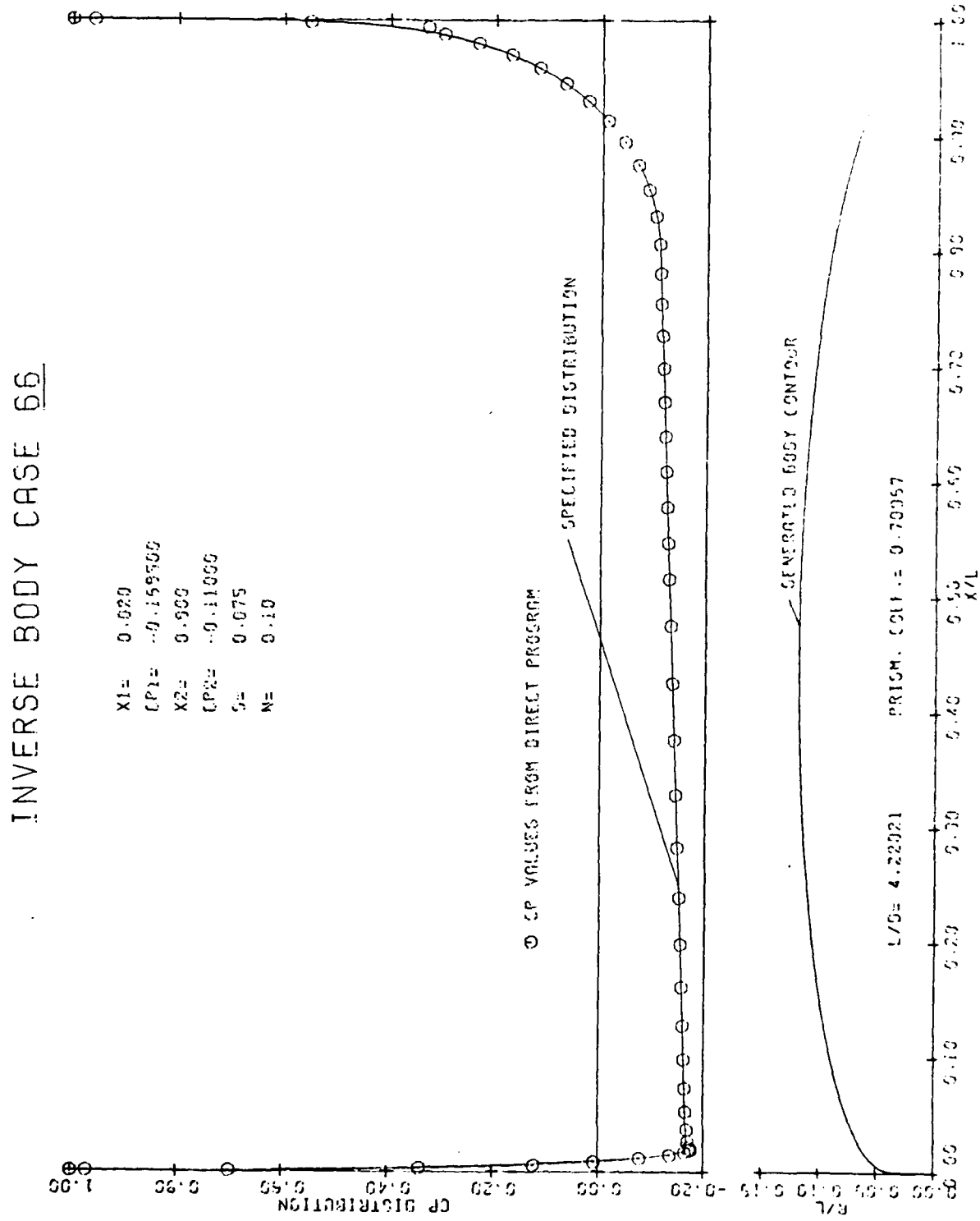

Figure 76. Pressure Distribution and Body Contour, Case No. 66.

19 August 1981
JJE:GHH:mmj

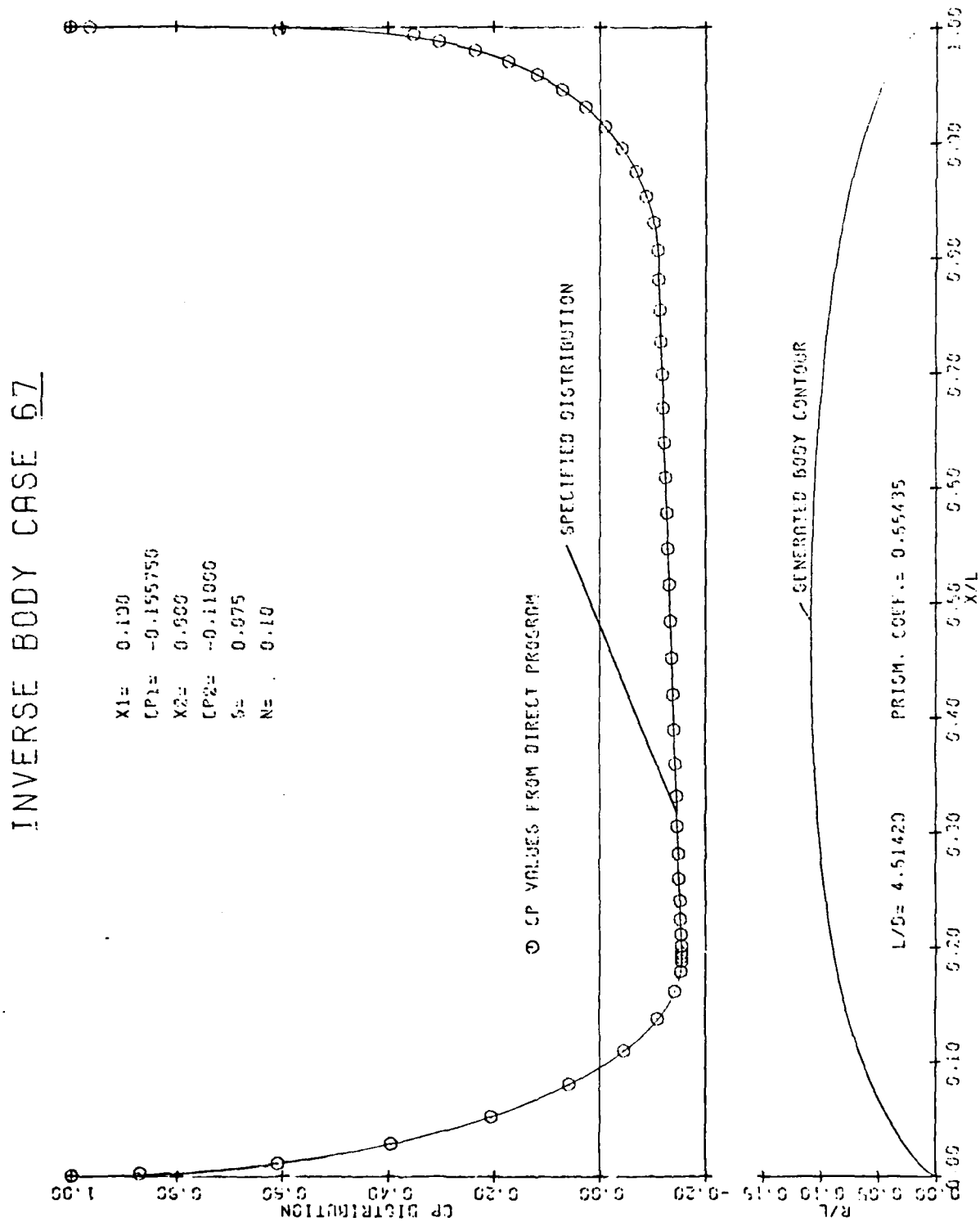

Figure 77. Pressure Distribution and Body Contour, Case No. 67.

19 August 1981
JJE:GHH:mmj

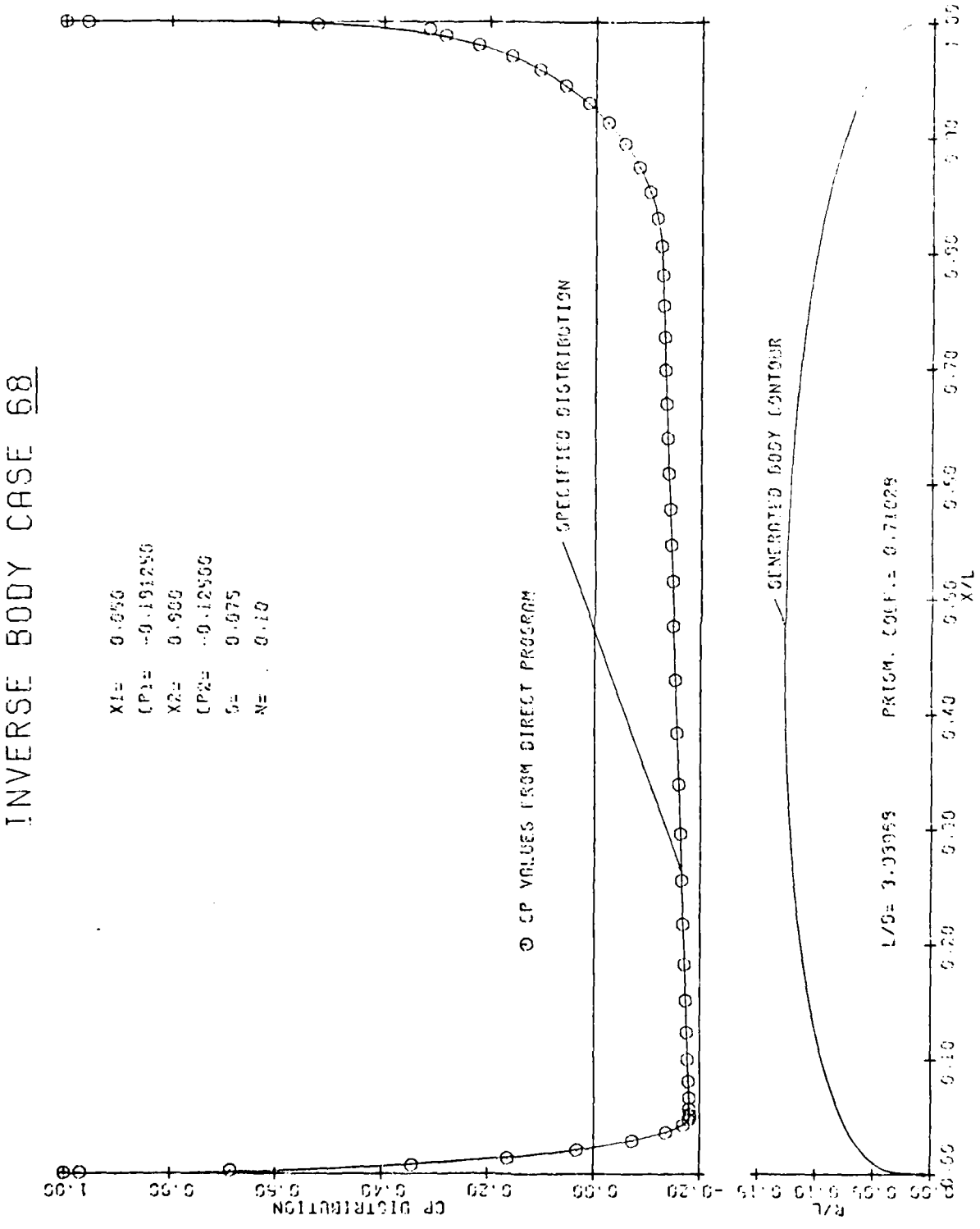

Figure 78. Pressure Distribution and Body Contour, Case No. 68.

19 August 1981
JJE:GHH:mmj

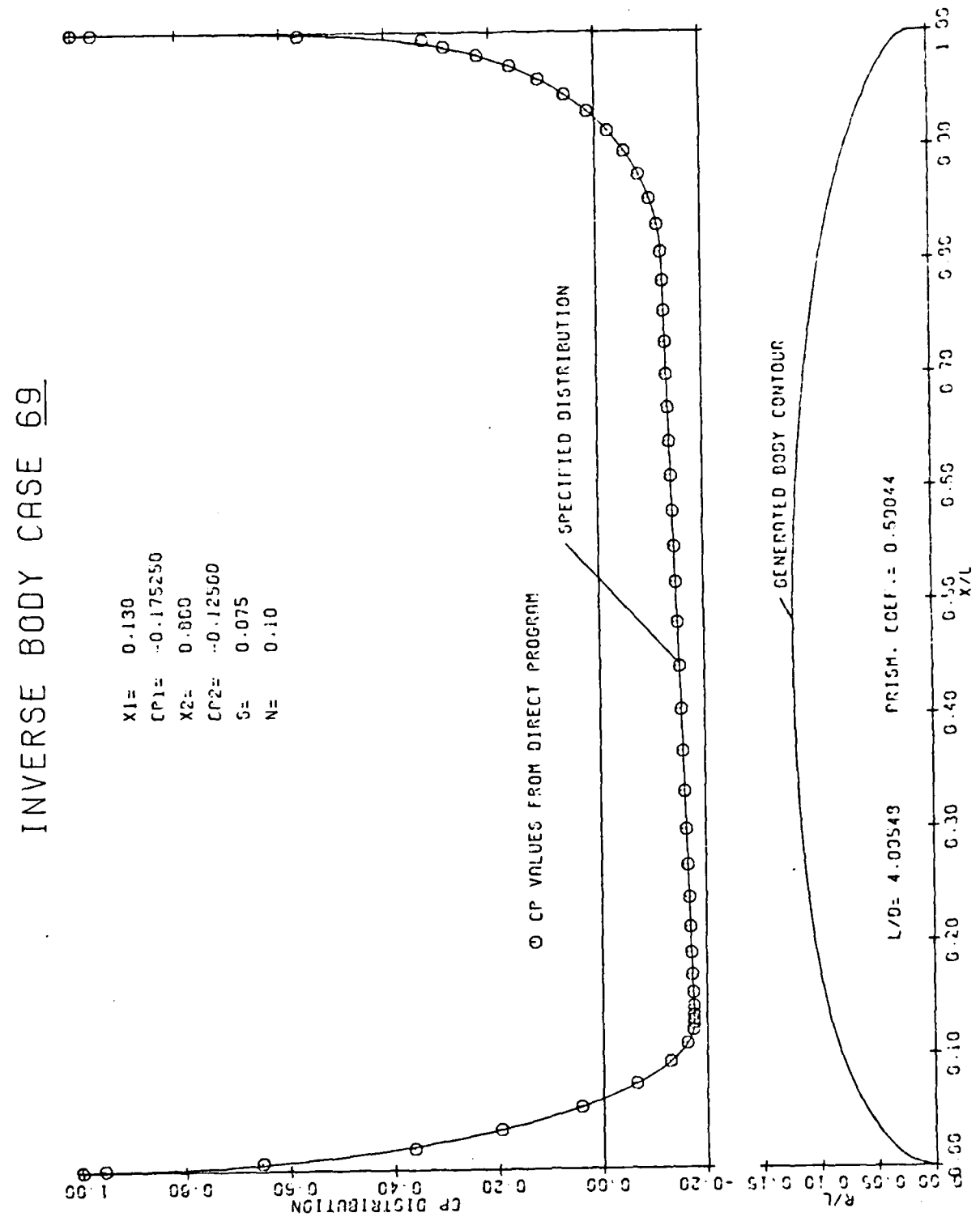

Figure 79. Pressure Distribution and Body Contour, Case No. 69.

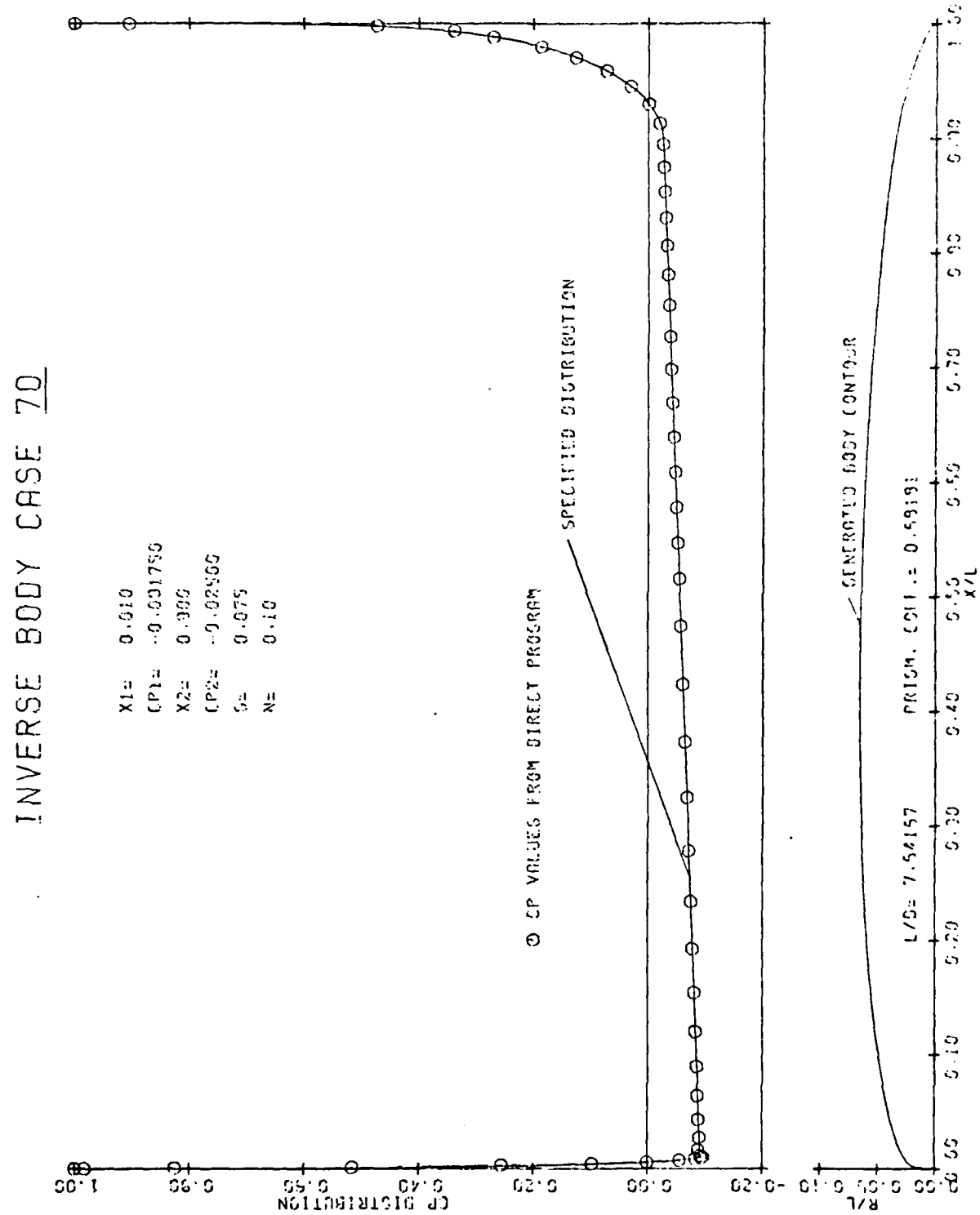

Figure 80. Pressure Distribution and Body Contour, Case No. 70.

19 August 1981
JJE:GHH:mmj

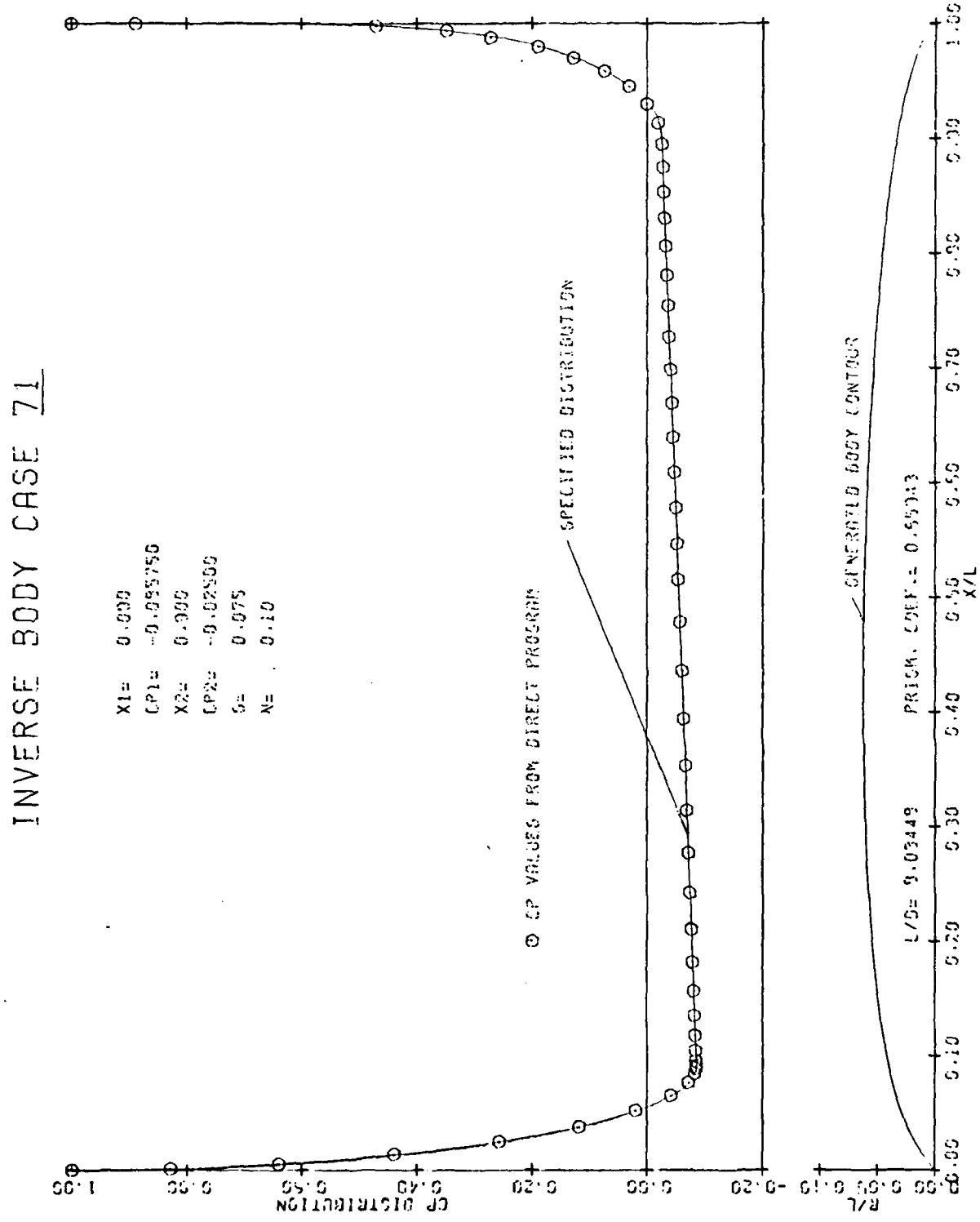

Figure 81. Pressure Distribution and Body Contour, Case No. 71.

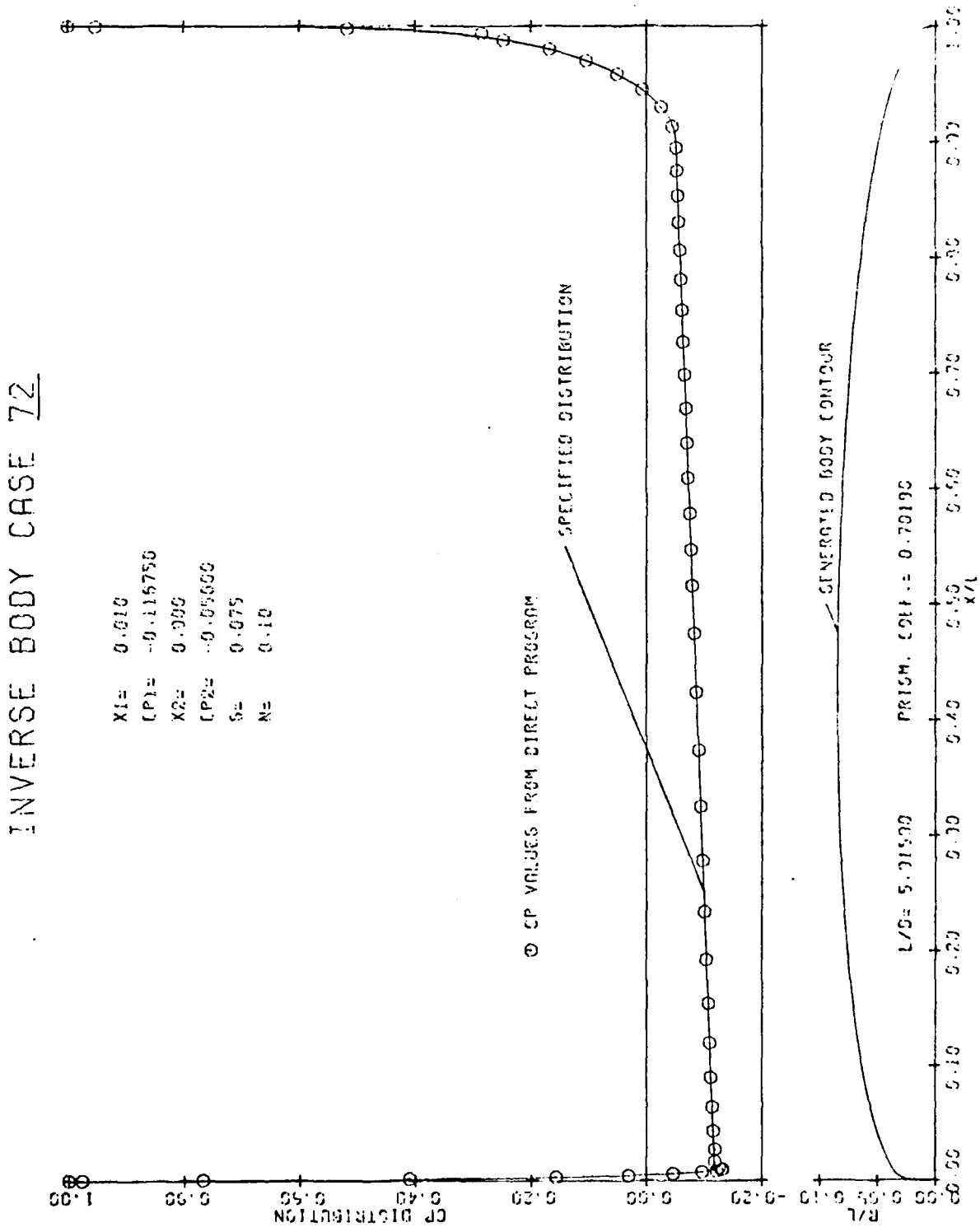

Figure 82. Pressure Distribution and Body Contour, Case No. 72.

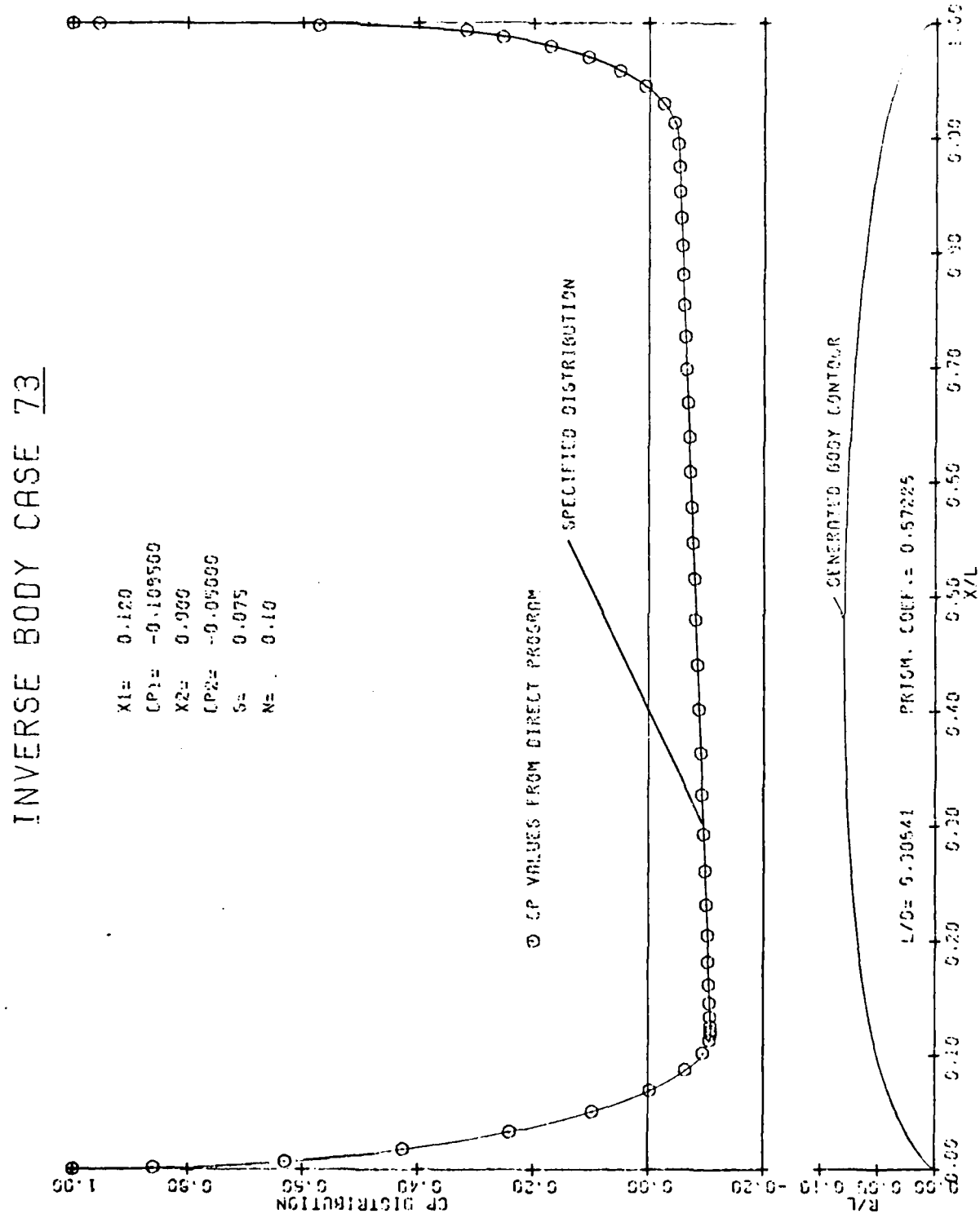

Figure 83. Pressure Distribution and Body Contour, Case No. 73.

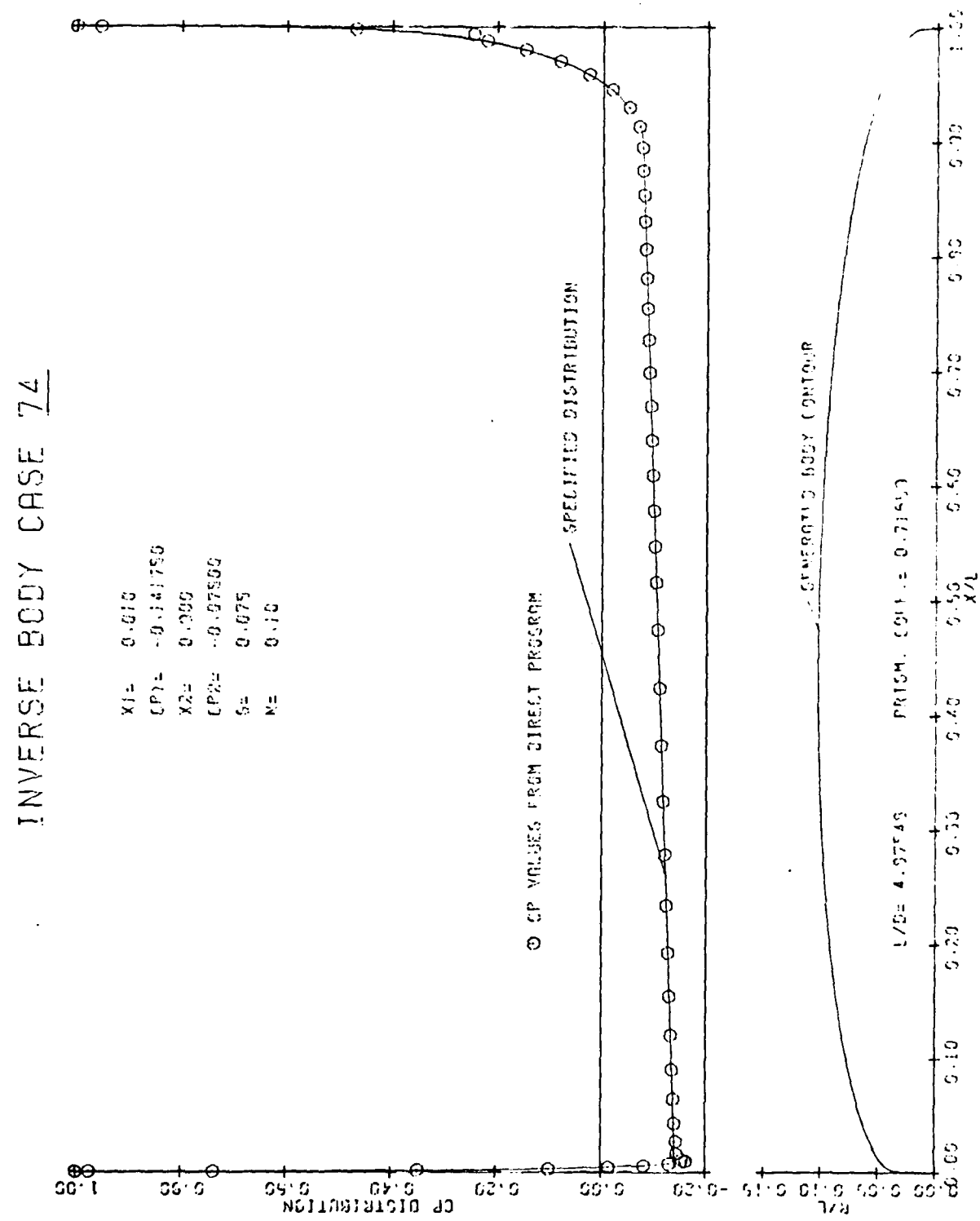

Figure 84. Pressure Distribution and Body Contour, Case No. 74.

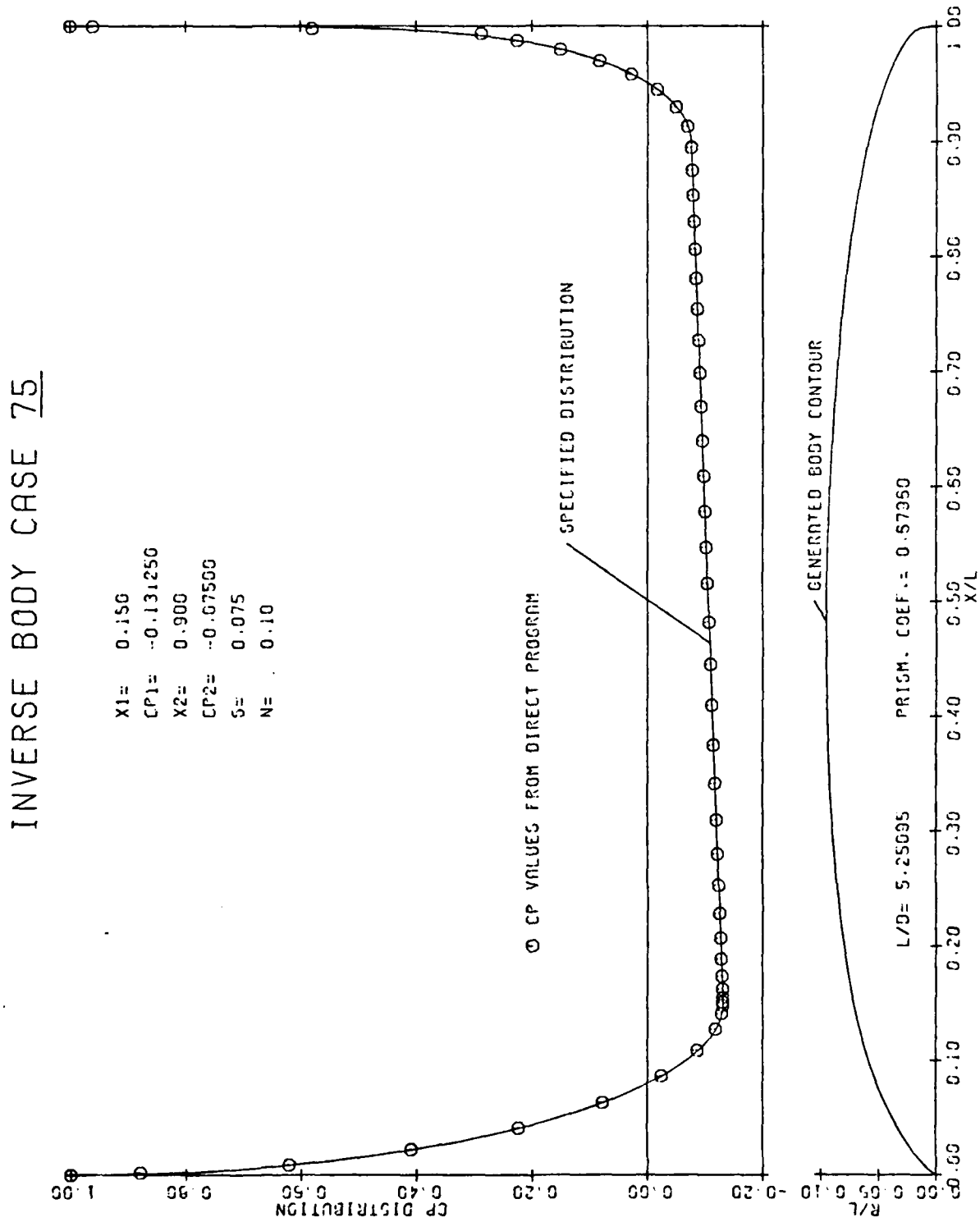

Figure 85. Pressure Distribution and Body Contour, Case No. 75.

19 August 1981
J.E:GHH:mmj

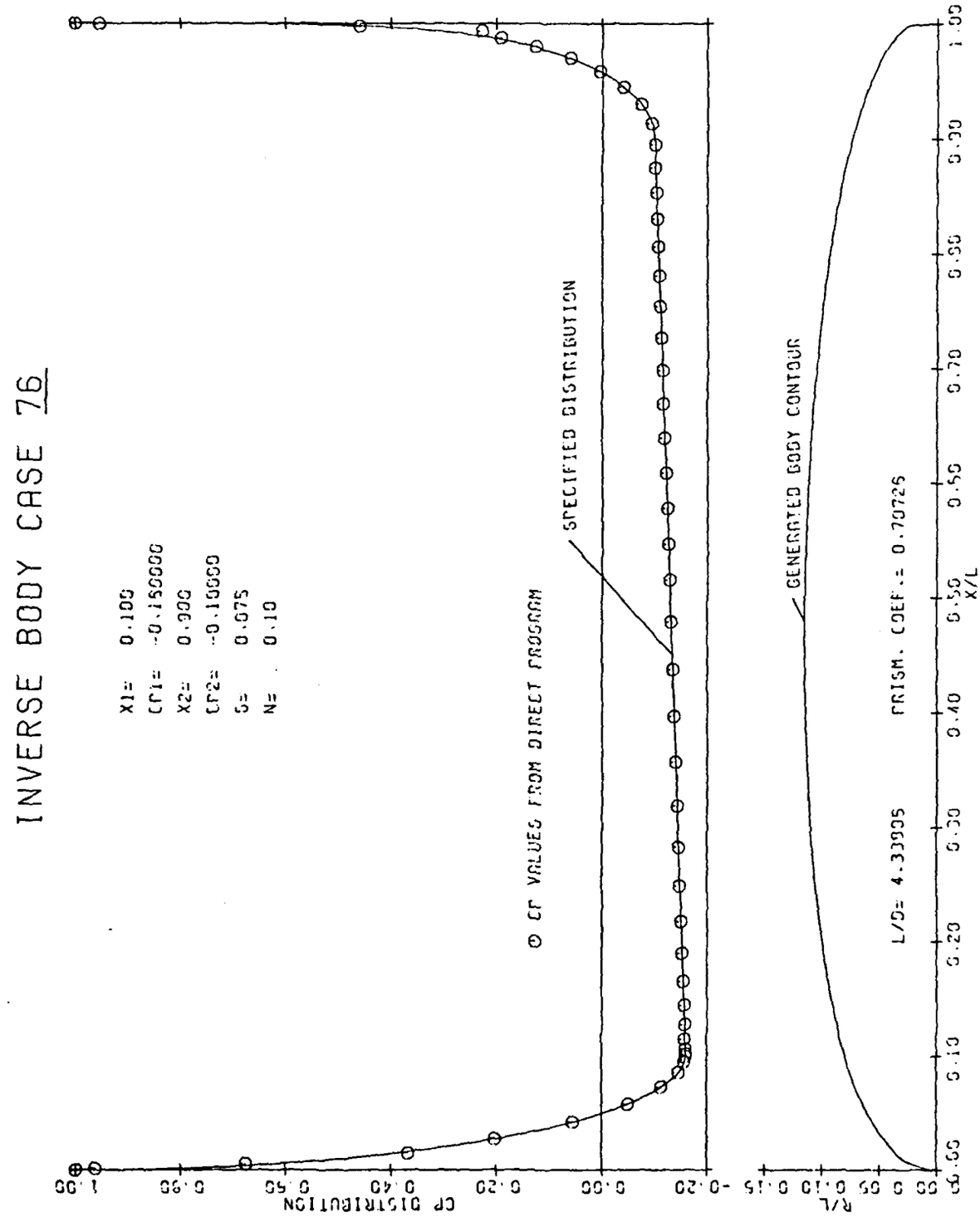

Figure 86. Pressure Distribution and Body Contour, Case No. 76.

19 August 1981
JJE:GHH:mmj

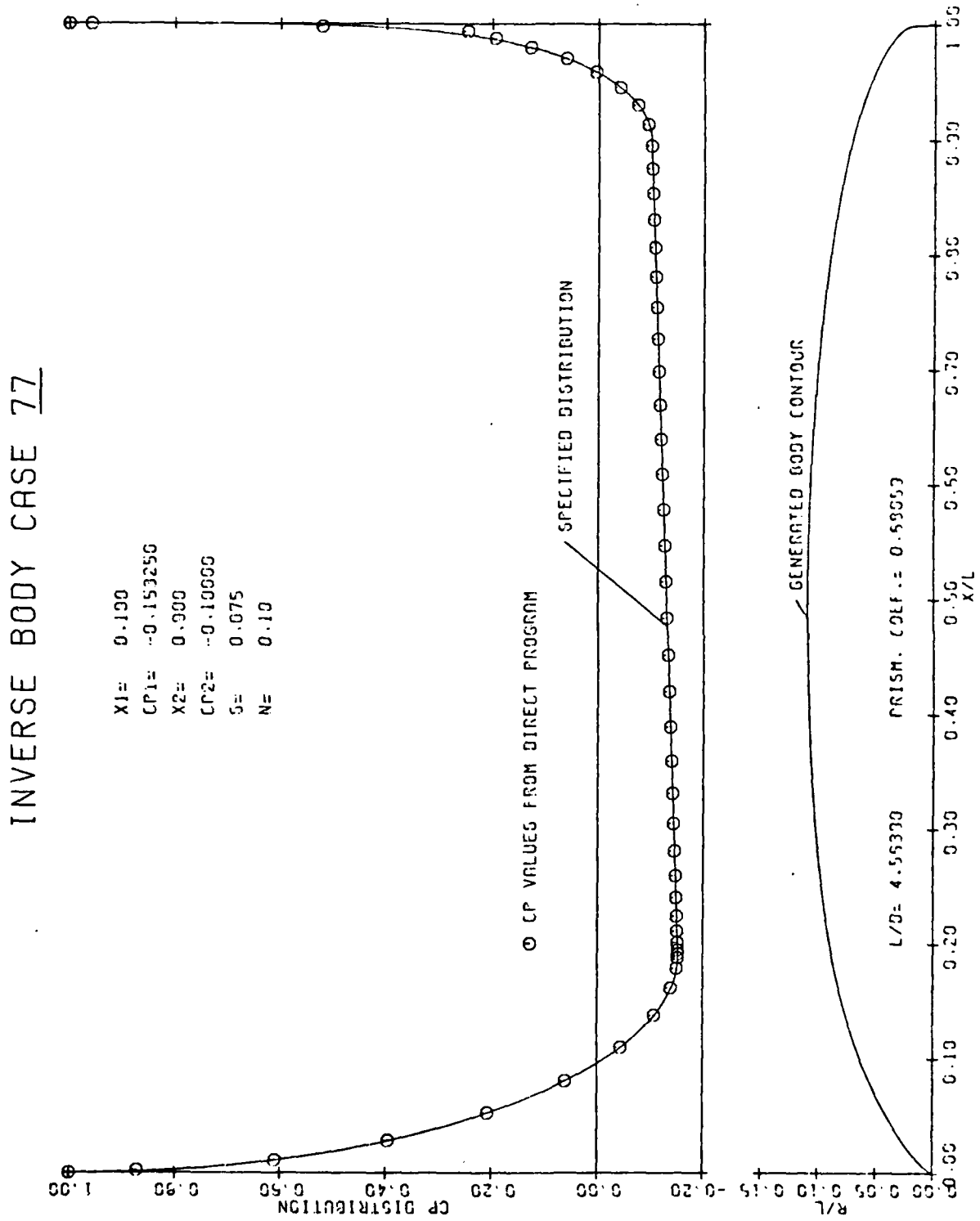

Figure 87. Pressure Distribution and Body Contour, Case No. 77.

19 August 1981
JJE:GHH:mmj

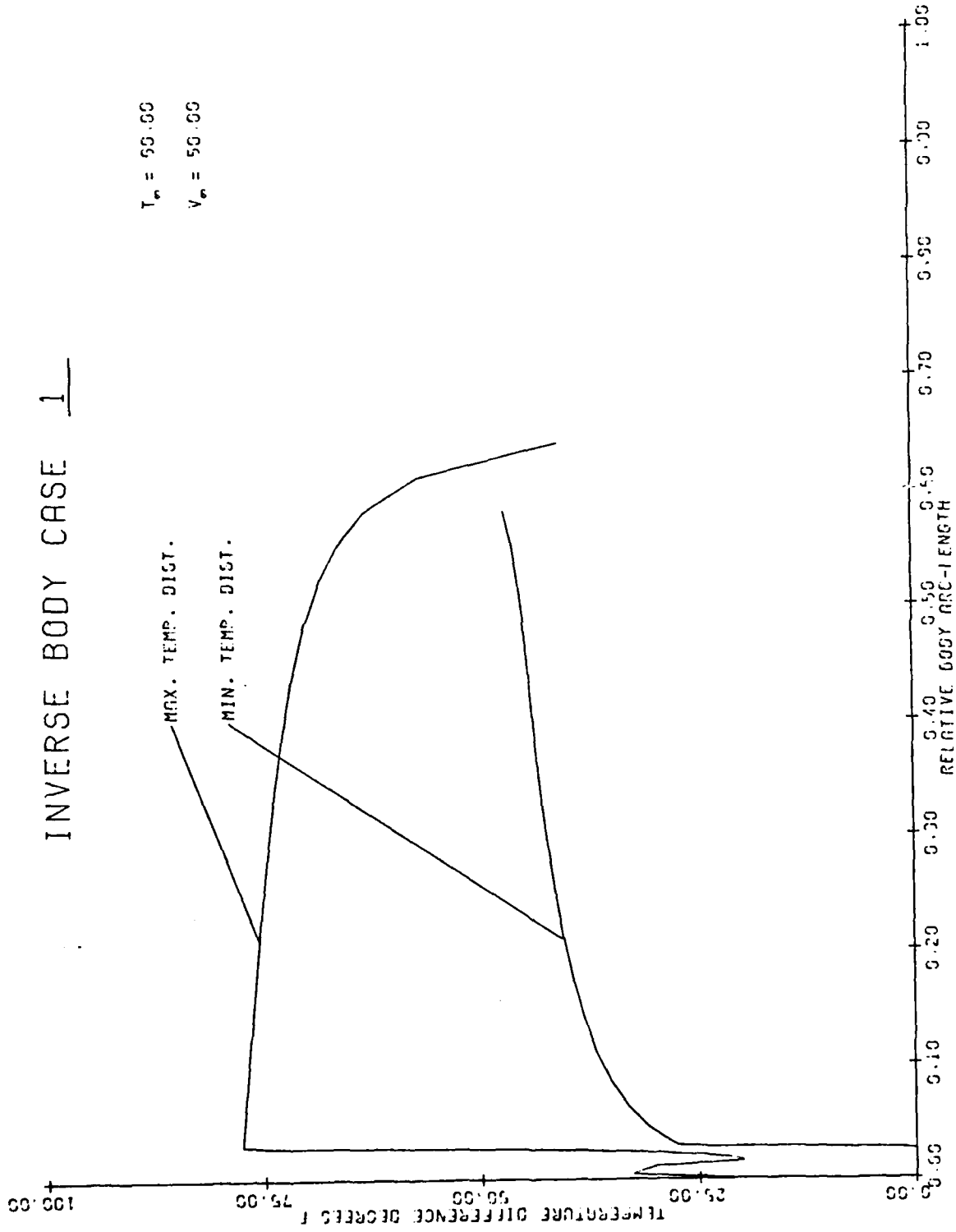

Figure 88. Temperature Distributions, Case No. 1.

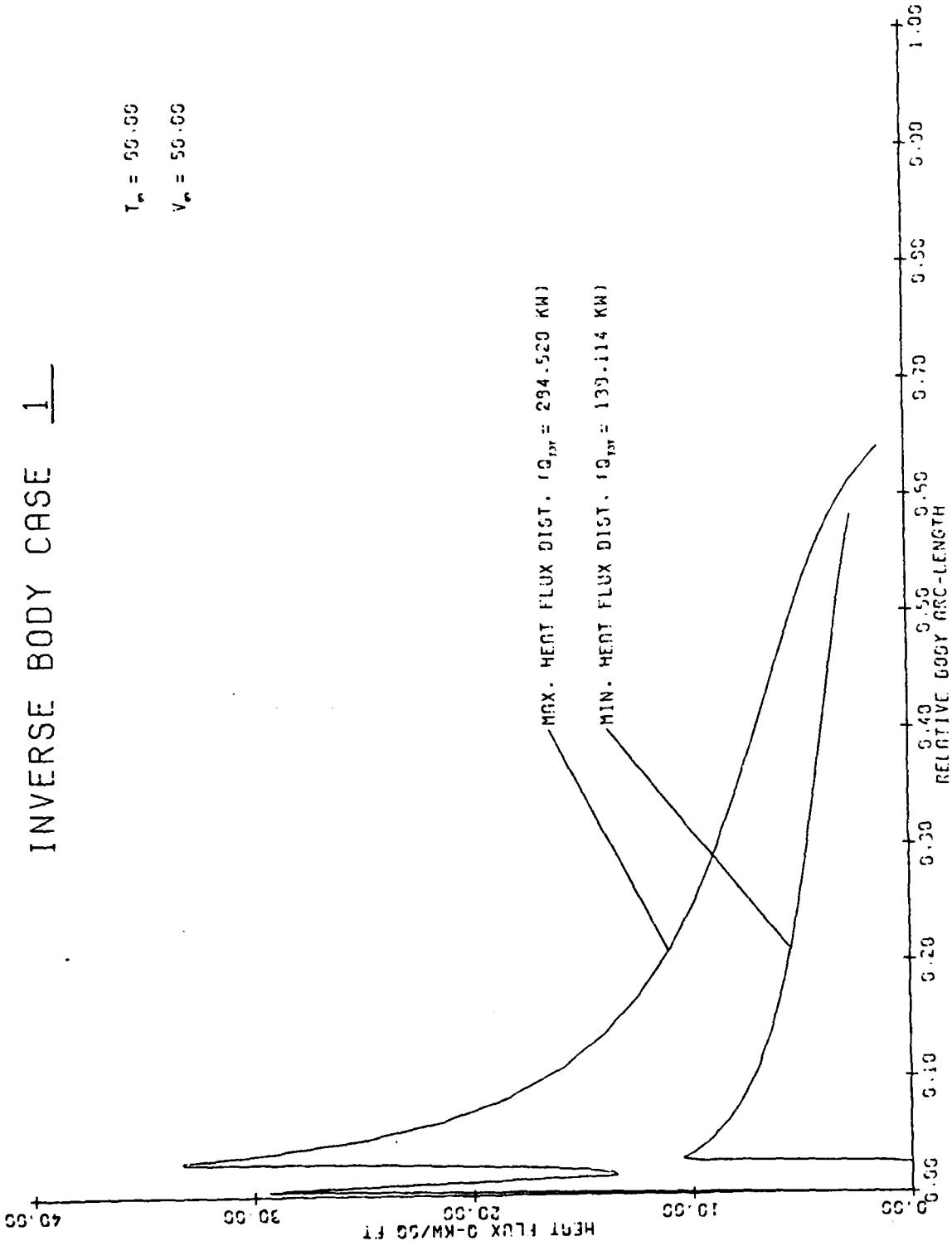

Figure 89. Heat Flux Distributions, Case No. 1.

19 August 1981
JJE:GHH:mmj

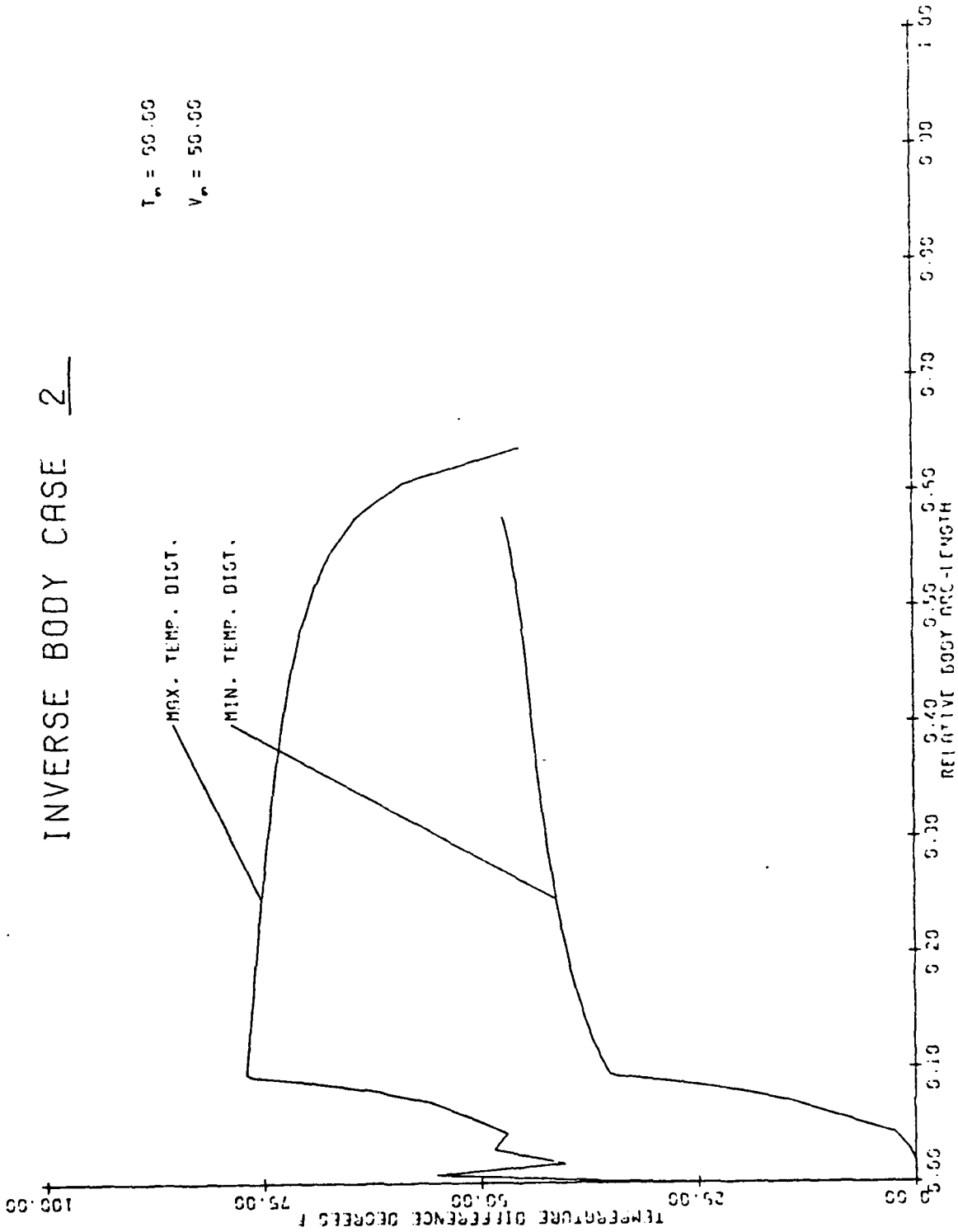

Figure 90. Temperature Distributions, Case No. 2.

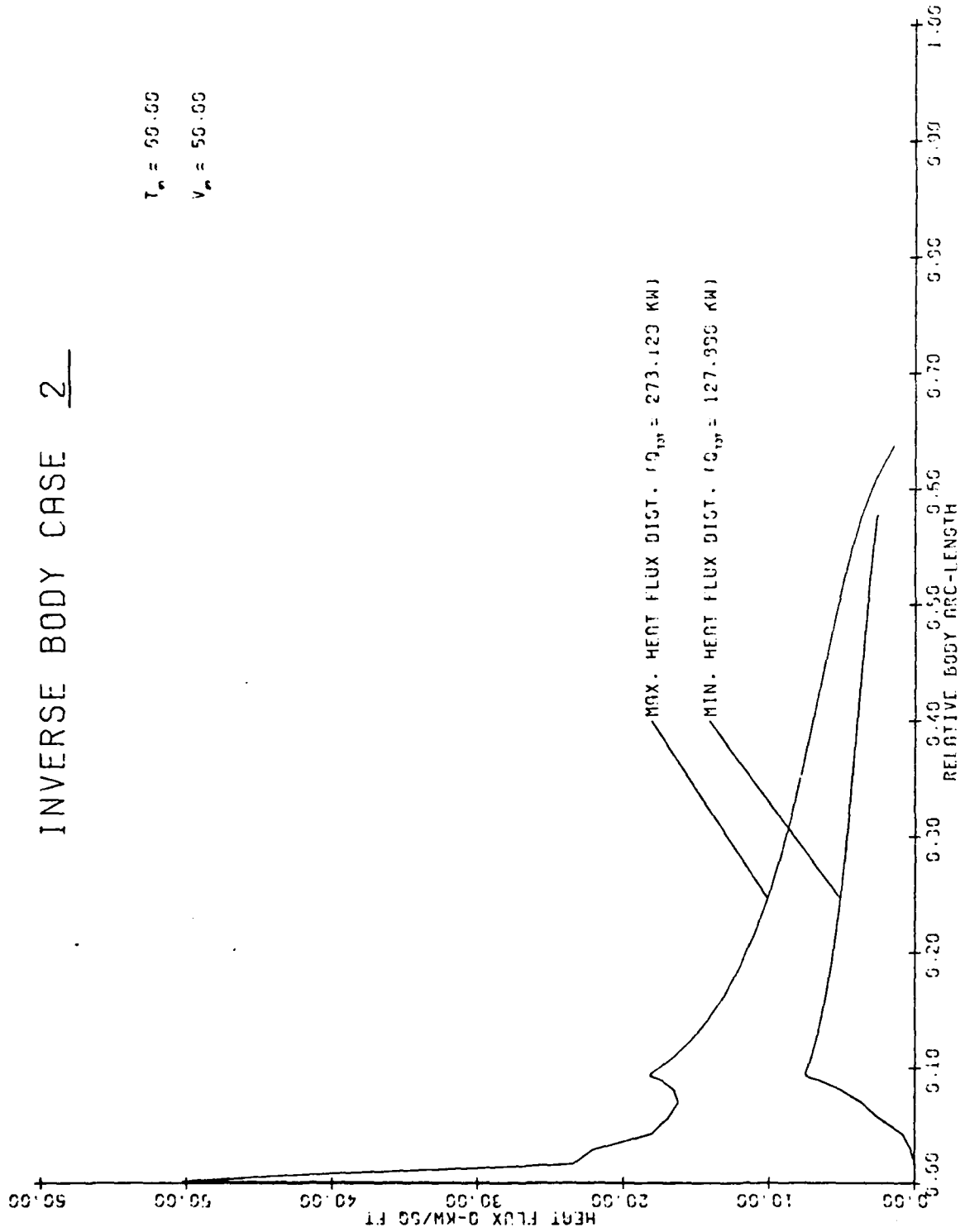

Figure 91. Heat Flux Distributions, Case No. 2.

19 August 1981
JJE:GHH:mmj

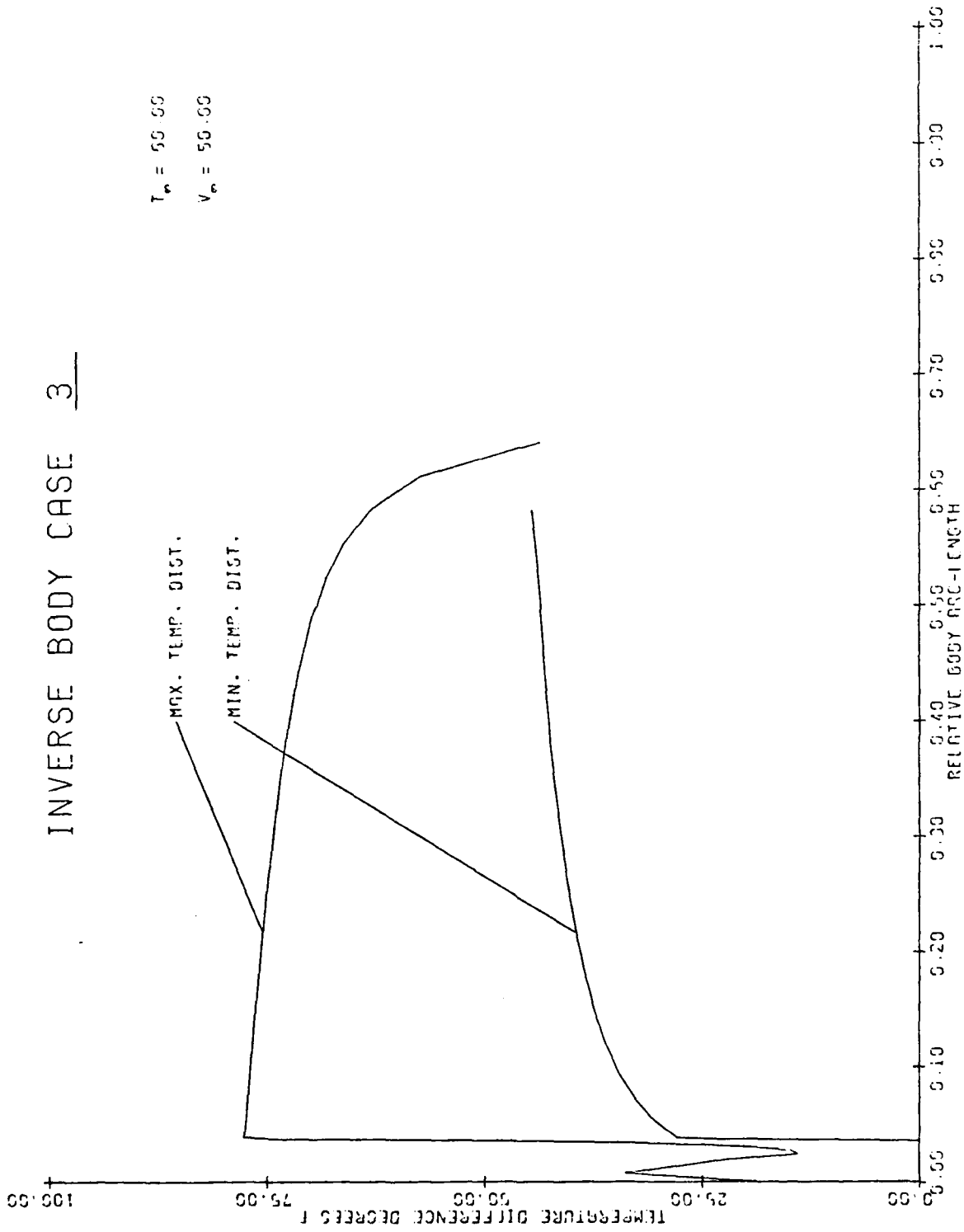

Figure 92. Temperature Distributions, Case No. 3.

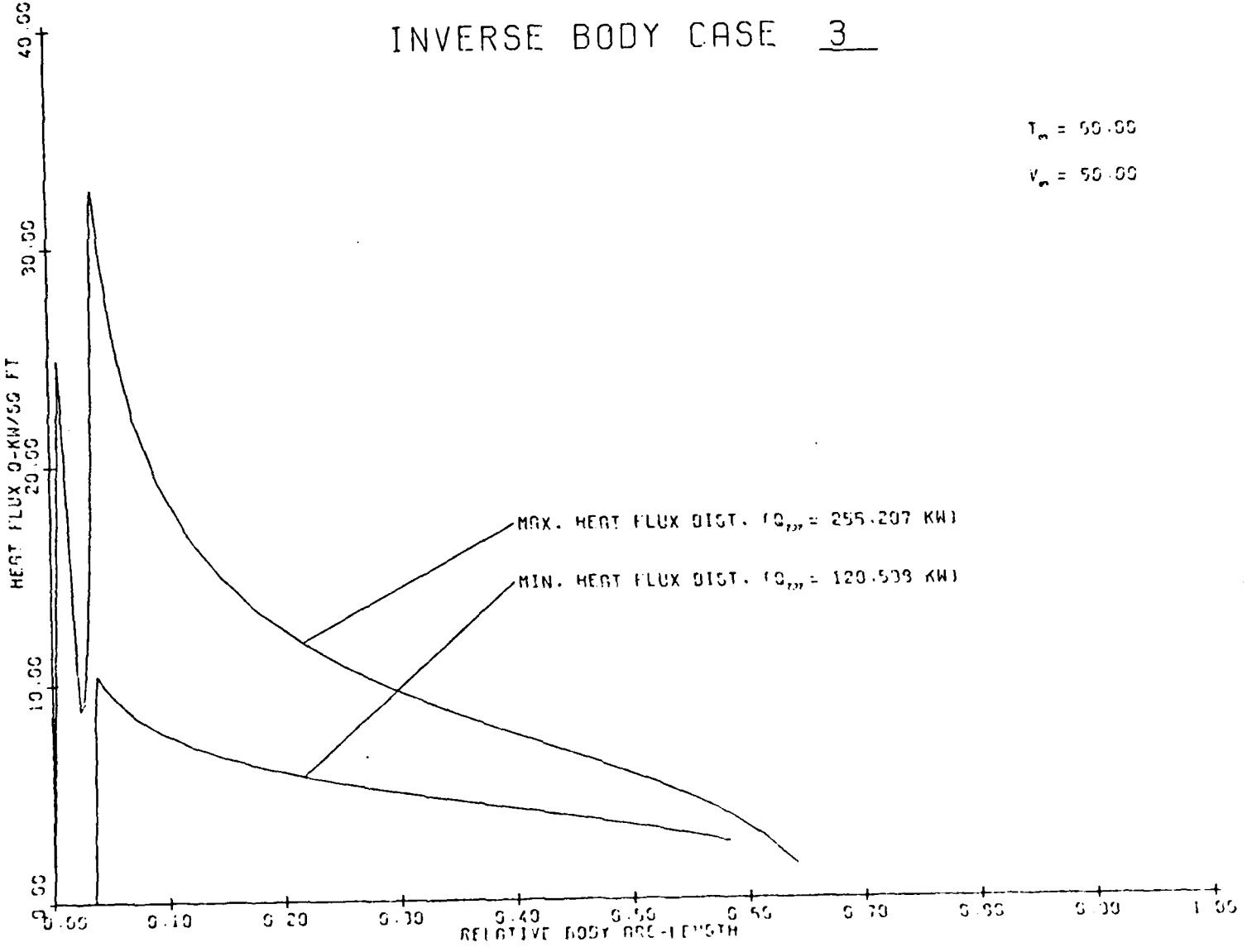

Figure 93. Heat Flux Distributions, Case No. 3.

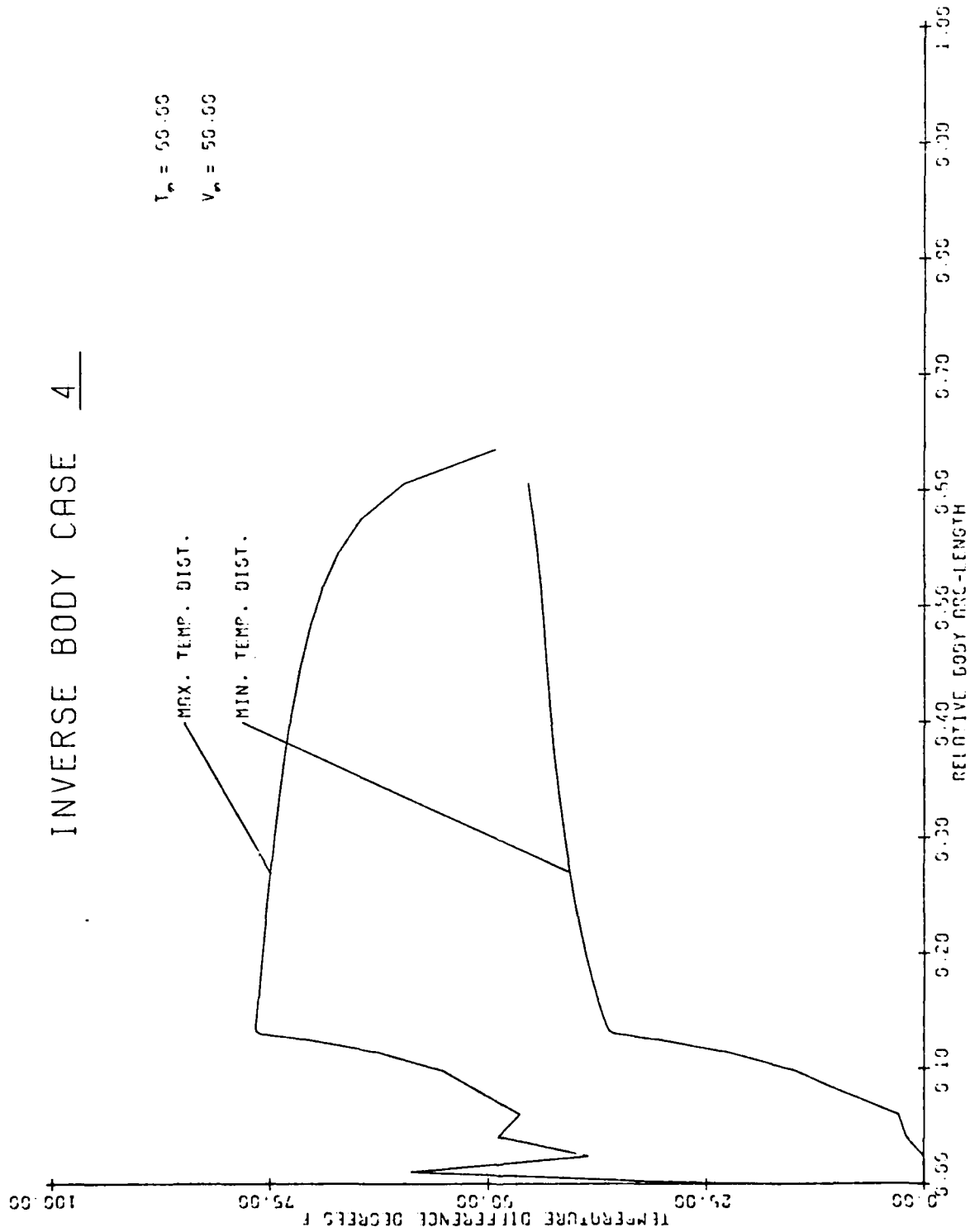

Figure 94. Temperature Distributions, Case No. 4.

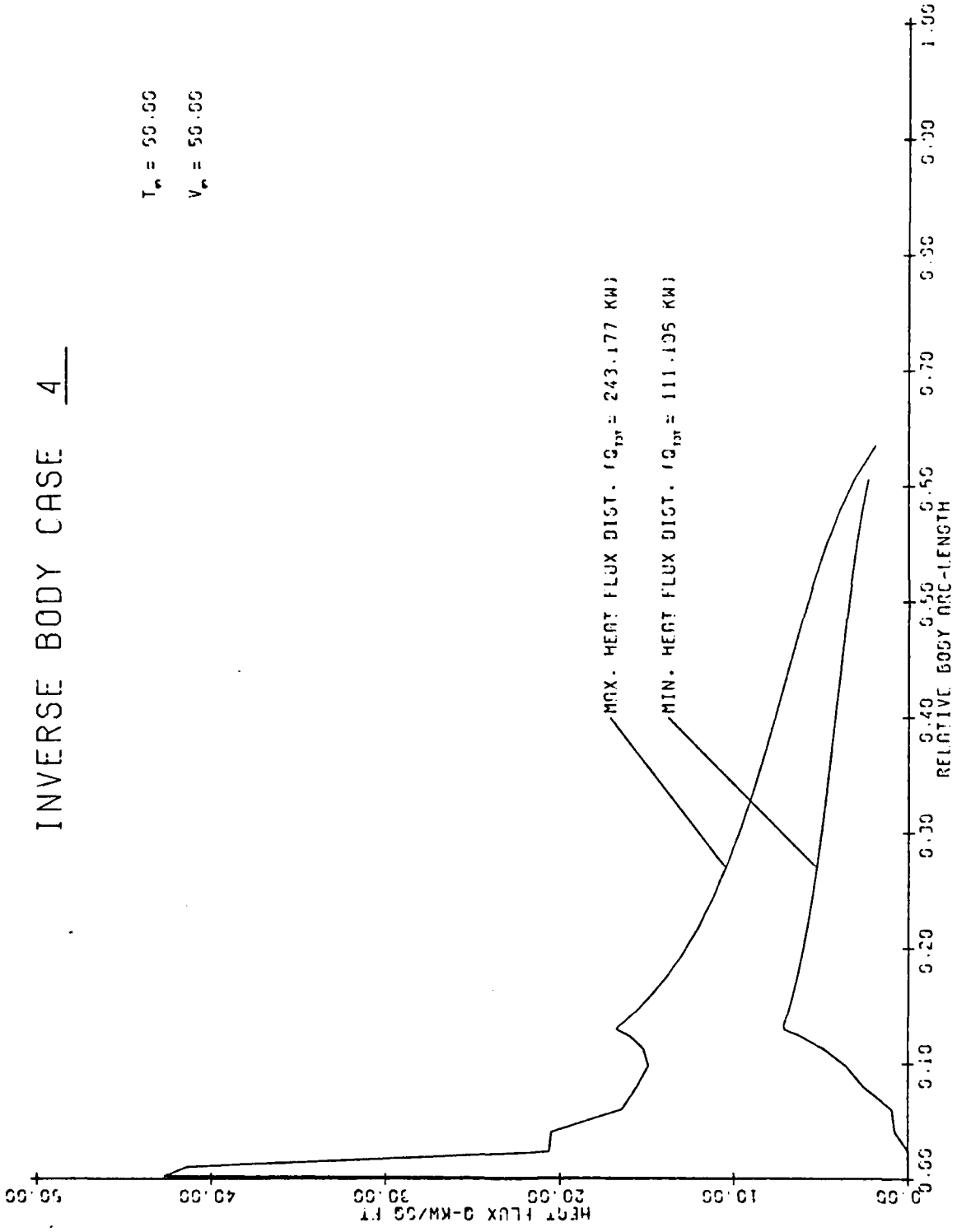

Figure 95. Heat Flux Distributions, Case No. 4.

19 August 1981
JJE:GHH:mmj

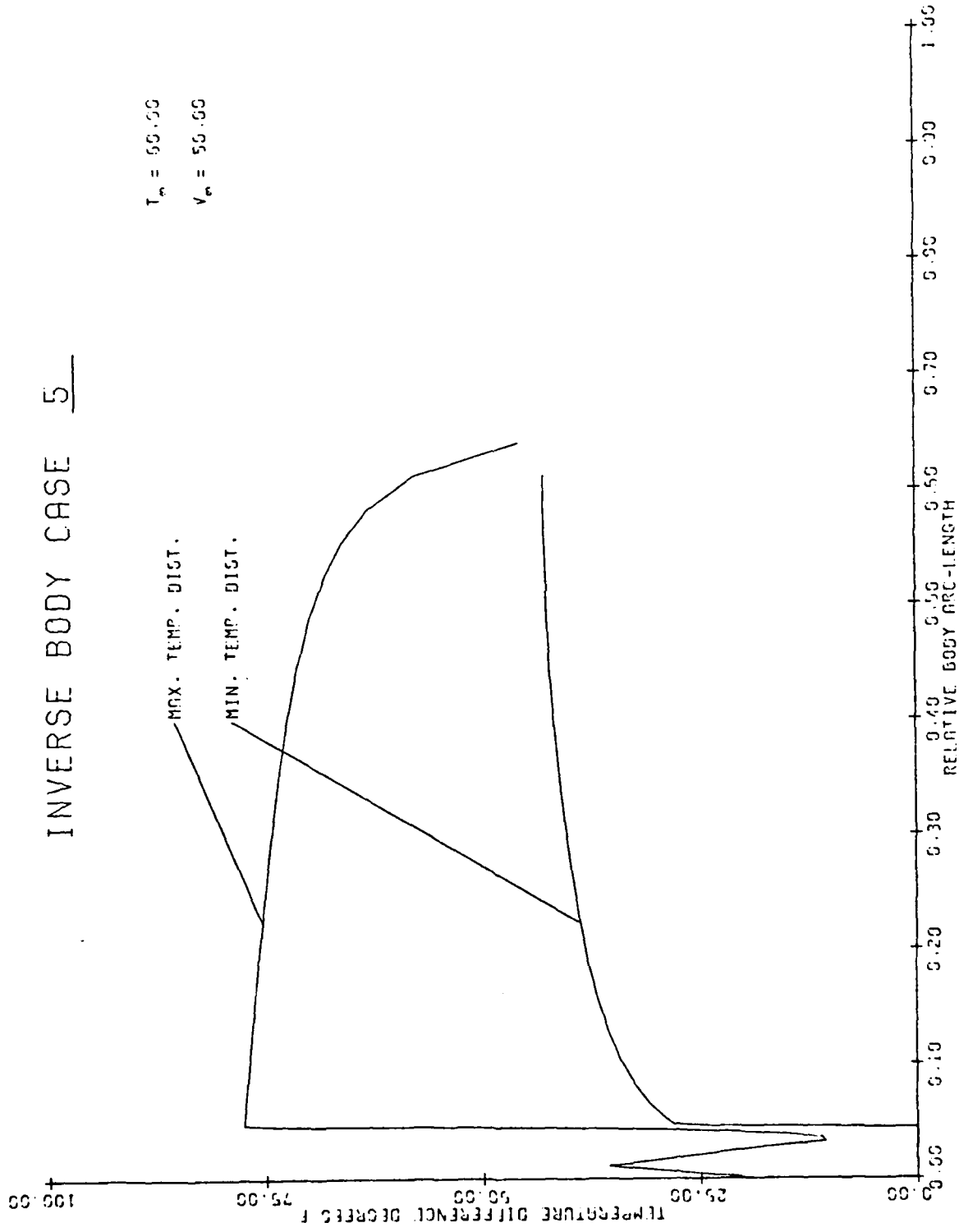

Figure 96. Temperature Distributions, Case No. 5.

19 August 1981
JJE:GHH:mmj

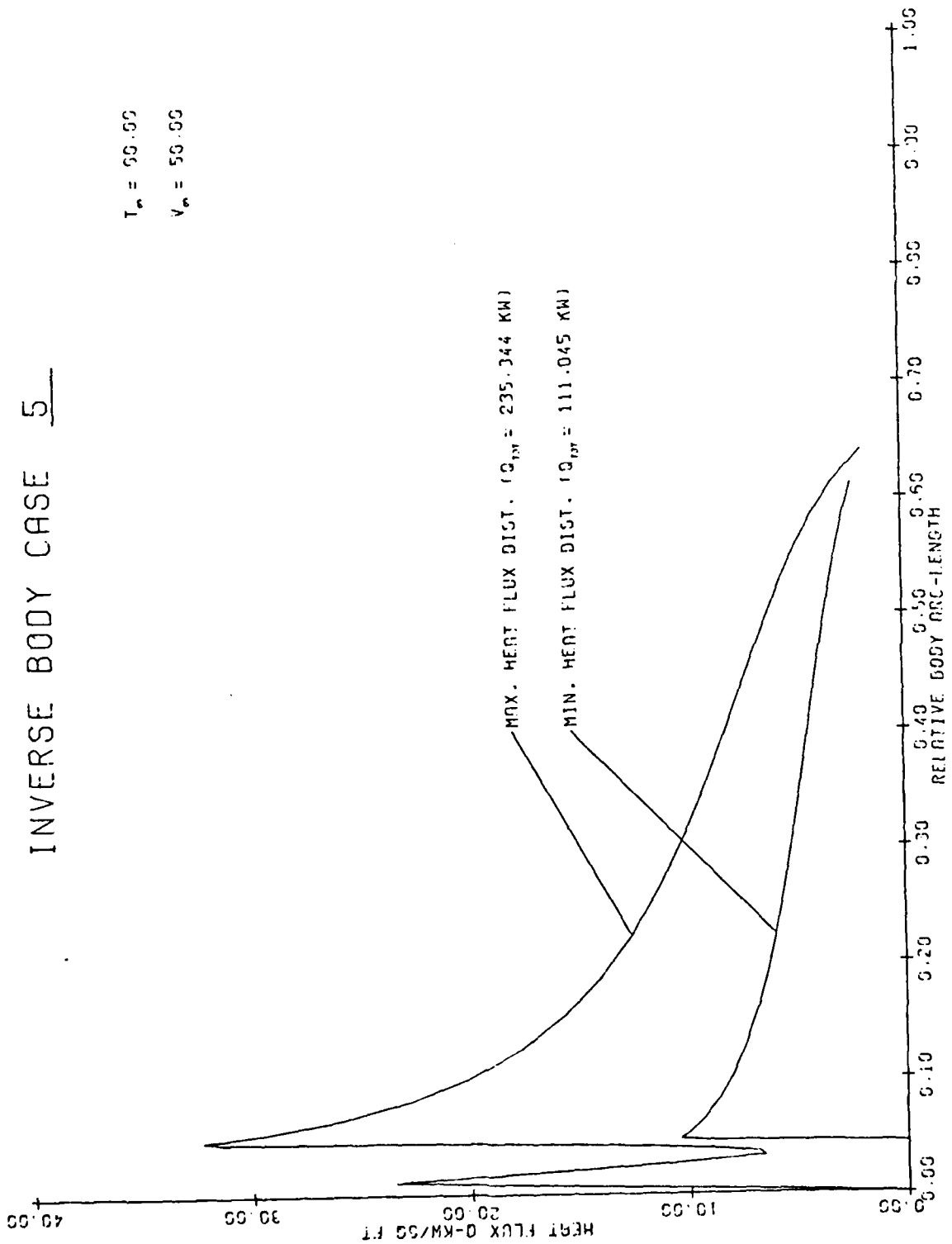

Figure 97. Heat Flux Distributions, Case No. 5.

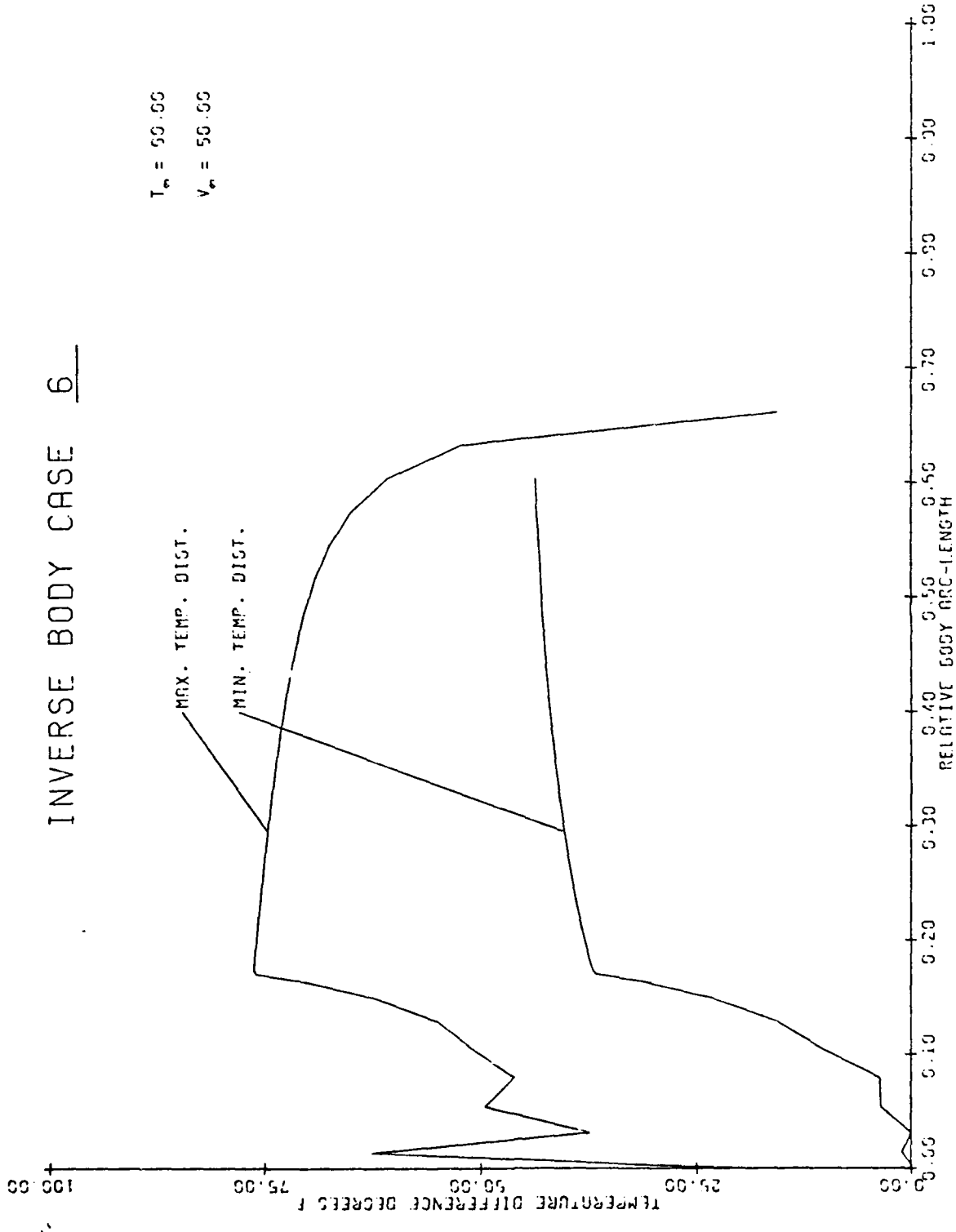

Figure 98. Temperature Distributions, Case No. 6.

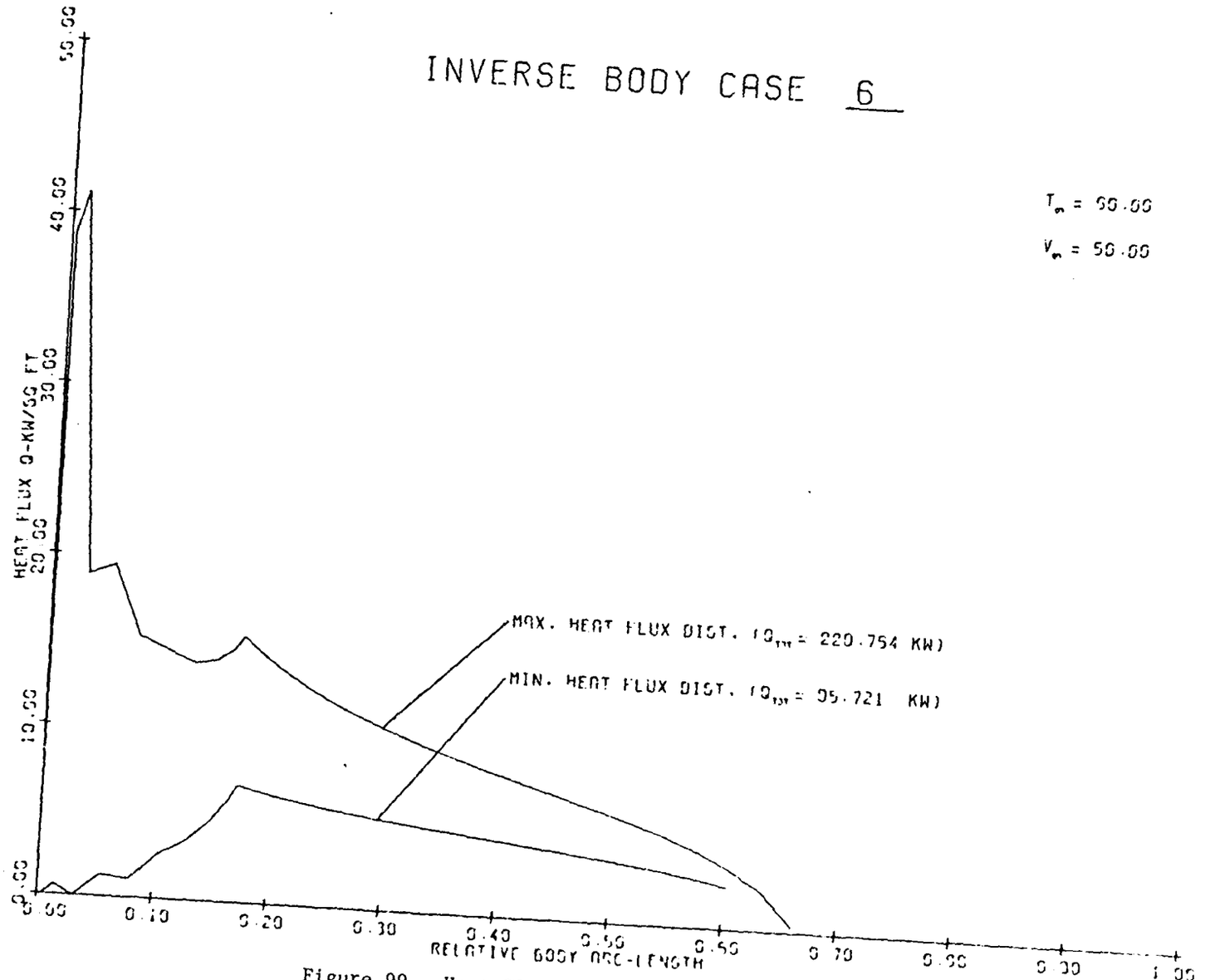

Figure 99. Heat Flux Distributions, Case No. 6.

19 August 1981
JJE:GHH:mmj

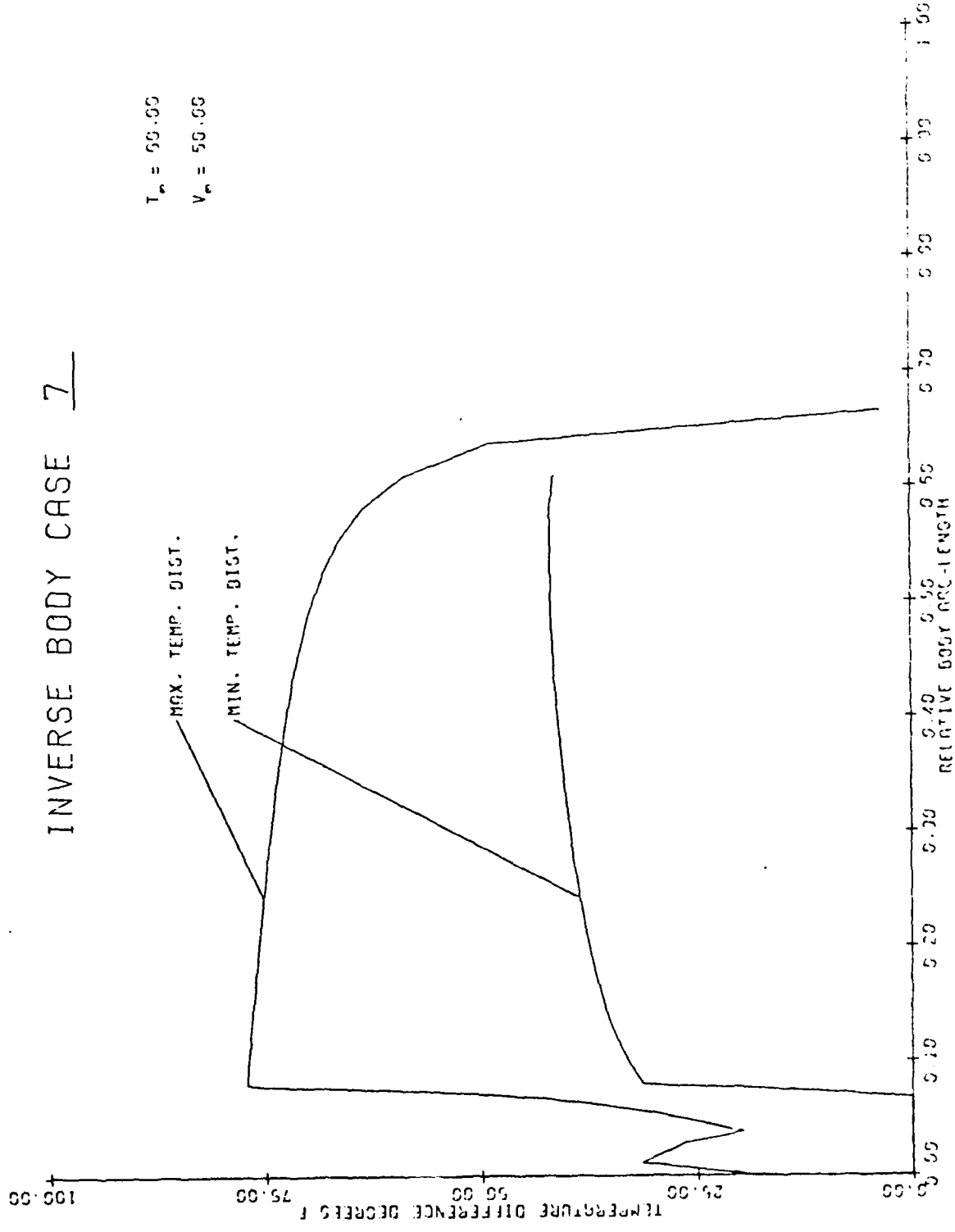

Figure 100. Temperature Distributions, Case No. 7.

19 August 1981
JJE:GHH:mmj

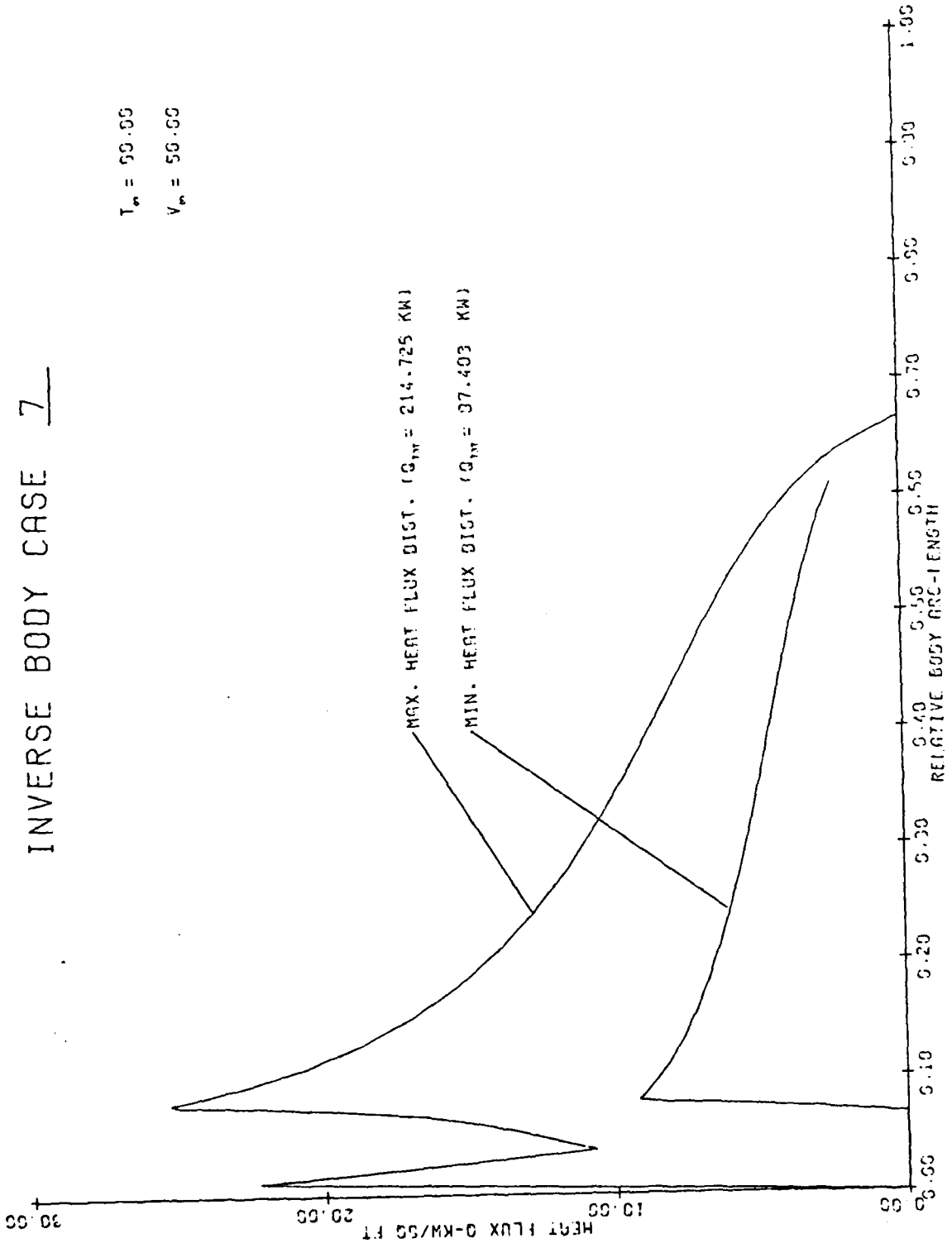

Figure 101. Heat Flux Distributions, Case No. 7.

19 August 1981
JJE:GHH:mmj

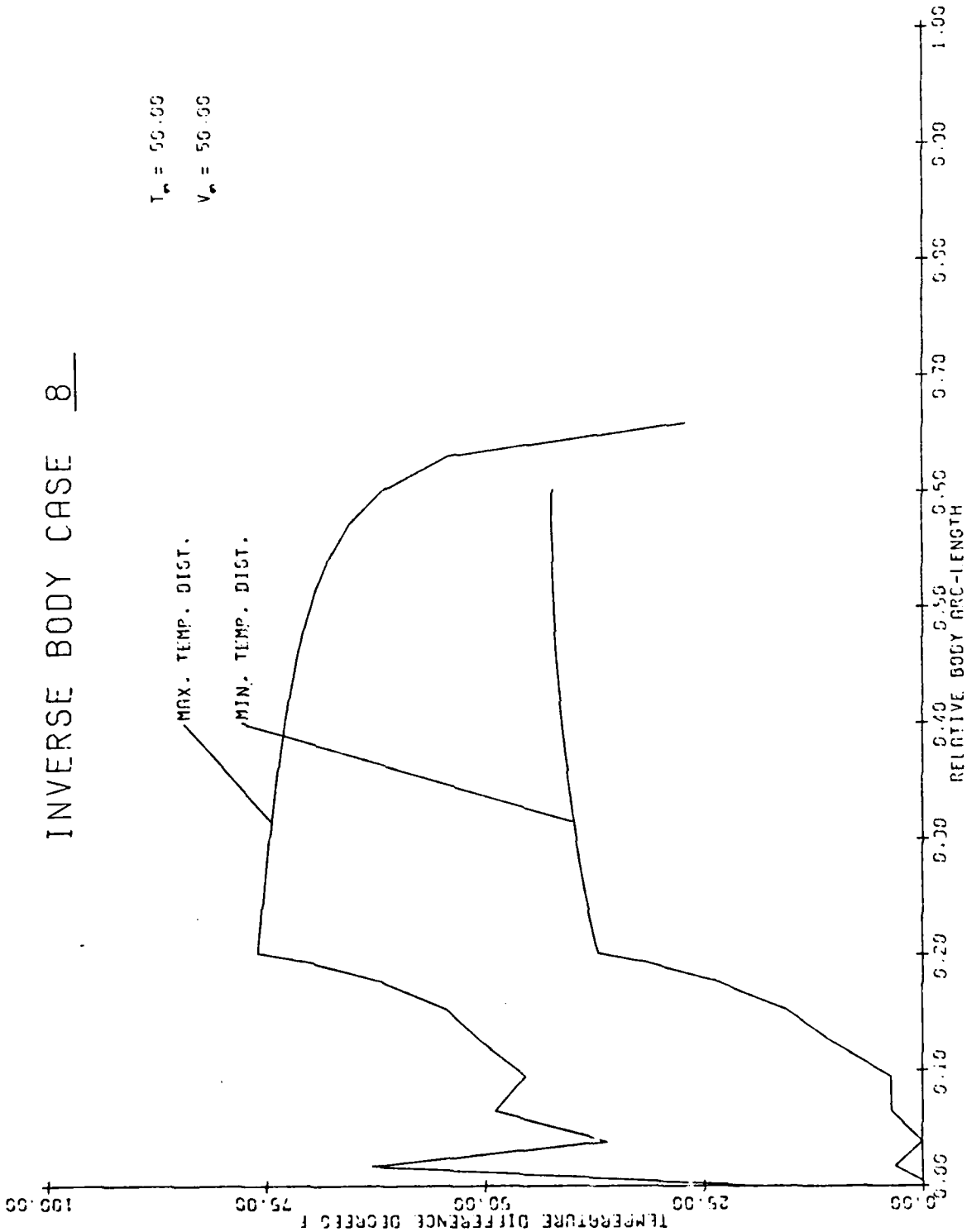

Figure 102. Temperature Distributions, Case No. 8.

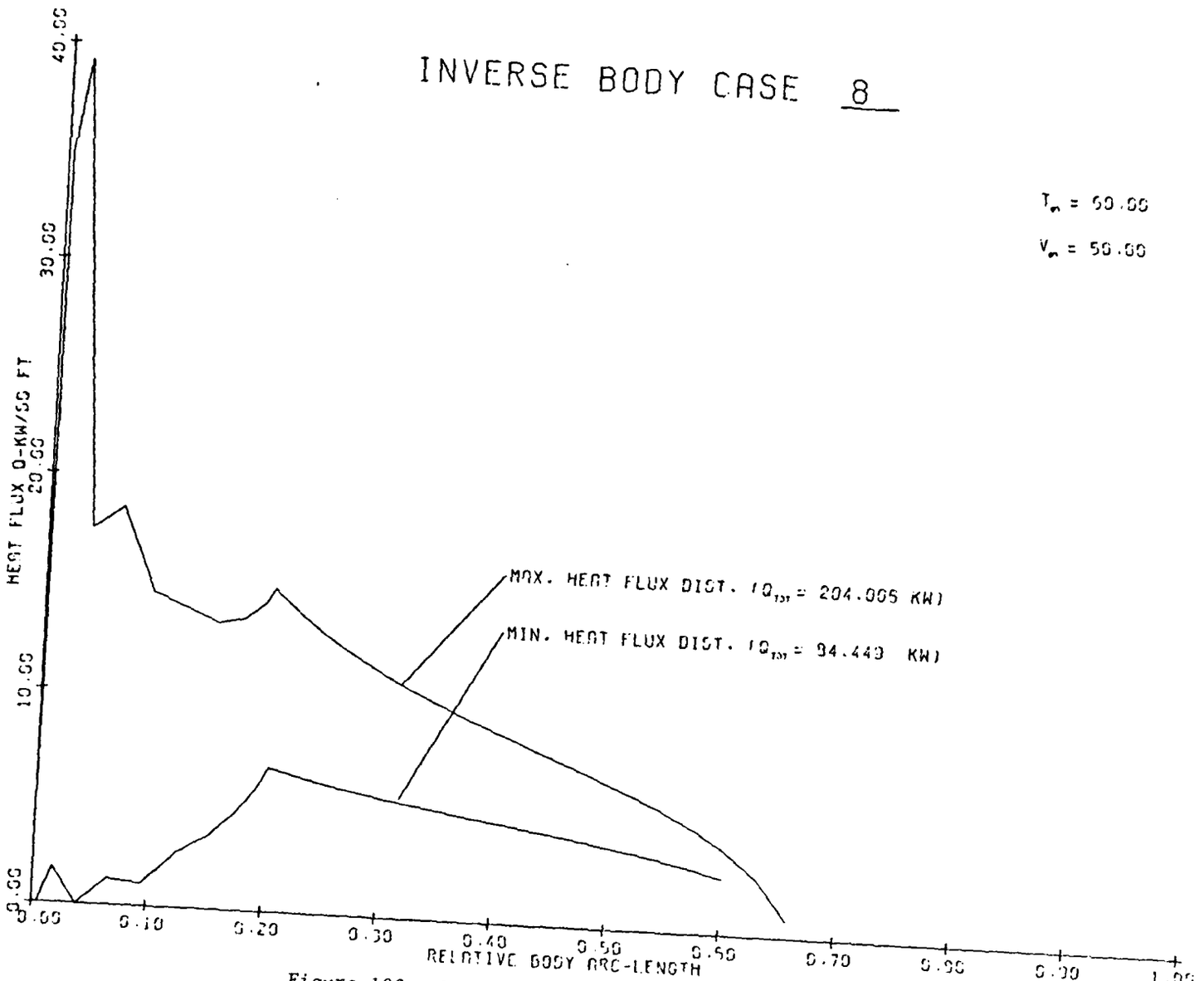

Figure 103. Heat Flux Distributions, Case No. 8.

19 August 1981
JJE:GHH:mmj

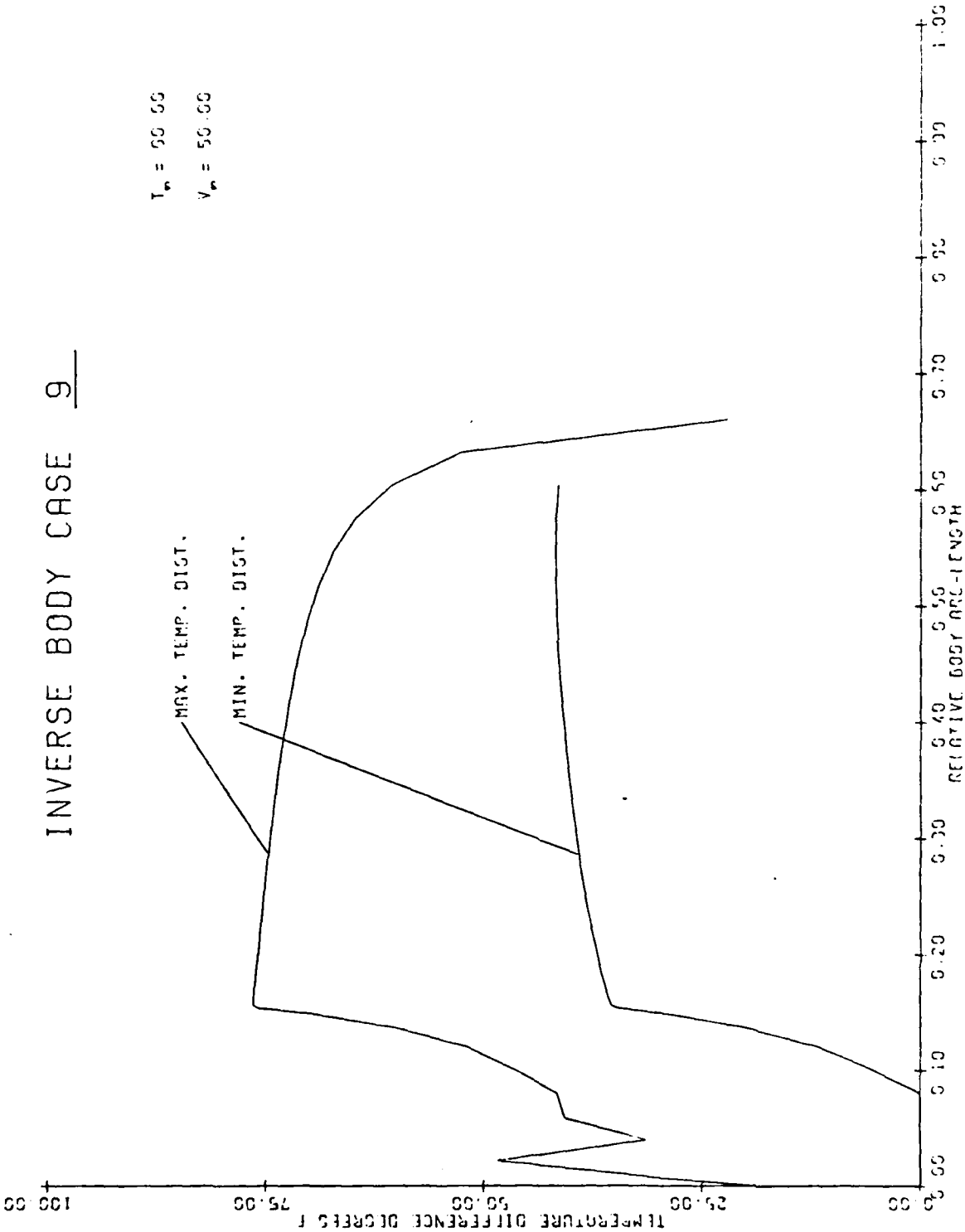

Figure 104. Temperature Distributions, Case No. 9.

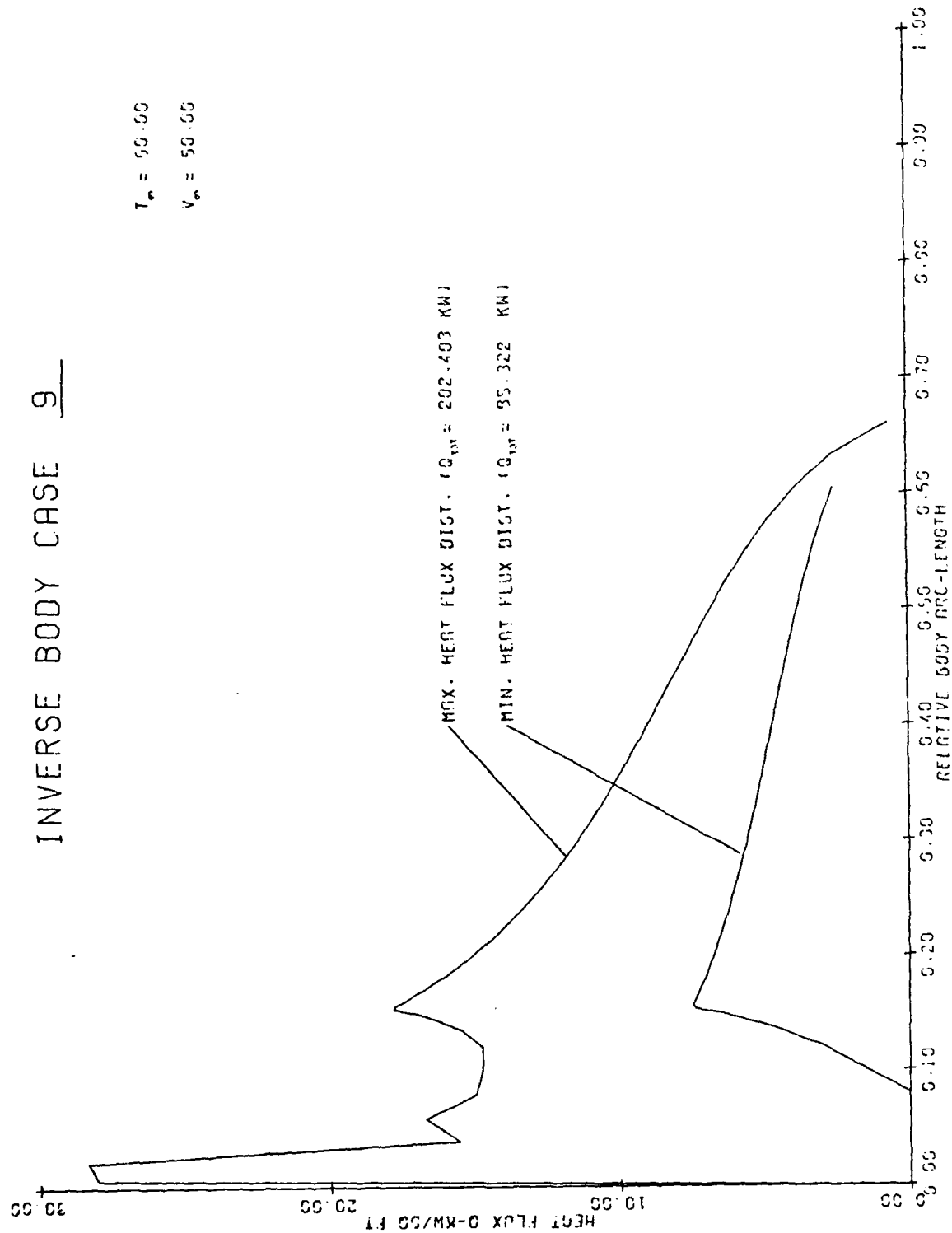

Figure 105. Heat Flux Distributions, Case No. 9.

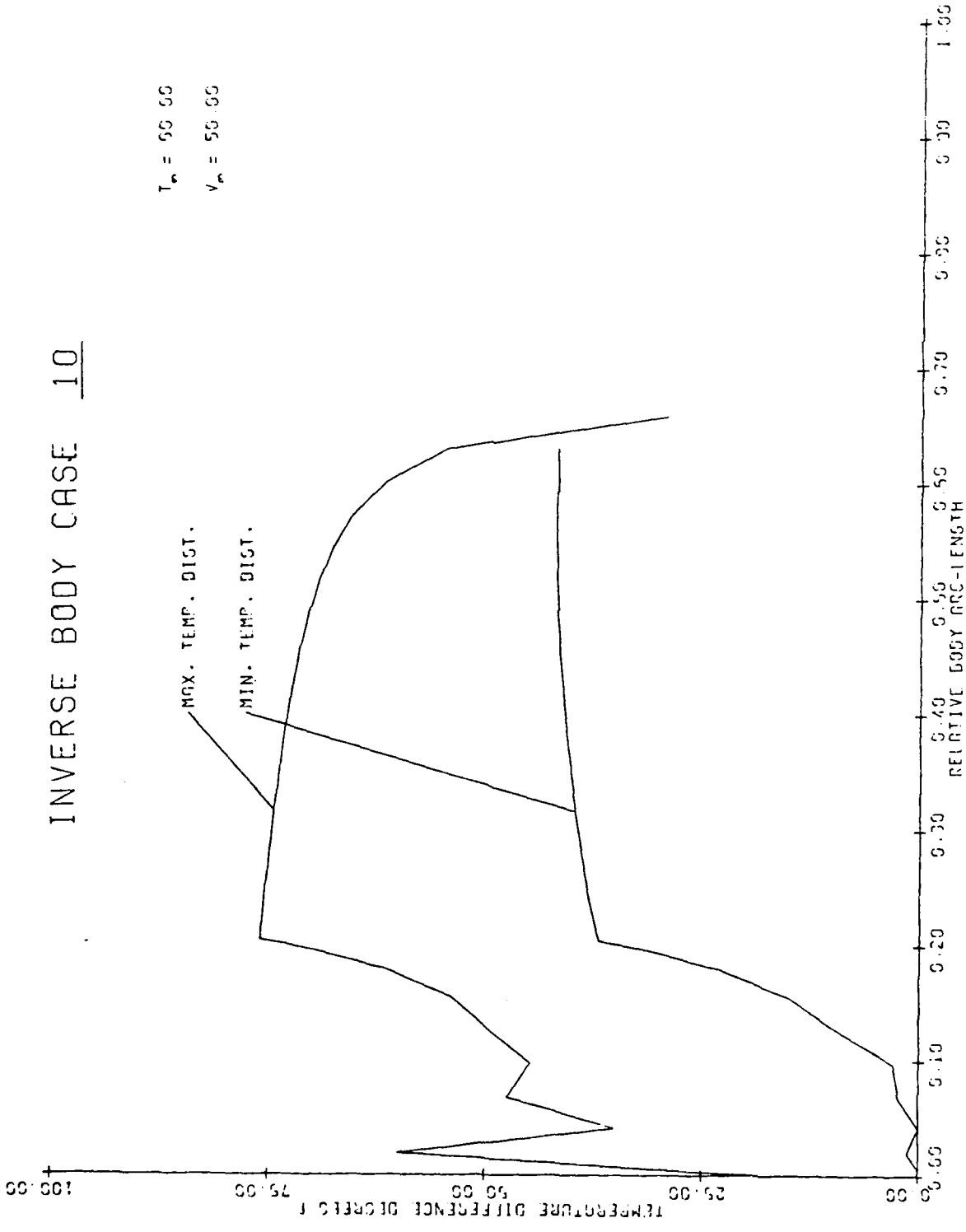

Figure 106. Temperature Distributions, Case No. 10.

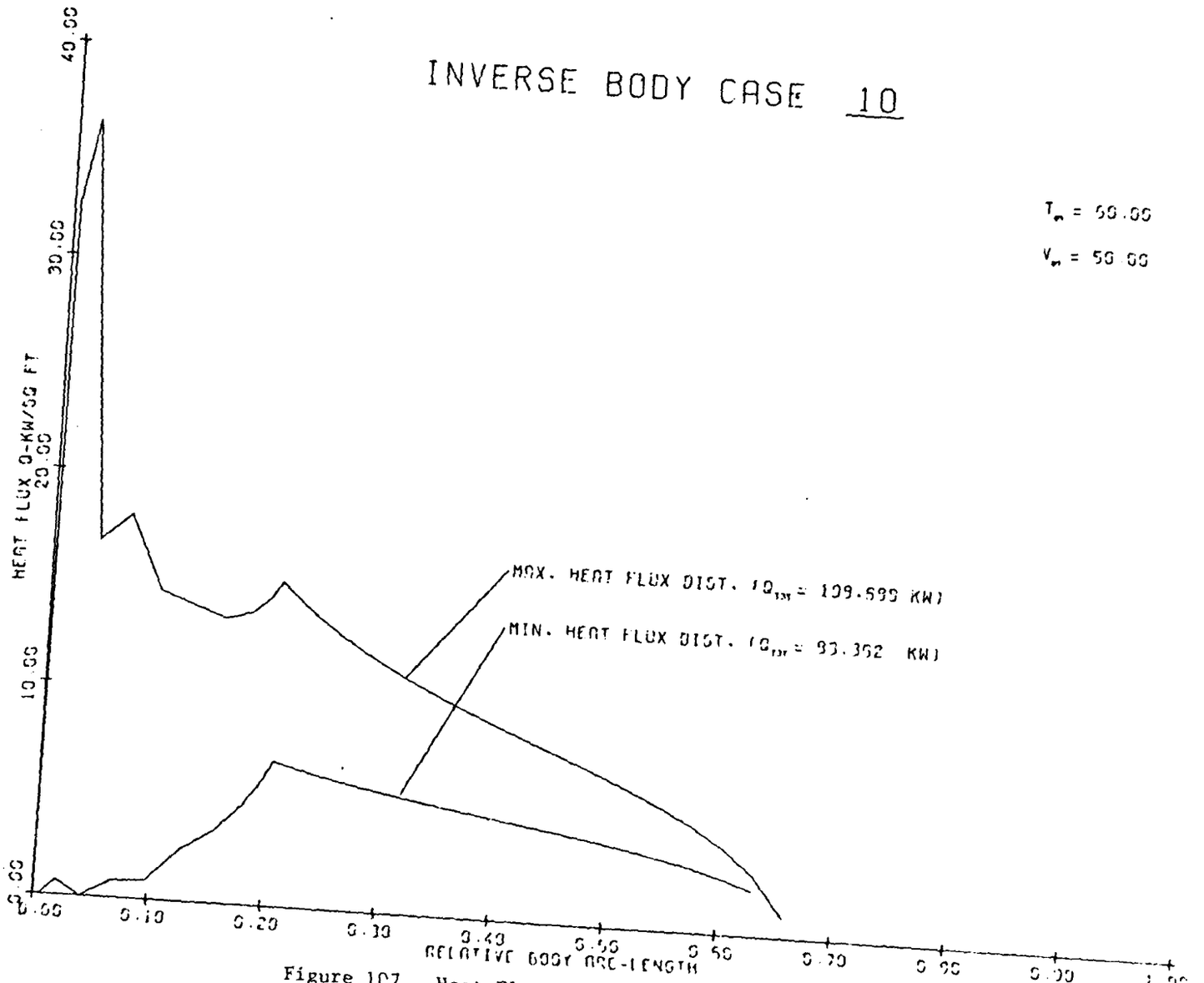

Figure 107. Heat Flux Distributions, Case No. 10.

19 August 1981
JJE:GHH:mmj

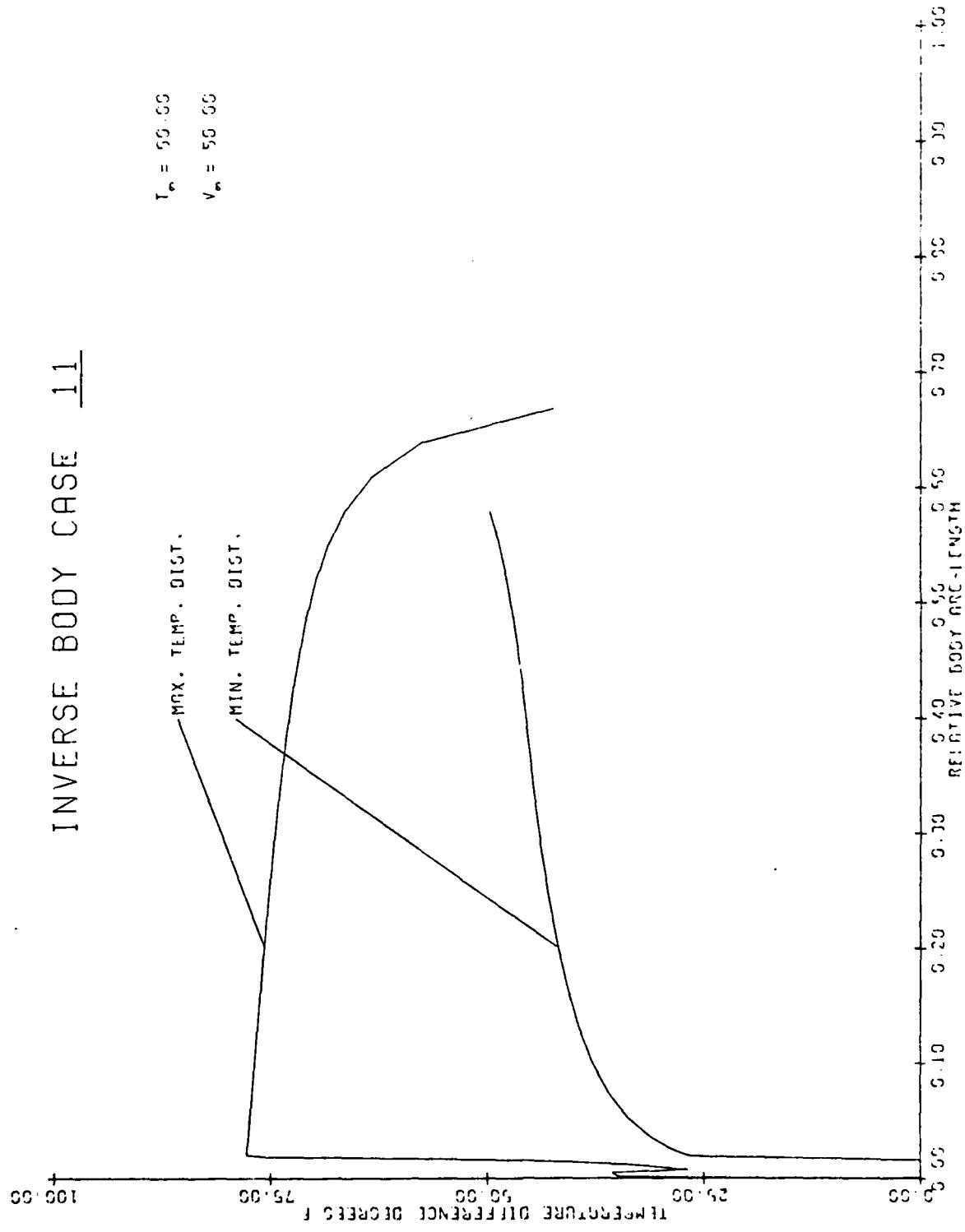

Figure 108. Temperature Distributions, Case No. 11.

19 August 1981
JJE:GHH:mmj

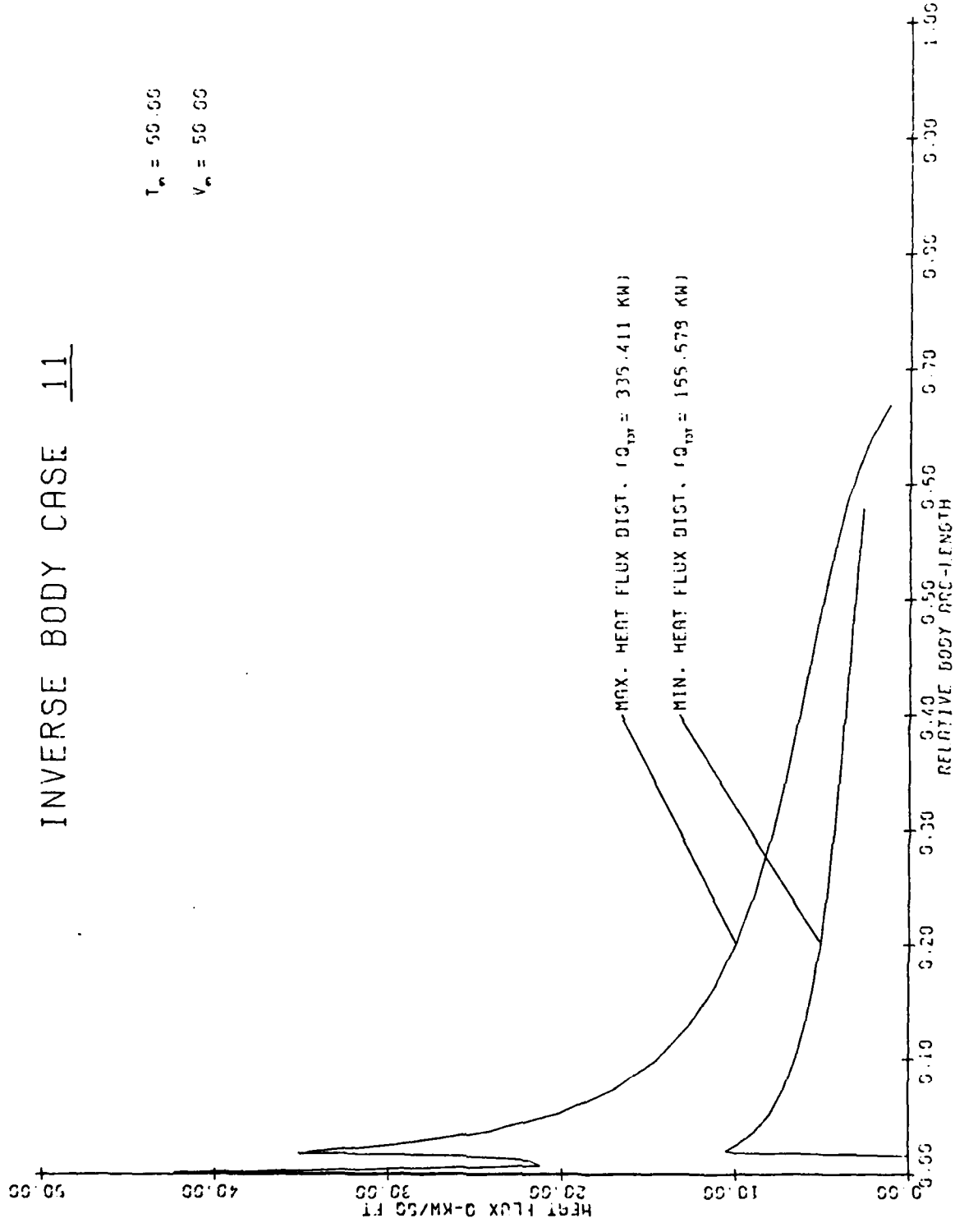

Figure 109. Heat Flux Distributions, Case No. 11.

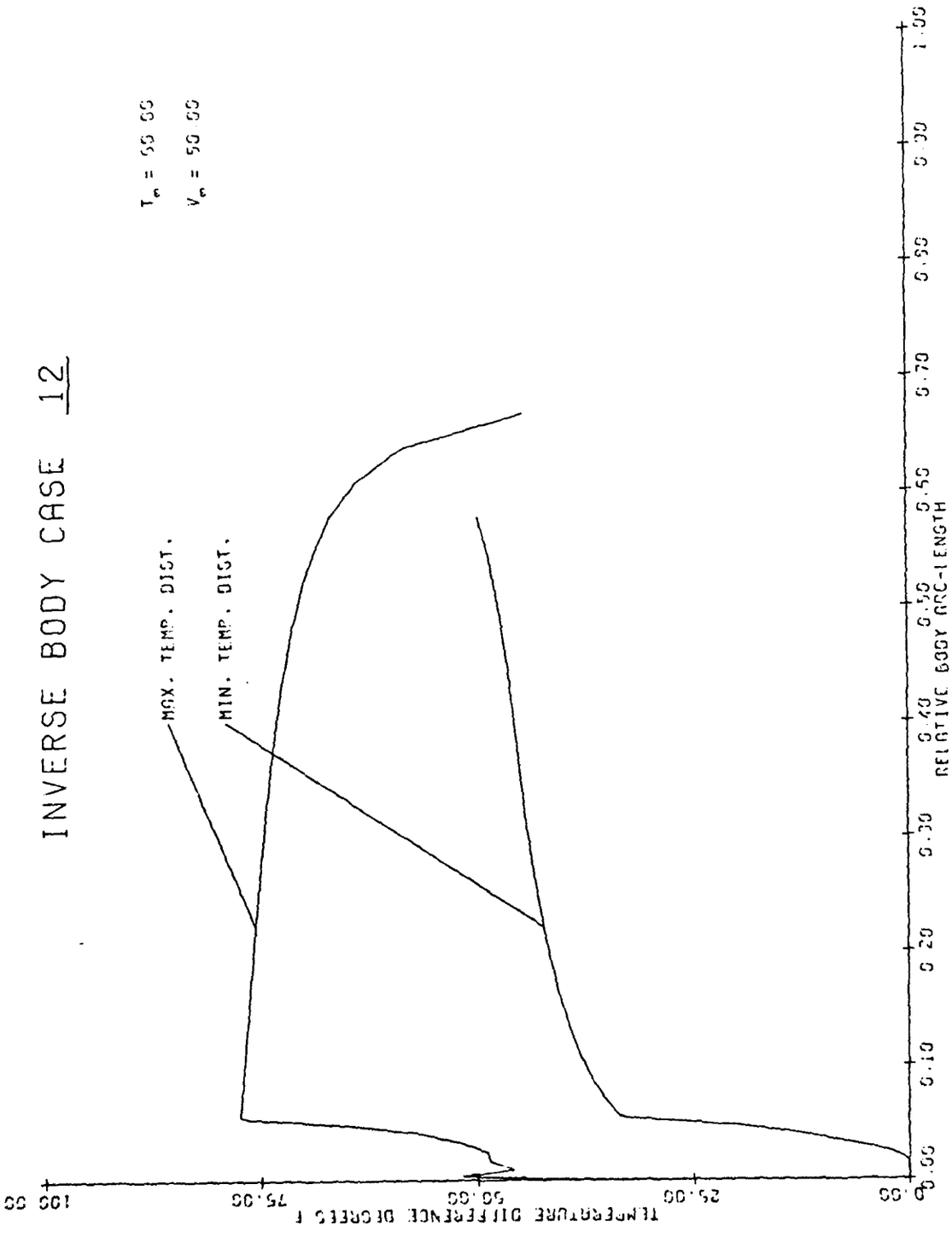

Figure 110. Temperature Distributions, Case No. 12.

19 August 1981
JJE:GHH:mmj

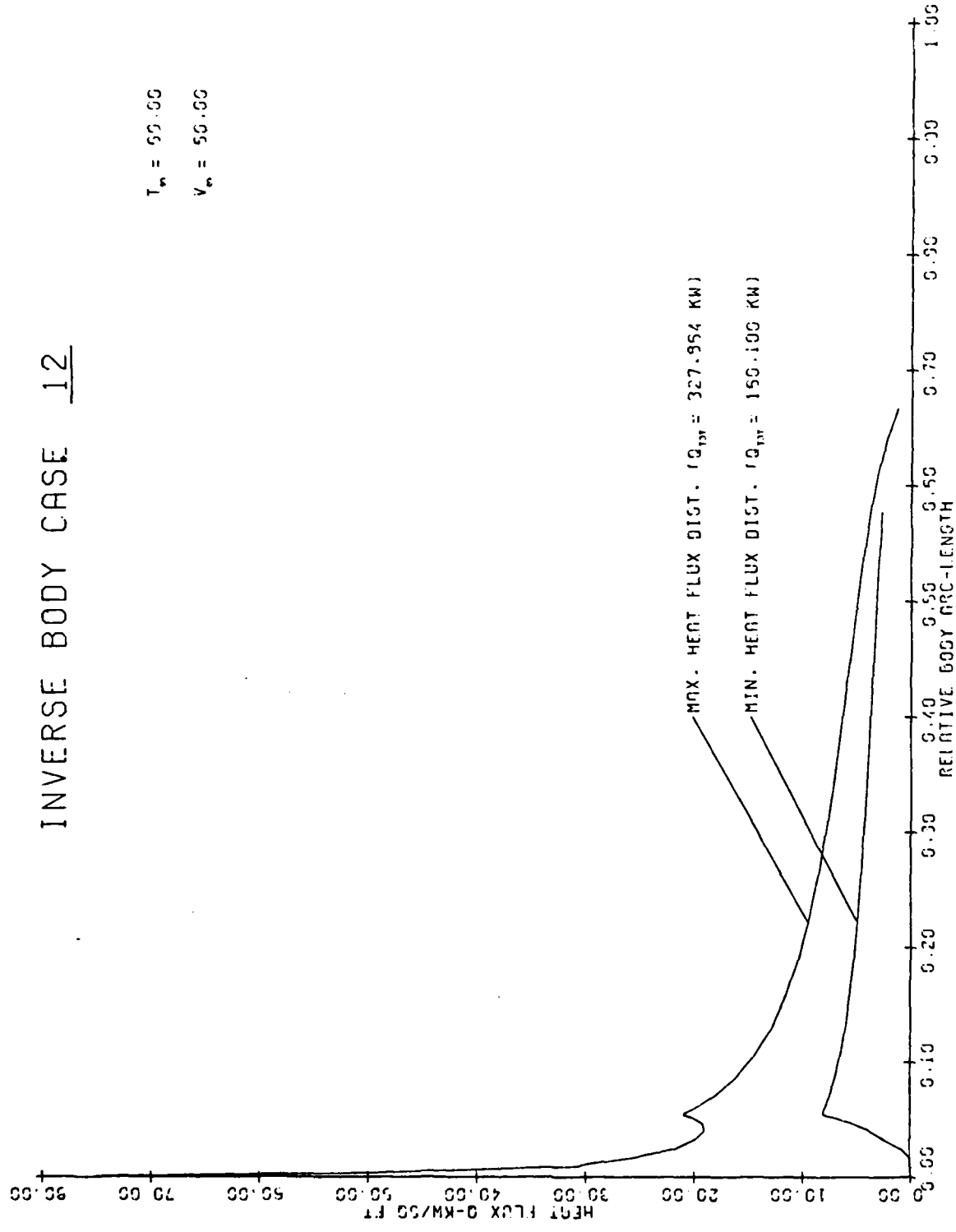

Figure III. Heat Flux Distributions, Case No. 12.

19 August 1981
JJE:GHH:mmj

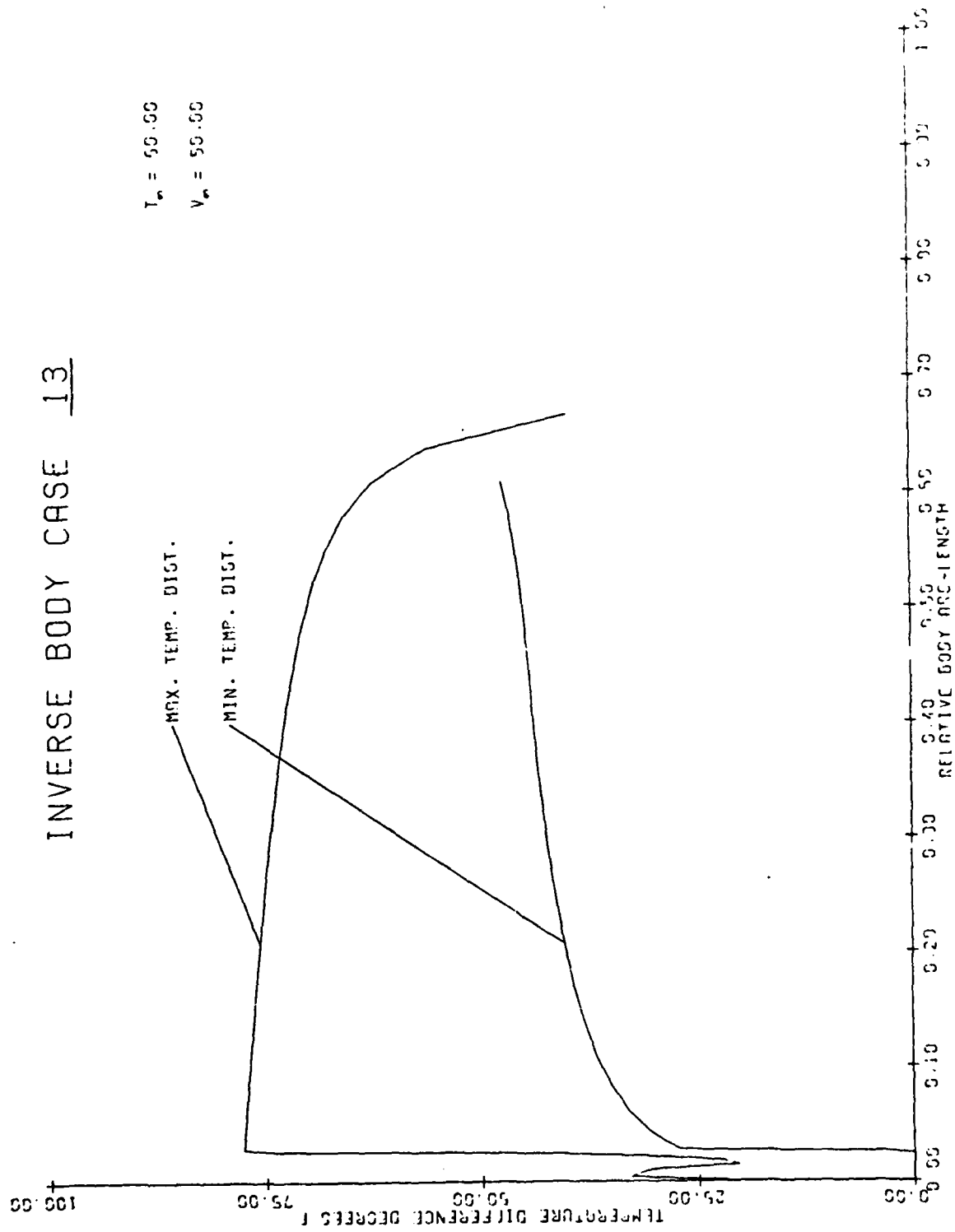

Figure 112. Temperature Distributions, CAse No. 13.

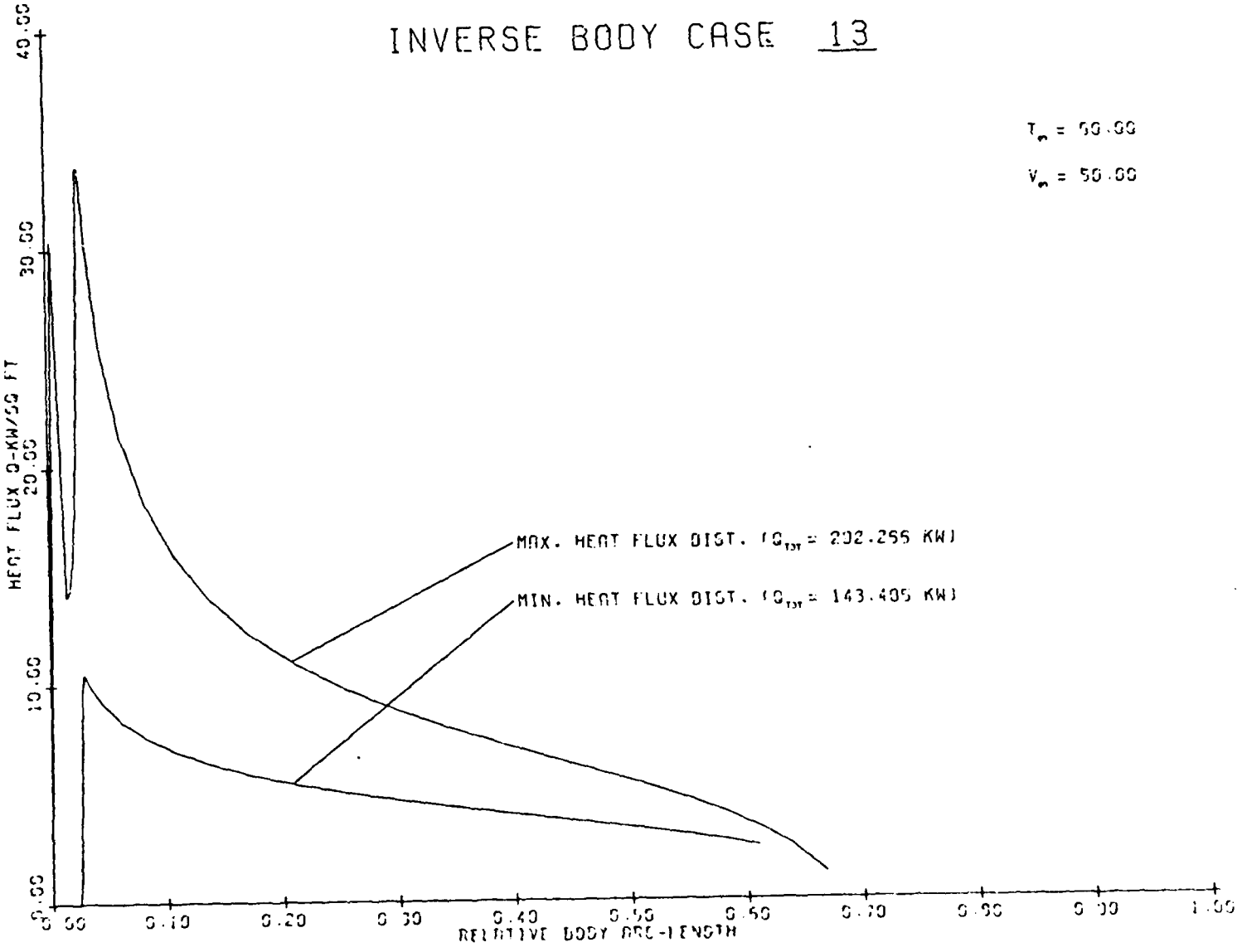

Figure 113. Heat Flux Distributions, Case No. 13.

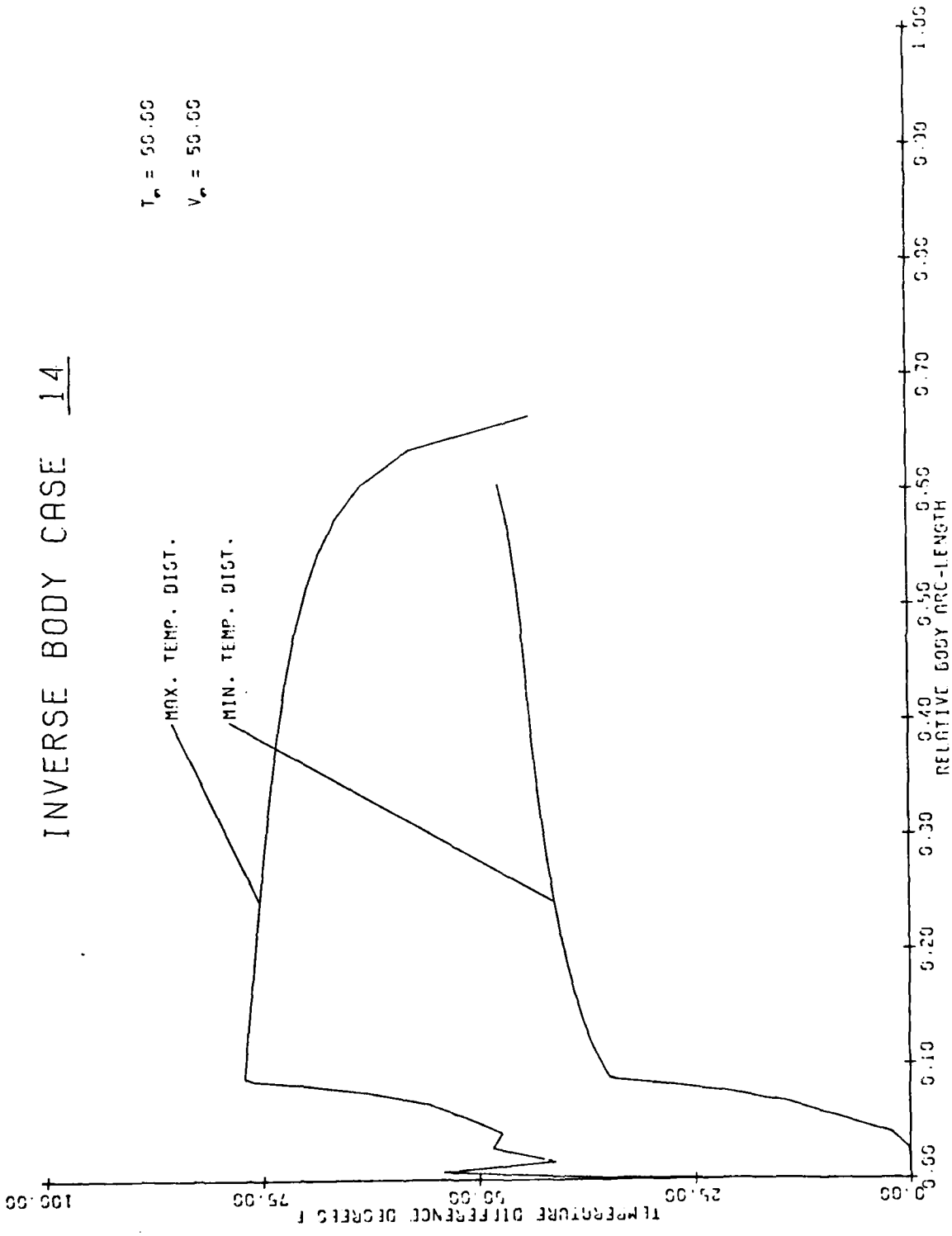

Figure 114. Temperature Distributions, Case No. 14.

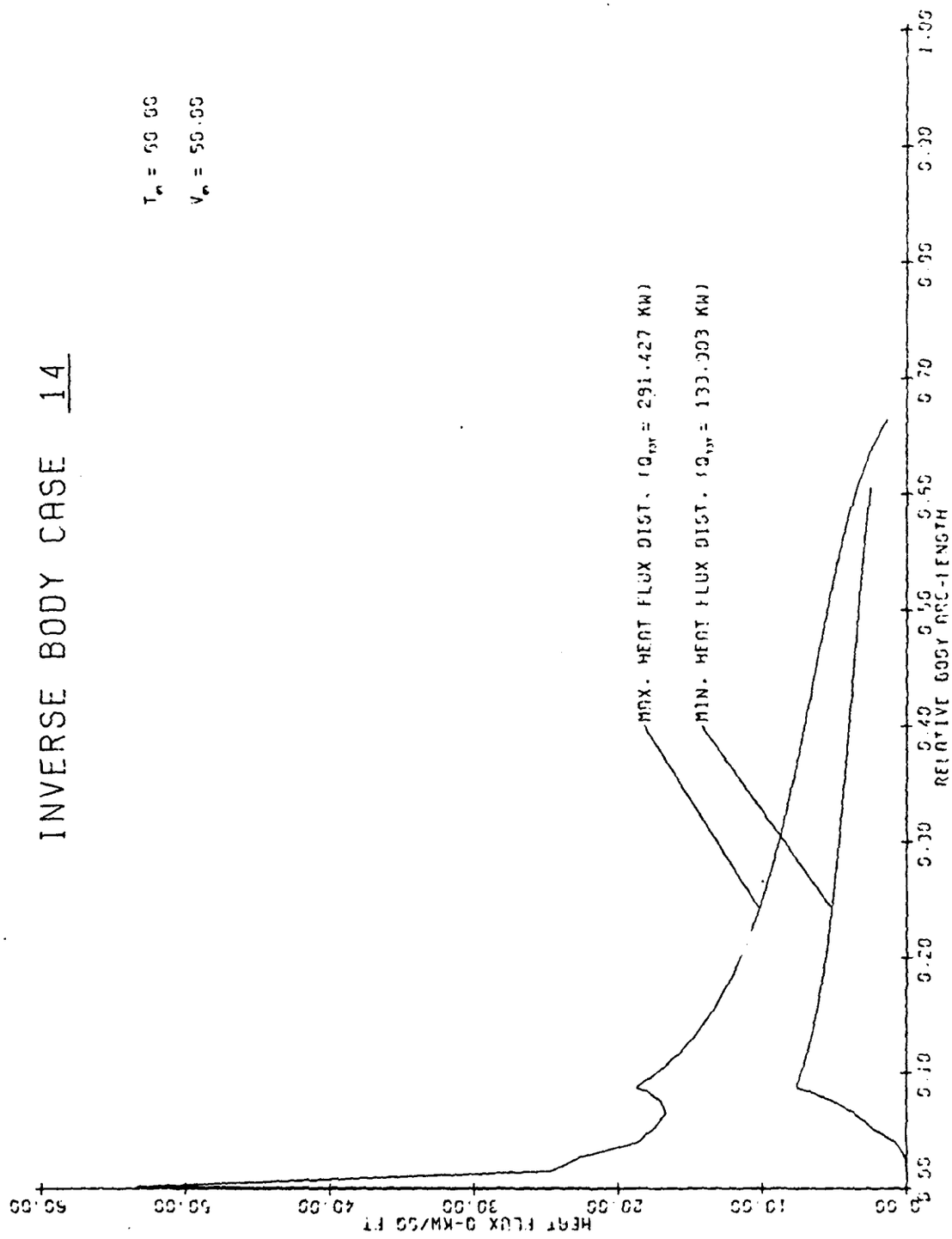

Figure 115. Heat Flux Distributions, Case No. 14.

19 August 1981
JJE:GHH:mmj

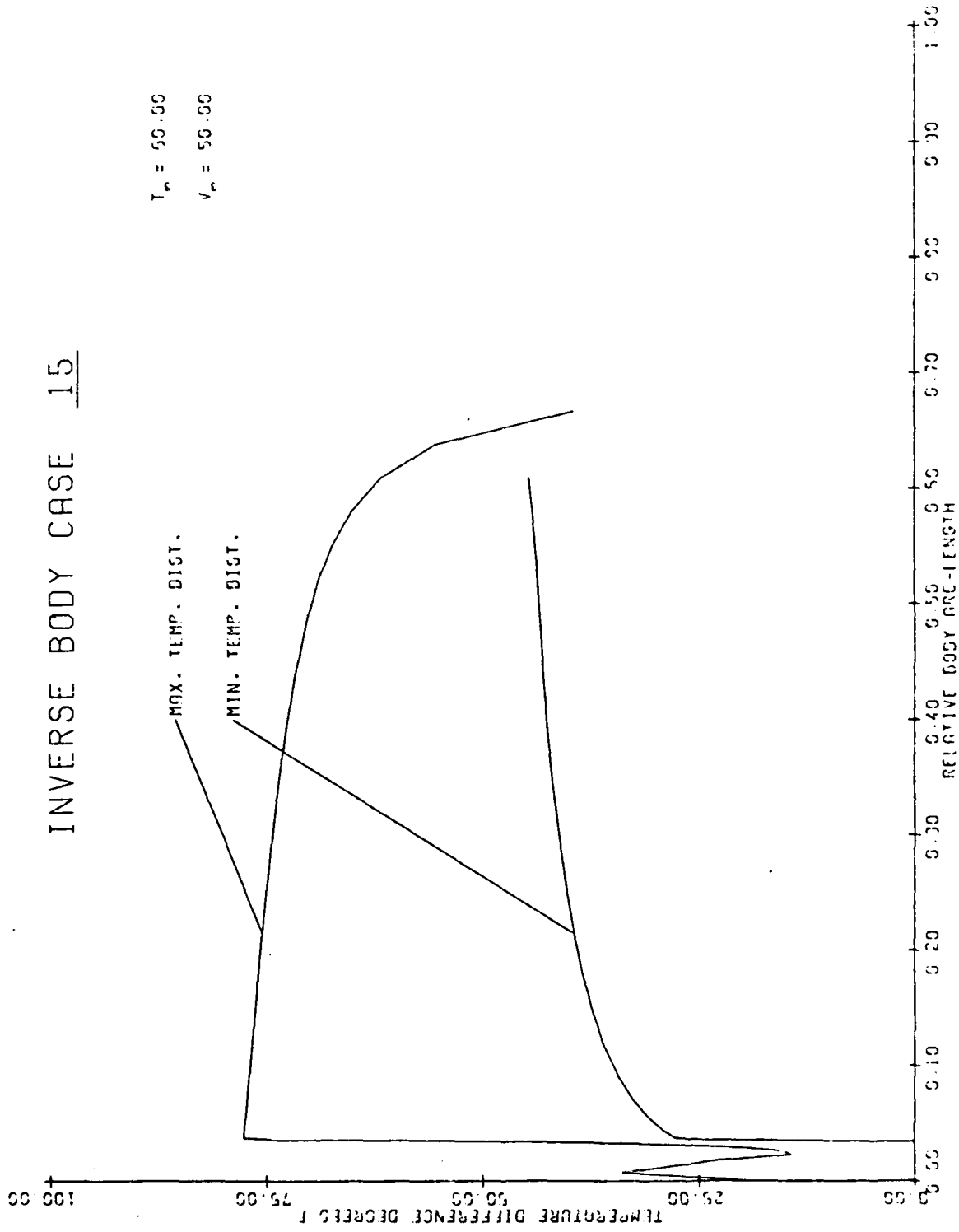

Figure 116. Temperature Distributions, Case No. 15.

19 August 1981
JJE:GHH:mmj

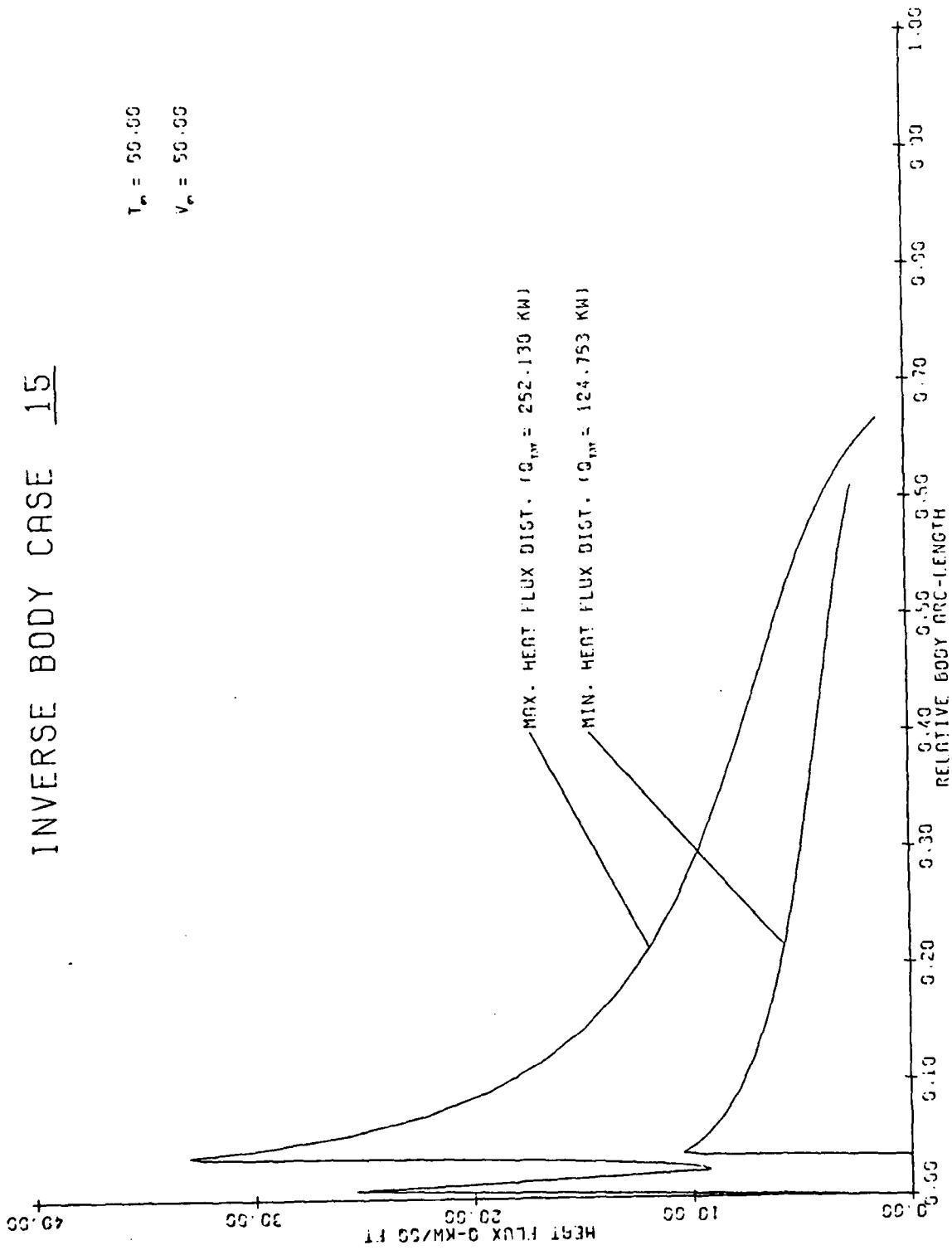

Figure 117. Heat Flux Distributions, Case No. 15.

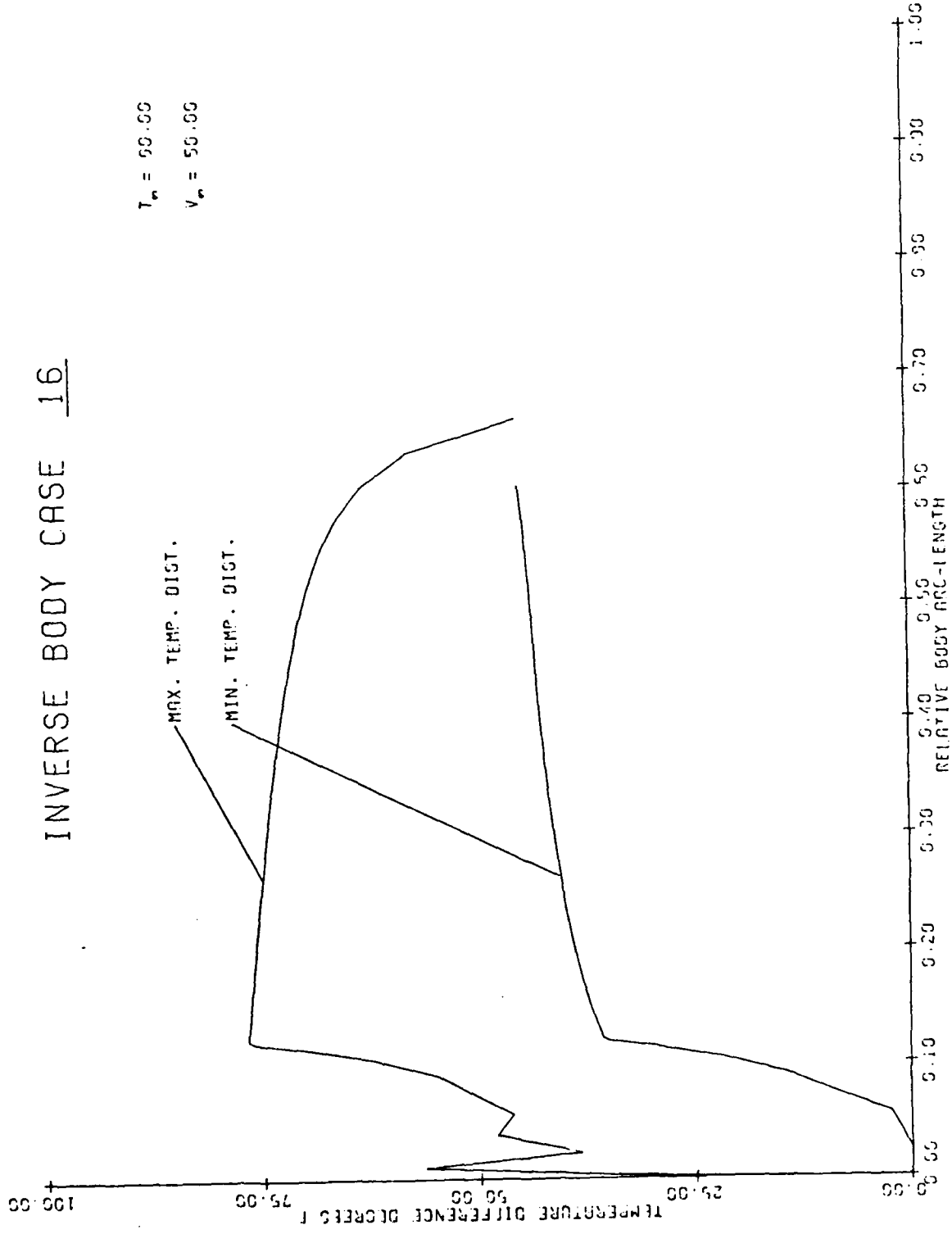

Figure 118, Temperature Distributions, Case No. 16.

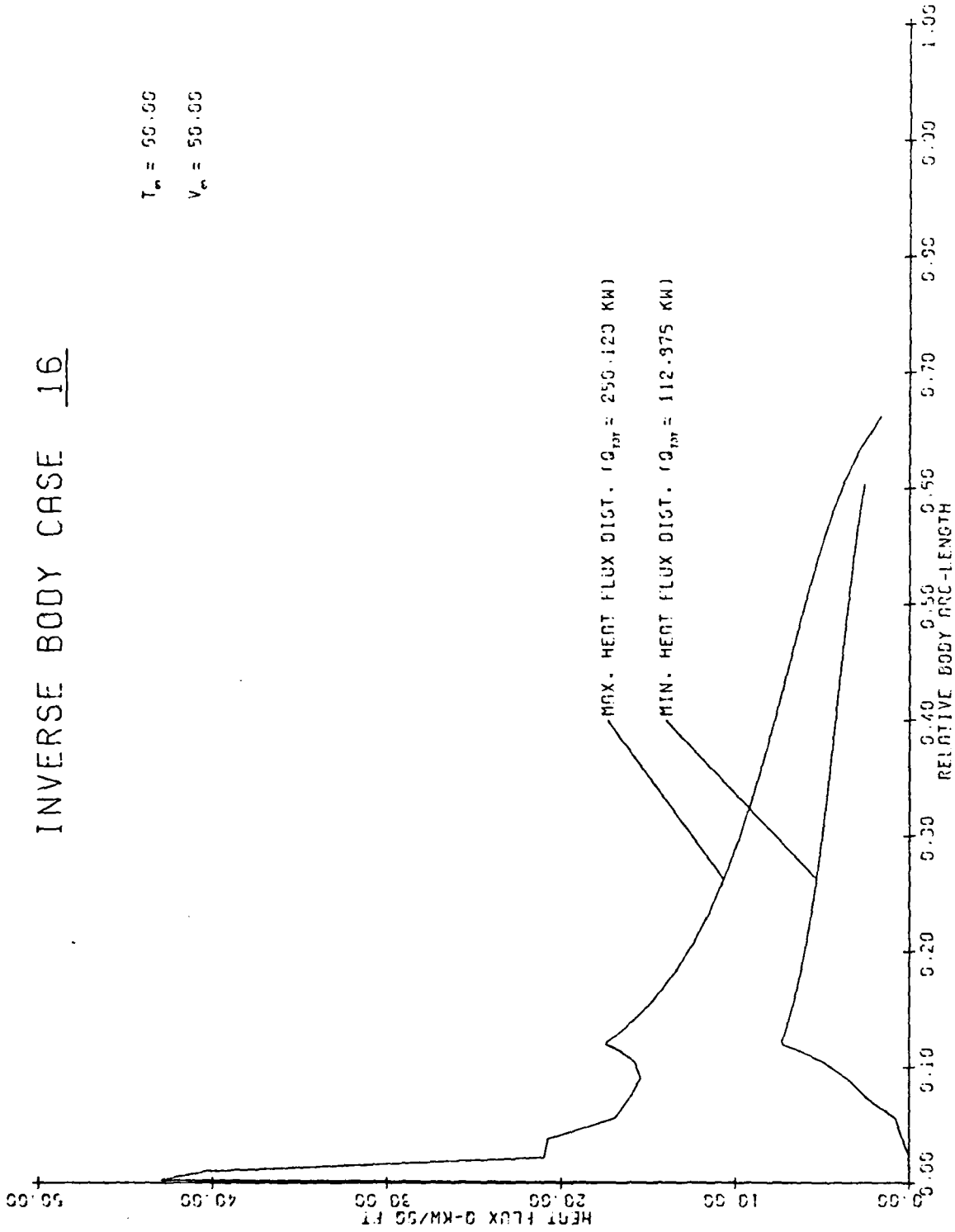

Figure 119. Heat Flux Distributions, Case No. 16.

19 August 1981
JJE:GHH:mmj

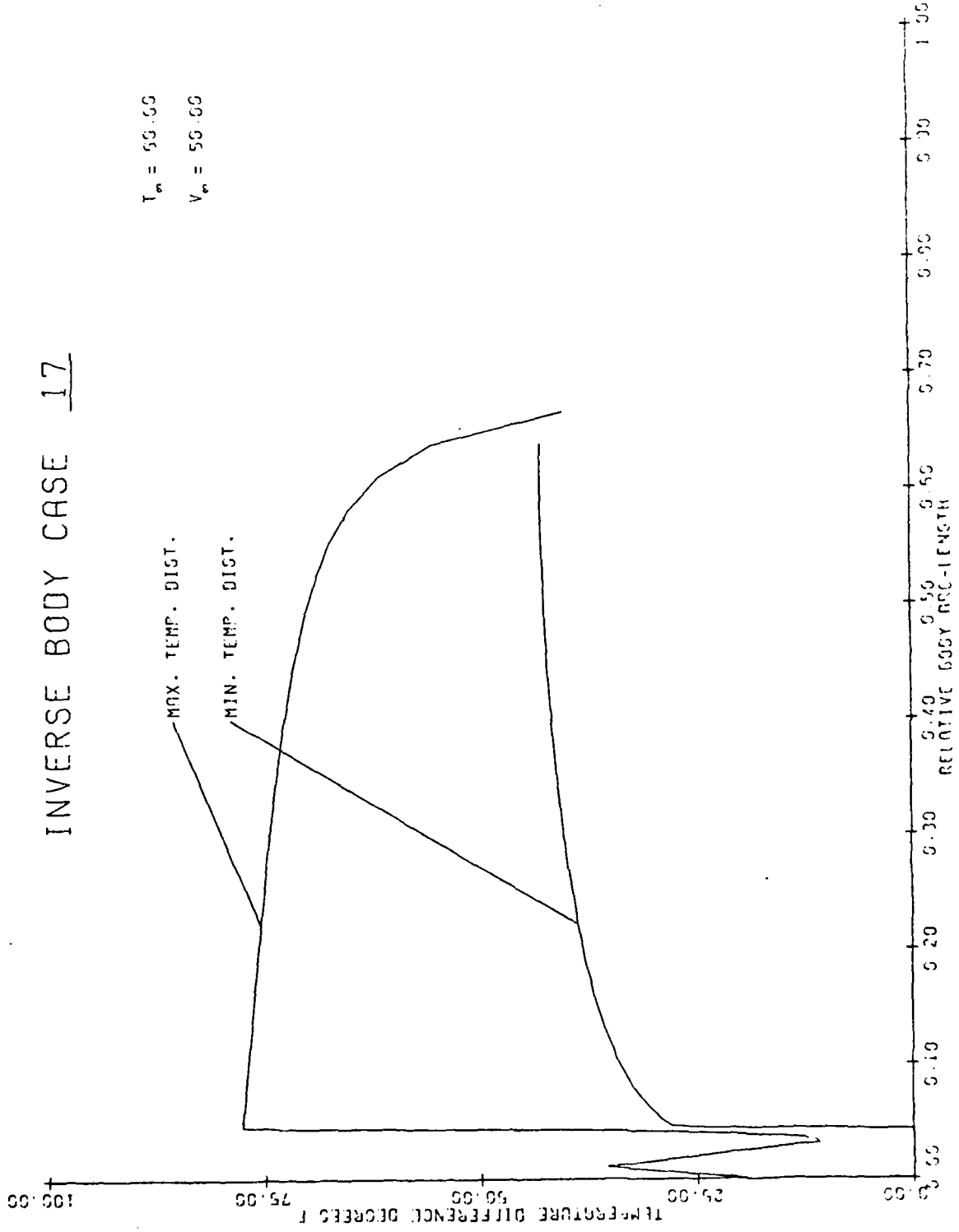

Figure 120. Temperature Distributions, Case No. 17.

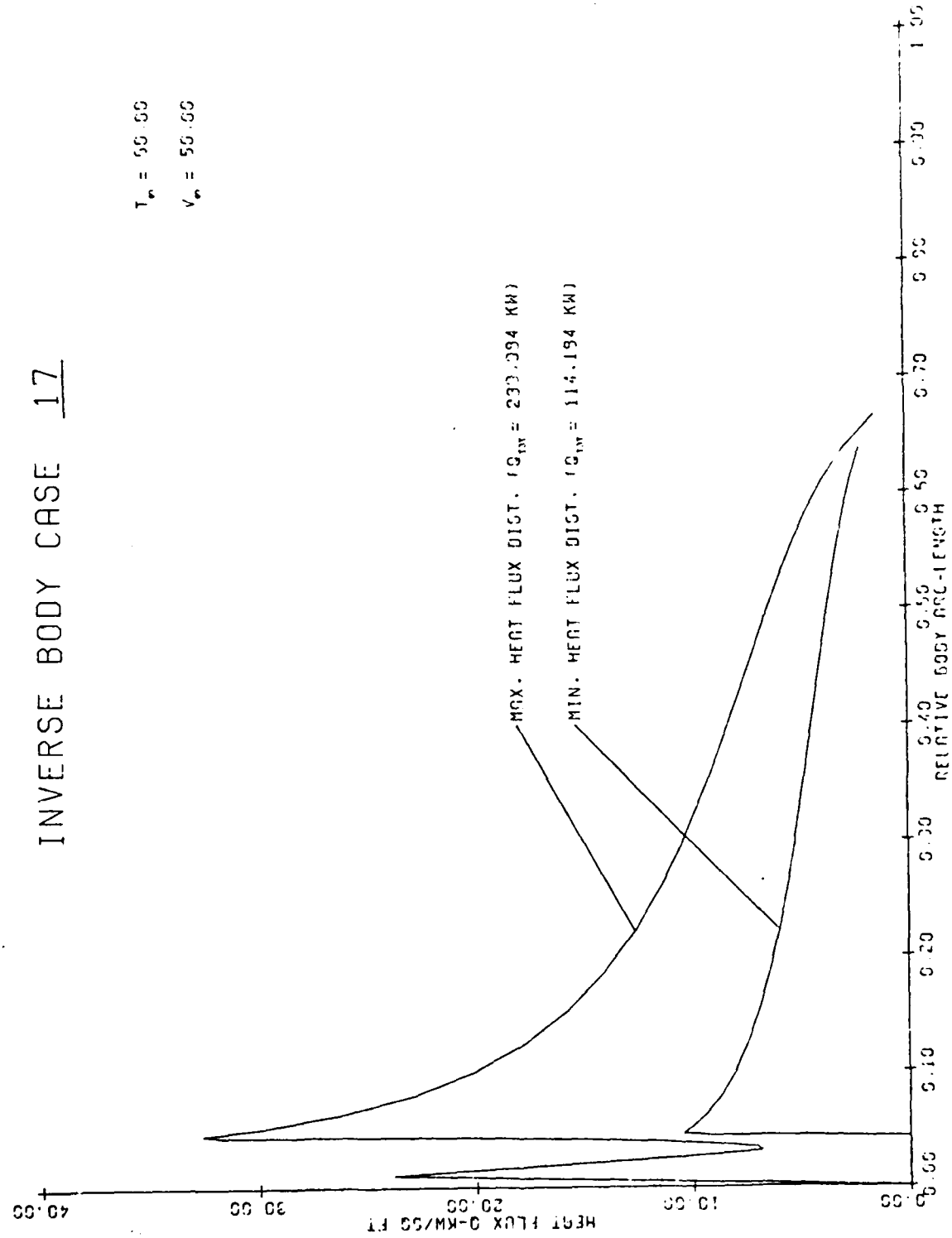

Figure 121. Heat Flux Distributions, Case No. 17

19 August 1981
JJE:GHH:mmj

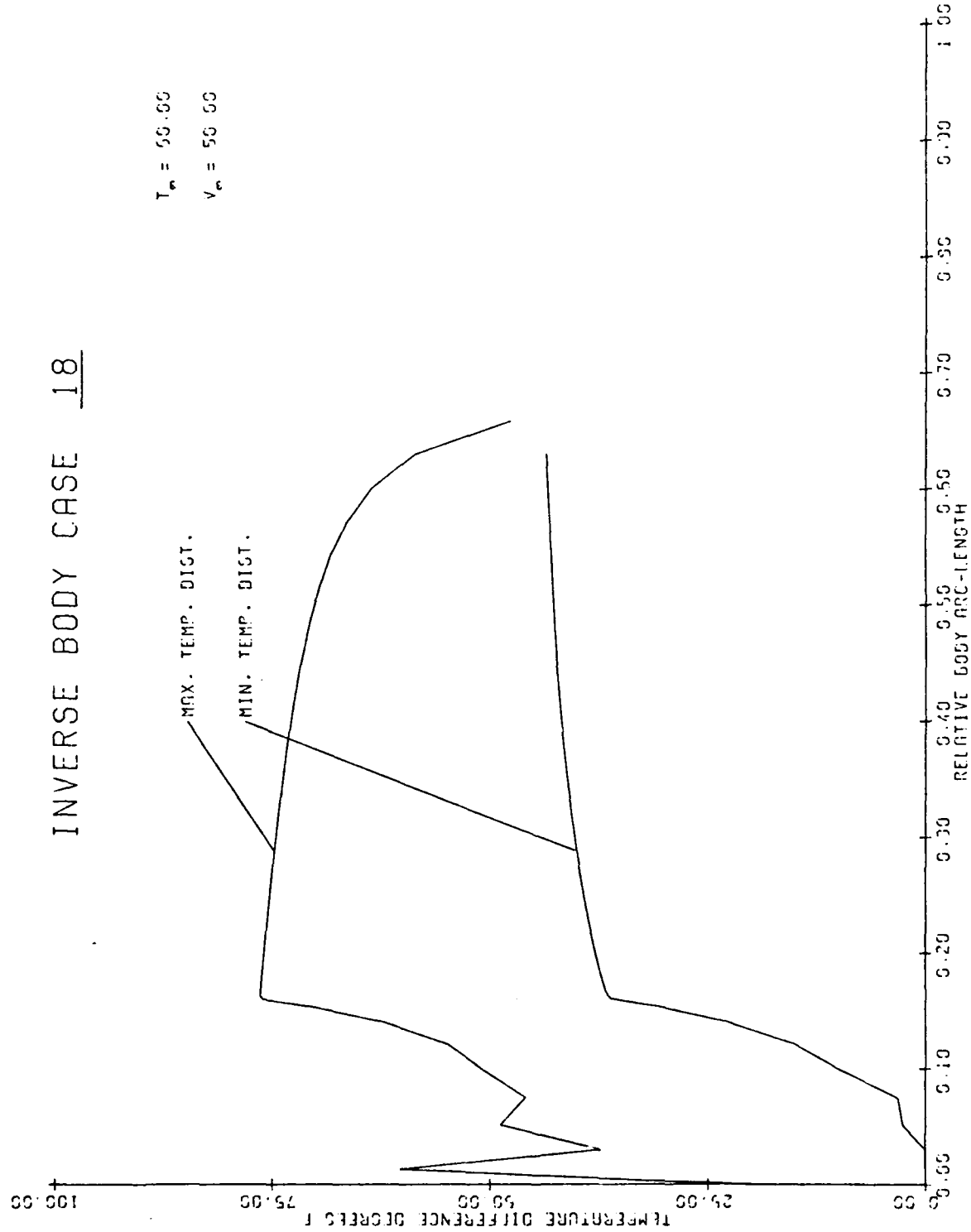

Figure 122. Temperature Distributions, Case No. 18.

19 August 1981
JJE:GHH:mmj

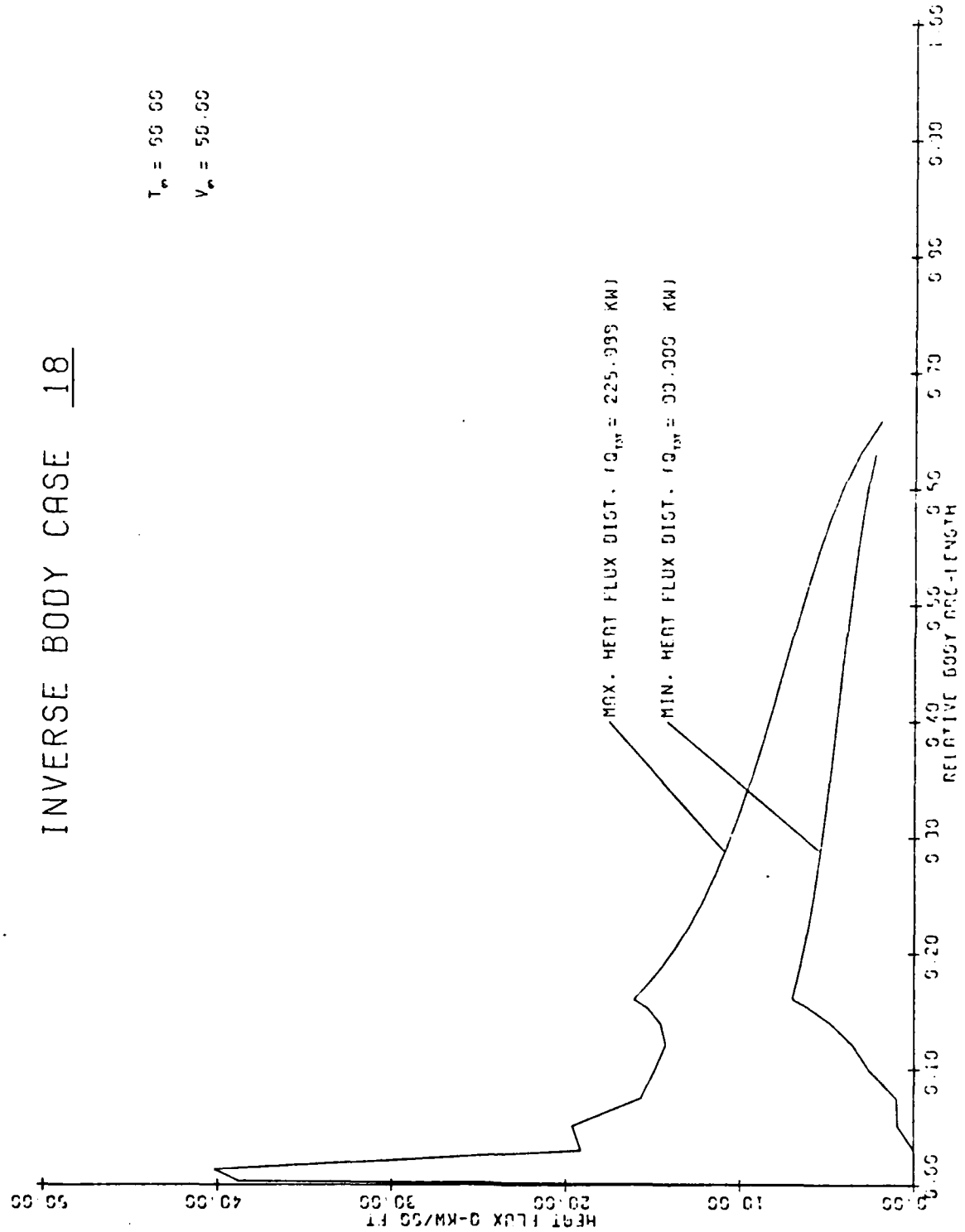

Figure 123. Heat Flux Distributions, Case No. 18.

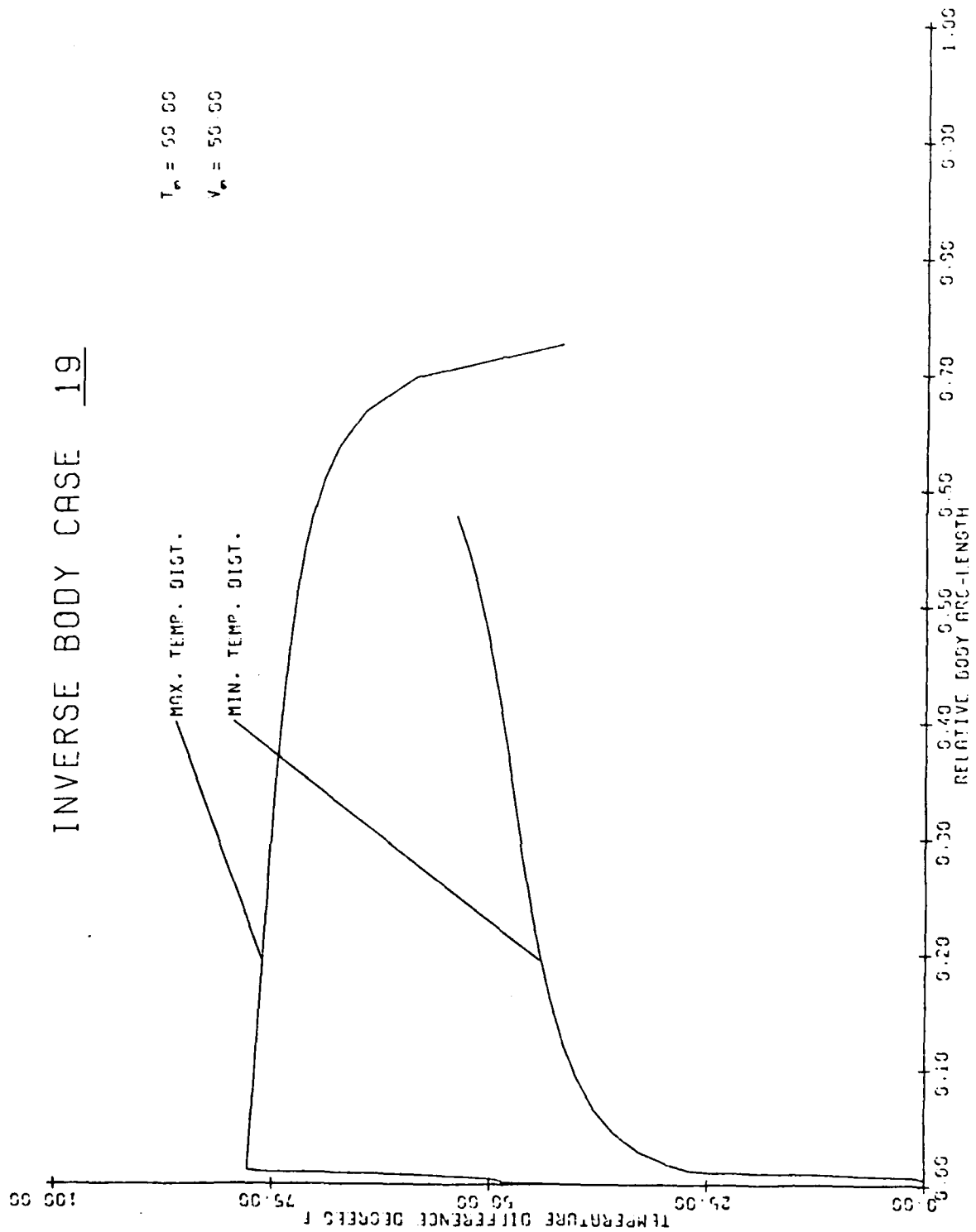

Figure 124. Temperature Distributions, Case No. 19.

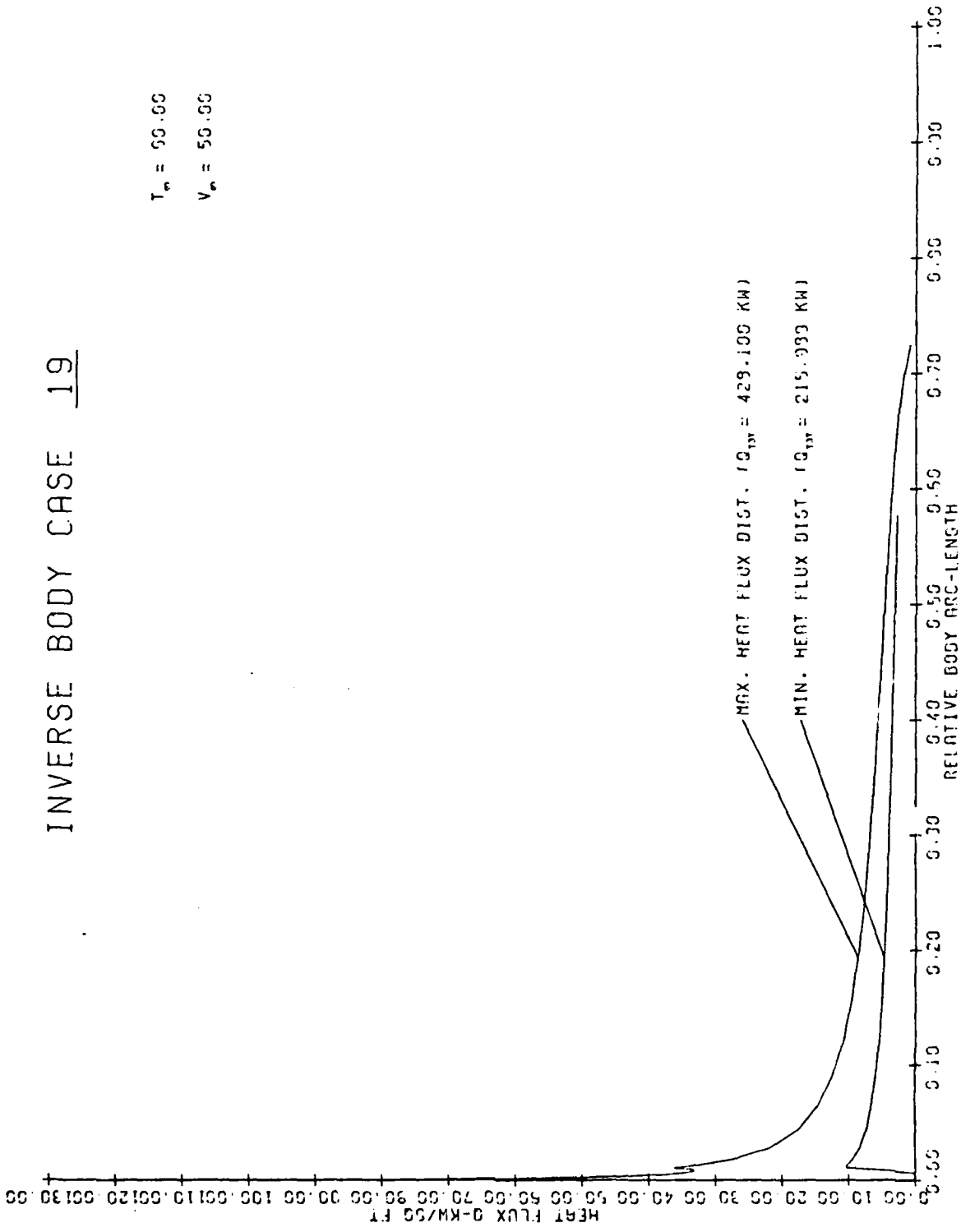

Figure 125. Heat Flux Distributions, Case No. 19.

19 August 1981
JJE:GHH:mmj

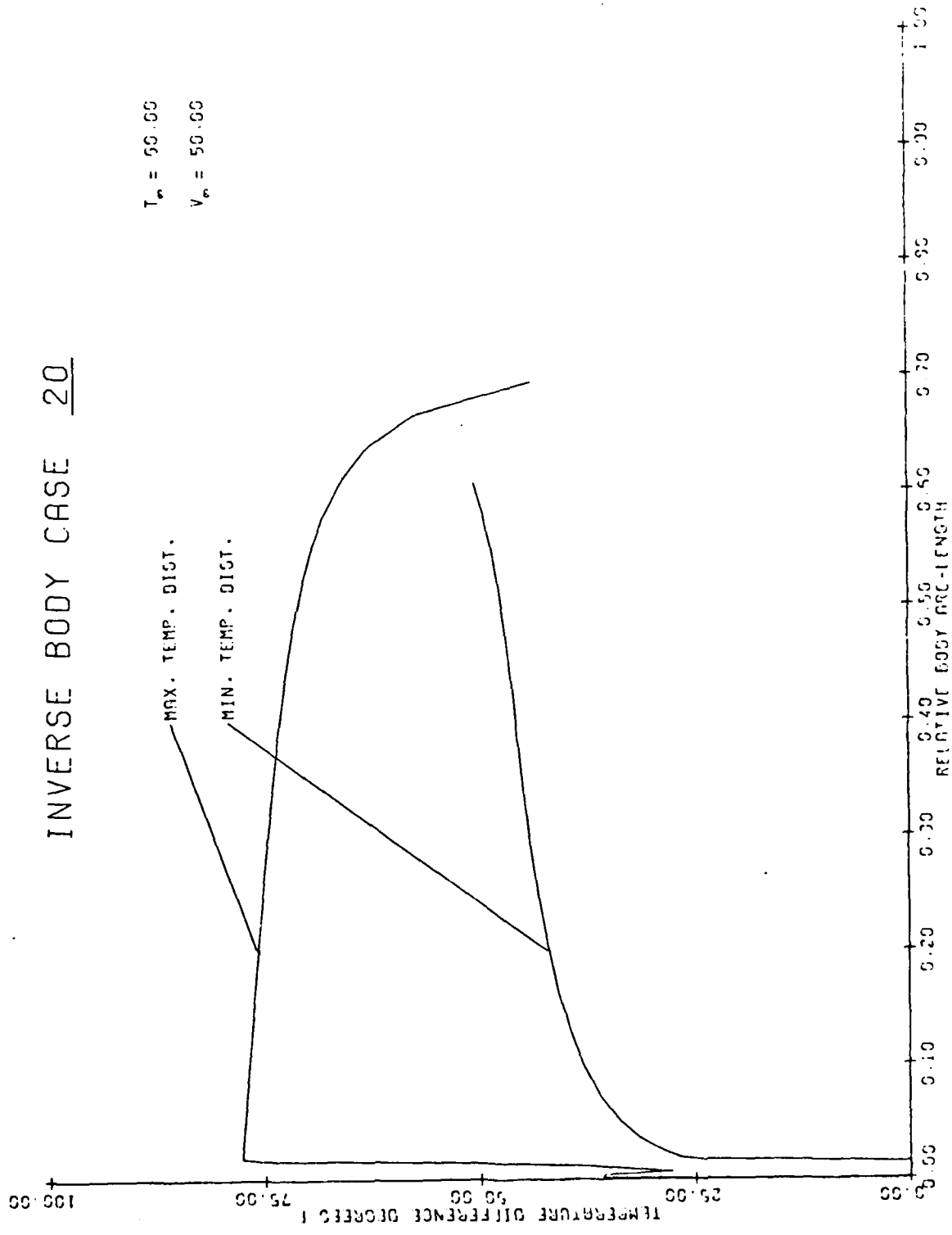

Figure 126. Temperature Distributions, Case No. 20.

19 August 1981
JJE:GHH:mmj

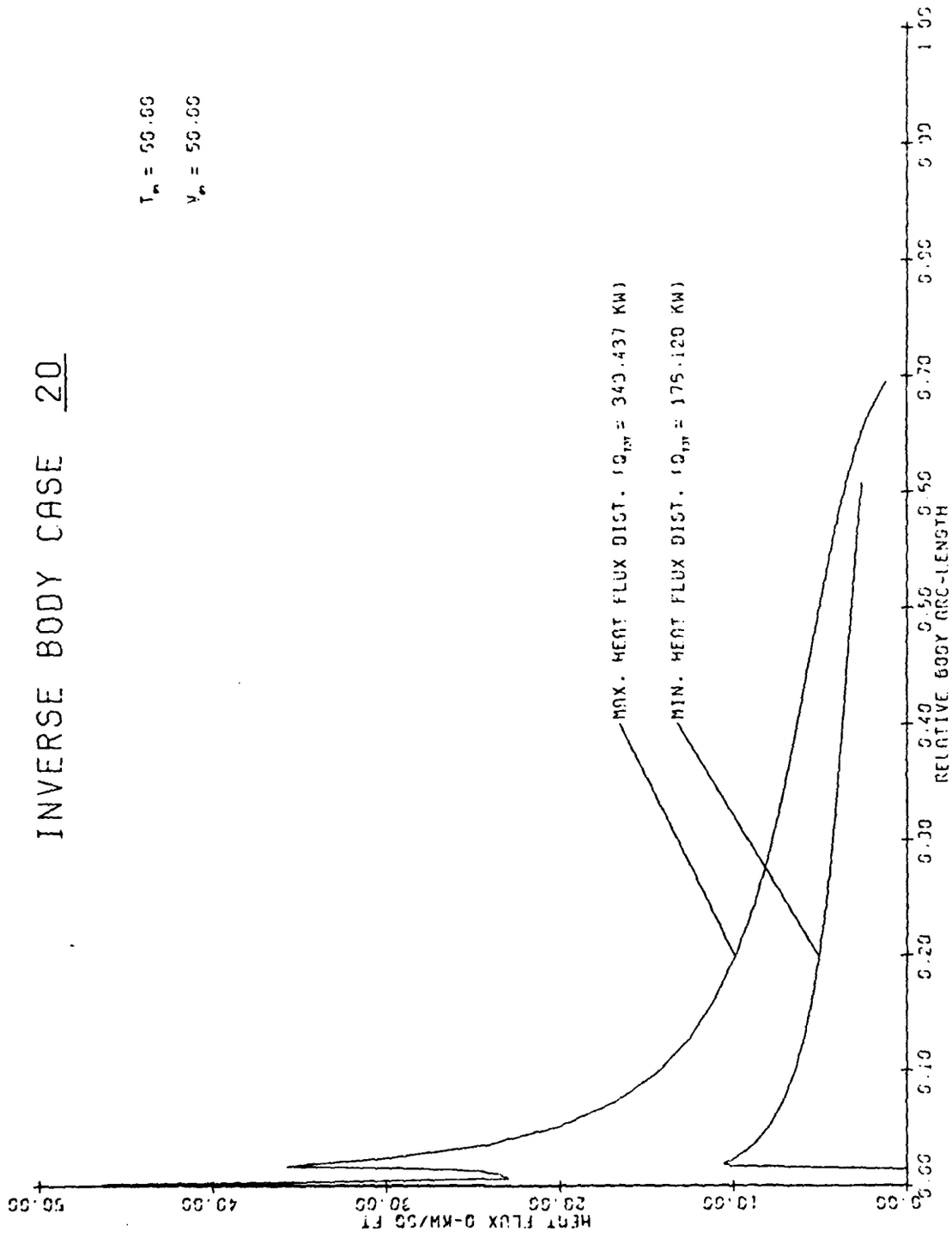

Figure 127. Heat Flux Distributions, Case No. 20.

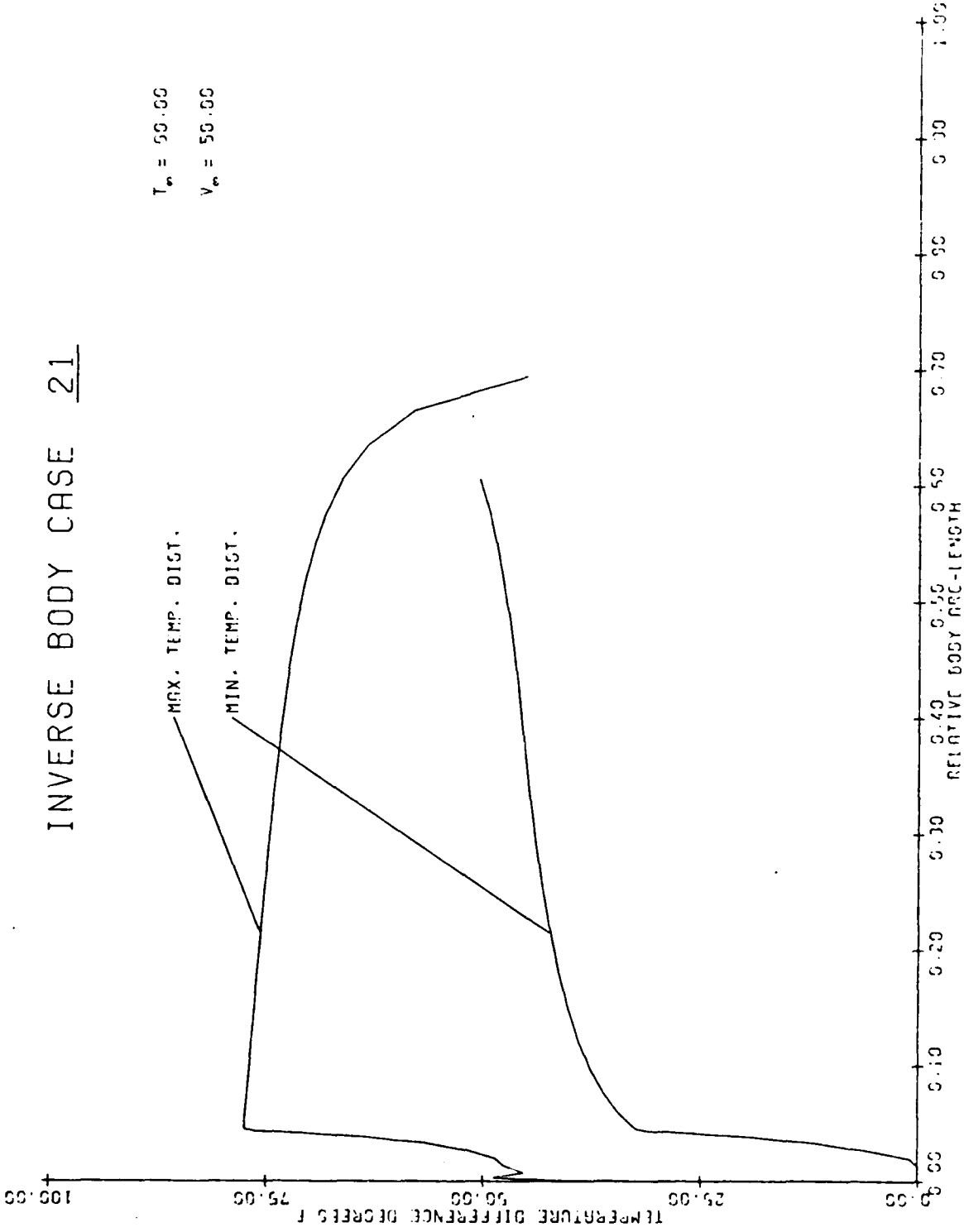

Figure 128. Temperature Distributions, Case No. 21.

19 August 1981
JJE:GHH:mmj

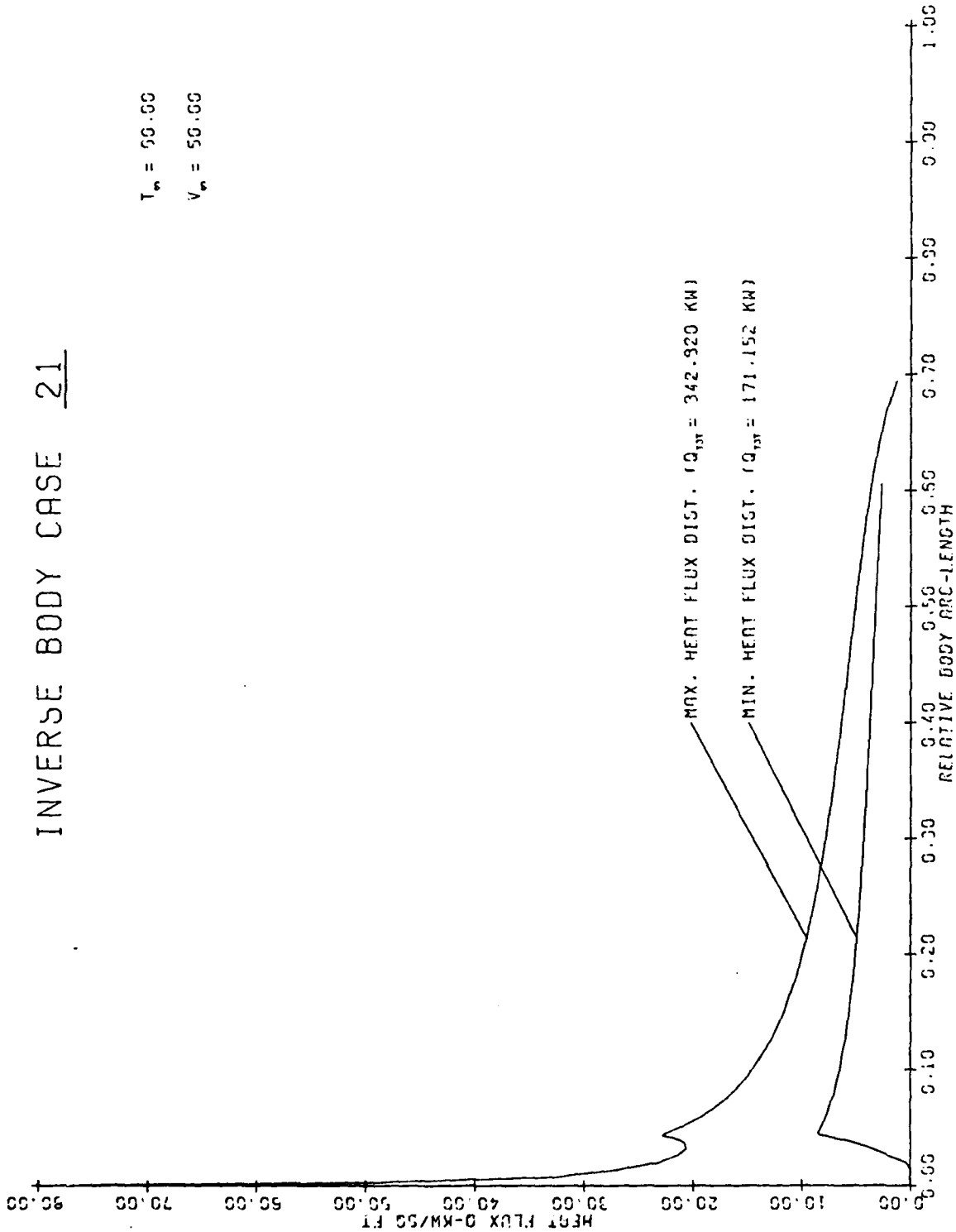

Figure 129. Heat Flux Distributions, Case No. 21.

19 August 1981
JJE:GHH:mmj

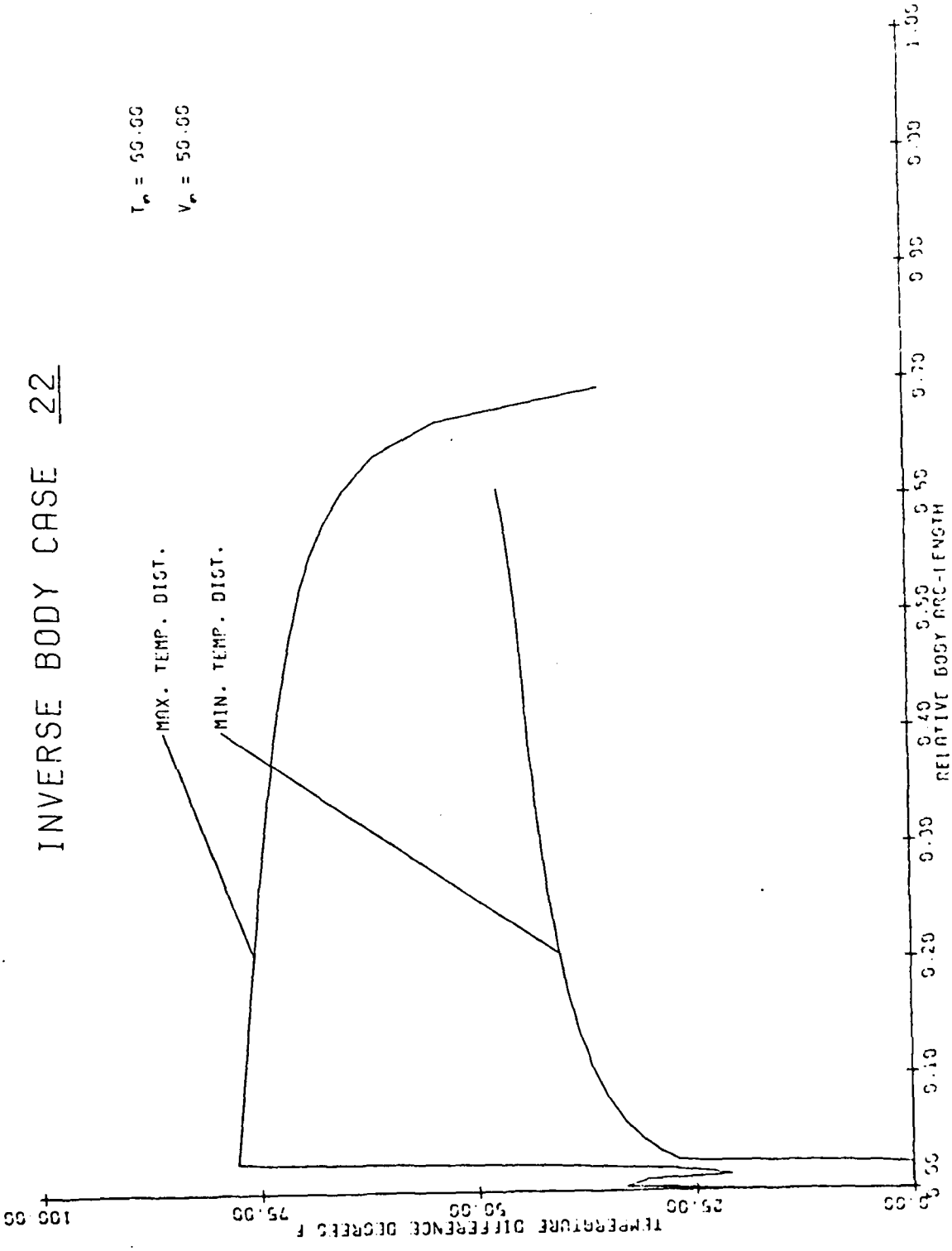

Figure 130. Temperature Distributions, Case No. 22.

19 August 1981
JJE:GHH:mmj

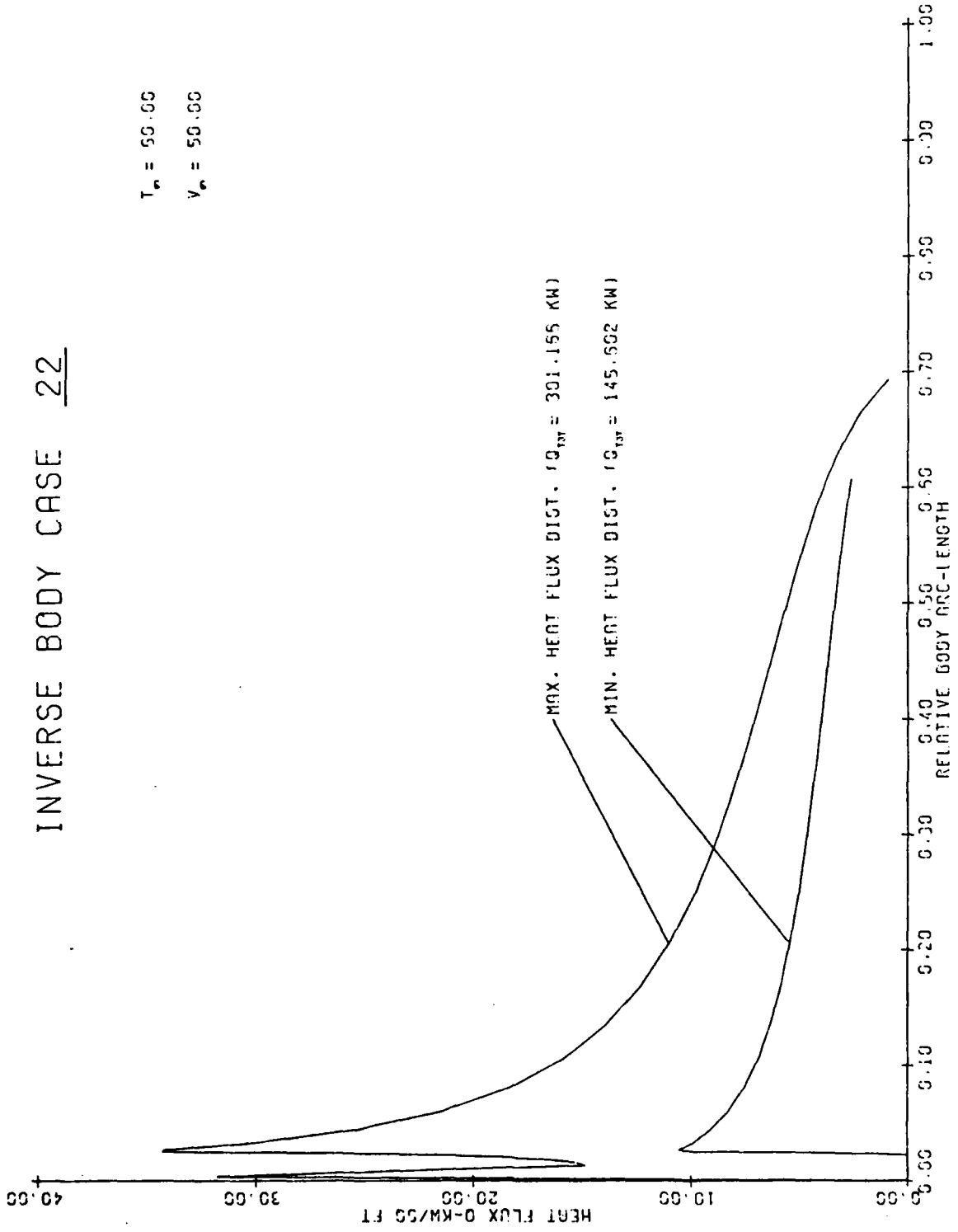

Figure 131. Heat Flux Distributions, Case No. 22.

19 August 1981
JJE:GHH:mmj

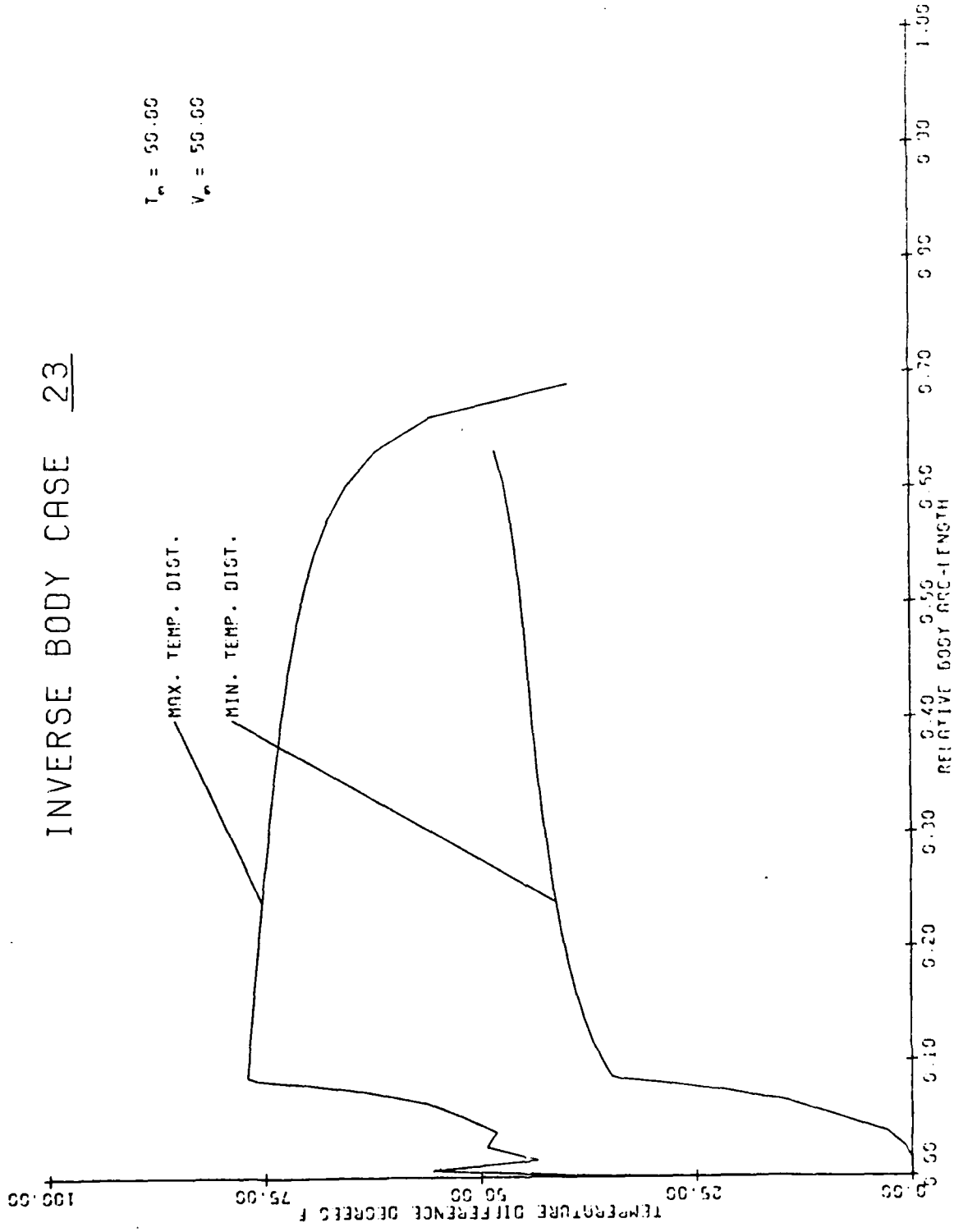

Figure 132. Temperature Distributions, Case No. 23.

19 August 1981
JJE:GHH:mmj

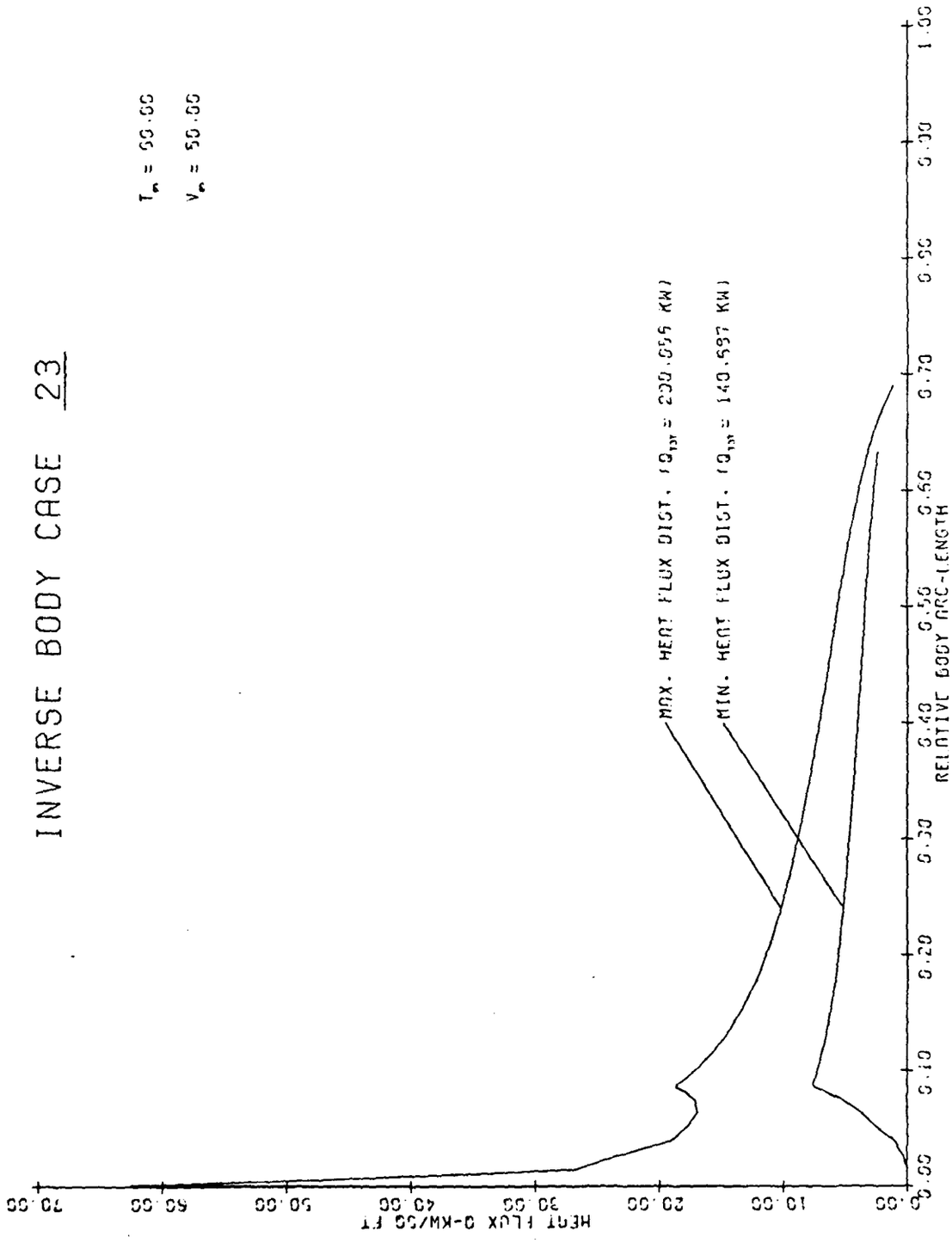

Figure 133. Heat Flux Distributions, Case No. 23.

19 August 1981
JJE:GHH:mmj

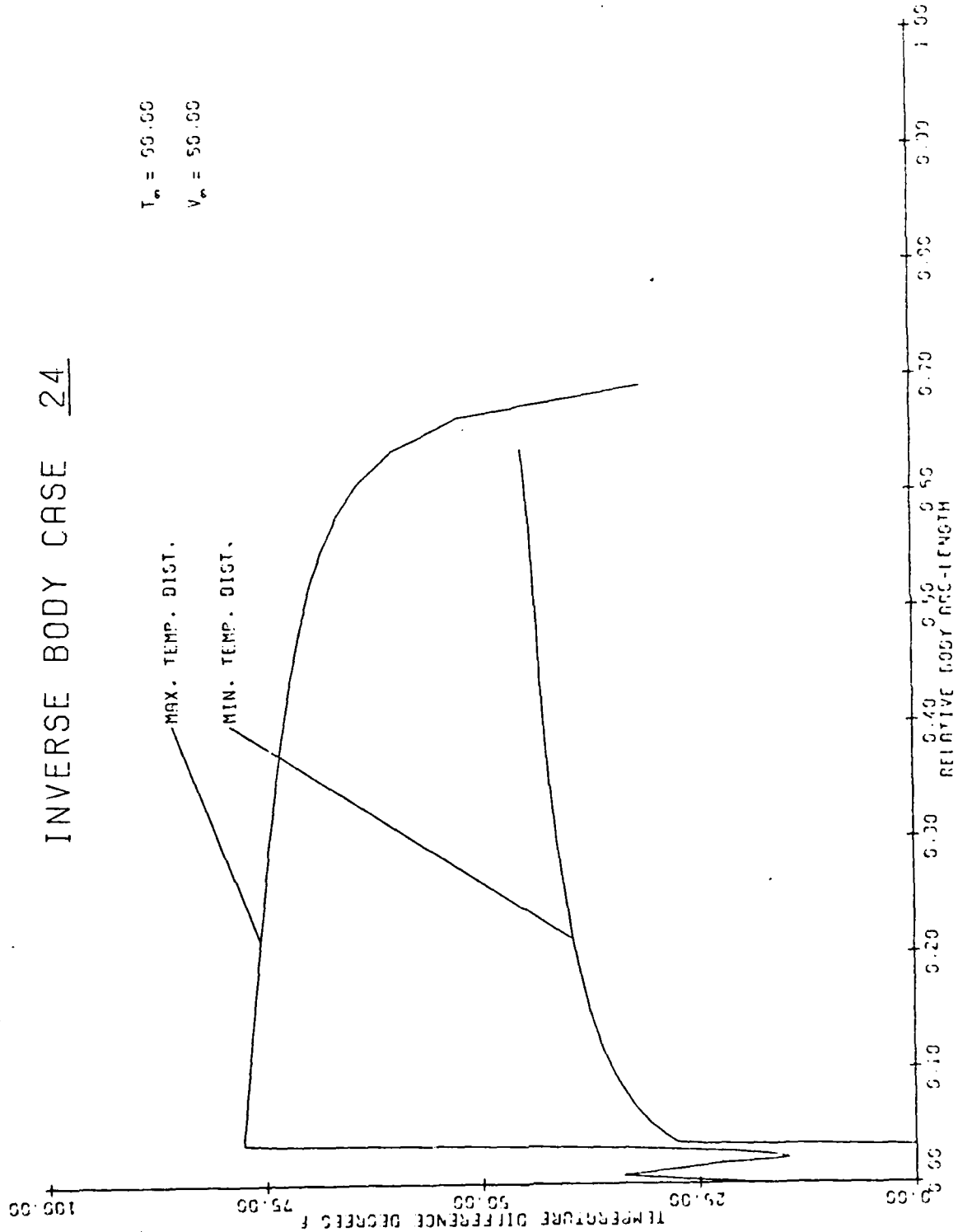

Figure 134. Temperature Distributions, Case No. 24.

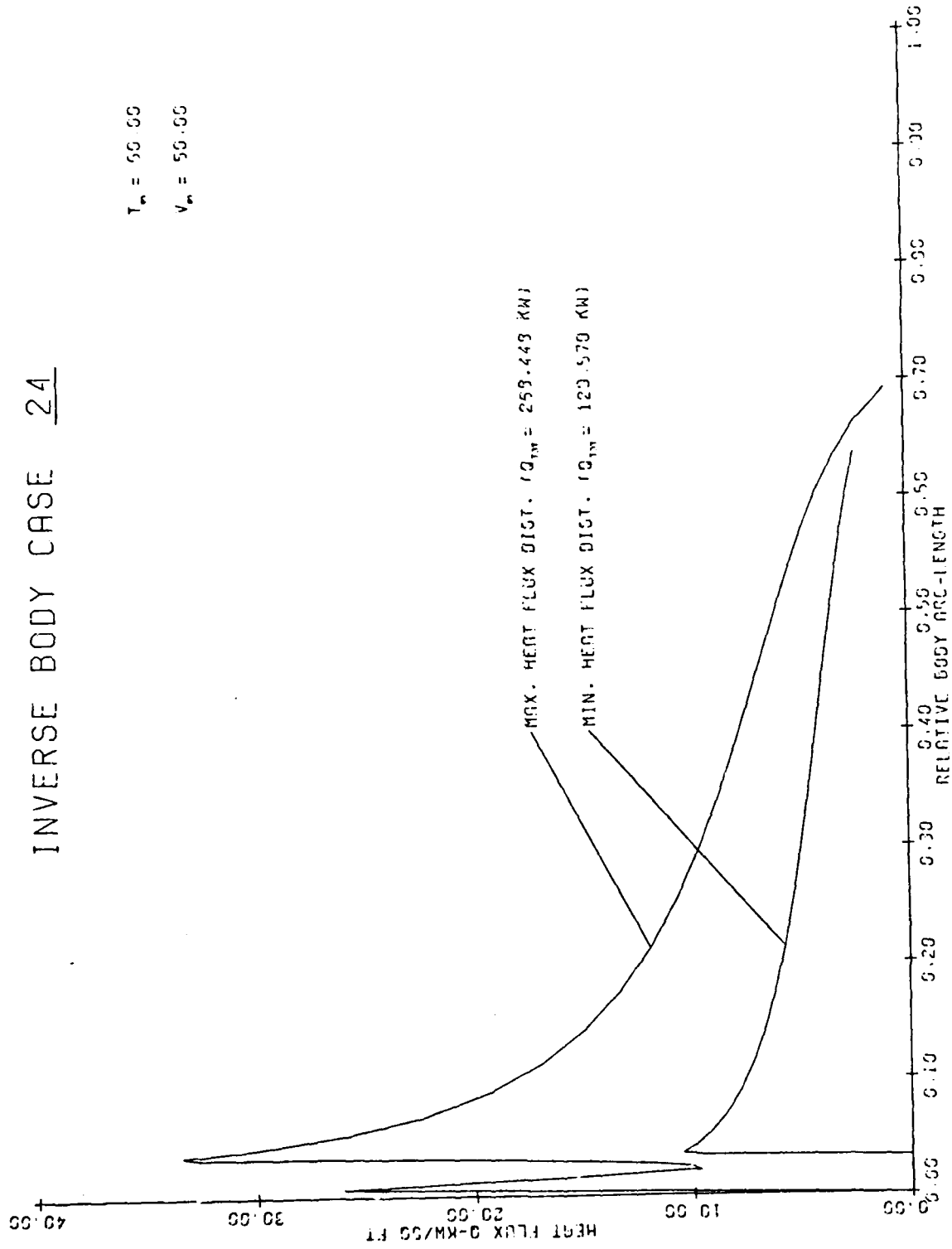

Figure 135. Heat Flux Distributinons, Case No. 24.

19 August 1981
JJE:GHH:mmj

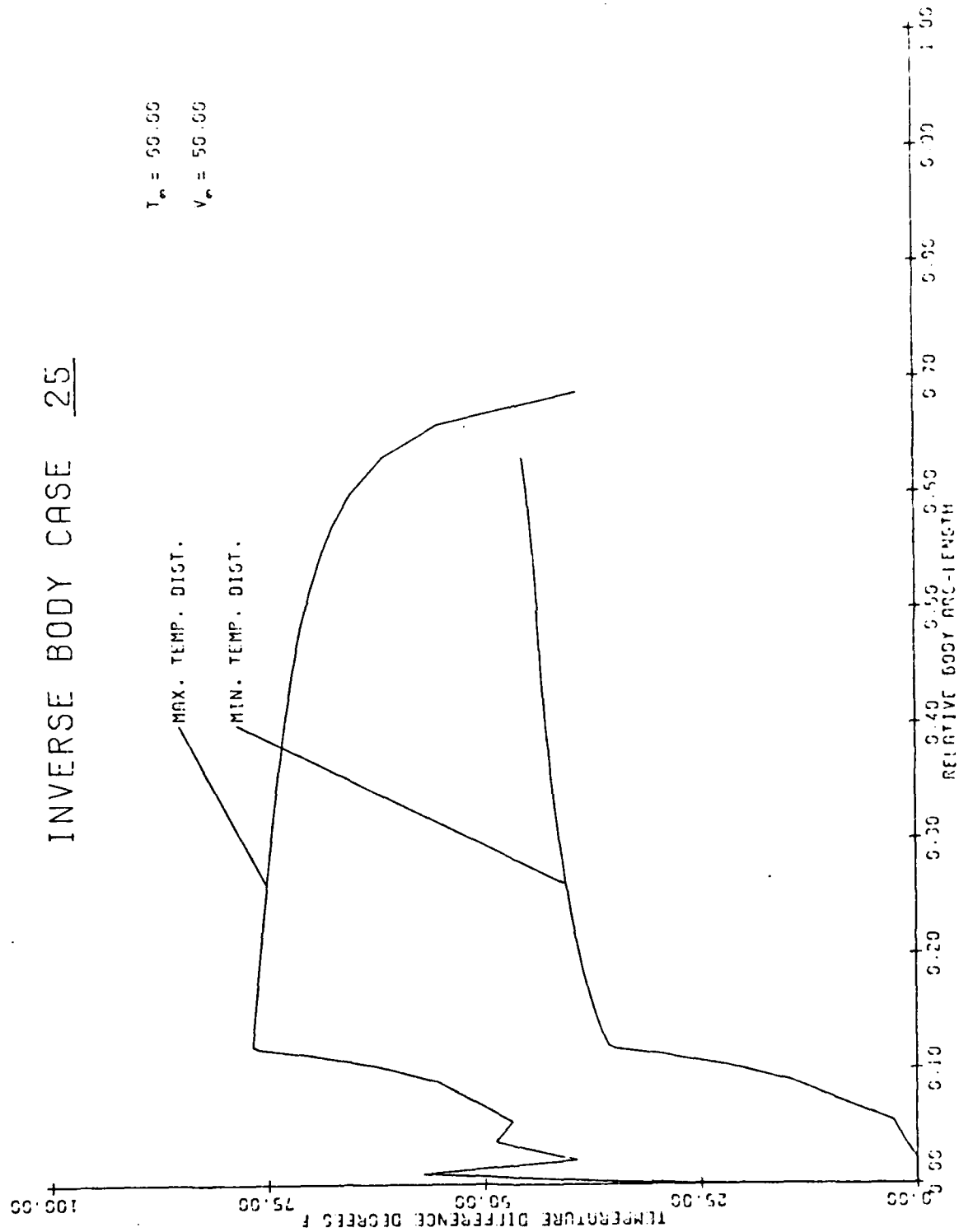

Figure 136. Temperature Distributions, Case No. 25.

19 August 1981
JJE:GHH:mmj

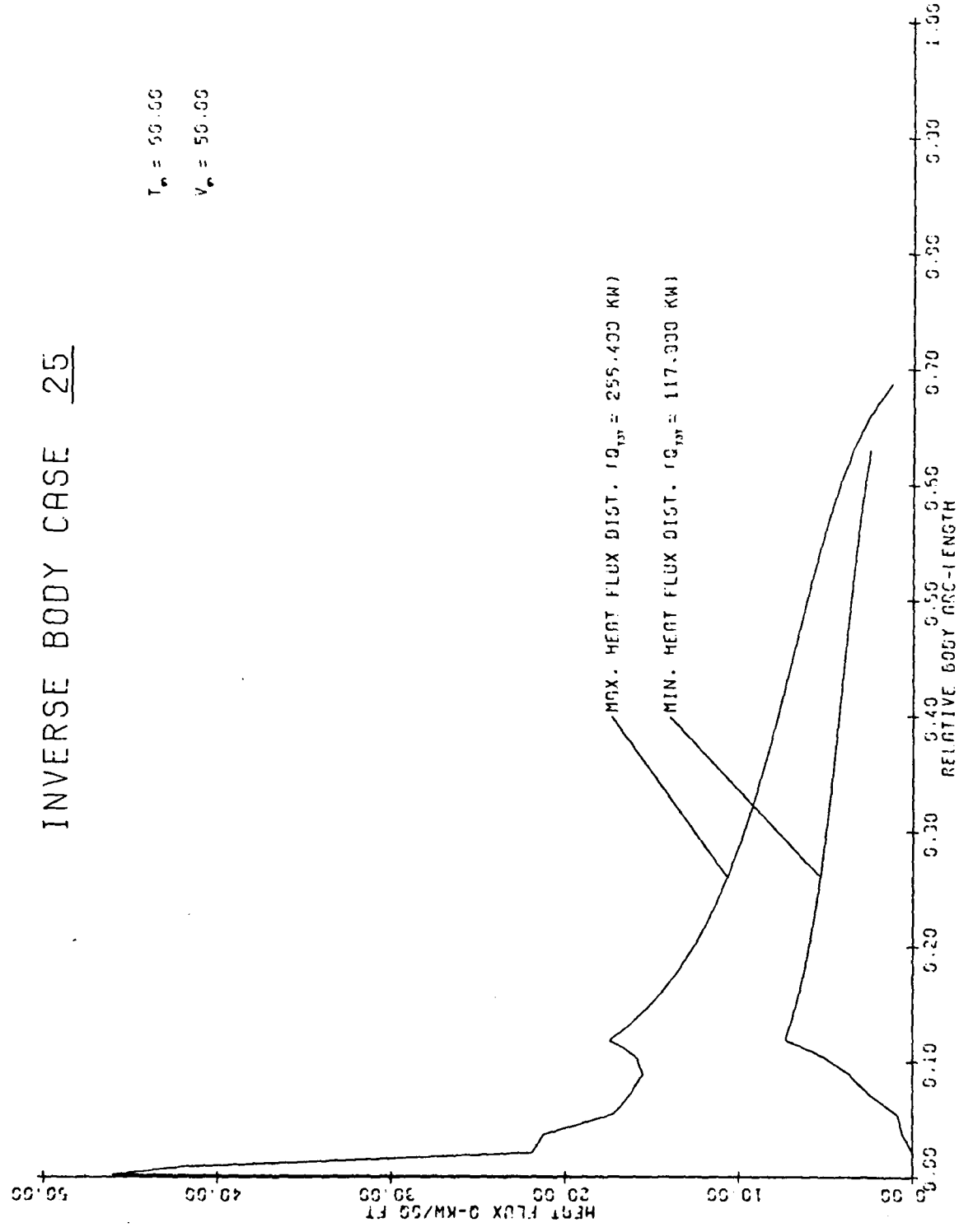

Figure 137. Heat Flux Distributions, Case No. 25.

19 August 1981
JJE:GHH:mmj

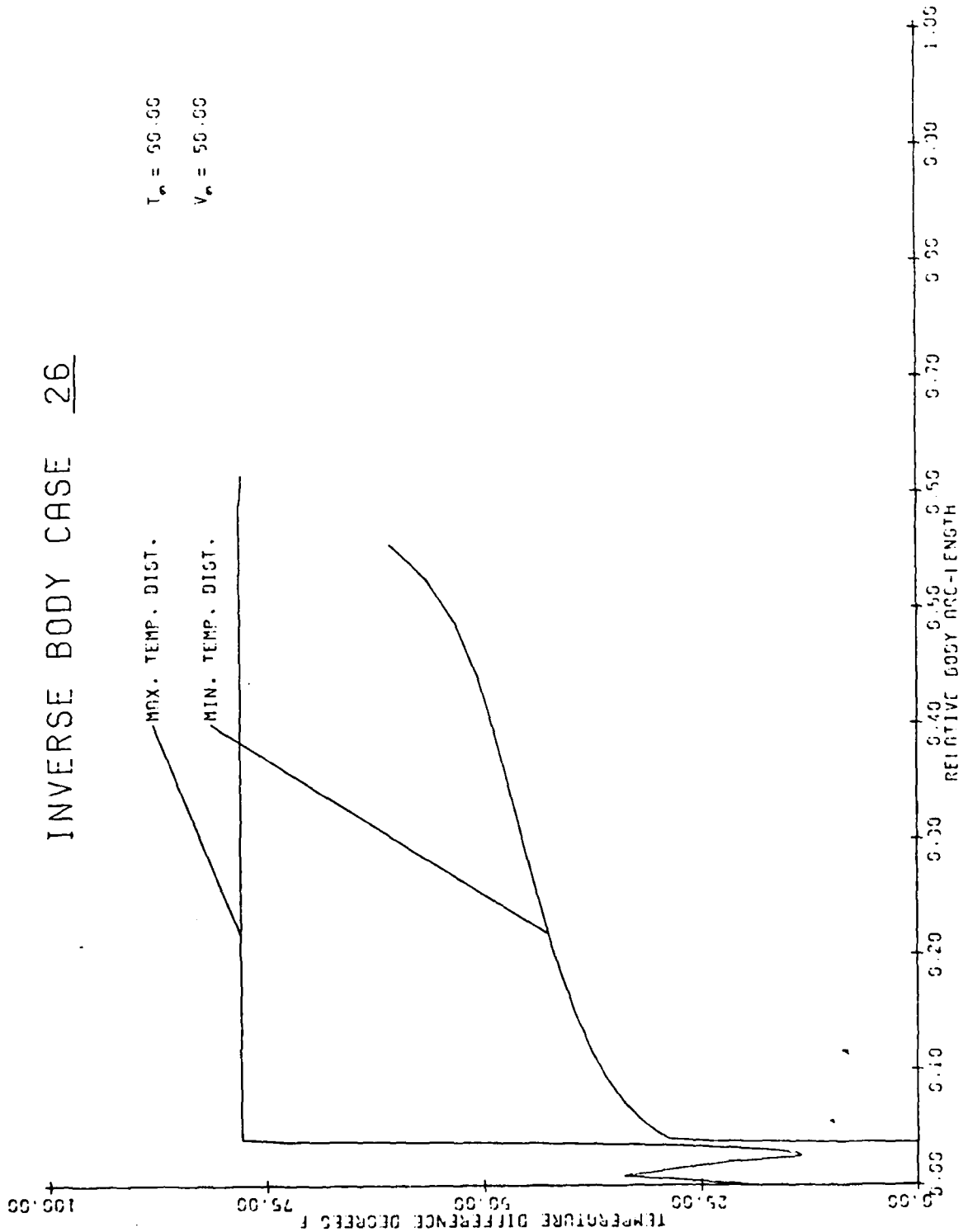

Figure 138. Temperature Distributions, Case No. 26.

19 August 1981
JJE:GHH:mmj

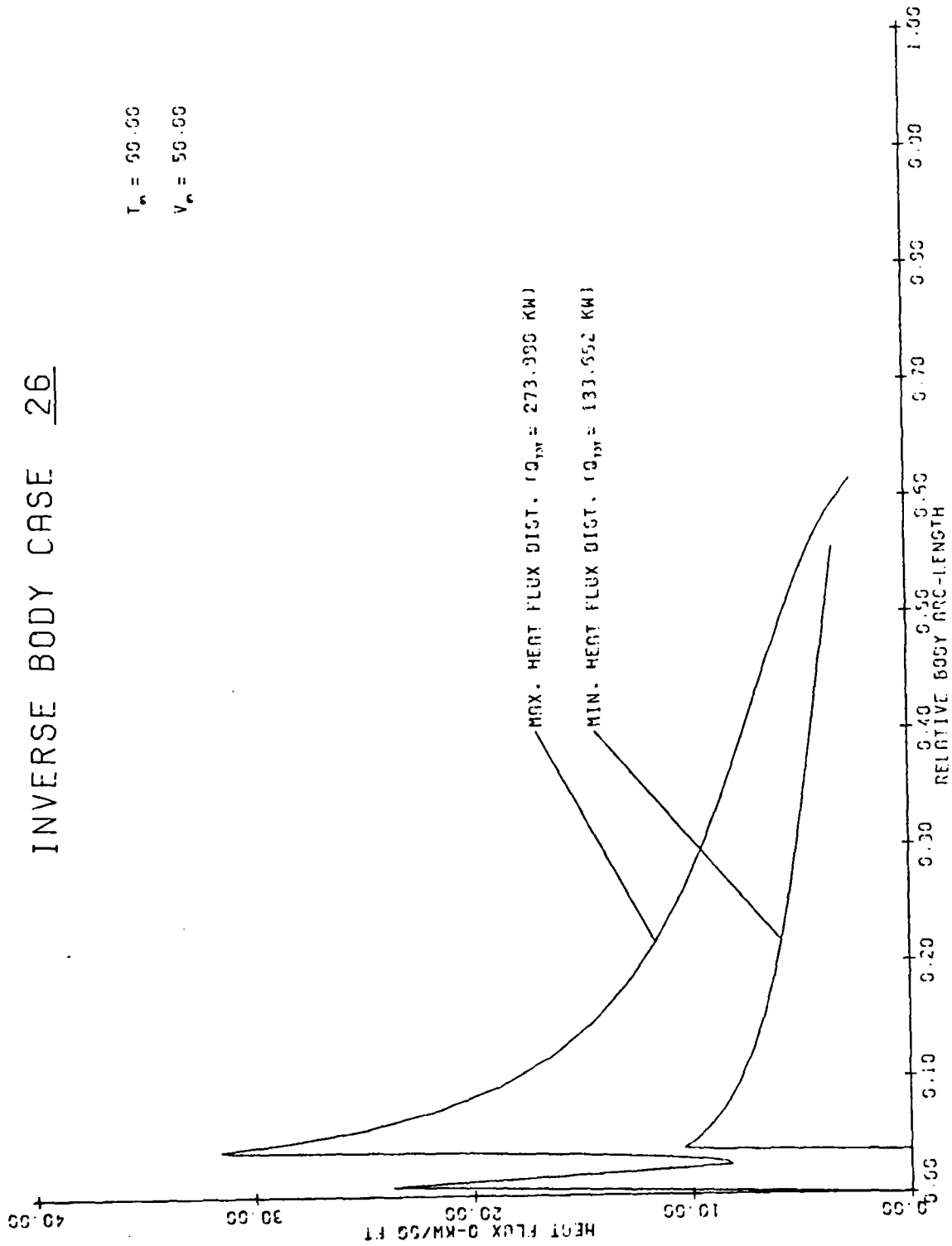

Figure 139. Heat Flux Distributions, Case No. 26.

19 August 1981
JJE:GHH:mmj

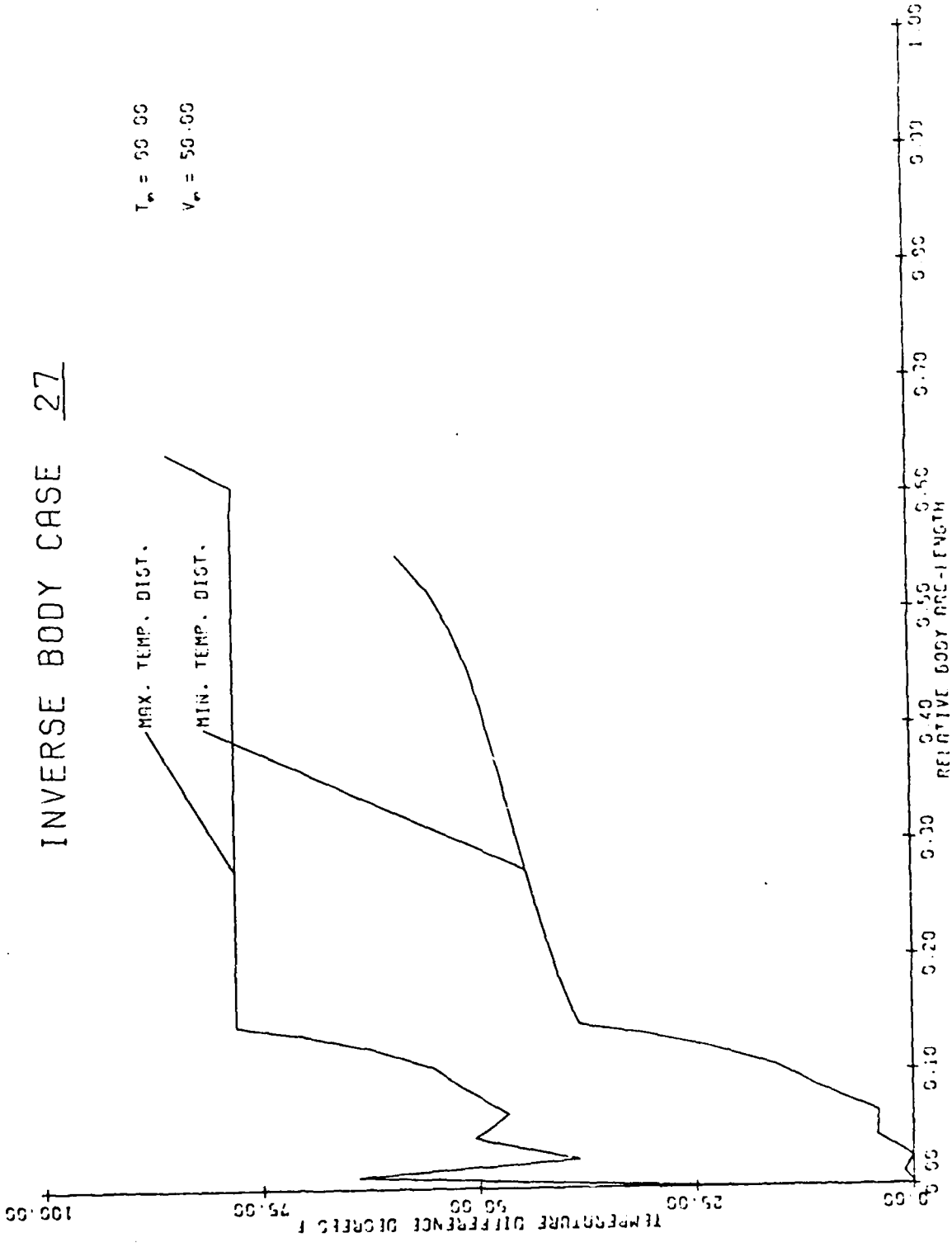

Figure 140. Temperature Distributions, Case No. 27.

19 August 1981
JJE:GHH:mmj

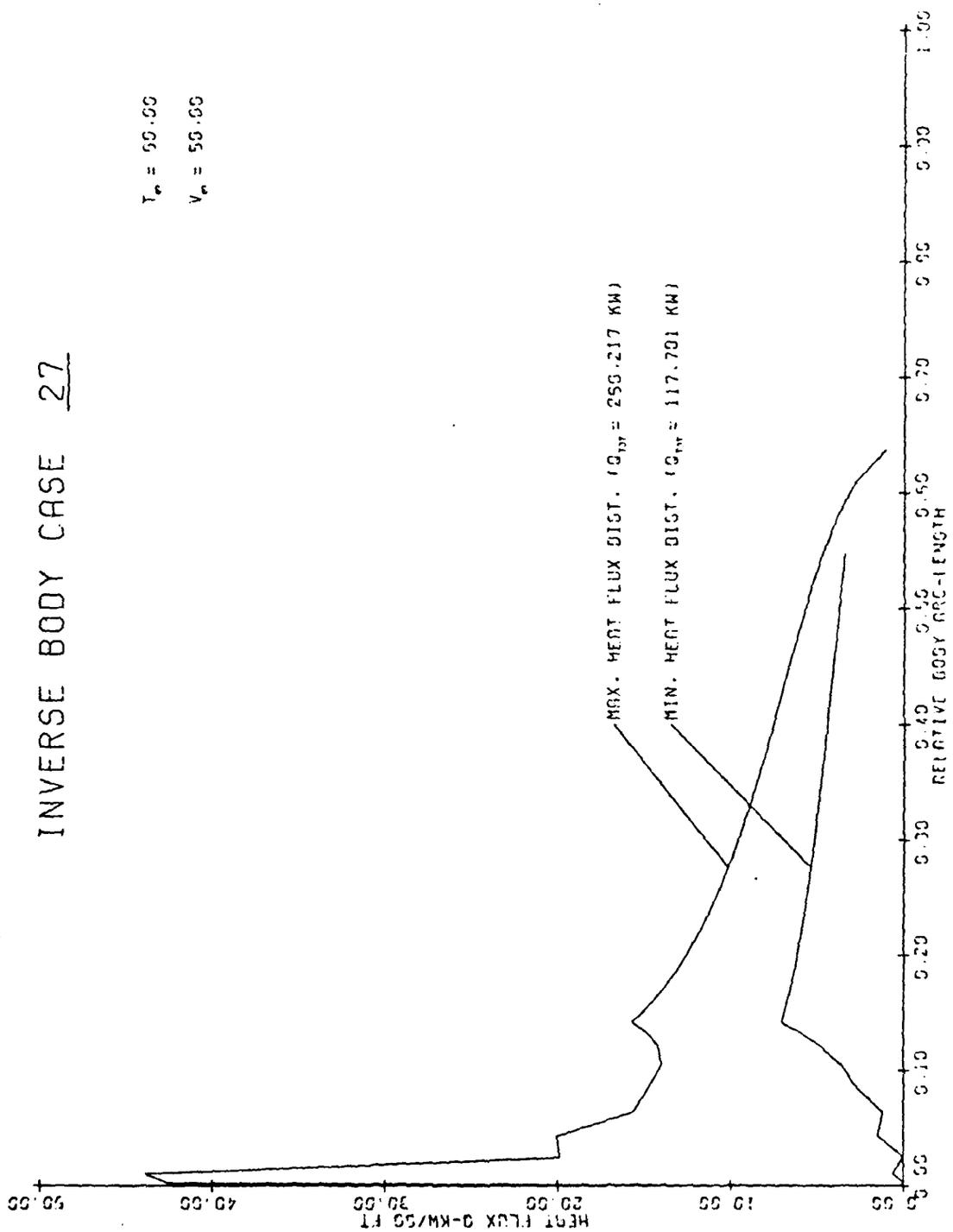

Figure 141. Heat Flux Distributions, Case No. 27.

19 August 1981
JJE:GHH:mmj

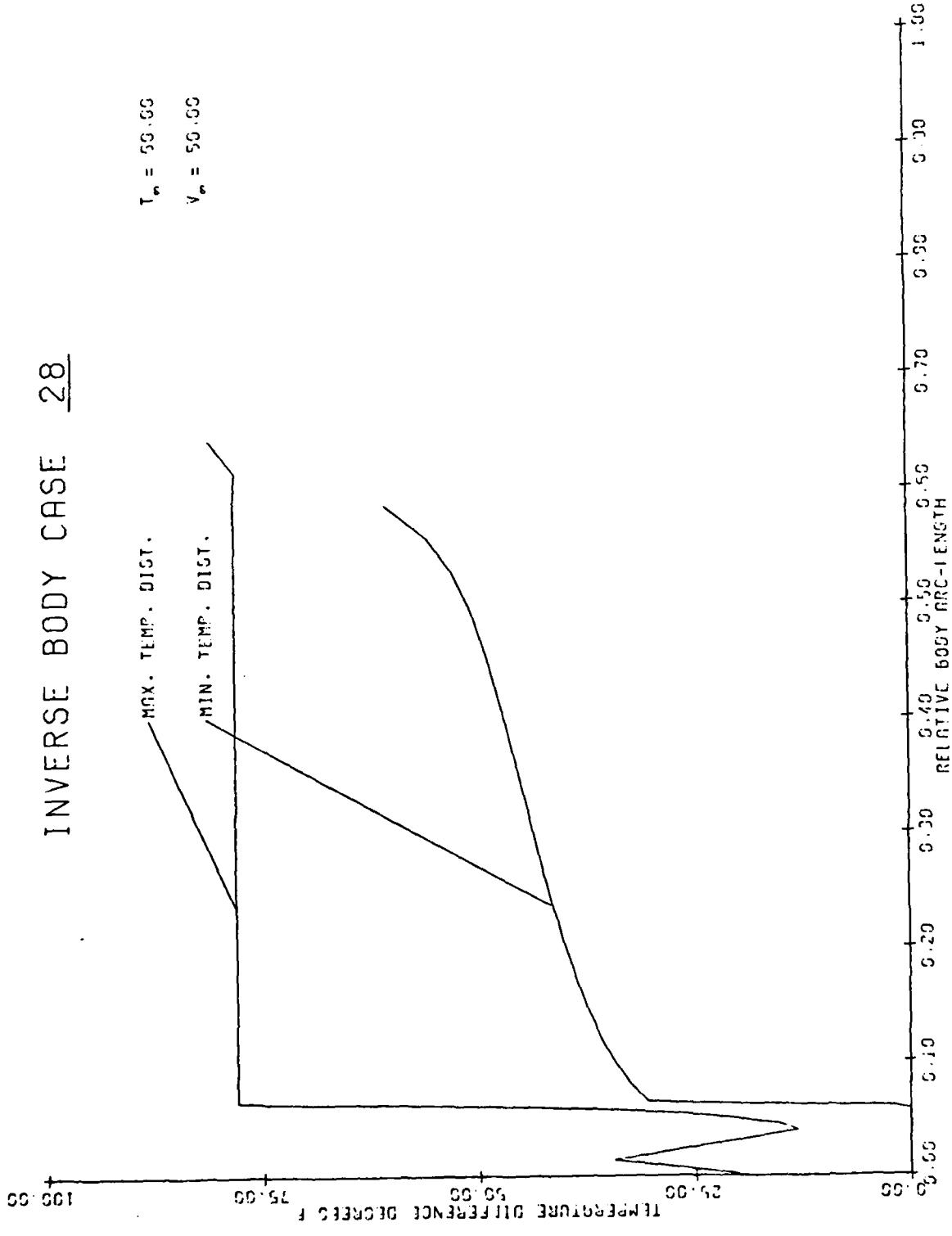

Figure 142. Temperature Distributions, Case No. 28.

19 August 1981
JJE:GHH:mmj

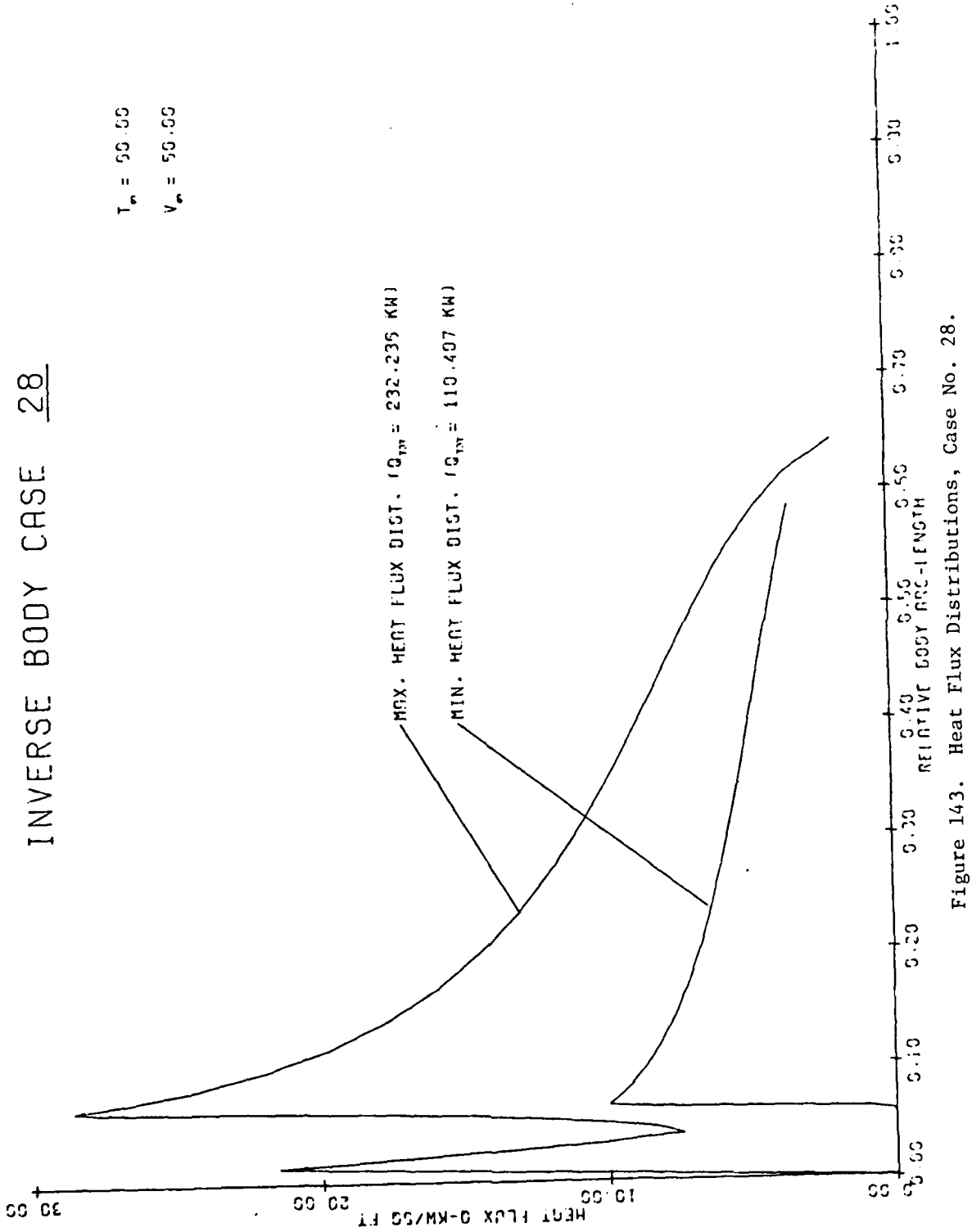

Figure 143. Heat Flux Distributions, Case No. 28.

19 August 1981
JJE:GHH:mmj

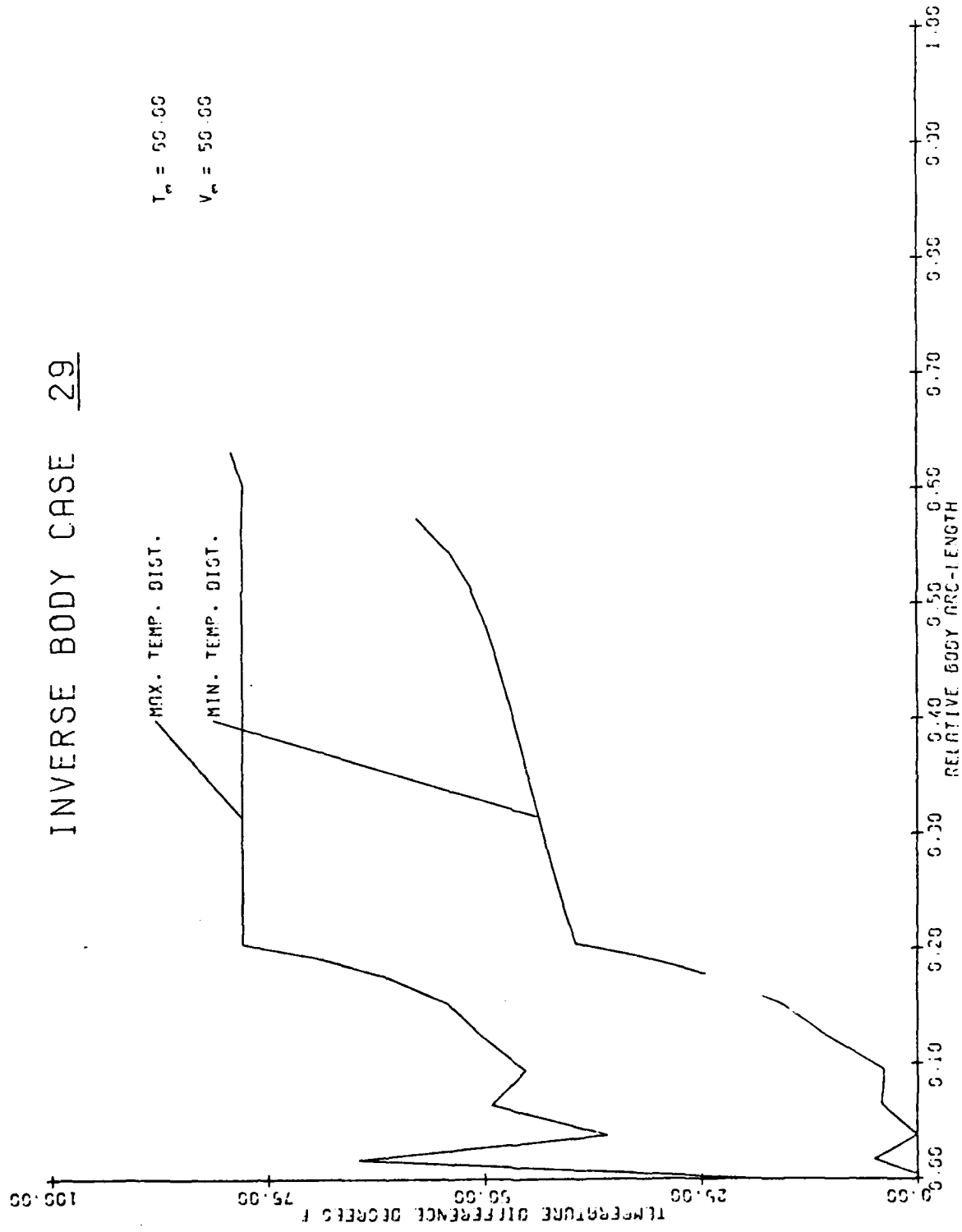

Figure 144. Temperature Distributions, Case No. 29.

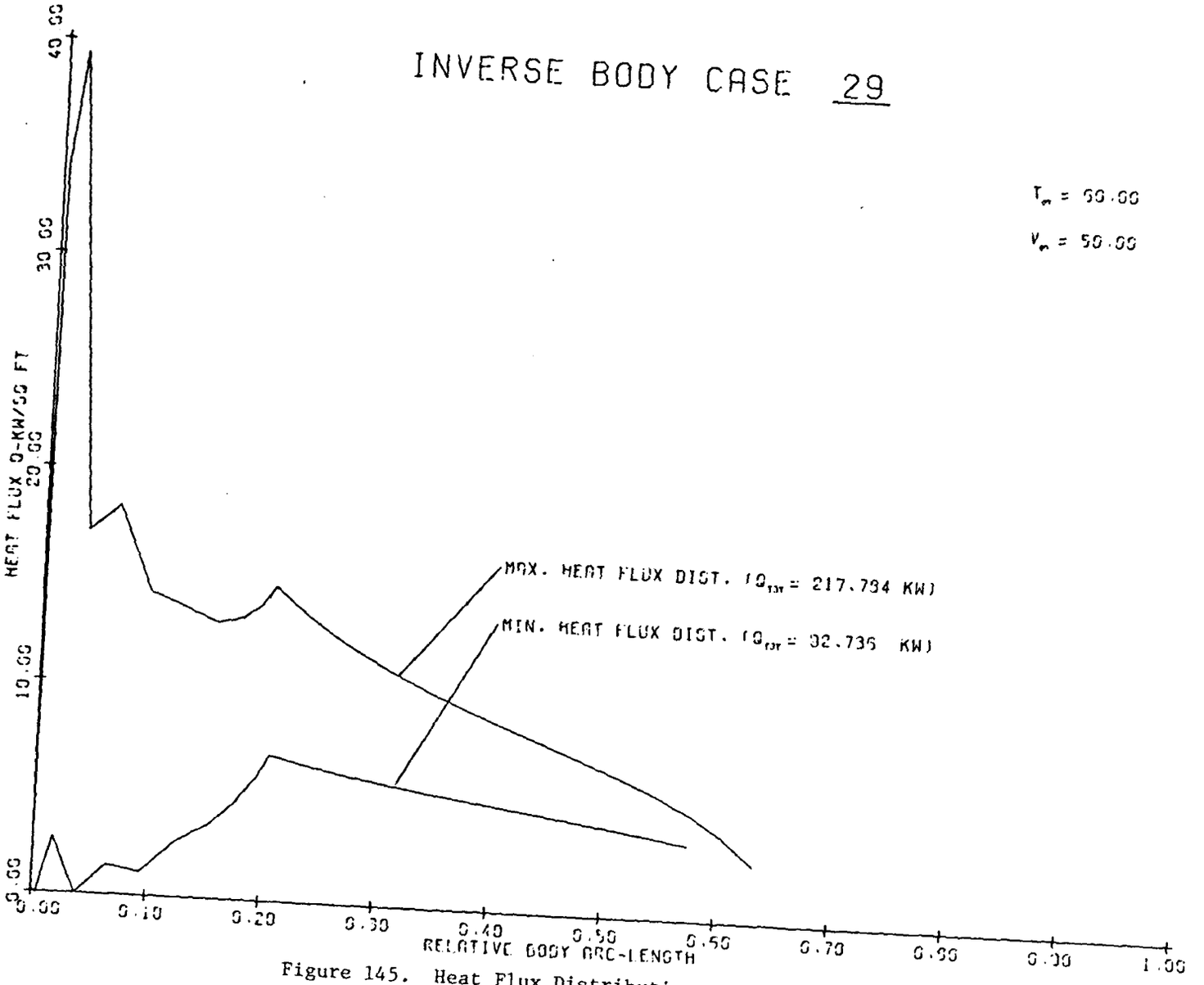

Figure 145. Heat Flux Distributions, Case No. 29.

19 August 1981
JJE:GHH:mmj

19 August 1981
JJE:GHH:mmj

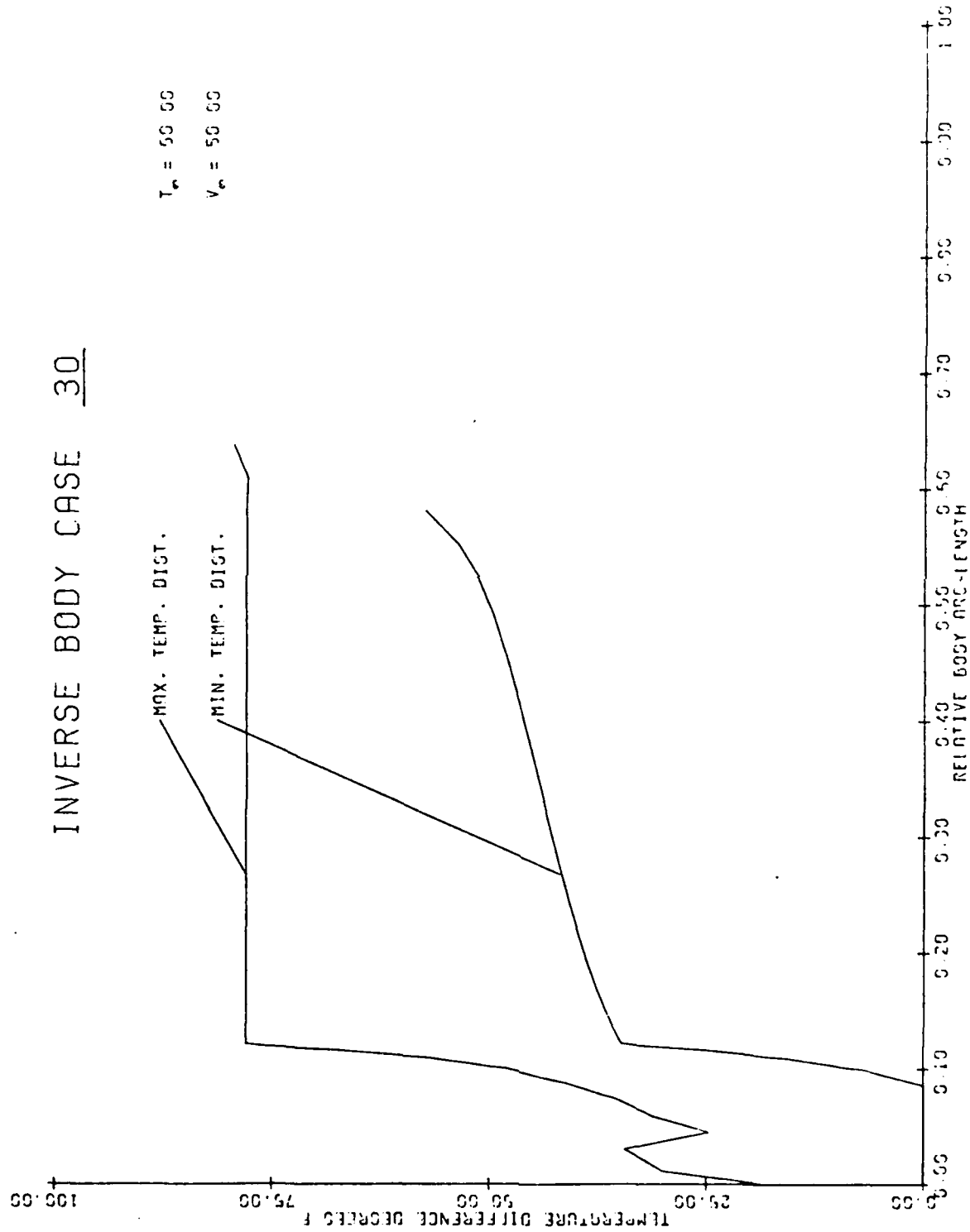

Figure 146. Temperature Distributions, Case No. 30.

19 August 1981
JJE:GHH:mmj

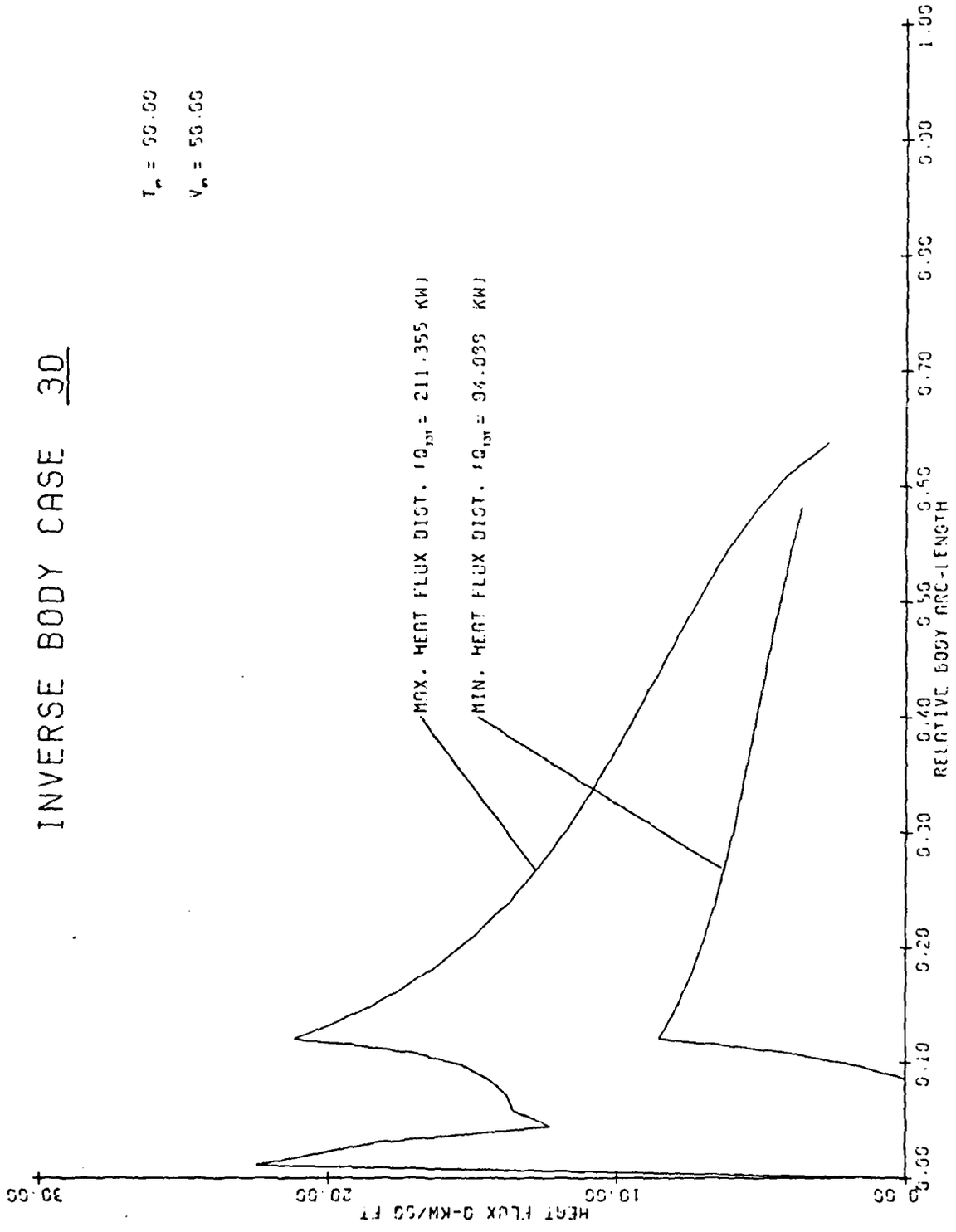

Figure 147. Heat Flux Distributions, Case No. 30.

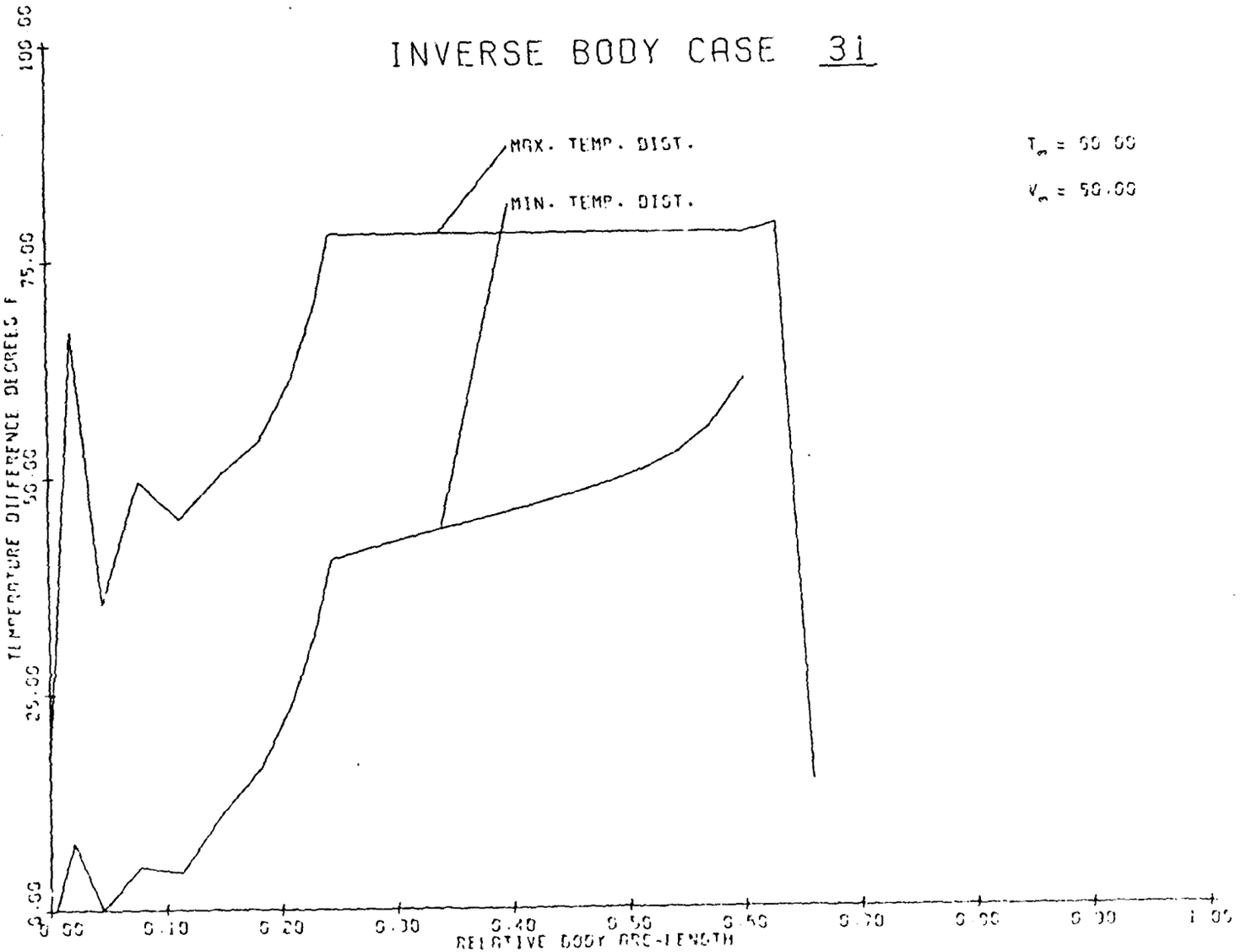

Figure 148. Temperature Distributions, Case No. 31.

19 August 1981
JJE:GHH:mmj

INVERSE BODY CASE 31

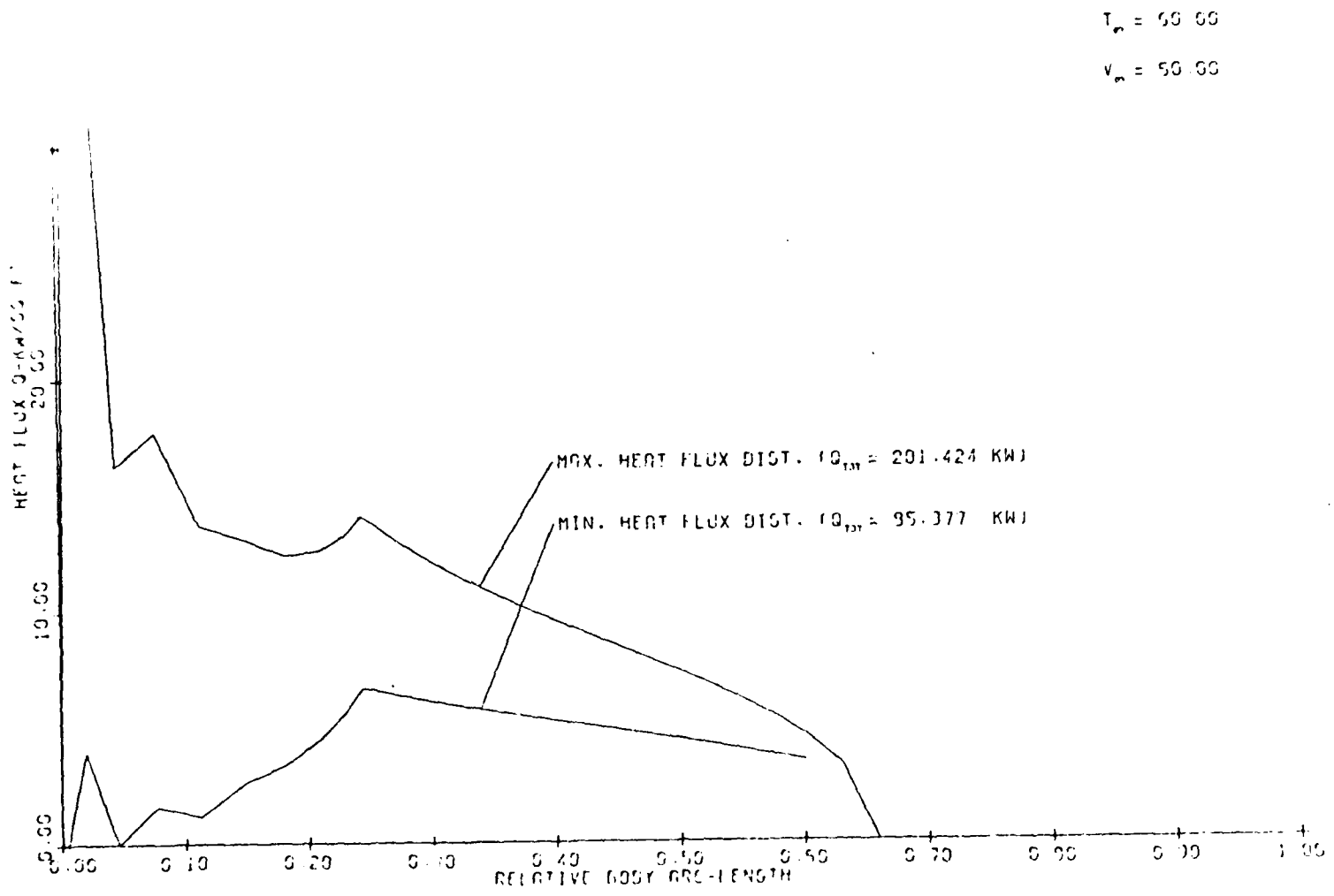

Figure 149. Heat Flux Distributions, Case No. 31.

19 August 1981
JJE:GHH:mmj

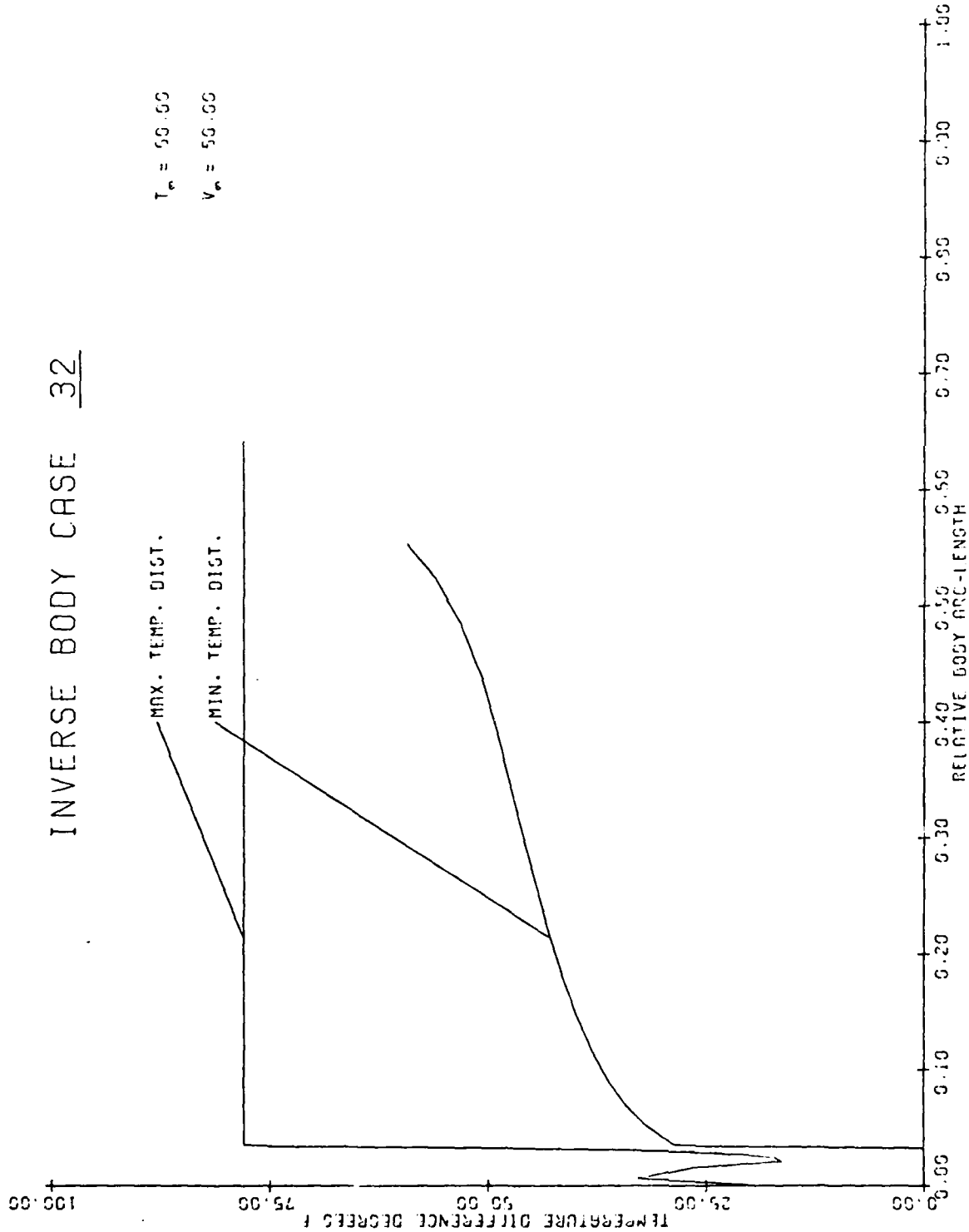

Figure 150. Temperature Distributions, Case No. 32.

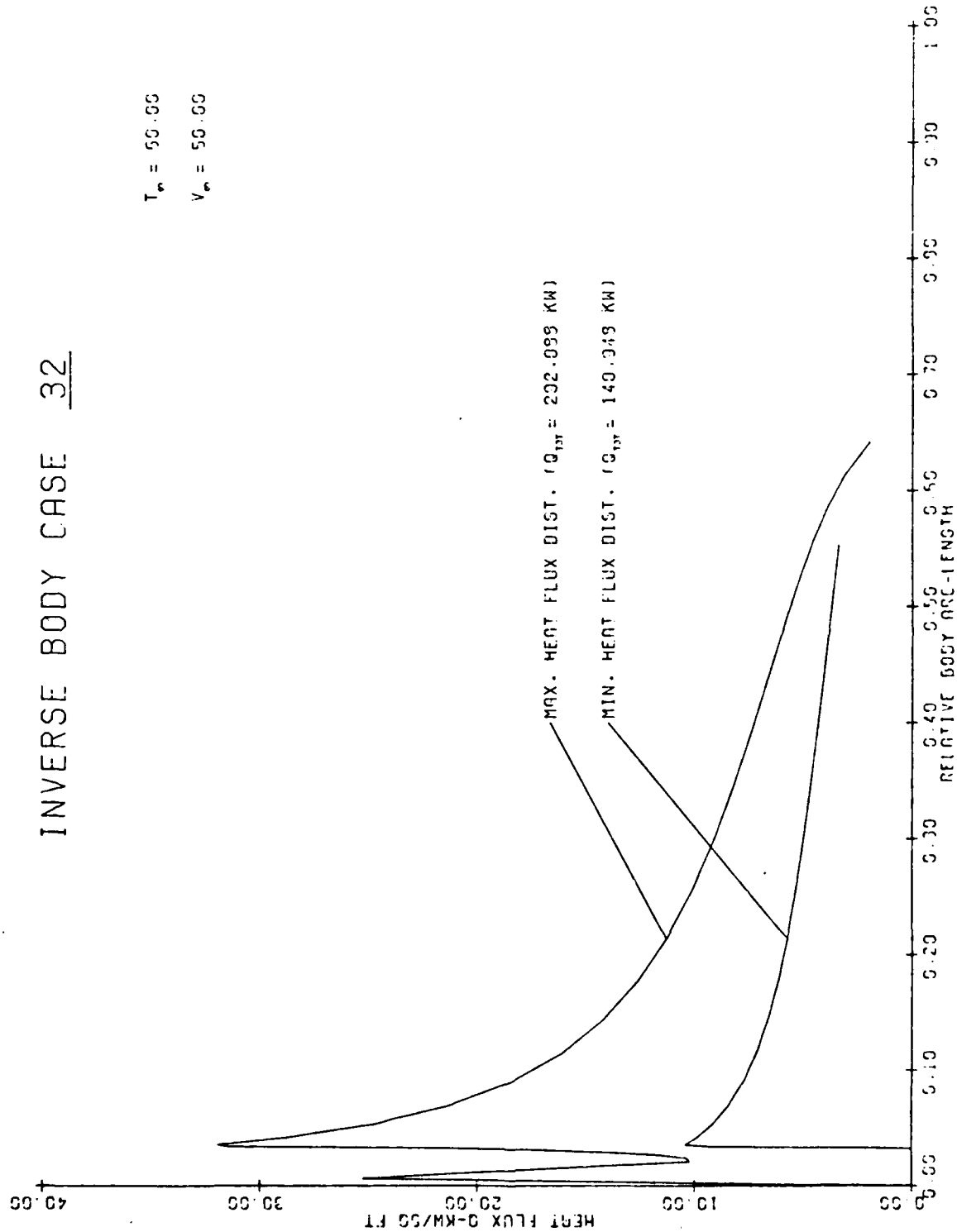

Figure 151. Heat Flux Distributions, Case No. 32.

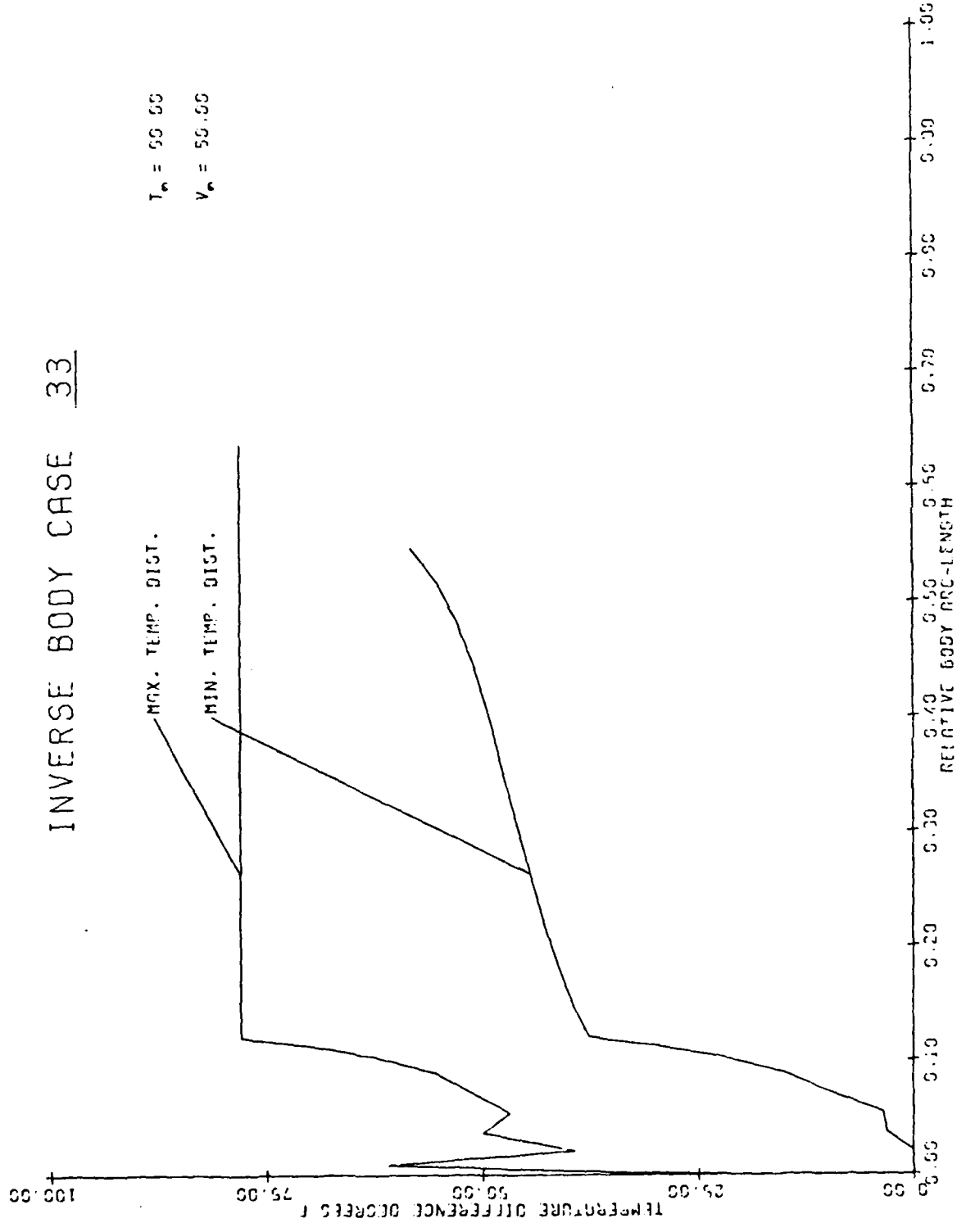

Figure 152. Temperature Distributions, Case No. 33.

19 August 1981
JJE:GHH:mmj

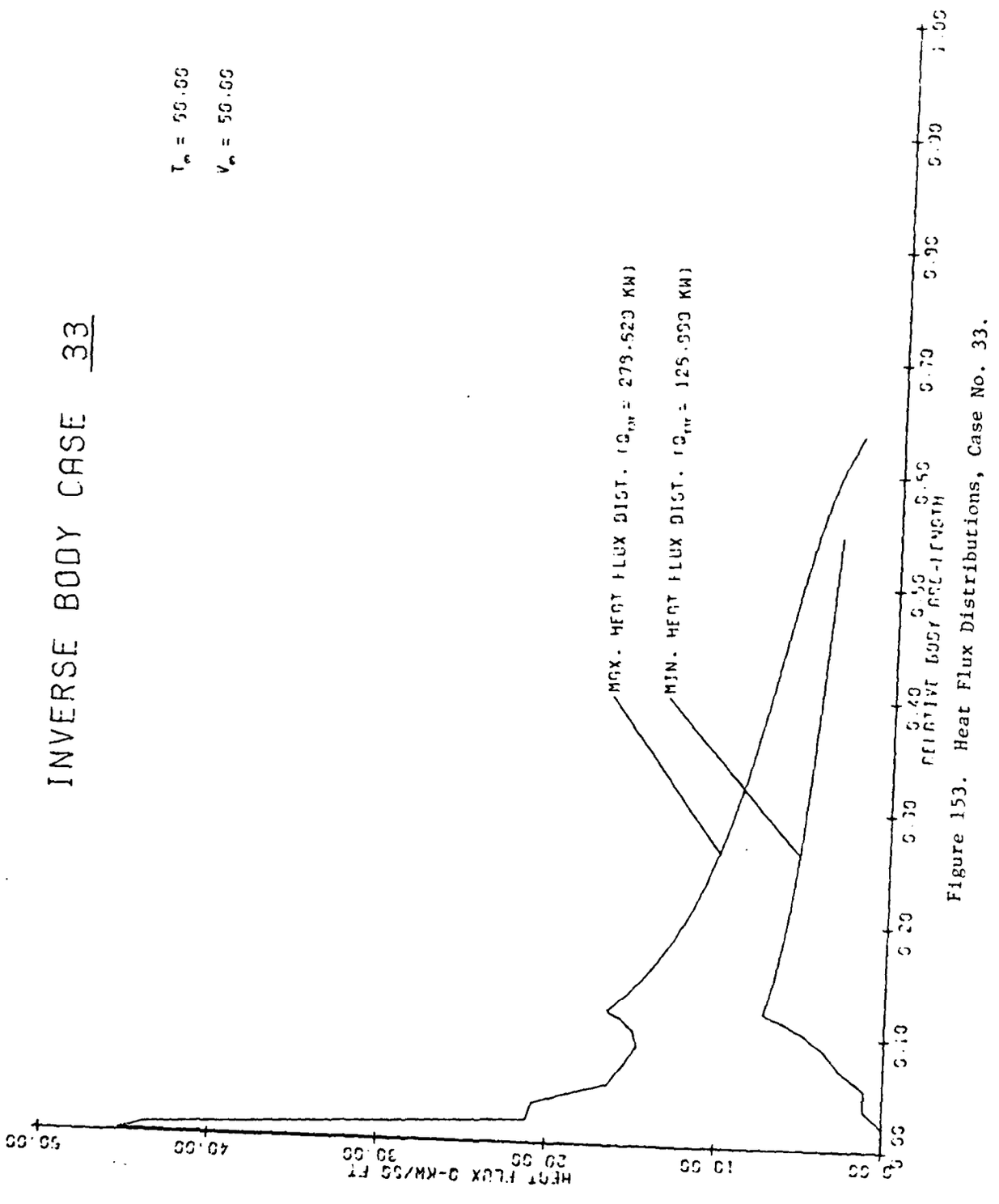

Figure 153. Heat Flux Distributions, Case No. 33.

19 August 1981
JJE:GHH:mmj

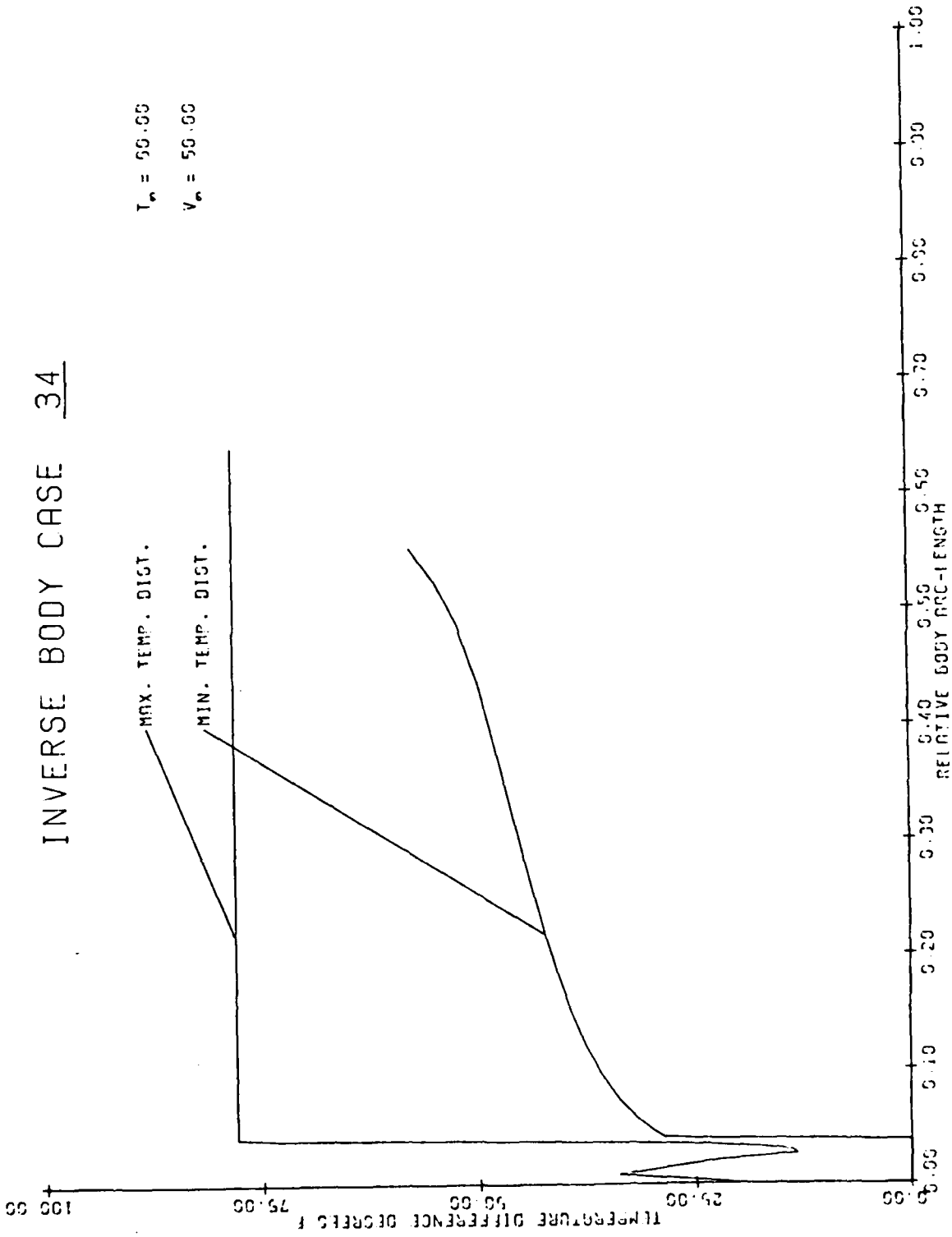

Figure 154. Temperature Distributions, Case No. 34.

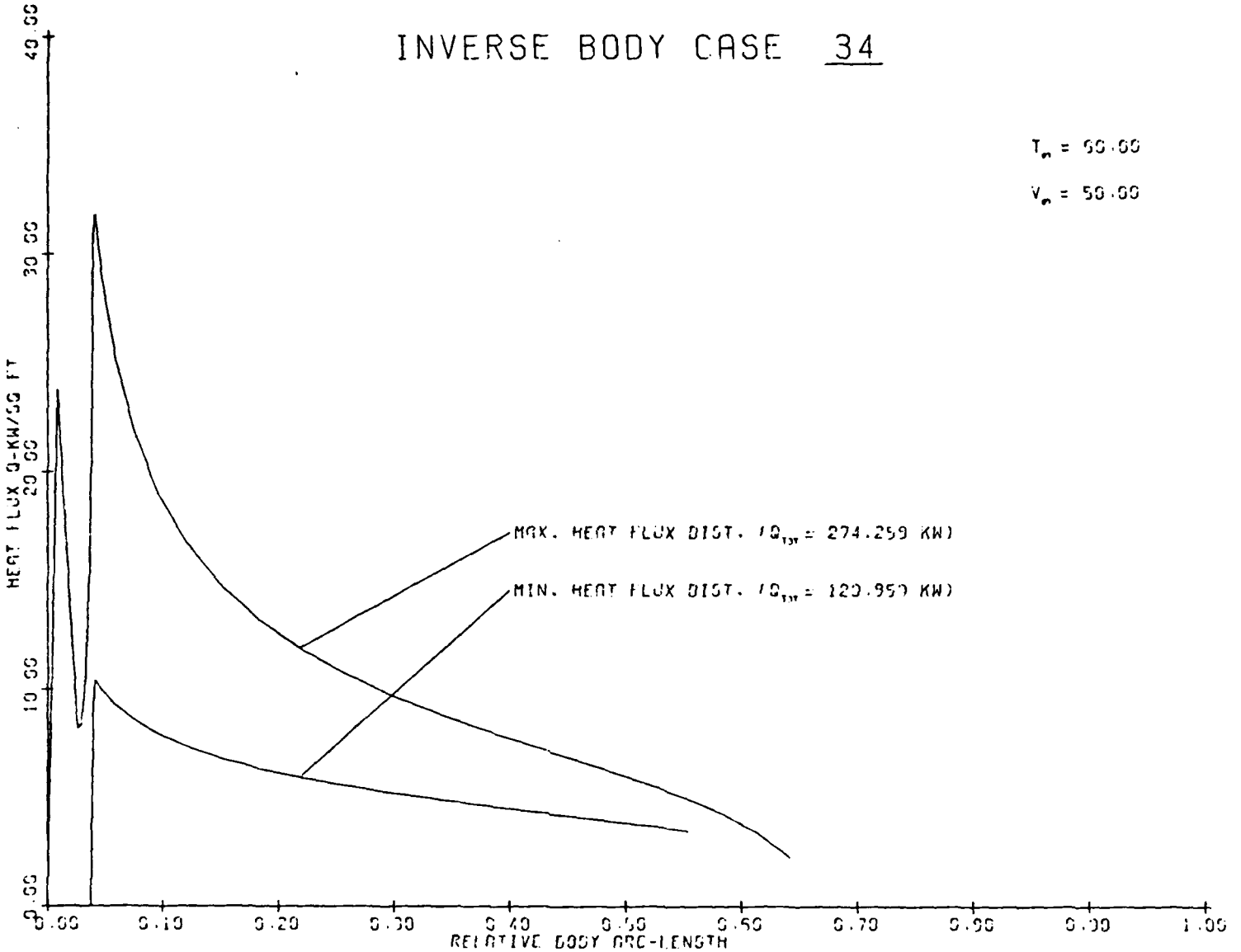

Figure 155. Heat Flux Distributions, Case No. 34.

19 August 1981
JJE:GHH:mmj

19 August 1981
JJE:GHH:mmj

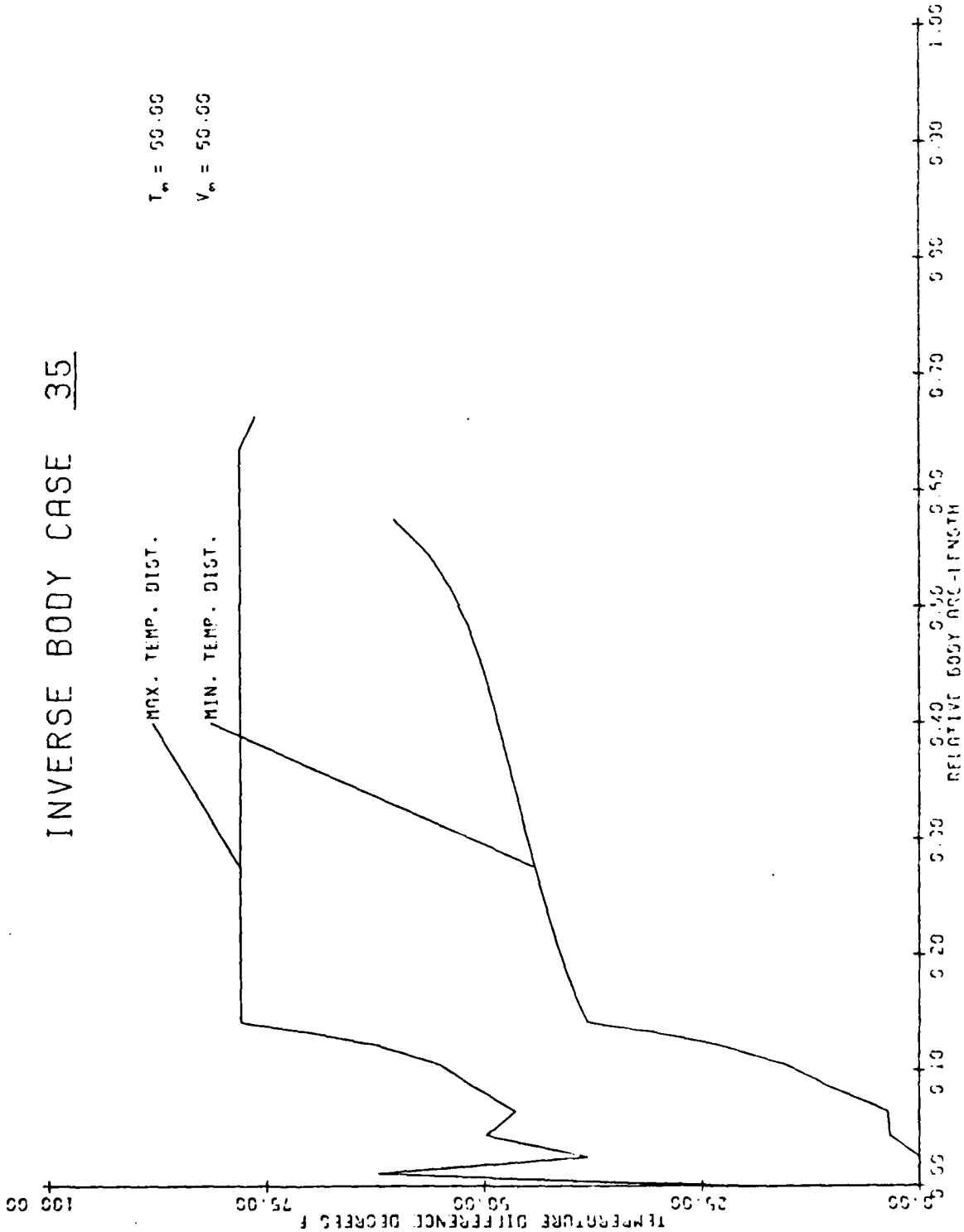

156. Temperature Distributions, Case No. 35.

19 August 1981
JJE:GHH:mmj

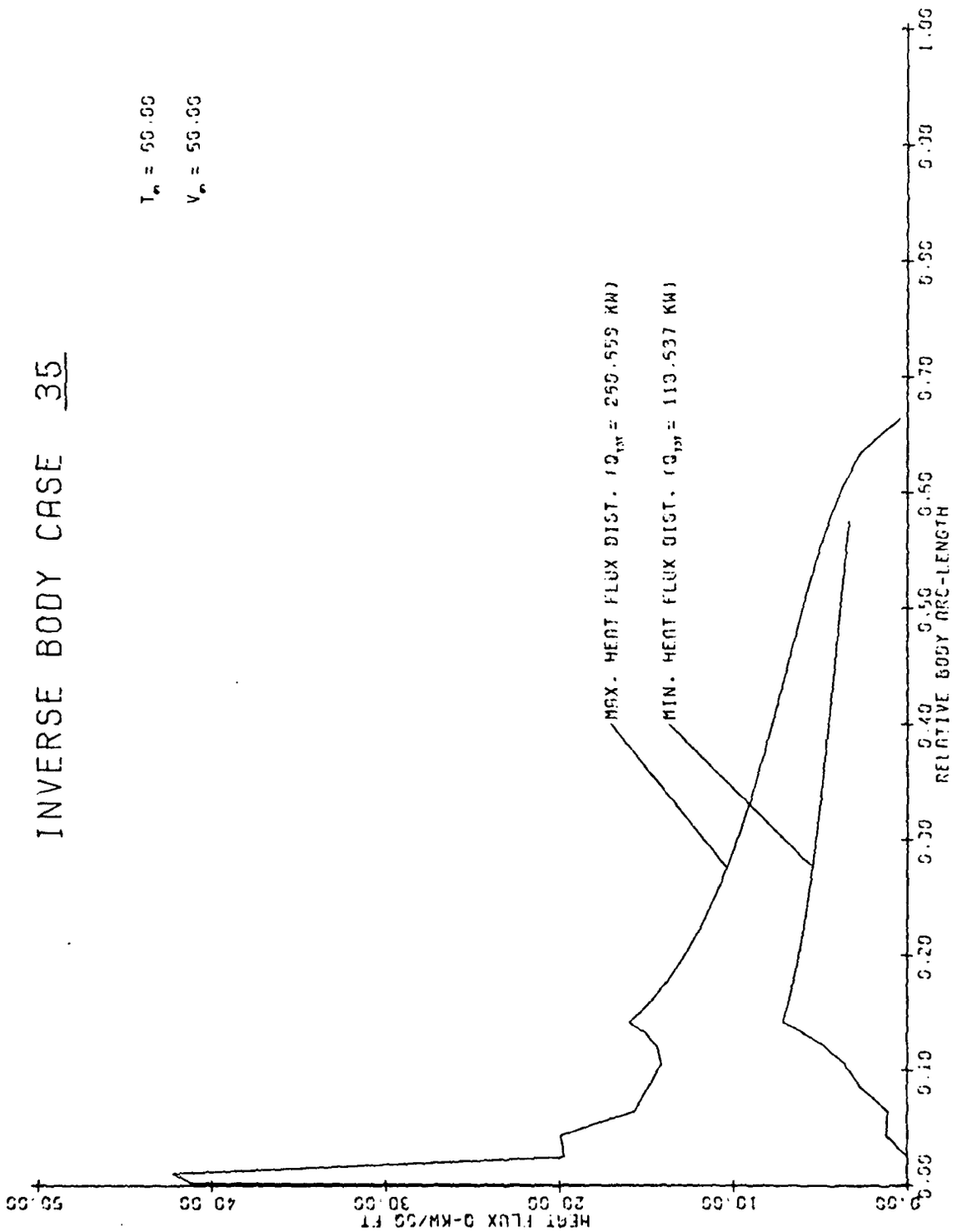

Figure 157. Heat Flux Distributions, Case No. 35.

19 August 1981
JJE:GHH:mmj

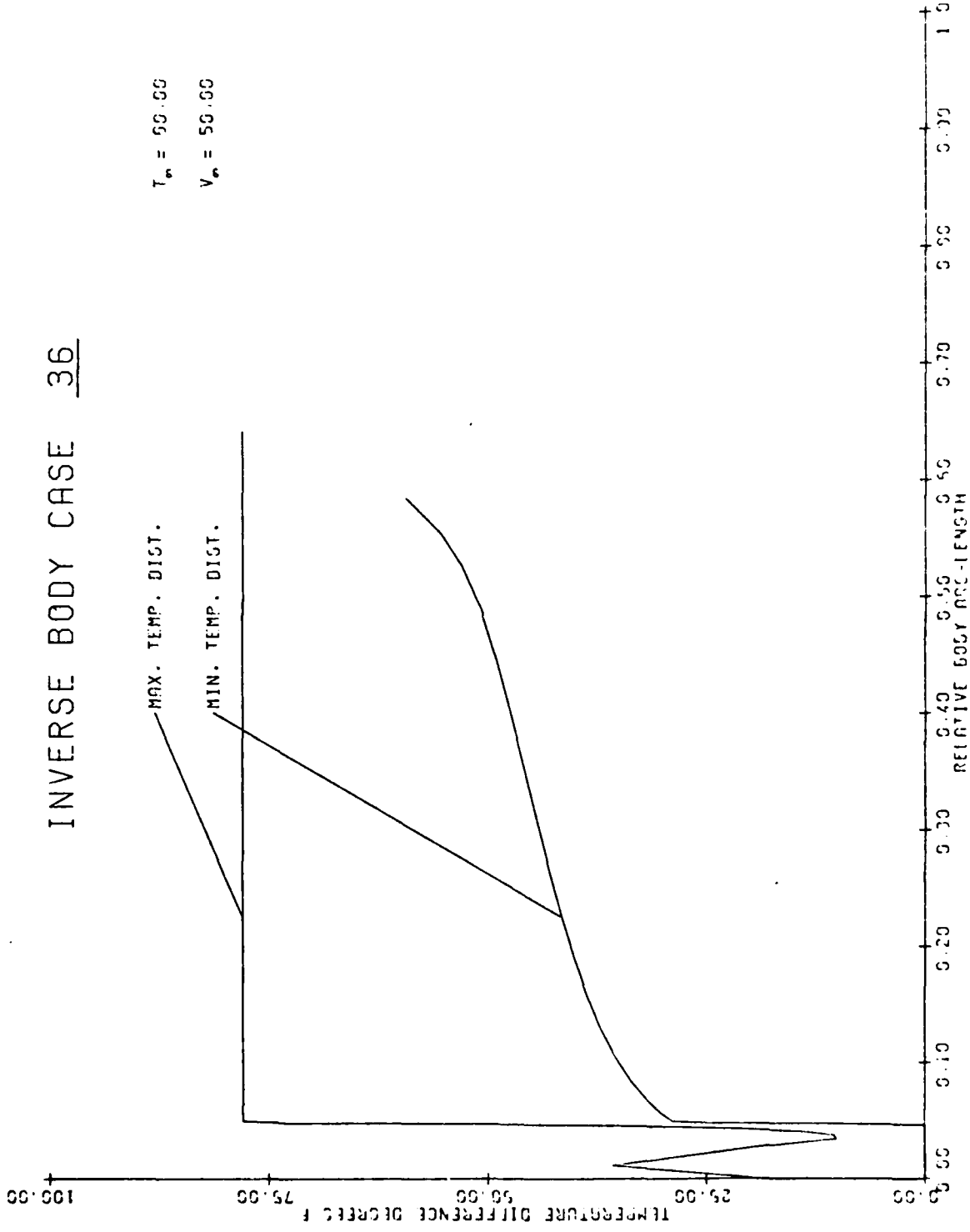

Figure 158. Temperature Distributions, Case No. 36.

19 August 1981
JJE:GHH:mmj

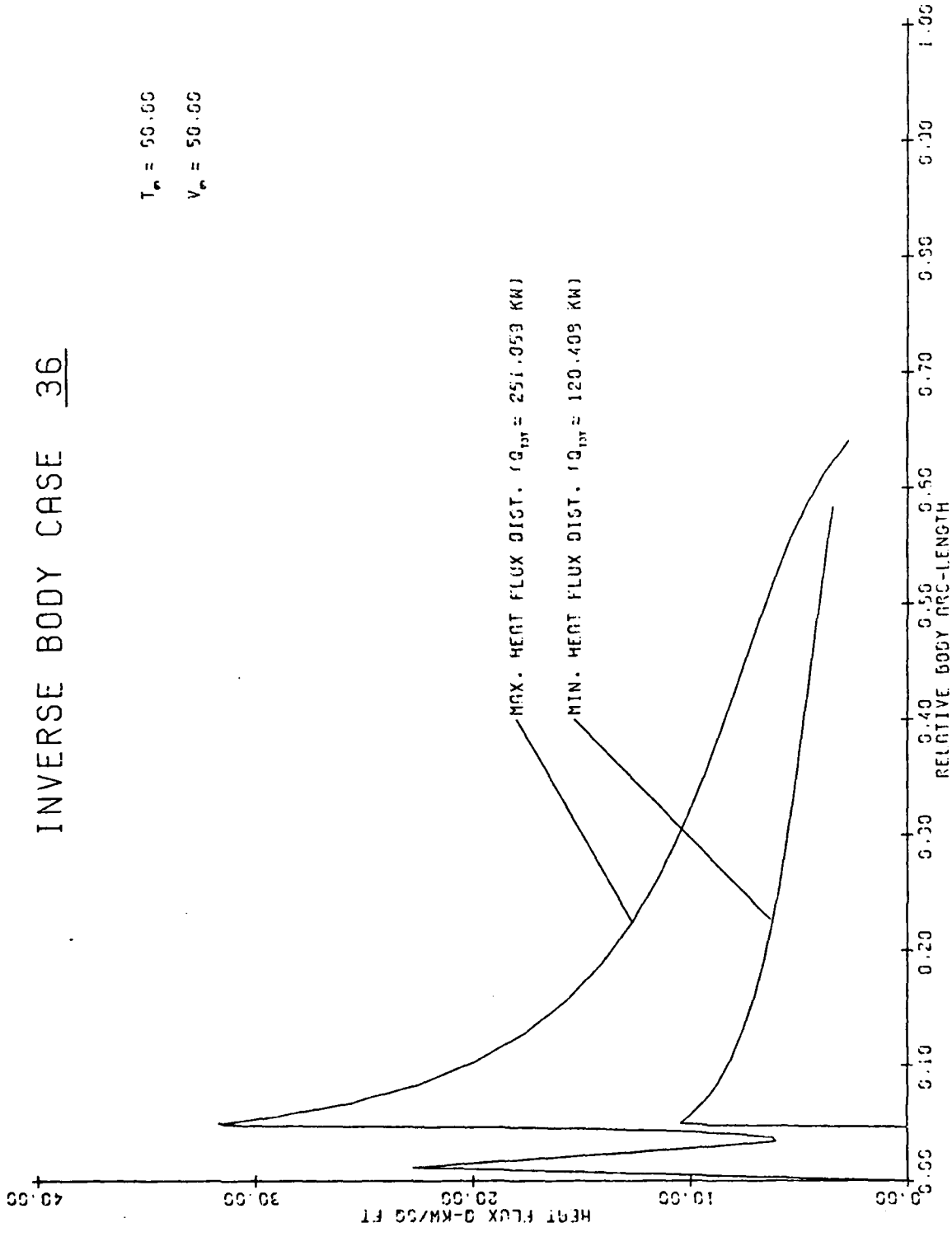

Figure 159. Heat Flux Distributions, Case No. 36.

19 August 1981
JJE:GHH:mmj

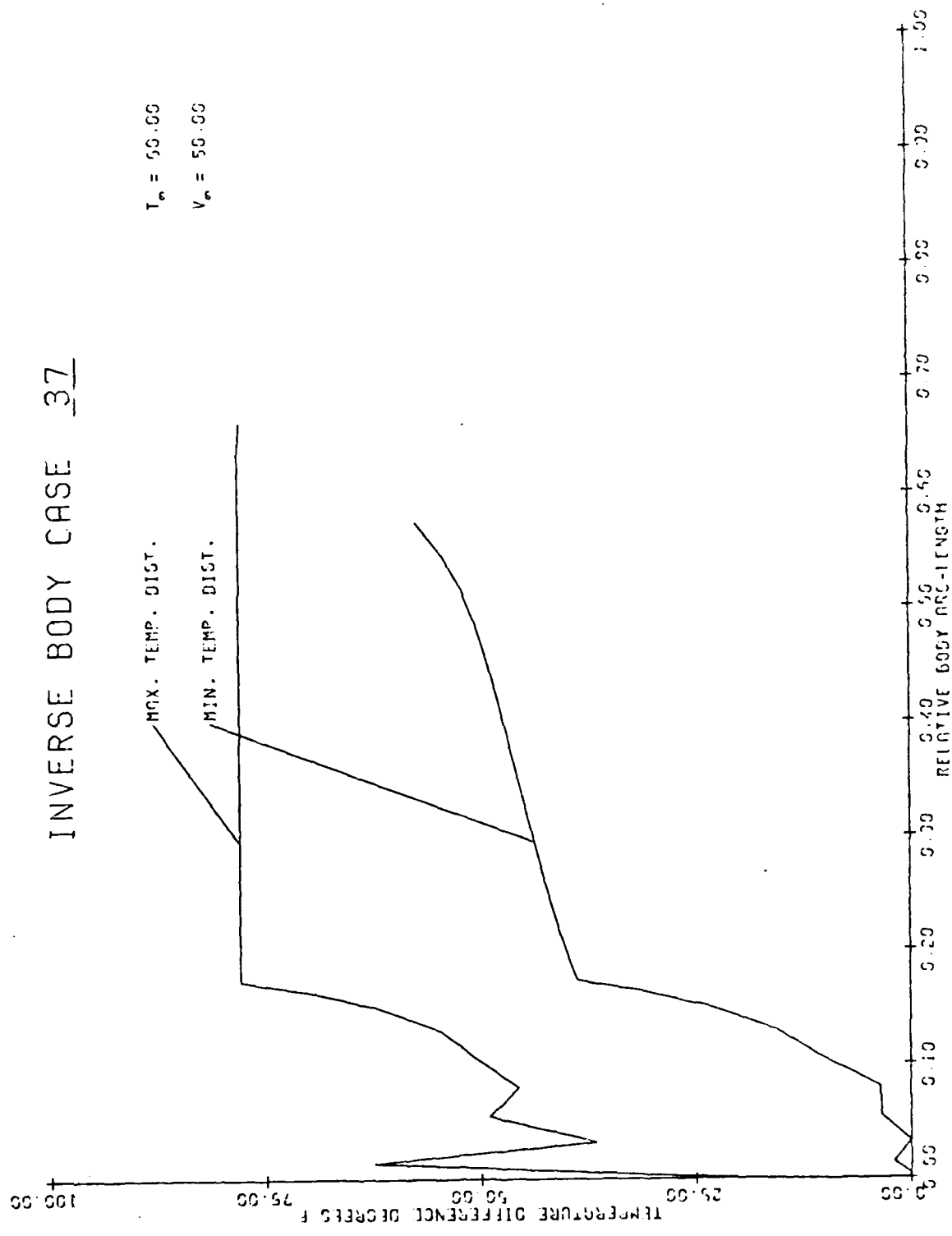

Figure 160. Temperature Distributions, Case No. 37.

19 August 1981
JJE:GHH:mmj

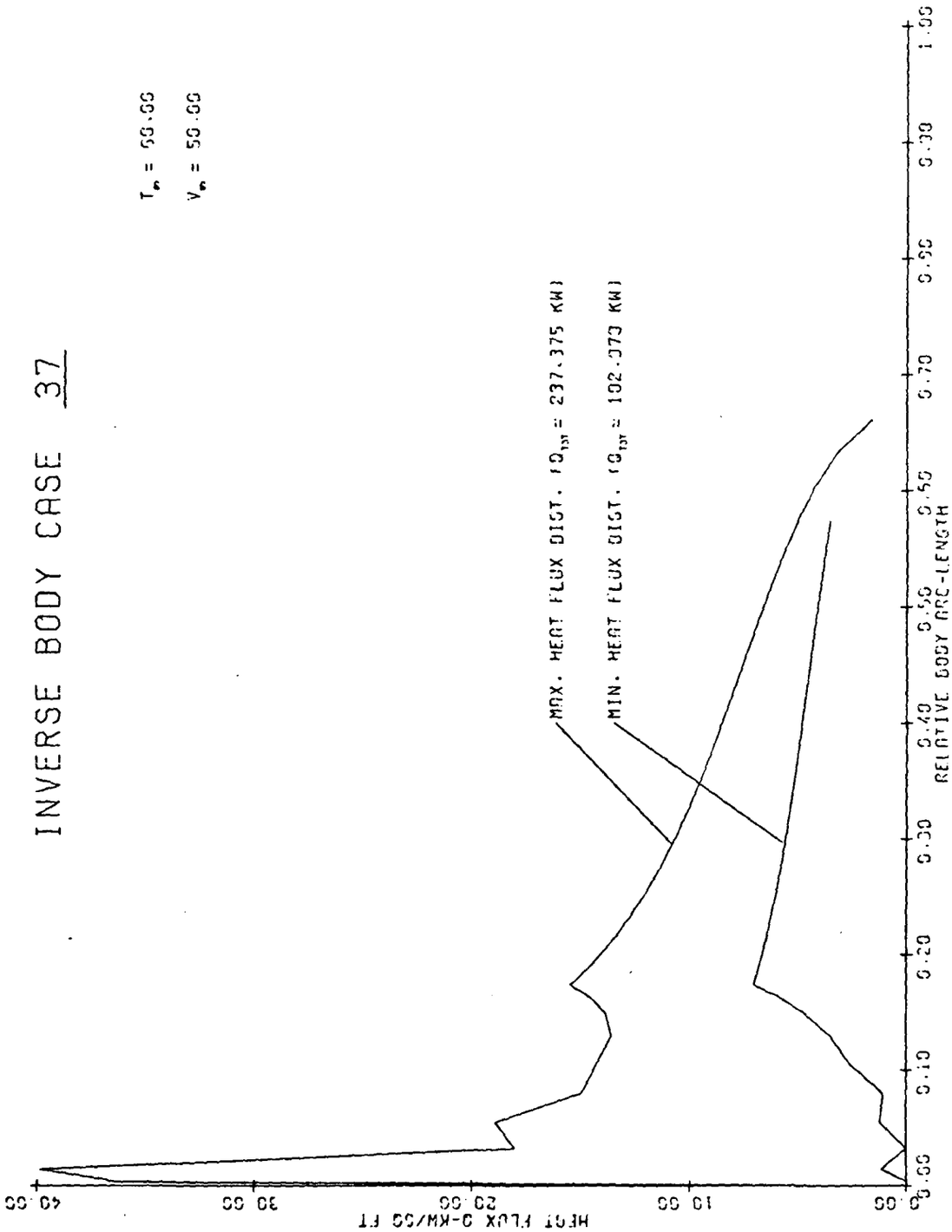

Figure 161. Heat Flux Distributions, Case No. 37.

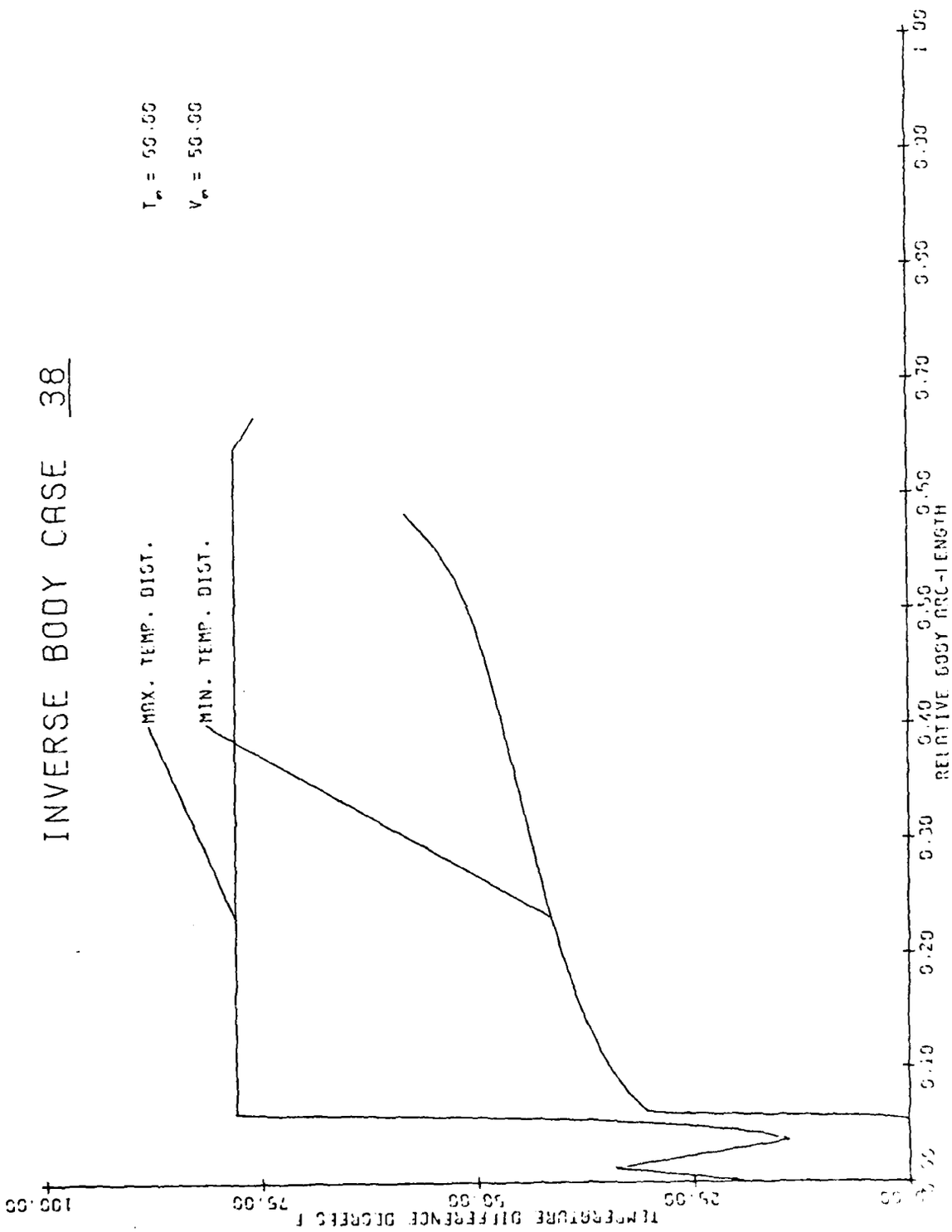

Figure 162. Temperature Distributions, Case No. 38.

AD-A107 662 PENNSYLVANIA STATE UNIV UNIVERSITY PARK APPLIED RESE--ETC F/G 20/4
INVERSE AXISYMMETRIC BODY STUDY.(U)
AUG 81 J J EISENHUTH, G H HOFFMAN N00024-79-C-6043
UNCLASSIFIED ARL/PSU/TM-81-177 NL

3 OF 3
AD A
107662

END
DATE FILMED
11-82
DTIC

19 August 1981
JJE:GHH:mmj

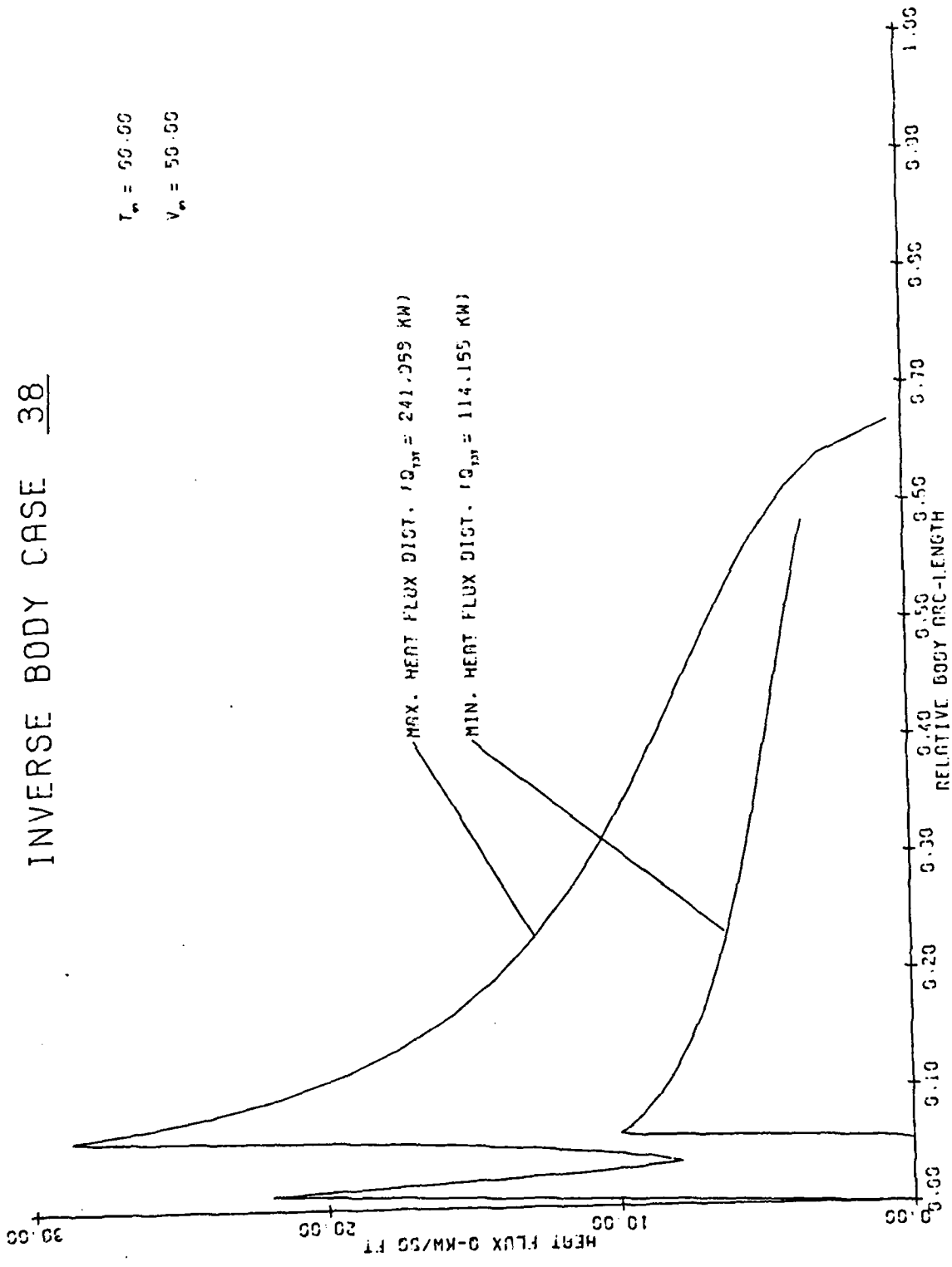

Figure 163. Heat Flux Distributions, Case No. 38.

19 August 1981
JJE:GHH:mmj

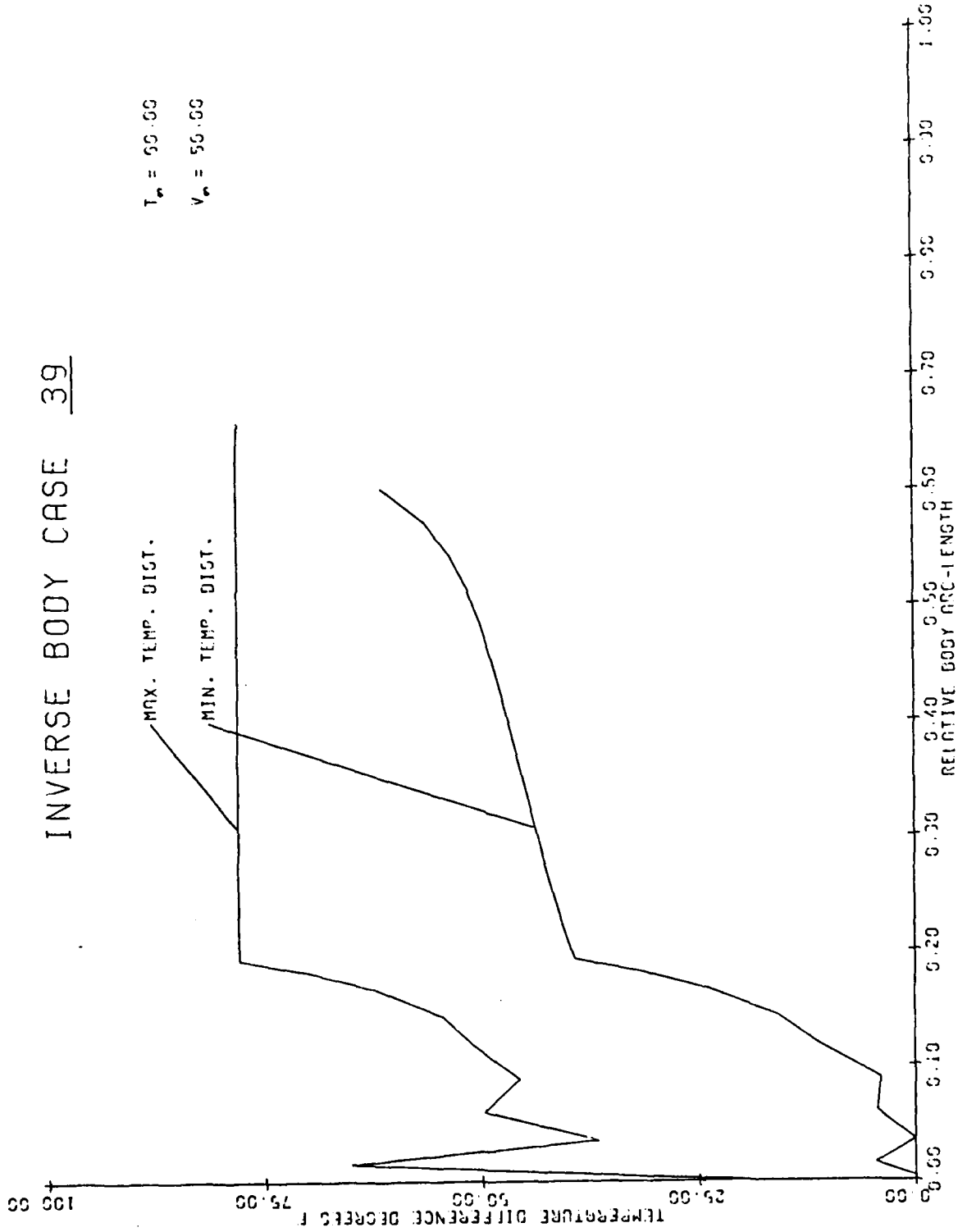

Figure 164. Temperature Distributions, Case No. 39.

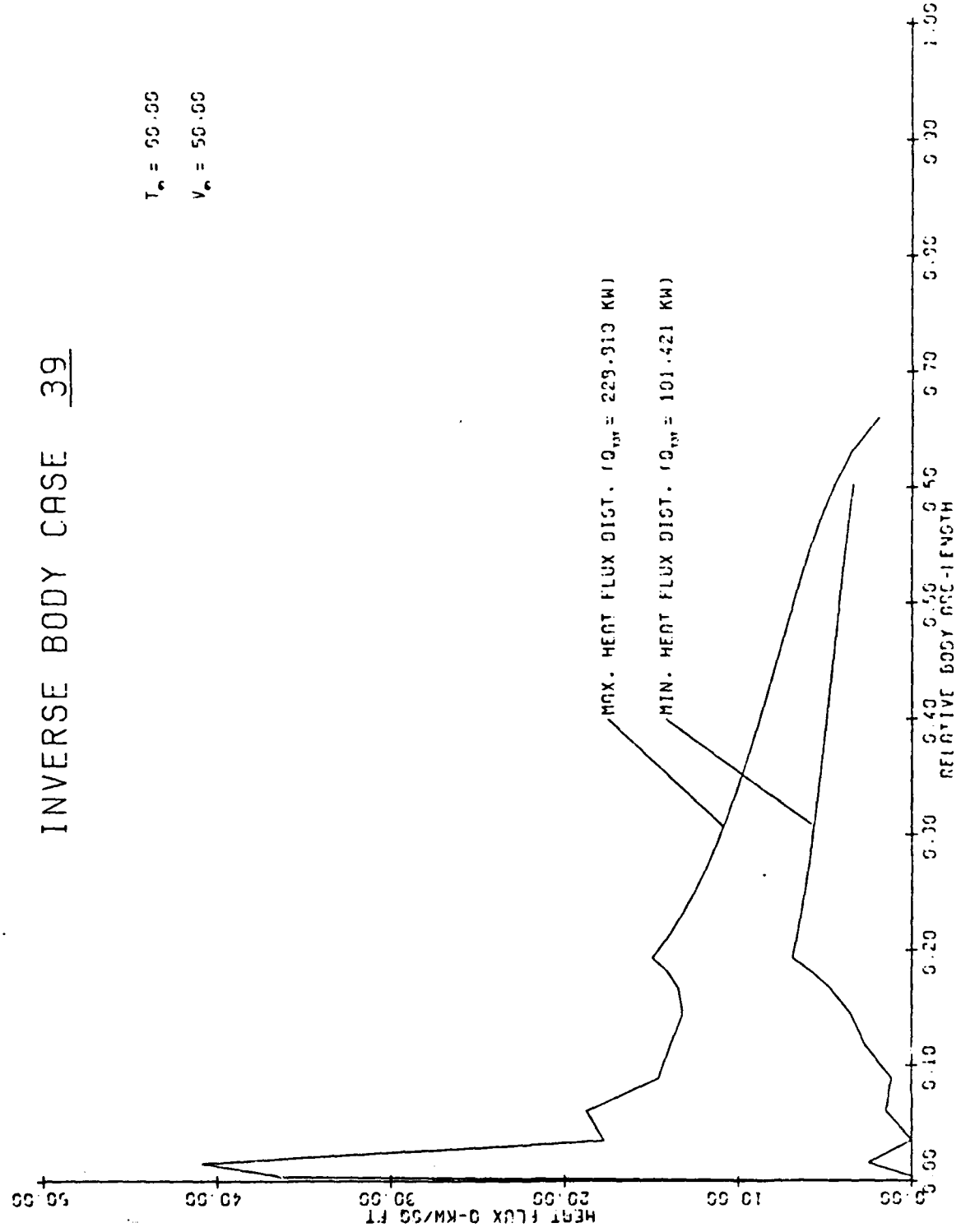

Figure 165. Heat Flux Distributions, Case No. 39.

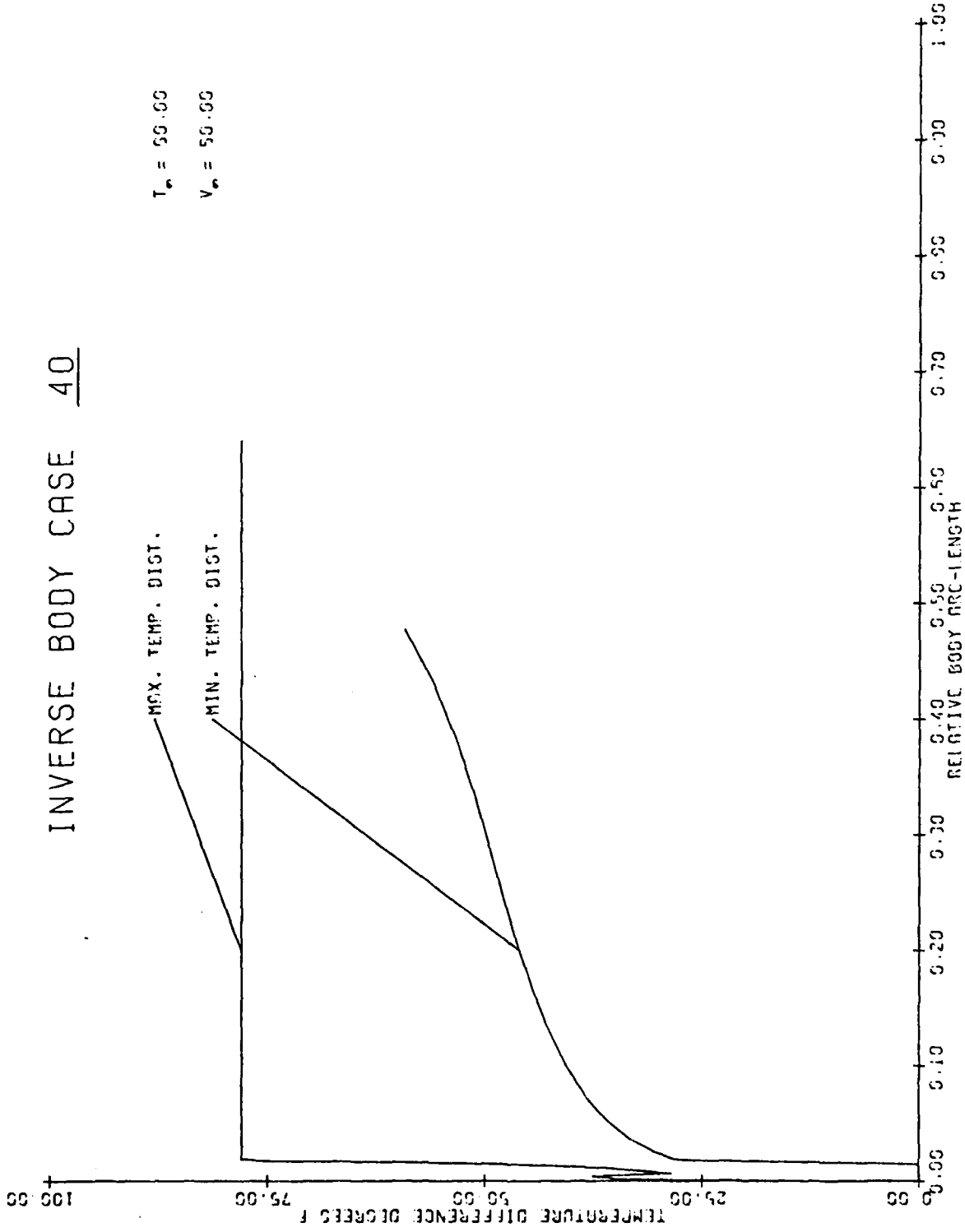

Figure 166. Temperature Distributions, Case No. 40.

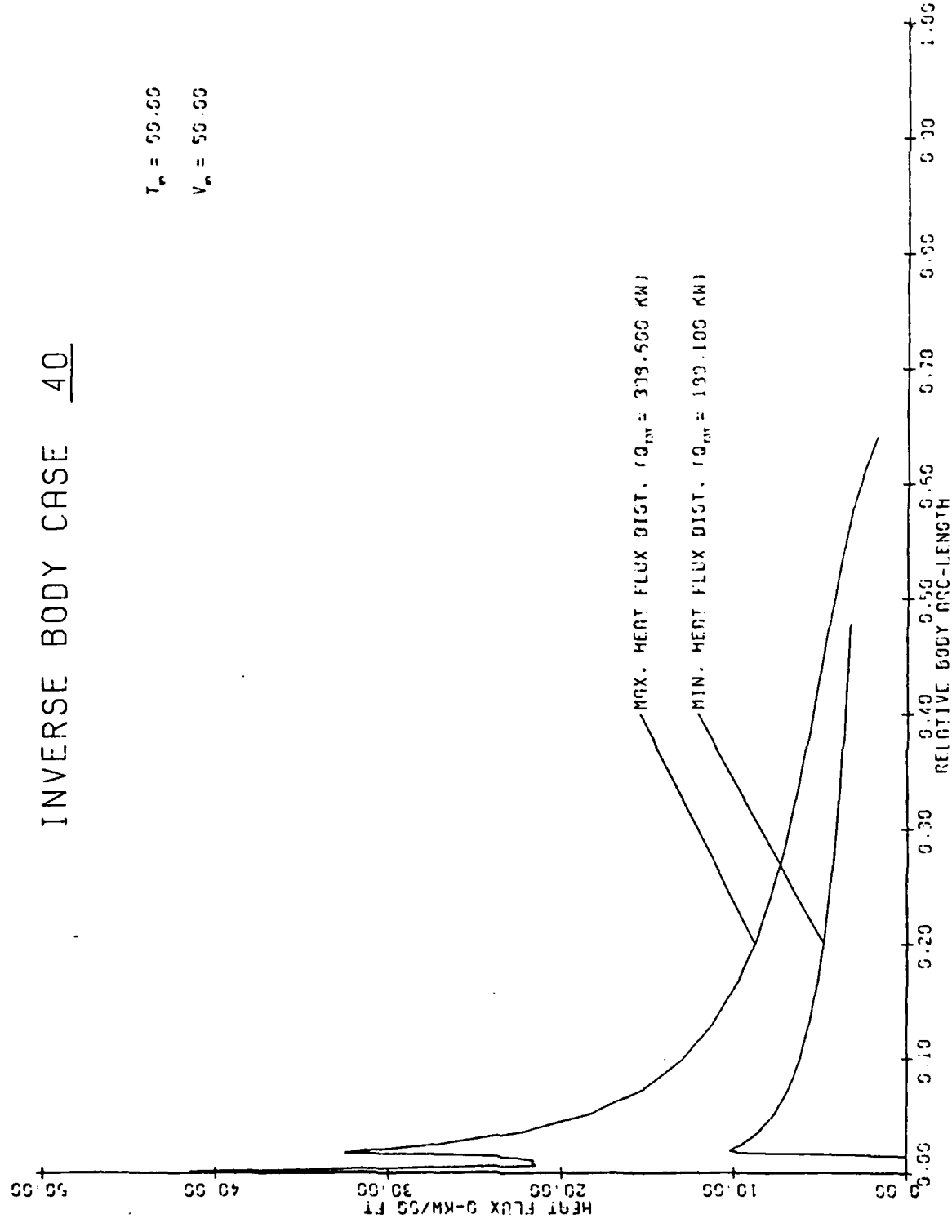

Figure 167. Heat Flux Distributions, Case No. 40.

19 August 1981
JJE:GHH:mmj

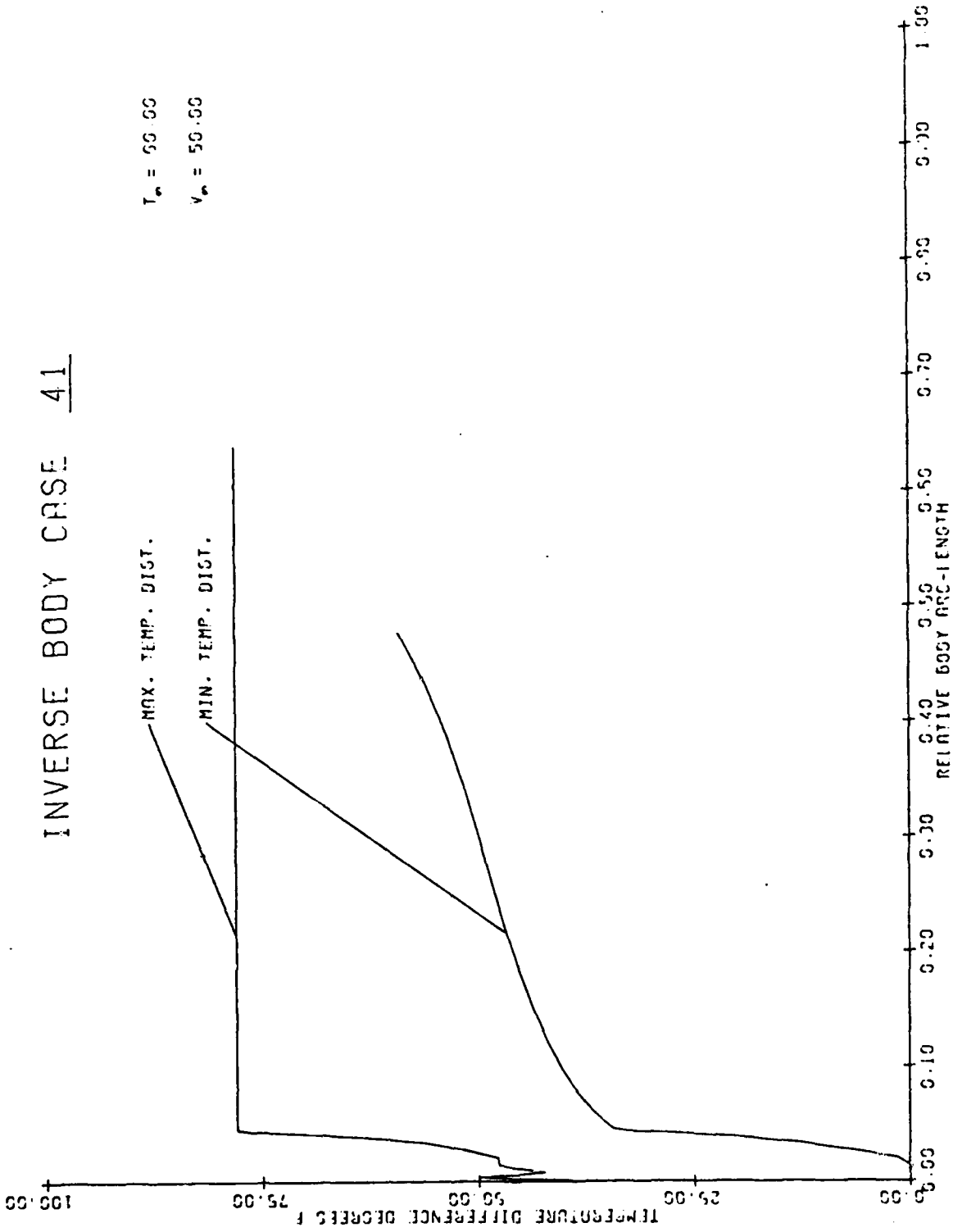

Figure 168. Temperature Distributions, Case No. 41.

19 August 1981
JJE:GHH:mmj

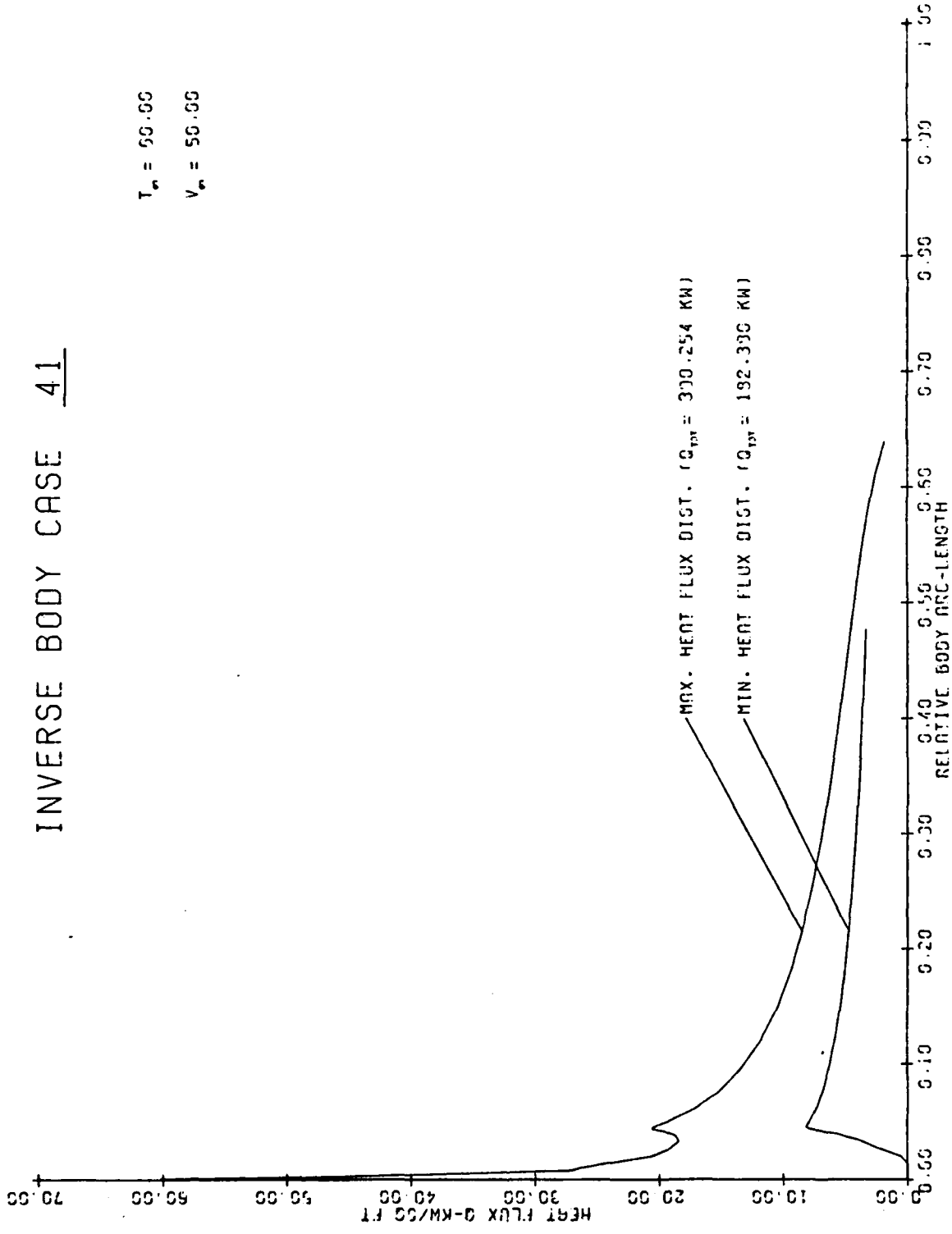

Figure 169. Heat Flux Distributions, Case No. 41.

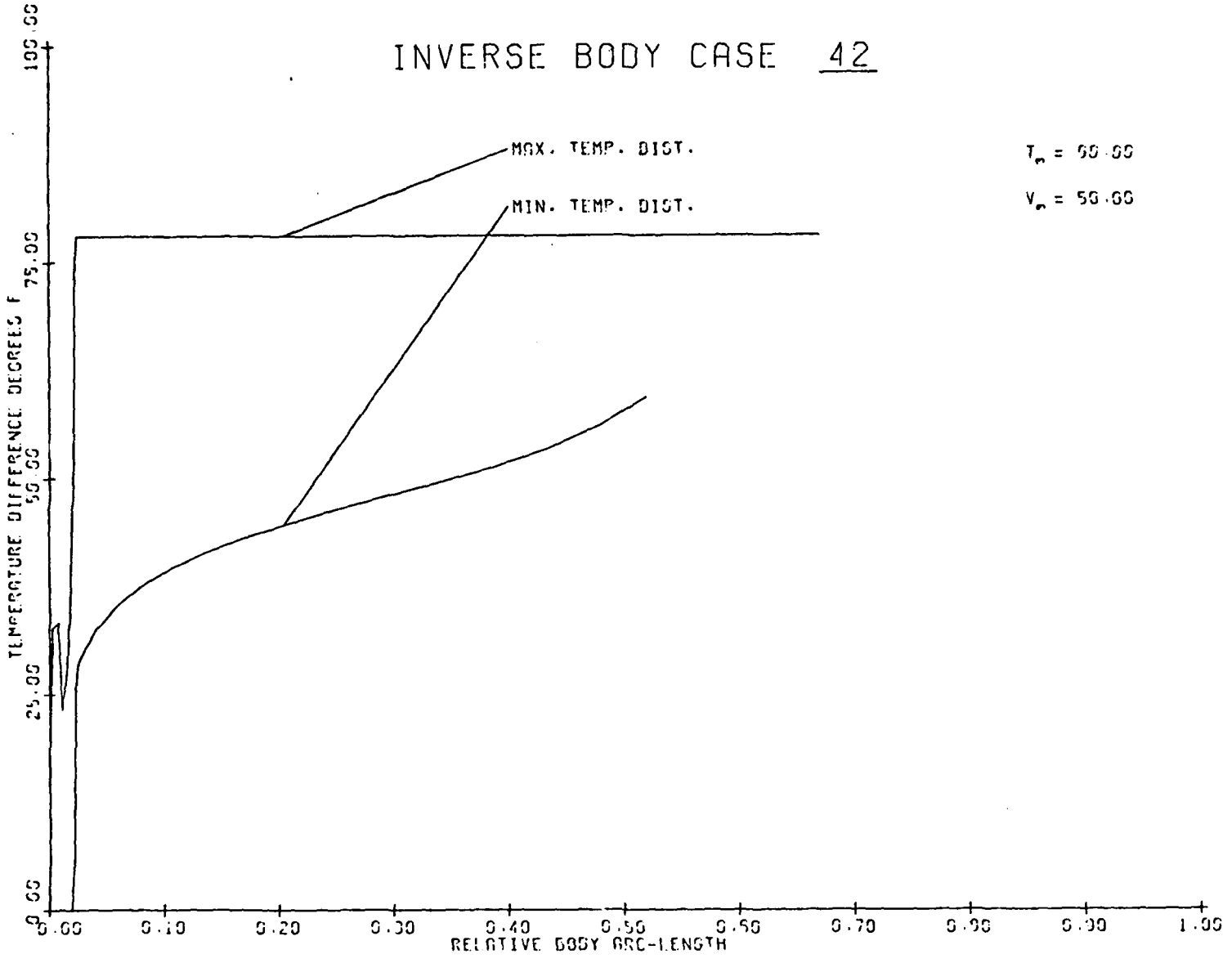

Figure 170. Temperature Distributions, Case No. 42.

19 August 1981
JJE:GHH:mmj

19 August 1981
JJE:GHH:mmj

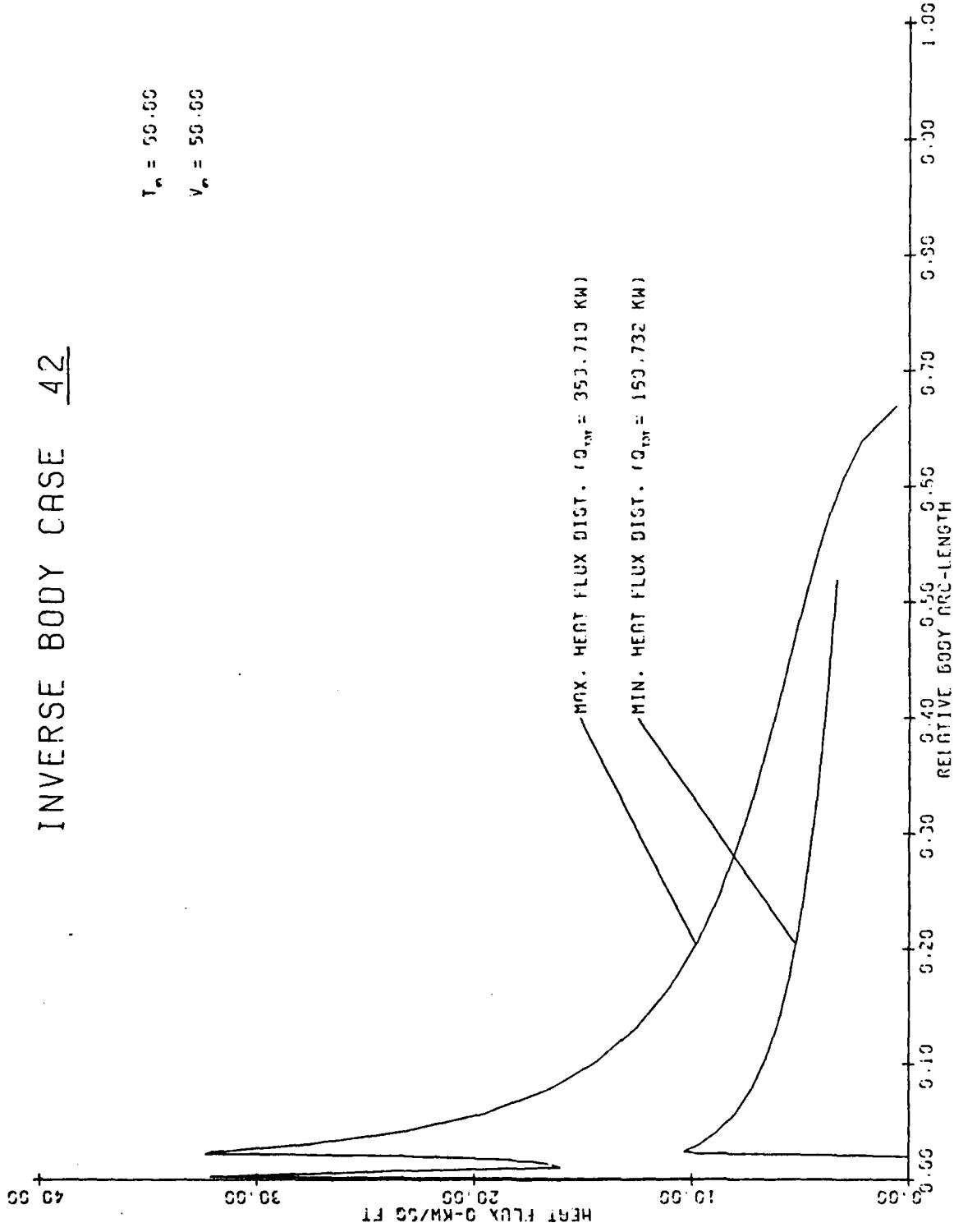

Figure 171. Heat Flux Distributions, Case No. 42.

19 August 1981
JJE:GHH:mmj

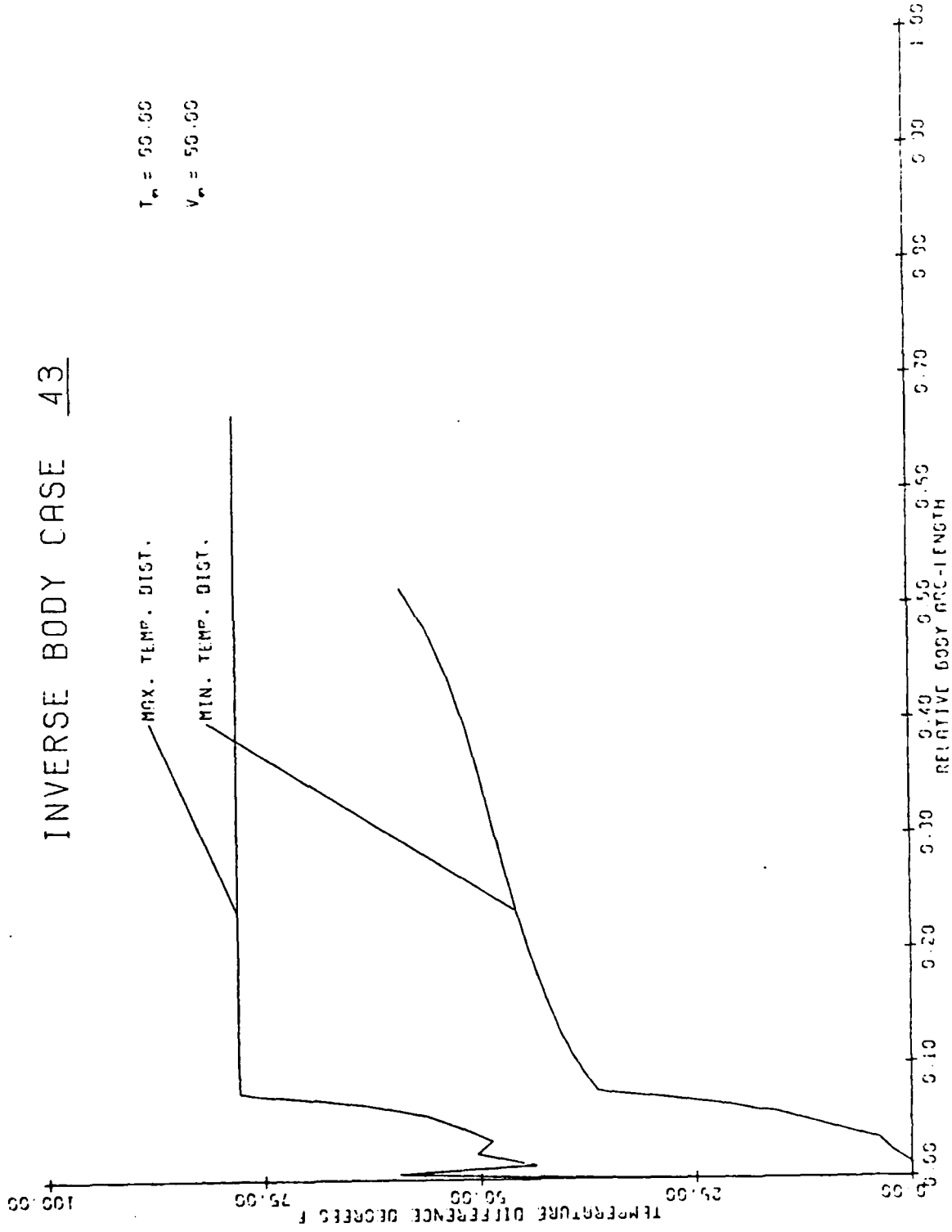

Figure 172. Temperature Distributions, Case No. 43.

19 August 1981
JJE:GHH:mmj

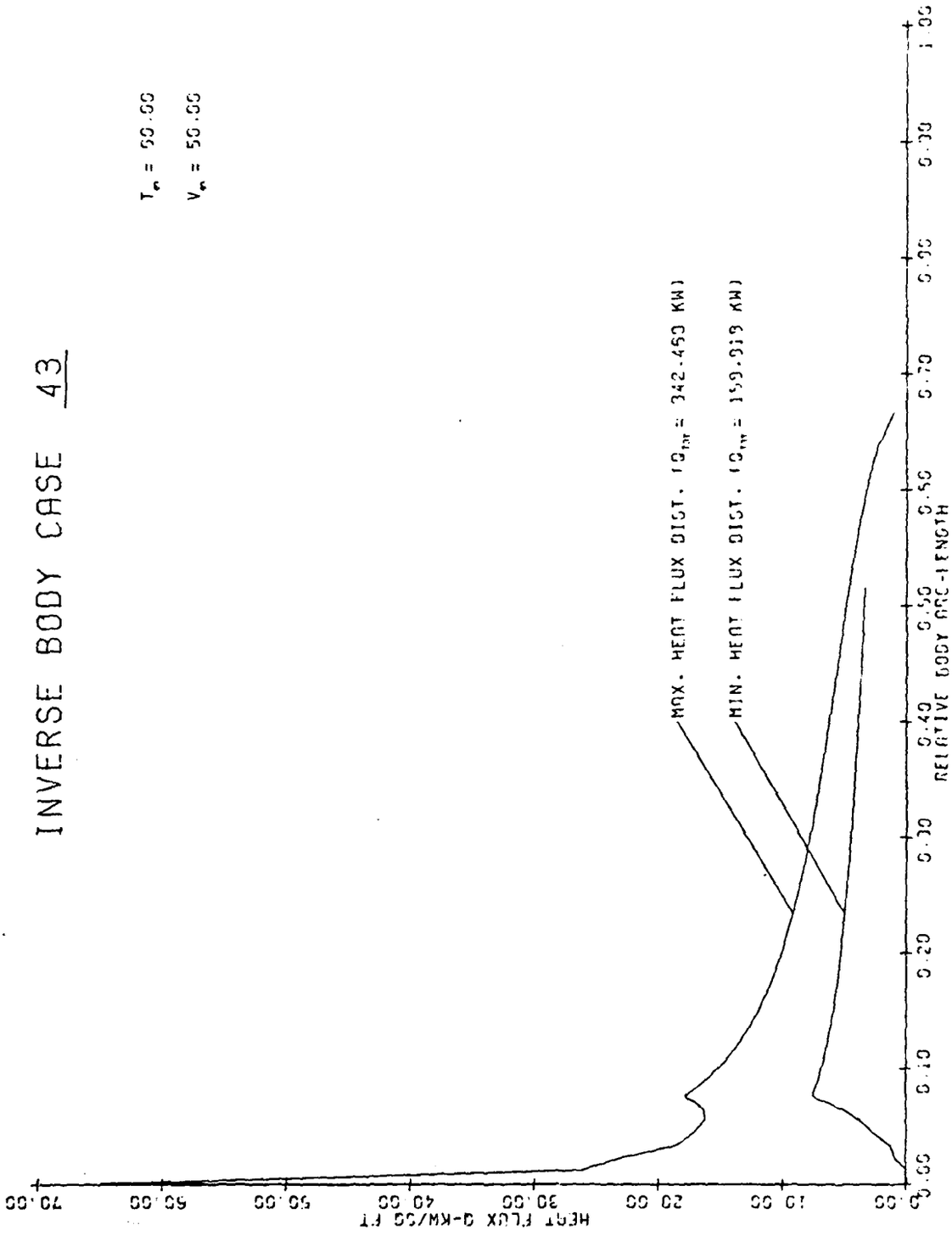

Figure 173. Heat Flux Distributions, Case No. 43.

19 August 1981
JJE:GHH:mmj

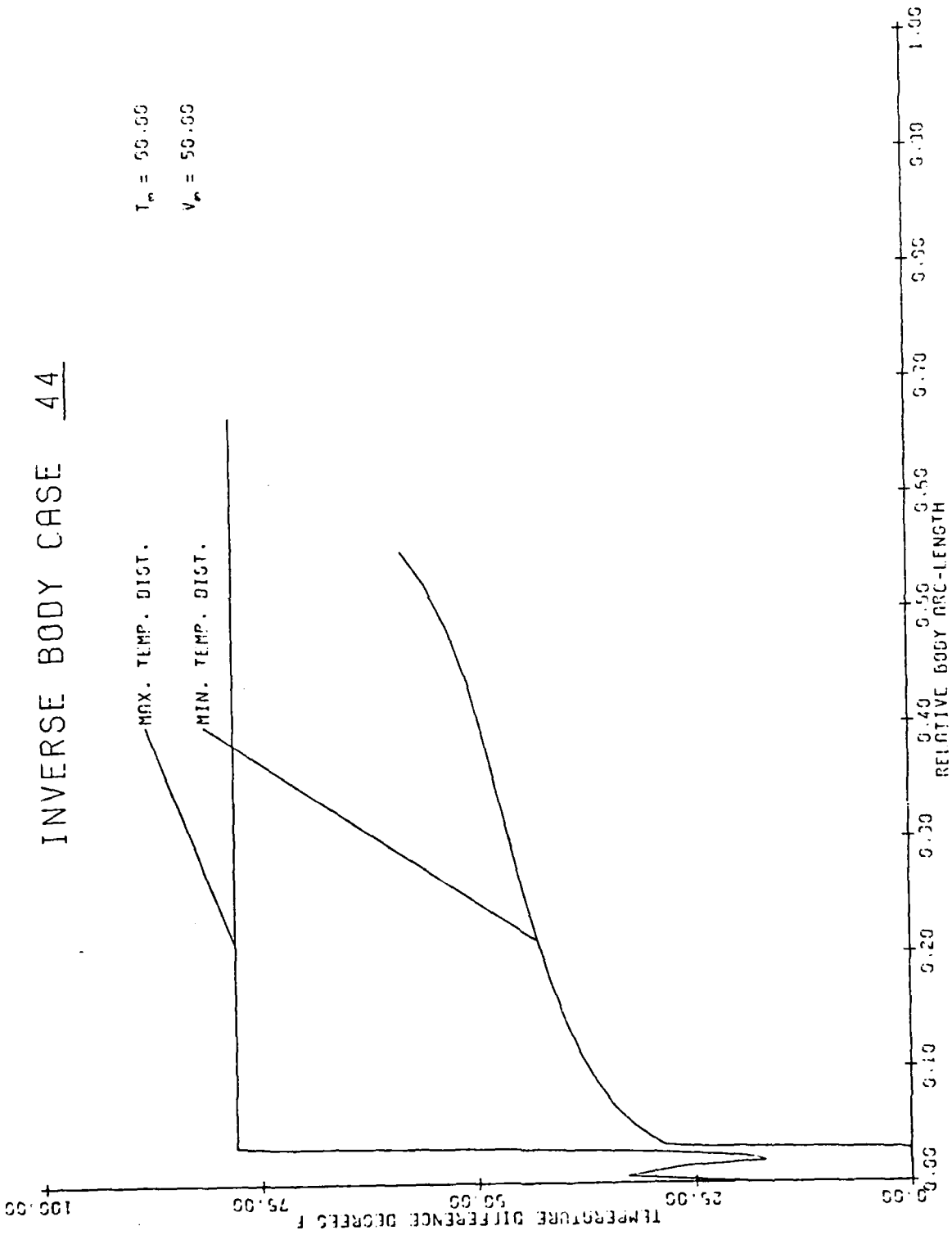

Figure 174. Temperature Distributions, Case No. 44.

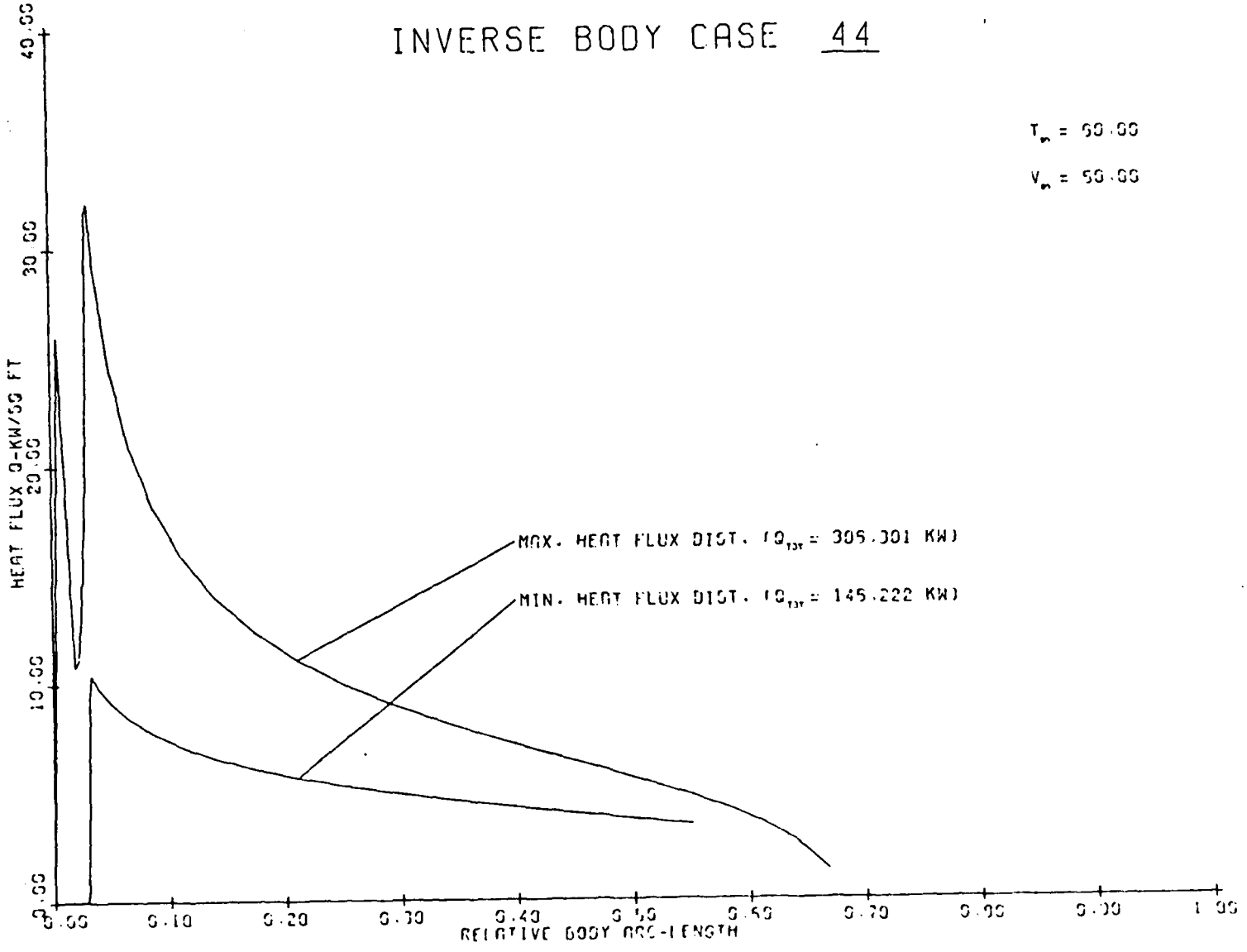

Figure 175. Heat Flux Distributions, Case No. 44.

19 August 1981
JJE:GHH:mmj

19 August 1981
JJE:GHH:mmj

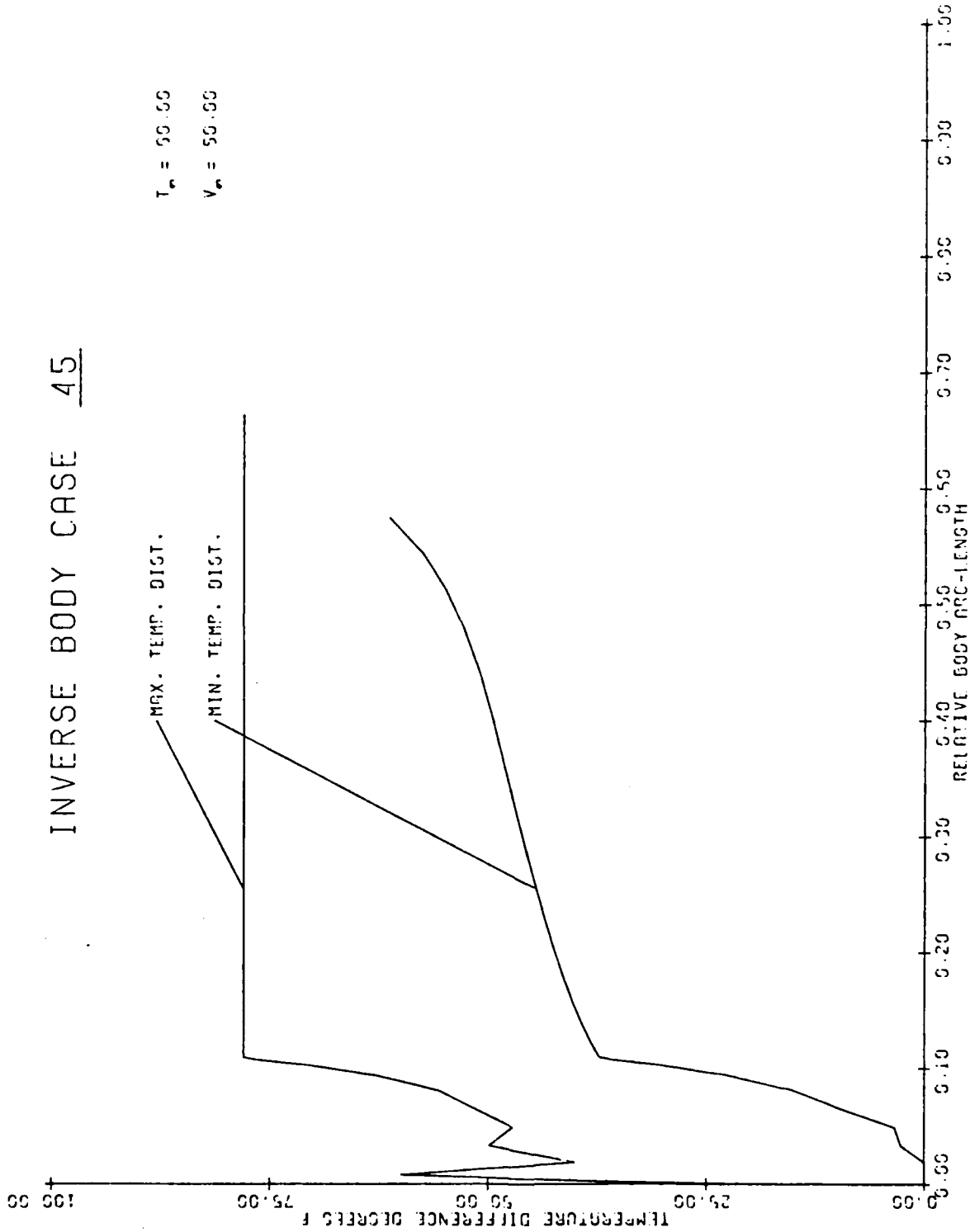

Figure 176. Temperature Distributions, Case No. 45.

19 August 1981
JJE:GHH:mmj

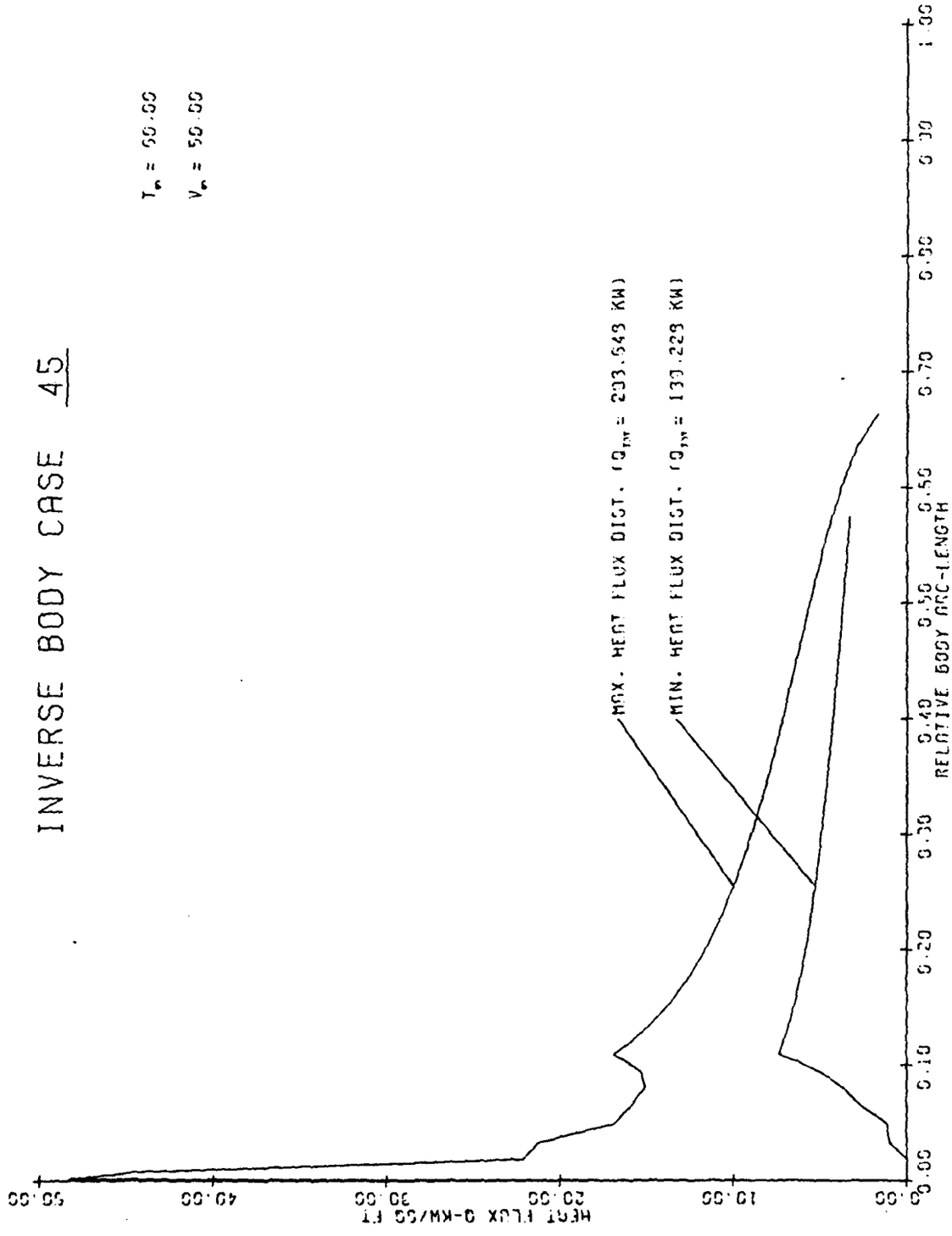

Figure 177. Heat Flux Distributions, Case No. 45.

19 August 1981
JJE:GHH:mmj

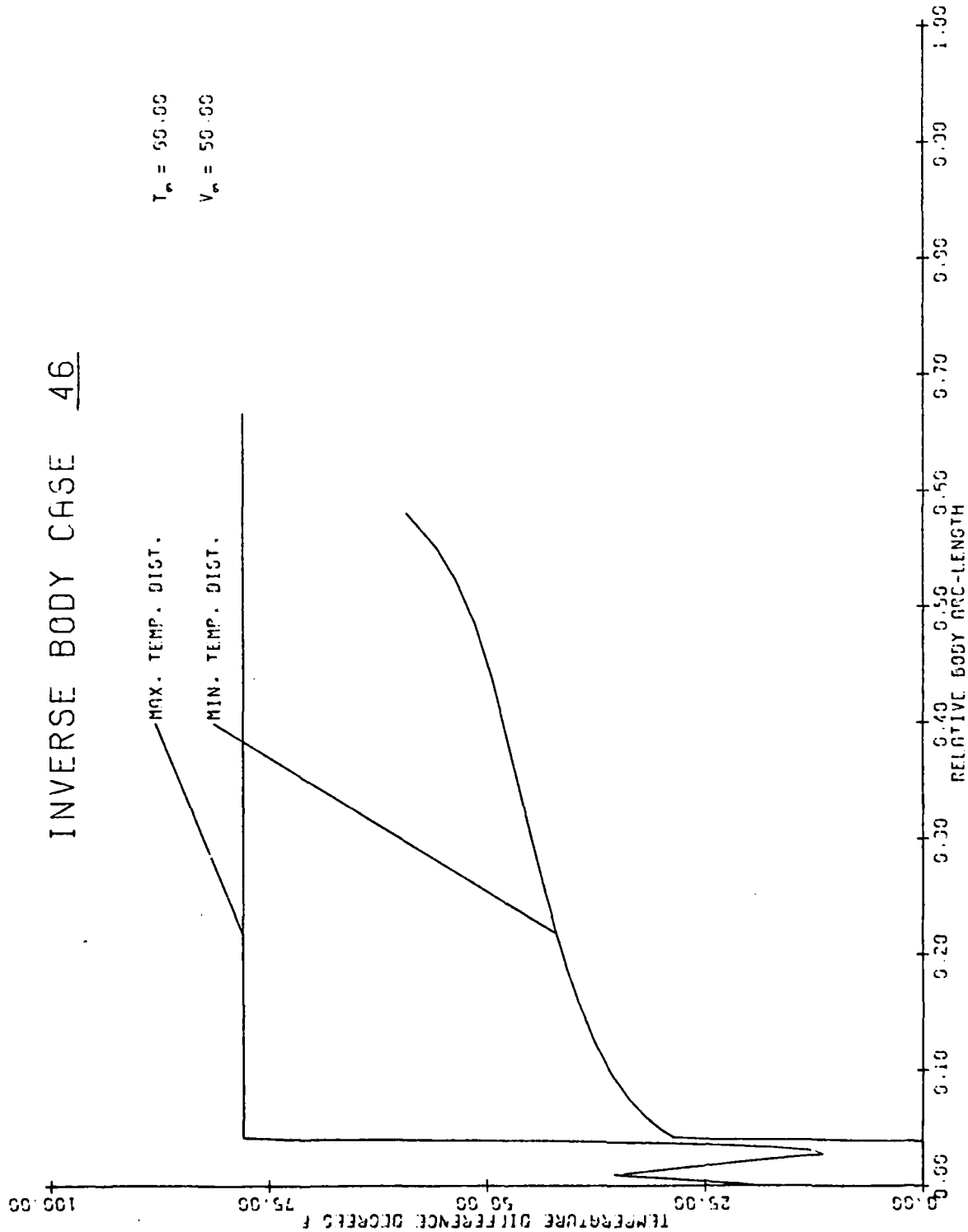

Figure 178. Temperature Distributions, Case No. 46.

19 August 1981
JJE:GHH:mmj

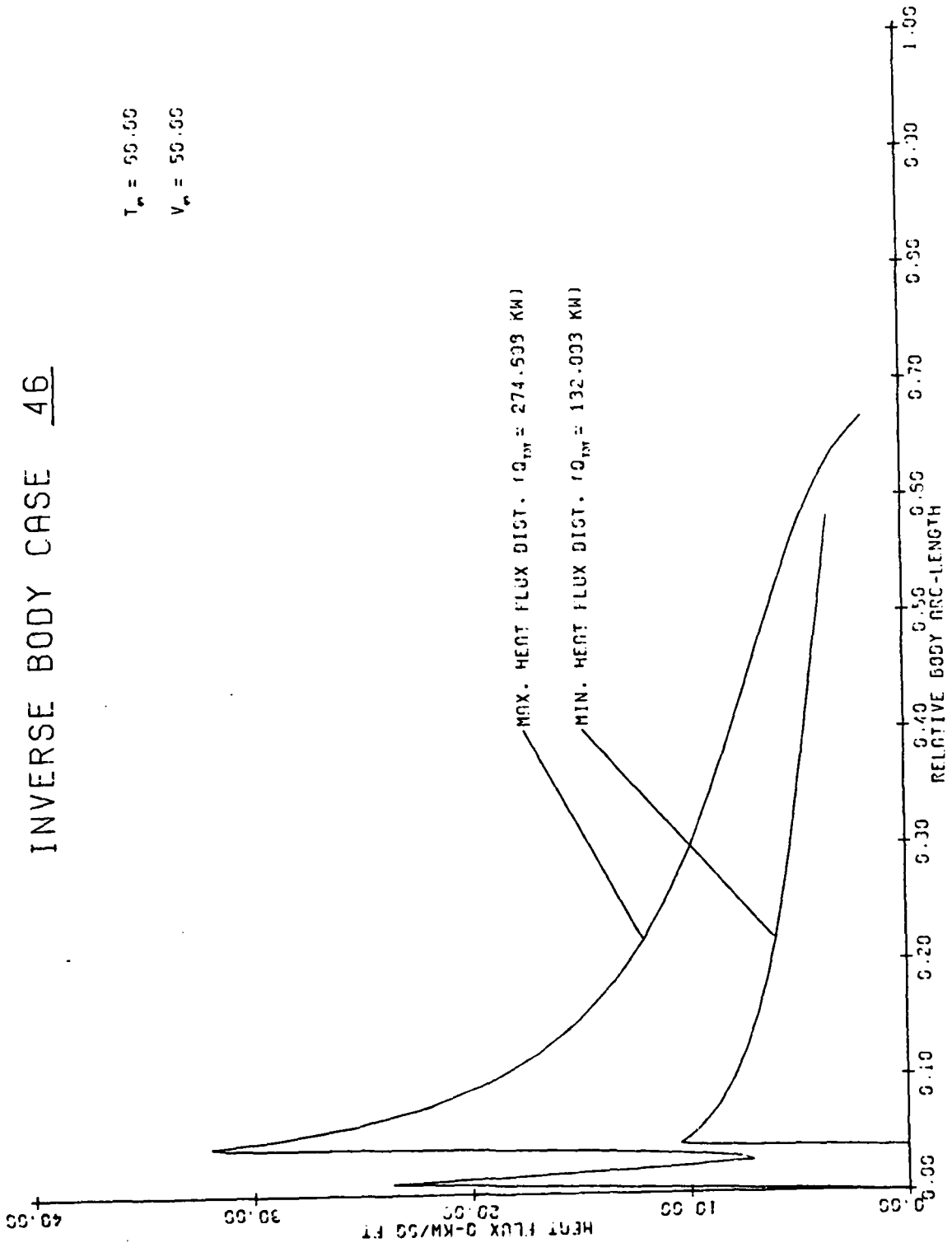

Figure 179. Heat Flux Distributions, Case No. 46.

19 August 1981
JJE:GHH:mmj

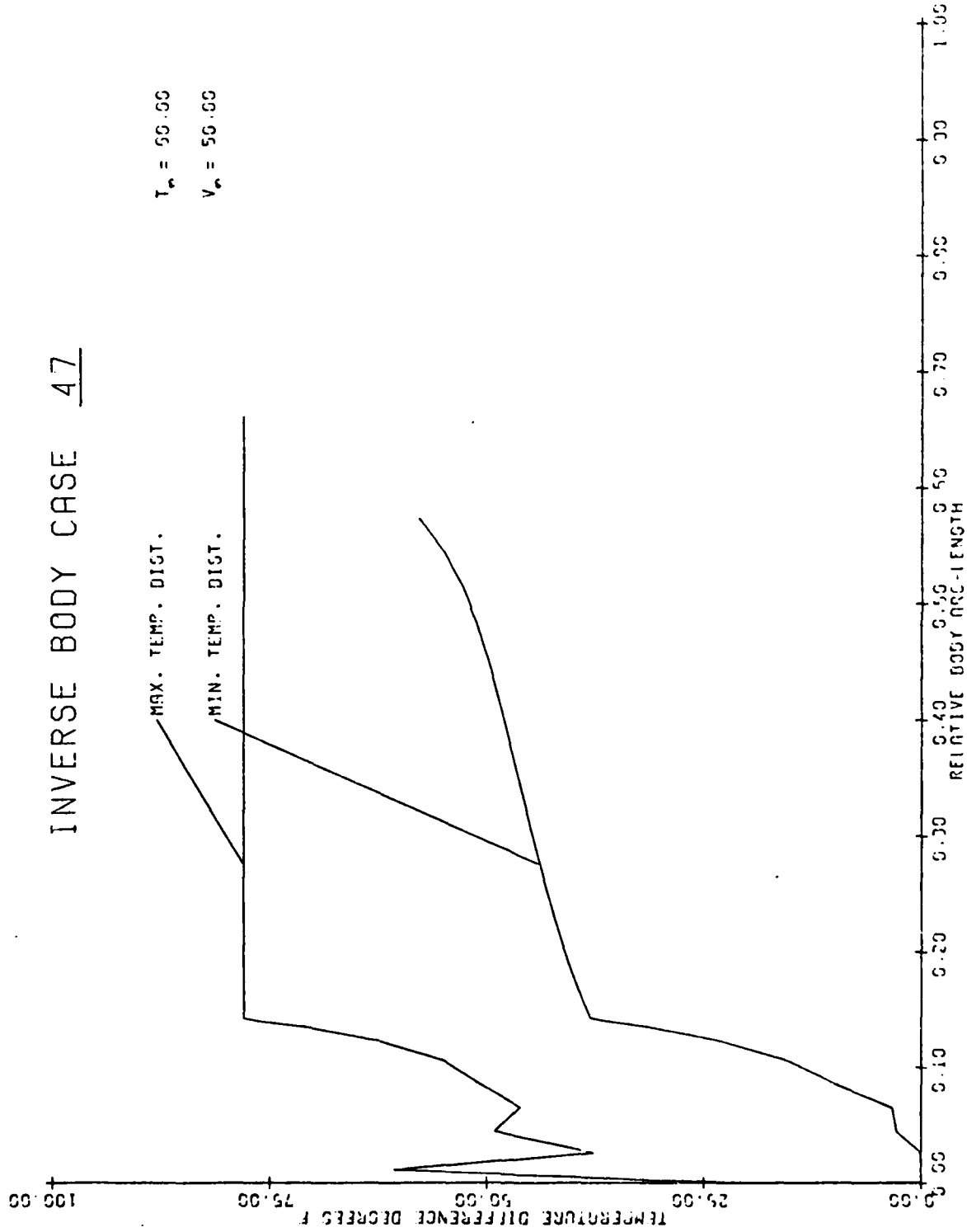

Figure 180. Temperature Distributions, Case No. 47.

19 August 1981
JJE:GHH:mmj

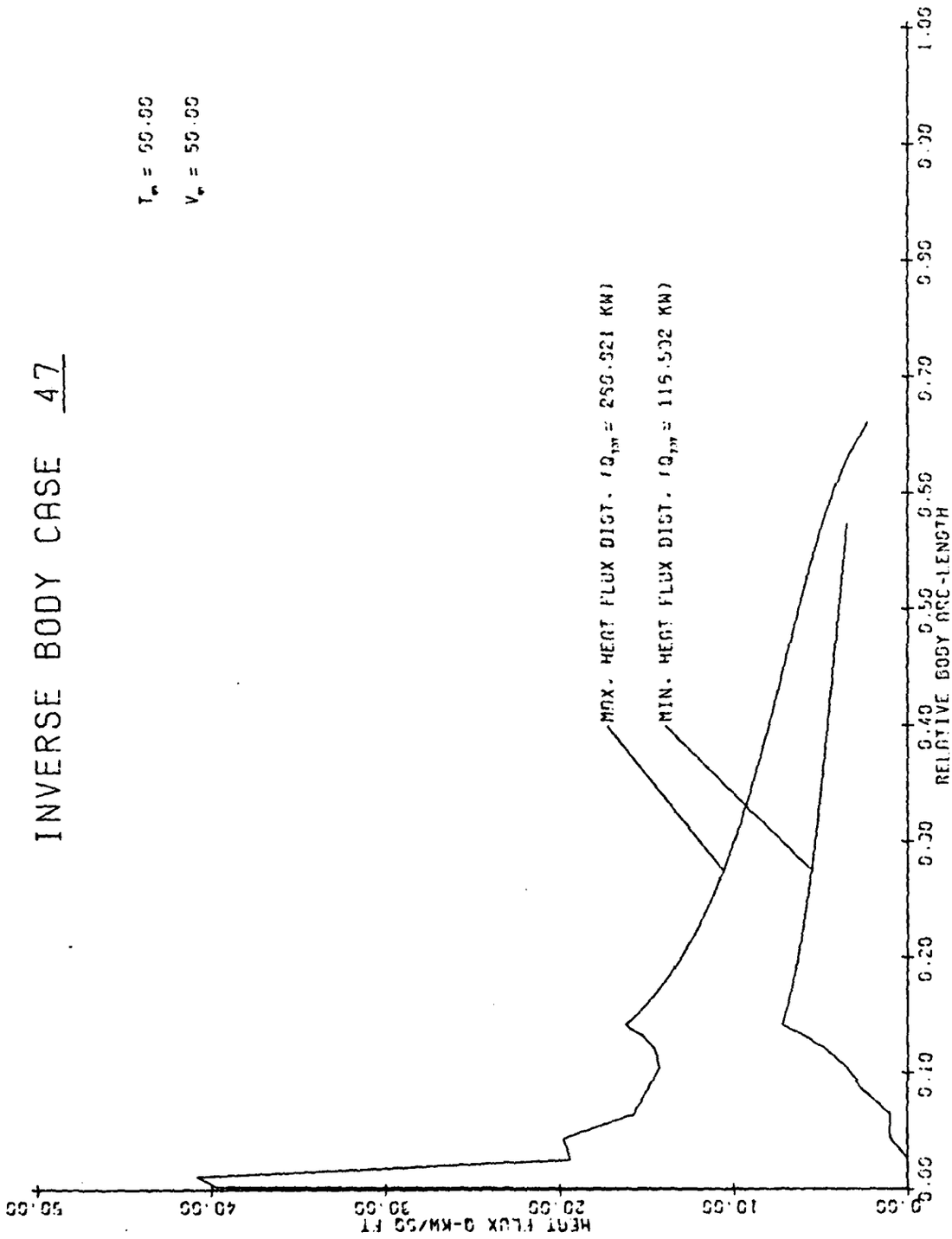

Figure 181. Heat Flux Distributions, Case No. 47.

19 August 1981
JJE:GHP:mmj

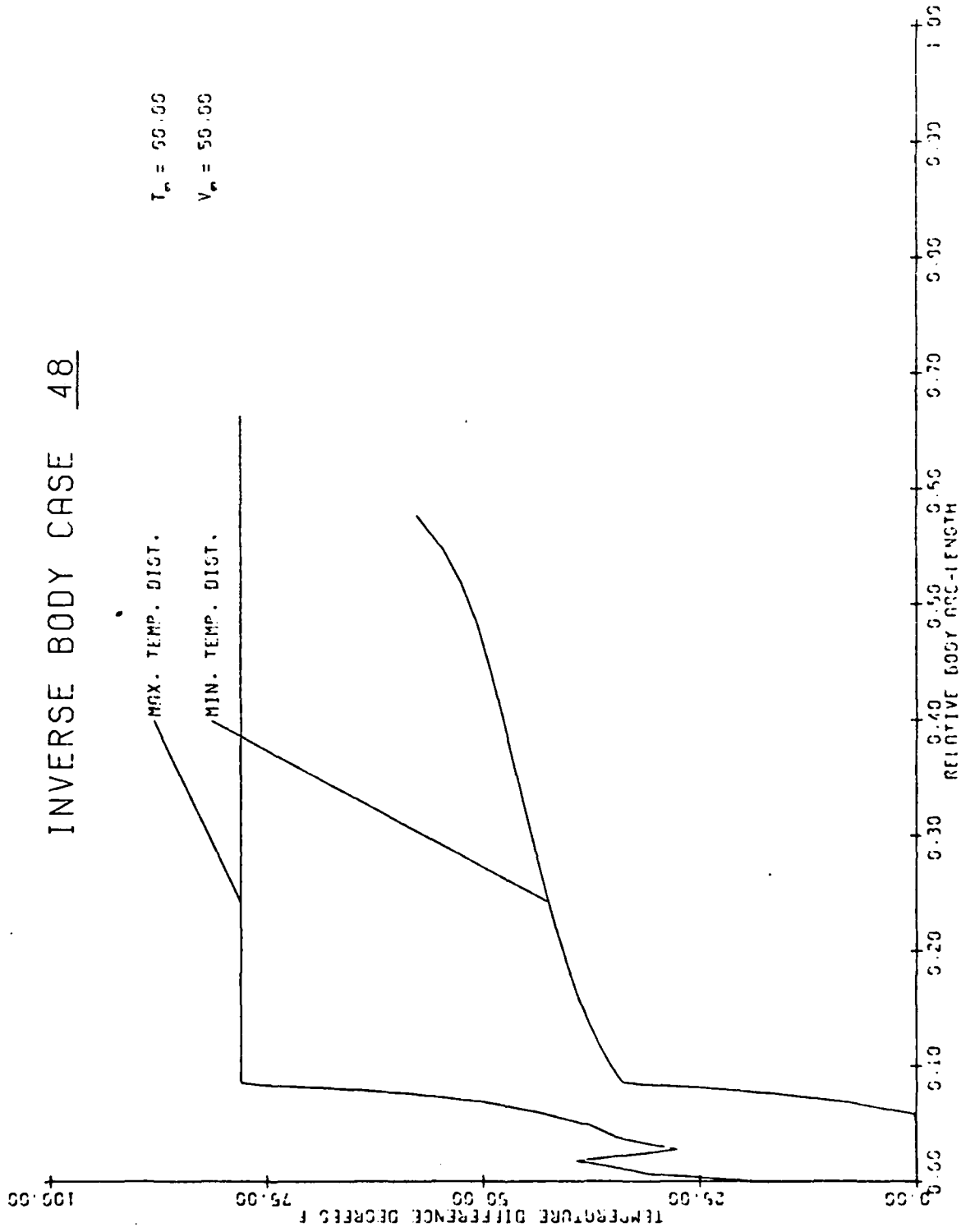

Figure 182. Temperature Distributions, Case No. 48.

19 August 1981
JJE:GHH:mmj

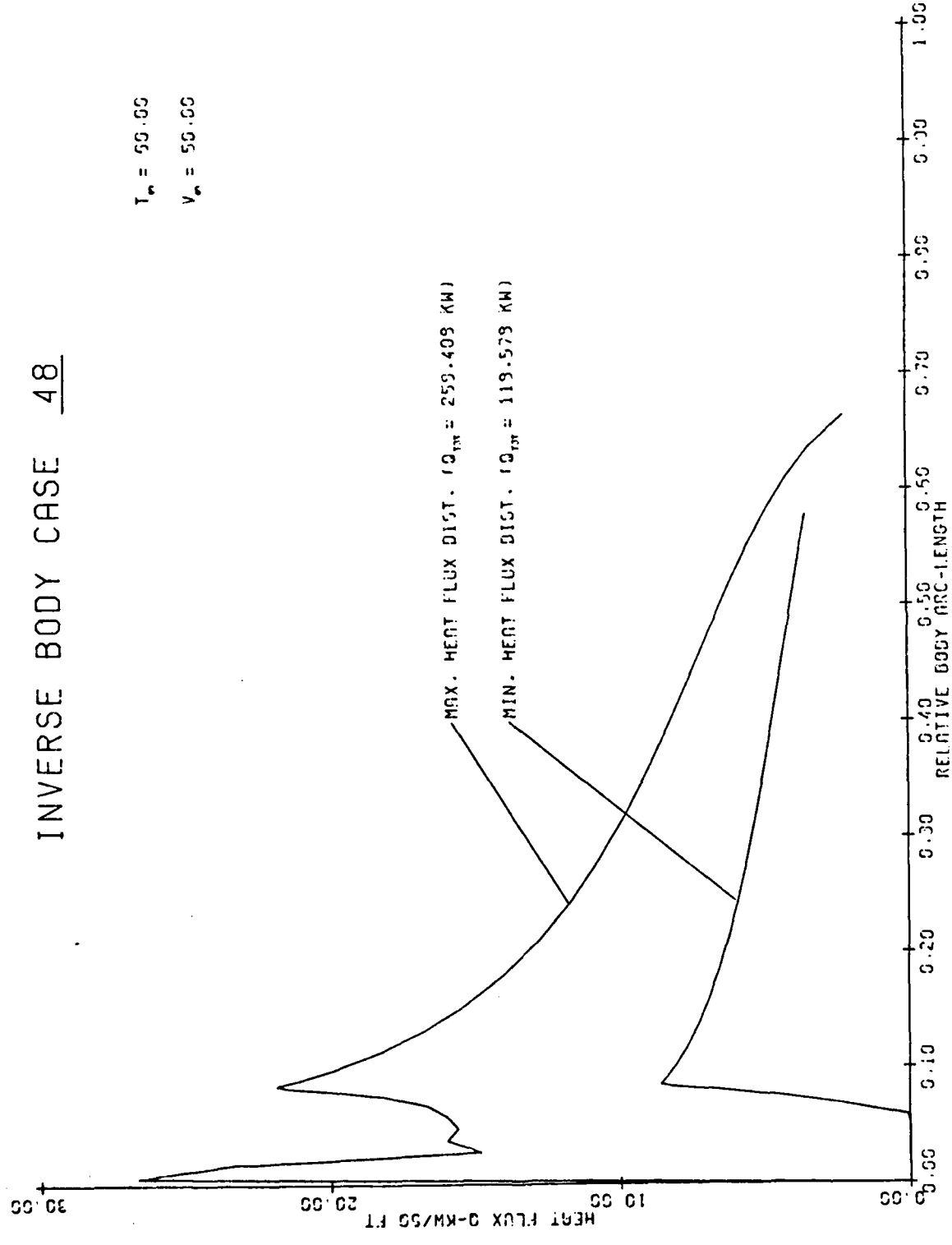

Figure 183. Heat Flux Distributions, Case No. 48.

19 August 1981
JJE:GHH:mmj

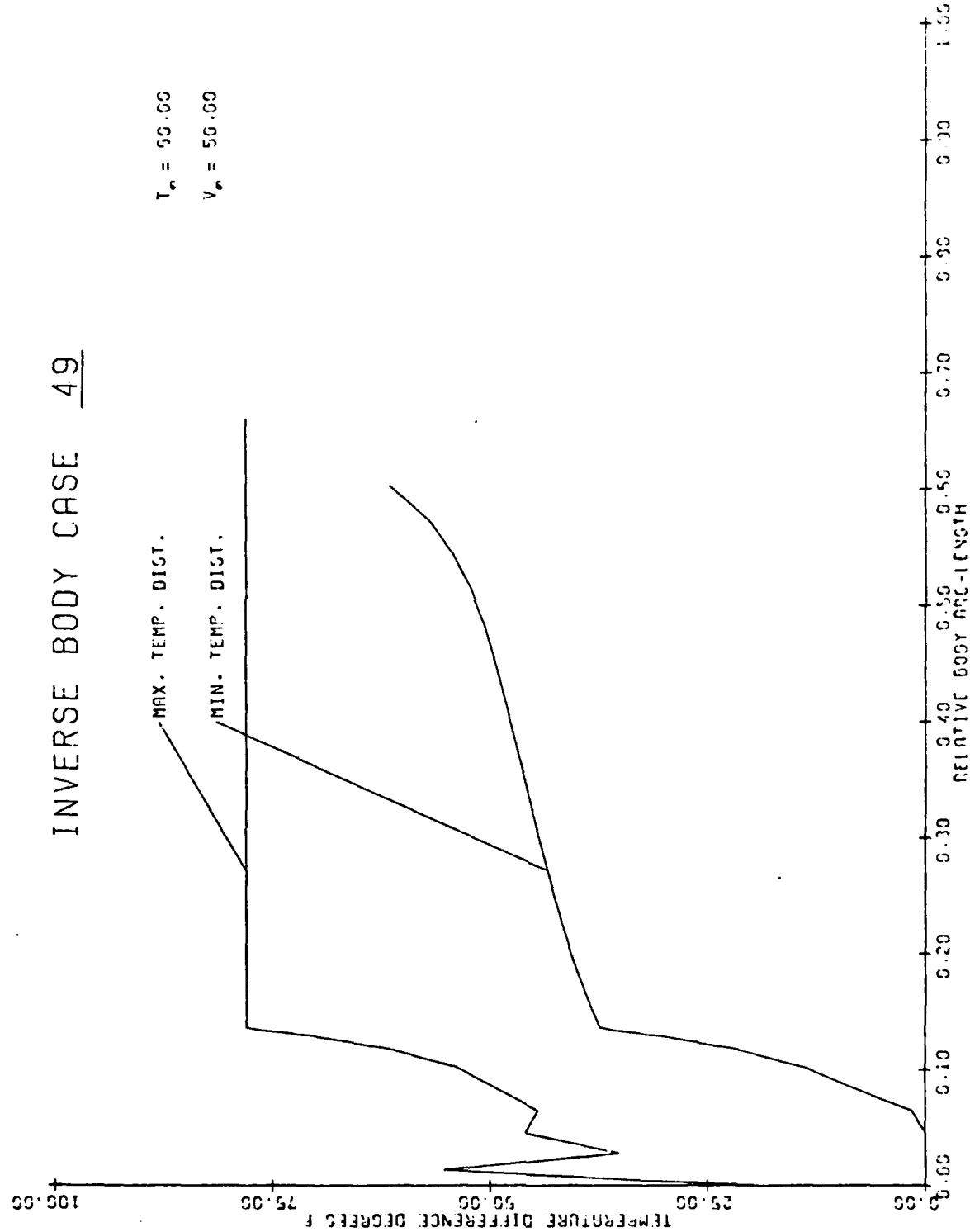

Figure 184. Temperature Distributions, Case No. 49.

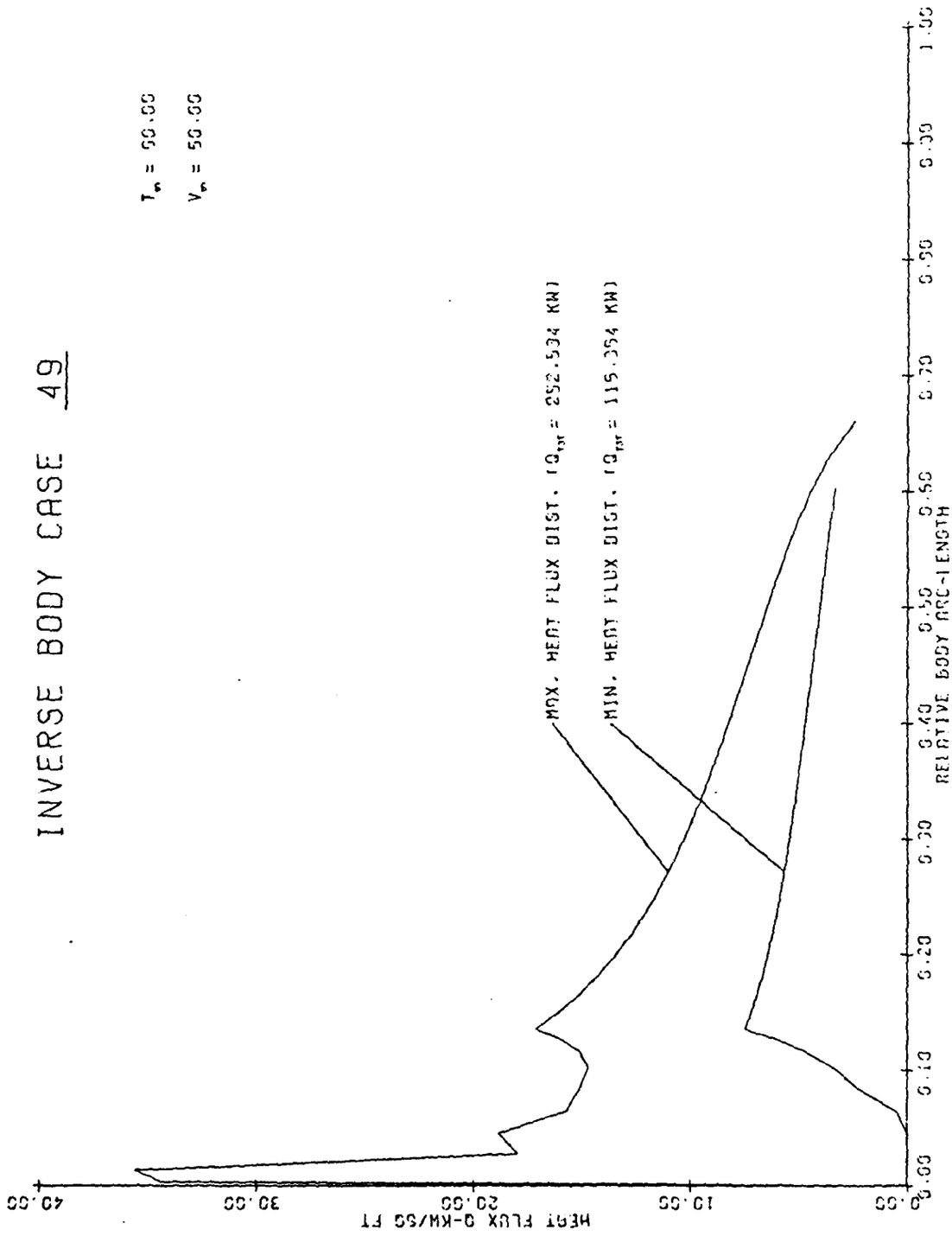

Figure 185. Heat Flux Distributions, Case No. 49.

19 August 1981
JJE:GHH:mmj

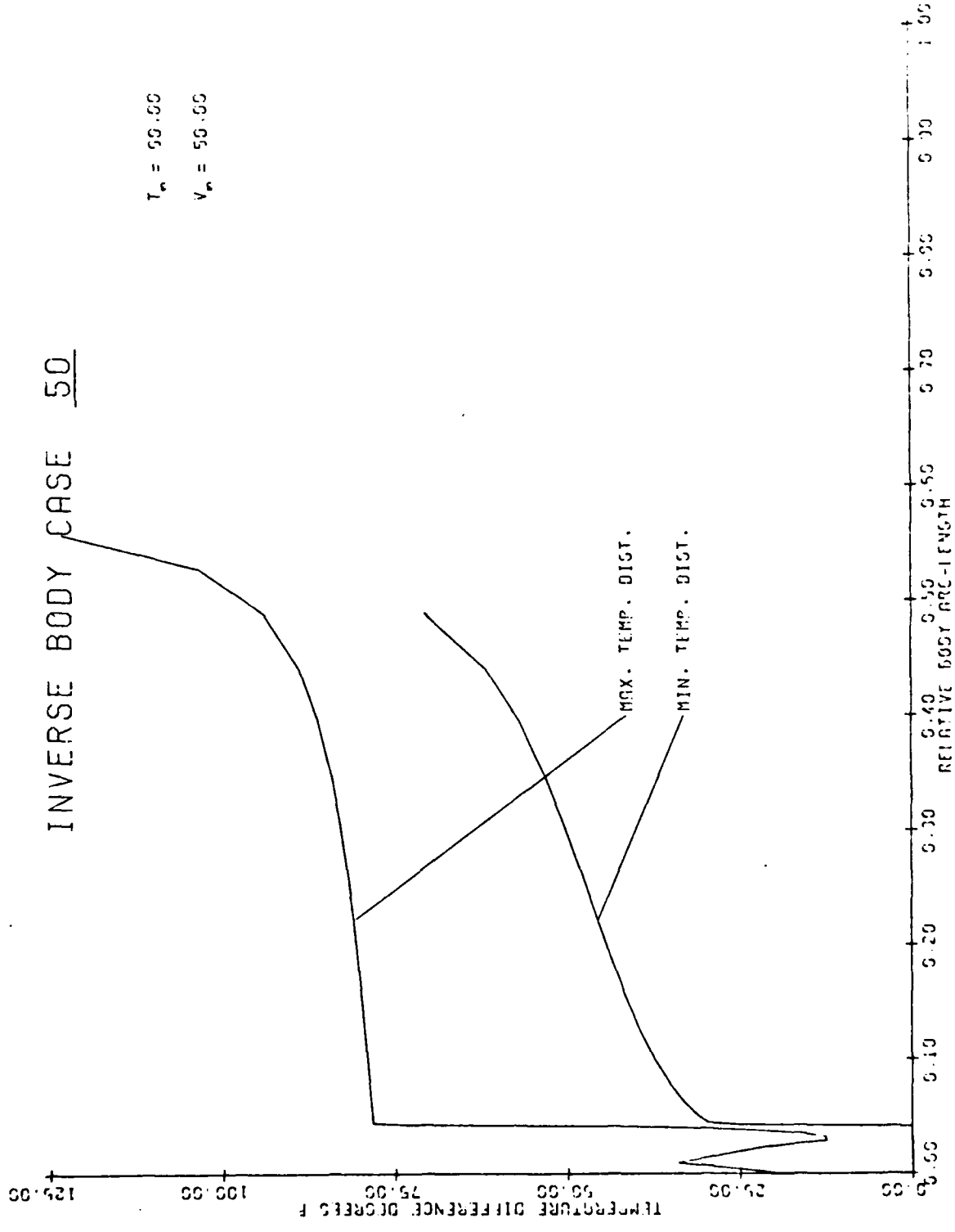

Figure 186. Temperature Distributions, Case No. 50.

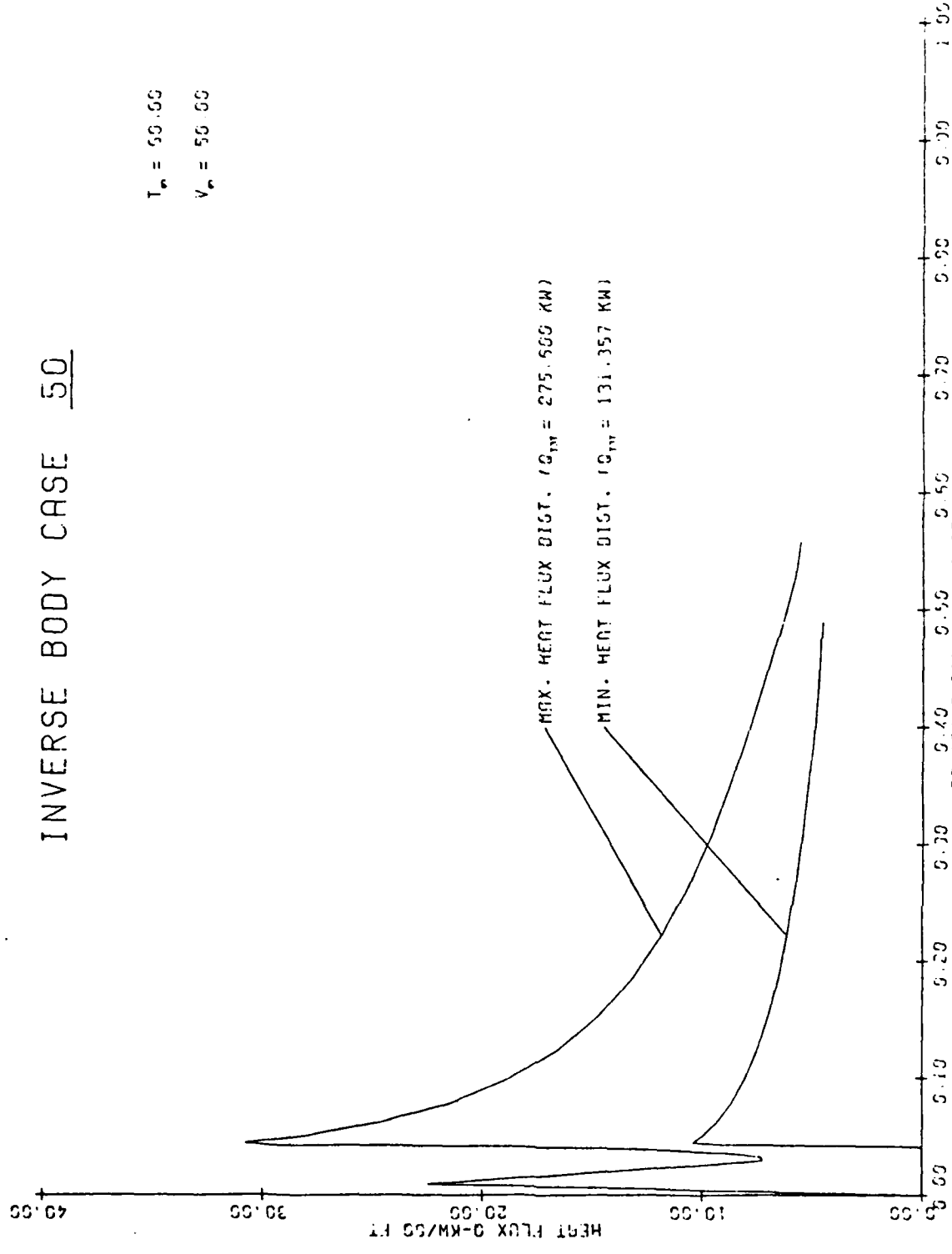

Figure 187. Heat Flux Distributions, Case No. 50.

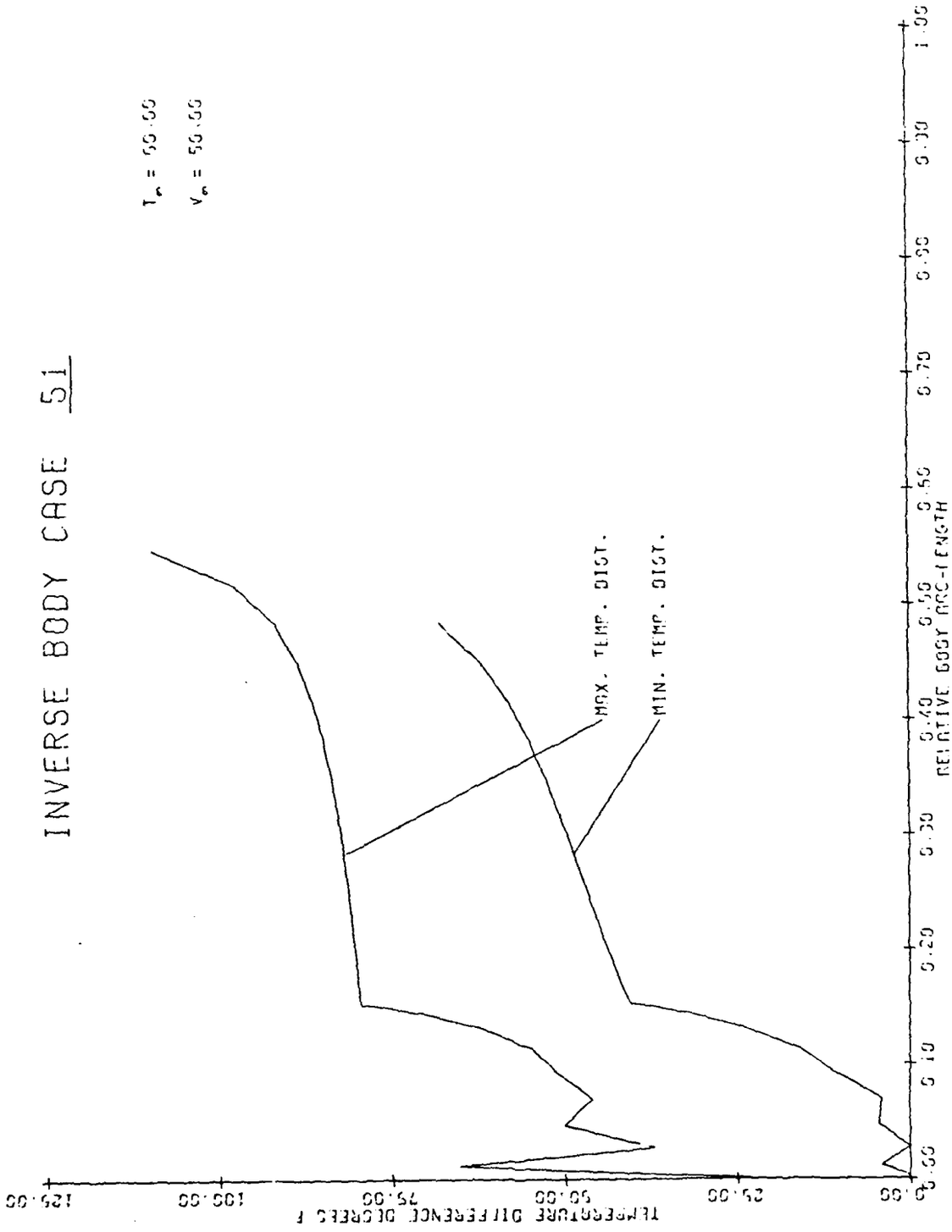

Figure 188. Temperature Distributions, Case No. 51.

19 August 1981
JJE:GHH:mmj

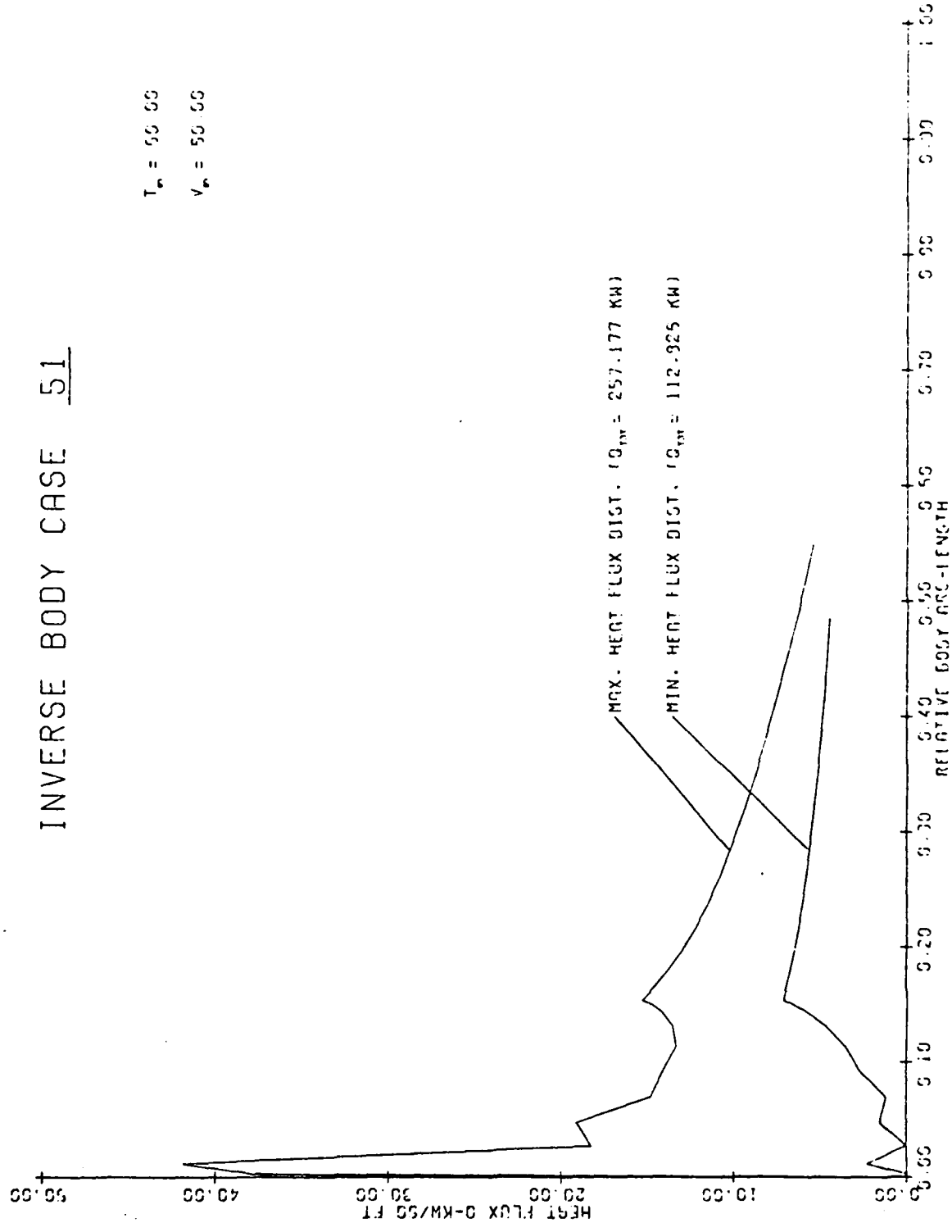

Figure 189. Heat Flux Distributions, Case No. 51.

19 August 1981
JJE:GHH:mmj

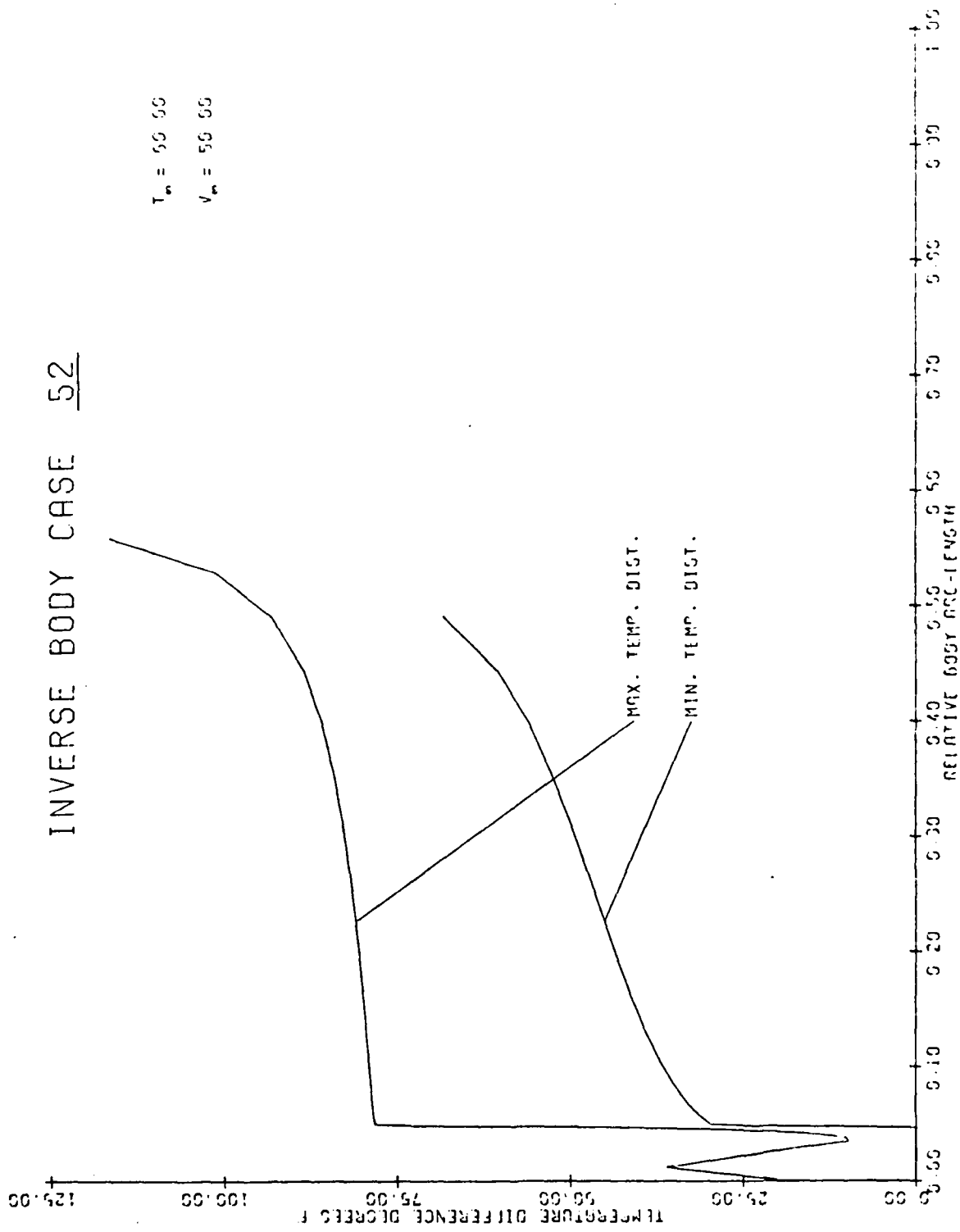

Figure 190. Temperature Distributions, Case No. 52.

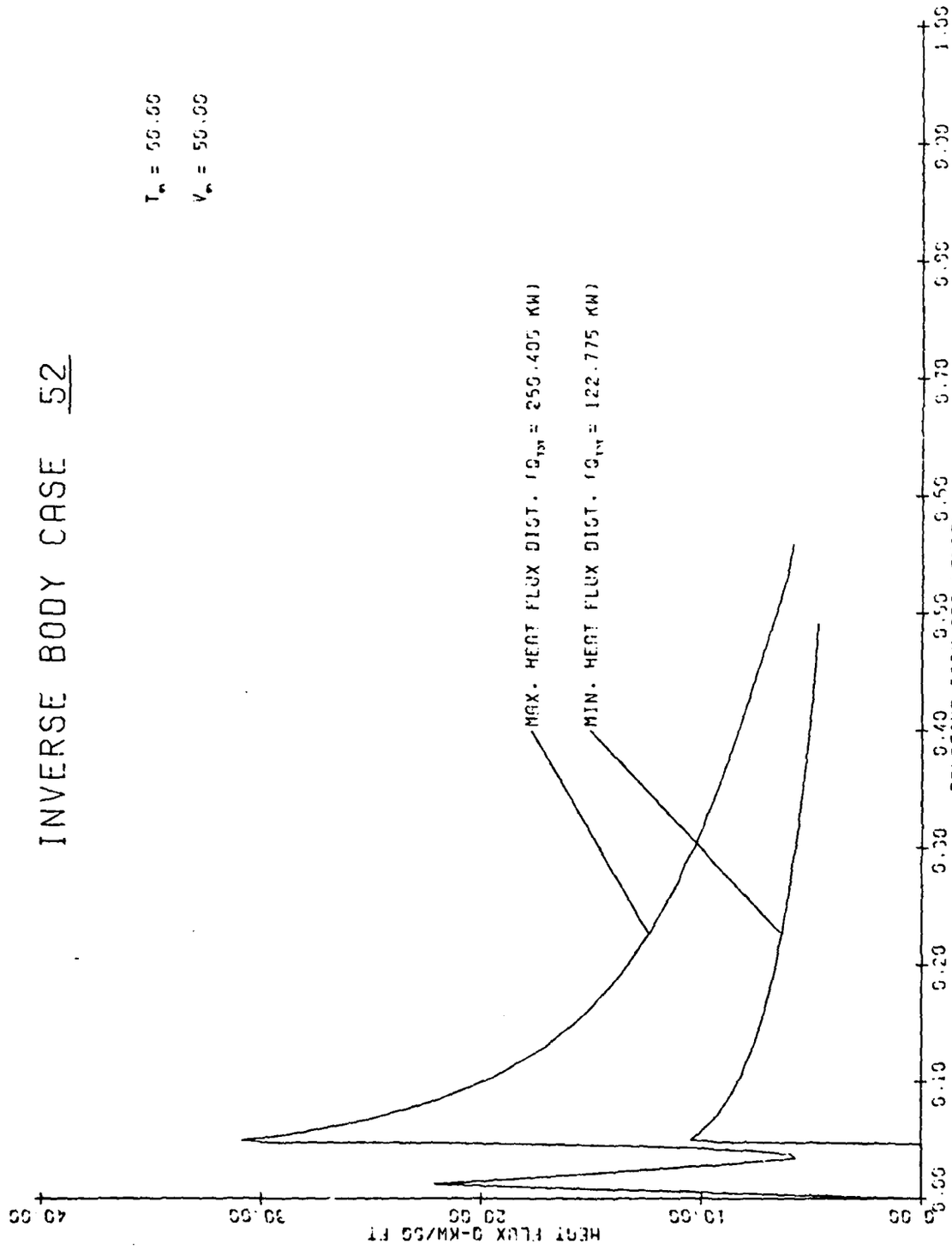

Figure 191. Heat Flux Distributions, Case No. 52.

19 August 1981
JJE:GHH:mmj

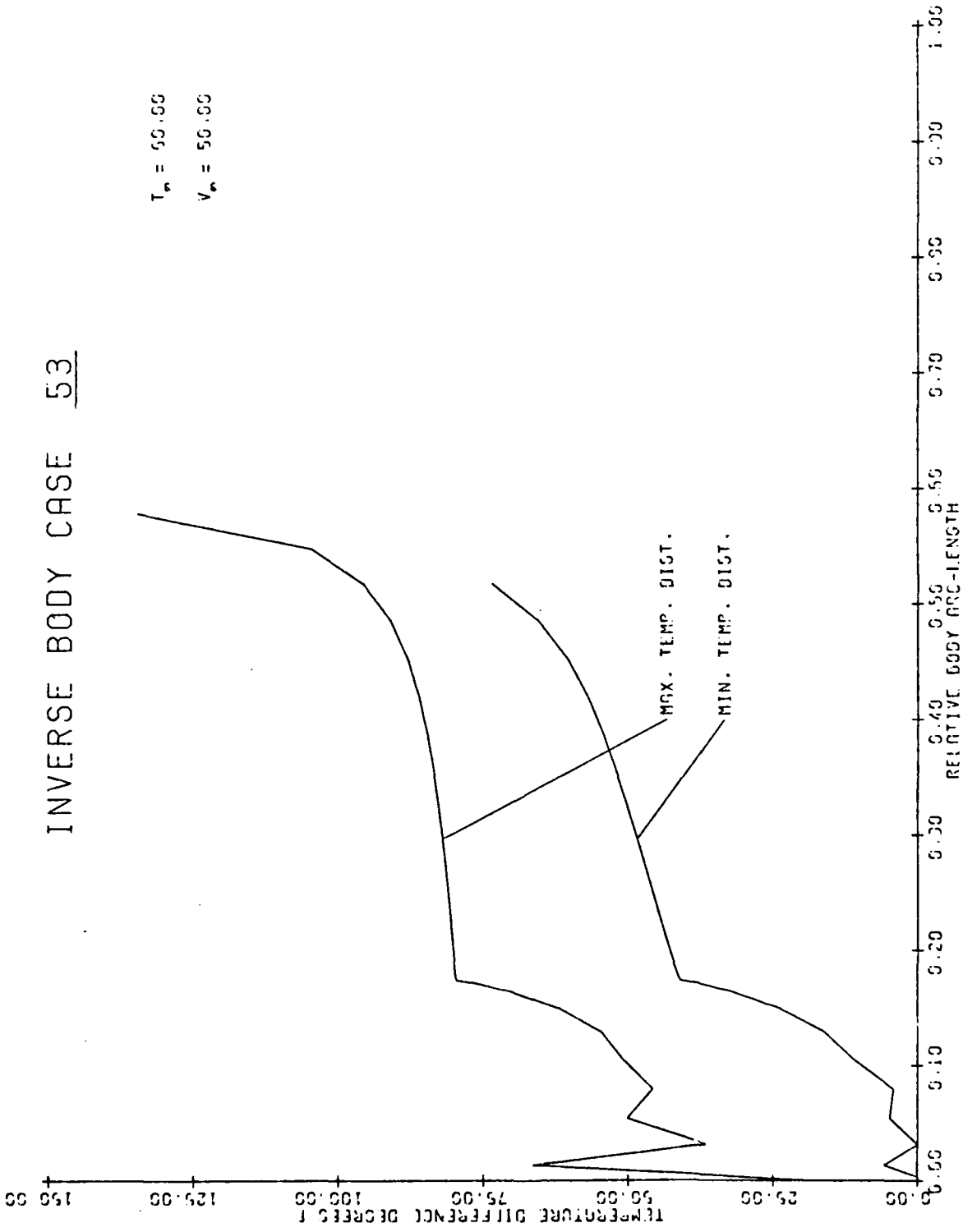

Figure 192. Temperature Distributions, CAse No. 53.

19 August 1981
JJE:GHH:mmj

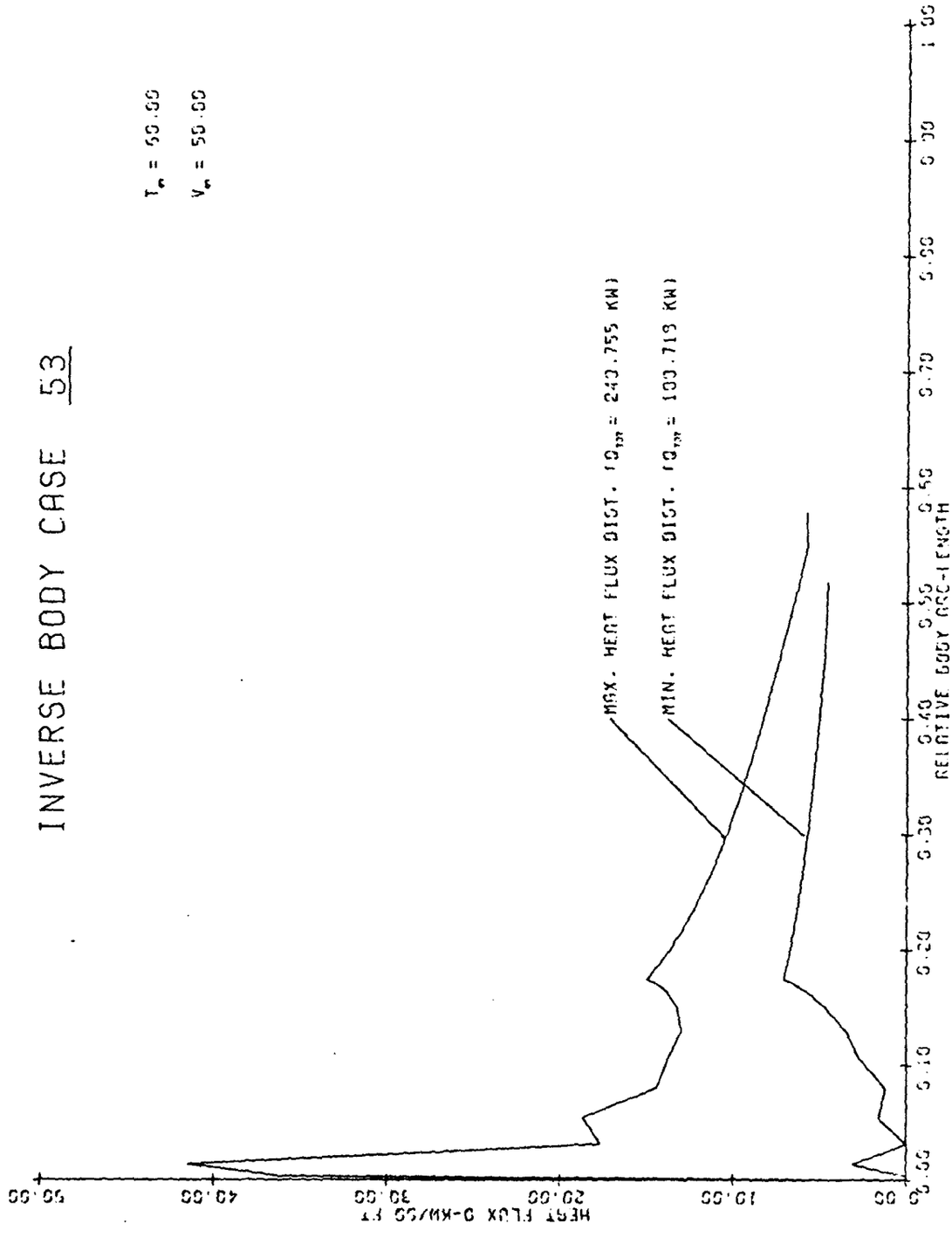

Figure 193. Heat Flux Distributions, Case No. 53.

19 August 1981
JJE:GHH;mmj

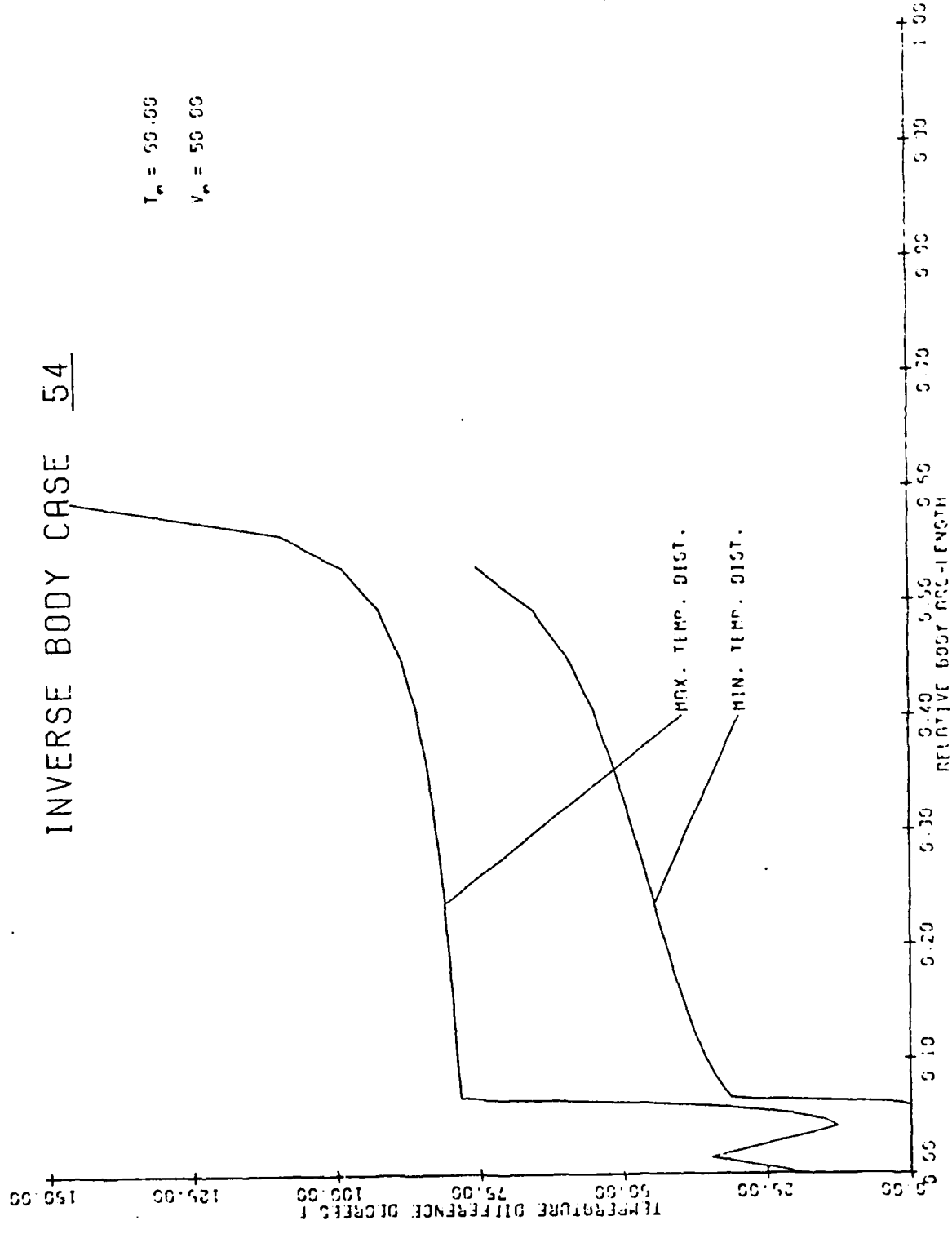

Figure 194. Temperature Distributions, CAse No. 54.

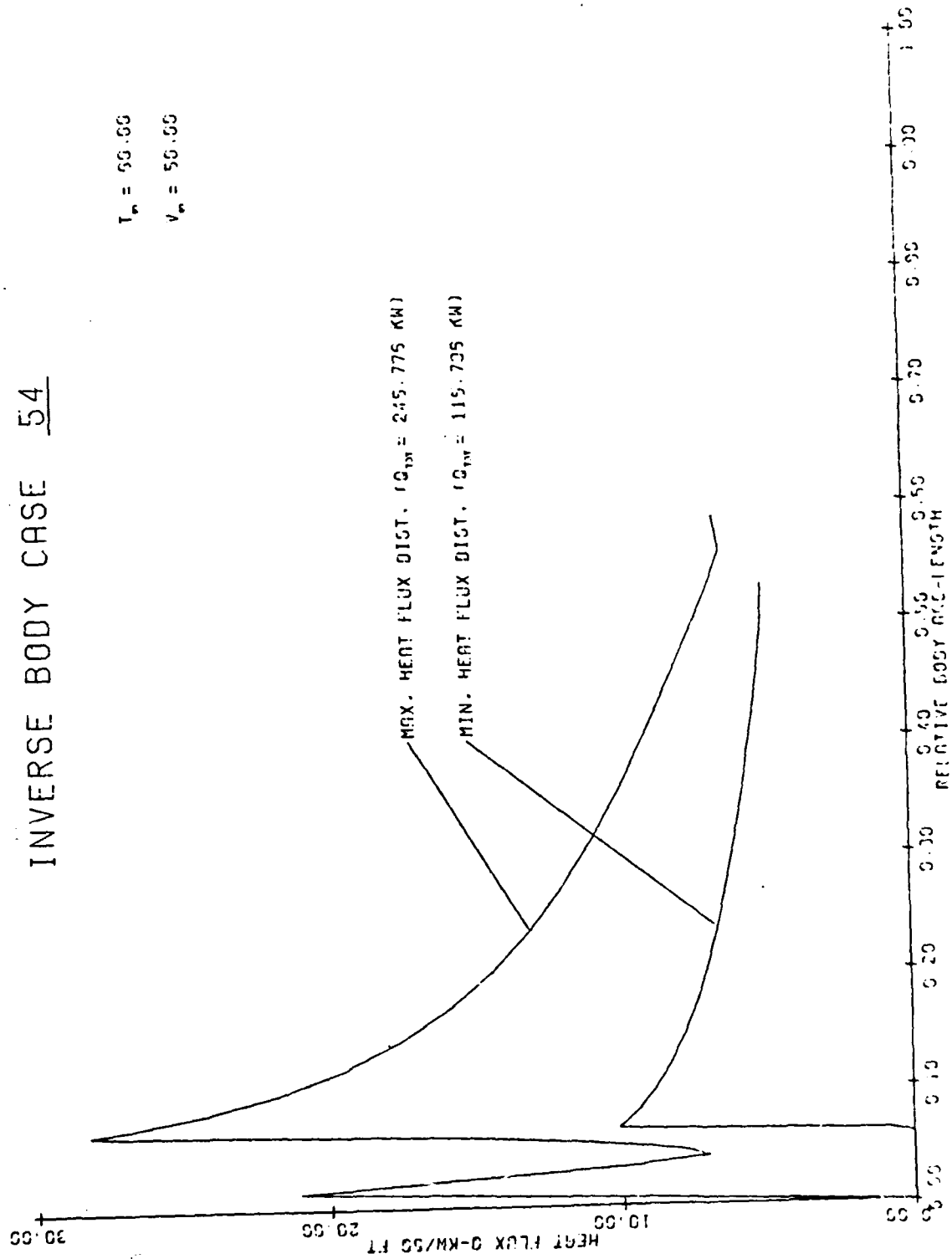

Figure 195. Heat Flux Distributions, Case No. 54.

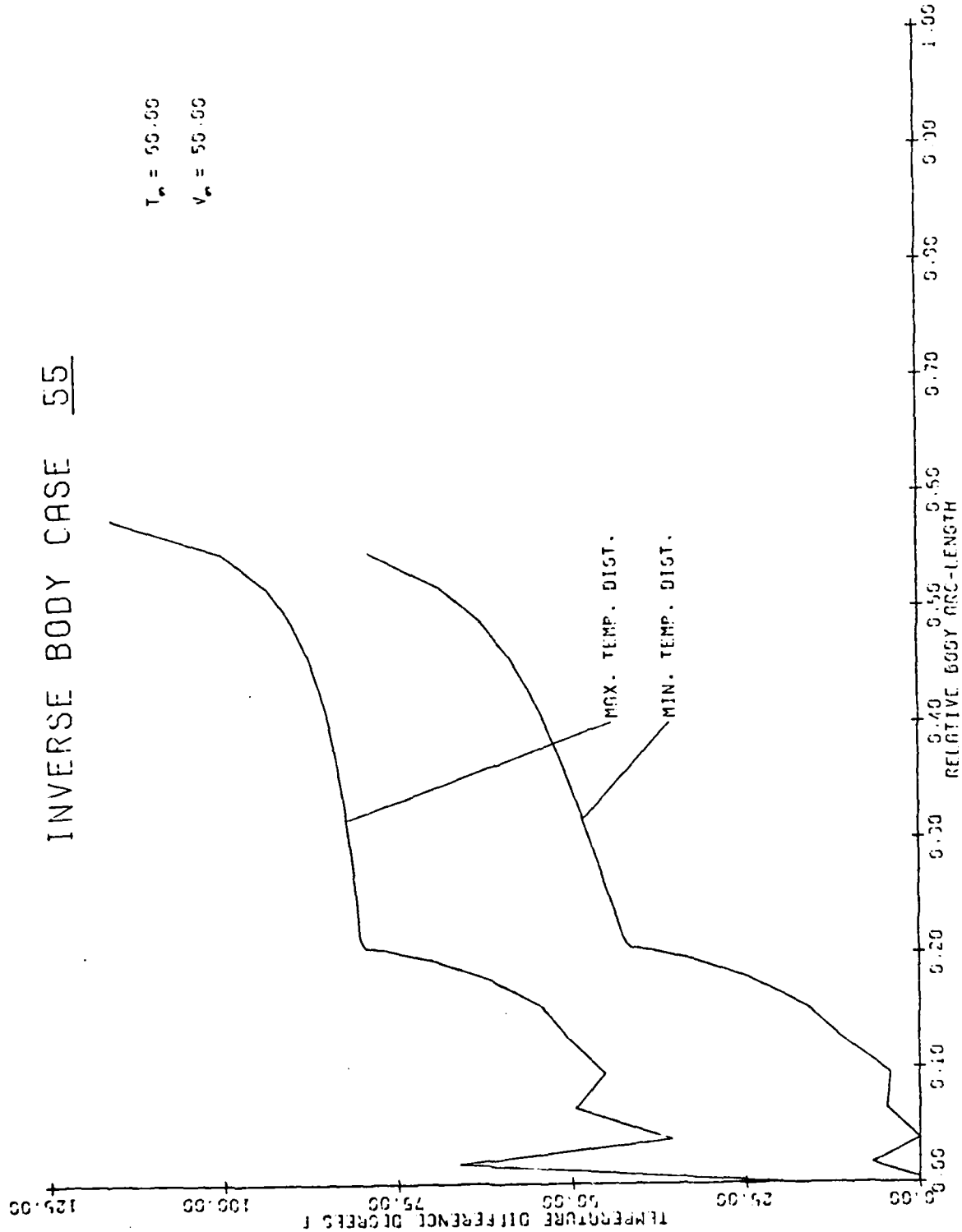

Figure 196. Temperature Distributions, Case No. 55.

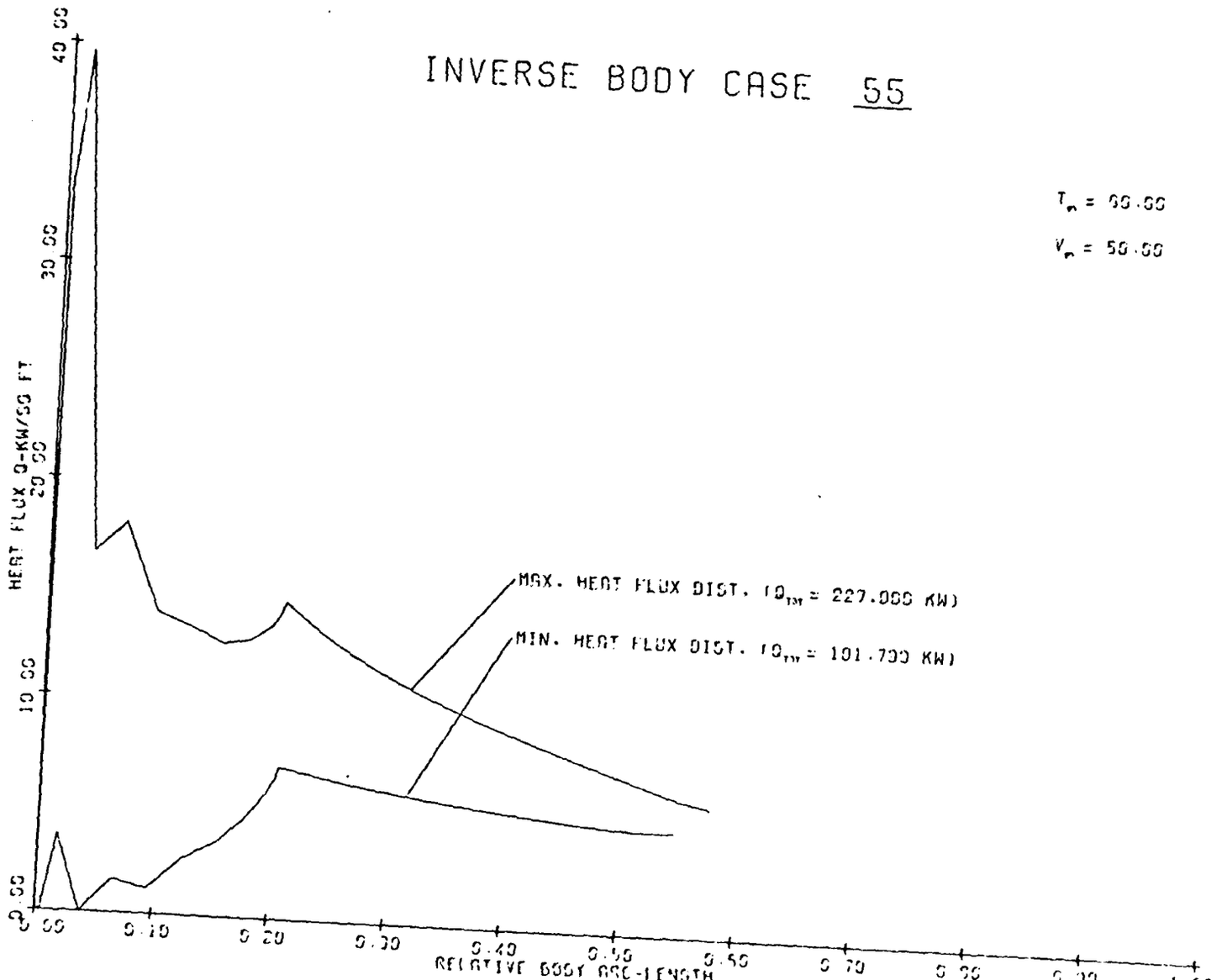

Figure 197. Heat Flux Distributions, Case No. 55.

19 August 1981
JJE:GHH:mmj

19 August 1981
JJE:GHH:mmj

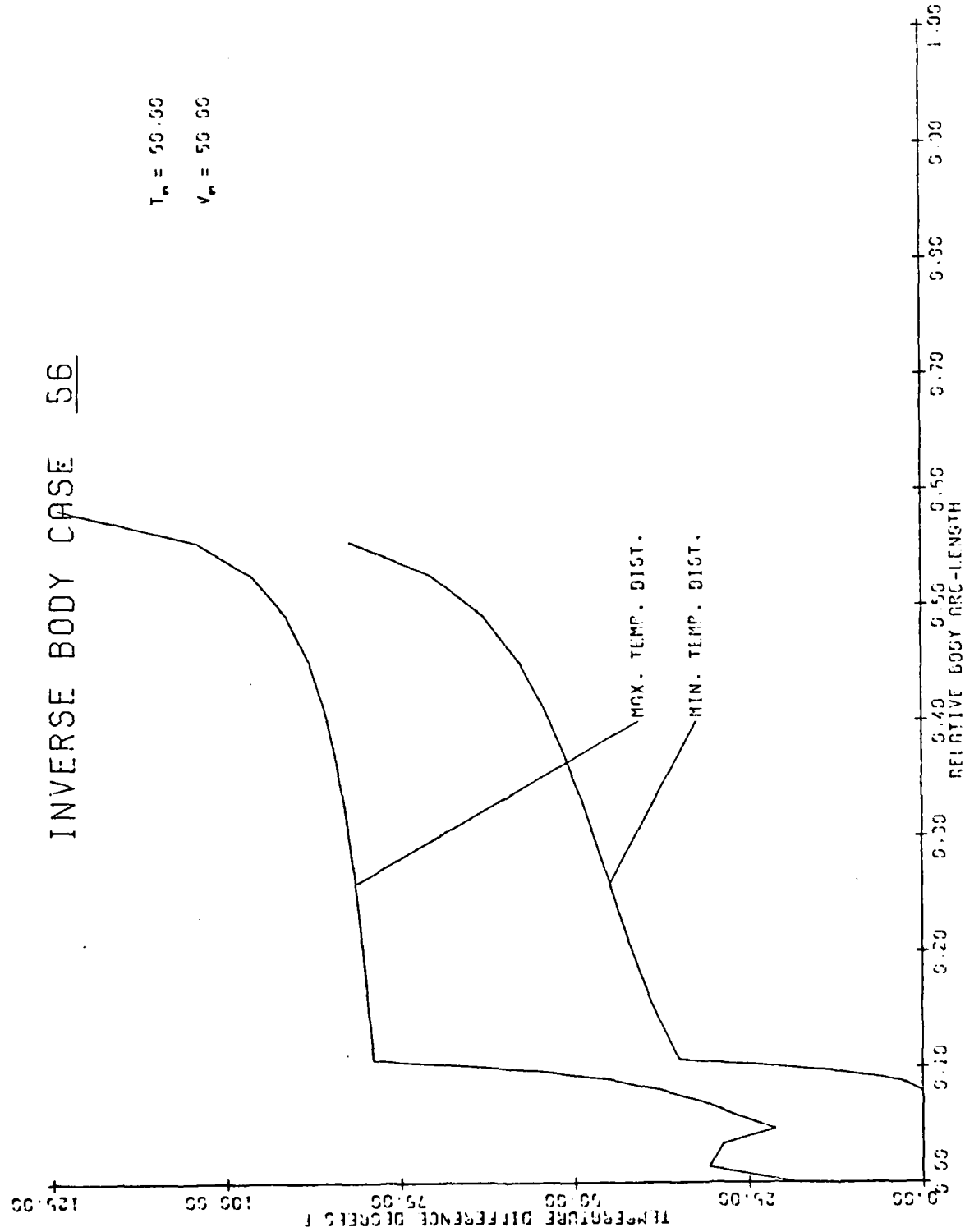

Figure 198. Temperature Distributions, Case No. 56.

19 August 1981
JJE:GHH:mmj

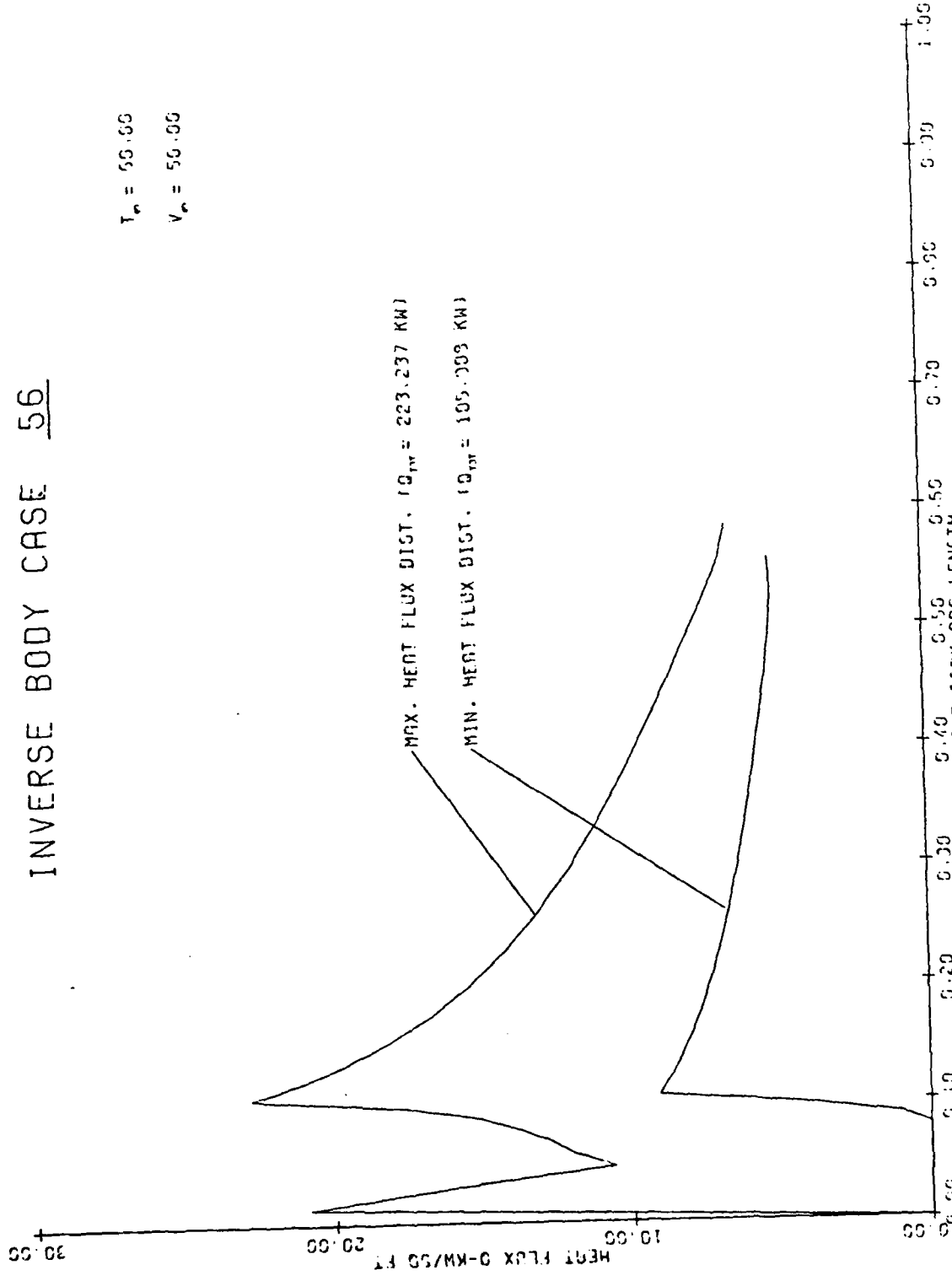

Figure 199. Heat Flux Distributions, Case No. 56.

19 August 1981
JJE:GHH:mmj

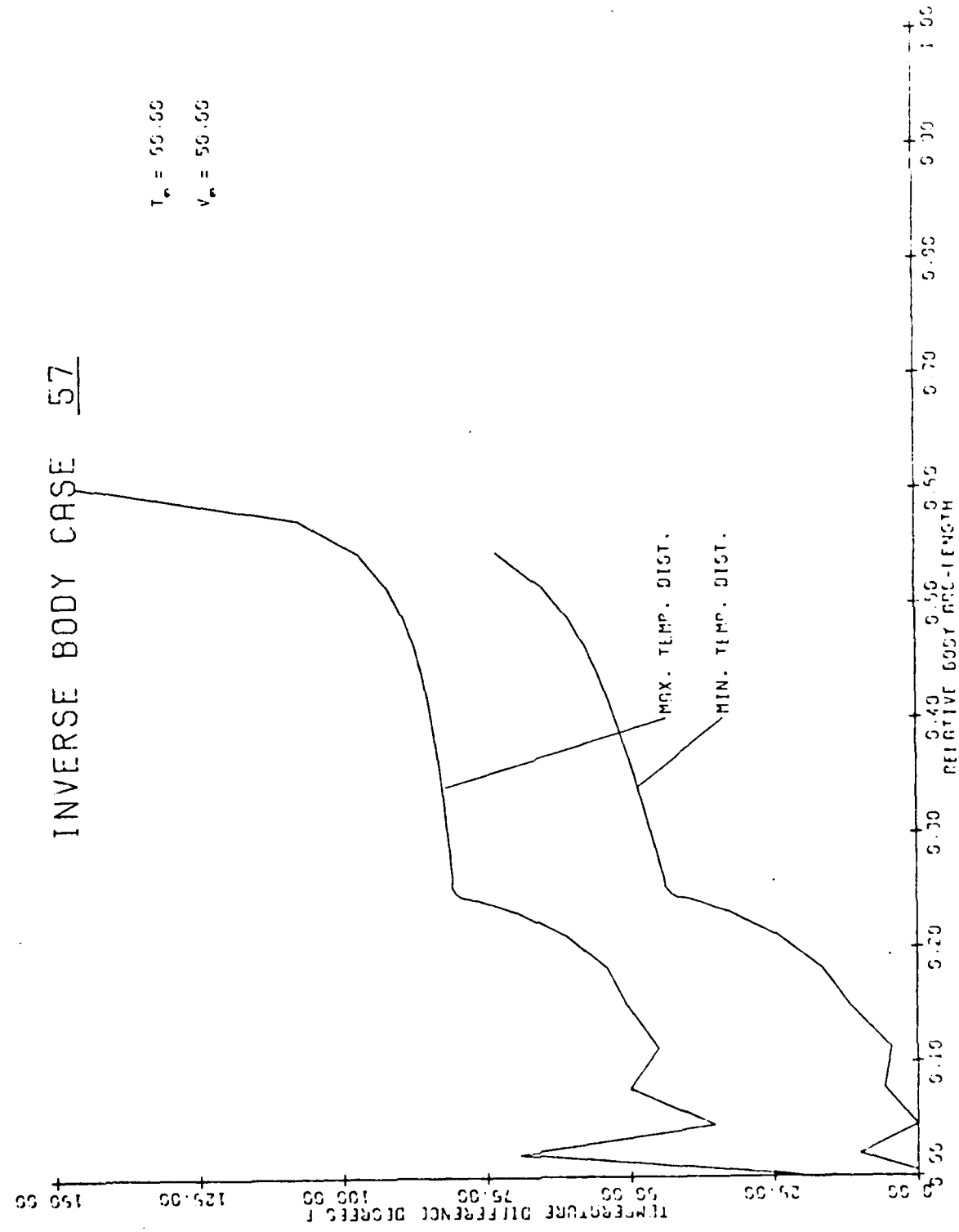

Figure 200. Temperature Distributions, Case No. 57.

19 August 1981
JJE:GHH:mmj

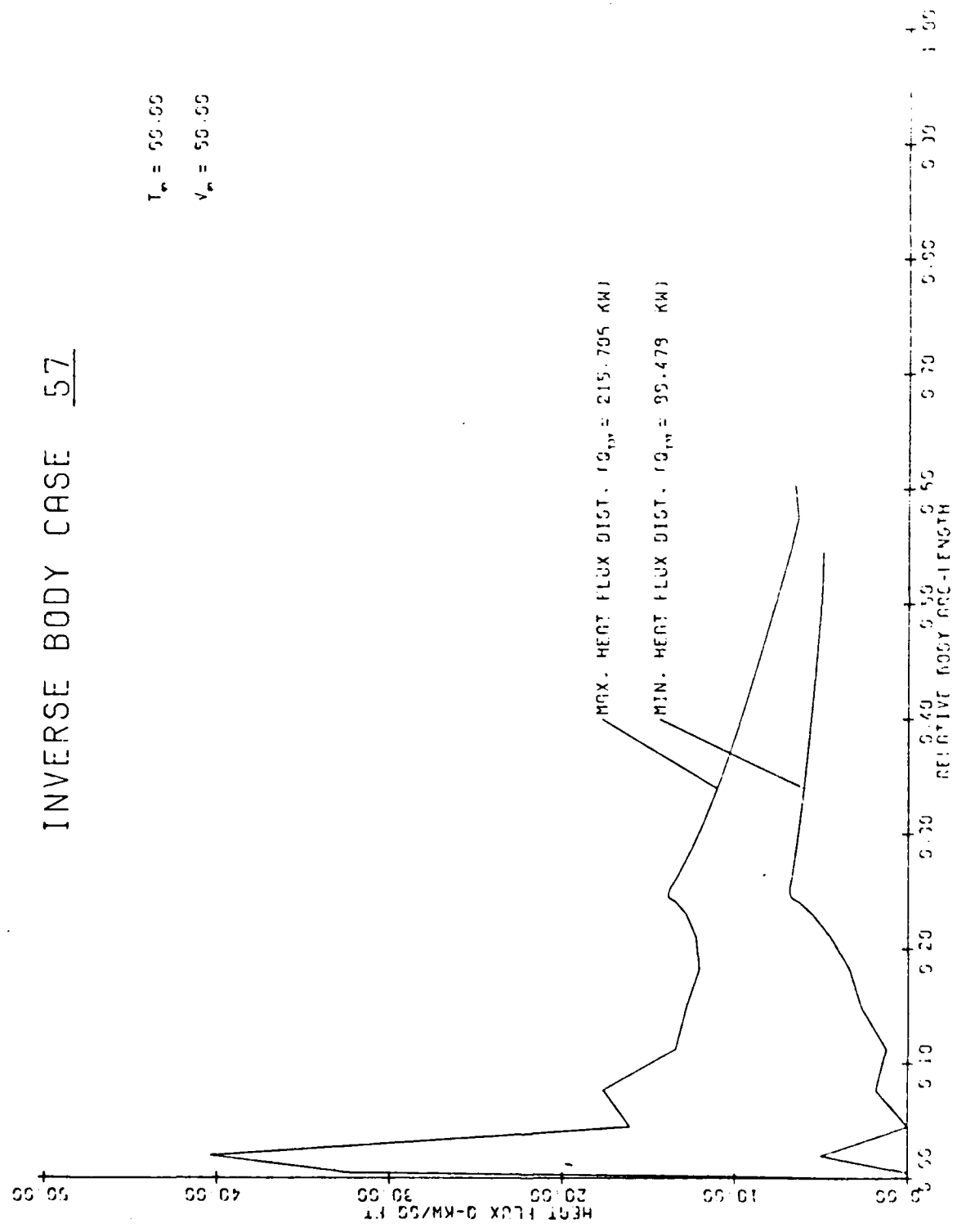

Figure 201. Heat Flux Distributions, Case No. 57.

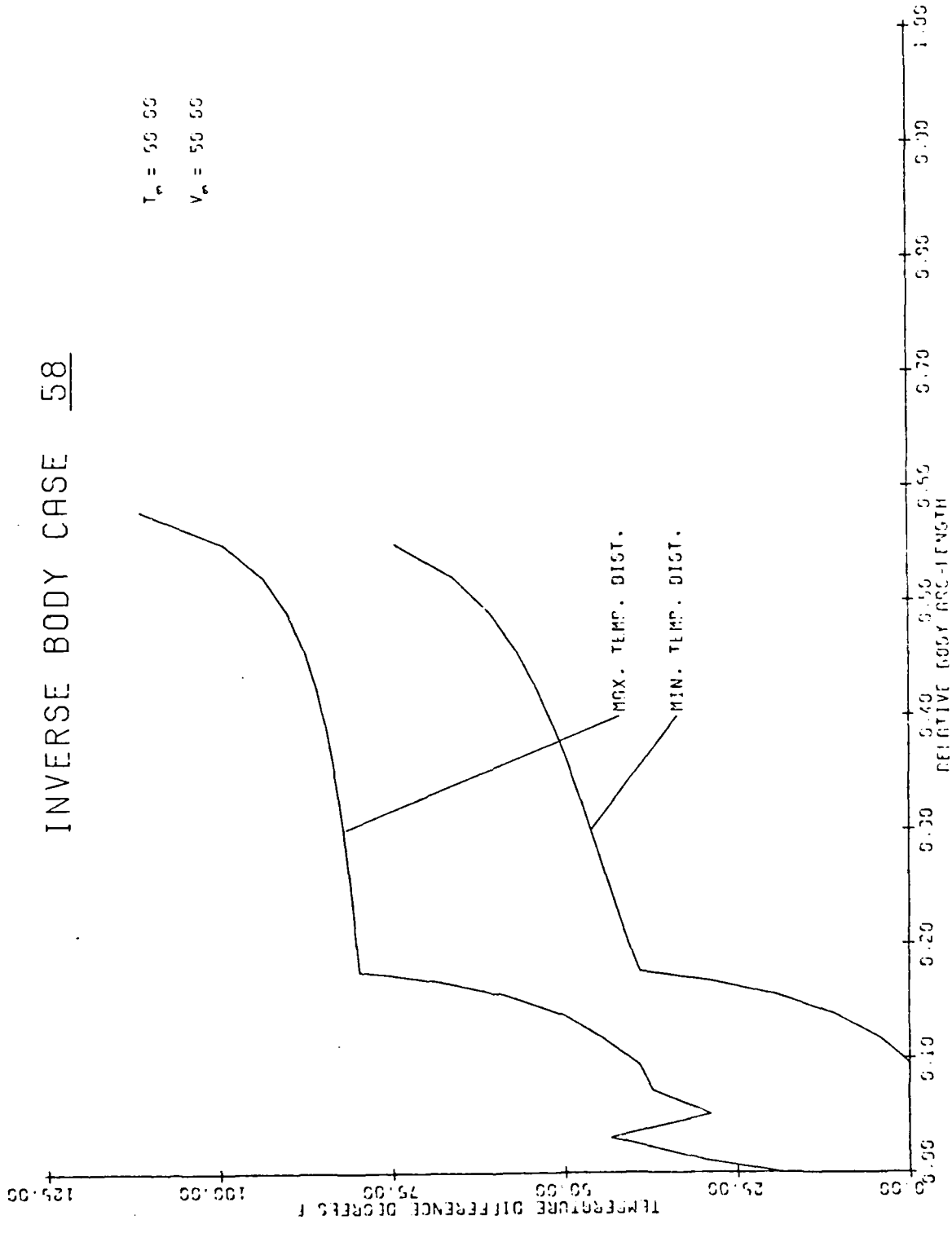

Figure 202. Temperature Distributions, Case No. 58.

19 August 1981
JJE:GHH:mmj

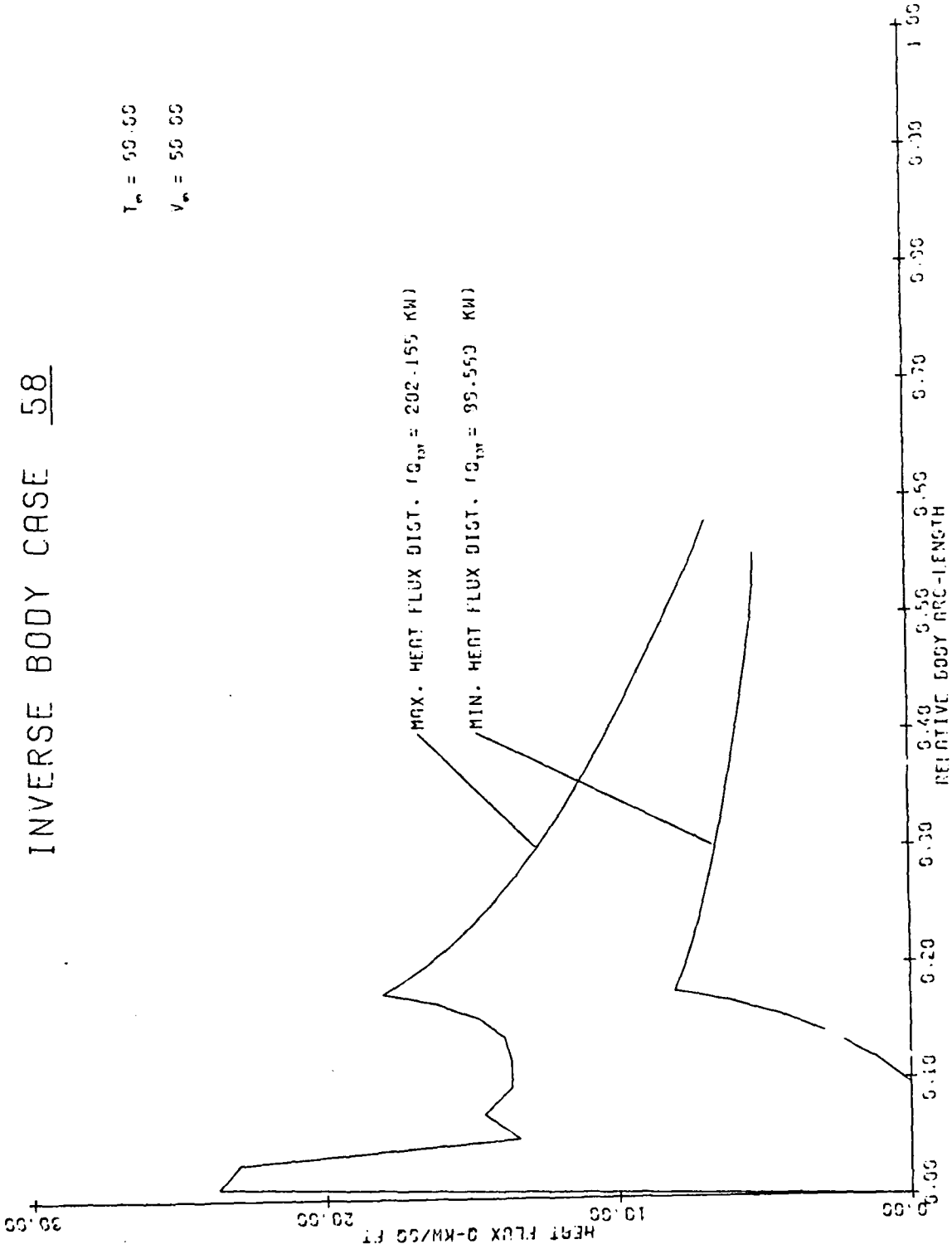

Figure 203. Heat Flux Distributions, Case No. 58.

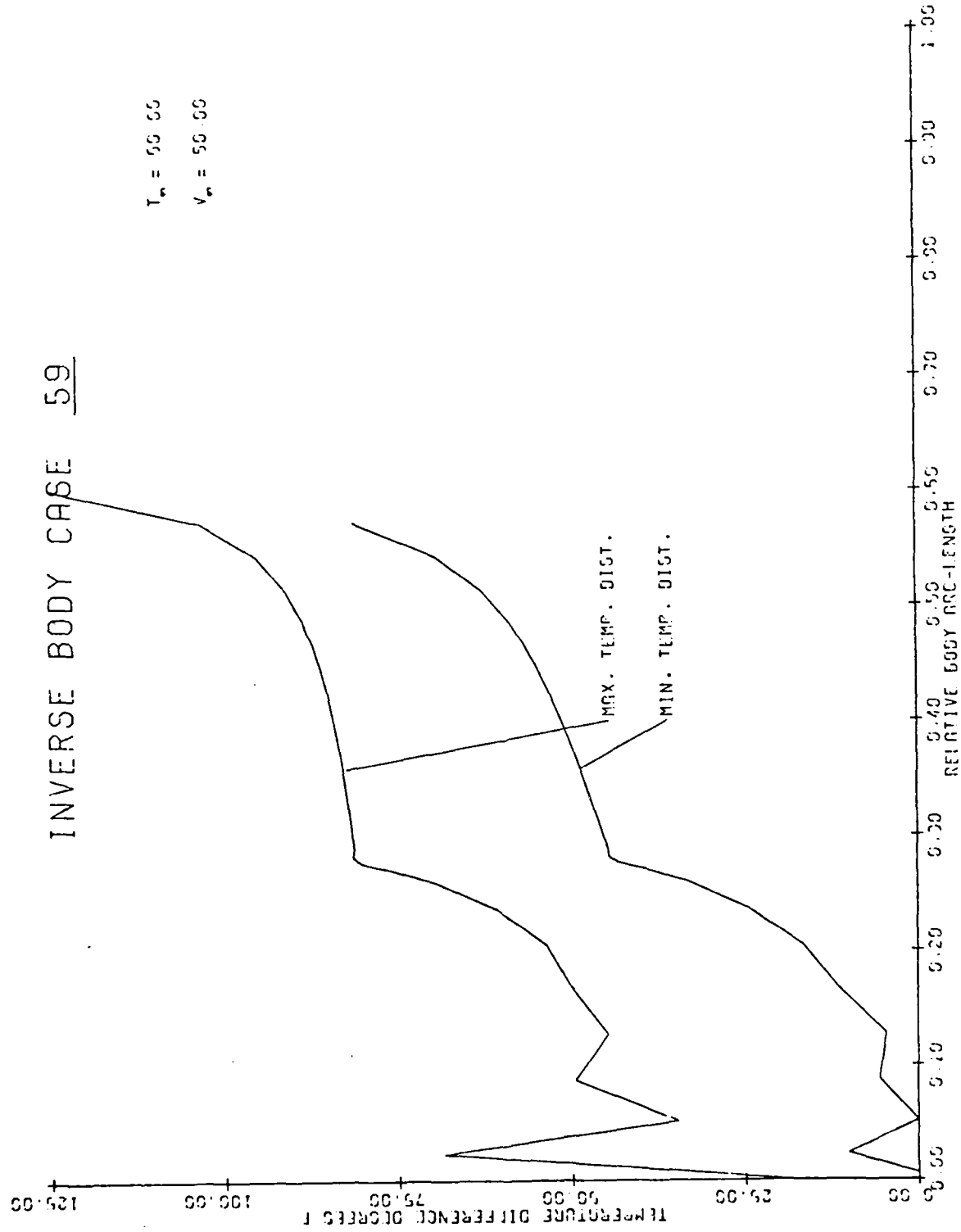

Figure 204. Temperature Distributions, Case No. 59.

19 August 1981
JJE:GHH:mmj

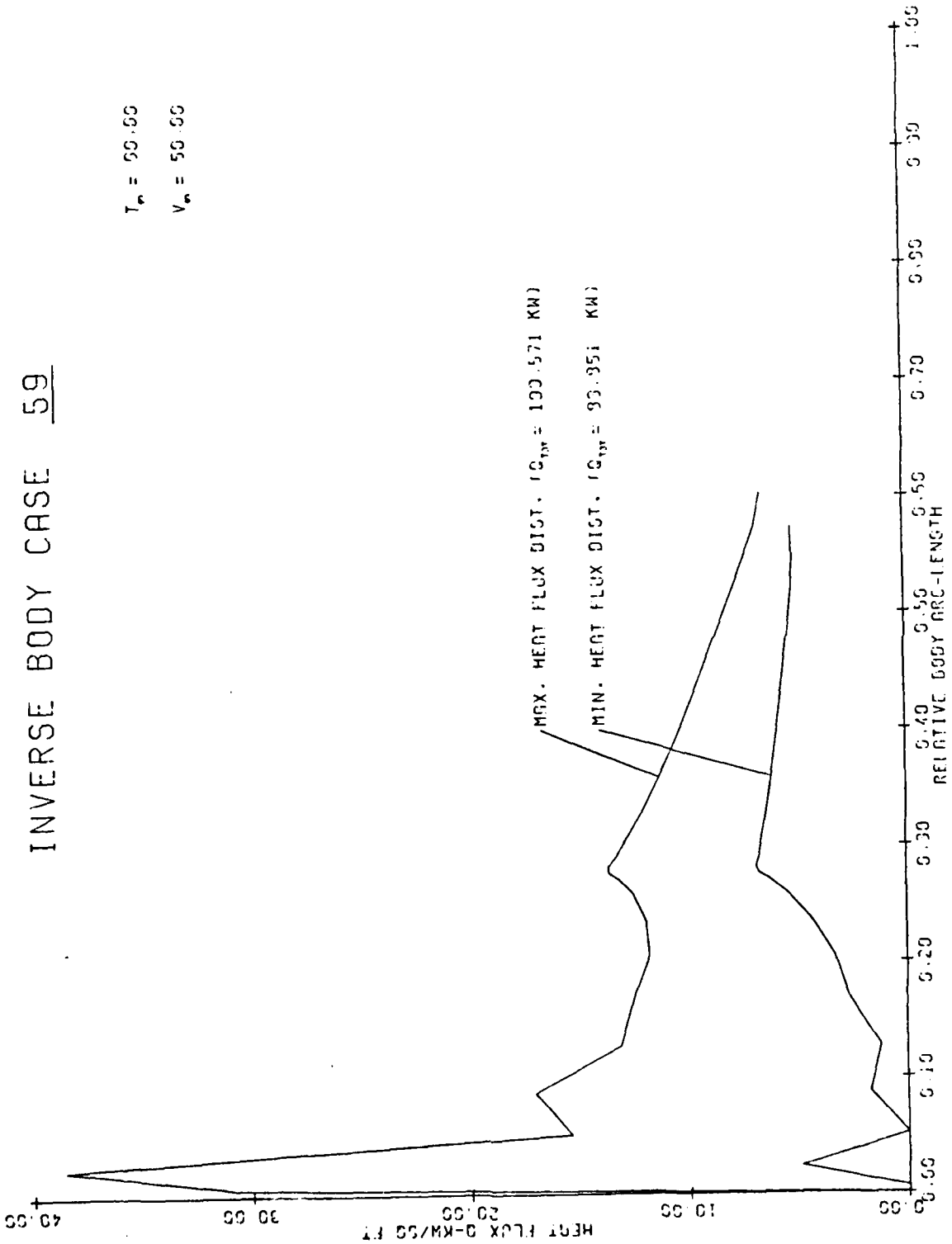

Figure 205. Heat Flux Distributions, Case No. 59.

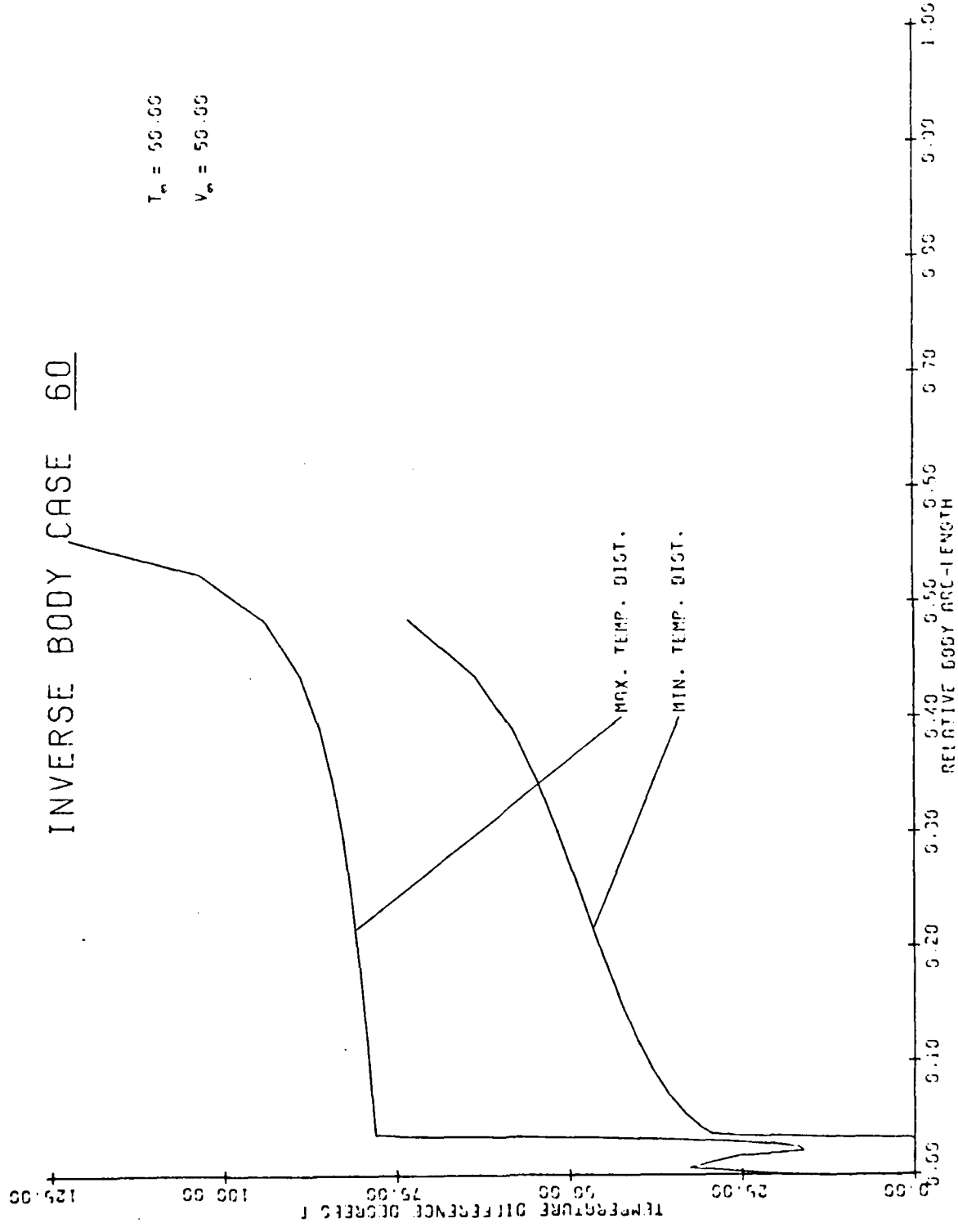

Figure 206. Temperature Distributions, Case No. 60.

19 August 1981
JJE:GHH:mmj

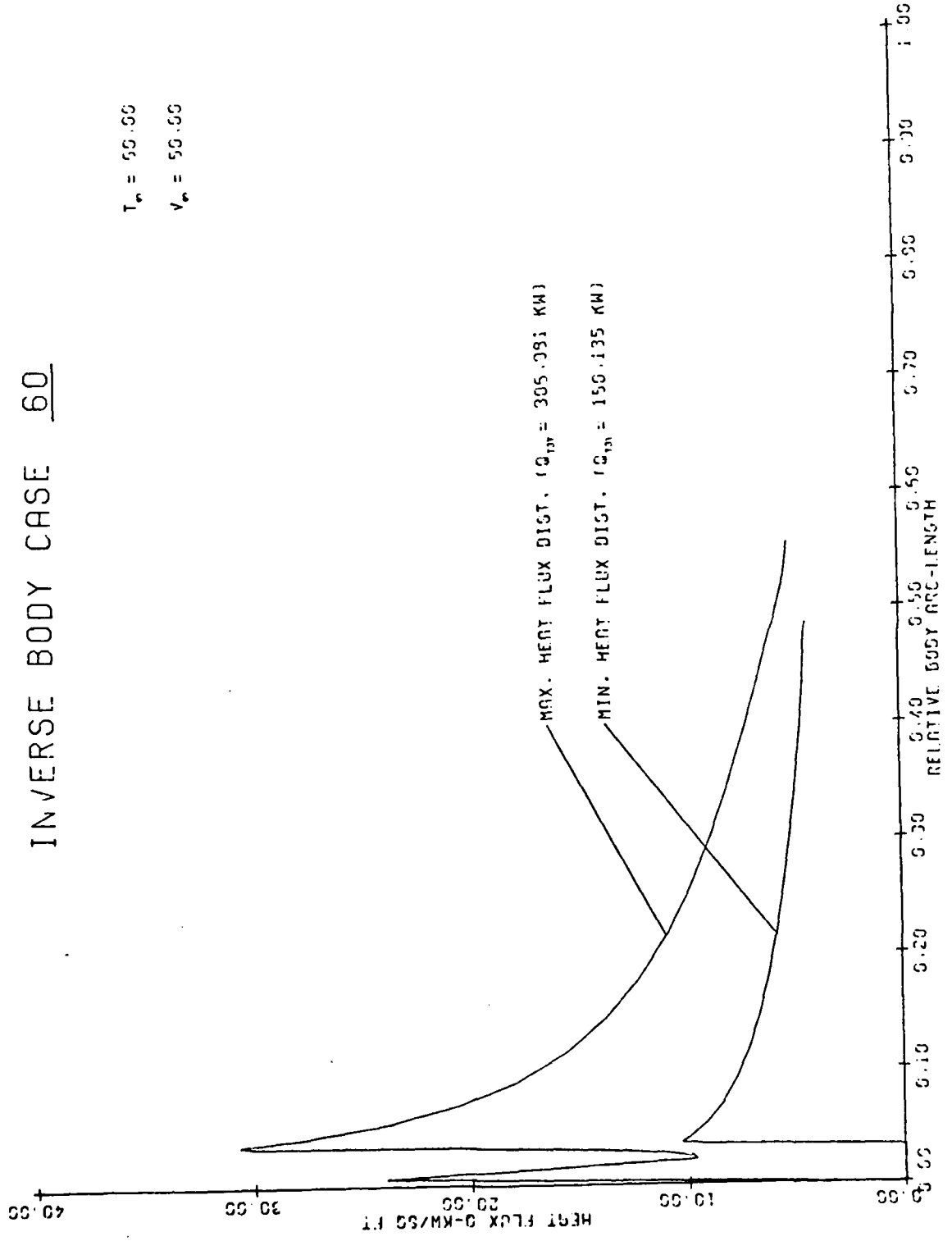

Figure 207. Heat Flux Distributions, Case No. 60.

19 August 1981
JJE:GHH:mmj

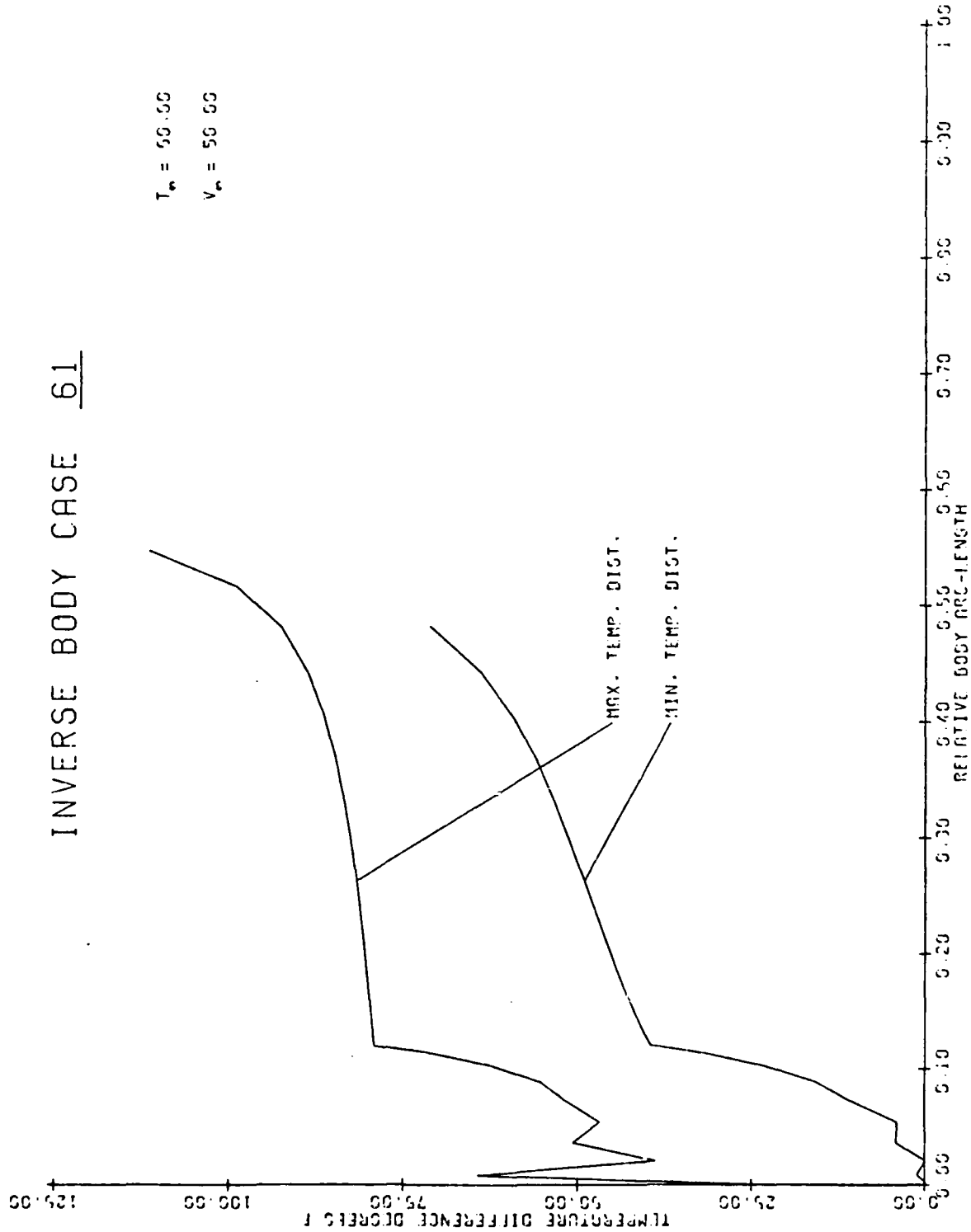

Figure 208. Temperature Distributions, Case No. 61.

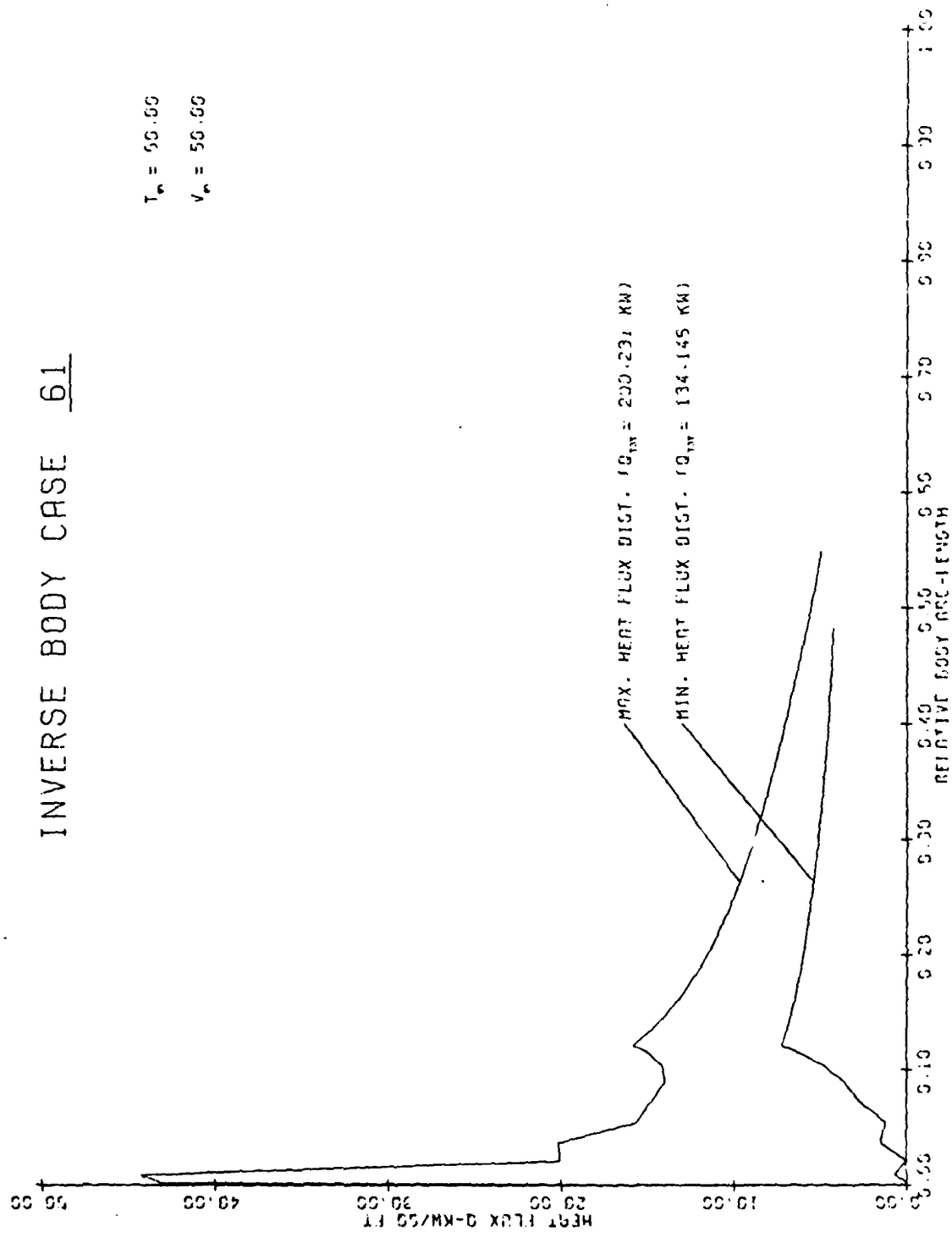

Figure 209. Heat Flux Distributions, CAse No. 61.

19 August 1981
JJE:GHH:mmj

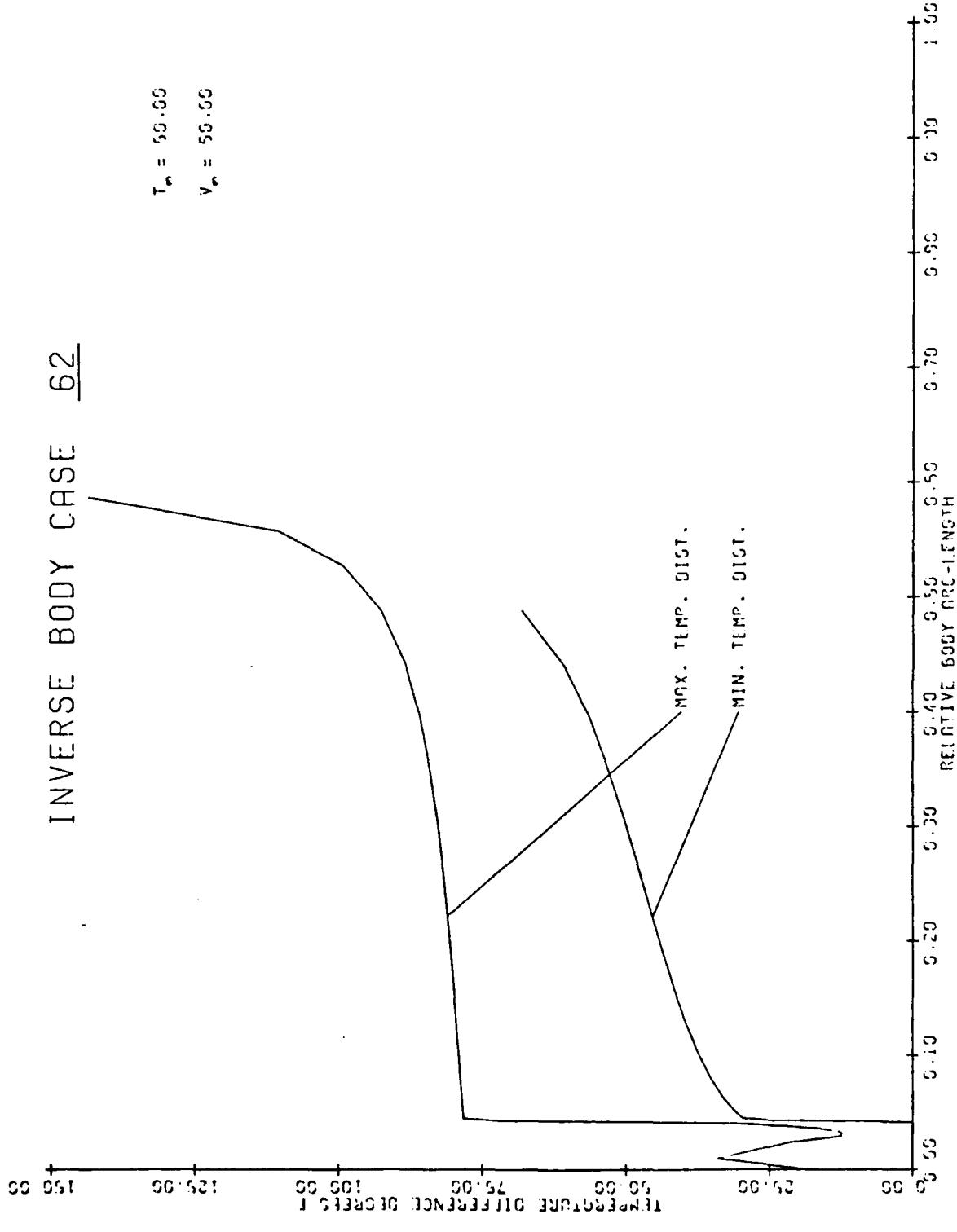

Figure 210. Temperature Distributions, Case No. 62.

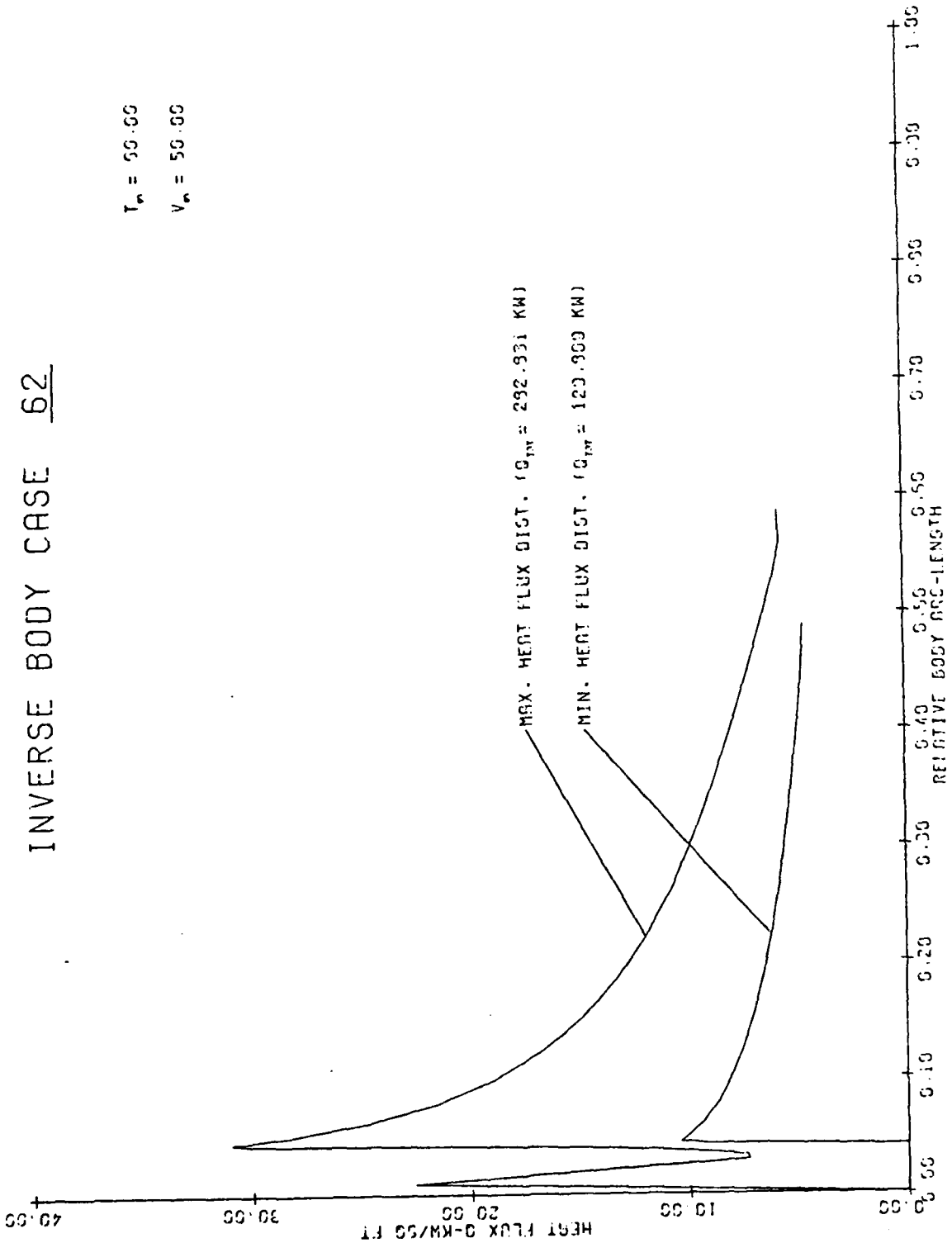

Figure 211. Heat Flux Distributions, Case No. 62.

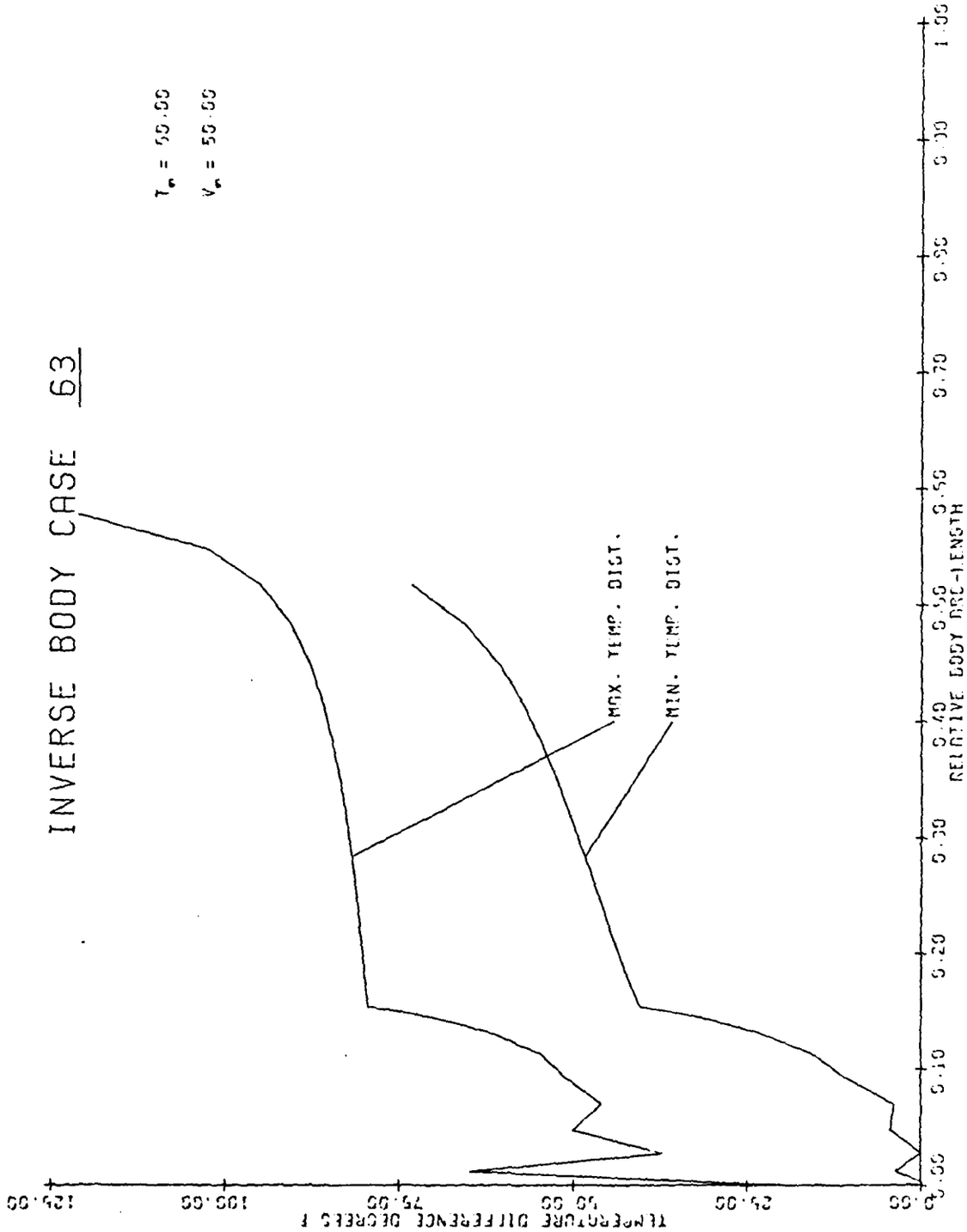

Figure 212. Temperature Distributions, Case No. 63.

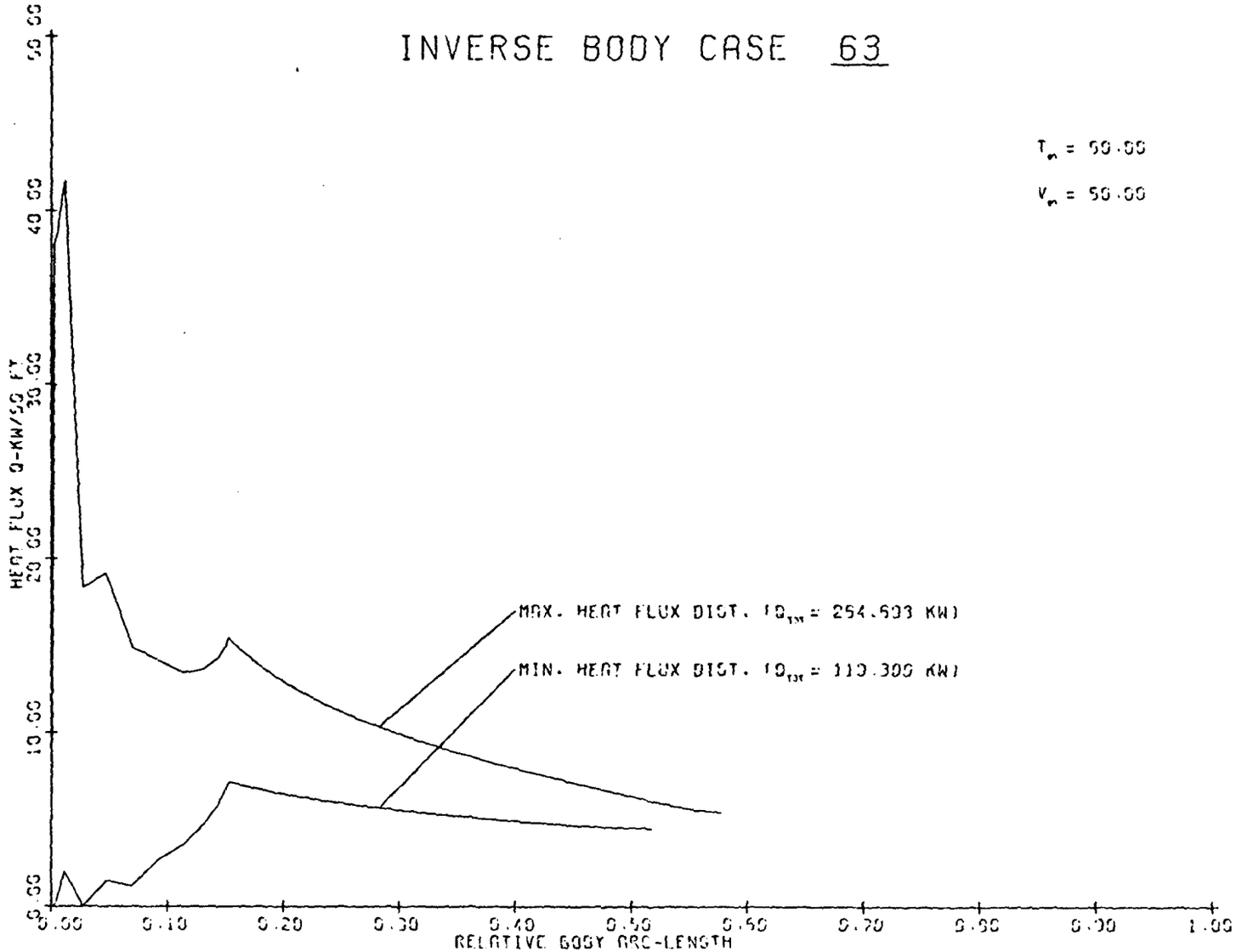

Figure 213. Heat Flux Distributions, Case No. 63.

19 August 1981
JJE:CHH:mmj

19 August 1981
JJE:GHH:mmj

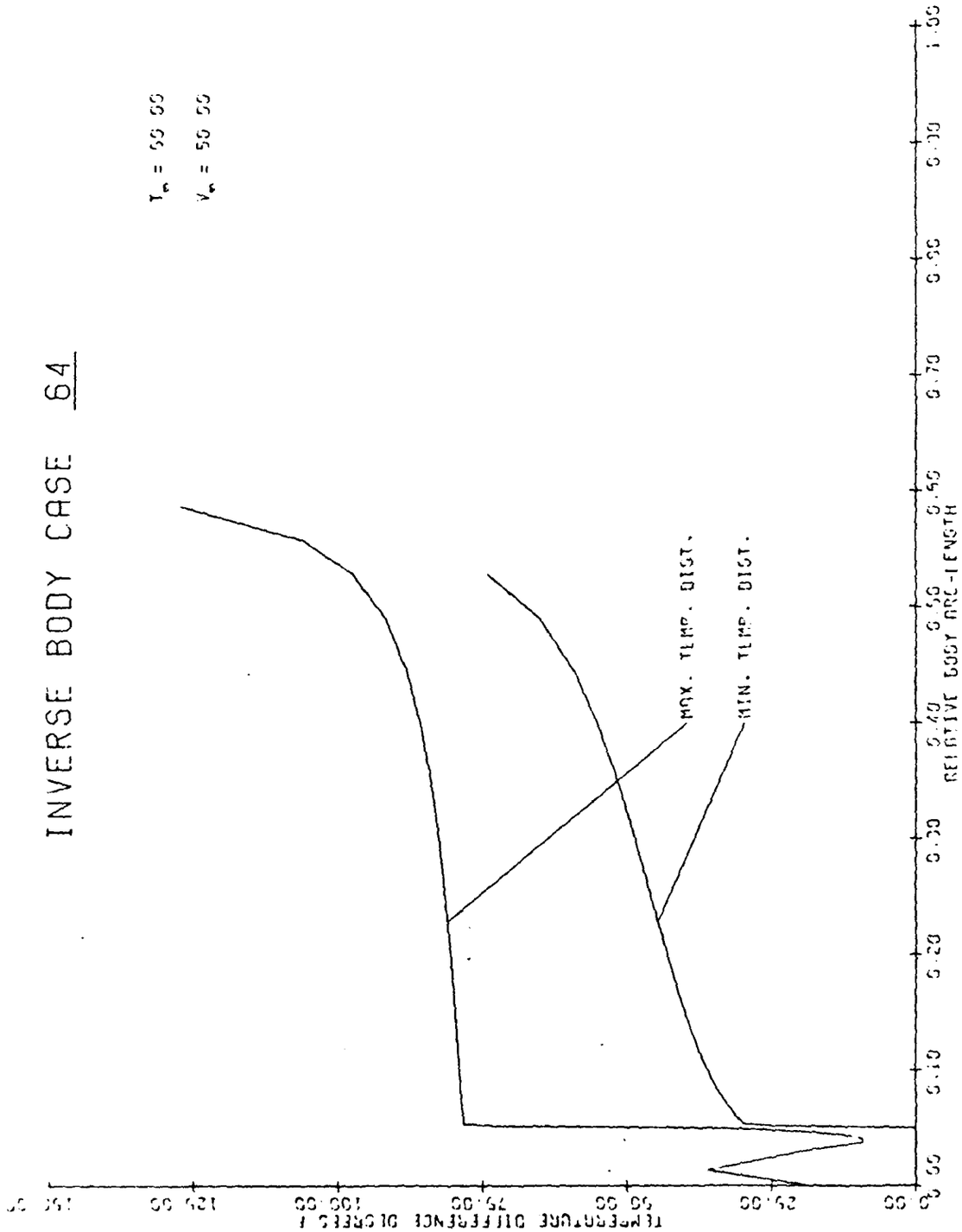

Figure 214. Temperature Distributions, Case No. 64.

19 August 1981
JJE:GHH:mmj

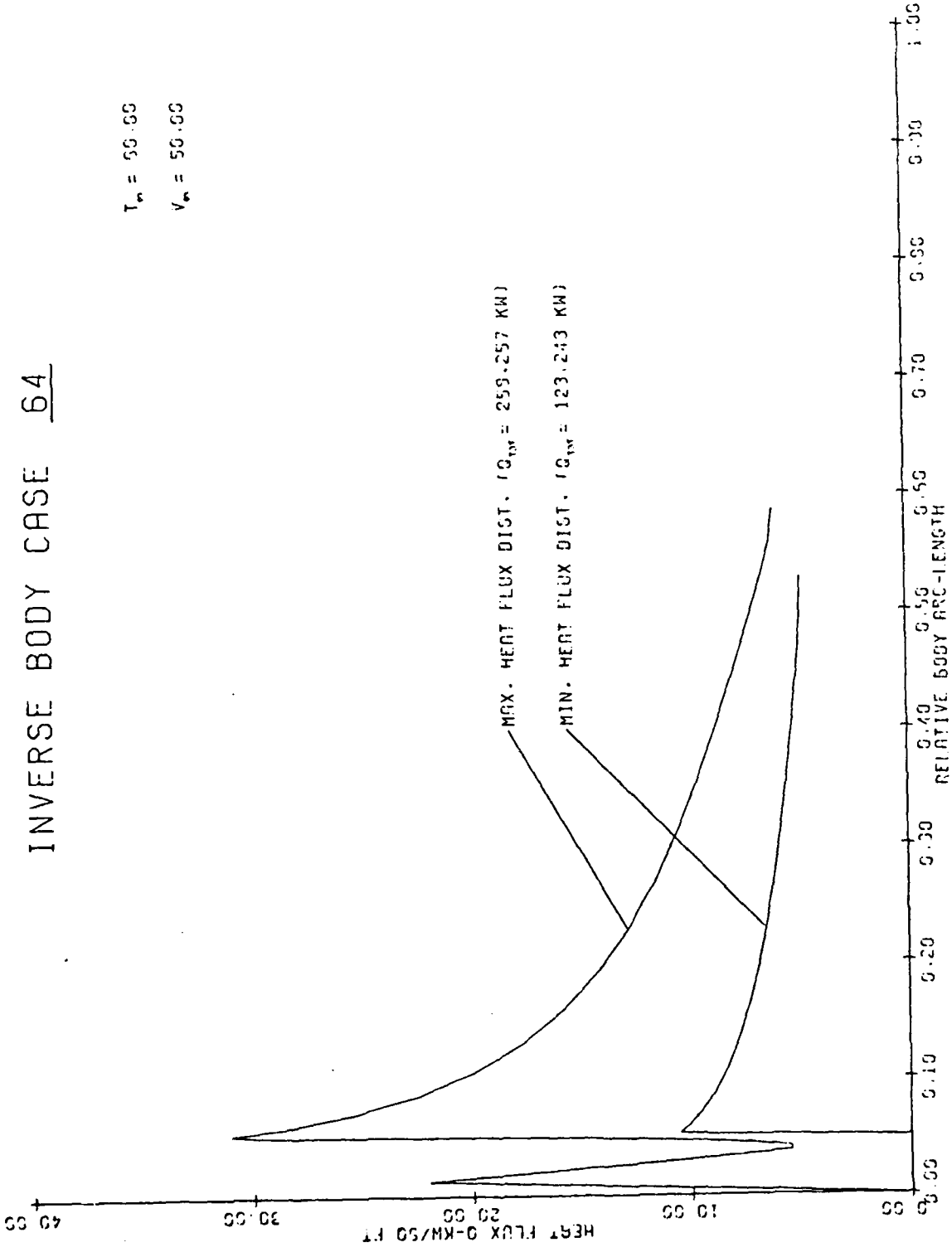

Figure 215. Heat Flux Distributions, Case No. 64.

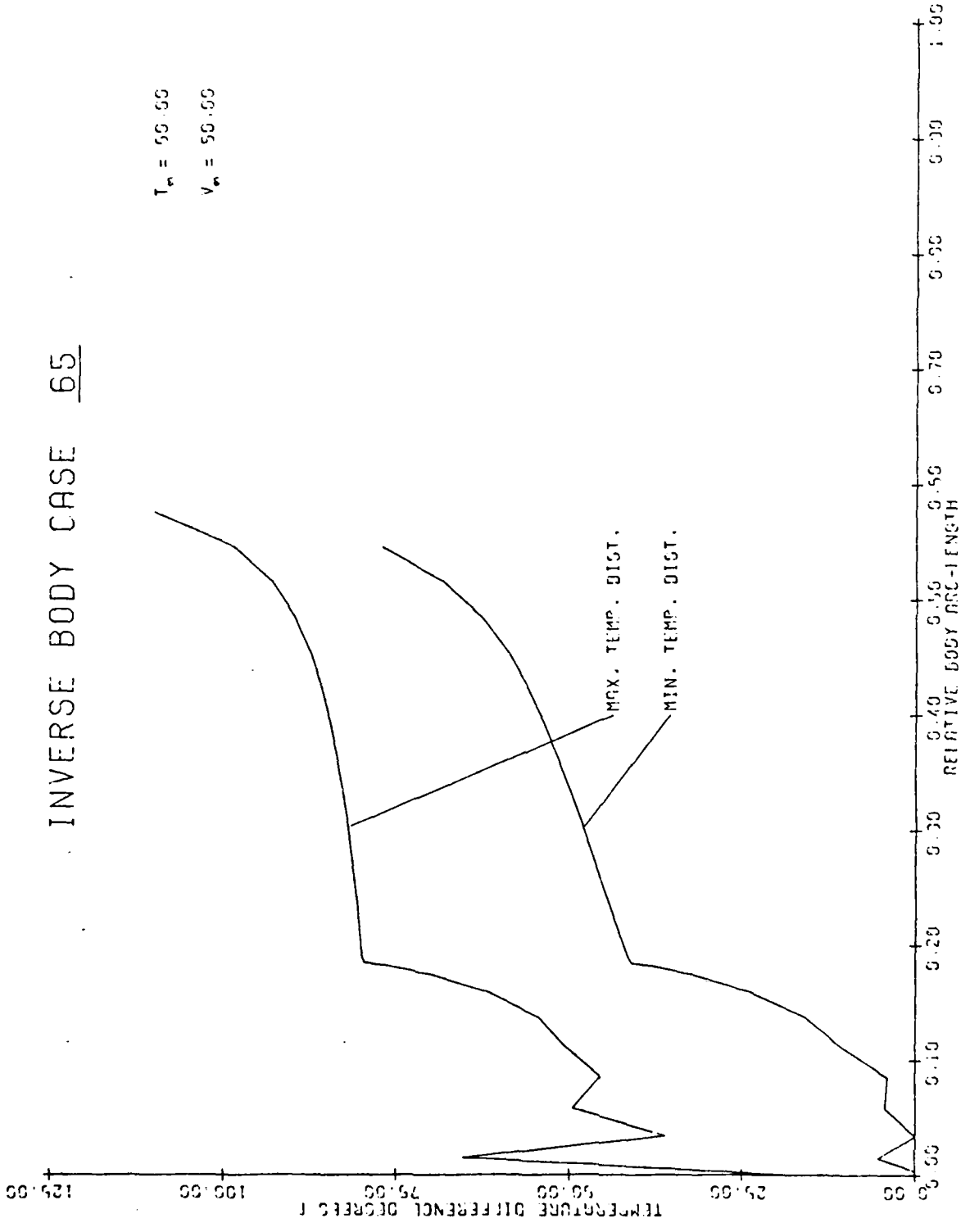

Figure 216. Temperature Distributions, Case No. 65.

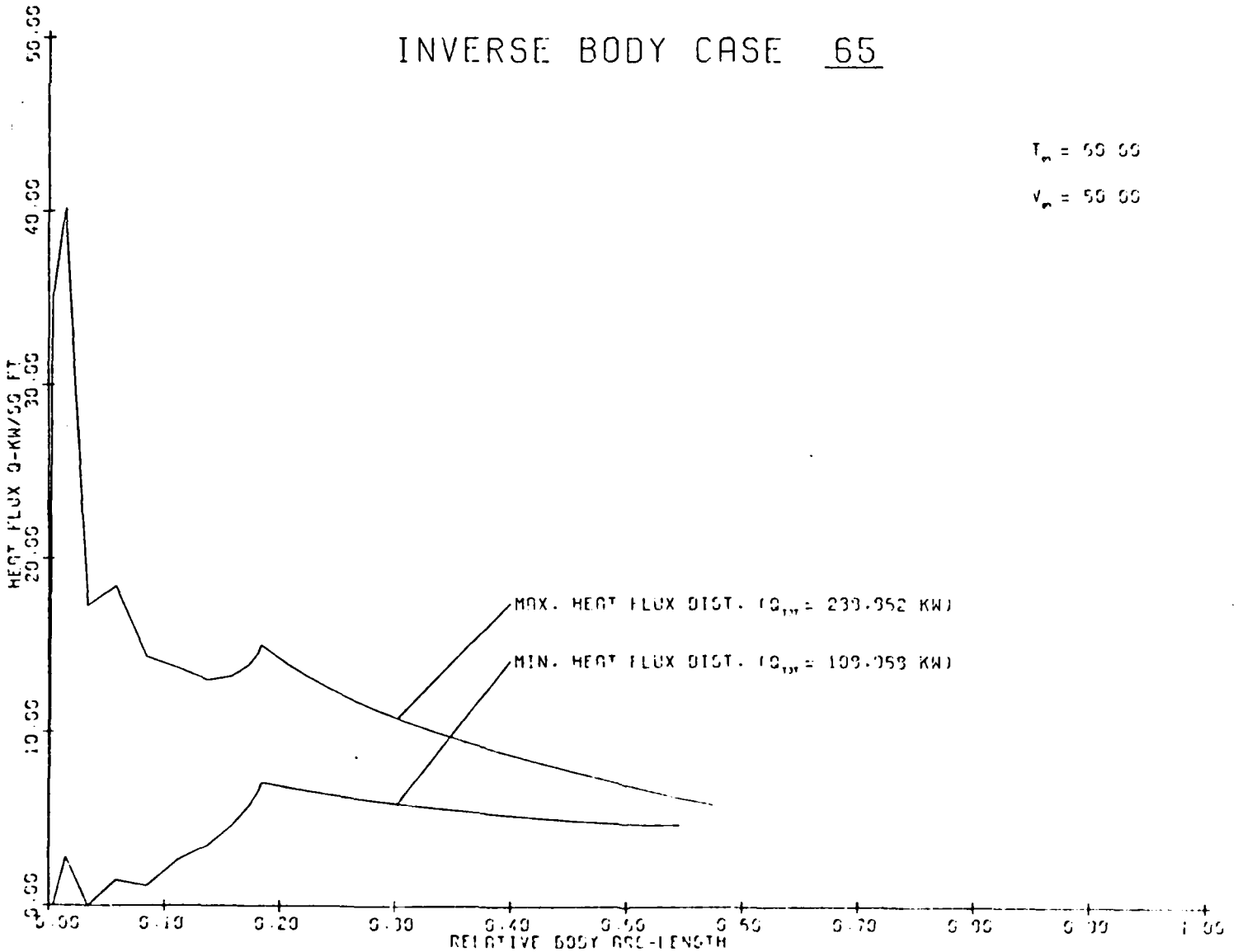

Figure 217. Heat Flux Distributions, Case No. 65.

19 August 1981
JJE:GHH:mmj

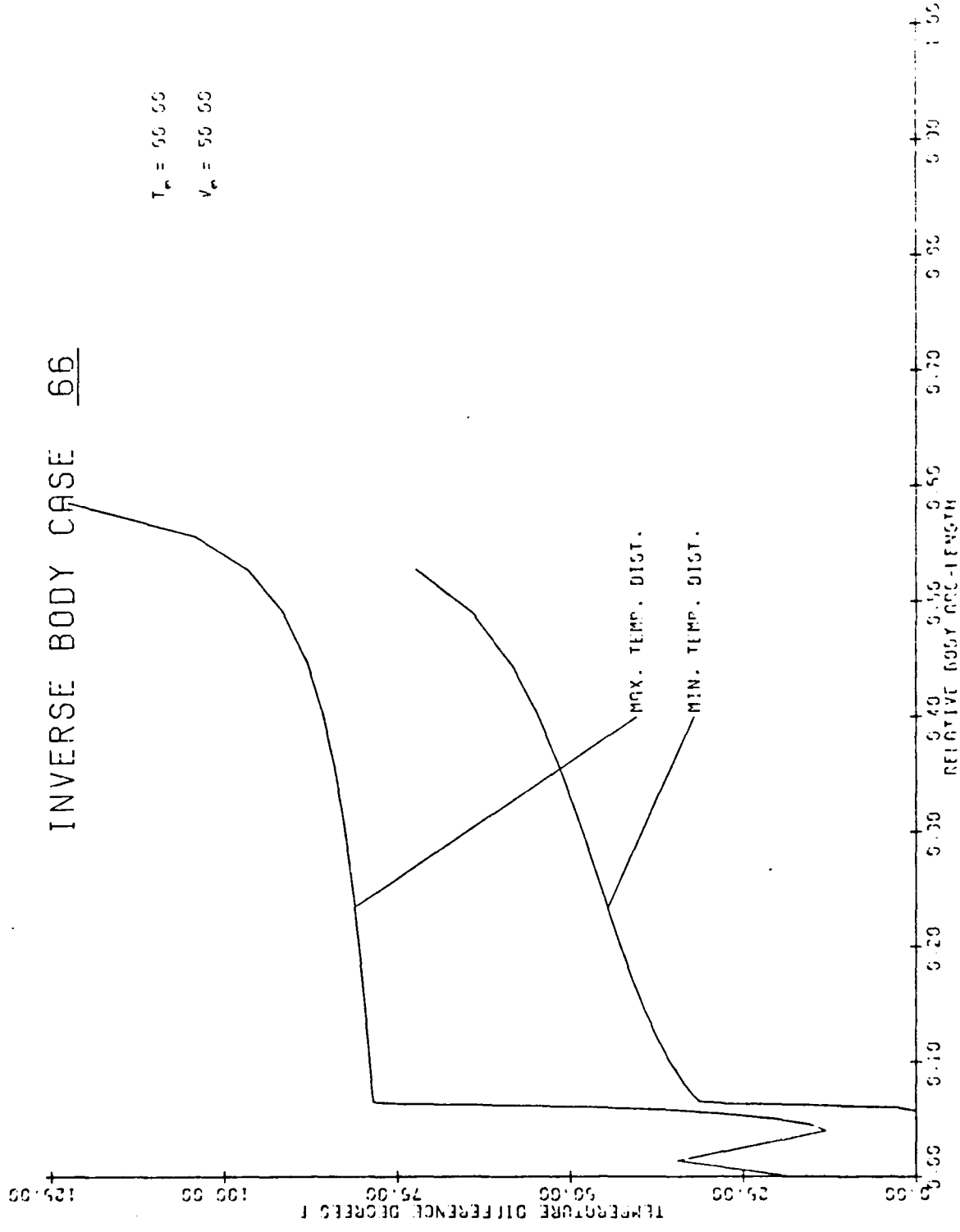

Figure 218. Temperature Distributions, Case No. 66.

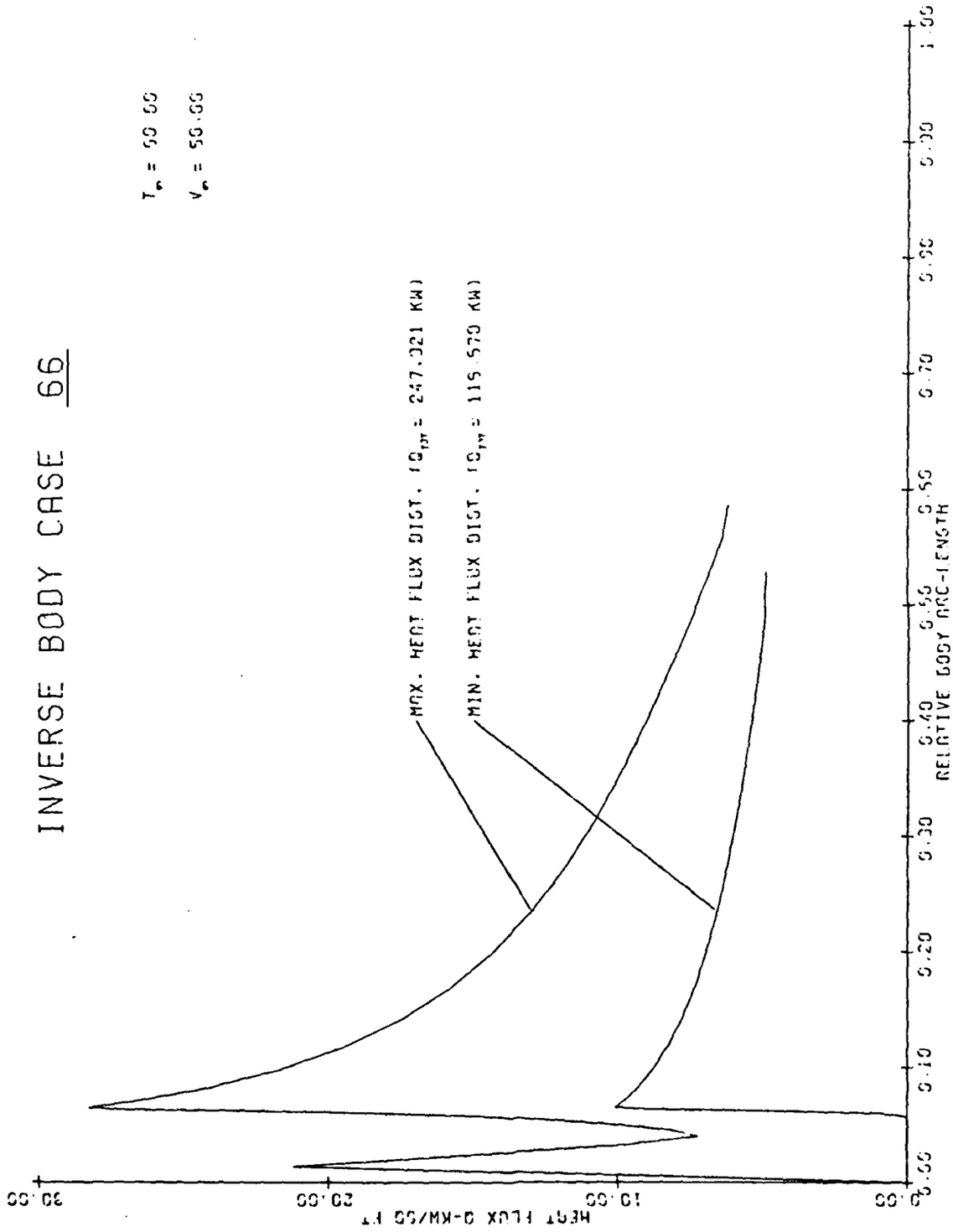

Figure 219. Heat Flux Distributions, Case No. 66.

19 August 1981
JJE:GHH:mmj

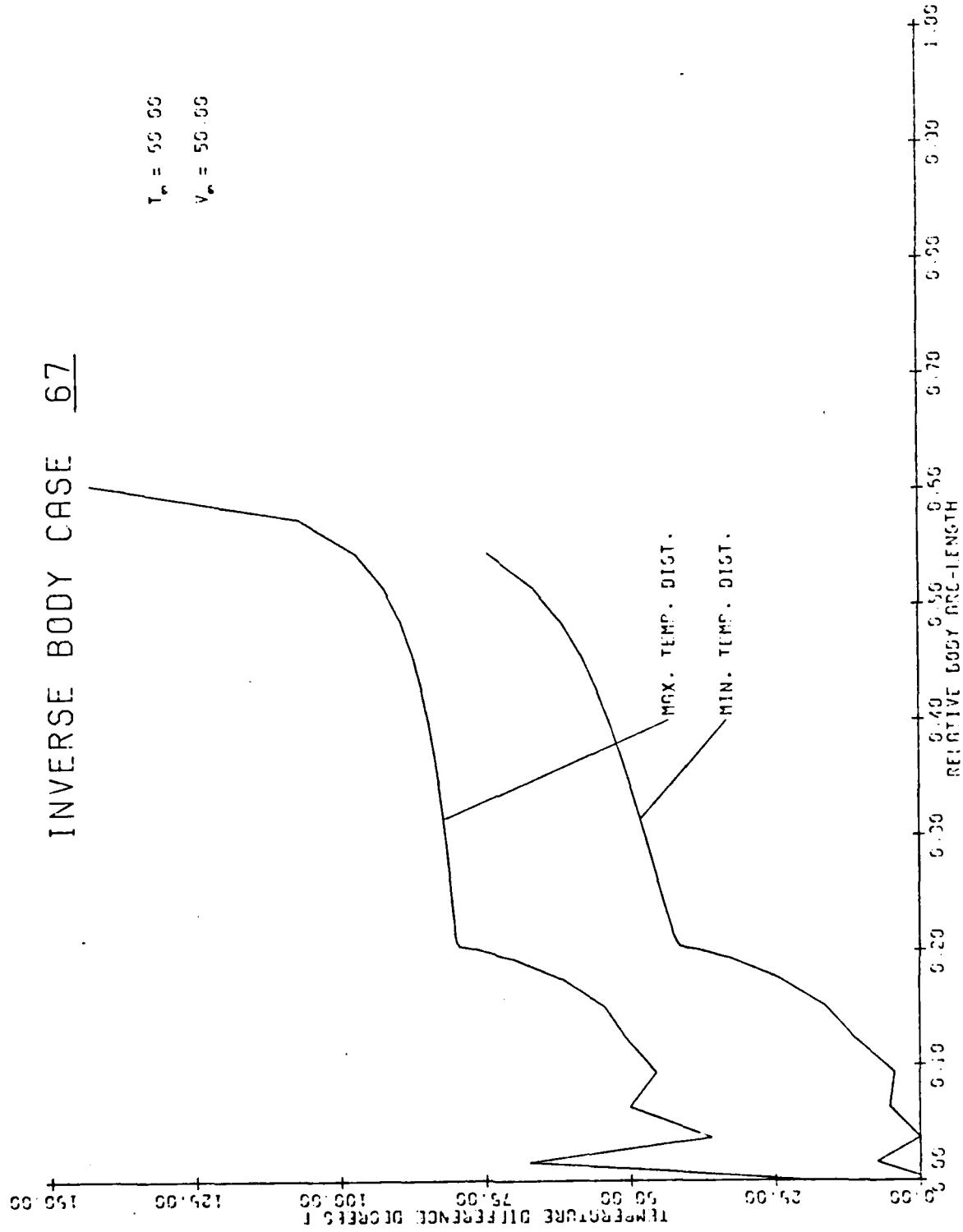

Figure 220. Temperature Distributions, Case No. 67.

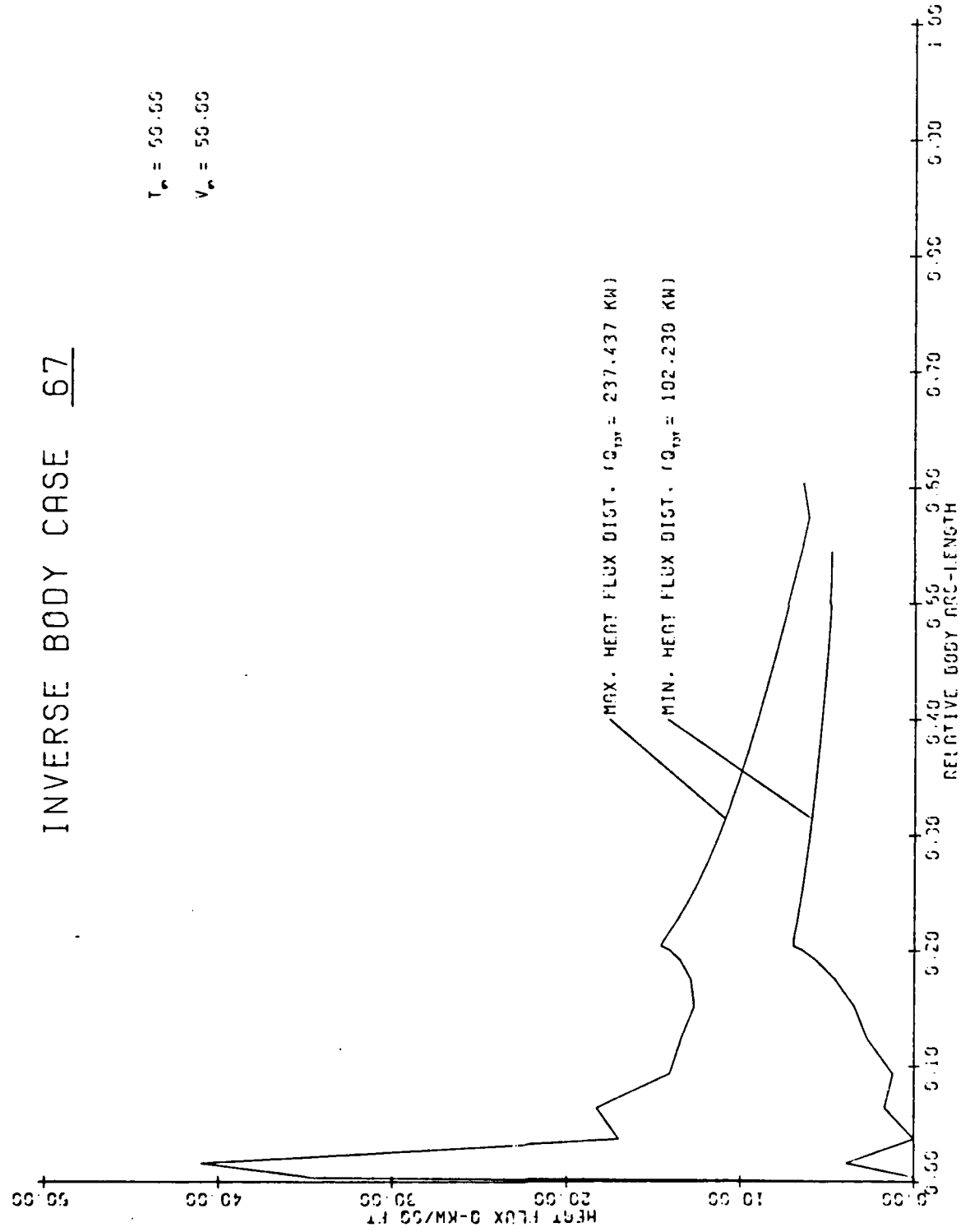

Figure 221. Heat Flux Distributions, Case No. 67.

19 August 1981
JJE:GHH:mmj

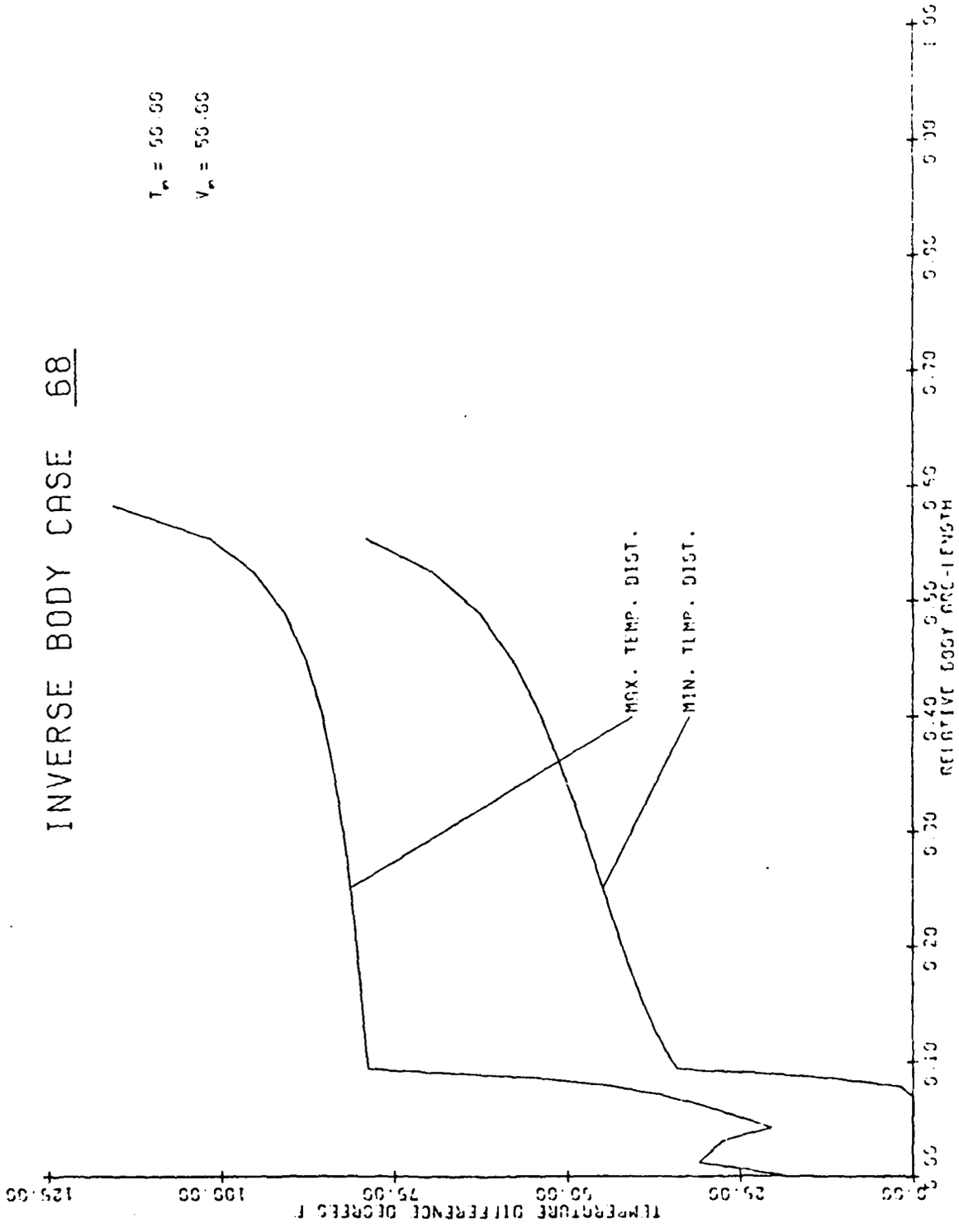

Figure 222. Temperature Distributions, Case No. 68.

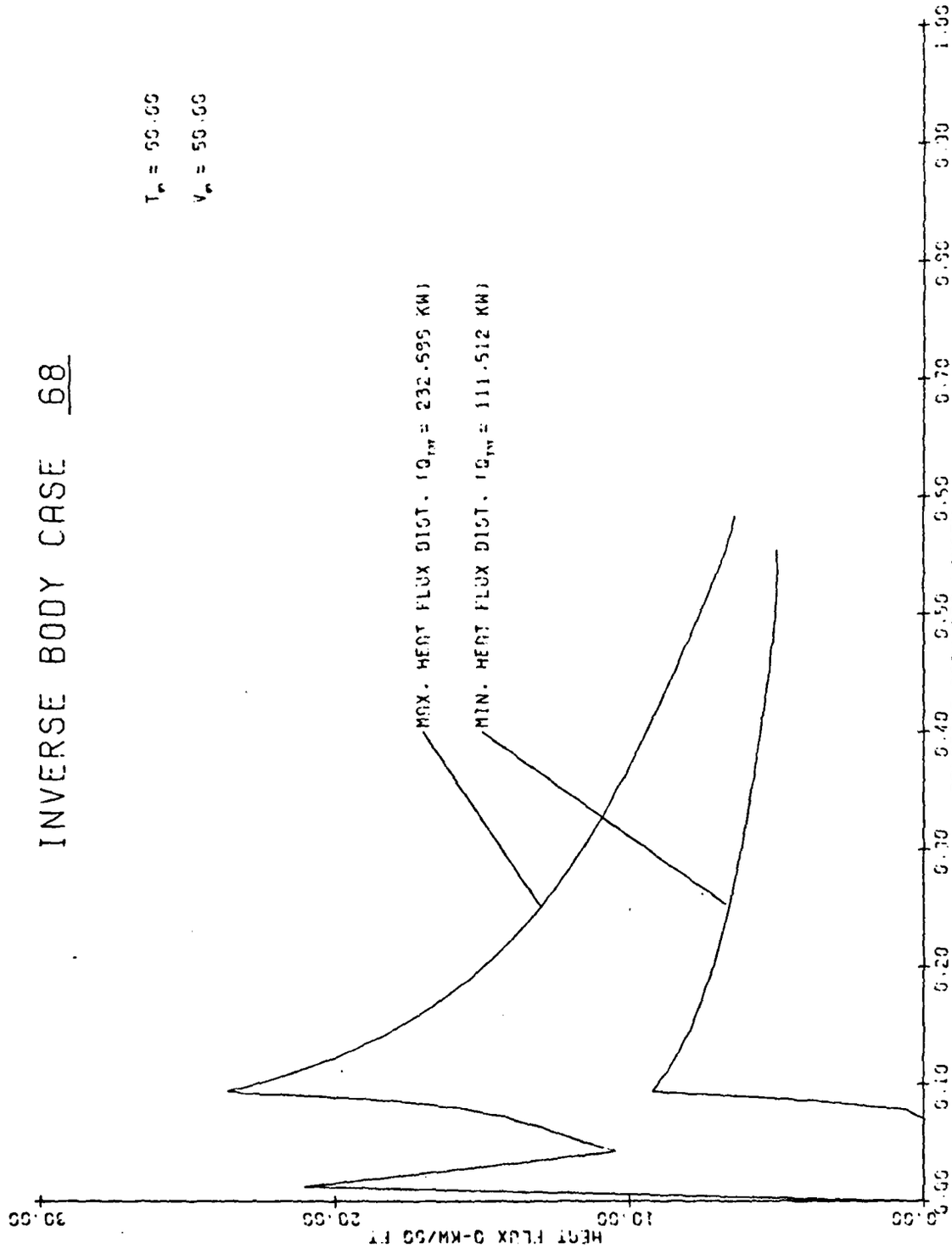

Figure 223. Heat Flux Distributions, Case No. 68.

19 August 1981
JJE:GHH:mmj

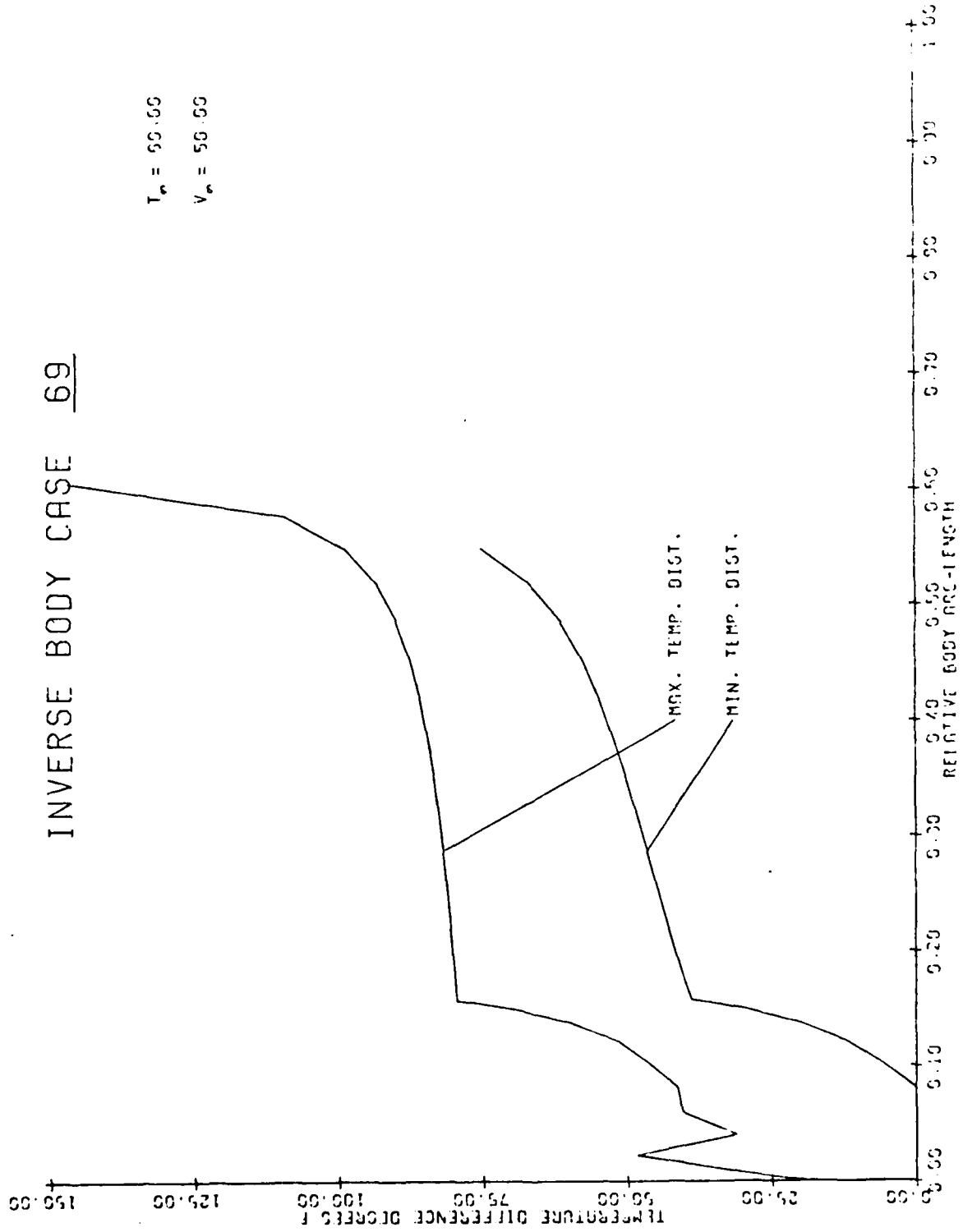

Figure 224. Temperature Distributions, Case No. 69.

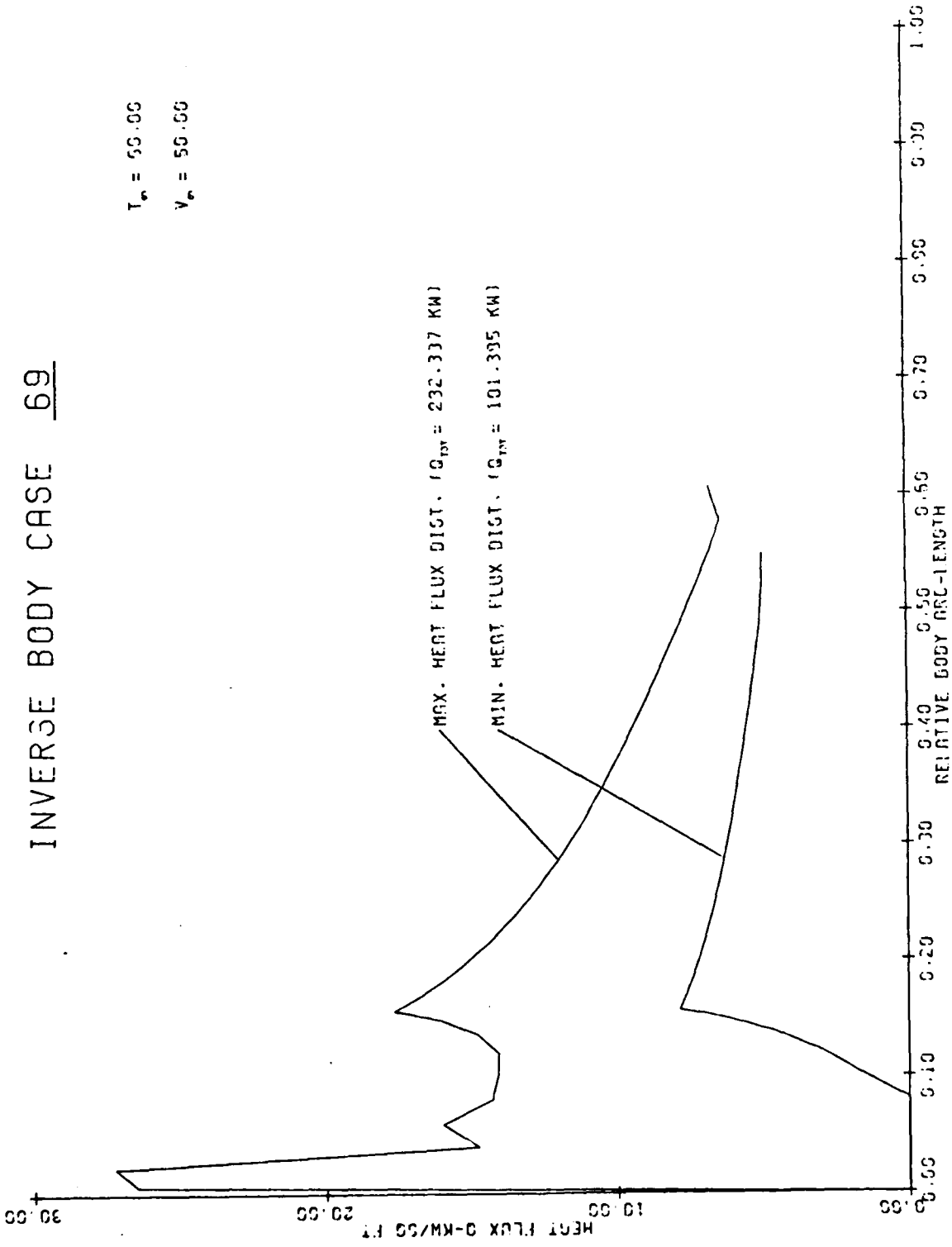

Figure 225. Heat Flux Distributions, Case No. 69.

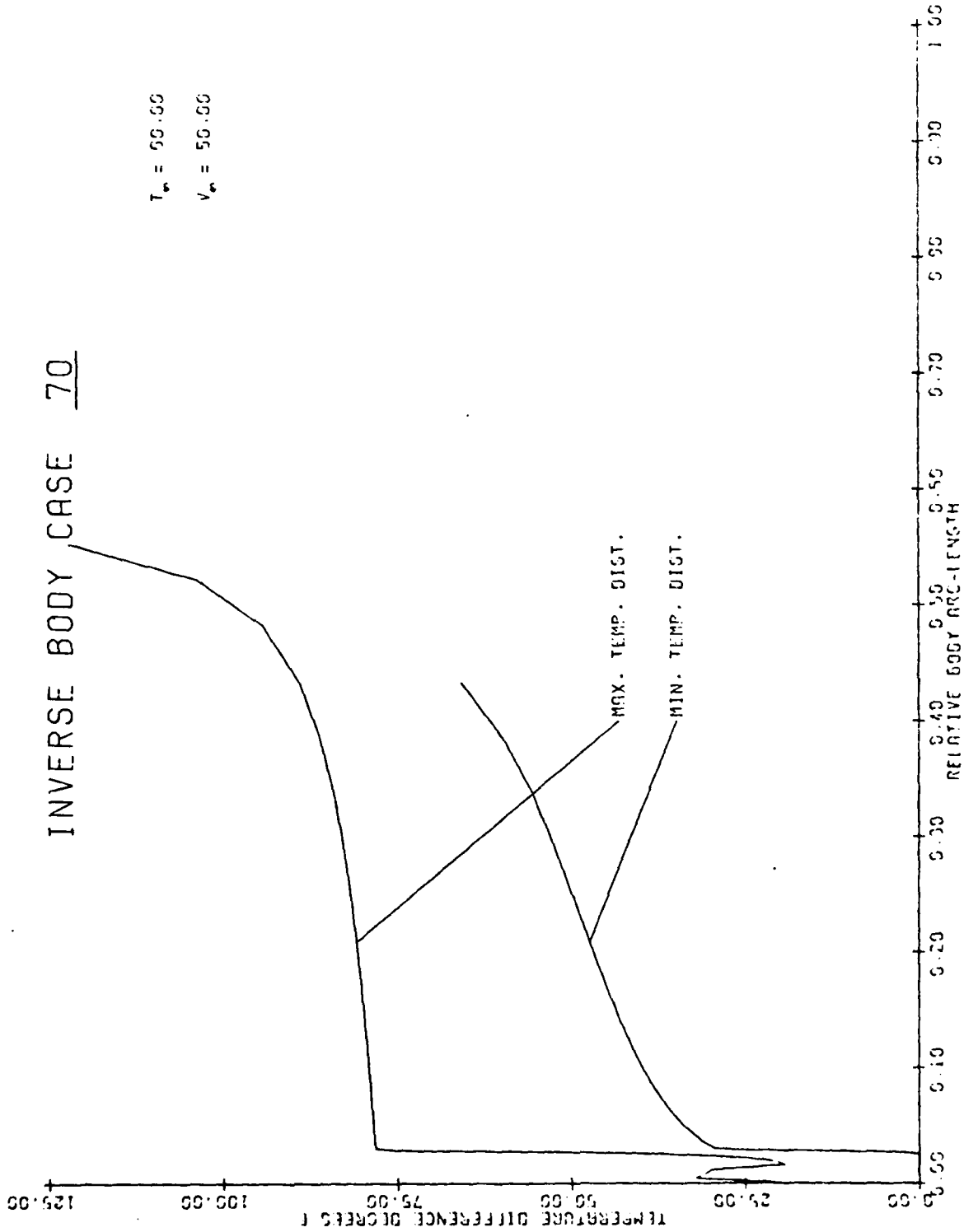

Figure 226. Temperature Distributions, Case No. 70.

19 August 1981
JJE:GHH:mmj

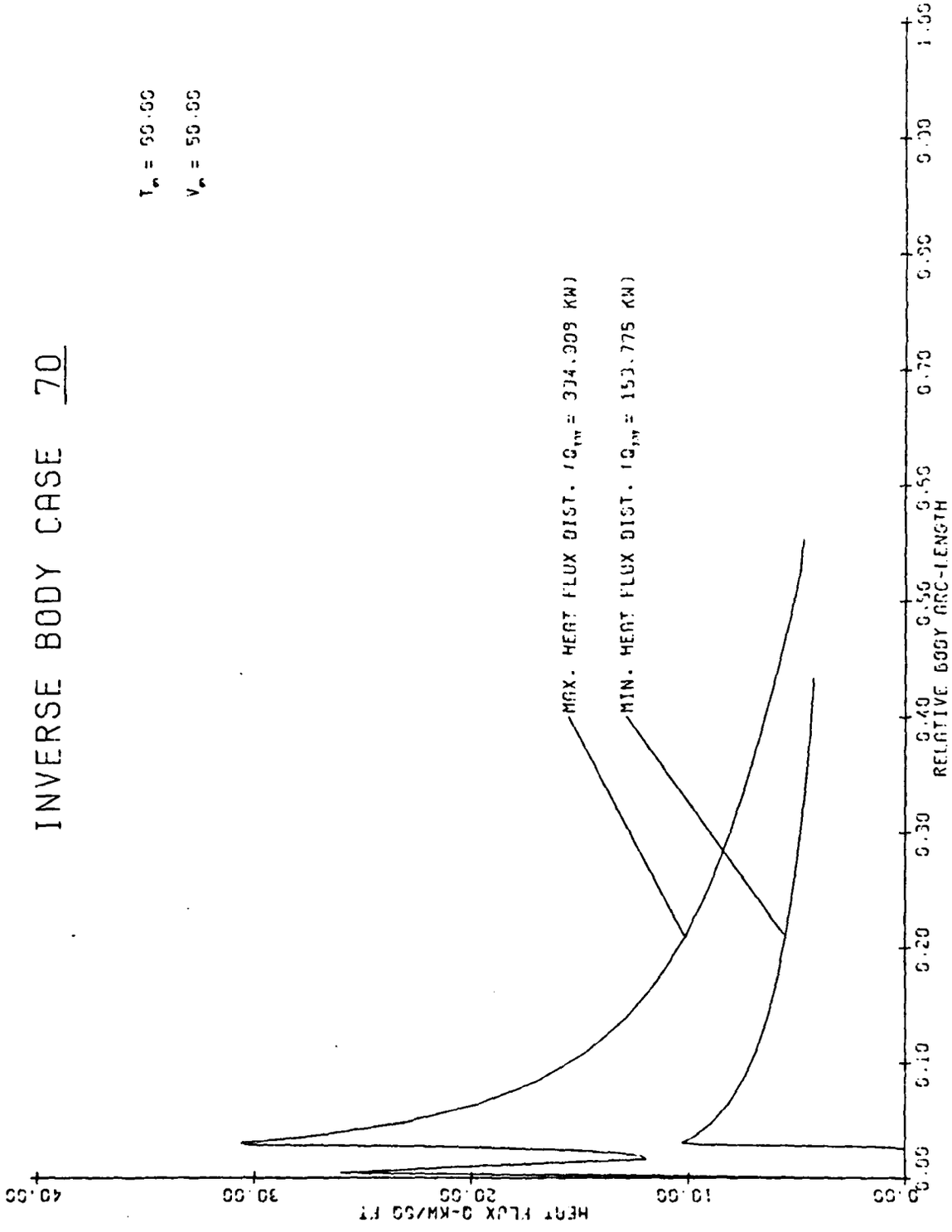

Figure 227. Heat Flux Distributions, Case No. 70.

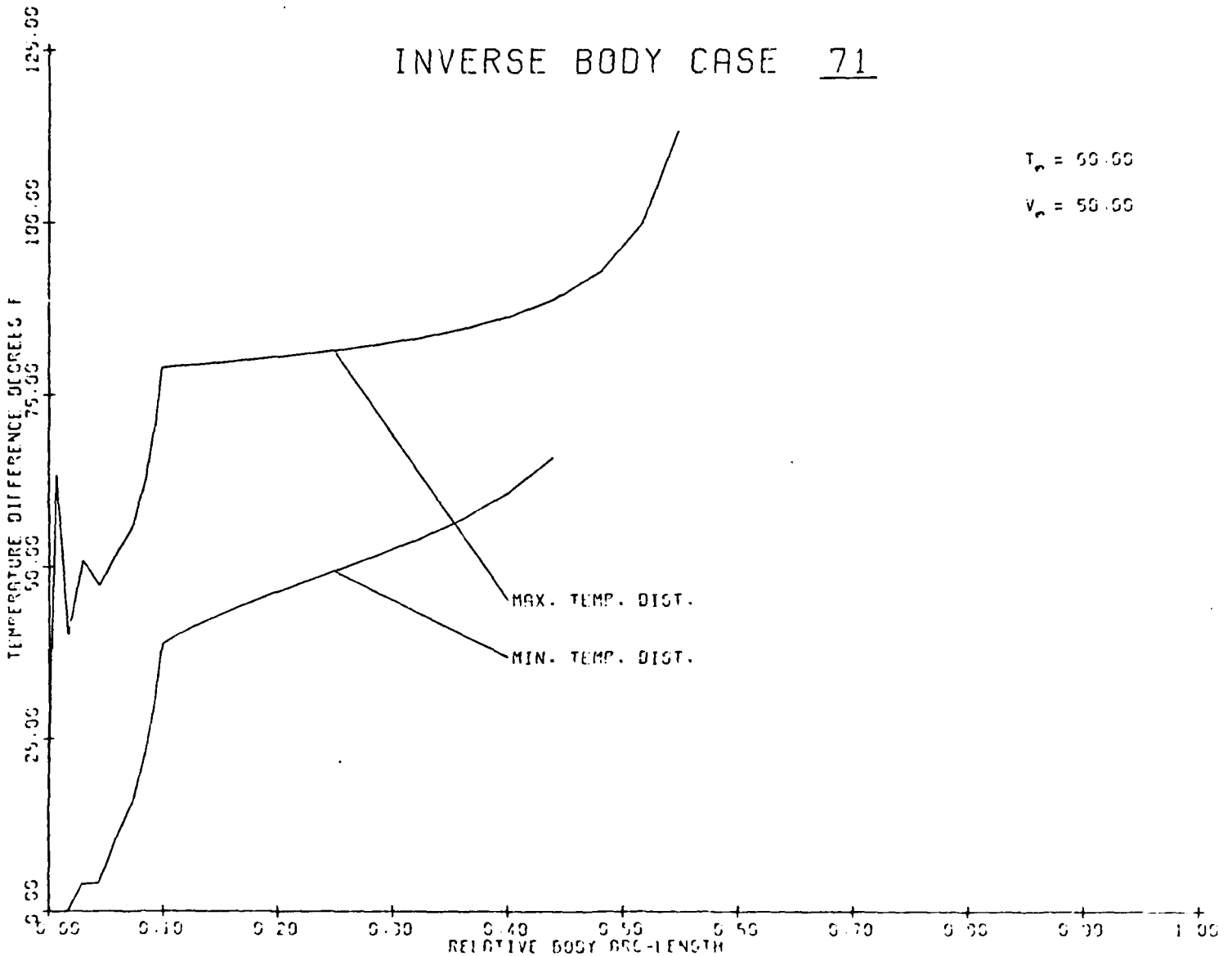

Figure 228. Temperature Distributions, Case No. 71

19 August 1981
JJE:CHH:mmj

19 August 1981
JJE:GHH:mmj

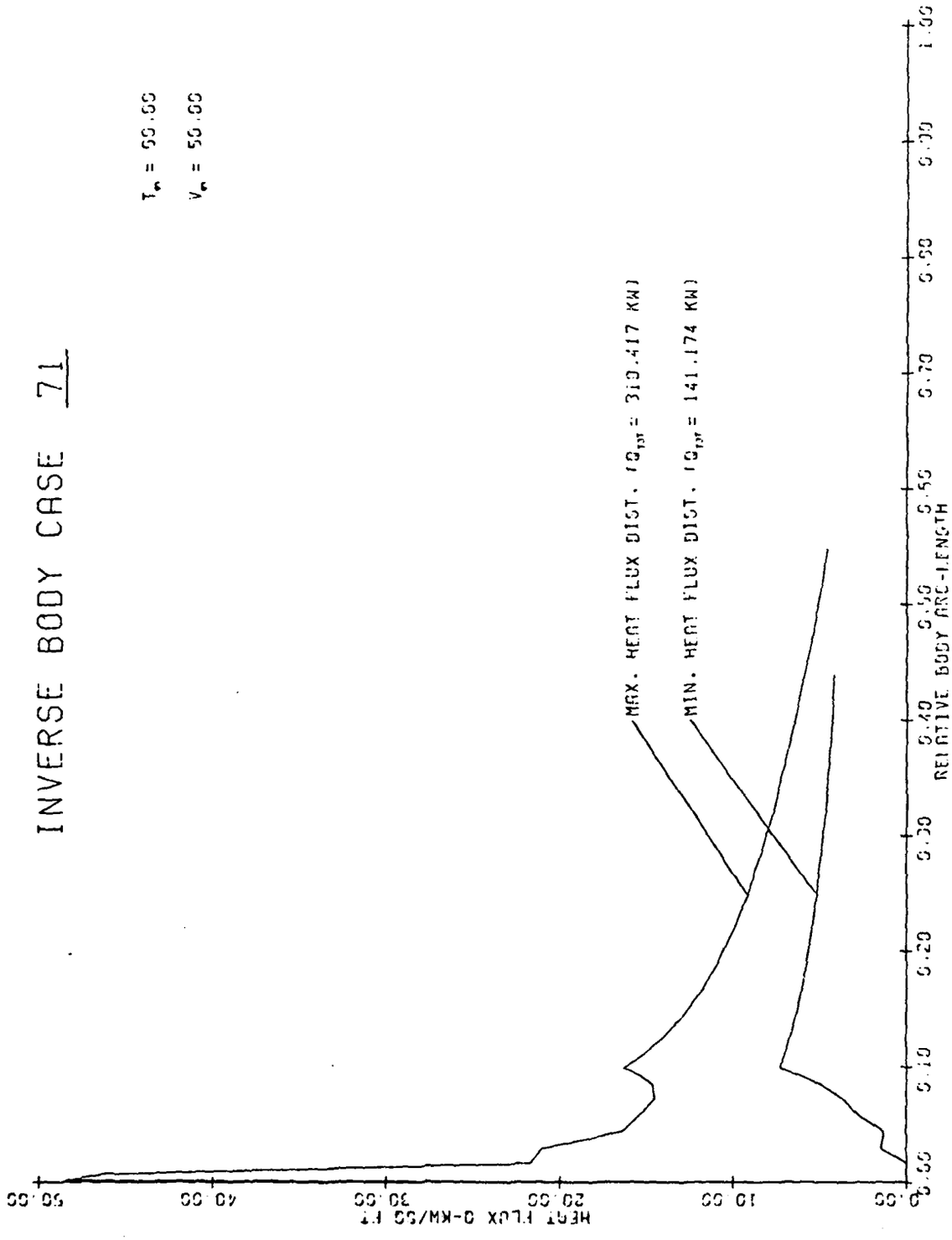

Figure 229. Heat Flux Distributions, Case No. 71.

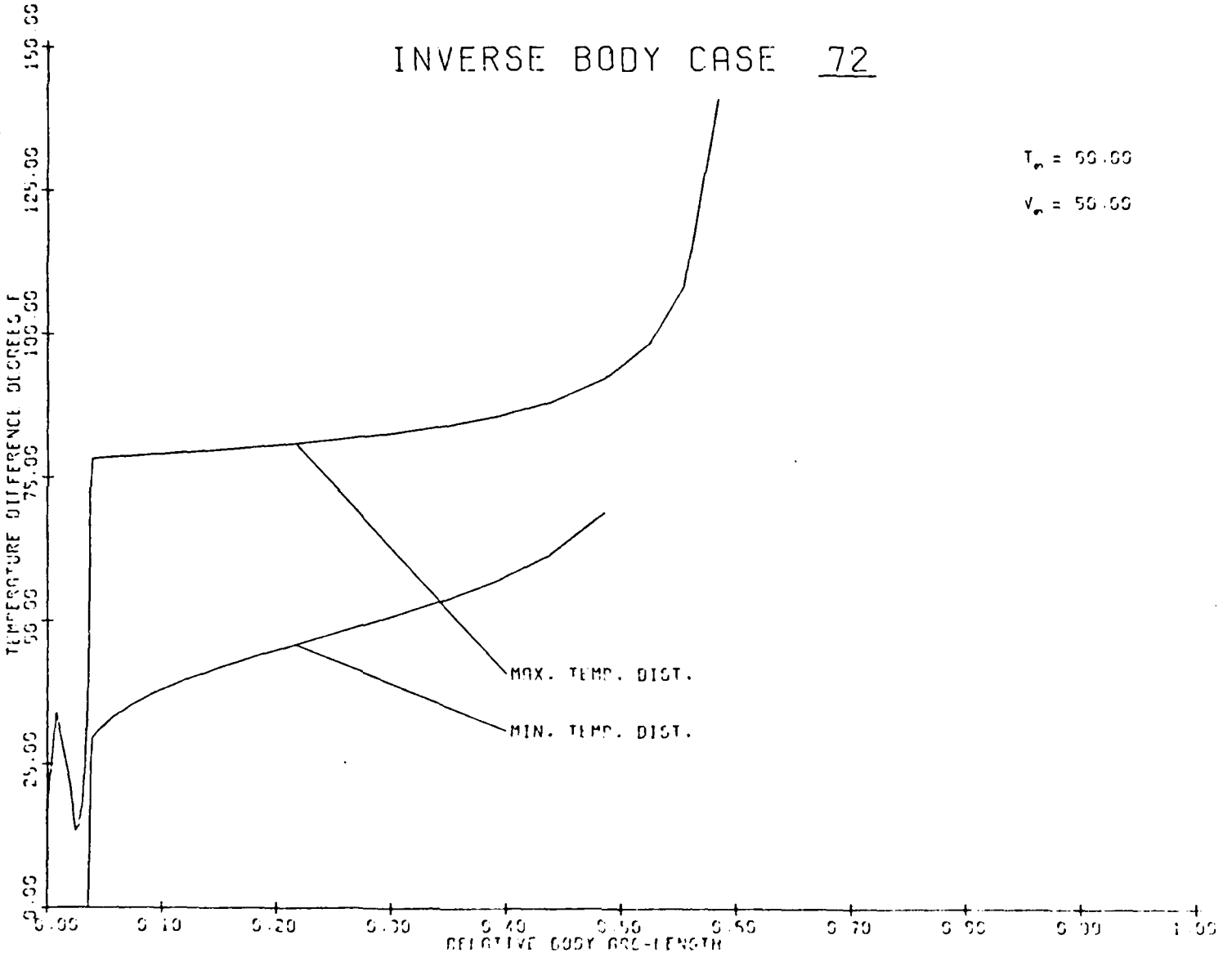

Figure 230. Temperature Distributions, Case No. 72.

19 August 1981
JJE:GHH:mmj

19 August 1981
JJE:GHH:mmj

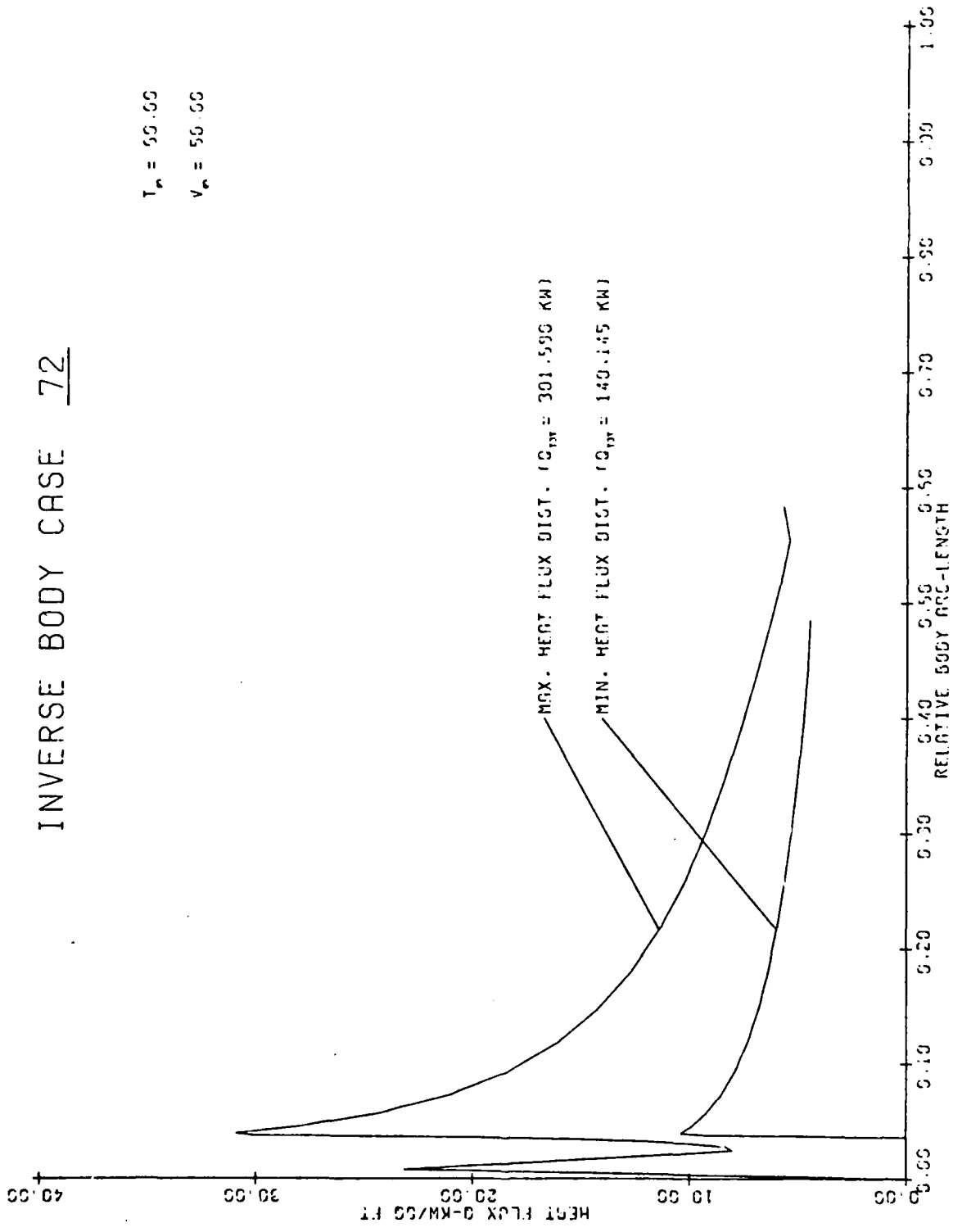

Figure 231. Heat Flux Distributions, Case No. 72.

19 August 1981
JJE:GHH:mmj

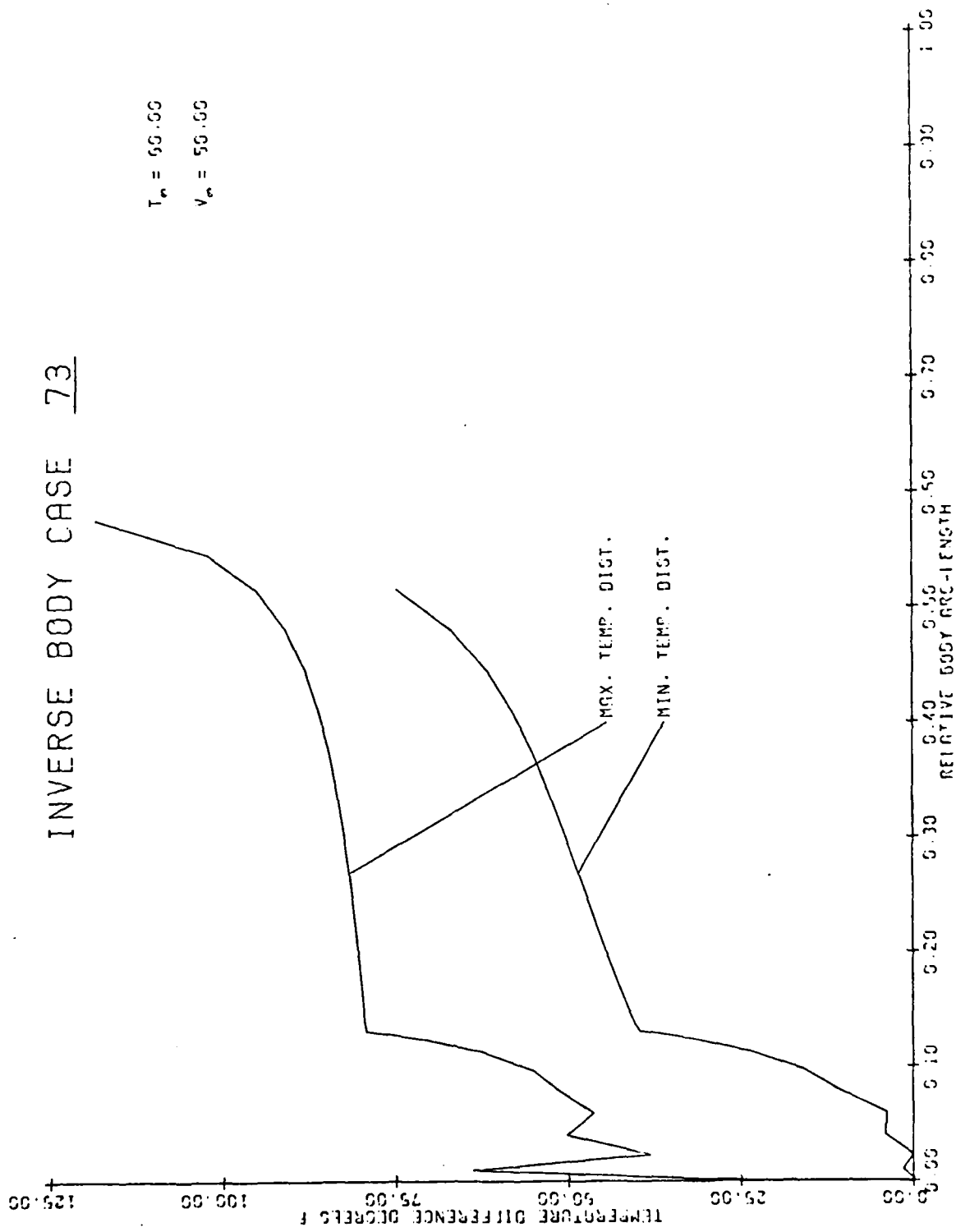

Figure 232. Temperature Distributions, Case No. 73.

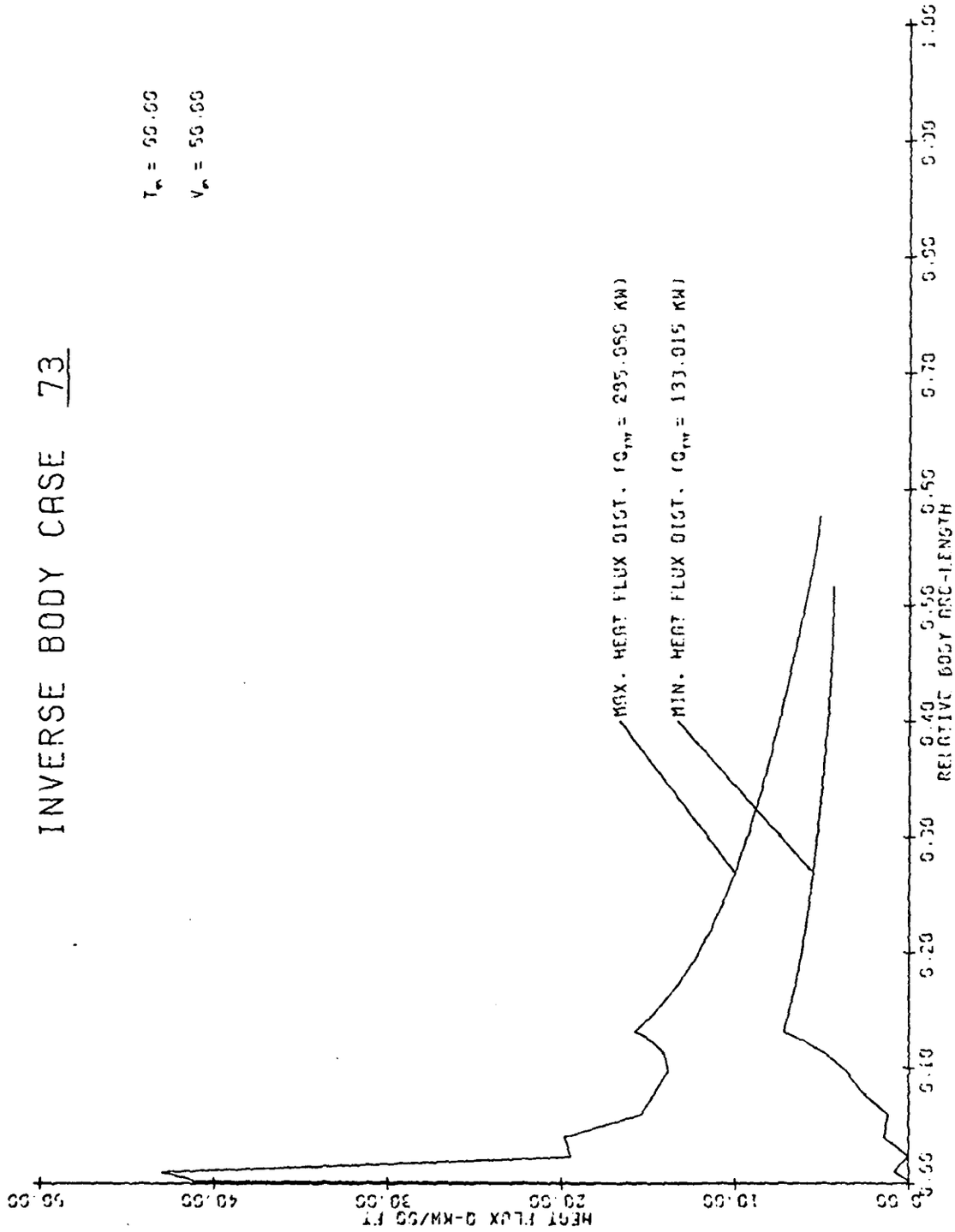

Figure 233. Heat Flux Distributions, Case No. 73.

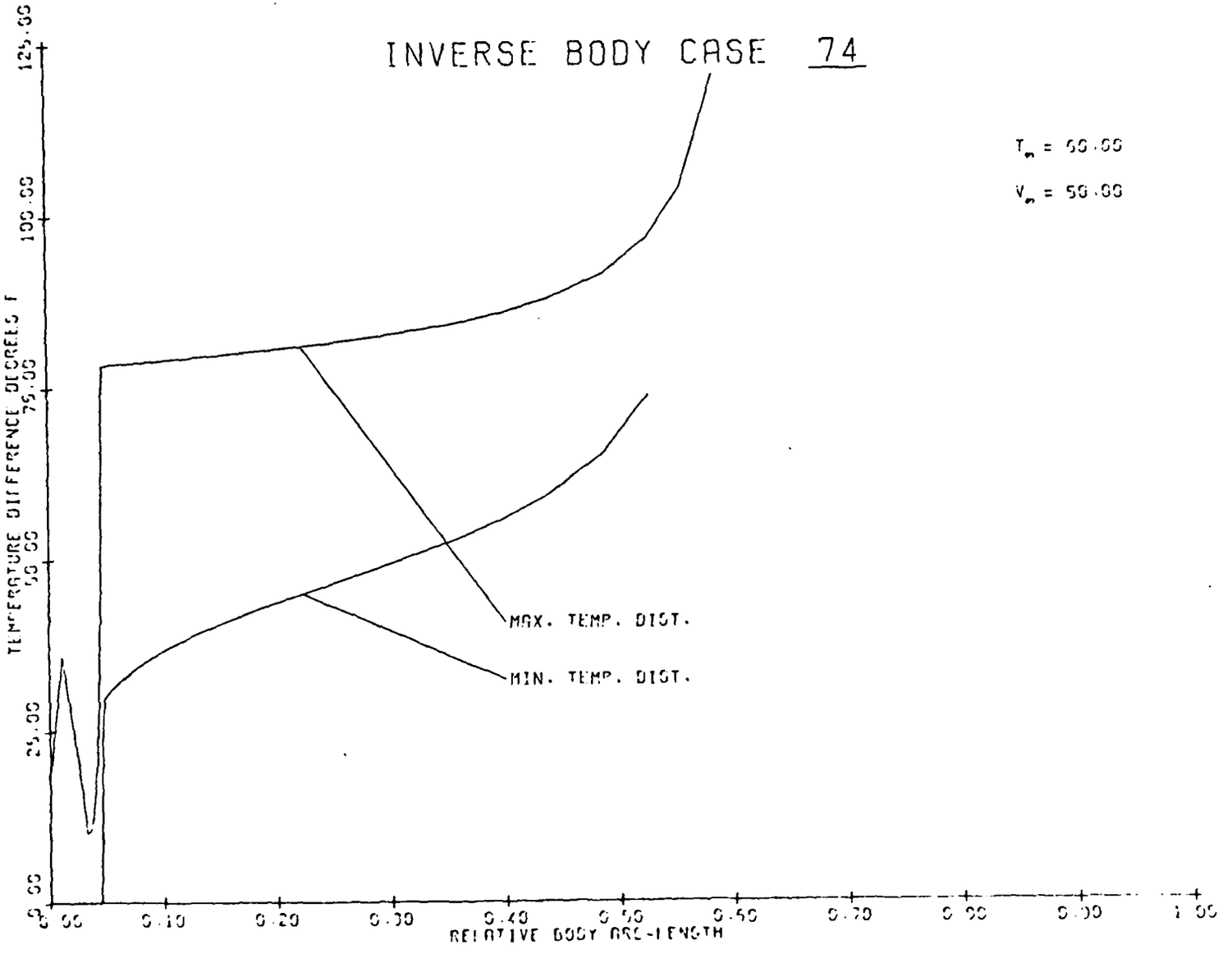

Figure 234. Temperature Distributions, Case No. 74.

19 August 1981
JJE:GHH:mmj

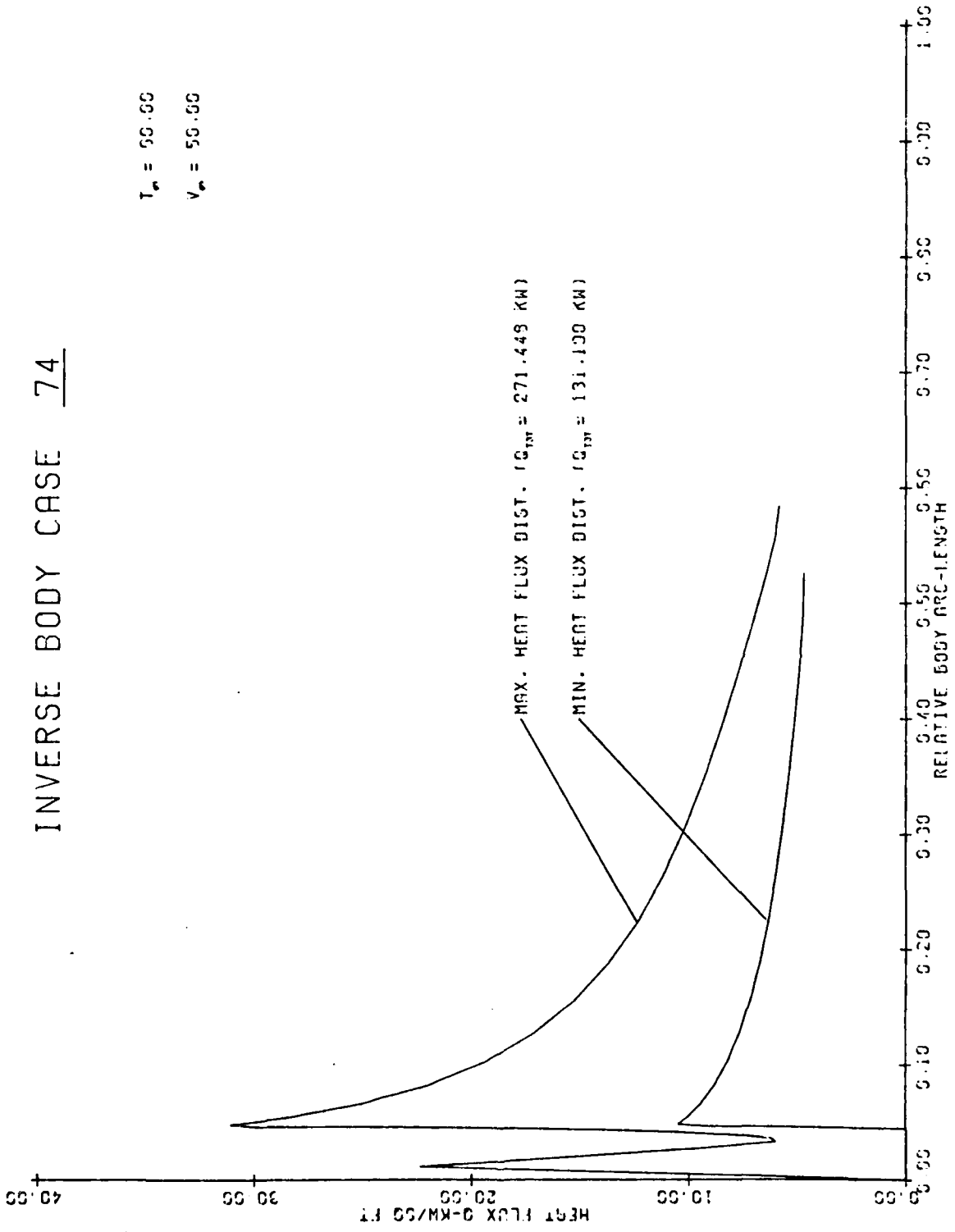

Figure 235. Heat Flux Distributions, Case No. 74.

19 August 1981
JJE:GHH:mmj

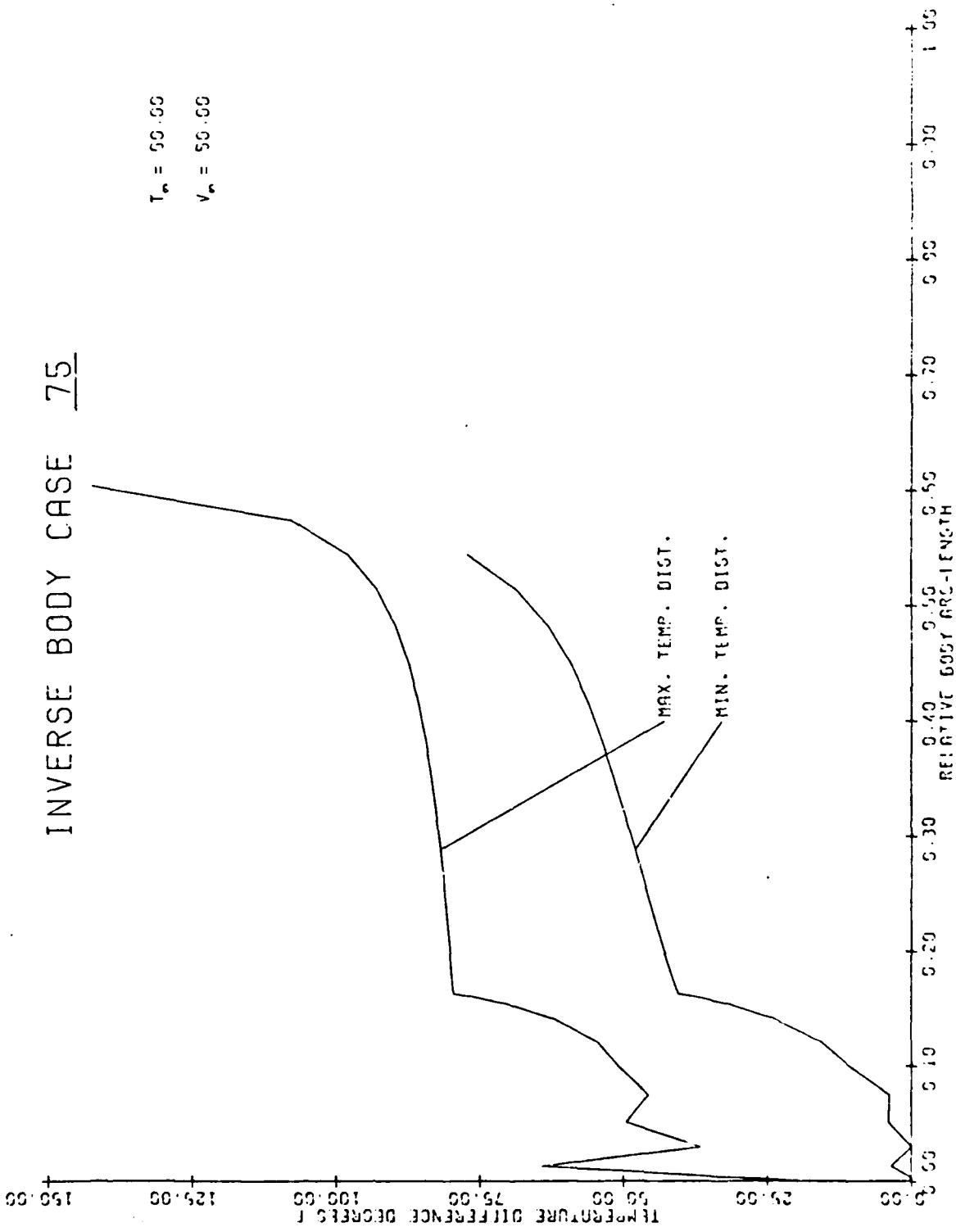

Figure 236. Temperature Distributions, Case No. 75.

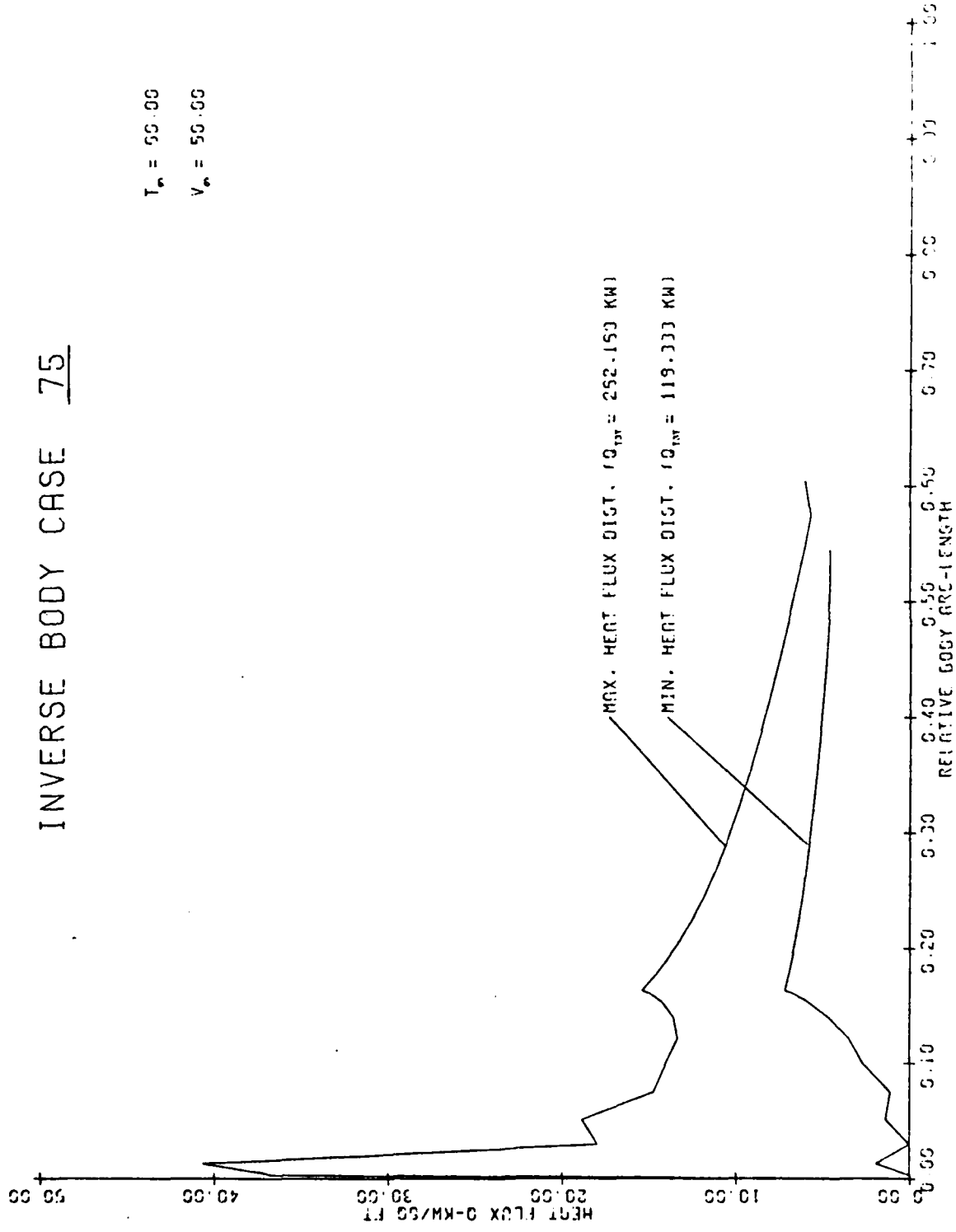

Figure 237. Heat Flux Distributions, Case No. 75.

19 August 1981
. JJE:GHH:mmj

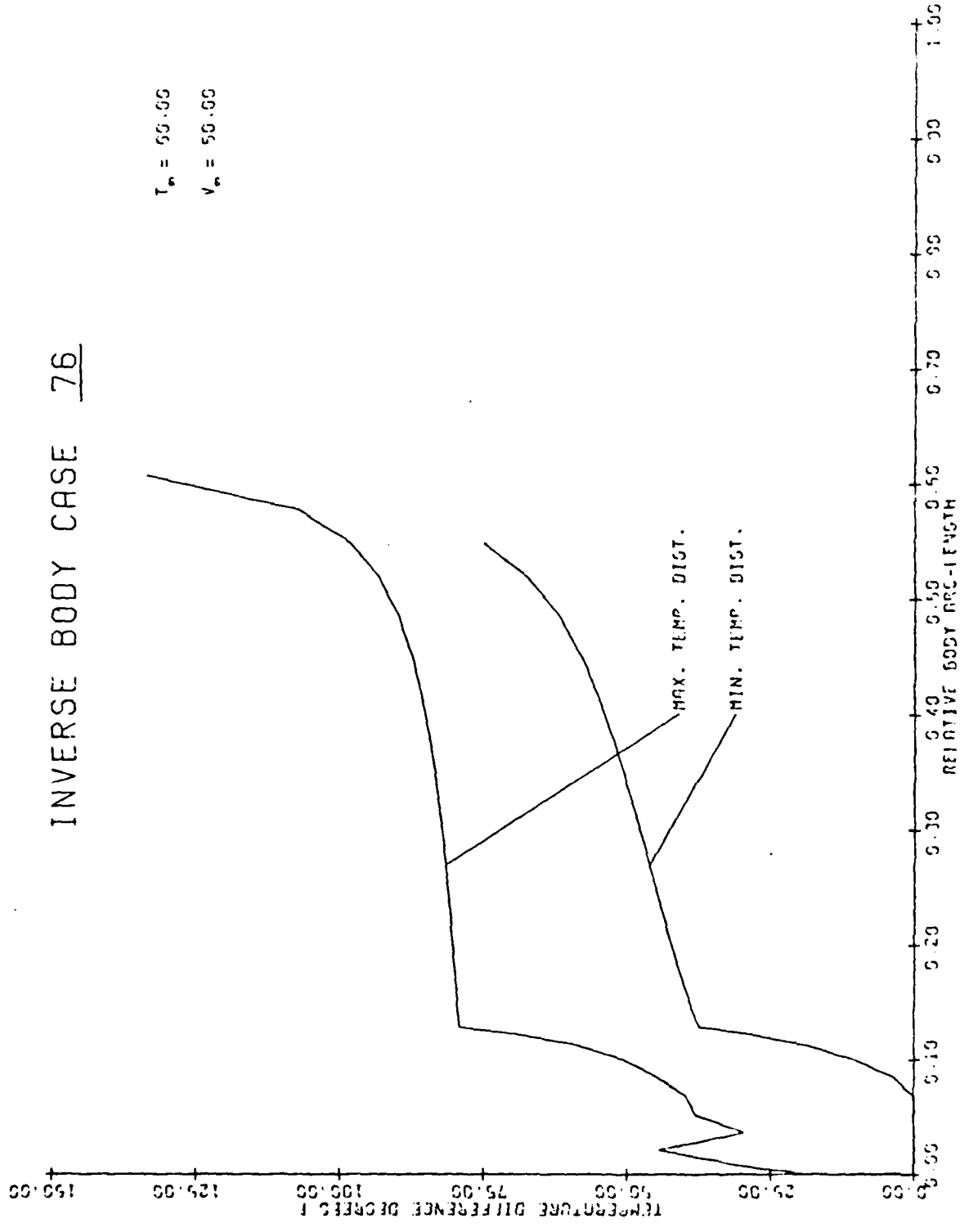

Figure 238. Temperature Distributions, Case No. 76.

19 August 1981
JJE:GHH:mmj

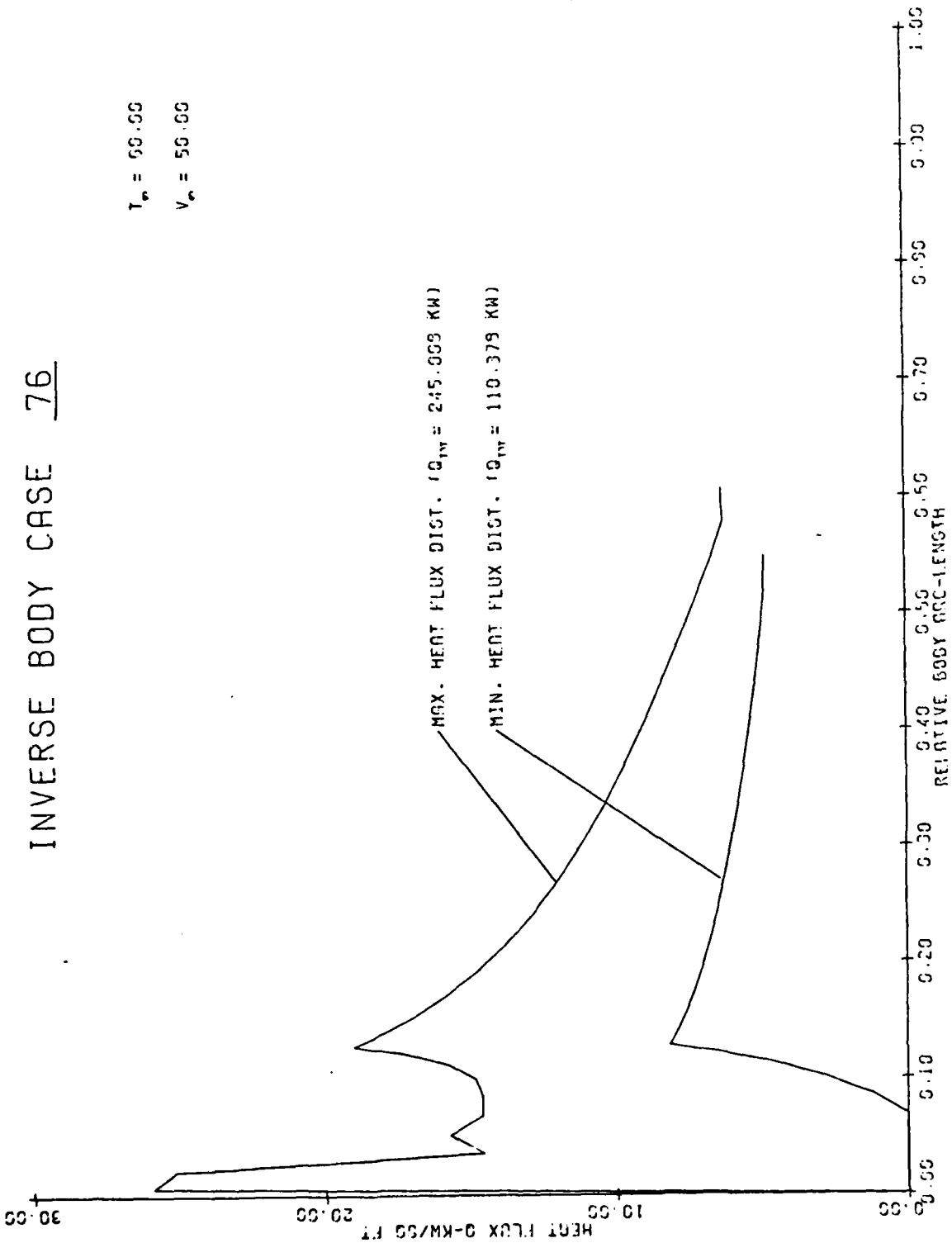

Figure 239. Heat Flux Distributions, Case No. 76.

19 August 1981
JJE:GHH:mmj

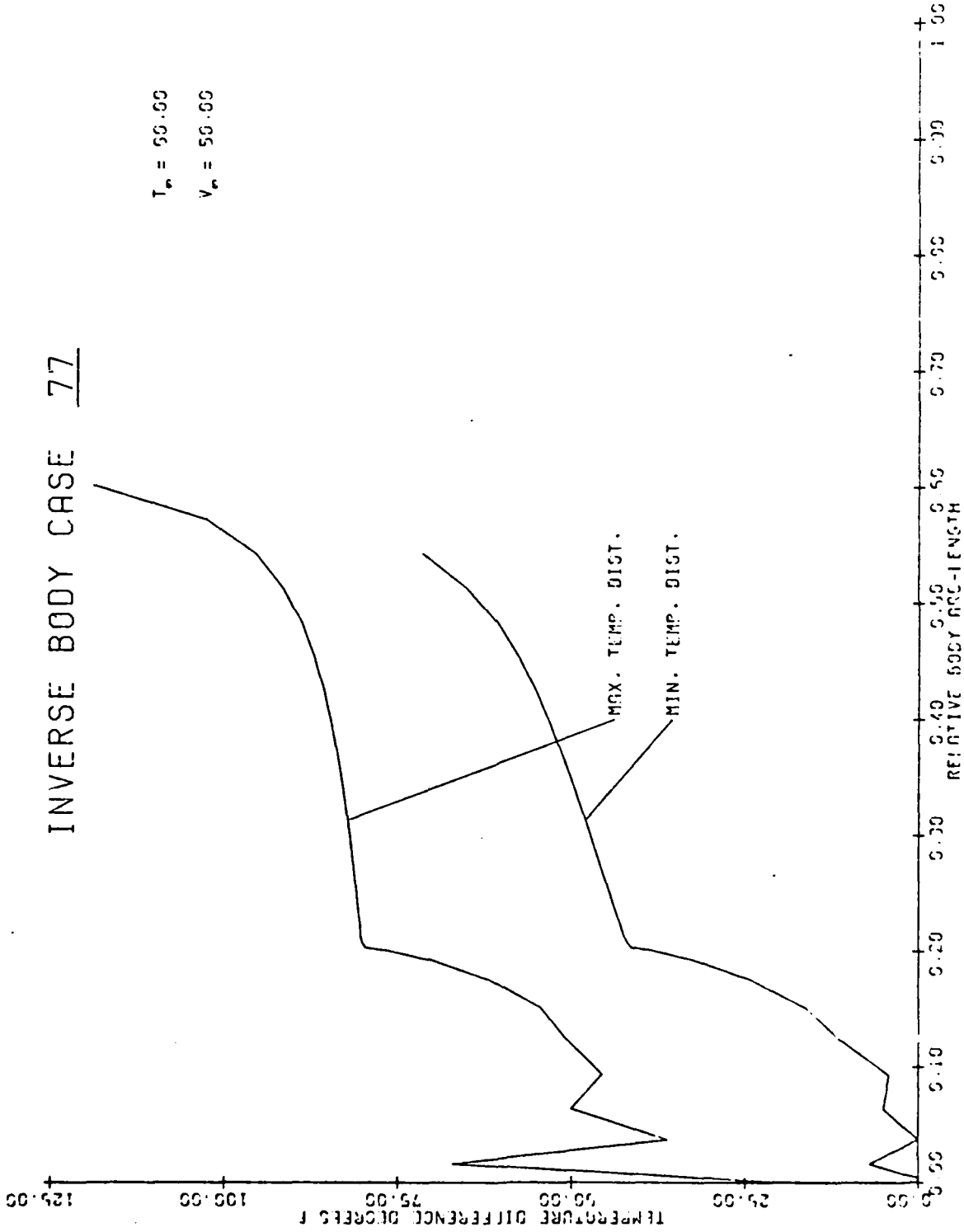

Figure 240. Temperature Distributions, Case No. 77.

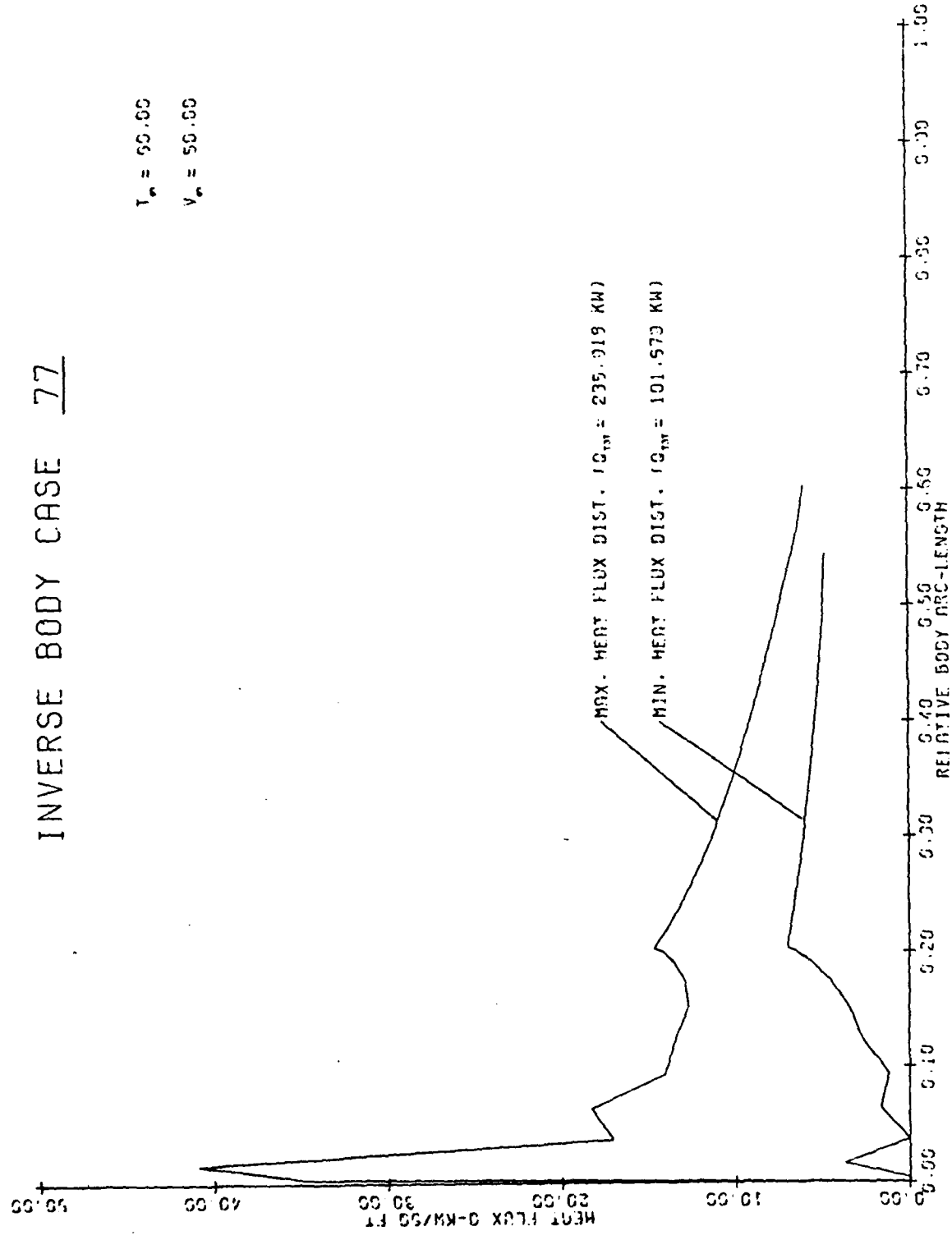

Figure 241. Heat Flux Distributions, Case No. 77.

19 August 1981
JJE:GHH:mmj

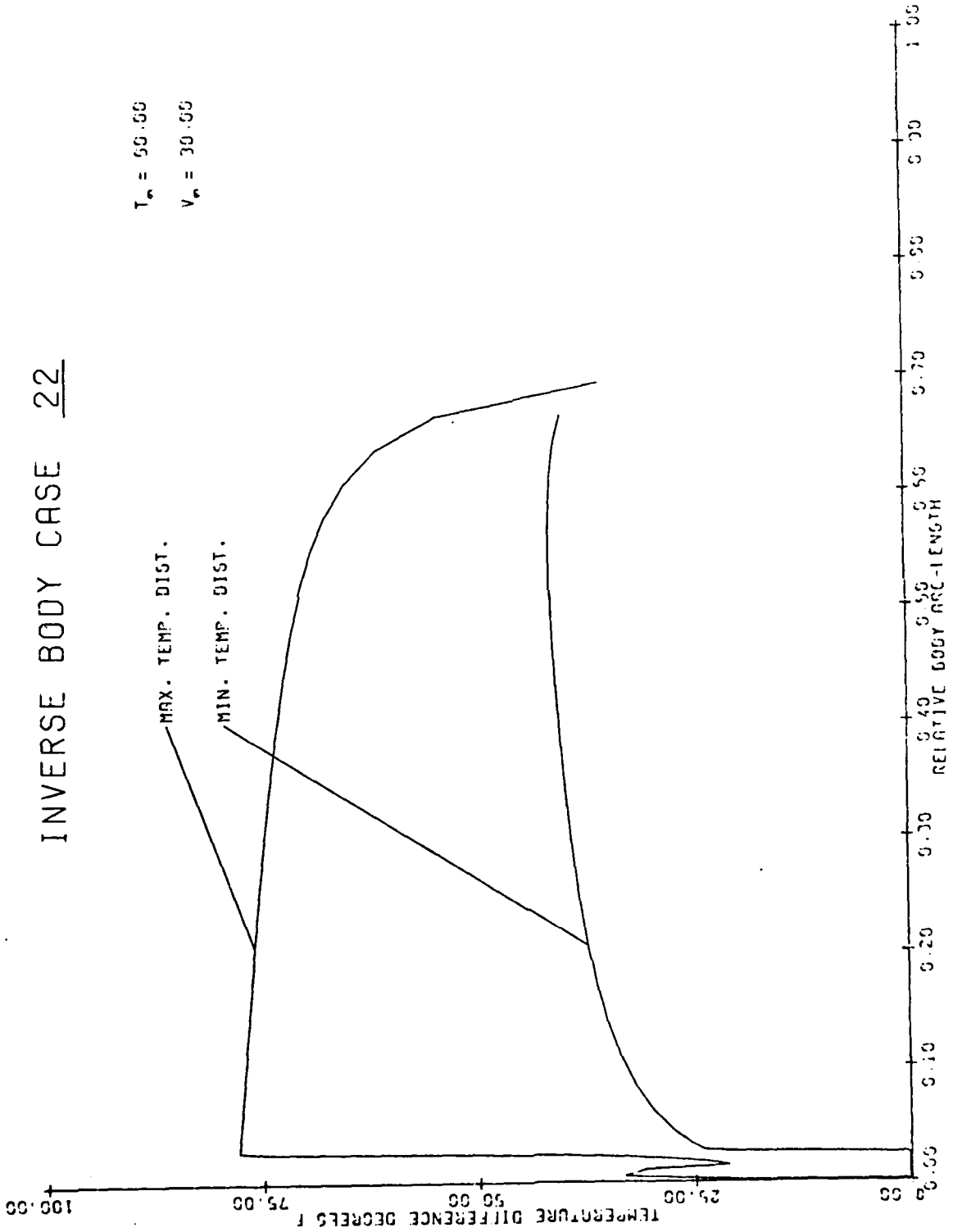

Figure 242. Temperature Distributions, Case No. 22, (V_∞ = 30 fps, D = 21 in.).

19 August 1981
JJE:GHH:mmj

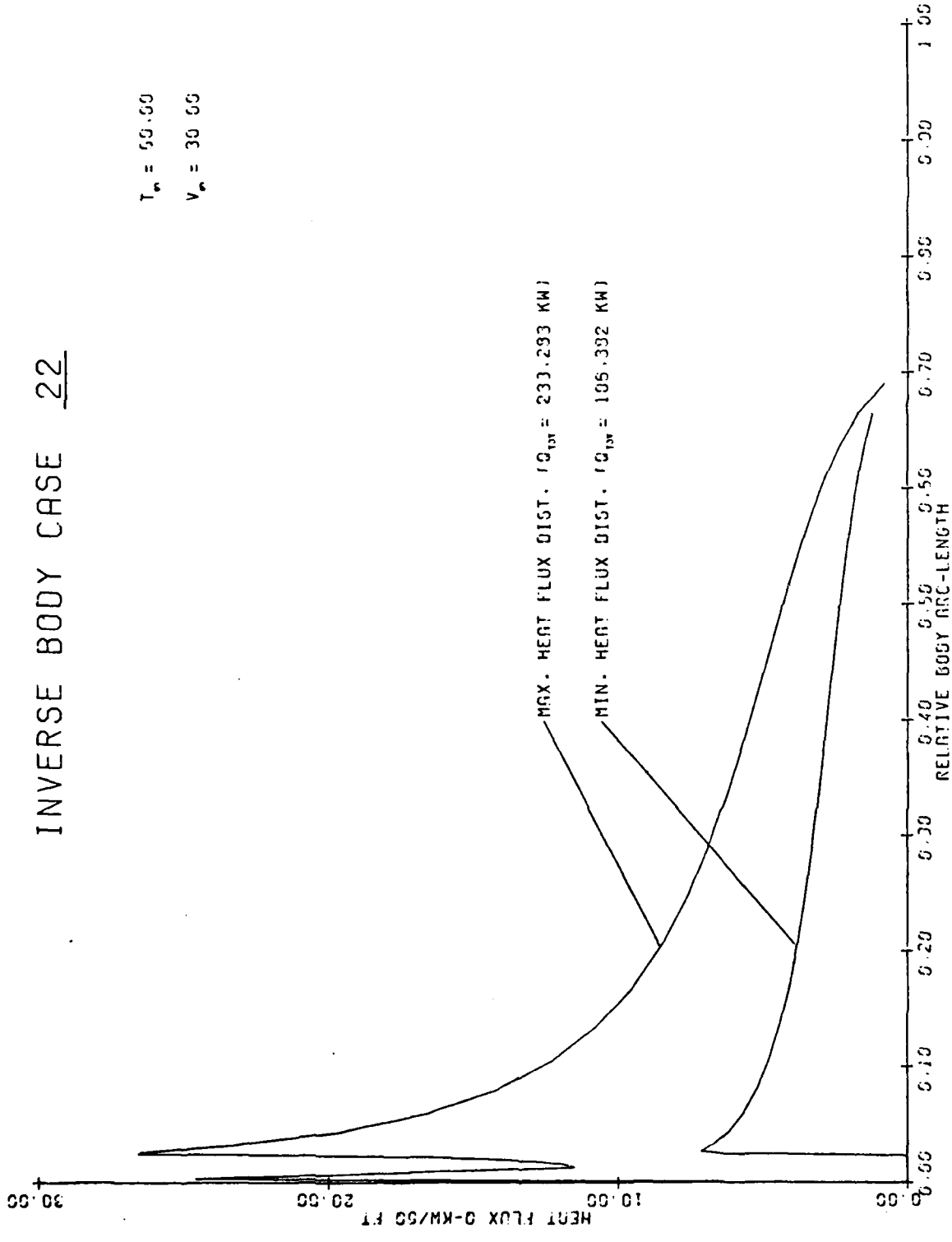

Figure 243. Heat Flux Distributions, Case No. 22, (V_∞ = 30 fps, D = 21 in.).

19 August 1981
JJE:GHH:mmj

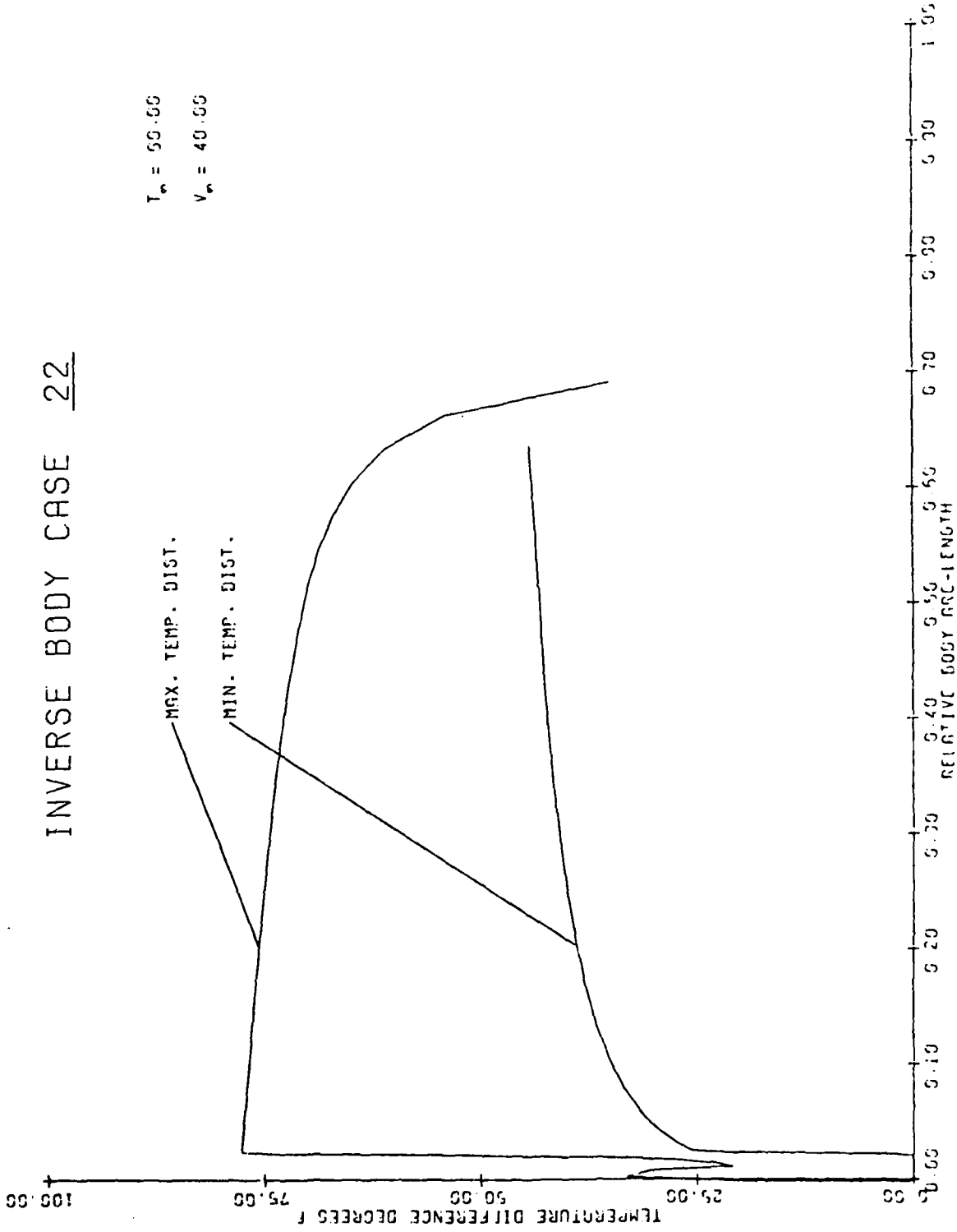

Figure 244. Temperature Distributions, Case No. 22, (V_∞ = 40 fps, D = 21 in.).

19 August 1981
JJE:GHH:mmj

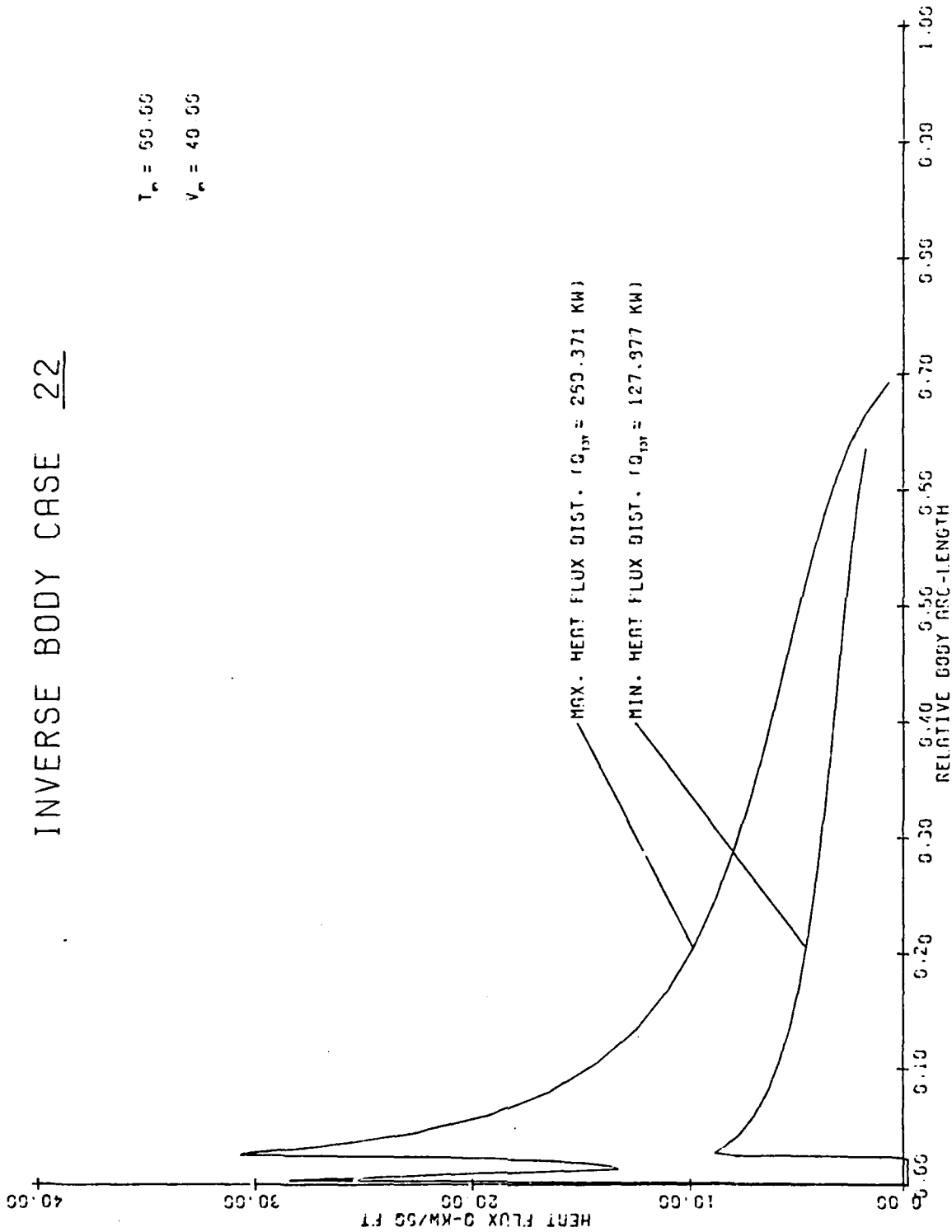

Figure 245. Heat Flux Distributions, Case No. 22, (V_∞ = 40 fps, D = 21 in.).

19 August 1981
JJE:GHH:mmj

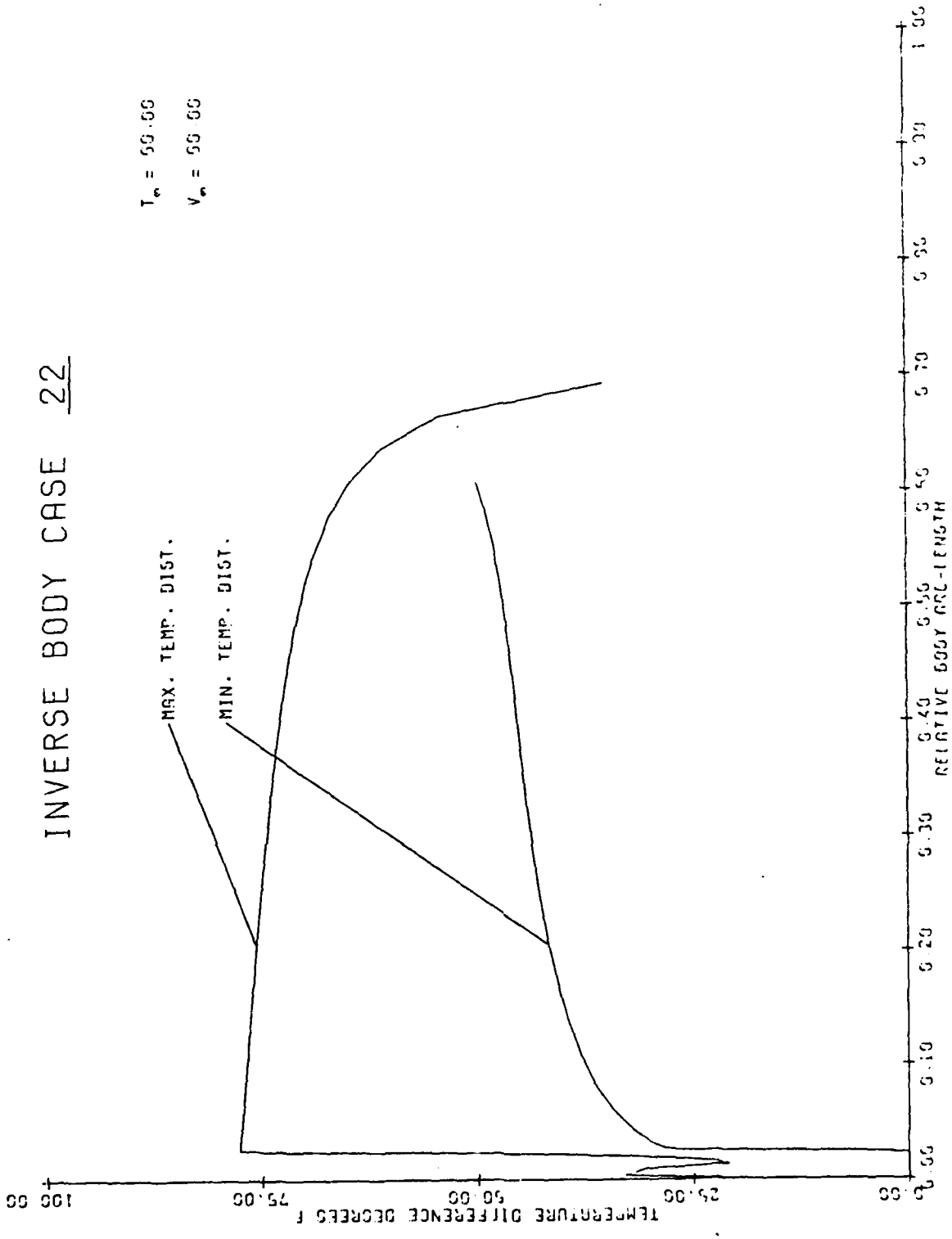

Figure 246. Temperature Distributions, Case No. 22, (V_∞ = 60 fps, D = 21 in.).

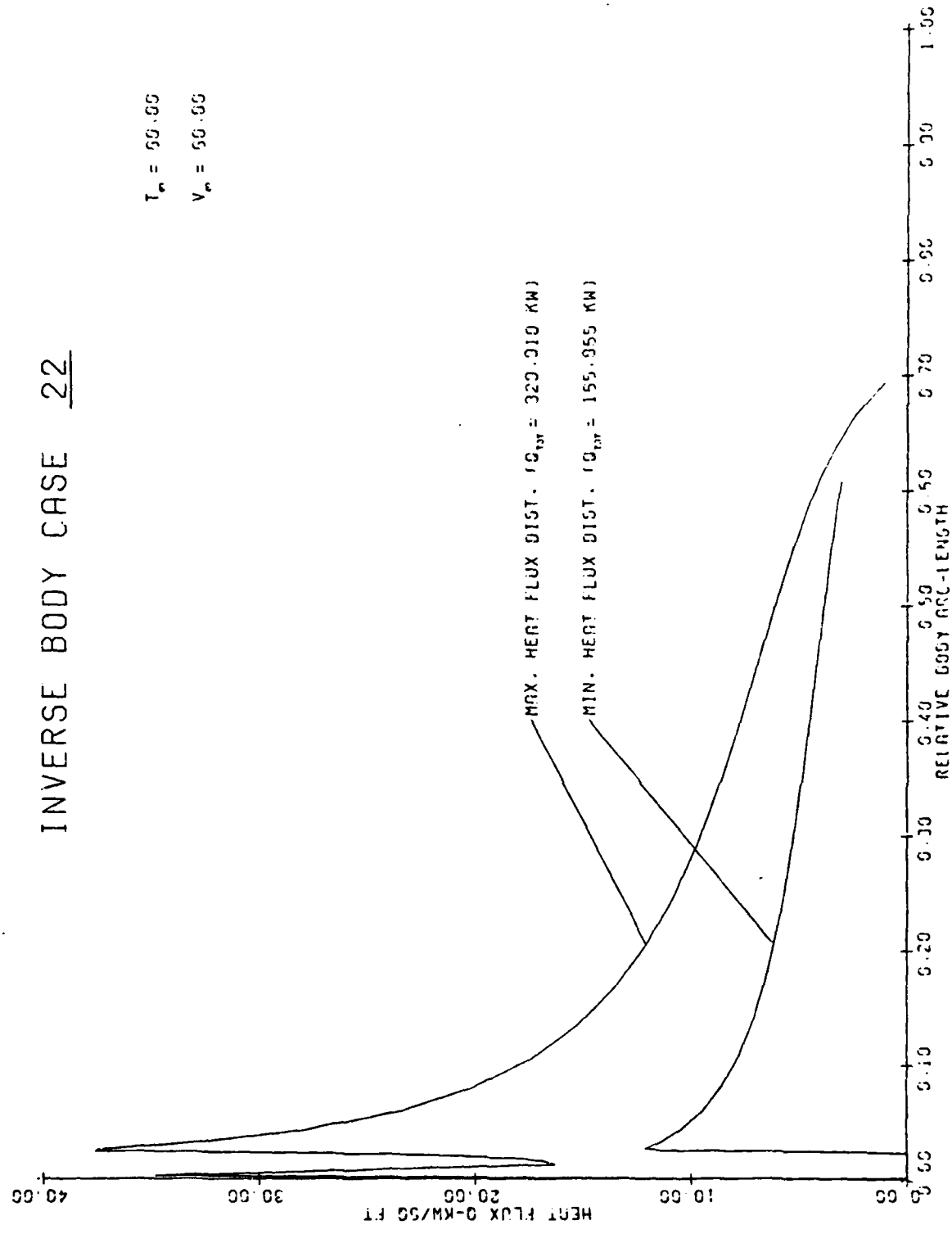

Figure 247. Heat Flux Distributions, Case No. 22, (V_∞ = 60 fps, D = 21 in.).

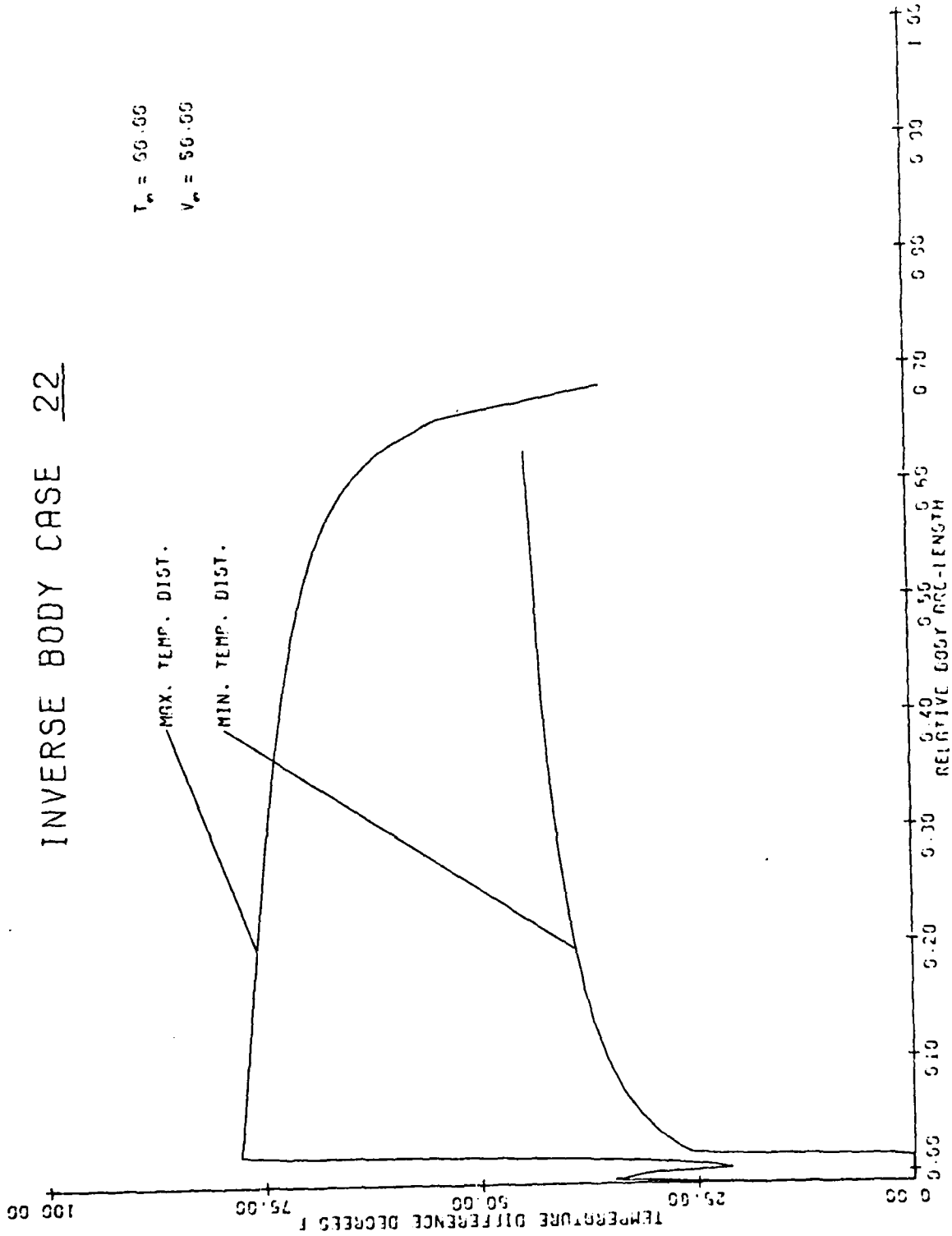

Figure 248. Temperature Distributions, Case No. 22, (V_∞ = 50 fps, D = 16.5 in.).

19 August 1981
JJE:GHH:mmj

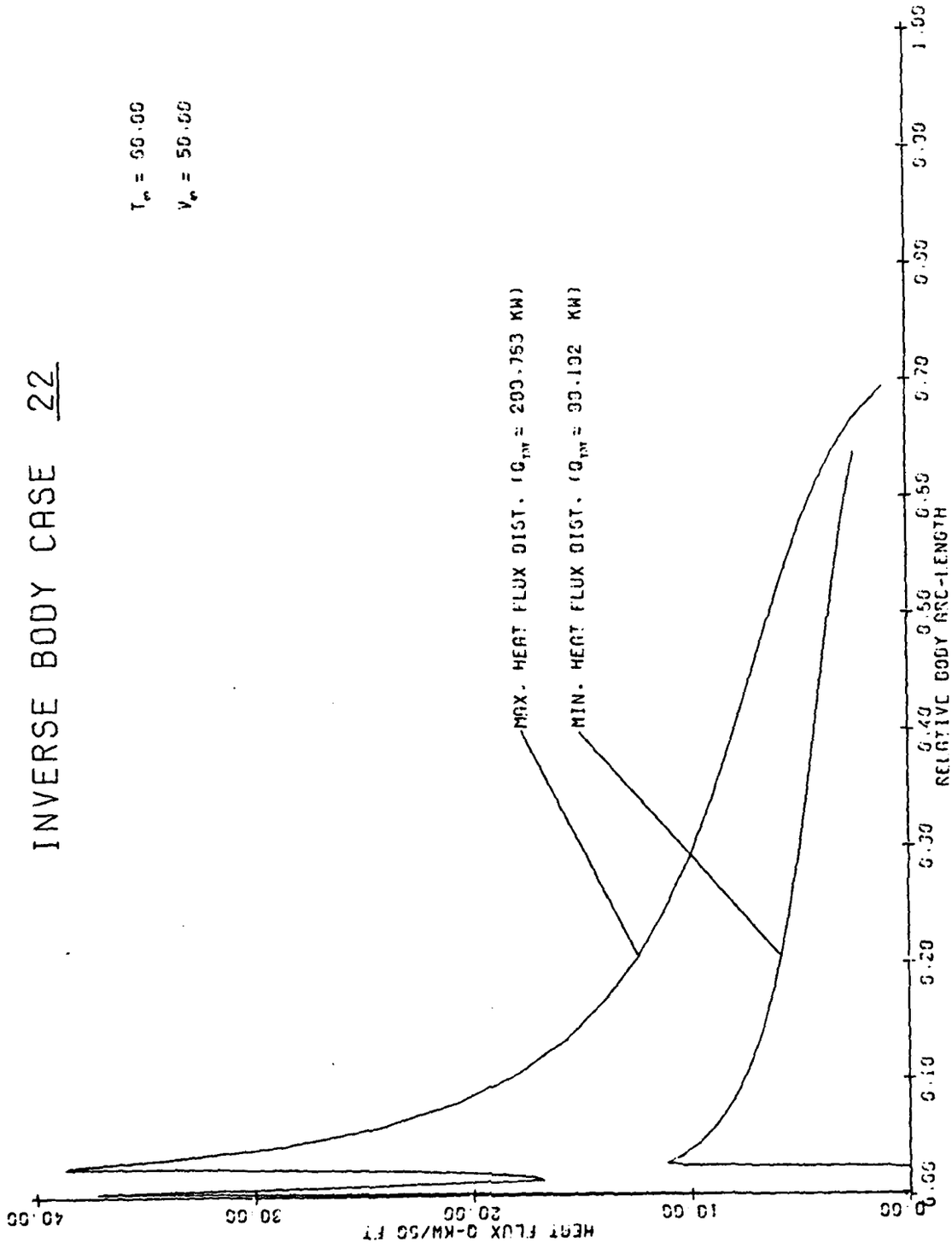

Figure 249. Heat Flux Distributions, Case No. 22, (V_∞ = 50 fps, D = 16.5 in.).

19 August 1981
JJE:GHH:mmj

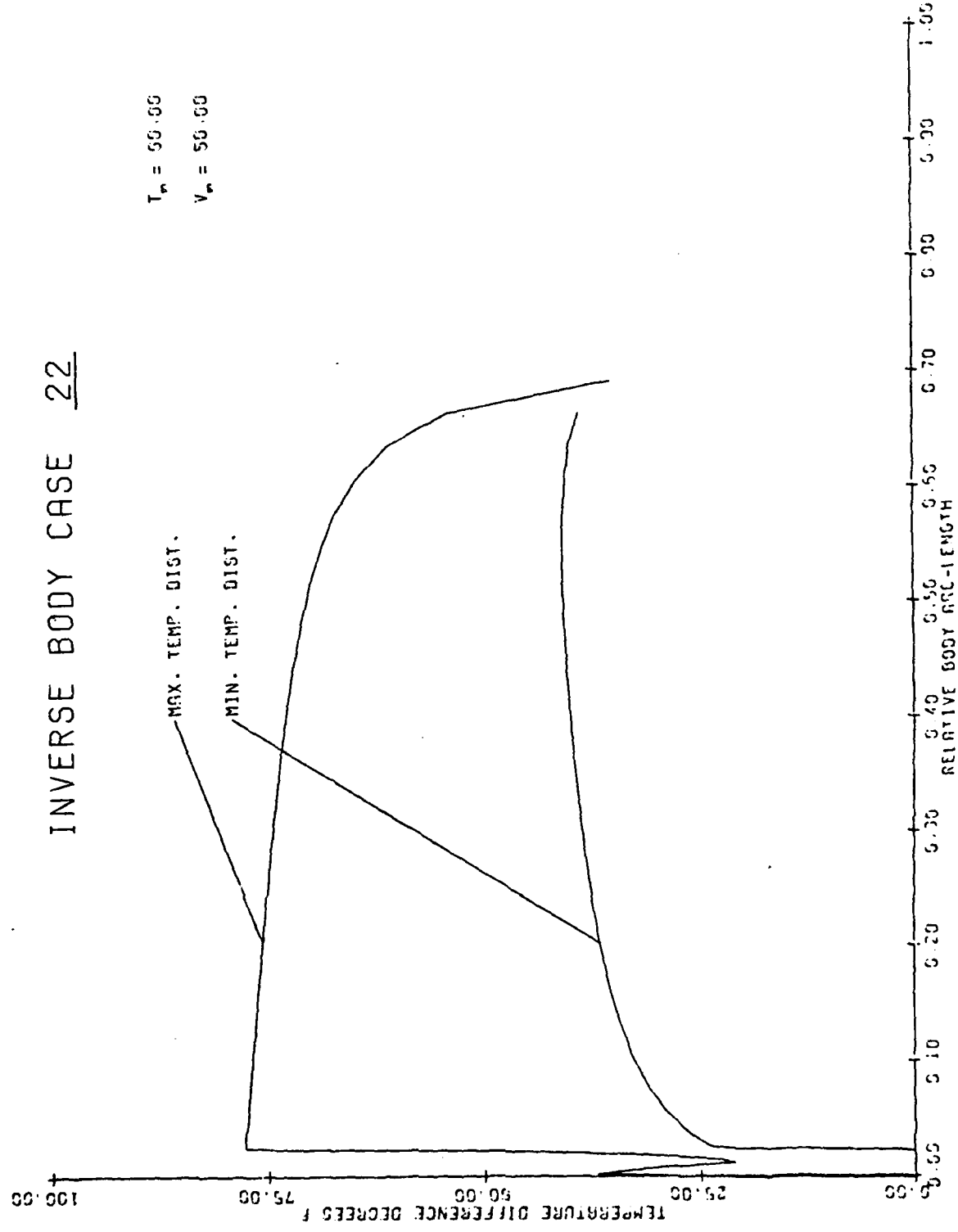

Figure 250. Temperature Distributions, Case No. 22, (V_∞ = 50 fps, D = 12 in.).

19 August 1981
JJE:GHH:mmj

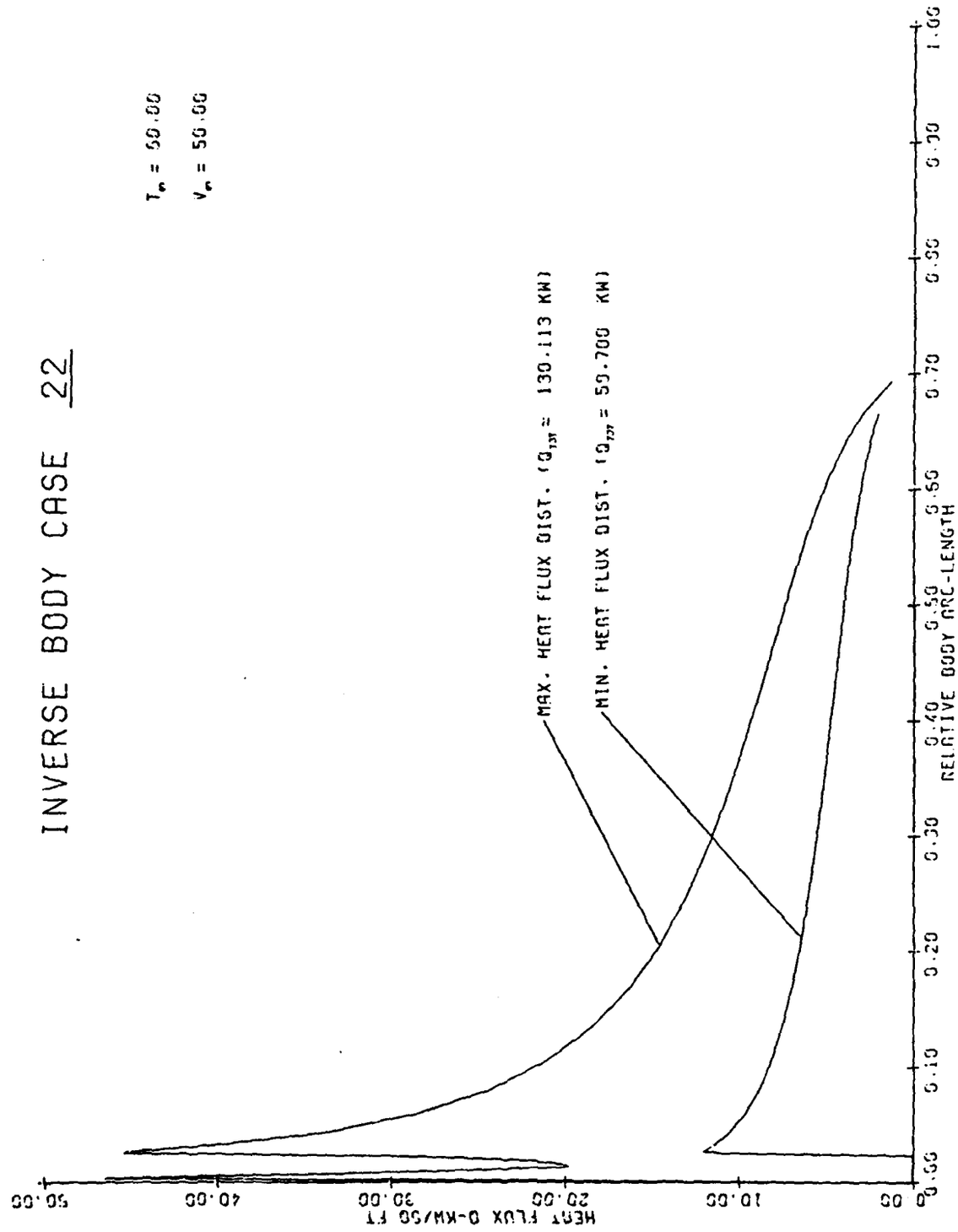

Figure 251. Heat Flux Distributions, Case No. 22, (V_∞ = 50 fps, D = 12 in.).

DISTRIBUTION LIST FOR UNCLASSIFIED TM 81-177 by J. J. Eisenhuth and G. H. Hoffman, dated 19 August 1981

Commander
Naval Sea Systems Command
Department of the Navy
Washington, DC 20362
Attn: Library
Code NSEA-09G32
(Copy Nos. 1 and 2)

Naval Sea Systems Command
Attn: S. M. Blazek
Code NSEA-05HB
(Copy No. 3)

Naval Sea Systems Command
Attn: F. E. Eissing
Code NSEA-05H
(Copy No. 4)

Naval Sea Systems Command
Attn: E. G. Liszka
Code NSEA-63R1
(Copy No. 5)

Naval Sea Systems Command
Attn: C. G. McGuigan
Code NSEA-63R2
(Copy No. 6)

Naval Sea Systems Command
Attn: A. R. Paladino
Code NSEA-05H1
(Copy No. 7)

Naval Sea Systems Command
Attn: T. E. Peirce
Code NSEA-63R3
(Copy No. 8)

Naval Sea Systems Command
Attn: F. J. Romano
Code NSEA-63R3
(Copy No. 9)

Naval Sea Systems Command
Attn: A. D. Whitt
Code PMS-406E
(Copy No. 10)

Naval Sea Systems Command
Attn: F. Peterson
Code NSEA-052P
(Copy No. 11)

Commanding Officer
Naval Underwater Systems Center
Newport, RI 02840
Attn: Library
Code 54
(Copy No. 12)

Naval Underwater Systems Center
Attn: D. Goodrich
Code 3634
(Copy No. 13)

Naval Underwater Systems Center
Attn: T. A. Davis
Code 36314
(Copy No. 14)

Naval Underwater Systems Center
Attn: R. J. Kittredge
Code 36301
(Copy No. 15)

Naval Underwater Systems Center
Attn: B. J. Myers
Code 36311
(Copy No. 16)

Naval Underwater Systems Center
Attn: R. H. Nadolink
Code 3634
(Copy No. 17)

Naval Underwater Systems Center
Attn: R. Trainor
Code 36314
(Copy No. 18)

Naval Underwater Systems Center
Attn: C. Hervey
Code 3634
(Copy No. 19)

Commanding Officer
Naval Ocean Systems Center
San Diego, CA 92152
Attn: D. Nelson
Code 6342
(Copy No. 20)

DISTRIBUTION LIST FOR UNCLASSIFIED TM 81-177 by J. J. Eisenhuth and G. H. Hoffman, dated 19 August 1981

Commander
David W. Taylor Naval Ship R&D Center
Department of the Navy
Bethesda, MD 20084
Attn: W. K. Blake
Code 1905
(Copy No. 21)

David W. Taylor Naval Ship R&D Center
Attn: T. E. Brockett
Code 1544
(Copy No. 22)

David W. Taylor Naval Ship R&D Center
Attn: M. J. Casarella
Code 1942
(Copy No. 23)

David W. Taylor Naval Ship R&D Center
Attn: T. M. Farabee
Code 1942
(Copy No. 24)

David W. Taylor Naval Ship R&D Center
Attn: J. H. McCarthy
Code 154
(Copy No. 25)

David W. Taylor Naval Ship R&D Center
Attn: W. B. Morgan
Code 15
(Copy No. 26)

David W. Taylor Naval Ship R&D Center
Attn: M. M. Sevik
Code 19
(Copy No. 27)

David W. Taylor Naval Ship R&D Center
Attn: J. Shen
Code 194
(Copy No. 28)

David W. Taylor Naval Ship R&D Center
Attn: Code 1505
(Copy No. 29)

David W. Taylor Naval Ship R&D Center
Attn: T. T. Huang
Code 1552
(Copy No. 30)

David W. Taylor Naval Ship R&D Center
Attn: Y. T. Shen
Code 1552
(Copy No. 31)

Commander
Naval Surface Weapons Center
Silver Spring, MD 20910
Attn: J. L. Baldwin
Code WA-42
(Copy No. 32)

Naval Surface Weapons Center
Attn: V. C. D. Dawson
Code U-1
(Copy No. 32)

Naval Surface Weapons Center
Attn: G. C. Gaunaurd
Code R-31
(Copy No. 33)

Naval Surface Weapons Center
Attn: J. E. Goeller
Code WA-42
(Copy No. 34)

Office of Naval Research
Department of the Navy
800 N. Quincy Street
Arlington, VA 22217
Attn: H. Fitzpatrick
Code 438
(Copy No. 35)

Office of Naval Research
Attn: R. H. Imus
Code 102 IP
(Copy No. 36)

Office of Naval Research
Attn: M. M. Reischmann
(Copy No. 37)

Office of Naval Research
Attn: A. H. Gilmore
(Copy No. 38)

Defense Technical Information Center
5010 Duke Street
Cameron Station
Alexandria, VA 22314
(Copy Nos. 39 through 44)

Dynamics Technology, Inc.
22939 Hawthorne Blvd. Suite 200
Torrance, CA 90505
Attn: W. W. Haigh
(Copy No. 45)

Dynamics Technology, Inc.
Attn: G. L. Donohue
(Copy No. 46)

DISTRIBUTION LIST FOR UNCLASSIFIED TM 81-177 by J. J. Eisenhuth and G. H. Hoffman, dated 19 August 1981

National Bureau of Standards
Aerodynamics Section
Washington, DC 20234
Attn: P. S. Klebanoff
(Copy No. 47)

Naval Research Laboratory
Washington, DC 20390
Attn: R. J. Hansen
(Copy No. 48)

NASA Lewis Research Center
21000 Brookpark Road
Cleveland, Ohio 44135
Attn: M. J. Hartmann
MS 5-9
(Copy No. 49)

NASA Lewis Research Center
Attn: W. M. McNally
MS 5-9
(Copy No. 50)

NASA Lewis Research Center
Attn: N. C. Sanger
MS 5-9
(Copy No. 51)

Applied Physics Laboratory/
University of Washington (APL/UW)
1013 NE 40th Street
Seattle, WA 98105
(Copy No. 52)

Applied Research Laboratories/
University of Texas (ARL/UT)
Austin, TX 78712
(Copy No. 53)

Rand Corporation
1700 Main Street
Santa Monica, CA 90406
Attn: C. Gazley
(Copy No. 54)

Martin Marietta Aerospace
Denver Division
P. O. Box 179
Denver, CO 80201
Attn: Leslie Lantz
(Copy No. 55)

The Pennsylvania State University
APPLIED RESEARCH LABORATORY
P. O. Box 30
State College, PA 16801
Attn: J. J. Eisenhuth
(Copy No. 56)

Applied Research Laboratory
Attn: W. S. Gearhart
(Copy No. 57)

Applied Research Laboratory
Attn: G. H. Hoffman
(Copy No. 58)

Applied Research Laboratory
Attn: K. C. Kaufman
(Copy No. 59)

Applied Research Laboratory
Attn: D. H. Kiely
(Copy No. 60)

Applied Research Laboratory
Attn: P. H. Kurtz
(Copy No. 61)

Applied Research Laboratory
Attn: G. C. Lauchle
(Copy No. 62)

Applied Research Laboratory
Attn: B. R. Parkin
(Copy No. 63)

Applied Research Laboratory
Attn: R. B. Smith
(Copy No. 64)

Applied Research Laboratory
Attn: GTWT Files
(Copy No. 65)

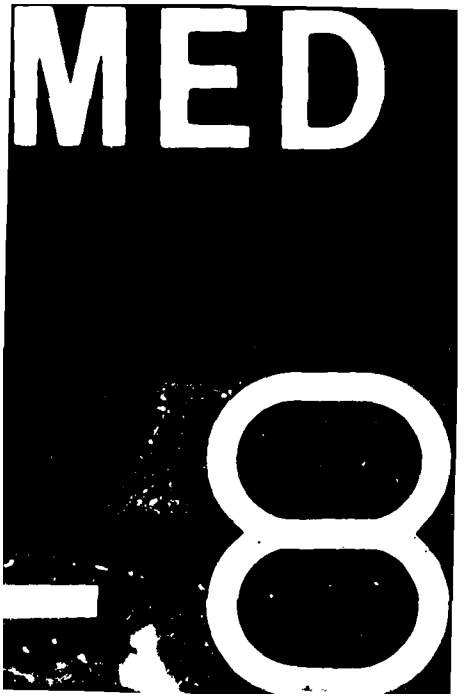
MED
8